LITHOPROBE

Slave-***NOR***thern **C**ordillera ***L***ithospheric ***E***volution (***SNORCLE***)

and

CORDILLERAN TECTONICS WORKSHOP

Report of the 1999 Combined Meeting
March 5-7, 1999
University of Calgary

LITHOPROBE Report No. 69

Recommended Citation:

Cook, F. and P. Erdmer (compilers), 1999, Slave-Northern Cordillera Lithospheric Evolution (SNORCLE) Transect and Cordilleran Tectonics Workshop Meeting (March 5-7), University of Calgary, Lithoprobe Report No. 69, 340 pp.

LITHOPROBE SLAVE/NORTHERN CORDILLERA LITHOSPHERIC EVOLUTION WORKSHOP
and
CORDILLERAN TECTONICS WORKSHOP

University of Calgary, March 5-7, 1999

FRIDAY, March 5, 1999

SESSION 1 - INTRODUCTION AND RESULTS FROM THE WESTERN SLAVE PROVINCE TO CORDILLERA

Page

08:30-08:45 Introduction and Welcome
F.A. Cook and P. Erdmer

08:45-09:00 1)LITHOPROBE update
R.M. Clowes (Project Director)

09:00-09:15 2)Evidence of crustal attenuation in the Archean Beniah formation, Northwest Territories
W.U. Mueller and C. Pickett.....14

09:15-09:30 3)Sedimentology and tectonic setting of the Burwash formation, Hearne Lake - Gordon Lake area
M. Ferguson, J. Waldron and W. Bleeker.....16

09:30-09:45 4)Seamount architecture of Archean volcanic sequences in the Slave province, Northwest Territories
P.L. Corcoran and J. Dostal.....20

09:45-10:15 5)The central Slave cover group and the central Slave basement complex: A progress report on U-Pb geochronological studies
J. Ketchum and W. Bleeker.....21

(next three talks)

6)Timing of plutonism, deformation and metamorphism in the Yellowknife domain, Slave province
W.J. Davis and W. Bleeker.....30

7)Crustal architecture of the Slave craton
W. Bleeker, B. Davis and J. Ketchum.....32

10:15-10:45 COFFEE

Page

10:45-11:00 8)Towards an integrated geological-geophysical interpretation of the Slave portion of the SNORCLE transect
W. Bleeker, D. Snyder, B. Roberts, W. Roest and K. Hendry.....34

11:00-11:15 9)More thoughts about the nature of bright reflections in the upper crust near Yellowknife
D. Snyder, B. Roberts and W. Bleeker.....37

11:15-11:30 10)Modeling of gravity profiles in the southern Slave province, - Are greenstones underlying the Yellowknife basin?
K.A.B. Hendry, W. Bleeker and W.R. Roest.....40

11:30-11:45 11)Syn - D_2 plutonism in the southern Slave province: Evidence from magnetic fabrics and field mapping
R. Spark, K. Benn, W. Bleeker and W. Roest.....42

11:45-12:00 12)U- Pb geochronology of lower crustal xenoliths - A window into the deep crust of the central Slave province
W. J. Davis, J. Mackenzie and D. Canil.....46

12:00-12:30 DISCUSSION

12:30-13:30 LUNCH

13:30-13:45 13)Mantle garnets from the Drybones Bay kimberlite and the nature of the on/off craton transition beneath the Slave province, NWT
G.B. Carbno and D. Canil.....48

13:45-14:00 14)U-Pb zircon, Sm-Nd and geochemical study of eclogite xenoliths, Jericho kimberlite pipe: The case for extensive Proterozoic metasomatism beneath the Slave craton
L.M. Heaman, R.A. Creaser and H.O. Cookenboo.....52

14:00-14:15 15)Electromagnetic studies of the Slave craton: Preliminary results and ongoing experiments
A.G. Jones, I. Ferguson, G. McNeice, R. Evans and A. Chave.....56

14:15-14:30 16)Deep EM studies of the Slave craton
R.L. Evans, A.G. Jones and A.D. Chave.....72

14:30-14:45 17)Lithospheric velocity structure beneath the Slave province and Wopmay orogen from the SNORCLE refraction experiment
G. Fernandez Viejo, R.M. Clowes, J.R. Amor and the SNORE Working Group.....73

14:45-15:15 COFFEE

Page

15:15-15:30 18)Characterization of the upper mantle beneath the Archean Slave craton using teleseismic methods
C-G. Bank, M. Bostock, R.M. Ellis and J.F. Cassidy.....81

15:30-15:45 19)Northwestern Canada seismic experiment
M. Bostock, J.B. Gaherty, E.J. Garnero and J.S. Revenaugh.....82

15:45-16:00 20)High heat flow along the SNORCLE transect
T.J. Lewis and R. Hyndman.....83

16:00-16:15 21)The Cordillera-craton thermal transition in northern and southern Canada
R.D. Hyndman and T.J. Lewis.....85

16:15-16:30 22)Thermomechanical modelling of convergent orogens
O. Vanderhaeghe, C. Beaumont, P. Fullsack and R.A. Jamieson..86

16:30-17:30 DISCUSSION

SATURDAY, March 6, 1999

SESSION 2 - NORTHERN CORDILLERA

08:30-08:45 23)Preliminary report on the lower Paleozoic stratigraphy and conodont biostratigraphy, platform to basin transect, in the Trutch, Halfway River and Ware map areas (94G, B, F), British Columbia
C.R. Barnes and L.J. Pyle.....87

08:45-09:00 24)Tectono-stratigraphic framework of Triassic strata, northeastern British Columbia: Ichthyolith biostratigraphy and regional thermal maturation studies
M.J. Johns, C.R. Barnes and M.J. Orchard.....94

09:00-09:15 25)A re-examination of the type section of the Backbone Ranges formation, Mackenzie Mountains, NW Canada: Stratigraphic and tectonic implications
R.B. MacNaughton, G.M. Narbonne and R.W. Dalrymple.....99

09:15-09:30 26)Tectonostratigraphic framework of the Mesoproterozoic Muskwa assemblage, northern British Columbia
D.G.F. Long, J.R. Devaney and B.R. Pratt.....112

Page

09:30-09:45 27)Mid-Cretaceous granites of the southern Yukon: Initial report
G.A. Morris and R.A. Creaser.....120

09:45-10:00 28)Cretaceous extension and regional calcic metasomatism in the Cassiar terrane south of the d'Abbadie pluton, south-central Yukon
M. de Keijzer and P.F. Williams.....122

10:00-10:30 COFFEE

10:30-10:45 29)New terrane interpretation for the St. Cyr klippe, south-central Yukon
K.M. Fallas, P. Erdmer, R.A. Creaser, D.A. Archibald and L.M. Heaman.....130

10:45-11:00 30)Yukon-Tanana terrane and its relationship to Slide Mountain 'terrane', Finlayson Lake area, southeastern Yukon
D.C. Murphy.....138

11:00-11:15 31)Volcanic probes of the craton's edge beneath the northern Canadian Cordillera
D. Francis, A-C. Abraham and M. Polve.....142

11:15-11:30 32)Mantle signature versus crustal contamination in arc-magmatism: An example from Zippa Mountain
M. Westphal, I.M. Coulson, G.M. Dipple and J.K. Russell.....146

11:30-11:45 33)Geotectonic motion history of the Yukon-Tanana terrane: Preliminary paleomagnetic results from the Big Creek and Seymour Creek intrusions
D.T.A. Symons, P.J.A. McCausland, C.J.R. Hart, W.H. Blackburn, M.J. Harris and P.R. Williams.....153

11:45-12:00 34)Crustal seismic velocity structure of the northern Cordillera, southern Yukon Territory - Lithoprobe SNORE line 31
B. Creaser and G. Spence.....163

12:00-12:30 DISCUSSION

12:30-13:30 LUNCH

13:30-13:45 35)Deformation processes along the Denali fault system
J.C. White.....168

Page

13:45-14:00 36)Migmatization in the central gneiss complex, coastal northwestern British Columbia and southeastern Alaska
N.K. Sokol and M.L. Crawford.....169

14:00-14:15 37)Implications of Early Miocene or younger normal faults on interpretation of ACCRETE reflection data, northwest Canadian Cordillera
C.A. Evenchick, M.L. Crawford and V.J. McNicoll.....171

14:15-14:30 38)Crustal structure across the Coast plutonic complex and Stikinia in northwestern British Columbia: Wide-angle P- and S-wave velocity models from ACCRETE and Lithoprobe SNORE line 22
P.T.C. Hammer and R.M. Clowes.....172

14:40-14:45 39)The Omineca belt: A crustal scale shear zone or a zone of thrusting?
P.F. Williams and D. Jiang.....179

14:45-15:00 40)Slip and deformation path partitioning in orogenic belts: Implications for kinematic analysis of geological structures
D. Jiang and P.F. Williams.....180

15:00-15:30 COFFEE

15:30-16:30 DISCUSSION/SNORCLE SYNTHESIS

16:30-??? POSTERS

SUNDAY, March 7, 1999

SESSION 3 - CENTRAL AND SOUTHERN CORDILLERA

08:30-08:45 41)Tectonics of central British Columbia and a proposal for a three-dimensional mapping transect across the Cordillera at 55° latitude
L.C. Struik.....181

08:45-09:00 42)Mid-Jurassic Hobson Lake pluton of the central Cariboo Mountains, British Columbia: Re-examination of critical field relationships
L. Reid.....186

Page

09:00-09:15 43)New structural and stratigraphic data from the Purcell thrust zone and some implications
P.S. Simony, K.J.E. Boggs and S.L. Acton.....188

09:15-09:30 44)The Josh Creek diorite, Christina Lake, southeastern British Columbia: A deformed Late Triassic body within Quesnellia
S.L. Acton, P.S. Simony and L. Heaman.....190

09:30-09:45 45)U-Th-Pb geochronologic constraints on diachronous metamorphism and deformation in the Mica Creek area, southeastern Canadian Cordillera
J.L. Crowley, E.D. Ghent, S.D. Carr, M.A. Hamilton and P.S. Simony.....192

09:45-10:00 46)The Nicola horst: An update and unresolved problems
J.M. Moore.....193

10:00-10:30 COFFEE

10:30-10:45 47)Tracking North American basement west of the Okanagan Valley: Insights from the Vernon, Ashcroft and Hope map areas
R.I. Thompson, P. Erdmer, K.L. Daughtry, L.M. Heaman and R.A. Creaser.....195

10:45-11:00 48)Preliminary U-Pb geochronology results from the Vernon area, British Columbia
L.M. Heaman, P. Erdmer, R.I. Thompson and K.L. Daughtry.....196

11:00-11:15 49)Spatial relations between a mid-crustal ductile shear zone, the sub-Eocene unconformity, and asymmetric Eocene normal faults, Vernon map area
P. Glombick.....202

11:15-11:30 50)Transition from Proterozoic to Triassic stratigraphy, Vernon map sheet: Is the Quesnellia terrane autochthonous or allochthonous on Silver Star Mountain?
J. Unterschutz.....204

11:30-11:45 51)Devonian plutonism and pre-Devonian tectonism, Vernon map area, British Columbia
N. Slemko.....210

11:45-12:30 DISCUSSION

12:30-13:30 LUNCH

POSTERS

(listed alphabetically)

Page

1)Investigation of strain related to displacement-transfer and along-strike structural variation by 3-D seismic interpretation, physical modelling and computer-graphics visualization
E.O. Aydemir and J.M. Dixon.....214

2)Deformation features, and rheological behaviour of the Slave upper mantle
M.J. Begbie and L.A. Kennedy.....215

3)Meso- and Paleoarchean basement rocks of the Slave province: Distribution in space and time
W. Bleeker, J. Ketchum, B. Davis and R. Stern.....218

4)Progress report on U-Pb geochronology studies - Teslin zone and western Cassiar terrane, Yukon; Timing constraints on deformation and thermal history
S.D. Carr, M. de Keijzer and C. Gallagher.....219

5)Preliminary stratigraphy and structure of Yukon-Tanana terrane, Little Kalzas Lake area, central Yukon (NTS 105L/13)
M. Colpron.....221

6)Primitive arc-magmatism in Stikinia: Implications from the Zippa Mountain pluton
I.M. Coulson, M. Westphal, J.K. Russell and G.M. Dipple.....227

7)Physical modelling of hangingwall and footwall deformation near tear faults and lateral and oblique ramps
J.M. Dixon, M. Oliphant, J. Blackburn and S. Garneau.....235

8)Physical modelling of the influence of regional lithofacies gradients on fold-thrust structures
J.M. Dixon and M. Wardman.....236

9)U-Pb geochronologic evidence of Early Cretaceous large-scale folding in the Dycer Creek area, Pelly Mountains, Yukon
C. Gallagher, S.D. Carr and R.L. Brown.....237

10)Prestack time migration with relative amplitude preservation: Results from the SNORCLE transect
H.D. Geiger, R. Maier, A.J. van der Velden and F.A. Cook.....250

Page

11)Eocene Ootsa Lake group volcanics in the northern Nechako River and southern Fort Fraser map sheets, central British Columbia
N. Grainger and B. Anderson.....263

12)Early Tertiary forearc igneous and metamorphic activity recorded in the Leech River complex, southern Vancouver Island
W.G. Groome, D.J. Thorkelson, R.M. Friedman, J.K. Mortensen and N.W.D. Massey.....265

13)Relating potential field anomalies to Proterozoic structures in western Canada
K.W. Hall, F.A. Cook and C.E. Lynn.....274

14)Crustal structure across the Cordilleran orogen of northwest British Columbia, preliminary results of Lithoprobe SNORCLE refraction experiment line 22
P.T.C. Hammer and R.M. Clowes.....275

15)Reconstruction of motion along the Great Slave Lake shear zone, northwestern Canada, using regional aeromagnetic data
K.A.B. Hendry and W.R. Roest.....283

16)Plasticity of forsterite-enstatite composites at high temperature
S. Ji and Z. Wang.....285

17)Baja BC and Baja California: An evaluation of docking latitudes
J.D. Keppie, J. Dostal and E. Centeno-Garcia.....287

18)Composition of peridotitic mantle from below the Slave craton
M.G. Kopylova and J.K. Russell.....288

19)Geochronological, petrological and microstructural studies on the Thor-Odin dome, Monashee complex, southern Canadian Cordillera
Y.D. Kuiper, S.D. Carr and P.F. Williams.....296

20)Central Foreland NATMAP: Preliminary results of detailed mapping in the Trutch and Toad River areas, northeastern B.C.
L.S. Lane, J. Bednarski, M.P. Cecile, L.D. Currie, A. Legun, A.V. Okulitch and G.S. Stockmal.....297

Page

21)Preliminary sedimentological analysis of the Cambrian Atan group in northern B.C. - A rifted margin with fluvial cobble conglomerate to deep marine olistostromal carbonate facies
D.G.F. Long, J.R. Devaney and B.R. Pratt.....298

22)Continuity into the Cordilleran interior from the North American craton of Archean and Proterozoic transverse crustal structures: Evidence from geological and potential-field data
H. Lyatsky.....299

23)Comparative analyses of regional geological and geophysical data sets by application of geographical information systems
C.E. Lynn, F.A. Cook and K.W. Hall.....305

24)The Burmis thrust: A blind thrust in the southern Canadian Cordillera
P.A. Mackay.....306

25)The Volcanic Creek centre, northern British Columbia and the nature of the underlying lithosphere
J. Nicholls and M.Z. Stout.....307

26)Metamorphic constraints on the tectonic evolution of the Thor-Odin dome, Shuswap metamorphic core complex
B.H. Norlander, D.L. Whitney and C. Teyssier.....309

27)*Cyperus papyrus*, a key to the tectonic elucidation of the northern Cordillera and contiguous Canada basin
D.K. Norris.....310

28)The role of overturned panels in the tectonic evolution of the Phanerozoic section on the north flank of the Central anticlinorium, Ostrov Vrangelya
D.K. Norris.....311

29)Geochemistry of metavolcanic rocks from the Yukon-Tanana terrane and Campbell River belt, Finlayson Lake region, southeastern Yukon Territory: Preliminary results
S.J. Piercey, D.C. Murphy, J.K. Mortensen and J.A. Hunt.....312

30)Stratigraphy of the Hazelton group of southeastern Nechako River map area, central British Columbia
M.B. Quat and L.C. Struik.....313

Page

31)Upper crustal structure in the southwestern Slave province - A detailed look at the seismic results from SNORCLE line 1
B. Roberts, D. Snyder and E. Adam.....315

32)Faults in Lansing map area, Selwyn basin, Yukon: A transpressive squeeze
C.F. Roots.....317

33)Rapid Eocene cooling from peak metamorphic temperatures in the northern Monashee complex, southern Canadian Cordillera: Evidence from $^{40}Ar/^{39}Ar$ and U-Pb data
N.M. Sanborn, J.L. Crowley and D.A. Archibald.....318

34)Progress report: Geoscience studies in the northern Cordillera
V.Z. Sterenberg.....319

35)New geological maps of the Wernecke Mountains, Yukon Territory (106D/16, 106C/13, 106C/14)
D.J. Thorkelson and C.A. Wallace.....320

36)Role of partial melting during late-orogenic collapse: Structural and geochronological constraints in the Shuswap metamorphic core complex, Canadian Cordillera
O. Vanderhaeghe, C. Teyssier, W.J. Dunlap, R. Wysoczansky and I. McDougall.....324

37)Seismic skeletonization + empirical mode decomposition = A new hybrid approach to deep crustal seismic data interpretation
K. Vasudevan and F.A. Cook.....325

38)Towards a transect of the North American lithosphere
K. Vasudevan, F.A. Cook, A.J. van der Velden, C.E. Lynn and R.M. Clowes.....334

39)Results from Lithoprobe SNORE 97 experiment, line 21: Seismic velocity structure across the Canadian Cordillera of northeastern British Columbia
J.K. Welford and R.M. Clowes.....335

Preface

This volume includes the abstracts and short articles submitted for the 1999 LITHOPROBE Slave - Northern Cordillera Lithospheric Evolution (SNORCLE) transect meeting and Cordilleran Tectonics Workshop. These meetings were held concurrently at the University of Calgary. Accordingly, this volume includes several contributions related to both the southern and northern Cordillera. We sincerely thank Elissa Lynn for her assistance in organizing the meeting and compiling this volume.

Frederick A. Cook and Philippe Erdmer

ABSTRACTS of ORAL PRESENTATIONS

Evidence of crustal attenuation in the Archean Beniah Formation, Northwest Territories

W.U. Mueller and C. Pickett, Sciences de la terre, Univ. du Québec á Chicoutimi, Québec, Canada, G7H 2B1; wmueller@uqac.uquebec.ca

The Beniah Formation (63°20'N/112°19'W), in the south-central part of the Slave craton, is a 0.2-1 km-thick sedimentary succession that represents a well-defined, but unstable Archean shelf sequence. Several lithofacies are distinguished based on grain-size, composition, sedimentary structures, and stratigraphic position including: 1) a 2-13 m-thick (av. 6 m) siltstone-sandstone lithofacies with 5-28 m-thick (av. 14 m) banded iron-formation, 2) a 3-30 m-thick (av. 12 m) sandstone-siltstone ± volcaniclastics lithofacies, and 3) a 4-55 m-thick (av. 19 m) quartz-arenite lithofacies with 3-12 m-thick (av. 7 m) quartz-pebble conglomerate ± sedimentary breccia lithofacies, The metamorphic grade is greenschist to lower amphibolite, but primary volcanic and sedimentary textures are readily identified, except in areas of high strain or intense deformation. The Beniah Formation is the time- and lateral equivalent of the quartz-arenites at Bell, Dwyer and Brown Lakes. These sedimentary units are preserved preferentially adjacent to > 2.8 Ga basement highs and N-trending crustal-scale faults, represented by the Beniah Lake and ancestral Jackson Lake faults. The Beniah Lake sedimentary rocks are inferred to overlie a mafic layered complex and a tonalitic gneiss unconformably.

The best exposed outcrop zones, 160 m- and 75 m-thick, display a characteristic lithofacies architecture commencing with the basal siltstone-sandstone to the medial sandstone-siltstone which in turn grades into the summital quartz-arenite that collectively occur as 25-85 m-thick upward-coarsening sequences. The sedimentary lithofacies exhibit the salient characteristics of an unstable shallow-water shelf setting. The quartz-arenite and quartz-pebble conglomerate have an upper sharp depositional contact with the siltstone-sandstone lithofacies. Locally, minor pebble to granule lags were observed at the base of the siltstone-sandstone lithofacies. In contrast, other lithofacies relationships are generally gradational over 1-2 m.

The siltstone-sandstone lithofacies features 0.1-3 m-thick laminated siltstone, graded sandstone or siltstone-mudstone couplets with numerous rippled horizons. Coarse-grained, 5-20 cm-thick sandstone interbeds are planar bedded or low-angle planar bedded. The sedimentary structures are suggestive of low wave energy and suspension deposits that were affected sporadically by high wave surge and storms in a a shallow-water lower shoreface to proximal offshore setting. Interstratified banded iron-formation (BIF) containing 0.2-2 cm-thick, finely-laminated to rippled siltstone and fine-grained sandstone beds, alternating with laminated 0.5-2 cm-thick iron-rich beds, argue for the lateral shallow-water, offshore equivalent of the siltstone-sandstone lithofacies. Alternatively, the BIF may represent small protected coastal embayments that have direct access to weathered and uplifted mafic rocks.

The sandstone-siltstone ± volcaniclastic lithofacies is characterized by 5-50 cm-thick crossbeds, low-angle planar to planar beds with mudstone and siltstone drapes between bedforms, as well as superposed small-scale crossbeds, which collectively form composite 50-200 cm-thick cross-strata. Inferred tuffaceous-type beds of felsic composition crop out locally, and have similar sedimentary structures. The large- and small-scale sedimentary structures are considered to be wave-induced bedforms that developed during highly fluctuating energy conditions as suggested by mudstone and siltstone drapes. The drapes represent suspension sedimentation possibly related to tide-influence. A wave- and tide-influenced lower shoreface coastal sequence best explains the observed bedforms.

The up-section quartz-arenite lithofacies is organized into 0.25-2 m-thick composite beds that display a tabular geometry. Each tabular-shaped structure contains planar beds, low-angle planar

beds, tangential crossbeds and local tabular crossbeds that collectively form composite cross-strata. Green, chrome-rich micas and mud drapes develop on foresets and between individual beds. A complex nearshore-shoreface setting with tide- and wave-influenced sandwaves and large-scale dunes is envisaged. Quartz-pebble conglomerate containing well rounded quartz clasts and discontinuous clay drapes as well as displaying a massive to stratified nature, is considered the high-energy subaerial to subaqueous coastal counterpart of the quartz-arenite. The 3-5 m-thick sedimentary breccia sublithofacies, composed almost exclusively of angular sedimentary clasts (1-5 cm) in 0.5-2 m-thick massive beds, is interpreted as a subaqueous massflow deposit.

Cyclic repetition of Beniah lithofacies compares favourably with transgressive-progradational events that can be associated with first order allocyclic controls such as eustatic sea-level changes or tectonic influence. Both can develop similar cyclothems. Rifting and associated crustal thinning, is an appealing large-scale process which explains the abundant mafic dykes in the platformal quartz-arenite sequence, the up-section transition of the siltstone-sandstone lithofacies to mafic pillowed flows, and the overall lithofacies organization. Numerous coarsening-upward sequences developed in response to tectonic cyclicty. Transgression probably reflects the immediate response to tectonic extension in areas with direct sea access. Erosional processes and associated coarse clastic deposits should lag behind, but near the fault, clastic sedimentation must have been commensurate with tectonic uplift or basin subsidence.

Each phase of rifting in the study area commences with a basal shallow-water siltstone-sandstone lithofacies and represents flooding of the platform due to extensional tectonics, characterized by normal faulting, block rotations and floundering of the basin. Continued tectonic uplift in the hinterland and pronounced basin subsidence caused down-cutting along the fault and/or basin margin with increased erosion rates. The sandstone-siltstone and quartz-arenite lithofacies are sequencial products of this part of the rifting stage. Generally, upward-coarsening cycles related to alluvial fans suggest that tectonic activity exceeded the rate of stream incision and are easily identified. In contrast, subtle changes in lithofacies architecture or identification of progradational events in distal areas of broad platformal sequences removed from fault zones are difficult to detect. This study area is an exception, and the proposed elevated topography at basin highs or margins facilitated the development of well-defined coarsening-upward successions at distal coastal sites. The preserved rock record at Beniah Lake indicates drowning of an unstable quartz-arenite platform. Similar sequences at Brown, Dwyer and Bell Lakes support the inference of large-scale crustal attenuation and possibly the incipient breakup of an Archean proto-continent at 2.8 Ga.

Sedimentology and Tectonic Setting of the Burwash Formation, Hearne Lake - Gordon Lake area

Mark Ferguson[1], John Waldron[2], and Wouter Bleeker[3]

[1]Department of Earth Sciences, Dalhousie University, Halifax N.S. B3H 4J1
[2] Geology Department, Saint Mary's University, Halifax N.S. B3H 3C3
[3] Continental Geoscience Division, Geological Survey of Canada, Ottawa, Ont. K1A 0E8

The Burwash Formation is a thick slate-metagreywacke turbidite succession in the southern Slave Province. The formation and underlying volcanics have been deformed by two generations of folds, and were regionally metamorphosed. Although metamorphism reaches amphibolite facies near the Anton and Sleepy Dragon complexes, in other areas, the formation is metamorphosed only to greenschist facies and most sedimentary structures are preserved with relatively minor deformation. Interbedded tuff units have provided both an isotopic age (2661 +/- 2 Ma) and a means of correlating laterally within the thick package of sedimentary rocks. Field work in the summers of 1996-98 provided evidence of the depositional environment, source area, and tectonic setting.

Sedimentology

In thinly bedded units, abundant well-preserved sedimentary structures have been observed that are consistent with Bouma sequences. However, other features less commonly associated with turbidites are also observed. These include massive to amalgamated sandstones occasionally containing scour and fill structures. These features are similar to structures observed within turbidites of the Early Paleozoic Meguma Group (Waldron and Jensen, 1985), and are interpreted as having been deposited from high density turbidity currents.

Previously, channel-levee systems have been identified within the central Burwash (Waldron and Bleeker, 1997). Preliminary results from the summer of 1998 identified massive, deeply scoured, granule conglomerate beds along the west coast of Hearne Lake. Based on airphoto interpretation, and on paleocurrent indicators, we suggest that these channel fills extend beneath an F_1 syncline and re-emerge on the opposing limb as a granule conglomerate previously identified by Henderson (1985) (Figure 2).

We interpret the depositional environment to involve channel-levee systems formed by high density turbidity currents, and minor debris flows. These systems appear similar in scale and proportions to those of modern submarine fan environments.

Tectonic Setting: Paleocurrent Distributions

Previous work along the west coast of Yellowknife Bay indicated predominant eastward paleocurrents, and postulated a relatively symmetrical basin with sediment derivation from basement massifs to the east and west (Henderson, 1985). Paleocurrent data have been collected using outcrop measurements and oriented cross-lamination samples. These

samples were cut parallel to bedding to observe the crest forms, after which precise paleocurrent directions were determined. The resulting paleocurrent directions have been reoriented by rotation about the strike to remove the effects of local folding.

Our preliminary paleocurrent data, from the Hearne lake and Gordon lake areas, suggest northward flow directions, parallel and oblique to the axes of F1 folds (Figure 2 and 3). This may indicate that the pattern of paleocurrents cannot be related in a simple way to the present-day distribution of basement massifs.

Further work will involve more rigorous removal of tectonic strains from the paleocurrent distribution. Fieldwork east of Gordon Lake planned for the summer of 1999 should clarify the structural complexities and aid in the interpretation of the sediment source and depositional environment.

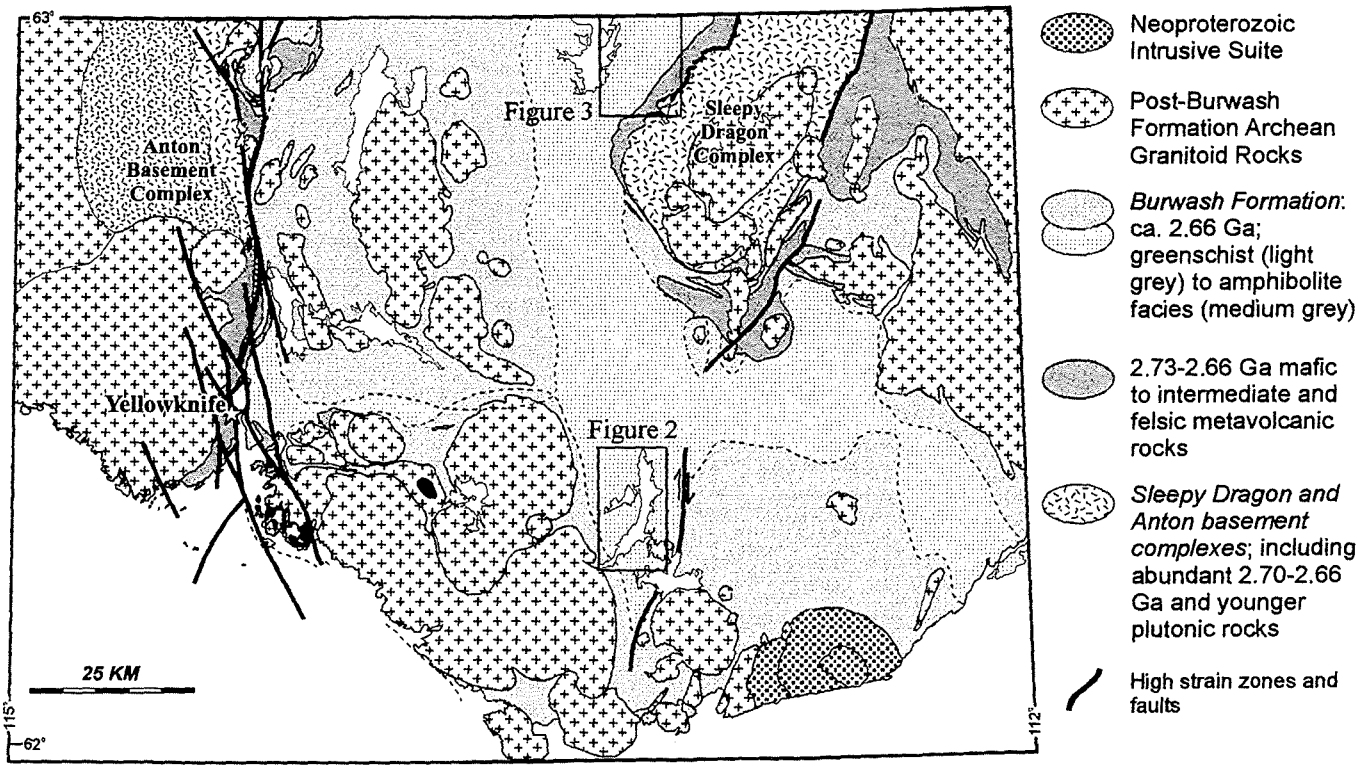

Figure 1: Geology of the Yellowknife Domain. Note the position of older sialic crust to east and west of the Burwash Formation (modified from Ketchum and Bleeker, 1997).

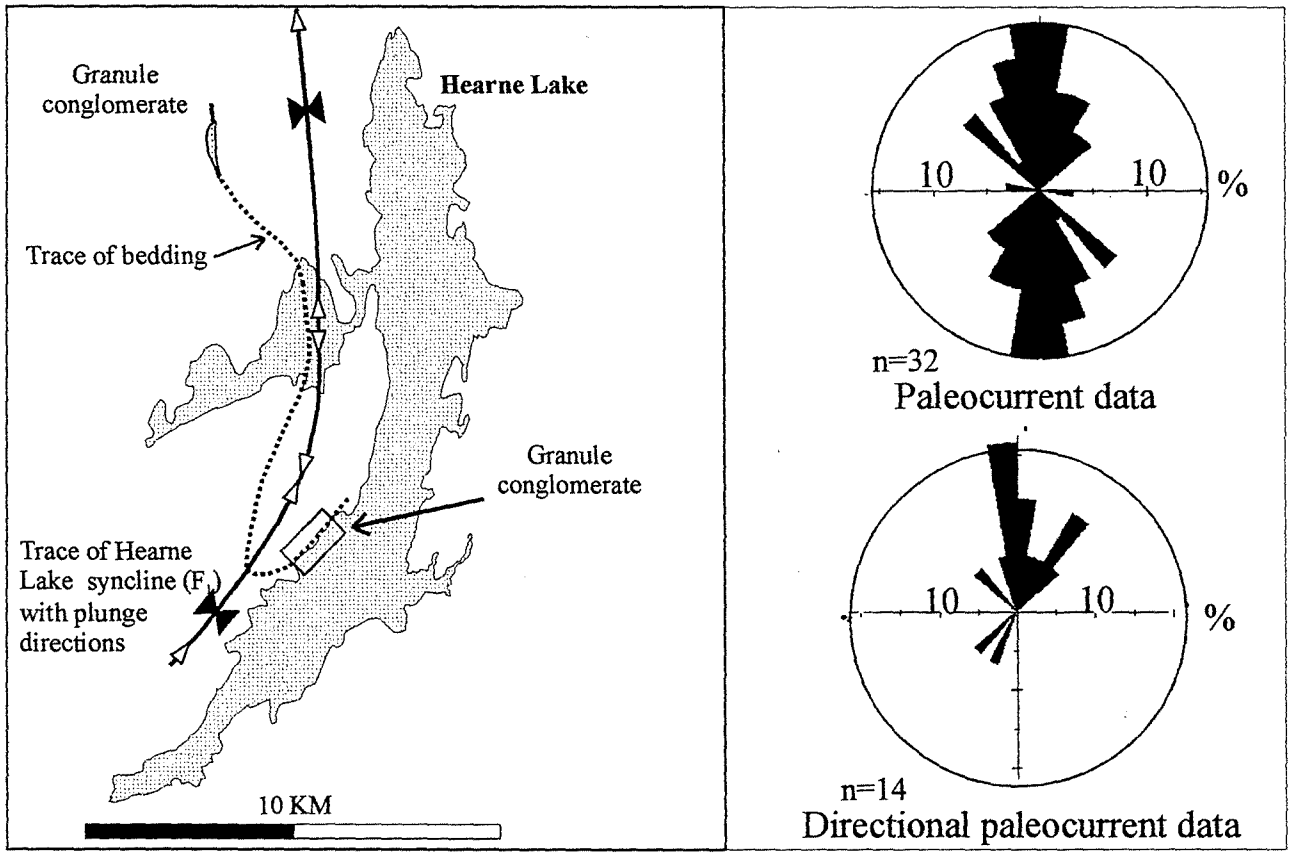

Figure 2: Map of Hearne Lake showing location of previously observed and recently mapped granule conglomerates, and suggested trace of bedding linking the two outcrops. Note also the consistent northerly paleocurrent distribution.

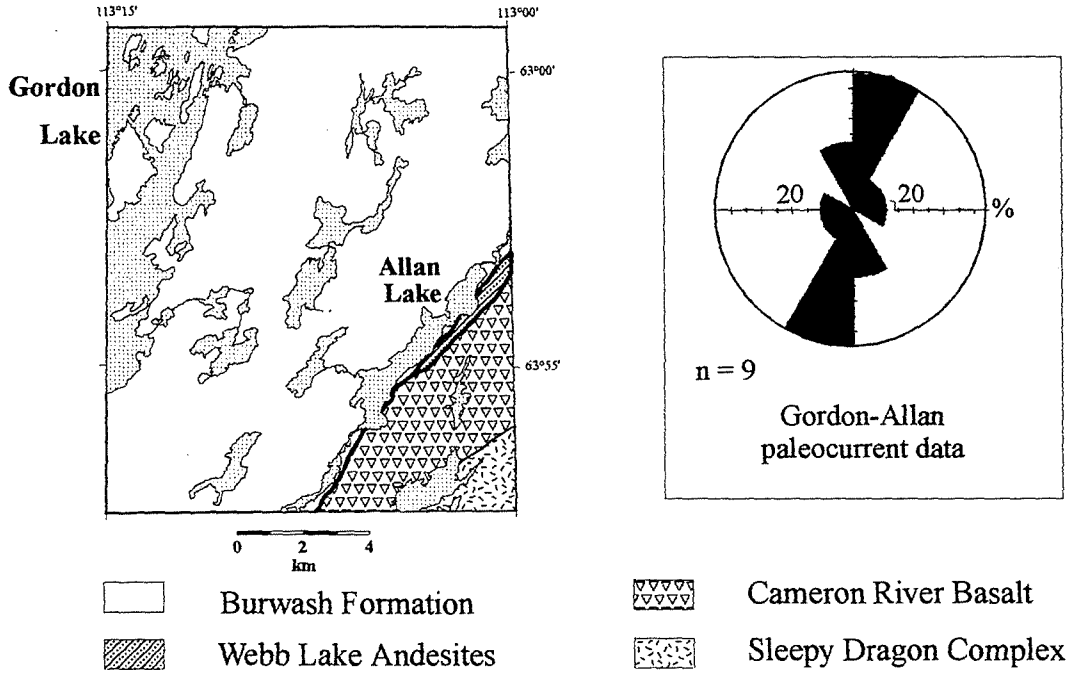

Figure 3: Map of Gordon-Allan Lake area with preliminary paleocurrent data. Geological boundaries from Henderson (1985).

References

Henderson, J.B., 1985. Geology of the Yellowknife-Hearne Lake area, District of Mackenzie: a segment across an Archean Basin; Geological Survey of Canada, Memoir 414, 135.

Ketchum, J., and Bleeker, W., 1997. Systematic U-Pb geochronological study of Slave Province "Basement" rocks along the SNORCLE Lithoprobe Transect: Preliminary results; in Cook, F., and Erdmer, P. (compilers), Slave-Northern Cordillera Lithospheric Evolution (SNORCLE) Transect and Cordilleran Tectonics Workshop Meeting, March 7-9, University of Calgary, Lithoprobe Report No. 56, 28-31.

Waldron, J.W.F., and Bleeker, W., 1997. Late Archean Turbidites and their Tectonic Setting in the Southern Slave Province; in Cook, F., and Erdmer, P. (compilers), Slave-Northern Cordillera Lithospheric Evolution (SNORCLE) Transect and Cordilleran Tectonics Workshop Meeting, March 7-9, University of Calgary, Lithoprobe Report No. 56, 21-27.

Waldron, J.W.F., and Jensen, L.R., 1985. Sedimentology of the Goldenville Formation, Eastern Shore, Nova Scotia. GSC Paper 85-15, 31.

SEAMOUNT ARCHITECTURE OF ARCHEAN VOLCANIC SEQUENCES IN THE SLAVE PROVINCE, NORTHWEST TERRITORIES

Corcoran, P.L. *Department of Earth Sciences, Dalhousie University, Halifax, Nova Scotia, Canada, B3H 3J5 E-mail: corcoran@is2.dal.ca;* **Dostal, J.** *Geology Department, Saint Mary's University, Nova Scotia, Canada, B3H 3C3*

The mafic volcanic-dominated, ca. 2.66-2.69 Ga Peltier Formation and Beaulieu River volcanic belt, in the Slave Province, Northwest Territories, are composed of volcanic facies characteristic of modern seamounts that develop at mid-oceanic and back-arc spreading centres. Two localities in the Peltier Formation represent 1) proximal, deep-water (locality A), and 2) medial to distal, deep-water (locality B) seamount settings, whereas one locality in the Beaulieu River volcanic belt demonstrates the facies architecture typical of the medial, shallow-water portion of a seamount. Locality A in the Peltier Formation is composed of a 55 m-thick, non-vesicular pillowed sequence cut by mafic, north-south-trending dykes and east-west-trending sills. Parallel dykes are characterized by mm-thick multiple chilled margins, indicating successive magma intrusion related to the construction of the edifice. Effusive facies, feeder conduits and the absence of vesicles are features characteristic of the central, deep water portion of seamounts where edifice growth is initiated. Locality B in the Peltier Formation, is represented by a 30-80 m-thick sequence of pillow breccia, and pillowed and massive flows with vesicularity ranging from 5-27%. Disorganized, non-vesicular hyaloclastite intermingled with sedimentary material (peperite), and shale units intercalated with pillow breccia and hyaloclastite, indicate that volcanism and deep-water sedimentation were contemporaneous. Increased vesicularity, pillow breccia, and hyaloclastite, in addition to thinner massive and pillowed flows, relative to locality A, suggests that locality B represents the medial to distal part of a seamount. Bedded tuffs, 10-35 m thick, are the on-strike equivalents of massive flows and further support a distal setting, where erosion and remobilization of flows and breccia resulted in turbiditic transport of volcaniclastic material. The third locality, in the Beaulieu River volcanic belt, is represented by a 5-85 m-thick sequence of vesicular lobate-pillowed and massive flows, stratified pillow breccia and hyaloclastite, and mafic dykes. A shallow water setting is inferred based on the presence of stratified pillow breccia and hyaloclastite, in addition to high vesicularity which ranges from 21-49% in pillowed flows, 5-40% in massive flows, and 20-35% in pillow breccia and hyaloclastite.

The Peltier Formation and Beaulieu River volcanic belt are two volcanic successions located approximately 300 km apart, along strike of the north-trending Beniah Lake fault. This 600 km-long lineament, along which several north-south-trending volcanic belts are located, may have played a role in flow emplacement and construction of seamounts because initial magma transport from chamber to dykes/sills is often facilitated by faults and fissures. The alignment of north-south-trending volcanic belts of similar ages, facies architecture, and geochemical signatures along fault strike suggest that a chain of seamounts may have been constructed 2.66-2.7 billion years ago. The volcanological facies architecture and preliminary geochemistry which indicates that the rocks range from tholeiitic to calc-alkaline in composition, enable the preferred interpretation of the study areas in the Peltier Formation and Beaulieu River volcanic belt as specific portions of Archean seamounts located in arc-back-arc settings. Crustal-scale faults spatially associated with similar volcanic facies are common to other Archean cratons, indicating that seamounts were possibly characteristic of ancient ocean floors.

The Central Slave Cover Group and Central Slave Basement Complex: a progress report on U-Pb geochronological studies

John Ketchum
Department of Earth Sciences, Memorial University, St. John's, Newfoundland, A1B 3X5
ketch@sparky2.esd.mun.ca

Wouter Bleeker
Geological Survey of Canada, 601 Booth Street, Ottawa, Ontario, K1A 0E8
wbleeker@NRCan.gc.ca

INTRODUCTION

The Central Slave Cover Group (CSCG) and its depositional basement, the Central Slave Basement Complex (CSBC) are regionally mappable tectonostratigraphic packages of Archean age recently identified in the southwestern Slave Province (Bleeker and Ketchum 1998; Bleeker et al. in press, parts I and II; Fig. 1). Both packages are physically discontinuous at surface, but much, if not all of this discontinuity can be explained by regional-scale folds, faults, voluminous younger plutonic suites, and younger supracrustal sequences. In the case of the CSCG, the lack of continuity can additionally be explained by local unconformities and potential areas of non-deposition.

The CSBC is dominated by mixed granitoid orthogneisses (dominantly tonalitic) with a complex history of high-grade metamorphism and deformation predating deposition of the CSCG. Supracrustal rocks of unknown age form an apparently minor component. The presently-known age range of CSBC plutonism is 3.33-2.83 Ga, but older components, perhaps as old as 3.6-4.0 Ga, are suspected based on field evidence, indirect isotopic data, and regional considerations. In many places, the CSBC is structurally overlain by the relatively thin CSCG, which consists mainly of clastic, quartz-rich sedimentary rocks, banded iron formation, and minor volcanic rocks. Although not everywhere present, this supracrustal package can be identified over a broad region based on stratigraphic correlation and the presence of distinctive lithologies (e.g., fuchsitic quartzite; Bleeker et al. in press, part I). Its contact with the CSBC is highly deformed in most places, but this contact is demonstrably unconformable in a number of lower-strain localities. The age of the CSCG is poorly constrained; a U-Pb age estimate of 2835 Ma (Isachsen and Bowring 1997) for a felsic volcanic component represents the only direct age constraint obtained thus far.

This report presents new results from an ongoing, multi-year project to map and characterize the CSBC and CSCG, two of the oldest lithotectonic elements in the Slave craton. A major part of this work involves determining the absolute time of plutonic, metamorphic, tectonic, and depositional events that formed and influenced these packages. This project addresses the early evolution of one of the oldest cratons on Earth, and attempts to shed light on the long-posed question of whether modern-style plate tectonic processes operated during the Archean. To provide an adequate database for speculation on this question, we have mapped in detail numerous areas where the CSBC and CSCG crop out together. U-Pb dating of primary and secondary mineral chronometers from a variety of samples in each location is an integral part of establishing a meaningful database, and is the focus of this progress report.

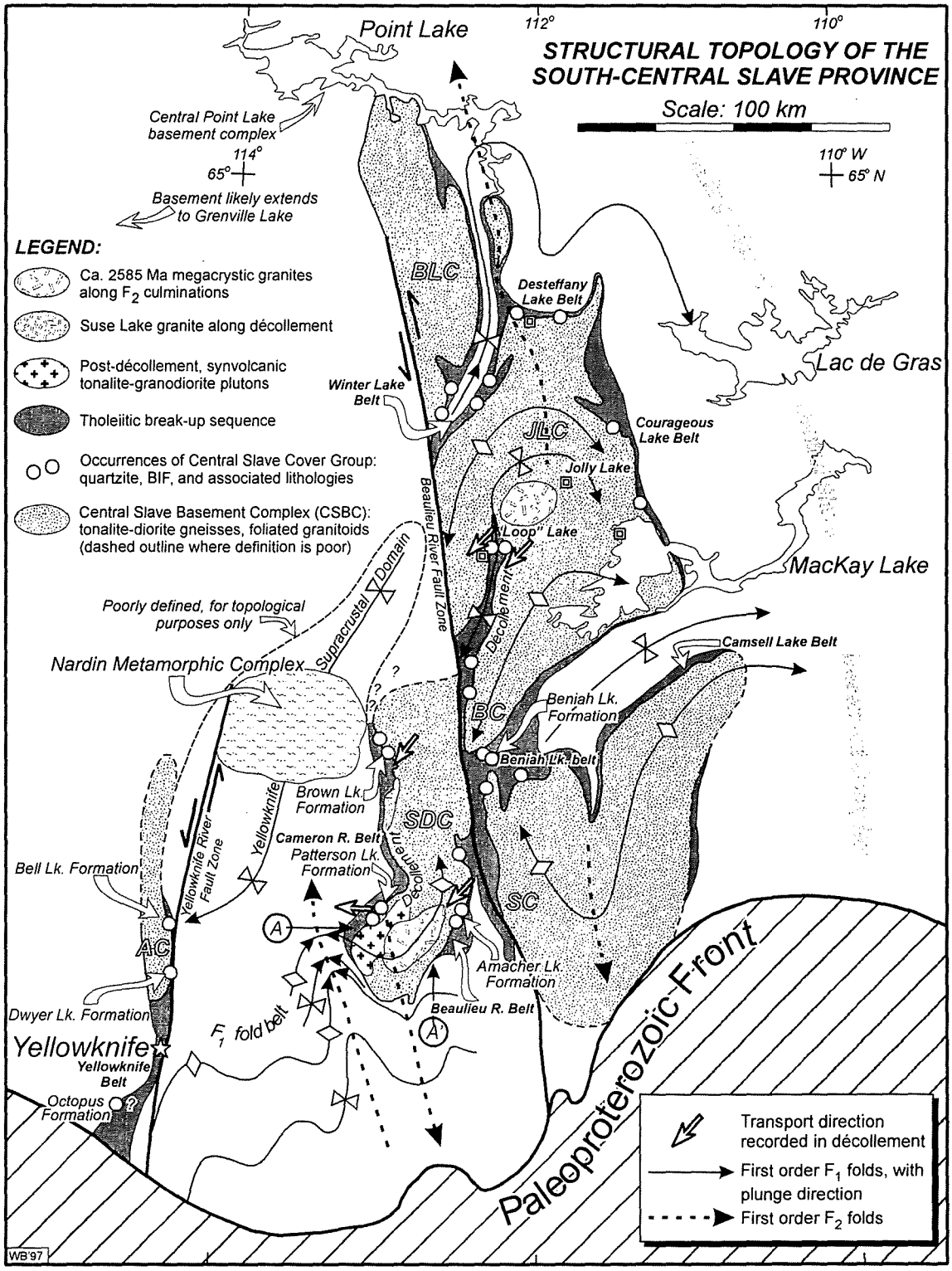

Figure 1. *Schematic illustration of the Central Slave Basement Complex, with numerous younger plutons omitted for clarity (after Bleeker and Ketchum 1998). Double box symbol indicates location of U-Pb geochronology samples discussed in text.*

SLEEPY DRAGON COMPLEX

In the area of Patterson Lake (Fig. 1), the ca. 2.94 Ga Sleepy Dragon Complex is overlain by (*i*) the Patterson Lake Formation, assigned by Bleeker et al. (in press, part I) to the CSCG, and by (*ii*) tholeiitic basalts and minor felsic volcanic rocks of the Cameron River volcanic belt (part of the clasically-defined Yellowknife Supergroup; Henderson 1970). Ketchum and Bleeker (1998) presented preliminary age data from eight samples collected in a transect across the CSBC and CSCG in this region; here we discuss the final results of this work.

Figure 2 shows the sample locations and ages of the principal map units in the area. Based on mapping and geochronology, the evolution of the Slave Province in this region can be summarized as follows (see also Bleeker et al. in press, parts I and II):

1.) deposition of a pillowed mafic volcanic unit before 2942 ± 3 Ma, the age of metamorphic titanite (Fig. 3), and likely before ca. 2950 Ma (W. Davis, unpublished data). This volcanic unit appears to predate the CSCG; its depositional basement is unknown.

2.) tonalitic to dioritic magmatism, dated here at 2936 +7/-6 Ma and 2933 +8/-7 Ma. Although older crust may be present, this is the main episode of CSBC plutonism in this region.

3.) deposition of the Patterson Lake Formation between 2.93-2.73 Ga.

4.) *emplacement of mafic dykes at 2734 ± 2 Ma into the CSBC and CSCG (possibly representing the onset of Cameron River tholeiitic volcanism).*

5.) granite plutonism in the CSBC at 2726 ± 3 Ma.

5.) regional deformation, with translation along the basement-cover contact.

6.) emplacement of a second mafic dyke swarm at 2687 ± 1 Ma (W. Davis data; see Bleeker et al. in press, part II) across the sheared basement-cover contact.

7.) continued granitoid plutonism (probably arc-related) in the CSBC between 2683 ± 2 Ma and 2672 +7/-6 Ma, coeval with continued volcanism in the Cameron River Belt.

8.) late granite emplacement at 2586 Ma (Davis and Bleeker in press).

Figure 4 provides a schematic tectonostratigraphic section for the Patterson Lake region. One of the more significant findings of the present study is that the CSCG does not directly overlie plutonic rocks of the CSBC in this area. The intervening, highly-deformed pillowed basalt appears to predate the CSCG and apparently also predates ca. 2.94 Ga tonalite structurally beneath it. Field observations suggest that this unit is intruded by the tonalite. It is possible that the mafic unit could correlate with a 3.14-3.12 Ga volcanic sequence documented elsewhere in the western Slave Province (Villeneuve et al. 1994), but this remains speculative in the absence of additional data. A goal of future work in this region is to determine the age of this volcanic

U-PB AGES, PATTERSON LAKE AREA

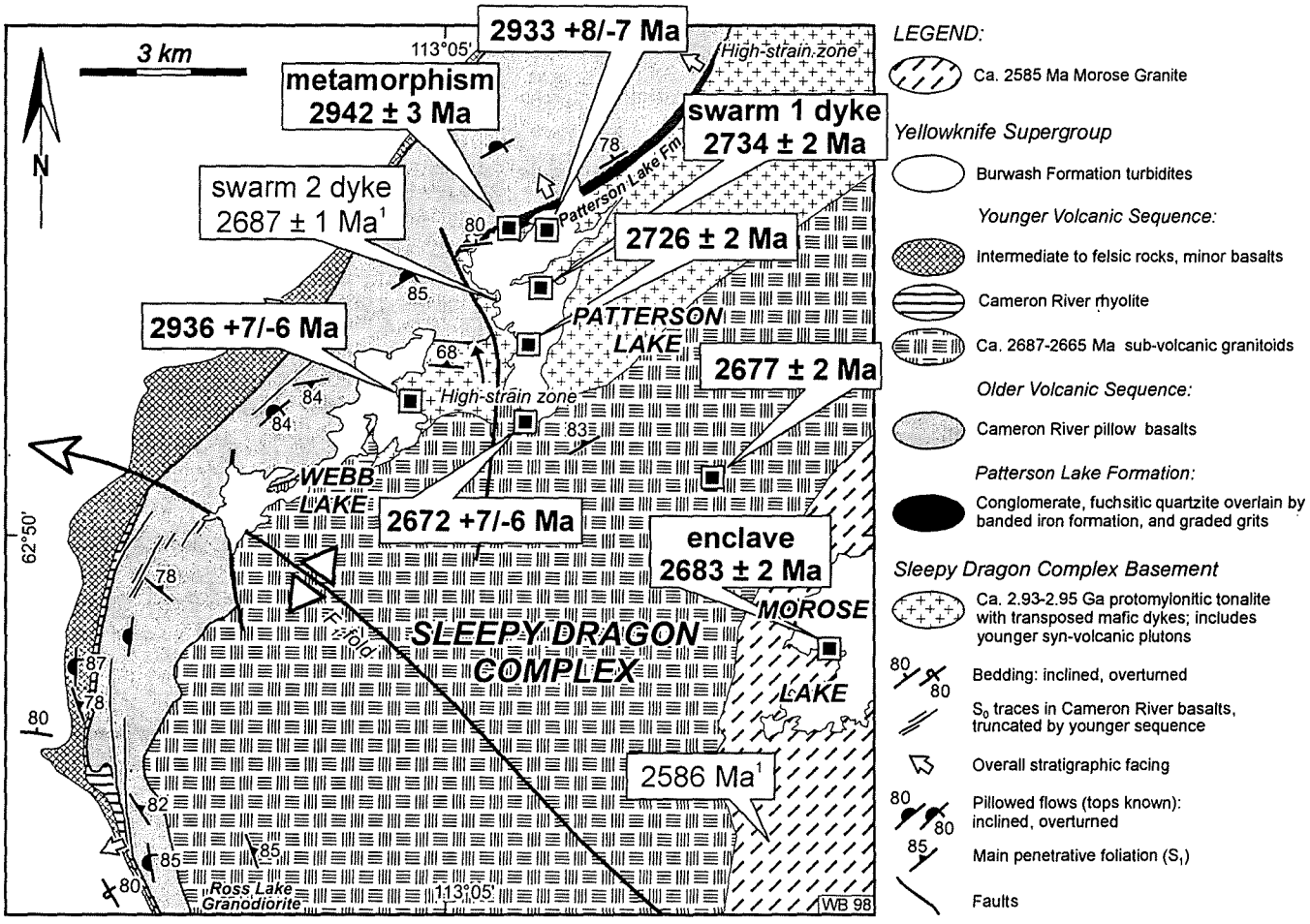

Figure 2. *U-Pb ages for the Morose-Patterson Lakes map area, western edge of the Sleepy Dragon complex, updated from Ketchum and Bleeker (1998). All ages denote primary crystallization age unless noted otherwise. (' age data of W. Davis, GSC.)*

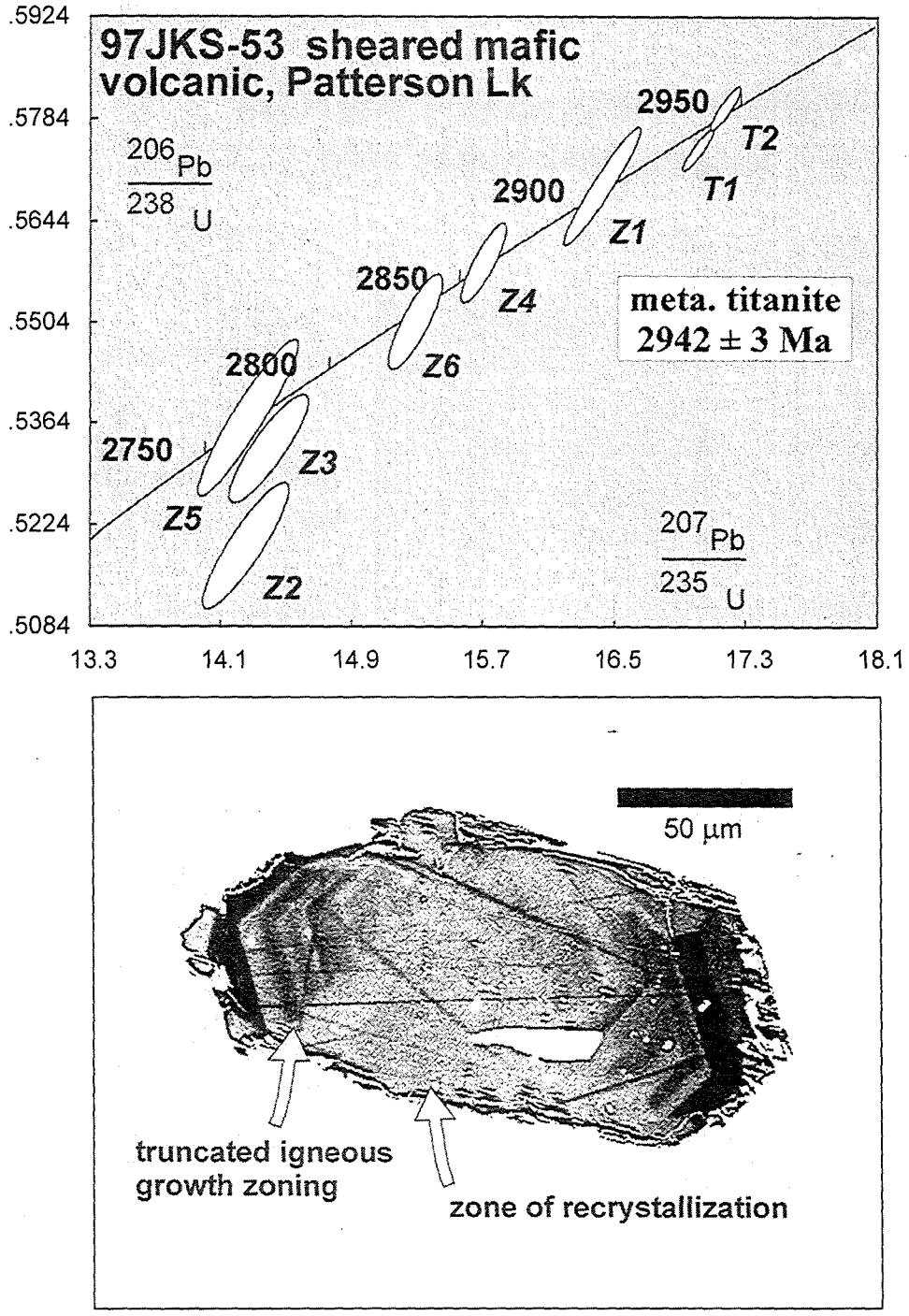

Figure 3. *Concordia diagram for sheared mafic volcanic unit with felsic layers (interpillow epiclastic material?) beneath Patterson Lake Formation, and back-scattered electron image of typical zircon from this sample. Internal recrystallization of zircon, suggested by truncated igneous growth zoning, may have led to Pb loss and a non-reproducable age for multigrain zircon fractions. Metamorphic titanite indicates that unit is older than 2942 Ma and may predate ca. 2935 Ma basement tonalite of the Sleepy Dragon Complex.*

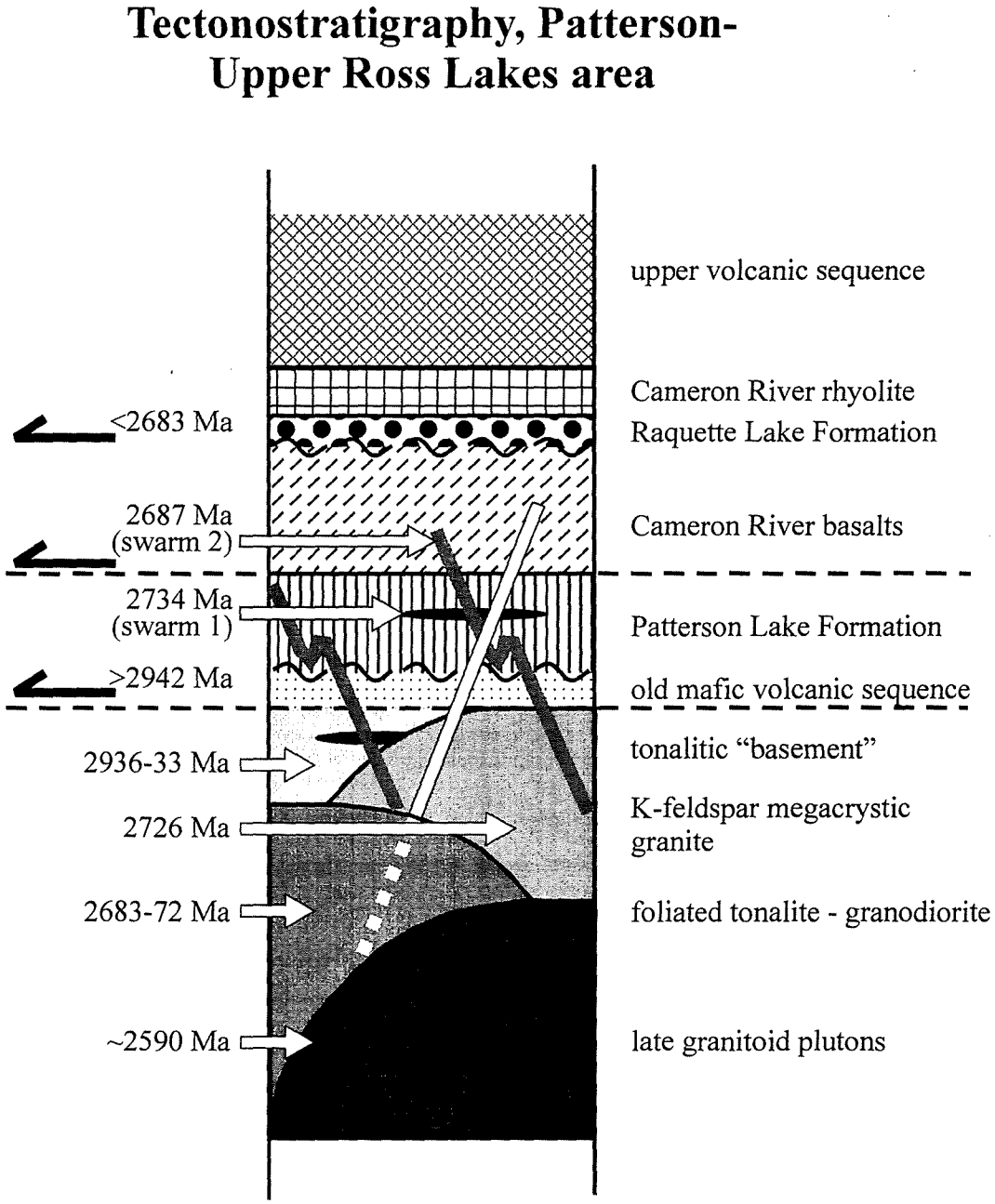

Figure 4. *Tectonostratigraphic units and ages of basement and cover rocks based on detailed mapping and U-Pb geochronology, southwestern Sleepy Dragon Complex. Diagram is entirely schematic and unit thicknesses are portrayed semi-quantitatively. Oldest unit in tectonostratigraphy appears to be a highly-thinned mafic volcanic sequence with metamorphic titanite dated at 2942 Ma. Patterson Lake formation (part of CSCG) may unconformably overlie this unit. See text for further discussion.*

unit and attempt to identify its depositional basement, if this basement in fact occurs within the Sleepy Dragon Complex.

Below we discuss U-Pb age results from several other areas within the proposed CSBC. Basement samples have been mainly collected from well-mapped areas where CSCG units are also present.

MACKAY LAKE

As reported by Bleeker and Ketchum (1998) and Bleeker et al. (in press, part I), a sample of migmatitic granodiorite gneiss from the footwall of the Courageous Lake greenstone belt at MacKay Lake was dated to confirm the antiquity of this unit and provide a link with the CSBC. The gneiss protolith is dated at 3325 ± 8 Ma, with growth of secondary zircon (perhaps related to leucosome development) at 2723 ± 3 Ma. Two fractions of metamorphic titanite with variable degrees of Pb loss suggest a ca. 2680 Ma thermal event. This is the easternmost CSBC unit dated thus far, and represents a critical sample for proposing the topologically simple basement distribution outlined in Figure 1.

JOLLY LAKE

A small island at the east end of Jolly Lake (Fig. 1) is underlain by interlayered biotite tonalite, hornblende-bearing tonalite, and hornblende diorite. These rocks, like the unit dated at MacKay Lake, are part of the Jolly Lake Complex of Thompson et al. (1994). In contrast to the MacKay Lake gneiss however, these units are not as strongly deformed or migmatitic and have a less pronounced gneissic foliation. Disrupted mafic dykes and cross-cutting granitic veins of at least two generations are common in this and other outcrops along the lakeshore.

A sample of biotite tonalite with a faint migmatitic appearance yields a U-Pb age of 2707 ± 2 Ma (Fig. 5), interpreted here as the time of igneous crystallization. A morphologically distinct population of small zircon prisms provide a younger age of ca. 2683 Ma (two slightly discordant analyses) that likely records metamorphism. Two discordant monazite analyses project to 2668 Ma and may record an even later metamorphic event, or perhaps cooling through the monazite closure temperature following protracted metamorphism. The data suggest that this tonalite is part of a younger suite of plutons within the CSBC that are coeval with early volcanic activity in the overlying Yellowknife Supergroup. Gneissic rocks observed at the west end of Jolly Lake may represent the host to the unit dated here.

"LOOP LAKE"

A migmatitic tonalite gneiss sampled one km west of the narrow, tightly-folded greenstone belt at "Loop Lake" (informal name; Fig. 1) is interpreted to have a primary crystallization age of 2939 ± 1 Ma, the age of a concordant, single-grain analysis (Fig. 5). This age is identical to that obtained for similar rocks in the Sleepy Dragon Complex (e.g., Lambert and van Breemen 1991; this report) and appears to be confirmed by additional zircon analyses that form two colinear arrays extending from 2939 Ma. The older colinear fractions suggest the presence of ca. 3.5 Ga inheritance in the tonalite, whereas two of the younger fractions are consistent with Pb loss at ca. 900 Ma (Fig. 5).

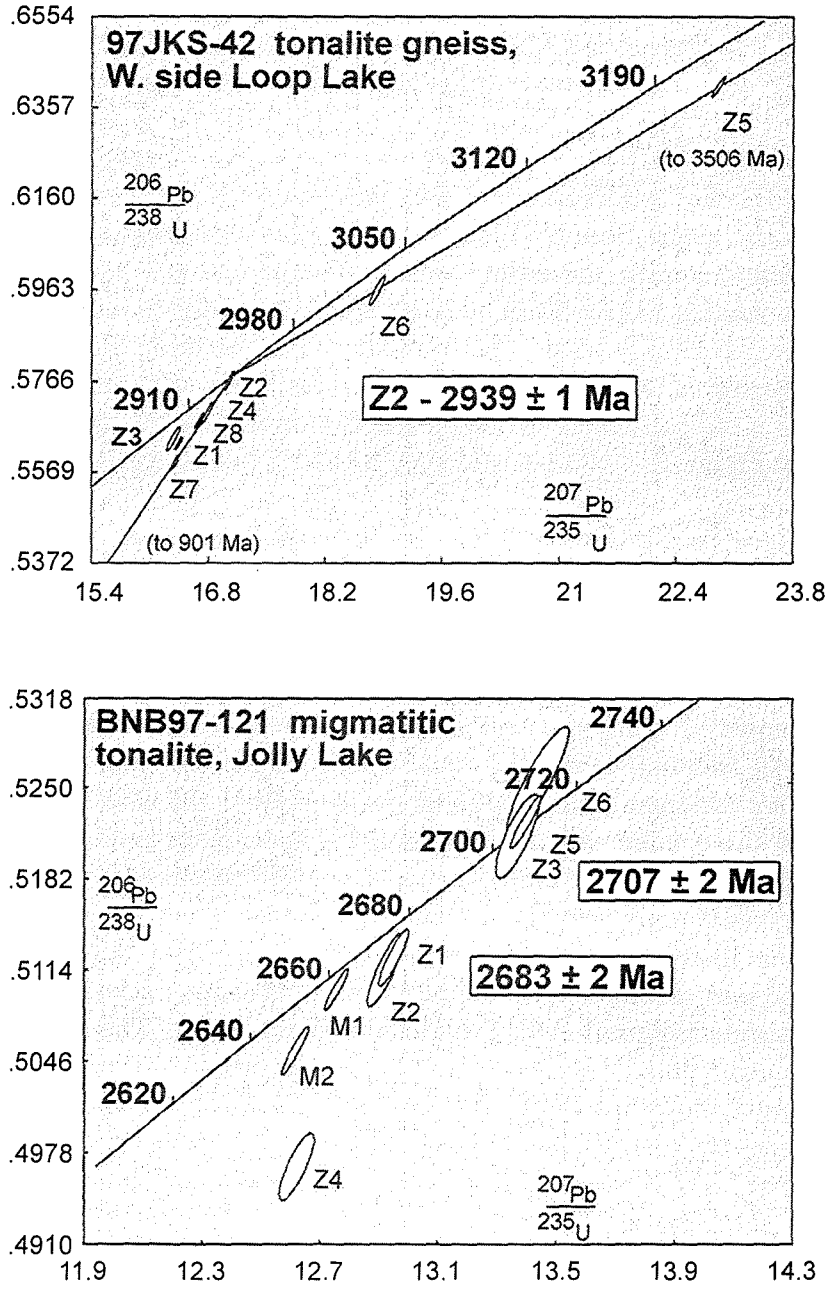

Figure 5. *U-Pb concordia diagrams for CSBC tonalite samples from "Loop" and Jolly Lakes. The Loop Lake sample is identical in age to tonalite from the Sleepy Dragon Complex, and appears to contain a ca. 3.5 Ga inherited zircon component. The 2707 Ma Jolly Lake tonalite is representative of magmatic activity in the CSBC that was coeval with volcanism in the overlying Yellowknife Supergroup. Younger zircon and monazite in this sample likely record metamorphism.*

DESTEFFANY LAKE

Three samples were collected for U-Pb geochronology from this location. Dating of biotite tonalite gneiss and younger, foliated to gneissic, K-feldspar megacrystic granite from the postulated CSBC is in progress. A sample of a fine-grained quartzofeldspathic paragneiss from the CSCG did not yield any minerals suitable for U-Pb dating. The unit is relatively quartz-rich and may represent a metamorphosed chert.

OTHER REGIONS

Samples of basement gneiss and supracrustal gneiss from other localities throughout the CSBC (from Point Lake to south of Beniah Lake) are currently being processed for U-Pb dating. The regional database created by this work, in addition to more detailed mapping and geochronological studies of selected areas (e.g, Patterson, Brown, Point Lakes), should provide a much better understanding of the early evolution of the south-central Slave Province, and a framework for comparison with other regions with "old" gneissic and supracrustal rocks in the western Slave Province. This is essential for determining the events that led to development of the western Slave protocraton prior to its amalgamation with juvenile rocks of the eastern Slave Province, and prior to deposition of the Yellowknife Supergroup.

REFERENCES

Bleeker, W., and Ketchum, J.W.F. 1998. Central Slave Basement Complex, Northwest Territories: its autochthonous cover, décollement, and structural topology. *In* Current Research 1998-C, Geological Survey of Canada, pp. 9-19.

Bleeker, W., Ketchum, J.W.F., Jackson, V.A., and Villeneuve, M. in press. The Central Slave Basement Complex, Part I: its structural topology and autochthonous cover. Canadian Journal of Earth Sciences.

Bleeker, W., Ketchum, J.W.F., and Davis, W.J. in press. The Central Slave Basement Complex, Part II: high-strain zones along the basement/cover contact. Canadian Journal of Earth Sciences.

Davis, W.J., and Bleeker, W., in press. Timing of plutonism, deformation and metamorphism in the Yellowknife Domain, Slave Province. Canadian Journal of Earth Sciences.

Henderson, J.B. 1970. Stratigraphy of the Archean Yellowknife Supergroup, Yellowknife Bay-Prosperous Lake area, District of MacKenzie (85 J/8, J/9). *In* Paper 70-26, Geological Survey of Canada, 12 p.

Isachsen, C.E., and Bowring, S.A. 1997. The Bell Lake group and Anton Complex: a basement-cover sequence beneath the Archean Yellowknife greenstone belt revealed and implicated in greenstone belt formation. Canadian Journal of Earth Sciences, **34**: 169-189.

Ketchum, J.W.F., and Bleeker, W. 1998. U-Pb Geochronology of the Sleepy Dragon Complex in the Morose - Patterson lakes area, southwestern Slave Province, with tectonic implications. *In* Slave-Northern Cordillera Lithospheric Evolution (SNORCLE) and Cordilleran Tectonics Workshop, Meeting March 6-8, Simon Fraser University. *Compiled by* F. Cook and P. Erdmer, Lithoprobe Report No. 64, pp. 25-30.

Lambert, M.B., and van Breemen, O. 1991. U-Pb zircon ages from the Sleepy Dragon Complex and new occurrence of basement rocks within the Meander Lake Plutonic Suite, Slave Province, N.W.T. *In* Radiogenic and Isotopic Studies: Report 4, Geological Survey of Canada, Paper 90-2, pp. 79-84.

Thompson, P.H., Ross, D., and Davidson, A. 1994. Regional geology of the Winter Lake - Lac de Gras area, central Slave Province, District of MacKenzie, Northwest Territories. *In* Current Research 1994-C, Geological Survey of Canada, pp. 1-12.

Villeneuve, M.E., Relf, C., Hrabi, B., and Jackson, V. 1994. Ages of detrital zircons from supracrustal sequences in the Slave province, NWT, Canada: implications for age of basement. *In* Abstracts with Programs, Geological Society of America 1994 Annual Meeting, v. 26, p. A-232.

Timing of Plutonism, Deformation, and Metamorphism in the Yellowknife Domain, Slave Province.

W.J. Davis and Wouter Bleeker

Geological Survey of Canada, 601 Booth St. Ottawa, ON. K1A 0E8
bidavis@nrcan.gc.ca

U-Pb zircon, titanite and monazite ages for plutonic rocks are used to provide a chronological framework for post-2.66 Ga deformational and metamorphic events in the Yellowknife Domain, southern Slave Province (Bleeker and Beaumont-Smith, 1995). Diorite and tonalite plutons of the Defeat Suite yield ages of 2628±3 Ma and 2624±4 Ma, older than previous, less precise estimates for this suite of ca. 2618-2620 Ma (Henderson et al. 1987). The Defeat Suite plutons cross-cut and post-date upright F_1 folds in turbidites of the ca. 2.68-2.66 Ga Burwash Formation (Bleeker and Villeneuve, 1995). D_1 deformation is therefore bracketed between 2.66 Ga and 2.63 Ga. A second folding event (F_2), represented by northwest- to north-trending steeply plunging folds of bedding and D_1 structures, affected the area after intrusion of the Hidden Lake pluton at 2606±2 Ma, and synchronously with intrusion of the 2596±2 Ma Sparrow Lake pluton, a member of the two-mica granite Prosperous Suite. Interpretation of the Sparrow Lake pluton as a syn-D_2 intrusion (Bleeker and Beaumont-Smith, 1995; Ham et al., 1997) requires D_2 folding to be in progress at 2596 Ma. However, initiation and duration of the D_2 event is not yet known. It may have affected units as young as the 2686±2 Ma Morose granite. Metamorphic isograds are spatially related to Defeat, Prosperous, or even younger plutonic complexes, and therefore may have formed at different times over a 30 m.y. period in different parts of the Yellowknife Domain.

A number of points can be emphasized with the new data within the broader context of the Slave Province. Firstly, the minimum age for D_1 in the Yellowknife Domain is similar to or older than depositional ages reported for some turbidite sequences elsewhere in the Slave Province, suggesting: 1) D_1 in the Yellowknife Domain was complete and post-D_1 Defeat plutons were being unroofed during sedimentation elsewhere in the Slave; or 2) D_1 was diachronous across the Slave Province. Secondly, diorite-tonalite plutonism (Defeat Suite) started in the Yellowknife Domain 10-15 m.y. earlier than compositionally similar intrusive events in the central and northern Slave Province. This highlights the potential for diachronous development of plutonism in the period from 2.63 to 2.61 Ga.. Defeat-type plutonic rocks in the Healy Lakes area, in the southeastern Slave Province have similar pre-2.62 Ga ages to those at Yellowknife (van Breemen et al., 1987; 1992), and one testable hypothesis is that 2.63-2.62 Ga plutons are

restricted to a zone extending across the southern portion of the Slave Province from the Yellowknife Domain to Healey Lake. The general orientation of such a plutonic zone would be broadly parallel to the northeast orientation of the D_1 fold belt in the Yellowknife Domain, after accounting for the effects of D_2 folding, and would be consistent with this phase of plutonism being related to the convergence (subduction?) which produced the D_1 fold belt. Further geochronological work is required in the southeastern Slave Province to confirm the older, but imprecise ages reported for that area to better delineate the extent and distribution of pre-2620 Ma Defeat-type plutons, and their relationship to early deformational fabrics.

Finally, the ages of younger two mica and k-spar megacrystic granites (Prosperous, Morose) show no evidence for diachroneity at the scale of the Slave Province, despite diachronous development of the older tonalitic magmatism. The cause of the widespread granite intrusive event and associated deformation remains speculative (lithospheric delamination, post-collisional extension, crustal thickening).

References

Bleeker, W. and Beaumont-Smith. C., 1995. in Current Research, 1995-C, Geological Survey of Canada, p. 87-96.

Bleeker, W. and Villeneuve, M., 1995. Lithoprobe Report No. 44, p. 8-13.

Ham, N, Benn, K, and Bleeker, W., 1997, GAC/MAC Abstract volume 22, A-61.

Henderson, J.B., van Breemen, O., and Loveridge, D., 1987, Geological Survey of Canada, Paper 87-2, 111-121.

van Breemen, O., Davis, W.J., and King, J.E, 1992, Canadian Journal of Earth Sciences, 26, 2186-2199.

van Breemen, O., Henderson, J.B., Sullivan, R.W., and Thompson, P.H., 1987, Geological Survey of Canada, Paper 87-2, 101-110

Crustal Architecture of the Slave Craton

Wouter Bleeker[1], Bill Davis[1], and John Ketchum[2]

[1]*Geological Survey of Canada, 601 Booth Street, Ottawa, ON, K1A 0E8 (wbleeker@nrcan.gc.ca)*
[2]*Memorial University of Newfoundland, St. John's, NF, A1B 3X5*

The lithotectonic framework of the Slave craton comprises a centrally situated Meso- to Paleoarchean basement domain (terrane?), flanked on either side by Neoarchean supracrustal domains (Fig.1). The ca. 2.7 Ga Neoarchean domain of the eastern Slave Province is considered to consist largely of juvenile crust (e.g., Davis and Hegner, 1992).

Basement rocks of the south-central Slave are overlain by a diagnostic, autochthonous cover sequence—the Central Slave Cover Group (Bleeker et al., 1999a). Structural continuity of the basement and correlation of the cover sequence show that all Mesoarchean basement rocks in this area, from Yellowknife to the east, and from the Sleepy Dragon Complex to Point Lake in the north, comprise a single contiguous basement block—the Central Slave Basement Complex (Bleeker et al., 1999a). Hence, terrane boundaries proposed by Kusky (1989, 1990) are no longer tenable. Nevertheless, a terrane-bounding suture remains a viable explanation for the apparent juxtaposition of old sialic crust and ca. 2.7 Ga juvenile crust, but this suture must be situated much further to the east, approximately on line with the Nd isotopic boundary of Davis and Hegner (1992).

The detailed outline of the Central Slave Basement Complex is becoming increasingly well defined, its boundaries almost everywhere being represented by significant high-strain zones (Bleeker et al., 1999a,b). The various basement/cover high-strain zones appear to be segments of a single structure that can be correlated over strike-lengths of 100's of kilometers and which has all the characteristics of a basal décollement that accommodated thrusting of autochthonous to parautochthonous cover units over older basement. Development of the high-strain zone, constrained to about 2690 Ma or possibly slightly earlier (Bleeker et al., 1999b), may have accompanied docking of a juvenile eastern Slave terrane.

The high-strain zones and juxtaposition of juvenile versus Mesoarchean crust predate deposition of ca. 2660-2685 Ma turbidites, which essentially form an overlap sequence across large parts of the Slave Province.

At least three important regional folding events, followed by major strike-slip faulting, overprint the turbidites. The three folding events (F_1, F_2, F_3) can be mapped and correlated as regional fold belts on scales approaching the dimensions of the craton, independently of the more random distribution, size, and shape of granitoid plutons that locally cause more complicated structural patterns. These fold belts record very large horizontal shortenings. F_1 deformation, which produced a northeast-trending belt of upright chevron folds, occurred prior to widespread Defeat Suite plutonism dated at 2624-2628 Ma (Davis and Bleeker, 1999). F_2 refolding, interpreted as a craton-wide transpressive event, was accompanied by voluminous granitoid magmatism dated at 2596 to 2586 Ma (Davis and Bleeker, 1999). F_3 remains less well documented.

In conclusion, the architecture of the Slave craton suggests that it grew and was subsequently deformed by several discrete collisional events. The first of these collision events juxtaposed juvenile crust against older Mesoarchean crust, whereas later collision events manifested themselves mainly by large horizontal shortenings. The principal shortening directions of these collisions varied in orientation, resulting in complex interference patterns. The coherent structural patterns on the scale of the craton suggest that the collisions involved micro-plates of considerable size and rigidity.

References

Bleeker, W., Ketchum, J.W.F., Jackson, V.A., and Villeneuve, M.E., 1999a. The Central Slave Basement Complex, Part I: Its structural topology and autochthonous cover sequence. Canadian Journal of Earth Sciences, *in press*.

Bleeker, W., Ketchum, J.W.F., and Davis, W.J., 1999b. The Central Slave Basement Complex, Part II: High-strain zones along the basement/cover contact. Canadian Journal of Earth Sciences, *in press*.

Davis, W.J., and Bleeker, W., 1999. Timing of plutonism, deformation and metamorphism in the Yellowknife Domain, Slave Province. Canadian Journal of Earth Sciences, *in press*.

Davis, W.J., and Hegner, E. 1992. Neodymium isotopic evidence for the tectonic assembly of Late Archean crust in the Slave province, northwest Canada. Contributions to Mineralogy and Petrology, **111**: 493-504.

Kusky, T.M. 1989. Accretion of the Archean Slave province. Geology, **17**: 63-67.

Kusky, T.M. 1990. Evidence for Archean ocean opening and closing in the southern Slave province. Tectonics, **9** (no.6): 1533-1563.

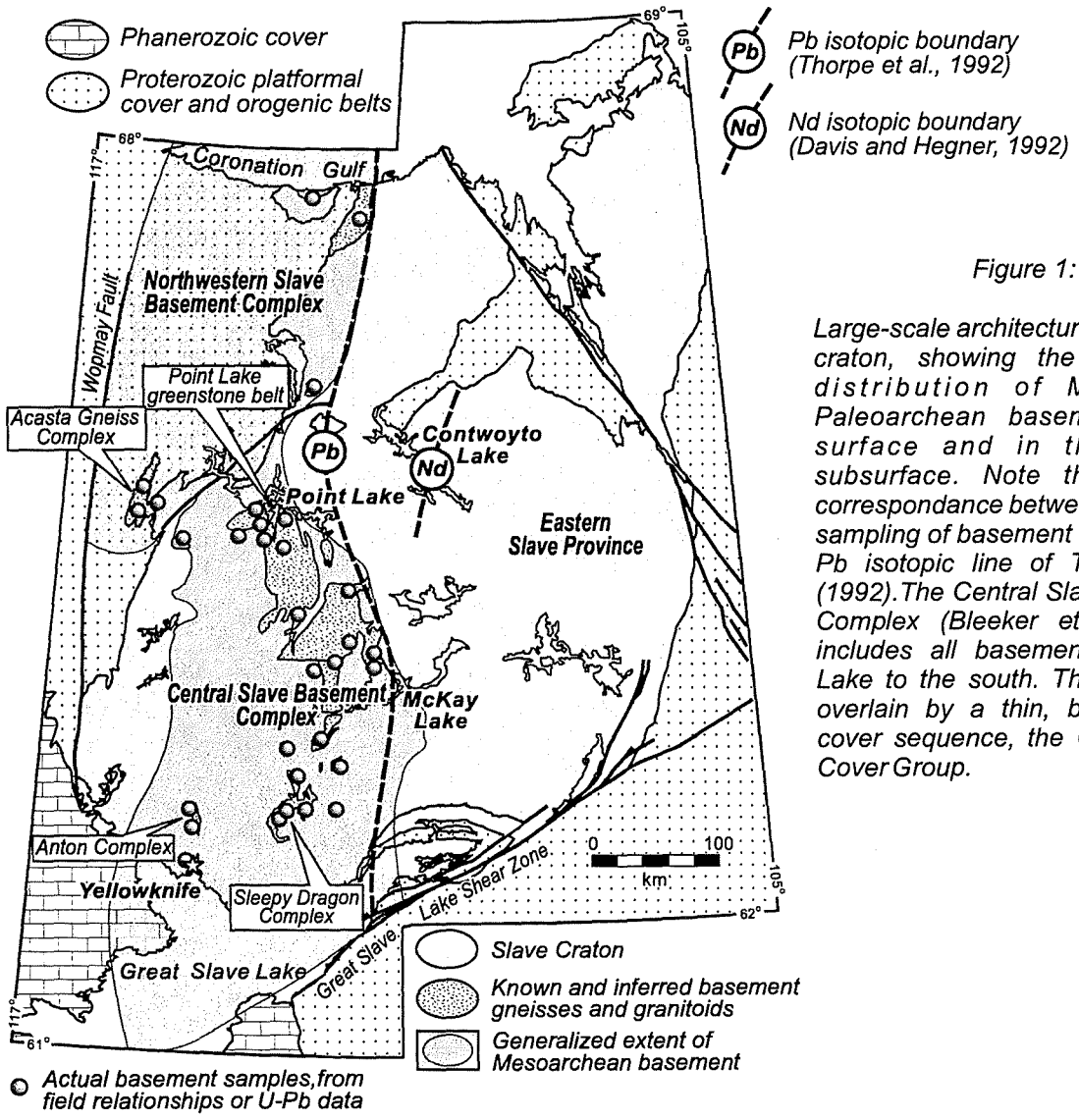

Figure 1:

Large-scale architecture of the Slave craton, showing the generalized distribution of Meso- and Paleoarchean basement at the surface and in the shallow subsurface. Note the excellent correspondance between the current sampling of basement rocks and the Pb isotopic line of Thorpe et al. (1992). The Central Slave Basement Complex (Bleeker et al., 1999a) includes all basement from Point Lake to the south. The complex is overlain by a thin, but diagnostic cover sequence, the Central Slave Cover Group.

Towards An Integrated Geological-Geophysical Interpretation Of The Slave Portion Of The SNORCLE Transect

Wouter Bleeker, David Snyder, Brian Roberts, Walter Roest, and Karen Hendry

Geological Survey of Canada
Continental Geoscience Division, 601 Booth Street, Ottawa, Ontario, K1A 0E8
email: wbleeker@nrcan.gc.ca; tel: (613) 995-7277

The Slave portion of the SNORCLE transect is generally well exposed, and from the end of the transect at Tibbit Lake to just west of Yellowknife the exposure level can only be described as exceptional. This portion of the transect should thus provide the strongest surface geological constraints on the interpretation of the seismic section. In general, this area has been well mapped and critical portions have been mapped in detail (e.g. Bleeker et al., 1999a,b). Furthermore, detailed gravity surveys have been acquired from the end of the road to the northeast, across the basement-cored Sleepy Dragon Complex, to provide additional constraints (Bleeker et al., 1998; see also Hendry et al., this volume). Following processing and a first complete analysis of the seismic data along SNORCLE Corridor 1 by Cook et al. (in press), we would like to attempt a more detailed analysis and geological-geophysical integration of the Slave portion of the transect. As a first step, we briefly review the characteristics of the main geological features that are likely to be important in any interpretation of the seismic data. Roberts et al. (this volume) and Snyder et al. (this volume) further expand on this and discuss the seismic data in detail.

Recent mapping, varying from regional to detailed scales (Bleeker et al., 1999a,b), has shown that the terrane boundaries proposed by Kusky (1990) are no longer tenable and that the entire Yellowknife Domain formed on Sleepy Dragon-like Mesoarchean crust. Bleeker et al. (1999a) refer to the large contiguous basement block underlying the south-central Slave craton as the Central Slave Basement Complex. The major domain (terrane?) boundary separating this Mesoarchean basement domain from the more juvenile eastern Slave lies much further to the east (eastern MacKay Lake) and, regrettably, this boundary is not currently addressed by the seismic transect. Burwash Formation turbidites in both the Yellowknife structural basin and east of the Sleepy Dragon Complex are indistinguishable in facies, detrital zircon population and age, further negating the model of a "Contwoyto terrane" accretionary prism (Kusky, 1990).

On a more local scale, the Yellowknife "basin" reflects structural relief created mainly during several regional, contractional, folding events. The Burwash Formation (s.s.) is preserved in a structural basin (synclinorium), rather than a sedimentary basin, flanked on either side by correlatable basement-cored antiforms (Anton and Sleepy Dragon complexes). The present asymmetry of the Yellowknife structural basin is attributed largely to a probable, crustal-scale fault zone of Archean age along the Yellowknife River lineament—the Yellowknife River Fault Zone. This near-vertical structure is inferred from significant tectonostratigraphic disontinuities, the presence of post-2600 Ma conglomerate panels, and a coincident major topographic lineament. It was

further overprinted during the Paleoproterozoic by north-northwest-trending, vertical brittle faults. This fault zone marked by disrupted, vertical panels of disparate lithostratigraphic units, should produce a poorly imagable seismic zone across which major reflectors (e.g., Y2, see Cook et al., in press) should not be expected to match.

East of Yellowknife, within the Burwash Formation metaturbidites, impedance contrasts may exist across the following contacts (qualitatively ranked in terms of decreasing contrast):

1) Paleoproterozoic mafic to ultramafic sills;
2) folded gabbro sills at Tibbit Lake;
3) possible volcanic intercalations within the turbidites;
4) the basal turbidite/volcanic contact;
5) deformed, domal or sheet-like granite plutons;
6) cryptic structural discontinuities;
7) pelite-dominated versus sand-dominated packages at 10-100 m scales.

Based on these expected impedance contrasts, the Duck Lake intrusive sheet, a differentiated mafic to ultramafic Paleoproterozoic intrusion that dips shallowly (20°) to the east at about the position of the Y1 reflector, should be highly imagable. New seismic processing by Roberts et al. (this volume) and additional arguments presented by Snyder et al. (this volume) lend credence to the interpretation of the Y1 reflector as shallowly dipping mafic sills (subhorizontal, but strictly speaking dykes since they are sharply cross-cutting). An additional argument is that there is no outcrop evidence for a shallowly cross-cutting detachment, the interpretation favoured by Cook et al. (in press). The down-dip continuity of the reflector, in an area where cross-cutting granitoid plutons are present, and the tabular (unfolded) geometry, indicate that the Y1 reflector is almost certainly post-2596 Ma in age, the age of the Prosperous Suite granites and associated D_2 deformation (Davis and Bleeker, 1999).

Below and adjacent to the Burwash Formation metaturbidites, major impedance contrasts are predicted across (again ranked in terms of decreasing contrast):

8) Turbidite/volcanic contacts, particularly where mafic volcanics are present;
9) the sheared basement/cover interface—an unconformity overlain by a thin package of quartzite and banded iron formation, and structurally enhanced by high shear strains;
10) gabbro sheets within basement;
11) mafic/felsic volcanic contacts;
12) younger cross-cutting plutons such as the Morose Granite, dated at 2586+/-2 (Davis and Bleeker, 1999).

Given these possibilities, we would interpret the prominent Y2 reflector as largely a stratigraphic reflector associated with volcanic rocks and the basement cover interface, and probably enhanced by tectonite fabrics. Bleeker et al. (1999b) have shown that the high strain in the basement/cover décollement is pre-2687 Ma and largely unrelated to late detachment-style faulting associated with core complexes (cf. Cook et al., in press).

The overall depth range of the Y2 reflector (up to 5 seconds) is in agreement with the folding-related structural relief predicted by Bleeker (1996). Cut-offs of deeper reflectors can be easily explained by truncation of basement structures (gabbro sheets?) along the sheared unconformity.

Future work will try to incorporate more data sets (e.g., gravity modelling) as well as expand the more detailed analysis to the entire Slave portion of the transect.

References

Bleeker, W., Cooper, R.V., Berrigan, M.E., Roest, W.R., and Hendry, K.A., 1998. Detailed gravity profiles across the Sleepy Dragon Complex and adjacent parts of the Yellowknife Domain, Slave structural province: preliminary data. *In* Current Research 1998-C, Geological Survey of Canada, pp. 1-8.

Bleeker, W., Ketchum, J.W.F., Jackson, V.A., and Villeneuve, M.E., 1999a. The Central Slave Basement Complex, Part I: Its structural topology and autochthonous cover sequence. Canadian Journal of Earth Sciences, **xx**: xxx-xxx.

Bleeker, W., Ketchum, J.W.F., and Davis, W.J., 1999b. The Central Slave Basement Complex, Part II: High-strain zones along the basement/cover contact. Canadian Journal of Earth Sciences, **xx**: xxx-xxx.

Davis, W.J., and Bleeker, W., 1999. Timing of plutonism, deformation and metamorphism in the Yellowknife Domain, Slave Province. Canadian Journal of Earth Sciences, **xx**: xxx-xxx.

Cook, F.A., van der Velden, A., Hall, K.W., and Roberts, B.J., in press. Frozen subduction in Canada's Northwest Territories: LITHOPROBE deep lithospheric reflection profiling of the western Canadian Shield. Tectonics.

Kusky, T.M. 1989. Accretion of the Archean Slave province. Geology, **17**: 63-67.

Kusky, T.M. 1990. Evidence for Archean ocean opening and closing in the southern Slave province. Tectonics, **9** (no.6): 1533-1563.

More thoughts about the nature of bright reflections in the upper crust near Yellowknife

David Snyder, Brian Roberts & Wouter Bleeker

Geological Survey of Canada
615 Booth Street
Ottawa, Ontario K1A 0E9
snyder@cg.NRCan.gc.ca

Among the many spectacular reflections observed in the data from corridor 1 of the SNORCLE transect are several prominent shallow dipping reflections within the upper 20 km of the oldest crust crossed by the transect. In this area, near Yellowknife, a pair of continuous bright reflections that dip in opposite directions were attributed to sheared rocks along detachment surfaces by Cook et al. (1999) (their reflections Y1 & Y2). The tectonic context for this interpretation is that of gneiss domes or metamorphic core complexes (i.e. the Sleepy Dragon Complex) unroofed by extension on shallow dipping shear zones. If the opposing detachments were active nearly simultaneously, Tertiary tectonics in the Betics of Spain may be an apt analogy (Vissers et al. 1995). These detachment surfaces may be particularly reflective due to coincident intrusions of magma or metasomatic fluids that deposited material with significant impedance contrast to the wall rocks or because the detachment reactivated an unconformity or earlier fault (Cook et al. 1999).

Reprocessing of the shallow seismic data near Yellowknife has revealed more information about these reflectors. We have been able to extend the shallower reflection Y1 closer to the surface (to ~ 100 ms) and to enhance some of the reflections above that horizon. These weak reflections have similar orientations to dips of structures observed in the metagreywackes of the Burwash Formation, but the prominent reflector cuts sharply across these steeply dipping structures (Figure 1). The dip of the prominent reflector is consistent with that of an intrusive sheet mapped at the surface along the profile directly along the extension of the Y1 reflector. We interpret this correlation as indicative that the Y1 reflector is primarily the ultramafic intrusion. At depths greater than one kilometer we rely on region seismic analysis. A discrete layer of high interval velocities is associated with this reflection, whereas a step increase in velocity would be more typical of a detachment surface. In addition, an mafic to ultramafic intrusive 100-200 m thick, surrounded by metagreywackes is ideally tuned to the seismic wavelengths (80-140 m) used in SNORCLE.

Because of its low dip, the deeper (Y2) reflection projects to the surface many tens of kilometers northeast of the end of the SNORCLE line (Figure 1), so its interpretation is less certain. The recently recognized regional extent of a thin package of quartzite and banded iron formation (Central Slave Cover Group), overlain by pillow lavas (Kam Group) of possible regional extent, together lying on top of basement gneiss complexes (Central Slave Basement Complex) (Bleeker et al. 1999) now makes this sequence an excellent candidate for a regional reflector. The juxtaposition of mafic volcanics (0-5 km thick) and tonalitic gneiss across an stratigraphic unconformity again provides ideal impedance contrasts for reflectors. Estimates of the thickness of the Burwash Formation from gravity (Gibb and Thomas 1980) and structural models are permissive of a 5-10 km thick unit along the SNORCLE profile.

The disappearance of this deeper reflector at 10-12 km depth to the west, near Yellowknife (Figure 1), is unlikely due solely to increased levels of noise because it occurs east of areas with demonstrable increased noise levels. Instead the reflector is likely truncated by a zone with a steeply dipping Archean ductile fault along the Yellowknife River overprinted by Proterozoic brittle left-lateral faults. A vintage refraction survey in Great Slave Lake (Clee et al. 1974) observed refractors at 8 km depth both east and west of Yellowknife Bay. SNORCLE reflection sections also image reflections at similar depths east and west of Yellowknife. This may indicate nearly pure strike-slip offset of a single southward dipping unconformity, or these refractors/reflectors may be very different features (the western one likely occurs within a late pluton). If the reflector represents a single regional unconformity, then a combination of uplift, possibly associated with the unroofing of the Anton Complex, and sinistral displacements of blocks of Kam Group and Central Slave Cover Group are required to produce the map patterns observed around Yellowknife Bay today. The SNORCLE line images just one section through this complex surface. Possible displacements along the unconformity surface are key to its geological understanding and may have enhanced its reflectivity, but these displacements are not resolvable with information available at present.

Reflections within crystalline and metamorphic rocks have remained largely enigmatic despite numerous surveys over the past few decades. This study encapsulates the problem. Reflectors are now recognized worldwide as primarily mafic intrusions into felsic basement, shear zones or sharp lithological changes. Here we argue that one reflector is due to an ultramafic intrusion and another is due to an unconformity or a detachment surface or a combination of the two. The deeper reflectors are more cryptic with respect to surface rocks.

References:

Bleeker, W., J. W. F. Ketchum, V. A. Jackson and M. Villeneuve, 1999, The Central Slave Basement Complex, Part I: its structural topology and authochthonous cover, *Canadian Journal of Earth Sciences*, in review.

Clee, T. E., K. G. Barr and M. J. Berry, 1974, Fine structure of the crust near Yellowknife, *Canadian Journal of Earth Sciences*, **11**, 1534-1549.

Cook, F. A., A. van der Velden, K. W. Hall and B. J. Roberts, 1999, Frozen subduction in Canada's Northwest Territories: LITHOPROBE deep lithospheric reflection profiling of the western Canadian Shield, *Tectonics*, in press.

Gibb, R. A. and M. D. Thomas, 1980, Correlation of gravity anomalies with Yellowknife Supergroup rocks, North Arm, Great Slave Lake, , *Canadian Journal of Earth Sciences*, **17**, 1506-1516.

Vissers, R. M., J. P. Platt and D. van der Wal. 1995, Late orogenic extension of the Betic Cordillera and the Alboran domain: a lithospheric view, *Tectonics*, **14**, 786-803.

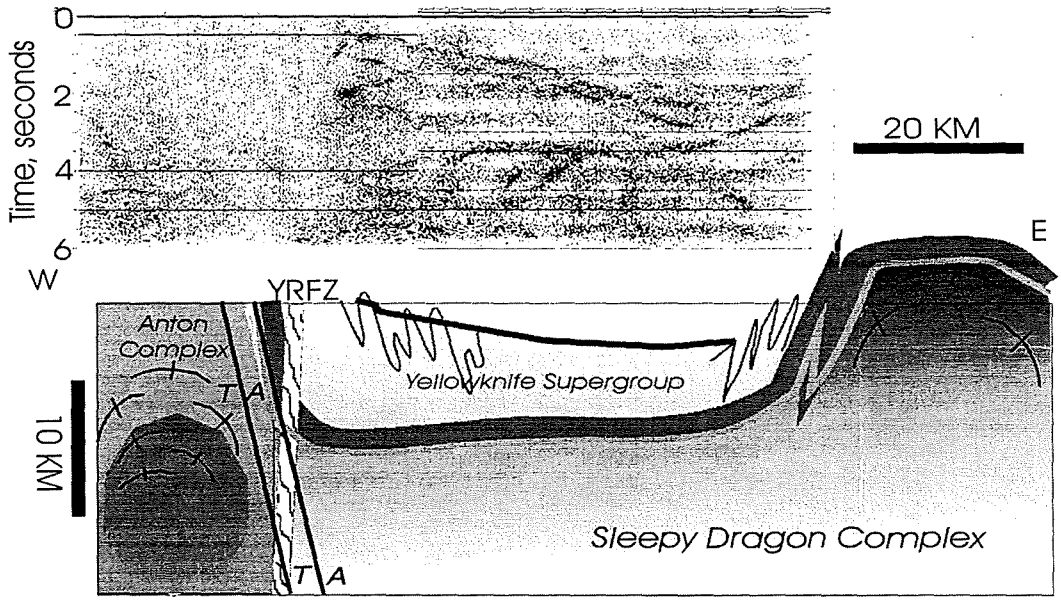

Figure 1. Cartoon interpretation of the SNORCLE section east of Yellowknife. YRFZ is the Yellowknife River fault zone; thin black lines represent Proterozoic faults with predominantly left-lateral offsets. The darker band separating the Yellowknife Supergroup (mostly Burwash Formation) and the two gneiss complexes is the proposed regional reflector composed primarily of the mafic Kam pillow lavas. At the top is the reprocessed SNORCLE seismic section (see Roberts et al. this volume).

Modeling of Gravity Profiles in the southern Slave Province, – Are Greenstones Underlying the Yellowknife Basin?

Karen A.B. Hendry [1,2], Wouter Bleeker [2], and Walter R. Roest [2]

[1] Ottawa-Carleton Geoscience Centre and Department of Earth Sciences, University of Ottawa, Ontario, K1N 6N5

[2] Geological Survey of Canada, 615 Booth St., Ottawa, Ontario, K1A 0E9

Targeted gravity data collection in the southern Slave Province was sponsored by the Geological Survey of Canada and its sister organization Geomatics Canada. Final GPS and gravity corrections are now complete for the data from two field seasons. In 1996, 700 gravity stations were measured along Corridor 1 of the SNORCLE transect. In 1997, a detailed gravity survey was carried out east of Yellowknife, across the Sleepy Dragon Complex, its flanking greenstone belts, and adjacent parts of the Yellowknife Domain (Bleeker et al., 1998). A total of 152 stations were recorded along three profiles that link up with the SNORCLE transect along the Ingraham Trail. Major gravity anomalies were recorded over the greenstone belts and over a variety of granitoid plutons of the Prosperous and Defeat Suites and the Morose Granite in the Sleepy Dragon Complex. In general, the gravity profiles show excellent correlation with the known geology (Bleeker et al., 1998) and help in constraining the deep structure of the area.

The geological evolution of the southern Slave Province has been studied for many years. One of the main issues under debate is the correlation between the various greenstone belts, and the relationship between greenstones and basement rock complexes. Detailed gravity modeling of the transects in the southern Slave Province may shed new light on these issues, by providing estimates for the overall subsurface dip and depth extend of contacts between the various rock units. The modeling also provides constraints on the shape of some of the plutons, which, combined with field and magnetic fabric studies may shed new light on the emplacement history (Spark et al., this volume).

Detailed 2.5-D gravity models are presented for the eastern portion of the SNORCLE transect and for the transect crossing the Sleepy Dragon Complex (Profile Cameron-1). Modeling of Cameron-1 shows that the Cameron River and the Beaulieu River greenstone belts can be

extended underneath the turbidites, which extend to the west and east respectively, as predicted by the model of Bleeker et al. (this volume). This supports that the Yellowknife "basin" is a large-scale synclinorium and the Sleepy Dragon Complex a large-scale anticline.

As part of an M.Sc. study by the first author, modeling of Cameron profiles 2 and 3 will be completed. Future work will include 3-D modeling of both gravity and magnetic data across the Yellowknife "basin", based on the GSC's regional data sets. This may give further constraints on the lateral extent of the greenstones and the final geometry resulting from protracted deformation.

Acknowledgments

This research is supported by an NSERC-Lithoprobe grant to Benn, Roest and Bleeker. K. Hendry acknowledges the use of GSC facilities and databases to carry out her research. We thank the gravity group, Geomatics Canada, for their role in gravity data acquisition.

Reference

Bleeker, W., Cooper, R.V., Berrigan, M.E., Roest, W.R., and Hendry K.A.B., 1998. Detailed gravity profiles across the Sleepy Dragon Complex and adjacent parts of the Yellowknife Domain, Slave Structural Province: preliminary data. In Current Research 1998-C, Geological Survey of Canada, p. 1-8.

Syn-D_2 plutonism in the southern Slave Province: evidence from magnetic fabrics and field mapping

Robert Spark and Keith Benn
Ottawa-Carleton Geoscience Centre
and
Department of Earth Sciences, University of Ottawa

Wouter Bleeker and Walter Roest
Geological Survey of Canada, 601 Booth Street, Ottawa

The magnetic fabric of a rock, derived from the *anisotropy of magnetic susceptibility* (AMS), provides a useful method of measuring mineral fabric where field measurements are scarce, such as within weakly deformed granitic plutons. AMS can provide information regarding the orientation and symmetry of rock fabric, and in some cases the intensity of strain. The magnetization induced in a weak applied field is a function of the magnetic susceptibility (K) of a rock specimen. In practice, a specimen is represented by a 25 mm diameter x 22 mm long piece of drill core. Since all rock specimens are magnetically anisotropic, the susceptibility differs as a function of the specimen orientation within the applied field. By measuring K in several different orientations with respect to the specimen, the susceptibility ellipsoid is defined, with its principal axes ($K_{max} \geq K_{int} \geq K_{min}$) corresponding to the three eigenvectors of the susceptibility tensor. The net result is a bulk magnetic fabric description that incorporates all the Fe-bearing minerals (mostly ferrosilicates and magnetite). The usefulness of the AMS technique lies in the fact that the magnetic fabric tends to be coaxial to the mineral fabric. Hence the AMS allows the quantification and mapping of mineral fabrics that cannot be measured by standard field techniques.

In our studies, the magnetic fabric is being used to document the mineral fabrics and the magmatic to subsolidus strain histories preserved within different suites of syntectonic plutons of the southern Slave Province. The plutonic rocks have recently been dated using high-resolution U-Pb techniques (Davis and Bleeker, in press). Recent mapping has suggested that much of the granitoid plutonism within the Yellowknife Domain of the southern Slave province is broadly contemporaneous with D_2 deformation (Bleeker and Beaumont-Smith, 1995). The magnetic fabric analyses, combined with field mapping and gravity modelling of the plutons, will provide new constraints on the regional deformation patterns associated with the D_2 transpressive tectonics concurrent with the different magmatic events, as well as on mechanisms of magma emplacement and exhumation of the plutons and their host rocks.

One of the main targets of our investigations is the Morose pluton, a large (25 km x 15 km), roughly elliptical, 2686 ± 2 Ma (Davis and Bleeker, in press) megacrystic granitoid situated within the Sleepy Dragon gneissic complex. SNORCLE-funded mapping and sampling of 70 stations was carried out in 1998, and the remainder of the field work on the Morose pluton is planned for the summer of 1999. The Morose pluton is particularly interesting since it was emplaced in the centre of the Sleepy Dragon complex, considered to be a regional-scale F_1/F_2

fold interference pattern (Bleeker, 1996) appearing as a tectonic window within surrounding higher-level Burwash Formation metasediments. Our magnetic fabric study offers insight into late stage kinematics within the complex; including possible elements of dextral transpression, and extension related with partial exhumation of this basement complex.

The Morose pluton consists of a white to pink-weathering coarse-grained biotite granite. Field observations and measurements, combined with the AMS results point to a syn-D_2 emplacement of the Morose pluton, refuting previous inferences of the Morose pluton and other late-stage megacrystic granites as being largely post-tectonic bodies that were not involved in regional deformation. It is becoming clear, through current work that much of the granitoid plutonism within the Yellowknife Domain of the southern Slave province is broadly contemporaneous with D_2 deformation (Bleeker and Beaumont-Smith, 1995).

Two fabric domains can be identified based on field measurements and magnetic fabrics. Megacrysts of K-feldspar,1-4 cm in size, are especially conspicuous and define a concentric, dome-like pattern of shallowly-dipping foliation, evident within the centre of the pluton. The magnetic foliation pattern is consistent with these observations. The magnetic lineations in the centre of the pluton are rather weak, but a pronounced NNW-SSE trending orientation is common. This orientation is essentially parallel to the regional F_2 fold axes that affect the host Sleepy Dragon complex (Bleeker, 1996). The mesoscopic-scale foliation intensifies and rotates into parallelism with the NW margin of the pluton, as does the magnetic foliation. The steep foliations at the margin are compatible with steeply dipping pluton contacts interpreted from gravity models (Hendry et al., 1998). The magnetic lineations also rotate into near-parallelism with the pluton margin, suggesting a dextral shearing along the NW margin that began late during crystallization of the magmas. The shallowly-dipping fabrics near the center of the pluton may be related to flow during emplacement of a horizontal, tabular pluton, or may record petrological (e.g. crystal settling, diffusion) processes. We interpret that the magnetic lineations record a tectonic reworking of an early-stage, shallowly-dipping fabric, that was reoriented late during crystallization.

The magnetic lineations in the (~2596 Ma) Ma Prosperous granite suite, further to the west in the southern Slave province, are also strongly oriented parallel to the regional F_2 trend (Benn et al., 1998; Ham et al., 1998). Our magnetic fabric studies of a small ~2624 Ma Defeat suite pluton at Upper Watta Lake also indicate primary igneous fabrics that were affected by D_2 shearing during emplacement, with no evidence of any D_1 deformation (Spark et al., 1998). The pluton is characterized by igneous textures and a steep magnetic lineation tentatively interpreted to record vertical magma flow during emplacement. Towards the eastern contact, the pluton is influenced by the D_2 Watta Lake Shear Zone, where the magnetic lineation is rotated into near-parallelism with the shear zone fabrics, possibly late during crystallization of the magma.

The reworking of igneous emplacement-related fabrics late in the crystallization histories of plutons may, in fact, be typical of plutons emplaced within actively deforming contractional belts. Magnetic fabric patterns similar to those found in the Morose, Prosperous and Defeat suite plutons have been documented from the Late Devonian syntectonic South Mountain batholith in the Meguma Terrane (Nova Scotia), which was emplaced during the advanced stages of Acadian transpression (Benn et al., 1997; 1999). This raises interesting questions regarding the

transpressional emplacement of granitic plutons — especially those regarding deep-level emplacement within a contractional orogenic belt, and their influence on tectonic denudation (e.g. Hill et al., 1992).

Large plutons, such as the Morose, comprise a significant component of the geology in the southern Slave Province, and therefore they should be considered when interpreting seismic and gravity profiles. In the coming year, the ongoing structural, magnetic fabric, gravity and geochronological studies of the Morose pluton and the Sleepy Dragon complex, should further our understanding of the shapes of large plutons that might be imaged by the SNORCLE geophysical transect, as well as aiding our interpretations of the mechanisms associated with syntectonic pluton emplacement, and the exhumation of the Sleepy Dragon complex.

References:

Bleeker, W., 1996. Thematic studies in the Slave Province, Northwest Territories: The Sleepy Dragon Complex; in Current Research 1996-C; Geological Survey of Canada: 37-48.

Bleeker, W., and Beaumont-Smith, C., 1995. Thematic structural studies in the Slave Province: Preliminary results and implications for the Yellowknife Domain, Northwest Territories; in Current Research 1995-C; Geological Survey of Canada: 87-96.

Benn, K, Ham, N.M., Pignotta, G.S. and Bleeker, W., 1998. Emplacement and deformation of granites during transpression: magnetic fabrics of the Archean Sparrow Pluton, Slave Province, Canada. J. Struct. Geol., v. 20: 1247-1259.

Benn, K., Horne, RJ, Kontak, D.J., Pignotta, G.S., and Evans, N.G. 1997. Syn-Acadian emplacement model for the South Mountain batholith, Meguma Terrane, Nova Scotia: Magnetic fabric and structural analyses. GSA Bull., 109: 1279-1293.

Benn, K., Roest, W.R., Rochette, P., Evans, N.G., and Pignotta, G.S. 1999. Geophysical and structural signatures of syntectonic batholith construction: the South Mountain Batholith, Meguma Terrane, Nova Scotia. Geophys. J. Int.: 144-158.

Davis, W.J. and Bleeker, W., in press. Timing of Plutonism, Deformation and Metamorphism in the Yellowknife Domain, Slave Province. C JES.

Ham, N.M., Benn, K., and Bleeker, W. 1998. The Late-Archean Prosperous Granite Suite: Syn-D2 laccoliths in the Yellowknife Domain, Slave province; in Slave-Northern Cordillera Lithospheric Evolution (SNORCLE) Transect and Cordilleran Tectonics Workshop Meeting, Lithoprobe Report No. 64: 36.

Hendry, K.A.B., Roest, W.R., Bleeker, W., and Benn, K., 1998. Geophysical data analysis and regional gravity modelling in the southern Slave province; in Slave-Northern Cordillera Lithospheric Evolution (SNORCLE) Transect and Cordilleran Tectonics Workshop Meeting,

Lithoprobe Report No. 64: 260-263.

Hill, E.J., Baldwin, S.L., and Lister, G.S. 1992. Unroofing of active metamorphic core complexes in the D'Entrecasteaux Islands, Papua New Guinea. Geology, 20: 907-910.

Spark, R., Benn, K., and Bleeker, W. (1998). The Magnetic Fabric of Granitoid Plutons: Evidence for the Late Archean Tectono-magmatic History of the Slave Province. Yellowknife Geoscience Forum Abstract 1998; p.103-104.

U-Pb Geochronology of Lower Crustal Xenoliths - A Window into the Deep Crust of the Central Slave Province

Davis W.J. Geological Survey of Canada, 601 Booth St. Ottawa, ON. K1A 0E8
Mackenzie, J. and Canil, D. School of Earth and Ocean Sciences, University of Victoria. Victoria, B.C. V8W 3P6

Lower crustal xenoliths entrained in kimberlites offer a unique opportunity to study the nature, age and thermal history of the lower crust of Archean cratons. We report results of a U-Pb geochronological study of lower crustal xenoliths from kimberlites in the central Slave Province, from the Lac des Gras, Yamba Lake, and Kennedy Lake areas. Granulite xenoliths include both felsic and mafic varieties. Some of the xenoliths are extensively altered during transport, particularly felsic varieties, and in some cases the original mineralogy and lithology cannot be determined with certainty. Mafic granulites typically consist of clinopyroxene, plagioclase, garnet, ilmenite, ± orthopyroxene, ± quartz, ± rutile, ± zircon and yield pressure and temperature estimates of 10-14 kbar and 700-900° C.

Zircons recovered from most granulite xenoliths record Neoarchean and/or younger ages. An older Mesoarchean history is preserved in two xenoliths from the Lac des Gras and Yamba Lake areas. An altered, leucocratic garnet-bearing gneiss (meta-tonalite?) contains ca. 3.1 Ga oscillatory zoned igneous zircon, possibly the protolith age, and at least three younger generations of metamorphic zircon at ca. 2.77, ca. 2.62 and 2.57 Ga. A mafic granulite from the Torrie pipe contains low Th/U metamorphic zircon with an age of ca. 2.97 overgrown by colourless higher Th/U zircon at some time after ca. 2.64 Ga. The Mesoarchean ages correlate with geological events documented in exposed basement localities in the western part of the province and their occurrence in the deep crust of the central region supports previously proposed hypothesis that basement rocks dips eastwards beneath the central part of the province, extending well to the east of the surface trace of the Pb isotopic line (Davis and Hegner 1992; Thorpe et al. 1992). Mesoarchean ages were not determined in xenoliths from Kennedy Lake, consistent with the eastern extent of Mesoarchean basement inferred from the isotopic composition of granites, however it must be noted that comparatively few samples have been studied from Kennedy Lake.

The majority of the xenoliths preserve Neoarchean zircon ages that cluster in distinct intervals; 2.63-2.61; 2.59-2.58 Ga, 2.55 Ga and 2.51 Ga . More than one episode of zircon growth is usually found within an individual xenolith, although no single xenolith records all events. Older ca 2.63-2.61 Ga zircon ages correlate with intrusion of dioritic to tonalitic plutons in the mid to upper crust, and zircon growth in lower crustal granulites may be related to crystallization during magmatic underplating and/or partial melting at that time. Younger zircon overgrowths at 2.59-2.58 Ga broadly overlap with granitic plutonism (ca. 2.6-2.58 Ga) and associated amphibolite grade, high-temperature low-pressure metamorphism (ca 2.60-2.59 Ga) documented in the exposed crust, and reflect zircon growth during peak metamorphism. The regional tectonic significance of the two younger Neoarchean zircon growth events at ca 2.55 and 2.51 Ga are more enigmatic and are not readily correlated with known geological events in the exposed crust. One possibility is that they are related to tectonic events that occurred in areas outside the present

margins of the province. For example, ca. 2.55 Ga granites locally form basement to the Wopmay orogen on the western margin of the Slave Province, and this event may have had an affect in the lower crust within the centre of the province. The protracted (>100 m.y) and apparently episodic nature of events affecting the lower crust during and following major orogenesis at 2.6 Ga is similar to that documented in the Kapuskasing lower crustal section (Krogh, 1993), and may be a characteristic feature of lower crustal evolution in the Neoarchean. In addition to the Neoarchean events discrete Paleoproterozic zircon growth is documented at ca. 2.22 and 1.28 Ga, and is interpreted to reflect thermal events related to mafic intrusive activity in the lower crust associated in time with major dyke swarm events. (Davis, 1997).

Information on the cooling and lower temperature thermal history of the crust can be inferred from U-Pb systematics in titanite and rutile (closure temperatures of ca 600-700° and 400° C, respectively). Titanites recovered from a mafic granulite at Lac des Gras yield discordant Paleoproterozoic ages that lie towards the lower end of a reference discordia line with intercepts at ca 2.55 and ca 1.66 Ga. Metamorphic zircon in this sample is of Neoarchean age and the younger titanite ages indicate either significant thermal resetting, or new growth of titanite in the Paleoproterozoic. This age is similar to Paleoproterozoic ca. 1.68 Ga zircon ages recorded in eclogite nodules from the Jericho pipe (Heaman et al., 1998) and may indicate that Proterozoic subduction/collisional events on the craton margins affected lower crust in the central part of the craton. Paleoproterozoic disturbances are also indicated by a range of Sm-Nd garnet whole rock isochron ages from 2.5 Ga to 1.8 Ga.

Rutile ages in all samples are discordant with $^{207}Pb/^{206}Pb$ ages ranging from ca. 1.0 to 1.8 Ga. U-Pb ages of rutiles from the majority of the xenoliths define a discordia line between 0.4 and 1.2 Ga. The older age provides a minimum estimate for when the lower crust cooled through 400° C, to lower crustal temperatures predicted for a stable cratonic geotherm. However, this 'age' may reflect a younger thermal disturbance, perhaps related to Mackenzie igneous events at 1.27 Ga, rather than steady-state cooling of the lithosphere. Rutile in some samples preserve older $^{207}Pb/^{206}Pb$ ages ranging from 1200 to 1860. The sample with the oldest rutile ages of ca 1.8 Ga occurs in the Kennedy Lake area, furthest from the proposed plume source of the Mackenzie igneous events at 1.27 Ga.

References

Davis, W.J. and Hegner, E. 1992. Contributions to Mineralogy and Petrology, 111:493-504.

Davis, W.J., 1997. Geology, 25:343-346.

Heaman, L.M., Creaser, R.A., and Cookenboo, H.O. 1998. Seventh International Kimberlite Conference, Extended Abstracts, Cape Town, 325-327.

Krogh, T.E., 1993, Earth and Planetary Science Letters, 119:1-19.

Thorpe, R., Cumming, G.L. and Mortensen, J.M. 1992. GSC Open File 2484, 179-184.

MANTLE GARNETS FROM THE DRYBONES BAY KIMBERLITE AND THE NATURE OF THE ON/OFF CRATON TRANSITION BENEATH THE SLAVE PROVINCE, NWT

CARBNO, G.B., and CANIL, D., School of Earth and Ocean Sciences, University of Victoria, PO Box 3500, Victoria, B.C., V8W 3P6, bcarbno@uvic.ca

The Drybones Bay kimberlite pipe (442-485 Ma) intrudes the Archean Defeat Plutonic Suite located beneath the north shore of Great Slave Lake, and is the largest kimberlite pipe (~36000 m^2) found to date in the Northwest Territories [1]. No local structure controls pipe emplacement, but the curious location of the kimberlite at the southwestern edge of the Slave Province makes it interesting with respect to the on/off craton transition in mantle lithosphere. Peridotite xenoliths and heavy mineral coarse concentrates were recovered from drill core, and 71 garnets were analyzed for both major (EMP) and trace elements (LAM-ICP-MS).

The xenoliths are coarse textured, with garnet grains as large as 6mm. Serpentinization and carbonatization has modified the primary mineralogy in the xenoliths, with the exception of garnet, spinel and phlogopite. Serpentine is the most common alteration product, and is found pseudomorphing many grains, most commonly olivine. Carbonate is a less significant alteration product found in some xenoliths, and is found pseudomorphing olivine and pyroxene. We distinguished olivine from pyroxene by preserved cleavage, but could not distinguish orthopyroxene from clinopyroxene.

Xenoliths of coarse garnet peridotite (0.65-8 cm^2) are composed of olivine (21-87 vol%), pyroxene (7-56 vol%), garnet (4-48%) and spinel (0.4-1.3 vol%), based on point counting 1500 to 6000 points per sample, depending upon sample size. The modal data revealed an interesting correlation between sample size and the amount of garnet, pyroxene and olivine in the sample. The larger the sample size, or grid area, the higher the modal abundance of olivine, and the lower the modal abundance of garnet and pyroxene (Figure 1). This observation has been noted by Cox et al. [2] to be a spatial relationship between garnet, olivine, orthopyroxene and clinopyroxene. Garnet and pyroxene are more closely associated spatially in an olivine-rich matrix. There is a definite bias in sampling for garnet and/or pyroxene-rich xenoliths, possibly due to judgement of the xenolith suite when sampling, or possibly due to the rhealogy of the xenoliths themselves during kimberlite emplacement. Extrapolation to the minimum scale recommended by Cox et al [2] also would suggest a mantle mineralogy with ~70-90% olivine beneath Drybones Bay. This olivine content is higher than that recognized for mantle lithosphere in the central Slave Province by Mackenzie and Canil [3], but their samples were relatively small (< 3 cm^2) and may have suffered a similar spatial association of pyroxene and garnet, which obscures the true mineralogy of the lithosphere.

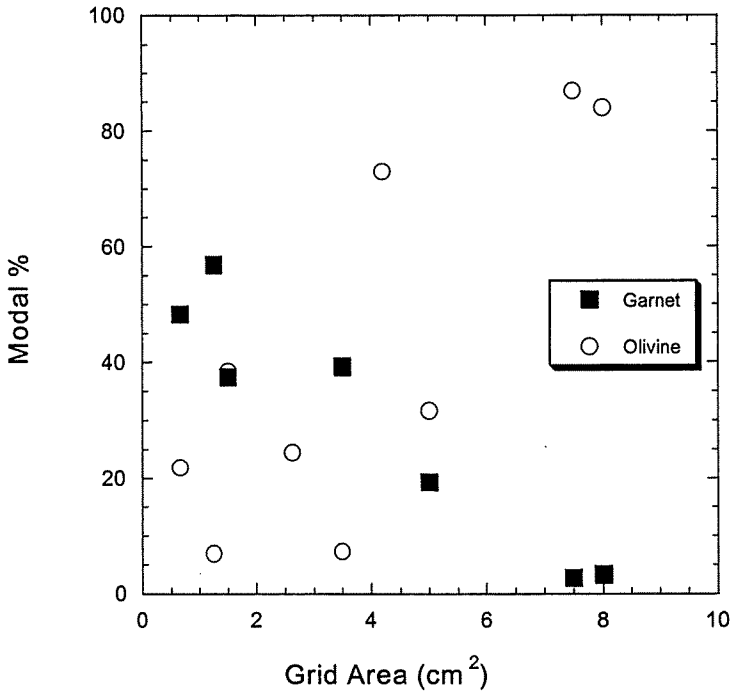

Figure 1. *Plot of modal percent olivine and garnet against grid area for Drybones Bay xenoliths.*

Garnets were chosen as the focus for the study because they show little sign of alteration in these samples, with some grains possessing kelyphite rims. Major element chemistry (CaO and Cr_2O_3) of the garnets in both xenoliths and concentrate indicate that they originate predominantly from lherzolite and wehrlite, with minor harzburgite also present. Because garnets from the drill core are the only reliable source of information, pressure and temperature estimates using conventional geothermobarometers for peridotites is not possible. Instead the Ni in garnet geothermometer after Canil [4] is used to estimate temperatures. Pressures are then calculated from an assumed geotherm. Two different geotherms with the same lithospheric heat generation were used with the Ni temperatures – a typical Archean cratonic value of 41 mWm^{-2} [5], and a measured value at Yellowknife of 53 mWm^{-2} [6]. The 41 mWm^{-2} geotherm yields the most reasonable lithospheric conditions, with a minimum lithospheric thickness of approximately 160-km (Figure 2). The 53 mWm^{-2} geotherm gives unreasonable results because it would predict that almost all of the samples came from the spinel stability field.

Concentrations of 24 trace elements in garnet were obtained by laser ablation microprobe (LAM-ICP-MS) at University of Victoria. The Rare Earth Element (REE) patterns observed in the garnets varies from a normal HREE enriched pattern typical of simple melting residues, to a sinusoidal pattern (Figure 3) indicative of disequilibrium and/or metasomatic effects. Clinopyroxene trace element abundances were calculated using distribution coefficients ($D^{GRT/CPX}$) for each trace element [7]. The sinusoidal pattern seen in the garnets, more specifically depletion in MREE and HREE, and

enrichment in LREE, signifies a mantle metasomatic process [8]. This metasomatic process is possibly carbonatite metasomatism when considering the REE patterns, along with the high Ca 'wehrlitic' nature of a large proportion of the garnets studied. The calculated clinopyroxene REE patterns also suggest a mantle process that follows a trend similar to garnet, with depletion in the HREE and MREE, along with enrichment in the LREE.

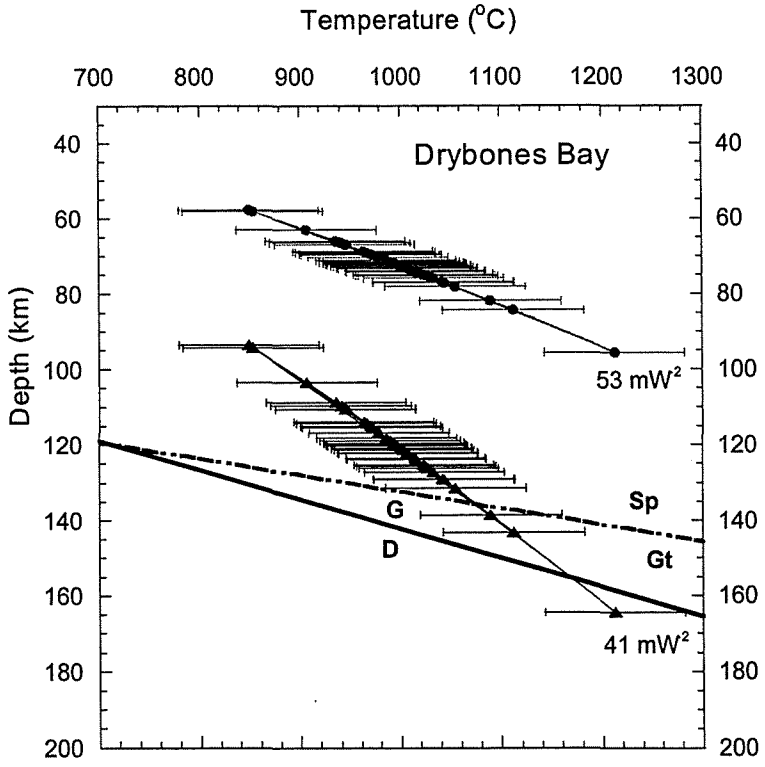

Figure 2. *Temperature versus depth plot based on Ni in Garnet temperatures (Canil, [4] and possible geotherms of 53 mWm^{-2} [5] and 41 mWm^{-2} [6]. Also shown is the diamond-graphite transition (Kennedy and Kennedy, [9]) and the spinel-garnet lherzolite transition for Cr-rich peridotite (Kopylova et al [10]).*

The location of the Drybones Bay kimberlite pipe is critical to understanding the nature of the on/off craton transition for the mantle lithosphere beneath the Southwest Slave Craton. Drybones Bay is at the edge of the craton as reflected in the surface geology, yet shows a minimum lithospheric depth within the stability field of diamond. Mantle lithosphere at Yellowknife and along SNORCLE Corridor 1 has been estimated by seismological [11] and magnetotelluric [12] methods at approximately 200 km. At Drybones Bay, only 50 km southeast, lithospheric thickness is ~160 km, implying that the base of the lithosphere may a have a ~40 degree dip from Drybones Bay to Yellowknife. The on/off craton transition could thus be quite steep, rather than forming a gradually tapered keel, or the craton could have suffered a tectonic process that somehow

deformed this edge of the craton. The Great Slave Lake Shear Zone could have played a major role in shaping the edge of the craton since its formation and stabilization.

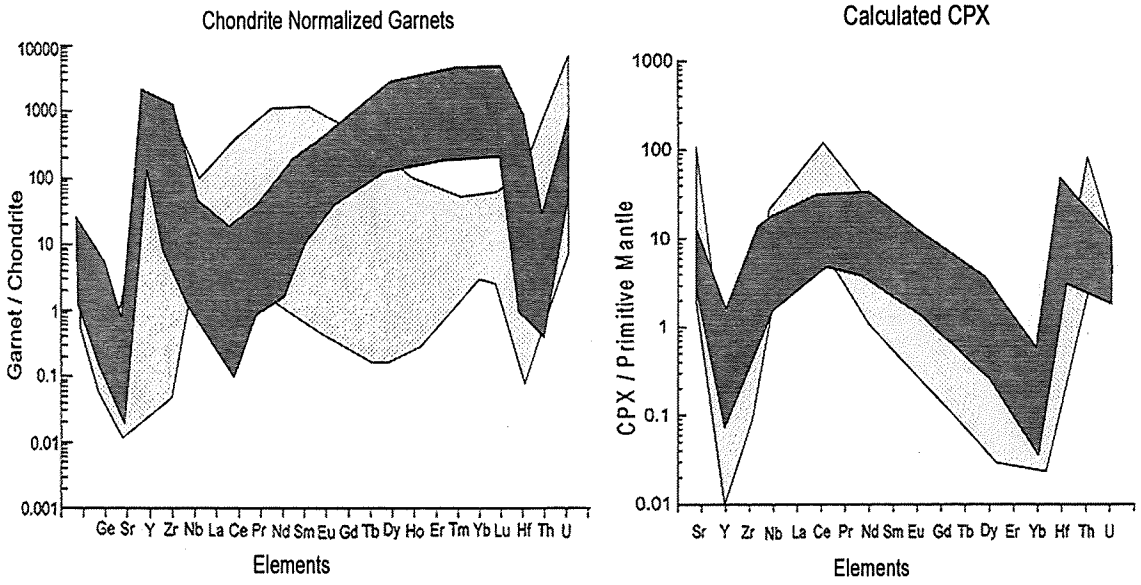

Figure 3. *REE patterns for garnet (chondrite normalized) and calculated clinopyroxene (primitive mantle normalized). The dark shaded patterns represent HREE enriched garnets, whereas the light patterns indicate some kind of mantle metasomatic process.*

References:

[1] Kretschmar, U., 1997, 1997 PDAC Exploration Summary, 9p.

[2] Cox, K.G., Smith, M.R., Beswetherick, S., 1987, In P.H. Nixon (Ed.), Mantle Xenoliths, Wiley, New York: pp. 537-550.

[3] MacKenzie J.M., Canil, D., 1999, Contrib Mineral Petrol (in press).

[4] Canil, D., 1994, Contrib Mineral Petrol 117: 410-420.

[5] Thompson, P.H., Judge, A.S., Charbonneau, B.W., Carson, J.M., Thomas, M.D., 1996, Geol Surv Can Current Research 1996-E: 135-146.

[6] Lewis, T.J., Wang, K., 1992, Palaeogeography, Palaeoclimatology, Palaeoecology 98: 87-100.

[7] Zack, T., Foley, F.F., Jenner, G.A., 1997, N Jb Miner Abh 172: 23-41.

[8] Stachel, T., Viljoen, K.S., Brey, G., Harris, J.W., 1998, Earth Planet Sci Lett 159: 1-12.

[9] Kennedy, S.C., Kennedy, G.C., 1976, J Geophysical Res 81: 2467-2470.

[10] Kopylova, M.G., Russell, J.K., Cookenboo, H., 1999, Journal of Petrology 40.

[11] Bostock, M.G., 1997, Nature 390: 392-395.

[12] Jones, A.G., Ferguson, I.J., 1997, LITHOPROBE Report No. 56: 42-47.

U-Pb Zircon, Sm-Nd and Geochemical Study of Eclogite Xenoliths, Jericho Kimberlite Pipe: The Case for Extensive Proterozoic Metasomatism Beneath the Slave Craton

Heaman, Larry M.[1], Creaser, Robert A.[1] and Cookenboo, Harrison O.[2]

[1]Dept. of Earth and Atmospheric Sciences, University of Alberta, Edmonton, Alberta, Canada T6G 2E3
[2]Canamera Geological Ltd., North Vancouver, British Columbia, Canada V7J 1G4

Eclogite xenoliths are abundant in the Jericho kimberlite of the Slave craton in northern Canada (e.g. Kopylova et al., 1998; Cookenboo et al., 1998) including a small proportion (2 to 3% out of a collection of 206 eclogites) that contain zircon. Although zircon-bearing eclogite xenoliths have been reported from a few orthogneiss localities, where both the timing of protolith formation and high pressure metamorphism are recorded in the U-Pb zircon systematics (e.g. Peucat et al., 1982; Paquette et al., 1985; 1995), zircon-bearing eclogites entrained in kimberlites are extremely rare (e.g. Chen et al., 1994). In this report, we will present an update on our isotopic studies of eclogite xenoliths entrained in the Jericho kimberlite including the following; 1) the U-Pb systematics of five zircon-bearing eclogites; 2) major and trace element whole rock geochemistry; and 3) Sm-Nd results on both whole rock and mineral separates.

GEOLOGICAL SETTING

The Jericho kimberlite (JD-1) is a diamondiferous pipe that intrudes ca. 2.6 Ga and older Archean granitoid rocks of the central Slave craton, approximately 150 km north of the main cluster of pipes located near the Lac de Gras, and 400 km northwest of Yellowknife, Northwest Territories. Four other kimberlites including the JD-3 pipe, 7 km southwest of Jericho, have been discovered in the area and, at present, all are interpreted to belong to a single kimberlite field spatially separated from pipes near Lac de Gras (Cookenboo et al., 1998). In addition to mantle xenoliths, the pipes in the Jericho kimberlite field entrained a distinctive population of crustal xenoliths which provide some geologic constraint to the emplacement age independent of radiometric dates. Most importantly, Middle Devonian (late Eifelian and early Givetian age) limestones that were deposited between approximately 375 to 385 Ma (Cookenboo et al., in press) provide a maximum geologic age for the pipe. More tenuously, the lack of wood fragments and Upper Cretaceous to Lower Tertiary mudstones at Jericho, which are common in the pipes near Lac de Gras (Nassichuk and McIntyre, 1996), implies a minimum emplacement age of pre-Late Cretaceous (roughly 100 Ma).

GEOCHEMICAL AND ISOTOPIC RESULTS

a) Rb-Sr emplacement age from phlogopite

We have obtained a total of eight Rb-Sr phlogopite analyses from various material, including five analyses from three macrocrysts hand-picked from kimberlite (four from JD-1 and one from JD-3); two analyses from different eclogite xenoliths (both from JD-1) and a single analysis from a peridotite xenolith from JD-3. The selected phlogopite macrocrysts were fresh crystals generally devoid of visible inclusions or alteration. The majority of fractions were given a dilute (0.75N) warm HCl leach prior to dissolution following the rationale of Brown et al. (1989). Phlogopite macrocrysts from kimberlite and the peridotite xenolith typically have high $^{87}Rb/^{86}Sr$ ratios (>180) with correspondingly high Rb

concentrations (up to 885 ppm), whereas phlogopite analyses from the two eclogite xenoliths have much lower $^{87}Rb/^{86}Sr$ ratios (<50), primarily a consequence of much higher Sr contents (18-24 ppm). Most of the Rb-Sr analyses are collinear with the exception of the peridotite and one eclogite (MX1) xenolith which plot below a reference isochron. Excluding the xenolith phlogopite analyses, the kimberlite phlogopite macrocrysts define an isochron age of 171.9±2.6 Ma (2σ) with an initial strontium ratio of 0.7086±0.0098 (MSWD=0.84). Considering the excellent fit of these kimberlitic phlogopite analyses to a single isochron, the 172 Ma age is interpreted to represent the best estimate for the time of kimberlite emplacement at Jericho. In fact, treating the JD-1 and JD-3 data independently indicates that the emplacement ages for both samples are indistinguishable within about 1 m.y. Interestingly, including the phlogopite analysis from one of the eclogite xenoliths (MX14) results in a very precise age of 173±1 Ma age with an initial strontium ratio of 0.7039±0.015 (MSWD=0.87) however these results could be misleading as there is evidence that the xenolith and kimberlite phlogopites do not have identical initial strontium ratios. If the 172±3 Ma Rb-Sr kimberlitic phlogopite age result obtained here is an accurate estimate of timing of Jericho kimberlite magmatism, then the Jericho pipes represent the first documented examples of mid-Jurassic kimberlite magmatism in the Slave Province.

U-Pb systematics of zircon from eclogite

The U-Pb results for single zircon crystals extracted from five eclogite xenoliths are in progress. The eclogitic zircon grains investigated so far generally have lower uranium abundances (10-70 ppm) compared to zircon from eclogite xenoliths within orthogneiss (100-300 ppm; e.g. Peucat et al., 1982). In detail, there are two distinct geochemical patterns preserved in the Jericho eclogitic zircon which are best seen on a plot of Th/U versus uranium content. The first pattern displays a strong inverse correlation between uranium content and Th/U ratio and occurs in moderate uranium level (>45 ppm) zircon grains analysed from xenoliths MX1 and MX10. In contrast, low-uranium (9-33 ppm) zircon crystals from two other eclogite xenoliths (MX8 and MX12) generally have very uniform Th/U ratios.

The U-Pb zircon results, for the most part, are unusual and do not define simple discordia or mixing lines. All the analyses are highly discordant (39-69%) and there is a large range in model $^{207}Pb/^{206}Pb$ ages for zircon suites from individual xenoliths. The most extreme range in $^{207}Pb/^{206}Pb$ ages was obtained for xenolith MX10 (403-1561 Ma). Of the five eclogite xenoliths analysed, only the zircon analyses from MX10 closely approach a linear relationship where three of four analyses define a regression line with an upper intercept age of 1679±10 Ma and a lower intercept age of 178±5 Ma (37% probability of fit), within error of the kimberlite emplacement age of 172±3 Ma established from Rb-Sr kimberlitic phlogopite analyses.

Sm-Nd whole rock, garnet and clinopyroxene results

The Sm-Nd isotopic composition of the eclogite xenoliths is currently under investigation to provide an independent estimate for the timing of eclogite metamorphism and/or metasomatism. A garnet-clinopyroxene internal Sm-Nd isochron from one eclogite xenolith indicates an age of 216 Ma with an epsilon Nd value of -5.5. At present, it is unclear whether this age has geological significance or represents partial equilibration of the Sm-Nd system in the xenoliths at the time of entrainment as has been documented previously by Richardson et al. (1985) for Bultfontein garnet lherzolite xenoliths. The model Nd ages for five eclogite xenoliths range from 1.0-1.3 Ga, however there is some uncertainty as to the geological significance of these ages as recent geochemical results indicate that a significant

metasomatic event has caused substantial enrichment in the LREE and other high field strength elements in these xenoliths prior to entrainment in the kimberlite.

DISCUSSION

The Rb-Sr results for phlogopite macrocrysts from kimberlite define an age of 172±3 Ma which is interpreted as the best estimate for the emplacement age of both the JD-1 and JD-3 pipes. These results also document for the first time the presence of Middle Jurassic kimberlite magmatism in the Slave Province which is distinct from Jurassic kimberlite magmatism elsewhere in North America (e.g. 155-160 Ma Kirkland Lake/Timiskaming field, Heaman and Kjarsgaard, in prep.).

The U-Pb systematics of zircon isolated from eclogite xenoliths entrained in JD-1 indicate an unusual behaviour. Three of the five xenoliths investigated in detail do not display a linear relationship and record either a complicated multi-stage Pb-loss history or represent paleo-diffusion curves such as those described by Peucat et al. (1982). In the latter case, combining the U-Pb zircon results obtained here with geothermometry data for the eclogite xenoliths could provide a natural example and indirect estimate for the closure temperature for Pb diffusion in zircon. The lower intercept age of 178±5 Ma for the mixing line obtained for zircon from xenolith MX10 is within error of the 172±3 Ma emplacement age obtained using Rb-Sr phlogopite macrocrysts and provides independent confirmation of the Middle Jurassic emplacement age. The U-Pb zircon data also indicate that a significant amount of Pb-loss in the zircon crystals occurred at the time of kimberlite emplacement. The upper intercept age of 1679 Ma for xenolith MX10 is intriguing and could be interpreted in at least two ways: 1) the protolith age for the eclogite precursor (as in the case for eclogitic pods in orthogneiss); or 2) a minimum estimate for the time of zircon growth during eclogite metamorphism. The large size of the zircon crystals (up to 3 mm), their low uranium content (<70 ppm) and low Th/U ratio (<0.2) are not typical of primary magmatic zircon crystallizing in mafic magmas (e.g. Bossart et al., 1986), thus we discount the first explanation, and favour the second alternative; that is, the 1679 Ma age reflects a minimum estimate for the timing of eclogite metamorphism. The origin of Paleoproterozoic eclogites beneath the Slave craton remains enigmatic, but could derive from east-dipping oceanic crust subducted during Great Bear Magmatic Arc time (1.88-1.84 Ga).

REFERENCES

Chen, Y.D., O'Reilly, S.Y., Kinny, P.D., and Griffin, W.L., 1994. Dating lower crust and upper mantle events: an ion microprobe study of xenoliths from kimberlitic pipes, South Australia: Lithos , 32, p. 77-94.

Cookenboo, H. O., Dupuis, J., and Foulkes J., 1998. Discovery and evaluation of the Jericho and 5034 kimberlite fields in the Slave Craton, northern Canada: Pathways'98. Extended Abstract Volume, p. 166-169.

Cookenboo, H. O., Kopylova, M. G., and Daoud, D.K. (1998). A chemically and texturally distinct layer of diamondiferous eclogite beneath the central Slave craton, northern Canada. 7th International Kimberlite Conference, Capetown. p.

Bossart, P.J., Meier, M., Oberli, F., and Steiger, R.H., 1986. Morphology versus U-Pb systematics in zircon: a high-resolution isotopic study of zircon population from a Variscan dike in Central Alps: Earth and Planetary Science Letters, 78, p. 339-354.

Brown, R.W., Allsopp, H.L., Bristow, J.W., & Smith, C.B., 1989. Improved precision of Rb-Sr dating of kimberlitic micas: an assessment of a leaching technique: Chemical Geology, 79, p. 125-136.

Heaman, L.M., Kjarsgaard, B.A., Creaser, R.A., Cookenboo, H.O., and Kretschmar, U., 1997. Multiple episodes of kimberlite magmatism in the Slave Province, North America: *Lithoprobe Workshop Report No.* 56, p. 14-17.

Heaman, L.M. and Kjarsgaard, B., (in prep.) Timing of Eastern North American Kimberlite Magmatism: Evidence for a Mesozoic Mantle Plume Track.

Kopylova M. G., Russell, J. K., and Cookenboo, H. O., (1998). Mantle xenoliths of the Jericho kimberlite: Implications for upper mantle stratigraphy and the thermal regime of the Slave Craton, Canada. 7th International Kimberlite Conference, Capetown. p.

Nassichuk, W.W., & McIntyre, D.J., 1995. Cretaceous and Tertiary fossils discovered in kimberlites at Lac de Gras in the Slave province, Northwest Territories: Geological Survey of Canada Current Research 1995-B, p. 109-114.

Paquette, J.L., Peucat, J.J., Bernard-Griffiths, J., and Marchand, J., 1985. Evidence for old Precambrian relics shown by U-Pb zircon dating of eclogites and associated rocks in the Hercynian belt of South Brittany, France: Chemical Geology, 52, p. 203-216.

Paquette, J.L., Monchoux, P., and Couturier, M., 1995. Geochemical and isotopic study of a norite-eclogite transition in the European Variscan belt: Implications for U-Pb zircon systematics in metabasic rocks: Geochimica et Cosmochimica Acta, 59, p. 1611-1622.

Peucat, J.J., Vidal, Ph., Godard, G., and Postaire, B., 1982. Precambrian U-Pb zircon ages in eclogites and garnet pyroxenites from South Brittany (France): an old oceanic crust in the West European Hercynian belt? Earth and Planetary Science Letters, 60, p. 70-78.

Richardson, S.H., Erlank, A.J. and Hart, S.R., 1985. Kimberlite-borne garnet peridotite xenoliths from old enriched subcontinental lithosphere: Earth and Planetary Science Letters, 75, p. 116-128.

Electromagnetic studies of the Slave craton: preliminary results and ongoing experiments

Alan G. Jones[1], Ian Ferguson[2], Gary McNeice[3], Rob Evans[4] and Alan Chave[4]

1: Geological Survey of Canada, 615 Booth St., Ottawa, Ontario, K1A 0E9, Canada

2: Department of Geological Sciences, University of Manitoba, Winnipeg, Manitoba, R3T 2N2, Canada

3: Phoenix Geophysics Ltd., 3781 Victoria Park Ave., Unit #3, Scarborough, Ontario, M1W 3K5, Canada

4: Woods Hole Oceanographic Institution, 360 Woods Hole Woods Hole

Introduction

LITHOPROBE's SNORCLE (Slave-NORthern Cordilleran Lithospheric Evolution) transect comprises three corridors beginning east of Yellowknife on the Slave craton, host to the oldest dated rocks in the world today (Bleeker et al. 1999), and traversing west to some of the youngest rocks in Canada on British Columbia's west coast. The ACCRETE program (Hollister and Andronicos 1997) extends this transect offshore to cross the active Queen Charlotte transform fault. Thus, the SNORCLE-ACCRETE studies capture all Earth's geological history along their combined length, and almost all tectonic settings, either in modern or ancient forms. The Archaean and Proterozoic components of the SNORCLE transect are crossed by profiles 1 and 1A of Corridor 1, and are shown in Fig. 1 on the terrane map of the region (Slave terranes based on Kusky 1990).

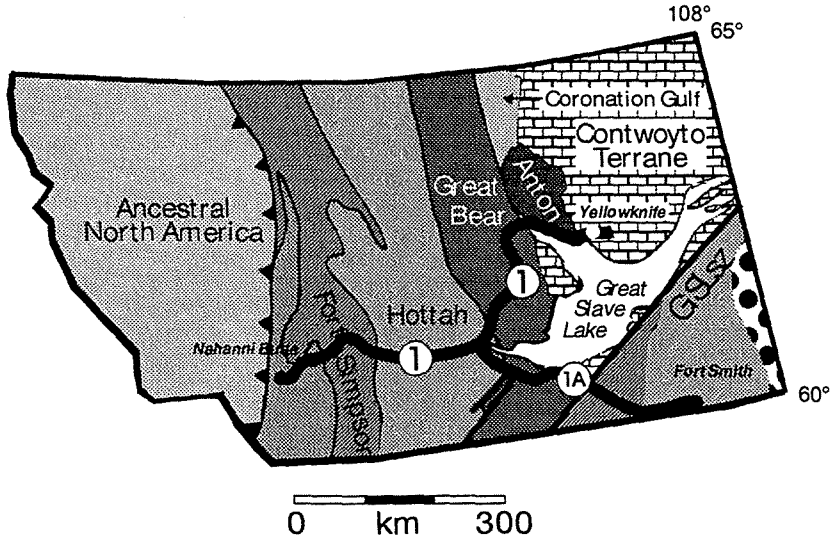

Critical to understanding the history, nature and relationships of the exposed or shallow subsurface crustal elements crossed by Corridor 1 is knowledge and understanding of lithospheric-scale processes, from lithospheric formation and deformation to destruction. Of particular interest within the Slave craton segment of SNORCLE transect activities is the debate concerning lithospheric formation and alleged differences between tectonic processes active during Archaean times compared to those during later Proterozoic and Phanerozoic times. Lithospheric growth models of Jordan (1988) and Ashwal and Burke (1989) advance modern-day processes as explanations of tectonic events that occurred during the entire history of the Earth. Conversely, Helmstaedt and Schulze (1989), with modifications by Kusky (1993), suggest more buoyant subduction occurred during Archaean times, leading to continental roots being formed by imbrication of shallowly-subducted lithospheric slabs. Alternative models are proposed by Thompson et al. (1995) and Polet and Anderson (1995) who appeal to non-tectonic processes, basal accretion of cooling mobile asthenospheric material and cold downwelling of lithosphere into the asthenosphere respectively, to explain lithospheric growth. Hoffman (1990) discussed aspects and implications of some of these models for the root of the Canadian Shield part of the North American craton, and concluded that the existing data are not adequate for discriminating between the various models.

High-quality, deep-probing electromagnetic (EM) studies are capable of addressing several questions regarding models of lithospheric formation, and thereby contributing to this debate. In particular, the natural-source magnetotelluric (MT) method is well-suited for probing the upper mantle, compared to controlled-source EM methods. This is due to its simpler logistics, sophisticated data analysis procedures, tensor information, and more tractable mathematics for forward modelling leading to effective two-dimensional (2D), and recently three-dimensional (3D), inversion codes. Jones (1999) demonstrates the contributions that MT studies have made and can make in imaging physical properties and geometrical relationships of the continental lithosphere, and lists the following hypotheses and tests:

Hypothesis 1: The cratonic lithosphere is Archaean in age and has been strongly coupled to its crust since that time.

Test 1: Electrical anisotropy, if present, must extend smoothly through the cratonic root and be approximately aligned with surface structures. A more exacting test would require that the obliquity between the seismic and EM anisotropy directions must define the same sense of movement as surface structures (Ji et al. 1996, hypothesis).

Hypothesis 2: The cratonic lithosphere is comprised of imbricate stacks formed in the Archaean (Helmstaedt and Schulze, 1989, model, with Kusky, 1993, modification).

Test 2: There will be a regional variation in electrical anisotropy direction and possibly in electrical parameters like conductivity or root thickness.

Hypothesis 3: The lithosphere has been added to the craton since the end of the Archaean by basal accretion (Thompson et al., 1996, model).

Test 3: There will be no anisotropy and no regional variation in electrical parameters. If either consistent anisotropy or regional variation is observed, then the hypothesis can be rejected.

Hypothesis 4: The old mantle root is of limited spatial extent and its apparent seismically-determined size is caused by transient cold downwelling (Polet and Anderson, 1995, model).

Test 4: There will be no consistent anisotropy direction, no deep anisotropy, and probably a weak electrical signature over most of the craton. The presence of deep anisotropy and an extensive low conductivity root is cause to reject this hypothesis.

One geometrical parameter that is well resolved by appropriate high quality MT studies is the thickness of the thermal lithosphere, the depth to the thermal lithosphere-asthenosphere boundary generally assumed to be around 1300 ^{o}C. This is due to the high sensitivity of electrical conductivity to the onset of ionic conductivity in an interconnected partial melt phase. Laboratory studies on H_2O ice - KCl aqueous solution, as an analogue for partially molten Earth materials, demonstrate that electrical conductivity rises very rapidly by many (>2) orders of magnitude at the onset of interconnected partial melt (Watanabe and Kurita 1993). Laboratory studies on mantle materials have generally concentrated on olivine, particularly peridotite.

Deep-probing EM studies of the Slave craton are occurring at a time when there is much interest in obtaining knowledge about the deep lithosphere to aid exploration activities for Canada's fledgling diamond-industry (Jones et al. 1996). Current models for diamondiferous kimberlite emplacement require a thick (>150 km), cold lithosphere, whereas thinner lithosphere will result in barren kimberlites (Mitchell 1991). Given the presently-known distribution of diamondiferous kimberlites across the Slave, imaging the geometry of the base of the lithosphere, and its spatial variation, may lead to further understanding of mantle processes, such as focusing of upwelling material.

This paper summarises the EM experiments that have been, and are being, conducted on the Slave craton and adjacent Proterozoic terranes to the west. Four different types of experiments have been, or are, underway, and the site locations on the Slave are shown on Fig. 2, together with the locations of the teleseismic sites of Bostock and Cassidy (1997). The EM studies began in 1996, and will continue until the year 2000, and perhaps beyond if problems and interest remain.

Objectives of the SNORCLE EM program on the Slave craton

The general objective of the SNORCLE program are given in the LITHOPROBE Phase V proposal (Clowes 1997). Many of these objectives are pertinent to the Slave craton and adjacent Proterozoic terranes, and can be directly addressed using electromagnetic methods. We have classified these objectives into three groups, which are discussed below.

Characterising the deep crust and mantle between the oldest rocks to the younger Proterozoic terranes

This component will permit addressing the following stated transect objectives:

- What kind of deep crust and mantle underlie the oldest rocks on Earth?
- Is the tectonic style of Early Archaean protocontiental nuclei unique?

- Are deep structural and stratigraphic characteristics of Proterozoic orogens fundamentally different from those of Phanerozoic orogens and, if so, why?

- How have deep Precambrian structures been significant in controlling the stratigraphic and structural evolution of Phanerozoic orogens?

- What is the nature of the Anton terrane (Kusky 1990)?

This is being accomplished by the acquisition of contracted wide-band MT sites together with long period MT sites installed at the same locations, and using the same electrode array. The wide-band data measure frequencies in the range 0.01 – 1,000 Hz (or periods of 0.001 – 100 s), and give information primarily about the crust. The long period data measure periods in the range 10 – 10,000 s, and can give information about the mantle to depths in excess of 200 km. The MT site locations are nominally equi-spaced, with a station spacing of around 15 km, but the surveys are run in "dynamic" mode with in-field processing and modelling permitting identification of critical repeat and infill site locations.

In addition, in order to address the Slave mantle root geometry characterisation, two other experiments are underway and are discussed in detail below. The first involves making measurements along the 600-km-long winter road to the north-east of Yellowknife, and is in partnership with industry. The second is a joint U.S.-Canadian project that entails installing shallow-water ocean-bottom MT equipment in lakes across the Slave craton. Both of these are the first of their kind.

Characterising the geometry of the major vertical structures

Knowing the current geometry of vertical structures permits one to address such transect objectives as:

- What is the geometry of a probable Paleoproterozoic transform fault: the Great Slave Lakes shear zone?

EM studies have shown their superior effectiveness in determining the geometry of vertical structures to whole crustal depths over other geophysical methods (e.g., Fraser Fault, Jones et al. 1992; San Andreas fault, Unsworth et al., 1977). Following regional-scale data acquisition, closely-spaced (1 km) MT stations in the vicinity of each of the three major vertical structures, the Great Slave Lake Shear Zone, the Tintina-Rocky Mountain Trench Fault and the Denali Fault, are planned. Spatially-continuous electric field recording across the faults, using continuous electric-field dipoles, would yield the best image possible, and an excellent example is shown by the work across the San Andreas fault (Unsworth et al., 1977), but such surveys are not currently planned.

Auxiliary objectives

In addition to the stated SNORCLE objectives, there are additional objectives that can be addressed by EM studies on the Slave craton and adjacent terranes, and an objective related to processing of MT data from magnetically high latitudes:

- Does the Slave craton display similar strong mantle electrical anisotropy as are exhibited by the Abitibi region of the Superior (Mareschal et al. 1995)?

- Does the mantle beneath the Slave craton to depths of >1,000 km display the same electrical conductivity to that beneath the Superior craton (Schultz et al. 1993)? In particular, is there a discrete jump in conductivity at a depth of 410 km as predicted by laboratory studies (Xu et al. 1998)?

- Is there a difference between the mantle lithospheres on either side of the Pb and Nd isotope boundaries (Thorpe et al. 1992; Davis et al. 1996)?

- Is the lithosphere in the northern part different from the south as a result of modification caused by the emplacement of the plume that generated the MacKenzie dyke swarm (ca. 1267 +/- 2 Ma, LeCheminant and Heaman 1989)?

- Within the younger terranes in B.C., are there still fluids resident in the crust from the oblique subduction of the Kula plate which was cut off by the plate reorganisation at 55 Ma?

- Are current MT time series robust processing codes sufficient to remove the effects of highly non-uniform source fields?

The enigmatic long-period electrical anisotropy results of the Superior craton presented by Mareschal et al. (1995) require formation or deformation processes that result in mantle lithospheres with preferentially-aligned conducting fabrics. This observation parallels the seismically-observed time delays between arriving shear waves in orthogonal directions and interpreted as mantle anisotropy (Silver and Chan 1988, 1991). The small, but statistically-meaningful, obliquity between the direction of maximum conductivity and the shear-wave splitting fast directions (Senechal et al. 1996) were interpreted by Ji et al. (1997) as evidence for strong crustal-mantle coupling since lithospheric formation and as a potential indicator of the movement sense for ductile mantle shear zones. This thesis needs to be tested by making collocated MT and teleseismic observations at other locations and on other Archaean cratons.

Padgham and Fyson (1992) presented geological arguments that the Slave craton is geologically distinct compared to other Archaean cratons. How the electrical properties of the Slave cratonic mantle compare to others, particularly the Superior craton, addresses the question of the uniqueness of the Slave craton geophysically.

A very long period, high-quality, deep-probing experiment on the Superior craton demonstrated that the electrical conductivity of the mantle has discrete jumps at approximately 410 km and 660 km (Schultz et al. 1993). The former is consistent with recent laboratory work that shows a two orders of magnitude increase in conductivity as olivine undergoes a phase transformation to higher pressure mineralogy (wadsleyite) (Xu et al. 1998). This phase transformation is a pressure-effect, and accordingly should be seen at all localities. However, with the exception of the data of Schultz et al. (1993), the existing database of mantle MT response functions is insufficiently precise to be able to verify this laboratory inference. A step-like increase in conductivity is consistent with the EM responses observed in western United States of America, but not required by them (Egbert and Booker 1992). High quality very long period MT response functions need to be obtained for the Slave craton to compare with the results from the Superior craton, and with other cratons worldwide.

Finally, there is a lot of interest in making deep-probing MT measurements at high geomagnetic latitudes, both in Canada and elsewhere, to determine information about the lithosphere. The non-uniform field of the aurora borealis can have a severe effect on MT response function estimation, and an example is shown in Garcia et al. (1997). An experiment has

been performed to acquire almost a year of data under the auroral zone for analysis and development of appropriate processing methods (see below).

Electromagnetic experiments to date

Snorcle Corridor 1 acquisition

The first phase of acquisition of EM data along the SNORCLE transect began on August 1st, 1996, with a sixty (60) station contracted magnetotelluric (MT) survey along SNORCLE Corridor 1 (Figs. 1 and 2), including the Fort Providence - Wood Buffalo National Park profile (profile 1A, Fig. 1). The contractor (Phoenix Geophysics Ltd.) acquired the wide-band MT data pertinent primarily to the crust. In addition, longer period measurements were made at each location to image conductivity features in the sub-crustal lithosphere down to the conducting asthenosphere.

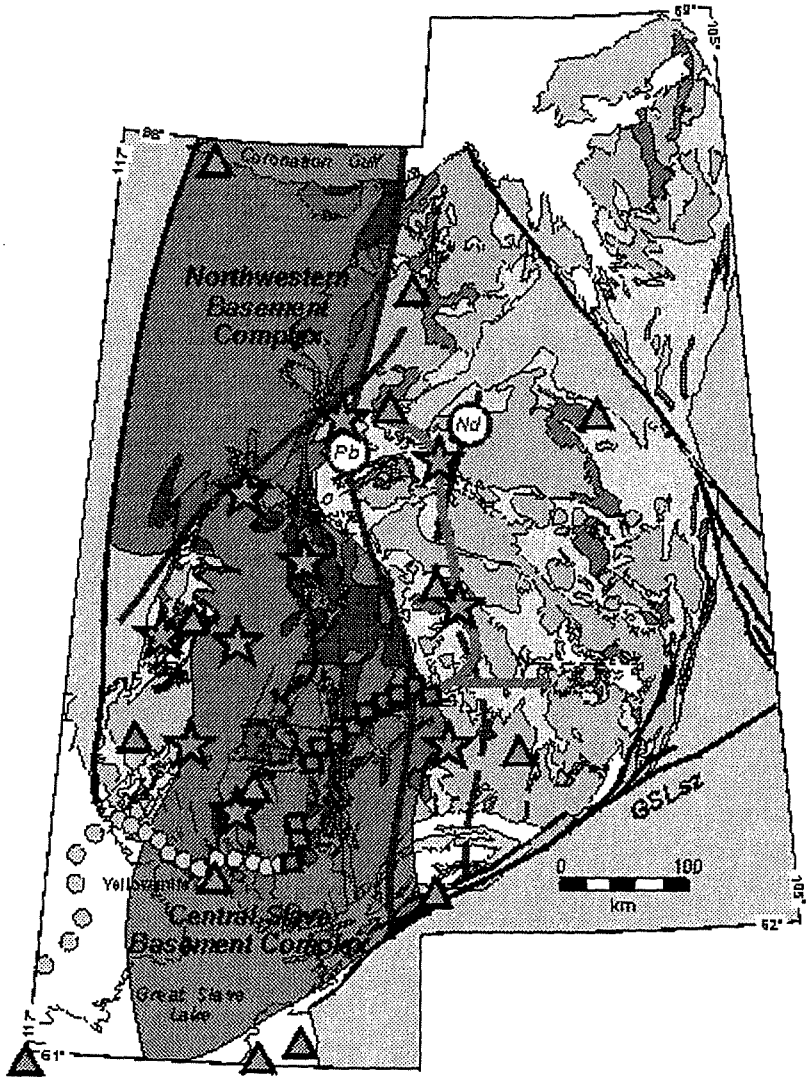

Thirteen sites were located on the exposed Slave craton, from Tibbit Lake to Rae, nine on the Great Bear magmatic arc, from Rae to Fort Providence, twenty-four on the Proterozoic section (Hottah, Fort Simpson and Nahanni terranes), from Fort Simpson to Nahanni Butte, and fifteen on the section crossing the Great Slave Lake shear zone, from Fort Simpson to within the boundaries of Wood Buffalo National Park. High frequency data (10 kHz to 0.01 Hz) were acquired by the commercial contractor with three nights of recording at all sites. There was one to four weeks recording of long period MT data (20 - 30,000 s), using fifteen GSC-built LiMS (Long period Magnetotelluric System) units, at each location by the scientist plus an assistant monitoring the contracted data acquisition.

The wide-band MT data (using Phoenix's V5 system) were processed in the field using a robust remote-reference code based on the algorithm of Jones and Jödicke (1984; method 6 in Jones et al. 1989). The LiMS data have only undergone preliminary processing, as final processing will include using data from the Yellowknife geomagnetic observatory and three sites operated as part of the Canada's Space Agency MARIA array (Contwoyto Lake, Fort Simpson and Fort Smith) as remote reference fields to remove noise effects and also reduce non-uniform source field contamination. Subsequent to data acquisition, a problem was identified trying to merge together the V5 and LiMS responses. After exhaustive and lengthy enquiry, it was discovered that there was an imprecision in the coil calibration procedures used by the contractor for extrapolating the coil response beyond the measured calibration range. The effects of this problem were such that the original V5 data at periods greater than 8 s were in error by up to 10^{o} in phase, and the equivalent value in apparent resistivity. This is far too large to be acceptable, and the V5 time series were all reprocessed using corrected calibration factors. The corrected data were delivered to the GSC/LITHOPROBE in December, 1998.

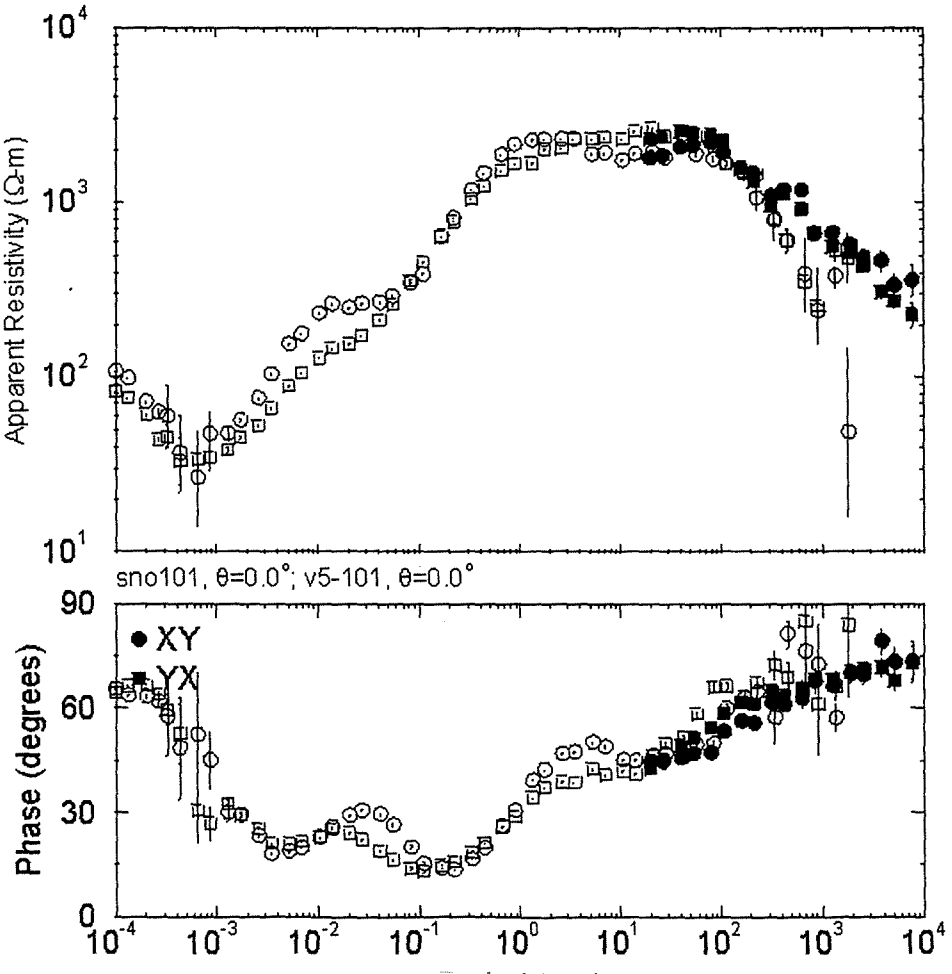

Figure 3 illustrates an example of the corrected V5 data together with the LiMS data from a site just to the west of Rae on the Great Bear magmatic arc (site 101). Even at this level of processing of the LiMS data, the overall data quality from both is excellent. Reasonable V5 data were even acquired in the high frequency "dead-band" of 1 kHz - 3 kHz, albeit with lower quality. There is a drop-off of the V5 data at the longest periods due to the inferior sensitivity at long periods of the coil magnetometer used for the V5 system compared to the ring-core fluxgate magnetometer used for the LiMS system (the opposite is true at high frequencies, >0.1 Hz). The absence of anthropogenic noise and low electric field distortion compound to give highly precise estimates of the magnetotelluric impedance tensor in all elements for almost all sites, which is rarely the case for MT data acquired on highly resistive regions (cratons, batholiths, etc.).

Winter Road acquisition

Vehicle access of the Slave craton is limited, and Echo Bay's 600-km-long winter road, from Tibbit Lake east of Yellowknife to the Lupin gold mine at Contwoyto Lake (Fig. 2), provides a logistical opportunity to extend the geophysical observations from around the south-west corner of the Slave craton to well into the interior. In particular, the winter road affords the possibility to cross the boundary between the Central Slave Basement Complex and the presumed juvenile eastern Slave (Bleeker et al. 1999), and to map electrically the lateral variation of the crust and sub-crustal lithosphere across the Slave craton. Secondary roads off the main winter road afford access to regions further to the east and west.

MT acquisition along the winter road is a relatively-affordable geophysical method for obtaining information on the regional-scale, lateral variation of the Slave lithosphere, and will contribute significantly to the objectives of the SNORCLE transect. The winter road has a total length of ca. 600 km, requiring a minimum of 40 MT sites to characterise the deep structure electrically. The results should provide an improved picture of the assembly of the Slave Province and allow evaluation of lithospheric growth models such as that of Helmstaedt and Schulze (1989) and Kusky (1989).

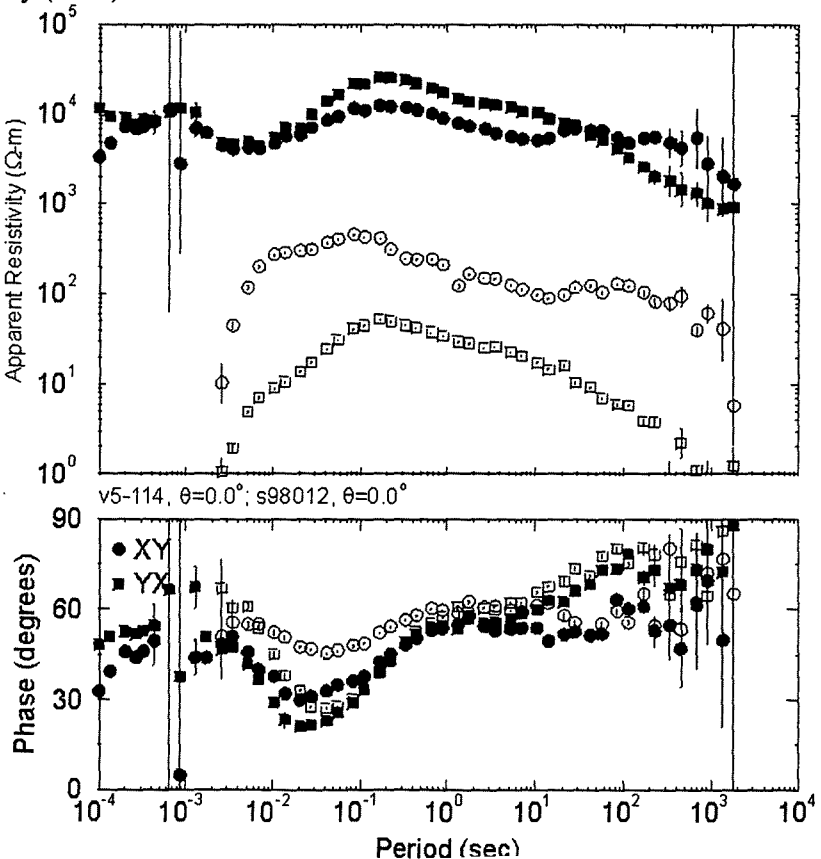

In April, 1997, a feasibility study was undertaken in northern Ontario of the logistical and scientific challenges faced by attempting to make measurements on a frozen lake surface. The tests undertaken demonstrated that it is important to make the telluric measurements with the electrodes in contact with the sediments at the lake bottom, whereas the magnetic field measurements need to be made on the lake shore due to the noise induced by ice movement (McNeice and Jones 1998). Subsequently, a pilot study along the winter road took place during March-April, 1998, of twelve sites. Three of these were at the southern terminus of the winter road close to Tibbet Lake, and the other nine were in an east-west profile from the northern end of Gordon Lake to the western end of MacKay Lake. A comparison of the data from this survey to the data from the 1996 land-based survey is shown in Fig. 4. There is a shift in the apparent resistivity curves due to local electric field distortion effects caused by the lake geometry. Such distortions are well-understood, and methods exist for identifying and removing the phase effects of these distortions (e.g., Groom et al. 1993). The amplitude effects, known as "static shifts" (Jones 1988; Sternberg et al. 1988), are more difficult to remove, but methods exist and are being developed further.

Slave Lakes experiment

Although the winter road work will give access to the interior of the Slave craton, it does run the danger of being in part along a possible mantle boundary, as inferred by the Pb and Nd isotope boundaries (Thorpe et al. 1992; Davis et al. 1996). In order to obtain broader regional coverage of the craton at as minimal a cost as possible, a novel experiment is in progress involving deploying shallow-water EM instrumentation designed to operate on the ocean bottom of the continental shelves in lakes on the craton. This type of instrumentation had only been deployed once before, as part of the SoAp (Southern Appalachians) experiment (Ogawa et al. 1996; Wannamaker et al. 1996), on the continental shelf off the coast of the Carolinas. The SoAp experiment was an onshore-offshore EM study of the Atlantic passive margin on a scale almost as large as the EMSLAB experiment of the active Pacific margin (Booker and Chave 1989; Wannamaker et al., 1989a, 1989b).

Using a float plane, the total compliment of ten instruments were deployed in lakes around the Slave craton during early July, 1998. The locations of the lake sites are shown in Fig. 2, and comprise roughly three east-west lines. The northern line comprises three lakes (Point Lake, Contwoyto Lake and Rockinghorse Lake), the central line four lakes (Indin Lake, Snare Lake, Big Lake and Lac de Gras), and the southern line also four lakes (Wheeler Lake, Duncan Lake and Lac Tet d'Ours). The systems have been set with a recording rate of one sample per second for the first two months (July and August, 1998), followed by a rate of one sample per minute for the remaining ten months. In July these instruments will be retrieved, and hopefully re-deployed in August, 1999 in another ten lakes.

Yellowknife Observatory long-term recording experiment

A single LiMS instrument was deployed close to the Yellowknife Geophysical Observatory for a year, from August 8th 1997 to August 28th 1998. Initial malfunctions were repaired, and continuous data exist from January 9th until August 28th 1998. The complete time series are shown in Fig. 5. For this installation, the analogue high-pass telluric filters, with their nominal –3 dB period set for 30,000 s, were bypassed in an attempt to obtain response function estimates to a day or longer. Such periods probe the deep mantle, and would allow for a comparison with the very long period measurements made on the Superior craton by Schultz et al. (1993).

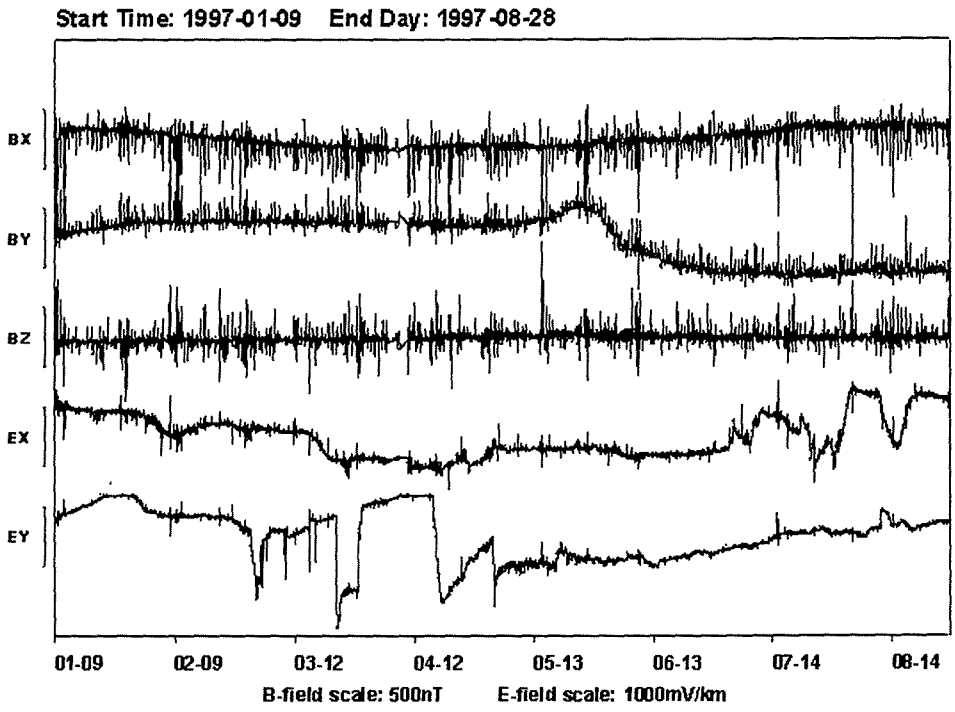

Preliminary results

The lateral variation of electrical properties of the subcrustal lithosphere can be derived from the lateral variation in the MT parameters. Figure 6 shows the apparent resistivities at a period that is sampling about 50 km into the lithosphere (30 s) for the MT sites along profile 1 (Fig. 1). The values rise from 100-300 Ω.m on the Proterozoic terranes to around 10,000 Ω.m on the Slave craton. This rise occurs mostly on the Fort Providence to Rae section of the profile across the Great Bear magmatic zone. These results imply that the lithosphere thins dramatically westward beneath the Great Bear magmatic zone. Preliminary modelling suggests that the lithosphere-asthenosphere boundary is 100+ km west of Fort providence, and around 200+ km beneath the Rae-Yellowknife section. To the east of Yellowknife the lithosphere may thin again, but only by a small amount.

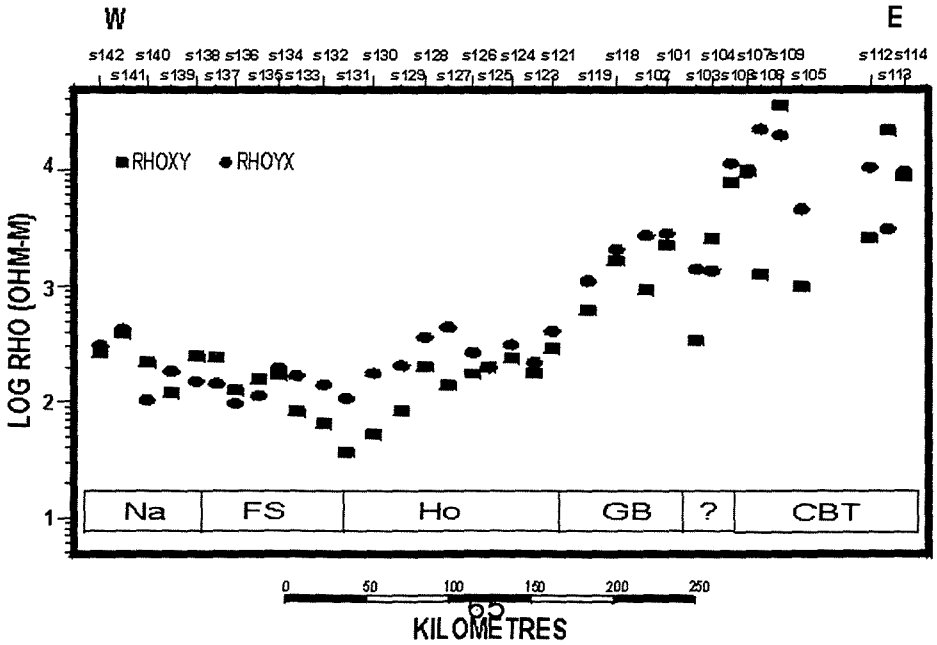

One-dimensional inversions of the averaged V5 MT data from two representative sites, one on the Proterozoic terranes (site 135, on the Fort Simpson terrane) and one on the Slave craton (site 106, on the western edge of the Central Slave Basement Complex), are shown in Fig. 7. At both sites there is high resistivity in the crust that drops at about the crust-mantle boundary. The resistivity of the mantle beneath the two regions is very different. There is a decrease to low values around 100 km beneath the Proterozoic terranes, whereas beneath the representative Slave craton site this decrease does not occur until depths of some hundreds of kilometres. Modelling this observation in the MT response as a step-like decrease would put the change at 350 km +/- 150 km. This boundary will be better resolved when the LiMS data are processed and merged with the V5 data.

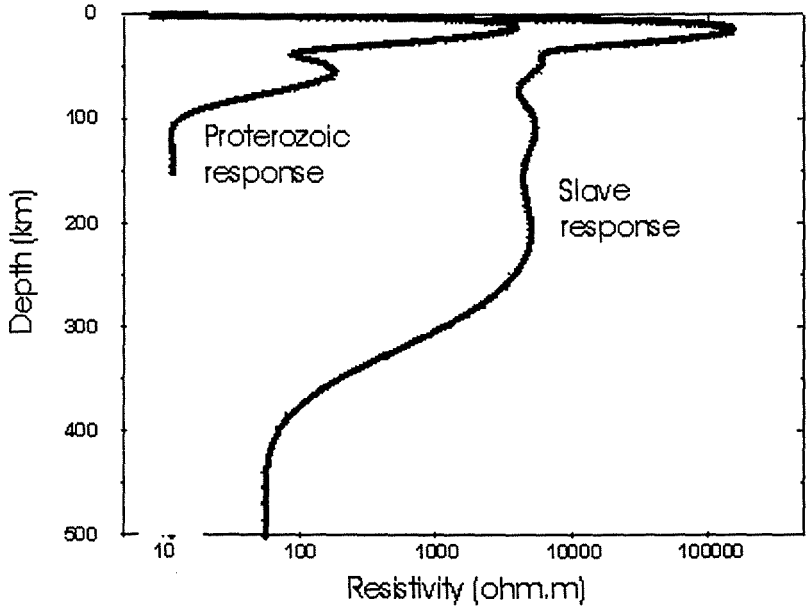

With the phase difference between orthogonal impedances of the MT tensor it is possible to determine whether there is any anisotropy in the measurements associated with structures, similar to the SKS technique in seismology. Figure 8 displays the phase differences for all stations at the same period as Fig. 6. Beneath stations from Yellowknife and further east, the lithosphere is electrically anisotropic, with the more conductive direction being around 105°,

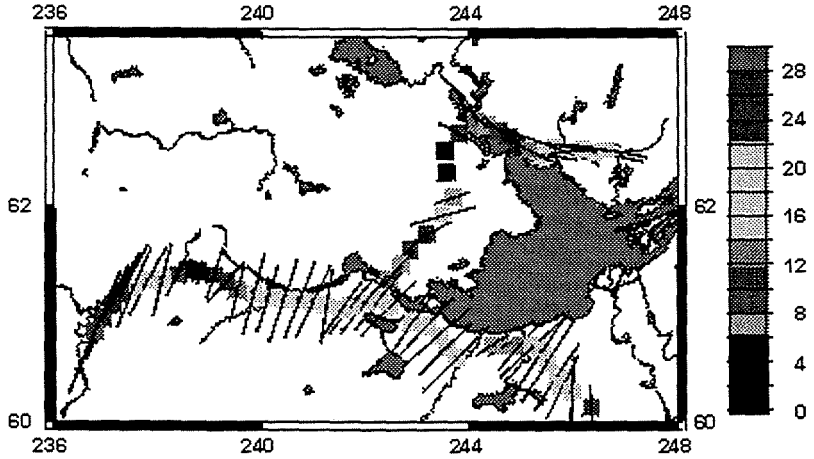

compared to the seismic SKS direction for the Yellowknife observatory of 048°. The lithosphere is laterally homogeneous between Fort Providence and Rae, but becomes anisotropic west of Fort Providence (Fig. 8). Sites around the Great Slave Lake shear zone display a strong anisotropy with a most conductive direction of 035°, i.e., oblique to the direction of the GSLsz of 045°. This anisotropy at such long periods suggests that the GSLsz penetrates deep into the mantle. The obliquity between the maximum conducting direction and the surface trace of the GSLsz is consistent with the dextral movement sense on the shear zone, following the hypothesis of Ji et al. (1996).

Further Work

The second phase of winter road acquisition will take place during Feb 22nd to early April, 1999. Phoenix Geophysics is being contracted for 30 acquisition days, and the expectation is that there will be a minimum of 25 MT soundings made during that time. The sites will be mainly along the northern section of the road from MacKay lake to the Lupin Mine on Contwoyto Lake. In addition, there will be two fill-in sites at the southern end of the line, plus sites along minor roads to the east and west. One in particular of interest is the road to Kennedy Lake, which is a property owned by Monopros.

A number of companies have offered logistical support for this survey. Giant Mine will allow the crew to stay in their field house whilst in Yellowknife. Diavik have offered board and lodging at their camp on Lac de Gras. BHP, Winspear and Monopros have offered the same at their camps at Ekati, Snap Lake and Kennady Lake respectively. Additional financial savings over the previous survey will be made by using government-owned snowmobiles, sleds, ice augers and batteries.

The Slave Lakes experiment was funded jointly by Lithoprobe and National Science Foundation's Continental Dynamics for one deployment. Lithoprobe committed to providing the field costs for the experiment, and allocated $25,000 for this. Total field costs for the installation were slightly under $15,000. The lakes into which the instruments are installed are shown in Fig. 2 on the new geological interpretation of the basement terranes from Wouter Bleeker. Unfortunately, as is apparent in the figure, we have no stations on the Northwestern Basement Complex, and little coverage into the eastern domain of the Slave.

We wish to rectify this situation by having a second deployment into ten other lakes. The locations of those ten are open for debate, but we propose that there should be two profiles with reasonable coverage crossing the isotope boundaries, one in the south and one in the north. A deployment configuration that would satisfy this is to have four instruments infill the current central line; two between Snare Lake and Lac de Gras, and two to the east of Lac de Gras, and a new profile of five sites at about the latitude of the Ulu mine (shown by the location of the teleseismic site). The tenth instrument would be reserved as a spare, and perhaps installed into the region west of the Central Slave Basement Complex.

A second deployment will in addition give us the opportunity to modify the instruments after they have been recovered. These instruments have never before been used in this way before, and that no experiment equivalent to this has ever taken place.

Also, the proposed northern line will give us an image of the lithosphere beneath the northern Slave craton which is thought to have been highly modified as a consequence of the mantle plume that gave rise to the MacKenzie dyke swarm (1267 Ma).

Information will be continually updated at the SNORCLE EM web page http://www.cg.NRCan.gc.ca/staff/jones/snorcle/snorcle.html.

Acknowledgements

The Winter road work is partially funded by Kennecott, Monopros, DIAND and B.H.P. Logistical support is provided by Royal Oak, Diavik, Winspear and Monopros.

The Slave Lakes project was funded by a National Science Foundation Continental Dynamics Program grant to Woods Hole Oceanographic Institution. Thanks to staff of Air Tindi for their design and construction of the winch.

Staff of the Yellowknife Geophysical Observatory, Bill Outhwaite and George Jensen, and former staff member Andy Langlois, provided much logistical support for all experiments.

References

Ashwal, L.D., and K. Burke, 1989. African lithospheric structure, volcanism, and topography, *Earth and Planetary Science Letters*, **96**, 8-14.

Bleeker, W., J.W.F. Ketchum, V.A. Jackson and M. Villeneuve, 1999. The Central Slave Basement Complex, Part I: Its structural topology and autochthonous cover. *Can J. Earth Sci.*, in press.

Booker, J.R. and Chave, A.D., 1989. Introduction to the Special Section on the EMSLAB-Juan de Fuca Experiment. *J. Geophys. Res.*, **94**: 14,093-14,098.

Bostock, M.G. and Cassidy, J.F., 1997. Upper mantle stratigraphy beneath the southern Slave Craton. *Can. J. Earth Sci.*, **34**, 577-587.

Clowes, R.M. (Editor), 1997. Lithoprobe Phase V Proposal - Evolution of a Continent Revealed. Publ. By Lithoprobe Secretariate, The University of British Columbia, Vancouver, B.C., pp. 292.

Davis, W.J., Gariepy, C. and Van-Breemen, O., 1996. Pb isotopic composition of late Archaean granites and the extent of recycling early Archaean crust in the Slave Province, northwest Canada. *Chemical Geology*, **130**, 255-269.

Egbert, G.D. and Booker, J.R., 1992. Very long period magnetotellurics at Tucson Observatory: Implications for mantle conductivity. *J. Geophys. Res.*, **97**, 15,099-15,112.

Garcia, X., Chave, A.D. and Jones, A.G., 1997. Robust processing of magnetotelluric data from the auroral zone. *J. Geomagn. Geoelectr.*, **49**, 1451-1468.

Groom, R.W., Kurtz, R.D., Jones, A.G. and Boerner, D.E., 1993. A quantitative methodology for determining the dimensionality of conductive structure from magnetotelluric data. *Geophys. J. Internat.*, **115**: 1095-1118.

Helmstaedt, H.H., and D.J. Schulze, Southern African kimberlites and their mantle sample: implications for Archean tectonics and lithosphere evolution, in J. Ross (ed.), Kimberlites and related rocks, vol. 1: Their composition, occurrence, origin, and emplacement, *Geol. Soc. Aust. Spec. Pub.*, **14**, 358-368, 1989.

Hoffman, P.F., 1990. Geological constraints on the origin of the mantle root beneath the Canadian shield. *Phil. Trans. R. Soc. London*, **A331**, 523-532.

Hollister, L.S., and Andronicos, C.L., 1997, A candidate for the Baja British Columbia fault system in the Coast Plutonic Complex. *GSA Today*, **7**, 1-7.

Ji, S., S. Rondenay, M. Mareschal and G. Senechal, 1996. Obliquity between seismic and electrical anisotropies as a potential indicator of movement sense for ductile mantle shear zones. *Geology*, **24**, 1033-1036.

Jones, A.G., 1988. Static shift of magnetotelluric data and its removal in a sedimentary basin environment. *Geophysics*, **53**: 967-978.

Jones, A.G., 1999. Imaging the continental upper mantle using electromagnetic methods Lithos, accepted.

Jones, A.G., Chave, A.D., Egbert, G., Auld, D., and Bahr, K.1989 A comparison of techniques for magnetotelluric response function estimation. *J. Geophys. Res.*, **94**: 14,201-14,213.

Jones, A.G., Eaton, D.W., White, D., Bostock, M., Mareschal, M. and Cassidy, J., 1996. Geophysical measurements for Lithospheric parameters. In: Searching for Diamonds in Canada, A.N. LeCheminant, R.N.W. DiLabio, and K.A. Richardson (ed.), Geological Survey of Canada, Open File 3228, 243-250.

Jones, A.G., Kurtz, R.D., Boerner, D.E., Craven, J.A., McNeice, G., Gough, D.I., DeLaurier, J.M., and Ellis, R.G., 1992. Electromagnetic constraints on strike-slip fault geometry -- the Fraser River fault system. *Geology*, **20:** 561-564.

Jordan, T.H., 1988. Structure and formation of the continental tectosphere, *J. Petrol.*, Special Lithosphere Issue, 11-37.

Kusky, T.M., 1989. Accretion of the Archaean Slave province. Geology, 17, 63-67.

Kusky, T.M., 1990. Evidence for Archean ocean opening and closing in the southern Slave province. *Tectonics*, **9**, 1533-1563.

Kusky, T.M., 1993. Collapse of Archean orogens and the generation of late- to postkinematic granitoids. *Geology*, **21**, 925-928.

LeCheminant, A.N. and Heaman, L.M., 1989. Mackenzie igneous events, Canada: middle Proterozoic hotspot magmatism associated with ocean opening. *Earth and Planetary Science Letters*, **96**, 38-48.

Mareschal, M., Kellett, R.L., Kurtz, R.D., Ludden, J.N. and Bailey, R.C.. 1995. Archean cratonic roots, mantle shear zones and deep electrical anisotropy. *Nature*, **373**: 134-137.

McNeice, G. and A.G. Jones, 1998. Magnetotellurics in the frozen north: measurements on lake ice. Contributed paper at: 14th EM Induction Workshop, Sinaia, Romania, August 16-23.

Mitchell, R.H., 1991. Kimberlites and lamproites: primary sources of diamond. *Geoscience Canada*, **18**, 1-16.

Ogawa, Y., Jones, A.G., Unsworth, M.J., Booker, J.R., Lu, X., Craven, J., Roberts, B., Parmelee, J. and Farquharson, C., 1996. Deep electrical conductivity structures of the Appalachian Orogen in the southeastern U.S. *Geophys. Res. Lett.*, **23**: 1597-1600.

Padgham, W.A. and W.K. Fyson, 1992. The Slave Province: a distinct Archaean craton. Can. J. Earth Sci., 29, 2072-2086.

Polet, J., and D.L. Anderson, Depth extent of cratons as inferred from tomographic studies, *Geology*, **23**, 205-208, 1995.

Schultz, A., R.D. Kurtz, A.D. Chave and A.G. Jones, 1993. Conductivity discontinuities in the upper mantle beneath a stable craton. Geophys. Res. Lett., 20, 2941-2944.

Senechal, G., Rondenay, S., Mareschal, M., Guilbert, J. and Poupinet, G., 1996. Seismic and electrical anisotropies in the lithosphere across the Grenville Front, Canada. *Geophys. Res. Lett.*, **23**: 2255-2258.

Silver, P.G., and W.W. Chan, Implications for continental structure and evolution from seismic anisotropy, *Nature*, **335**, 34-39, 1988.

Silver, P.G. and Chan, W.W., 1991. Shear-wave splitting and subcontinental mantle deformation. *J. Geophys. Res.*, **96**: 16,429-16,454

Sternberg, B.K., Washburne, J.C. and Pellerin, L., 1988. Correction for the static shift in magnetotellurics using transient electromagnetic soundings. *Geophysics*, **53**: 1459-1468.

Thompson, P.H., A.S. Judge, and T.J. Lewis, Thermal evolution of the lithosphere in the central Slave Province: Implications for diamond genesis, in Searching for Diamonds in Canada, A.N. LeCheminant, D.G. Richardson, R.N.W. DiLabio and K.A. Richardson (ed.), Geol. Surv. of Canada, Open File 3228, 151-160, 1996.

Thorpe, R.I., Cumming, G.L. and Mortensen, J.K., 1992. A significant Pb-isotope boundary in the Slave province and its probable relation to ancient basement in the western Slave province. *In* Project Summaries, Canada-Northwest Territories Mineral Development Subsidiary Agreement 1987-1991. *Edited by* D.G. Richardson and M. Irving. Geological Survey of Canada Open File 2484, 179-184.

Unsworth, M.J., P.E. Malin, G.D. Egbert and J.R. Booker, 1997. Internal structure of the San Andreas Fault at Parkfield, California. *Geology*, **25**: 359-362.

Wannamaker, P.E., Booker, J.R., Filloux, J.H., Jones, A.G., Jiracek, G.R., Chave, A.D., Waff, H.S., Young, C.T., Stodt, J.A., Martinez, M., Law, L.K., Yukitake, T., Segawa, J.S.,

White, A. and Green, A.W., 1989a. Magnetotelluric observations across the Juan de Fuca subduction system in the EMSLAB project. *J. Geophys. Res.*, **94**: 14,111-14,125.

Wannamaker, P.E., Booker, J.R., Jones, A.G., Chave, A.D., Filloux, J.H., Waff, H.S. and Law, L.K., 1989b. Resistivity cross-section through the Juan de Fuca subduction system and its tectonic implications. *J. Geophys. Res.*, **94**: 14,127-14,144.

Wannamaker, P.E., Chave, A.D., Booker, J.R., Jones, A.G., Filloux, J.H., Ogawa, Y., Unsworth, M. and Evans, R., 1996. Sutures and deep physical state of the SE U.S. Atlantic margin: The Southern Appalachians magnetotelluric experiment. *EOS.* **77**, 329-333.

Xu, Y. B.T. Poe, T.J. Shankland and D.C. Rubie, 1998. Electrical conductivity of olivine, wadsleyite and ringwoodite under upper-mantle conditions. *Science*, **280**, 1415-1418.

Deep EM Studies of the Slave Craton

Rob. L. Evans[1], Alan G. Jones[2] and Alan D. Chave[1]

1. Dept. of Geology and Geophysics, Woods Hole Oceanographic Institution

2. Geological Survey of Canada, Ottawa

A better understanding of how the mantle participated in the growth and stabilisation of ancient cratons is central to the evolution of the continents. There are several competing models for the formation of cratons, but they are in conflict, reflecting the limited data that can sense the structure at sufficient depth.

Deep-probing, natural source electromagnetic (EM) studies have demonstrated that they can contribute to such studies by defining both the base of the lithosphere and by determining structural features within the mantle. These studies can also define fossil foliation and lineation direction through detection of mantle electrical anisotropy. Comparison of deep electrical profiles collected across distinct tectonic regimes can provide insight into the chemical and thermal variations that control lithospheric evolution.

With this in mind, we deployed 10 magnetotelluric (MT) instruments in lakes across the Slave craton during a field program last summer. The instruments were left in place over the winter and are to be recovered this summer. By measuring a long time series of electric and magnetic fields, we hope to constrain the the electrical resistivity structure to depths of several hundred kilometres.

We will present some background motivation for our experiment and discuss some of the important issues that might govern electrical structure of the lithosphere and underlying mantle beneath the Slave craton. We will also give a brief overview of the instruments used and their deployment last August.

Lithospheric Velocity Structure beneath the Slave Province and Wopmay Orogen from the SNorCLE Refraction Experiment

Gabriela Fernandez Viejo ([1,2]), Ron M. Clowes ([1,3]), John R. Amor ([1]) and the SNORE Working Group

([1]) Department of Earth and Ocean Sciences, University of British Columbia, Vancouver, BC
([2]) Geological Institute, University of Copenhagen, Denmark
([3]) also LITHOPROBE, University of British Columbia, Vancouver, BC

ABSTRACT

During August-September 1997, LITHOPROBE conducted SNORE 97, a four-line seismic refraction/wide-angle reflection experiment in NW Canada. Here we present the results from Line 11, a ~700 km profile, which crosses the Archean Slave Province and the Proterozoic Wopmay Orogen in the SW Northwest Territories.

The Slave Province (4.0-2.5 Ga) is a small Archean craton including granite-greenstone, gneissic and basin domains, plus the Anton terrane, the oldest known sialic crust. The Wopmay Orogen (2.1-1.9 Ga), lies west of the Slave and includes a series of N-S oriented magmatic arcs (Great Bear, Fort Simpson) and accreted terranes (Hottah and Nahanni). Scientific goals include investigating the structure of early Archean crust, evolution of cratons, and transition and type of suturing between cratons and old Proterozoic orogens.

Line 11 comprises eleven shots (400-3000 kg) detonated along the profile and two additional shots (5000 and 10000 kg) located ~200 km off either end of the line. 594 seismographs were positioned every ~1.2 km. Data analysis include initial τ-p analysis, and subsequent 2-D velocity modelling with RAYINVR.

Velocity structure models show variations that can be related to the different domains sampled. Crustal thickness is ~32-35 km except in the western end where it shallows to 30 km. A discontinuity between lower and upper-middle crust at ~20 km depth is a general feature. Crustal velocities vary from 6 km/s in the basement to 6.9 km/s above the Moho. Anomalous velocity variations occur at the transition zone between Anton terrane and the Yellowknife basin in the Slave Province, and between Hottah and Fort Simpson terranes in the Wopmay Orogen.

All shots show a prominent reflection from the upper mantle. The interface is subhorizontal and located about 75 km depth. A low velocity region in the upper mantle beneath the transition zone between the Fort Simpson and Hottah terranes can be related to subduction processes associated with the welding of the terranes.

1. SNORE 97 - The Experiment

The seismic experiment took place during August-September 1997 and involved personnel from 15 different institutions. Four refraction/wide-angle reflection (R/WAR) lines were recorded (Figure 1). For Line 11, 594 seismographs were deployed with station spacing of about ~1.2 km and with 3-component instruments interspersed along the line. A total of 11 shots (400-3000 kg) were detonated. To provide deep sampling and information about mantle structures, two additional shots (5000 and 10000 kg) were placed ~200 km off either end of the line increasing the maximum offset to about 800 km (Figure 2).

The primary objectives of the R/WAR experiment are:

- determination of the velocity structure of the crust and sub-crustal lithospheric mantle of the tectonic elements crossed by the profile;
- integration of the results with coincident seismic reflection, magnetotelluric and other geophysical data; and
- the relationship of those results to the tectonic elements in the region.

2. LINE 11 - Geotectonic Setting

SNORE 97 Line 11 crosses the Archean Slave Province and the Paleoproterozoic Wopmay Orogen in northwestern Canada (Figure 2).

The Slave Province is a small Late Archean craton. It exhibits an abundance of sialic basement, sedimentary versus volcanic rocks, felsic versus mafic volcanics and poorly developed suture zones, which distinguish it from

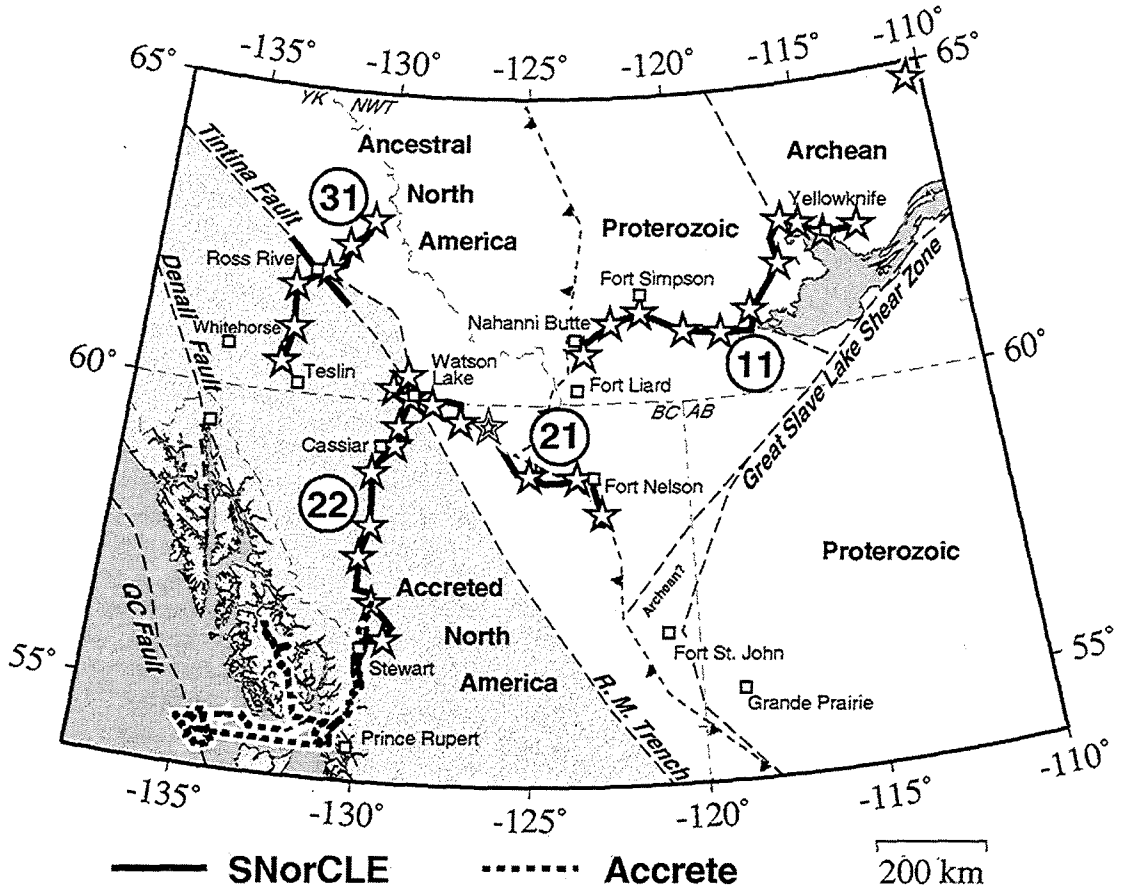

Figure 1. Topographic map showing the position of the refraction lines and shot locations for SNORE 97 experiment.

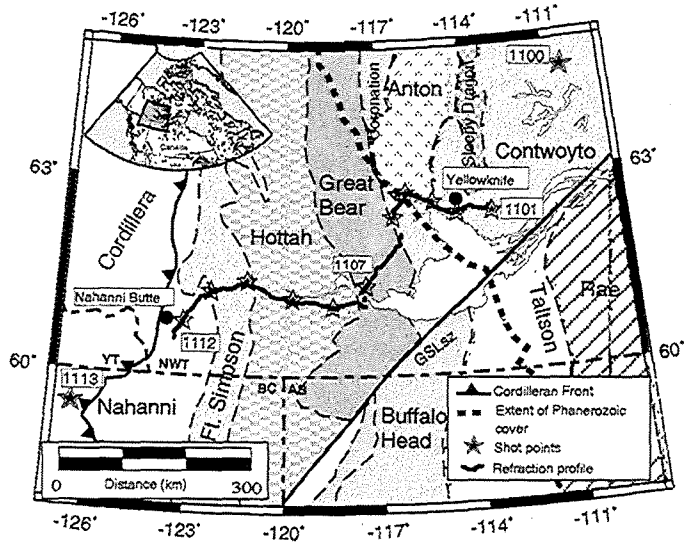

Figure 2. Tectonic element map for the study area and location of SNORE 97 Line 11. Note shot points 1100 and 1113 off the ends of the recording profile. Wopmay orogen includes Coronation, Great Bear, Hottah, Fort Simpson and Nahanni domains. Inset shows location of map within Canada.

other Archean cratons (Padgham & Fyson, 1992). Its history spans from 4.0-3.5 Ga, to 2.5 Ga, although basement older than 2.8 Ga has only been found on the western side of the province. The Slave Province is generally divided into a series of domains, distinguished by their geological characteristics.

- The Contwoyto domain in the east includes several greenstone belts and laterally continuous turbidites.
- The Sleepy Dragon Complex, composed of older gneisses and shallow water sediments, is bounded in the SW by the Yellowknife supracrustal sedimentary basin.
- The ancient Anton terrane in the west dips beneath Proterozoic rocks; its eastern contact is proposed as a major tectonic boundary.

The Wopmay Orogen is a Paleoproterozoic orogen formed between 1.92-1.84 Ga. It includes:

- the Coronation continental margin depositional prism that was shortened and thrust onto the craton during the Calderian orogeny (1.9-1.88 Ga);
- the Hottah terrane, a metamorphic plutonic arc-type complex inferred to have collided with Coronation;
- between these domains, the 100 km wide Great Bear Magmatic Zone, a continental calcalkaline magmatic arc that onlaps both previous elements and is the product of eastward subduction of oceanic lithosphere beneath the western margin of Hottah (Hildebrand et al., 1987);
- the Fort Simpson terrane which collided with Hottah after closure of the intervening ocean at 1.84 Ga, and now forms the autochthonous basement of the Cordillera; and
- the Nahanni terrane, an enigmatic domain defined by its prominent aeromagnetic signature.

A Mesoproterozoic orogenic event within the period 1.6-0.8 Ga, the Racklan orogeny, caused extensive deformation of rocks underlying a large area of northwestern Canada (Cook, 1992), including the western end of Line 11.

3. Data - Preliminary Studies

Data from the 13 record sections of Line 11 are high quality; good arrivals can be observed at the furthest offsets (Figure 3). The preliminary studies involved τ-p analyses, a quick method to obtain 1-D velocity depth functions without involving picking of arrivals (Gorman and Clowes, 1999).

Subsequent interpretation included picking of arrivals, correlation of phases and development of 2-D velocity models using RAYINVR (Zelt & Smith, 1992) to fit traveltimes and amplitudes. The main interpreted phases are: Pg, refracted wave in the upper-middle crust; PmP, wide-angle reflection at the crust-mantle boundary; Pn, refraction in the upper mantle; and PMP, wide-angle reflection in the lithospheric upper mantle. In many sections, intracrustal reflections from the upper limit of the lower crust also were used for the interpretation.

4. Crust and Mantle Interpretation - 2-D Velocity Models and Velocity Anomaly Images

4.1 Analysis procedures:

1) 2-d velocity model (Figure 4). The profile, due to its crooked geometry was divided into four segments that could be treated as straight lines. Velocity models were obtained through inversion of travel times, and forward modelling for amplitude fitting, using RAYINVR routines (Zelt and Smith, 1992).

2) Velocity anomaly image (Figure 5a). An average velocity model was obtained for the whole line and then subtracted from the final velocity models. The residual value gives a "velocity anomaly" cross section which is useful to elucidate velocity trends along the line. This image is compared with the coincident interpreted deep seismic reflection profile (Figure 5b).

4.2 Main results:

1) Velocity values for Line 11 (Figure 4) vary from 5.8-6.0 km/s in the upper crust to 6.9-7.0 km/s above Moho. Mantle velocities vary from 8.0 to 8.3 km/s, with an anomalously low velocity (7.6 km/s) beneath the transition between the Hottah and Fort Simpson terranes.

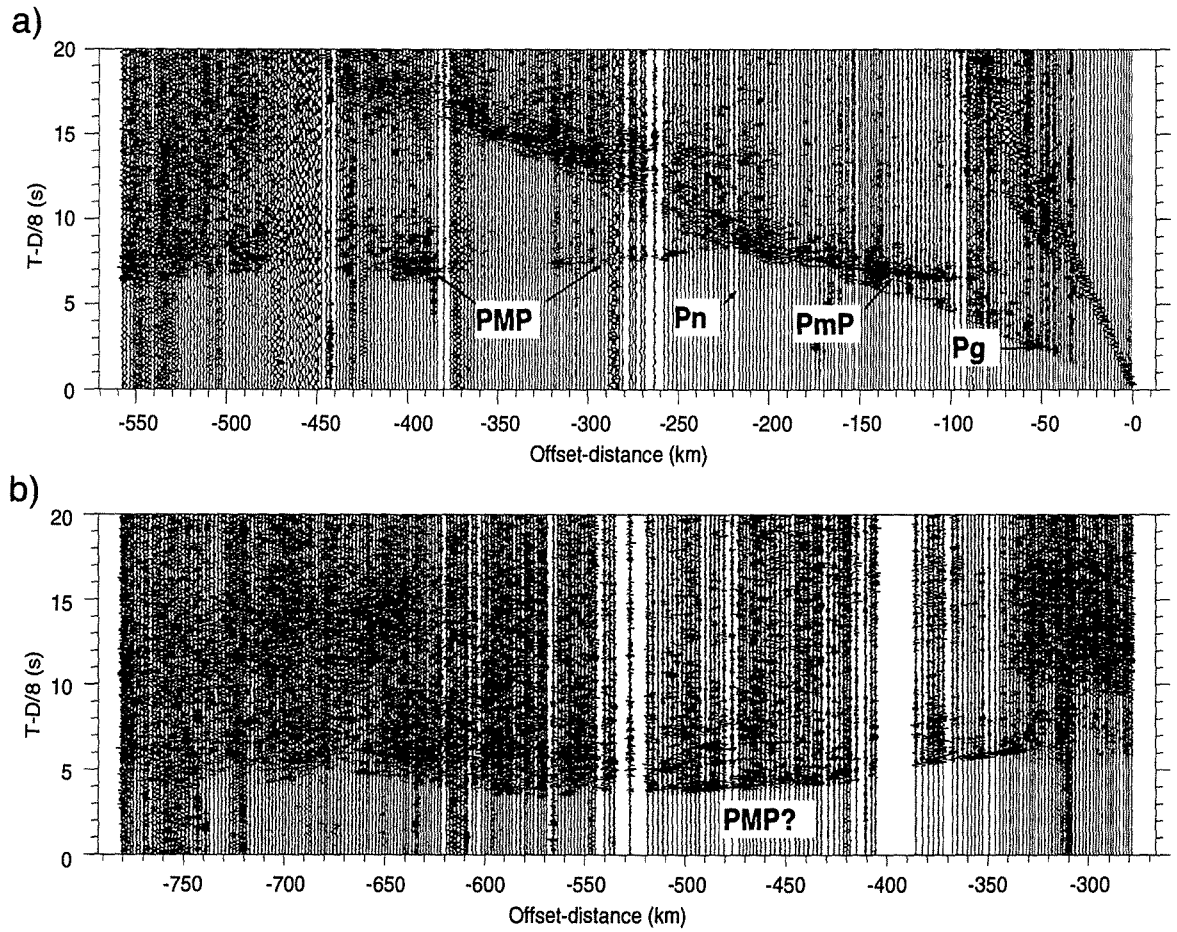

Figure 3. a) Record section from shot point 1101, showing the main interpreted phases. b) Shot point 1100, provided by BHP Diamonds, showing arrivals to offsets of ~800 km. Data are presented with a reduction velocity of 8 km/s, band-pass filtered from 3-13 Hz, and trace-amplitude normalized.

2) Three crustal discontinuities are defined by wide-angle reflections (Figure 4):
- The base of the upper crust is inconsistently imaged at 11-15 km depth.
- The top of the lower crust is clearly imaged along most of the profile at depths of 20-25 km.
- The Moho is well defined at depths of 32-35 km with no significant variations except at the western end.

3) Velocity anomaly image shows consistency with multichannel reflection image (Figure 5):
- In the Slave Province, the Anton terrane has higher velocities than the craton further east.
- The Hottah terrane shows higher crustal velocities in the east than in the west, perhaps indicating a different crustal block beneath the Great Bear magmatic zone.
- Prominent features are the low velocity upper crust (corresponding to a region of low stacking velocities) and the low velocity upper mantle (corresponding to a region of no multichannel Moho reflections) at the Fort Simpson-Hottah transition (~200 km distance) where delamination of the Fort Simpson crust occurs.
- Low velocity crust in the western side of the Fort Simpson terrane correlates with a deep Proterozoic sedimentary basin which thickens to the west.
- Mantle velocities are generally higher below the Slave craton than the Proterozoic terranes.

5. Lithospheric Mantle Interpretation - NMO-corrected and Stacked Wide-Angle Reflections from the Mantle

5.1 The PMP phase:

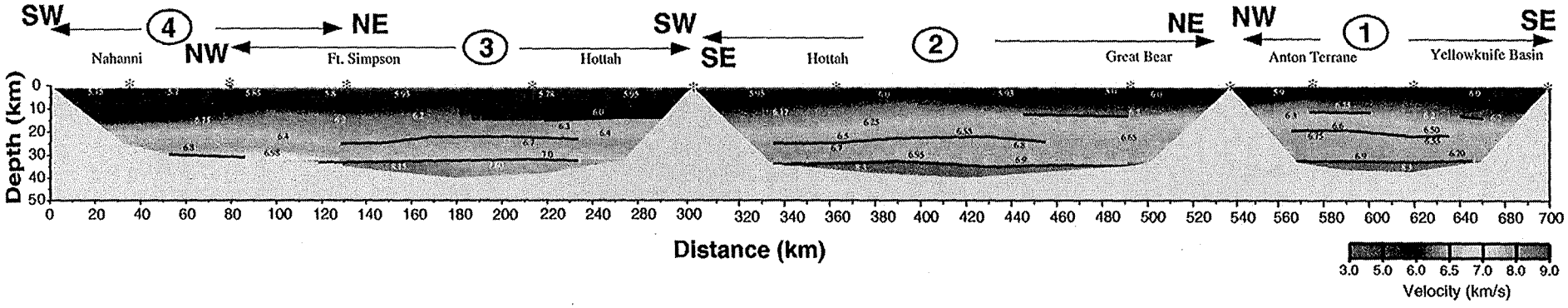

Figure 4. 2-D velocity structural models for the four segments of Line 11. Velocity values are shown by the colour scale (right); some values (km/s) are indicated directly by the numbers. Horizons well constrained by wide-angle reflections are marked by heavy lines. No vertical exaggeration.

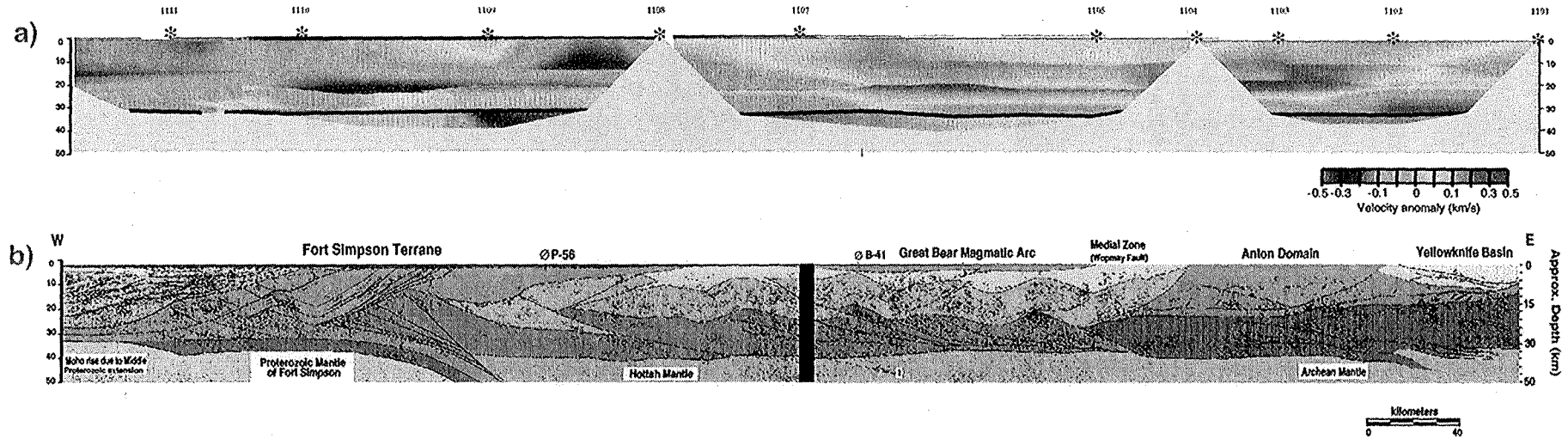

Figure 5. Comparison of images obtained from seismic refraction data and coincident deep reflection data along SNORCLE corridor 1. a) Composite velocity anomaly image from the four straight line segments modelled along Line 11. b) Intepreted deep seismic reflection profile acquired along the same road system (Cook et al., 1998). Note the good correlation between low velocity areas and sedimentary basins, the higher velocity in the eastern domains and the anomalously low mantle velocity in the area of the interpreted Paleoproterozoic subduction zone between Fort Simpson and Hottah terranes.

- To model the deep, wide-angle reflection labelled PMP, a full-length 2-D model had to be constructed. For this preliminary analysis, the crust is considered as one layer. Input velocities are derived from the detailed crustal models (Figure 4). The projection of the SNORE recording profile onto a straight line is shown in the small map of Figure 6.
- The resulting model (Figure 6) shows an interface located at about 75 km depth. A velocity contrast of 0.15 km/s gave enough amplitudes and fitted traveltimes for this phase. The low velocity zone just below Moho beneath the Hottah-Fort Simpson transition, outlined in the crustal models, appears to extend in depth to the mantle discontinuity.
- The mantle interface appears almost continuously beneath Hottah and Great Bear domains for more than 200 km with a slight westward dip. A somewhat less clear boundary was constrained beneath the Fort Simpson zone, dipping in the opposite direction for about 100 km between 300 and 400 km distance. Another reflector (dashed line) was introduced to match some consistent arrivals.
- On the western side of the profile, PMP arrivals from shot point 1113 constrained a flat reflector at about 75 km depth for 100 km distance beneath Nahanni terrane. This is in the region of the Racklan Orogen and the transition to the Cordillera.

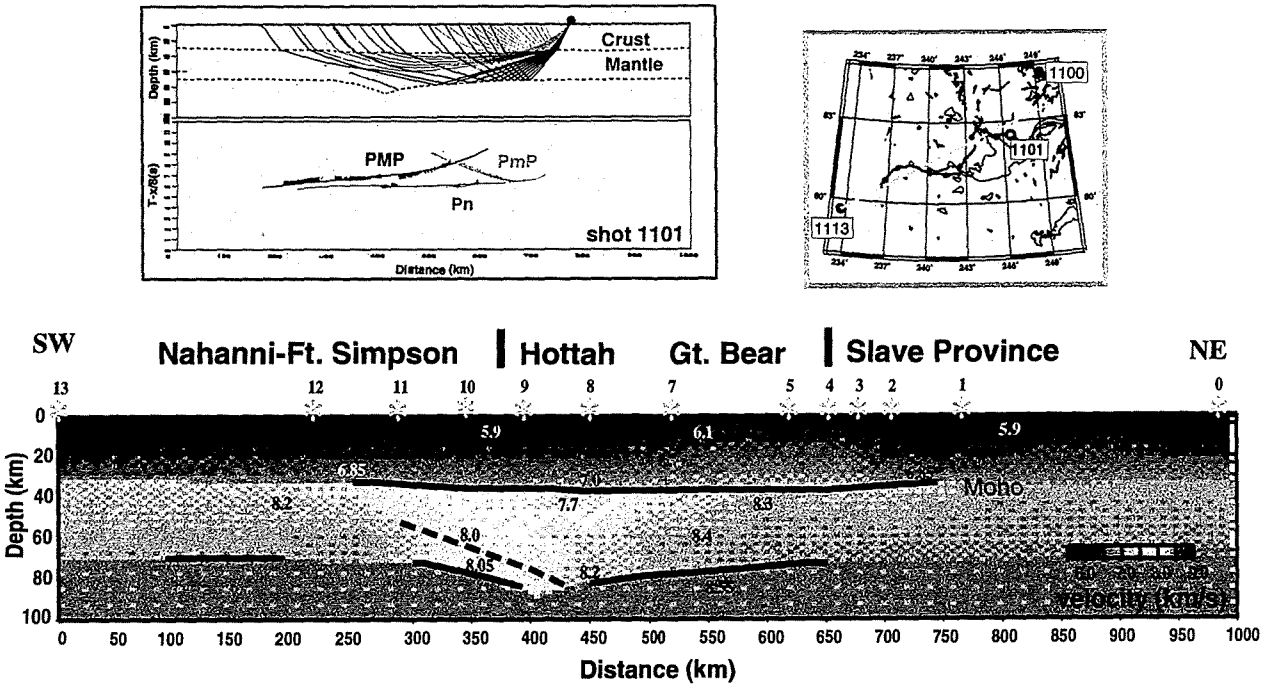

Figure 6. Preliminary 2-D velocity model for the Moho and subcrustal mantle. The profile extends from SP13 in NE B.C. to SP 0 which is 200 km N. of Yellowknife (map, upper right). Below the Moho, heavy black lines mark the segments of the mantle interface defined by wide-angle reflections. Ray paths and traveltimes for PMP are shown in the upper left panel.

5.2 NMO-corrected mantle reflections:

To obtain the equivalent zero-offset record section, an elementary wavefield processing sequence was applied. The procedure used several new routines added to the refraction package PLOTSEC (Amor, 1996).

- Direct wave and PmP multiples are muted.
- Data from all shots are gathered by offset: 50-300 km for PmP and 250 km to maximum offset for PMP.
- Gathers are NMO-corrected using a distance-varying velocity template. For PmP, NMO velocities range west to east from 6.45 to 6.6 km/s. For PMP, velocities range west to east from 7.55 to 7.9 km/s, except near the Fort Simpson-Hottah transition where a lower velocity (7.45 km/s) was needed (cf. Figure 4.).
- Traces are CMP stacked into bins 1 km long and sufficiently wide to capture all CMP points. The "0" km position is SP 13. See Figure 7b.
- A semblance filter is applied to the CMP stack. See Figure 7c.

While NMO-corrected images of the Moho from the PmP phase have been presented previously, the NMO-corrected image of a layer within the upper mantle from the PMP phase has not been reported previously. That

the layer is imaged and corresponds with that on the seismic reflection image (Figure 7a) confirms the existence of the layering within the upper mantle. We interpret the layering to be the result of subduction and/or continental collision processes.

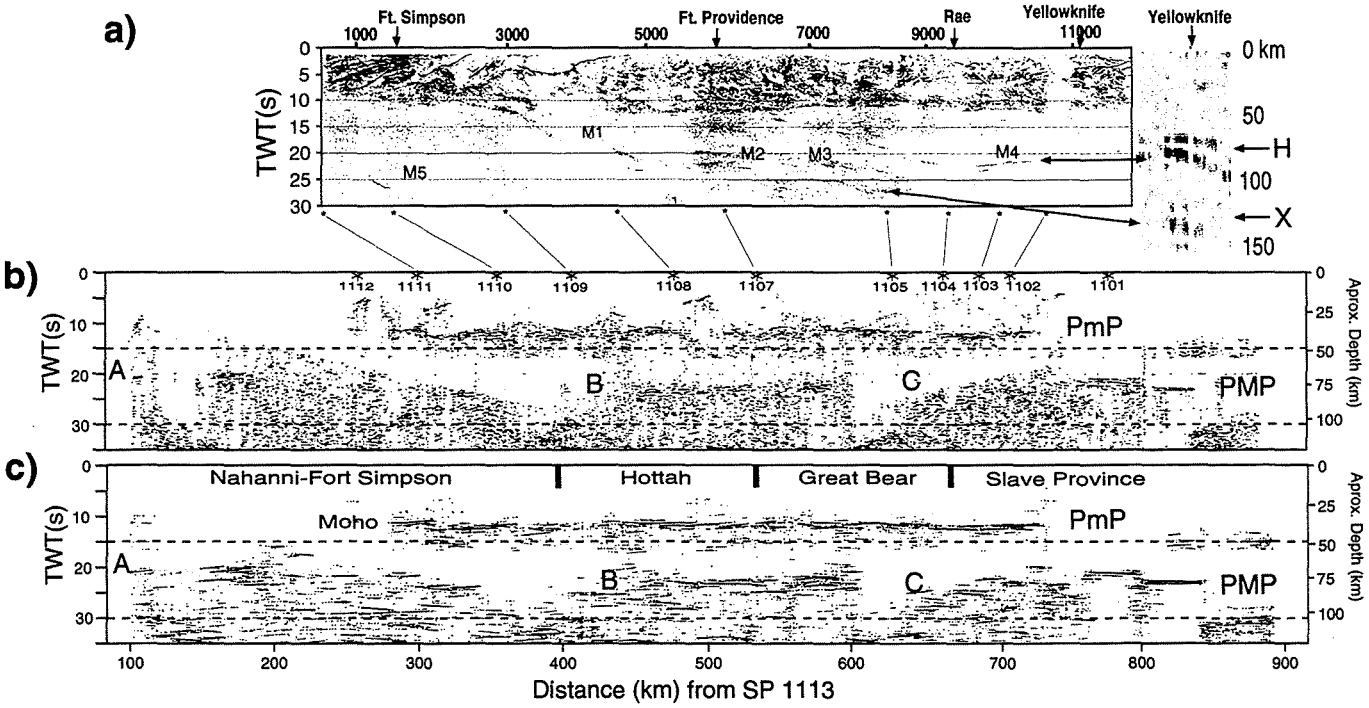

Figure 7. a) SNORCLE MCS line, showing deep seismic reflections from mantle (M1 to M5). To the right, the teleseismic image for the Slave craton shows the continuation of these reflectors to the east (Bostock, 1998). b) NMO-corrected and stacked section for wide-angle reflections PmP and PMP. c) Same image after applying a semblance filter. Note that the Moho image at 11-12s TWT corresponds closely with the MCS Moho reflectors. Mantle reflections are observed in three separate groups (A, B, and C). "C" is quasi-continuous and correlates well with M4 below the Slave Province, which relates to H from the teleseismic interpretation. "C" could represent a layer or fault associated with lithospheric collision of Hottah terrane with Slave craton. "B" is continuous for 150 km and corresponds closely with M2 and M3, which have been correlated with X from the teleseismic analysis of Bostock (1998). "B" is associated with Fort Simpson-Hottah collision and represents the subducted lower Fort Simpson crust. "A" shows coherent reflectivity from 20-22 s between 100 and 200 km distance. No equivalent MCS reflectors are observed; M5 is below 25s and dips moderately eastward. Explanations for "A" are speculative; they are possibly associated with Mesoproterozoic compression (Racklan orogeny) or Meso- to Neoproterozoic rifting of the western North American margin.

Conclusions

☞ Moho discontinuity appears as a flat, continuous interface at 32-35 km depth across different domains of different age. Both the Archean western Slave Province and Paleoproterozoic Wopmay Orogen have crustal thicknesses that are less than average.

☞ Crustal velocities for both Archean and Proterozoic domains vary between 6 and 6.9 km/s, with a differentiated lower crust ~10 km thick. However, different crustal blocks associated with the corresponding terranes can be distinguished on the bases of velocity trends. In the Slave craton, the Anton terrane can be distinguished as a higher velocity block than the eastern domains. The Yellowknife basin is outlined in the models. For the Wopmay orogen, the main feature corresponds to the Hottah-Fort Simpson transition where anomalous velocities are interpreted. The Proterozoic sedimentary basin west of the Fort Simpson zone is well defined in the refraction data. Hottah terrane seems to have higher velocity in the east. In general, mantle velocities increase to the east.

☞ Anomalously low mantle velocities below the transition between Hottah and Fort Simpson terranes, together with the image from the coincident reflection profile, can be attributed to collisional subduction processes and delamination of the lower crust of the colliding Fort Simpson block.

☞ Lithospheric mantle reflections are indicated in all the different methods used for interpretation of the refraction data. Located at about 75 km depth, the origin of this boundary(s) must be found in subduction and continental collision processes during Archean and Proterozoic times. Thus, plate tectonic processes active in Paleoproterozoic times appear similar to those active in the Phanerozoic, as also noted through a number of other studies.

References

Amor, J.R., PLOTSEC: generalized software for seismic refraction data, *LSPF Newsletter*, 9, 24-31, 1996. [see www.geop.ubc.ca/-amor/plotsec]

Bostock, M.G., Mantle stratigraphy and evolution of the Slave Province, *J. Geophys. Res.,* 103: 21183-212000, 1998.

Bowring, S.A., Williams, I.S., and W. Compston. 3.96 Ga gneisses from the Slave Province, NWT, Canada. *Geology*, 17: 971-975, 1989.

Cook, F.A., Racklan Orogen, *Can. J. Earth Sci.*, 29: 2490-2496, 1992.

Cook, F.A., Van der Velden, K.W. Hall and B.N. Roberts. Tectonic delamination and subcrustal imbrication of the Precambrian lithosphere in northwestern Canada mapped by LITHOPROBE. *Geology*, 26: 839-842, 1998.

Gorman, A.R. and Ron M. Clowes. Wave-field tau-*p* analysis for 2-D velocity models: Application to western North America lithosphere. *Geophys. Res. Lett*, in press, 1999.

Hildebrand, R.S., Hoffman, P.F., and S.A. Bowring. Tectono-magmatic evolution of the 1.9 Ga Great Bear Magmatic Zone, Wopmay Orogen, NW Canada. *J. Volc. Geothem. Res.*, 32: 99-118, 1984.

Padgham, W.A., and W.K. Fyson. The Slave Province: a distinct Archean craton. *Can. J. Earth Sci.*, 29: 2072-2086, 1992.

Zelt, C.A., and Smith, R.B., Seismic traveltime inversion for 2-D crustal velocity structure. *Geophys. J. Int.*, 108: 16-34, 1992.

Characterization of the upper mantle beneath the Archean Slave craton using teleseismic methods

C-G. Bank[1], M. Bostock[1], R.M. Ellis[1] and J.F. Cassidy[2]

[1]Department of Earth & Ocean Sciences, University of British Columbia
Vancouver, B.C., Canada V6T 1Z4
Phone: 604-822-2267, Fax: 604-822-6047, E-mail: bank@geop.ubc.ca

[2]Geological Survey of Canada
Sidney, B.C., Canada V8L 4B2
Phone: 250-363-6382, Fax: 250-363-6565
E-mail: cassidy@pgc.nrcan.gc.ca

A temporary array, consisting of 13 broadband seismic stations, recorded teleseisms between November 1996 and May 1998. This data set has been augmented by recordings from the Yellowknife seismic array. The objective of our study is to determine upper mantle structure below the Archean Slave craton, site of the oldest known rocks on Earth and numerous diamondiferous kimberlites, and thence gain an understanding of early crust formation and kimberlite genesis. Tomographic travel-time inversion indicates variations in P-wave velocity of up to $\sim$3%. A high velocity anomaly underlies much of the oldest portion of the Slave craton (the Anton terrane), and extends to $\sim$250 km depth. We interpret this to represent the approximate thickness of the cool subcratonic lithosphere, in agreement with results from magnetotelluric and petrological studies. Low velocities occur along an E-W trending corridor near 65°N, and may be associated with kimberlite magmatism in the Lac de Gras area. SKS-splitting analysis yields moderate delay times ($\sim$1s), and fast directions at all stations that are approximately parallel to the plate motion of North America. This direction is oblique to the Bathurst Fault and MacKenzie dike swarms, suggesting that neither continental collision to the east nor plume interaction to the north has had major effect on the bulk lithospheric fabric beneath the Slave province. A scatter in splitting direction of $\sim$ 30° for events from varying azimuths may be due to complex anisotropic stratification known to occur in the mantle beneath Yellowknife. Simultaneous deconvolution of P-coda for receiver functions reveals a Moho depth ranging from 36 to 42km within the Slave craton. P-to-S conversions from the 410 km and 660 km discontinuities can be identified at several stations and where present are $\sim$1s faster than predicted by IASP91. This is in accordance with high absolute velocities generally observed for upper mantle beneath cratons.

Northwestern Canada Seismic Experiment

M. Bostock[1], J.B. Gaherty[2], E.J. Garnero[3], J.S. Revenaugh[4]

[1]Department of Earth & Ocean Sciences, University of British Columbia
Vancouver, B.C., Canada V6T 1Z4
Phone: 604-822-2267, Fax: 604-822-6047, E-mail: bostock@geop.ubc.ca

[2]School of Earth & Atmospheric Sciences, Georgia Institute of Technology
Atlanta, GA, USA 30332-0340
Phone: 404-894-1992, Fax: 404-894-5638
E-mail: gaherty@eas.gatech.edu

[3]Department of Geology, Arizona State University
Box 871404 Tempe, AZ, USA

[4]Department of Earth Sciences, University of California
Santa Cruz, CA, USA 95064
Phone: 831-459-3055, Fax: 831-459-3074
E-mail: jsr@monk.ucsc.edu

A joint Canadian-U.S. experiment is proposed to study the nature of the upper mantle (35-660 km depth) beneath northwestern Canada and the role it has played in the evolution of the continent. A portable broadband seismic array comprising approximately 50 instruments will be deployed at 30 km intervals over portions of the Alaska Highway (Edmonton to Whitehorse) and the MacKenzie-Liard Highways (Fort Nelson to Yellowknife) for a 2-year period. The array's configuration and location with respect to global seismicity will allow acquisition of a data set ideally suited to examination of upper mantle lateral heterogeneity and anisotropy at a wide range of scales below the northern Cordillera and North American craton. Analysis of this data set using a comprehensive arsenal of seismological techniques will allow us to address a number of important geologic issues with both global and regional significance, namely i) What is the nature of contrasts between mantle underlying orogenies and that below old, stable continental interiors? ii) What effects has this had on the evolution of overlying crust and its expression in surface geology? iii) Do major fault zones mapped at the surface penetrate below crustal (30-40 km) levels? iv) What physical processes are responsible for the subhorizontal, shallow mantle boundaries observed on recent Lithoprobe reflection lines? v) What role has the plate tectonic evolution of the Pacific coast played in modifying the upper mantle beneath the Cordillera? and iv) What are the collective implications of i-iv) for our understanding of the assembly and evolution of continents?

High Heat Flow along the SNORCLE Transect

Trevor Lewis[1,2] and Roy Hyndman[1]

[1]Pacific Geoscience Centre, Geological Survey of Canada, Sidney, BC V8L 4B2
[2]Sidney Geophysical Consultants Ltd., 1107 Maple Road, Sidney, BC V8L 5P5
sgc_ltd@bc.sympatico.ca

New determinations based on measured temperatures and measured thermal conductivities from hydrocarbon exploration wells extend the region of high heat flow from northern B.C.-southern Yukon eastward across the Nahanni, Fort Simpson and Hottah terrains. Majorowicz (1996) first suggested high heat flows in the eastern part of this region based on BHT data and estimates of thermal conductivities from lithological descriptions of core cuttings (Majorowicz and Morrow, 1998). We measured the thermal conductivity of cuttings from 12 wells and of cores from two other sites, and we used recorded BHTs at 11 of these wells, and high precision temperature logs at three other sites. The thermal conductivity of shales which cannot be accurately be determined from cuttings was shown to be 1.25 W/m K in the Fort Providence well. The value previously assumed for shale (Majorowicz and Jessop, 1993), 1.4 W/m K, is 12% higher. Heat flows (Table 1) were determined using Bullard plots. The heat flow Majorowicz and Morrow (1998) determined previously in nine of these wells was on average 22% higher, reflecting differences in both the thermal conductivities and temperature gradients. The temperature gradients were the same only at one site. The heat flow from the three sites with high precision temperature logs was 97, 121 and 97 mW/m^2.

Proceeding westward along the transect, the heat flow increases from 54 mW/m^2 at Yellowknife to 89 +/- 17 mW/m^2 across the Hottah, Fort Simpson and Nahanni terrains, reaching 118-136 mW/m^2 in the Nahanni terrain. North of 59°N in B.C. and southern Yukon the average heat flow is 103.3 +/- 21.0 mW/m^2.

Lithospheric temperatures are a function of the surface heat flow, the thermal conductivity as a function of depth and the distributed crustal heat generation. The latter two parameters are not well defined as a function of depth, but constraints can be imposed to model the deep temperatures. The relative stability of this basement over 1.1Ga requires that much of the excess heat come from heat generation near the surface of the basement. A similar situation exists in Australia, where the

abnormally high heat flow is attributed to high heat generation in the upper crust. (Sandiford and Hand, 1998).

Very high heat generation was contained in the last magmatic phases of the Slave province: e.g., 33% of the Winter Lake map area is now covered by such a late granite having a heat production of 8-16 $\mu W/m^3$ (Thompson et al, 1995). Much of such an upper layer might have been eroded from the early craton, now forming part of the upper basement underlying this part of the Western Canada basin. Measurements on cuttings from wells penetrating the basement south of 60°N (Burwash and Cumming, 1976) do not reflect such high values. Jessop (1992) did show that the Rimbey Arc and the Slave had higher heat generation than other terrains south of 60°N

Table: Heat Flow Values

Location		Heat Flow
Lat. N	Long. W.	mW/m^3
62.508	114.422	54
61.437	117.375	97*
59.978	117.015	121*
59.847	117.088	97*
61.530	116.663	102
61.017	117.298	58
61.235	117.478	79
60.988	118.428	79
61.097	118.660	99
61.272	120.780	85
61.238	120.878	87
60.975	122.535	71
61.033	123.808	136
60.878	124.467	118
61.56	124.79	130

*high precision temperature logs

The Cordillera-Craton Thermal Transition in Northern and Southern Canada

R.D. Hyndman[1] and T.J. Lewis[1,2]
[1]Pacific Geoscience Centre, Geol. Surv. Canada, Sidney B.C., hyndman@pgc.nrcan.gc.ca
[2]Sidney Geophysical Consultants Ltd., 1107 Maple Rd. Sidney, B.C.

The heat flow and lithosphere temperatures increase abruptly across the transition from the stable North American Craton to the Canadian Cordillera. The heat flow increases from 40-60 mWm^{-2} in most of the Craton to 80-100 mWm^{-2} in the Cordillera. There are numerous reliable heat flow data in the Cordillera but measurements in the Western Canada Sedimentary Basin overlying the adjacent Craton are in petroleum exploration wells that have lower accuracy. However, additional thermal information is available from several other temperature sensitive geophysical parameters.

For the southern Canadian Cordillera, the thermal boundary is located 100 km west of the mountain front in the region of the Rocky Mountain Trench. Temperatures in the deep crust and upper mantle computed from the heat flow and radioactive heat generation data, from the temperature dependence of uppermost mantle seismic velocity, Pn, and from xenoliths in kimberlites for the Craton, and in Tertiary volcanics for the Cordillera all are in agreement. The temperatures just below the Moho are 400-500°C for the Craton and 900-1000°C beneath the Cordillera.

For the northern Cordillera in the region of the Lithoprobe SNORCLE transect, the Cordillera heat flow and inferred deep temperatures are high, similar or slightly higher than those in the south. However, the adjacent Craton to the west of Yellowknife (Hottah, Fort Simpson and Nahanni terranes) exhibits unexpected very high heat flow averaging 90 mW/m^2. The high heat flows in this area first suggested by Majorowicz (1996), are confirmed by our more detailed study of temperatures and thermal conductivity in 14 wells. We have detailed temperatures in three wells, and in one well (Ft. Providence) data extends to basement. Although these heat flows are similar to the Cordillera, other temperature sensitive indicators suggest that the deep crust and upper mantle temperatures are not as hot, and the source of the high heat flow must be unusually high radioactive heat generation in the upper crust. Although unusual, a similar conclusion has been made for an area of central Australia (Sandiford and Hand, 1998).

Two temperature sensitive changes across the thermal boundary are examined. In the south there is a westward decrease from a thick 40-50 km crust for the Craton to 32-34 km for the Cordillera, with no significant change in average elevation nor in gravity. Isostatic balance is maintained by thermal expansion and density reduction in the high temperature Cordillera lithosphere. The average temperature to a depth of 150 km is about 400°C higher for the Cordillera compared to the Craton. Upper mantle Pn velocities decrease from about 8.2 km/s for the Craton to 7.8 km/s for the Cordillera in response to the temperature difference. The northern Cordillera is similar to the south in both crustal thickness and Pn velocity. However, for the adjacent northern Craton, the relatively thin crust and the Pn velocity both suggest higher than normal Craton deep temperatures in agreement with the heat flow, although not as high as beneath the Cordillera. Detailed models have not yet been done, but the Moho may be at 600-700°C.

In the south, there is an abrupt westward decrease in lithosphere strength and thus deformation style across the Craton-Cordillera boundary. In the Craton, the crust and upper mantle are very strong to at least 100 km depth. As a result, the foreland belt deep crust and upper mantle have remained undeformed during Late Mesozoic to Early Tertiary tectonics. Shortening occurred primarily in overlying sedimentary thrust sheets, mediated by high pore fluid pressures. In the Cordillera hinterland, the high temperatures result in the rheological lithosphere with significant strength being limited to the upper 10-15 km of the crust. The upper mantle has negligible strength. Mesozoic-Cenozoic shortening deformation and subsequent extension included this whole thin lithosphere. In the north, the strength transition is more gradual and complex. The higher than normal deep temperatures beneath the western Craton result in a thinner and weaker lithosphere than normal. This weaker lithosphere may have allowed Cordilleran deformation to extend to the east, forming the large eastward bow in the mountain front in this region.

Thermomechanical modelling of convergent orogens

Vanderhaeghe O., Beaumont C., Fullsack P., and Jamieson R.A.

Oceanography and Earth Sciences, Dalhousie University, Halifax, Nova Scotia, Canada
(olivier@adder.ocean.dal)

Convergence of lithospheric plates is typically accommodated by crustal accretion and collision at the edge of continental margins. The evolution of large orogenic belts comprises a period of crustal thickening followed by the formation of a continental plateau and eventually a period of collapse of the zone of thickened crust. In a conceptual model, we infer that this evolution is controlled by the competition between tectonic and gravity forces combined with the role of the rheologic evolution of the crust, primarily as a function of temperature, on the traction at the base of the thickened orogenic belt (figure 1).

We test the pertinence of this conceptual model in reproducing first order features of orogenic belts, using a thermomechanical numerical model based on the finite element method. In the model, two-dimensional vertical plane strain deformation of the upper part of the system (the crust) is driven by the imposed velocity at its base (the subducting slab), and for each time step, the mechanical properties for each element are derived from the calculated temperature distribution. The imposed kinematic condition on the behavior of the mantle part of the lithsophere limits the investigation to crustal dynamics. Isostatic compensation is adjusted by the rigidity and density of elastic beams underlying the crustal part of the model, allowing to reproduce conditions of local isostasy as well as no isostatic compensation. Nevertheless, the thermal impact of lithospheric subduction is simulated and the thermal evolution of the zone of thickened crust is mainly controlled by the competition between cooling due to advection of cold subducted material beneath the crust and internal heat production related to radioactive decay concentrated in the zone of thickened crust.

Steady-state initial geotherms, calculated assuming either a diffusion or a diffusion/advection equilibrium, strongly influence the geometry of the models. In addition, the distribution and concentration of radioactive elements play a key role on the evolution of temperature during crustal thickening.

The comparision of experiments using simple constitutive equations (constant viscosity, Coulomb, temperature-dependant viscosity) provides some insights on the influence of the choice of the rheologic laws on orogenic evolution. In particular, crust with simple strength profiles controled by a constant viscosity or a Coulomb-plastic behavior show constant thickening and no development of continental plateau. The formation of a plateau implies mechanical decoupling at the crust/mantle interface and thus requires alteration of the basal traction. This is achieved for models with complex strength profiles including temperature-dependent rheologies and when crustal thickening is associated with an increase in temperature.

The transition from crustal thickening to the formation of a continental plateau is marked, in some cases, by a period of crustal thinning. This is interpreted as gravitational collapse of a thickened crust following the rapid decrease in strength at the base of the crust due to the increase in temperature.

PRELIMINARY REPORT ON THE LOWER PALEOZOIC STRATIGRAPHY AND CONODONT BIOSTRATIGRAPHY, PLATFORM TO BASIN TRANSECT, IN THE TRUTCH, HALFWAY RIVER AND WARE MAP AREAS (94G, B,F), BRITISH COLUMBIA

Christopher R. Barnes and Leanne J. Pyle
School of Earth and Ocean Sciences, University of Victoria,
P.O. Box 3055, Victoria, B.C. V8W 3P6
crbarnes@uvic.ca; leanne@uvic.ca

This is a preliminary report on a new project that was initiated in July, 1998, with support provided through a LITHOPROBE/SNORLCE grant and helicopter support in the field provided by the GSC's Central Foreland NATMAP project. Two field seasons are required to assemble all the stratigraphic and conodont biostratigraphic data. The principal objective is to reconstruct part of the Early Paleozoic evolution of the western margin of Laurentia through studies along a platform-outer miogeocline-basin transect. A general tectonic model was recently advanced by Cecile et al. (1997). This transect extends from north-east to south-west across three map areas and complements Line 2 of the SNORCLE transect.

Five main stratigraphic sections were measured in detail and sampled for conodont microfossils in the Trutch, Halfway River and Ware map areas (94G, B, F) (Fig.1). These sections are: Sikanni Chief River North (Fig. 2), Sikanni Chief River South (Fig. 2) (Trutch) , Section 9 of Thompson (1989) south of Mount Lady Laurier (Fig. 3), and near Section 6 of Thompson (1989) south-east of Mount Robb (Fig. 4) (Halfway River), and near Section 3 of Cecile and Norford (1979) east of the Ospika River (Fig. 5) (Ware). The stratigraphic units measured, described and sampled were the Kechika, Skoki, Beaverfoot, Unnamed Upper Ordovician quartzite and carbonaceous limestone units, Nonda, Unnamed Lower Silurian slope breccia unit, and Road River, together encompassing an Upper Cambrian through Lower Silurian interval. The overall stratigraphic framework along this transect is shown in Figure 6. A total of 137 4-5 kg conodont samples were collected and approximately 5050m of stratigraphic section were

described. The conodont samples are presently being processed: with large and argillaceous samples it will take about 9-15 months to dissolve, separate, pick and sort the conodonts prior to taxonomic identification and biostratigraphic-biofacies analysis of this first year's collections. Some key sampling intervals are being processed first to allow the second field season's sections and collections to be effectively integrated.

There was limited prior stratigraphic data and conodont data available for most of the sections studied. The thick (over 1000m) Kechika Formation (Upper Cambrian – Lower Ordovician) is primarily dolostone, limestone, and shale. It represents a gentle ramp facies but with little exposure of the underlying units. Trilobite packstones are present in the eastern, platform facies and should yield abundant conodonts; limestones are rare in the western, more basinal facies. The massive dolostones and subordinate limestones of the Skoki Formation, about 200-750m thick and of Lower to Middle Ordovician age, represent a shallow subtidal environment in which some horizons are characterized by abundant oncolites. Section 9 of Thompson (1989), south of Mt. Lady Laurier (Halfway River map area), includes substantial limestones especially in the lower half and lies just east of the ancient shelfbreak. Near Section 6 of Thompson (1989), south-east of Mount Robb, are exposed late Middle (?) to Upper Ordovician quartzite, and black shale and carbonaceous limestone units (c. 500m and 200m, respectively), bearing rare graptolites. These two units are probably laterally equivalent in part to the Beaverfoot Formation dolostones, a shallow water platformal facies, to the east (Trutch map area). Their relationship to the Advance Formation (Norford, 1996), that has a resticted outcrop belt to the south, is not clear at this point. Above the Beaverfoot Formation (c. 350m), shallow water dolostones, locally with abundant coral and brachiopod faunas, predominate in the Nonda Formation (c. 330m). Traced westwards, the Nonda appears to correlate with the Unnamed Breccia unit (c. 150m) – a complex of dolomitized slope breccias, composed largely of monomictic Nonda-type clasts. In the eastern Ware map area, representing a more basinal setting, the Kechika is entirely dolomitic with higher proportions of interbedded shales and rare sandstones. It is overlain by the Road River Group (c. 1000m) that was sampled west of the shelfbreak

where the sequence is particularly rich in crinoidal carbonate turbidites with rare sandstones, shales and volcanics. The orange-weathering Silurian(?) Siltstone unit lies above these carbonates and shales.

Although the general stratigraphic framework (Fig. 6) is understood from earlier regional mapping and will be further refined through the current NATMAP project, the present detailed stratigraphic and conodont biostratigraphic work should clarify the sequence stratigraphy and the east-west temporal and facies relationships.The provisional interpretations of the stratigraphic and facies relationships are illustrated in Figure 7. However, there is barely any biostratigraphic control across this transect in the Central Rockies. The conodont biostratigraphic and paleoecologic work will be able to constrain these interpreted relationships and allow a more precise interpretation of wider tectonic and eustatic effects and events. At present, without the conodont data, many stratigraphic and tectono-stratigraphic questions remain to be resolved and some of these are noted in Figure 8.

It is planned to continue the project next year (1999-2000). About three weeks field work is planned to examine about a further five composite sections and to collect about 120-150 additional samples. More intense sampling will be undertaken of critical intervals and for others as indicated by preliminary results from conodonts recovered from the 1998 collections; the work will likely be extended north to the Muncho Lake area. The two field seasons will therefore provide a north-east to south-west transect from the ancient platform though miogeocline over the shelfbreak to the basin with stratigraphic control based on about 10-12 composite stratigraphic sections and with detailed conodont sampling for biostratigraphic control. The 1999 samples will take about a year to process, pick, and analyse and then to integrate with the data from the 1998 field studies.

Acknowledgments

We gratefully acknowledge financial support for the project provided by LITHOPROBE/SNORCLE and of the logistical support for field work provided by the GSC's Central Foreland NATMAP Project. Particular thanks are extended to Michelle Landry who has cheerfully assisted in both the field work and the laboratory processing work.

References

Cecile, M.P., Morrow, D.W. and Williams, G.K. 1997: Lower Paleozoic tectonic history, northern Cordillera. Canadian Society of Petroleum Geologists Bulletin, v. 45, pp. 54- 73.

Norford, B. S. 1996. Stratigraphy and biostratigraphy of the Advance Formation, a new upper Middle Ordovician unit, northern Rocky Mountains, British Columbia. Geological Survey of Canada, Bulletin 491, p.5-19.

Thompson, R. I., 1989. Stratigraphy, tectonic evolution and structural analysis of the Halfway River map area (94B), northern Rocky Mountains. Geological Survey of Canada, Memoir 425, 119p.

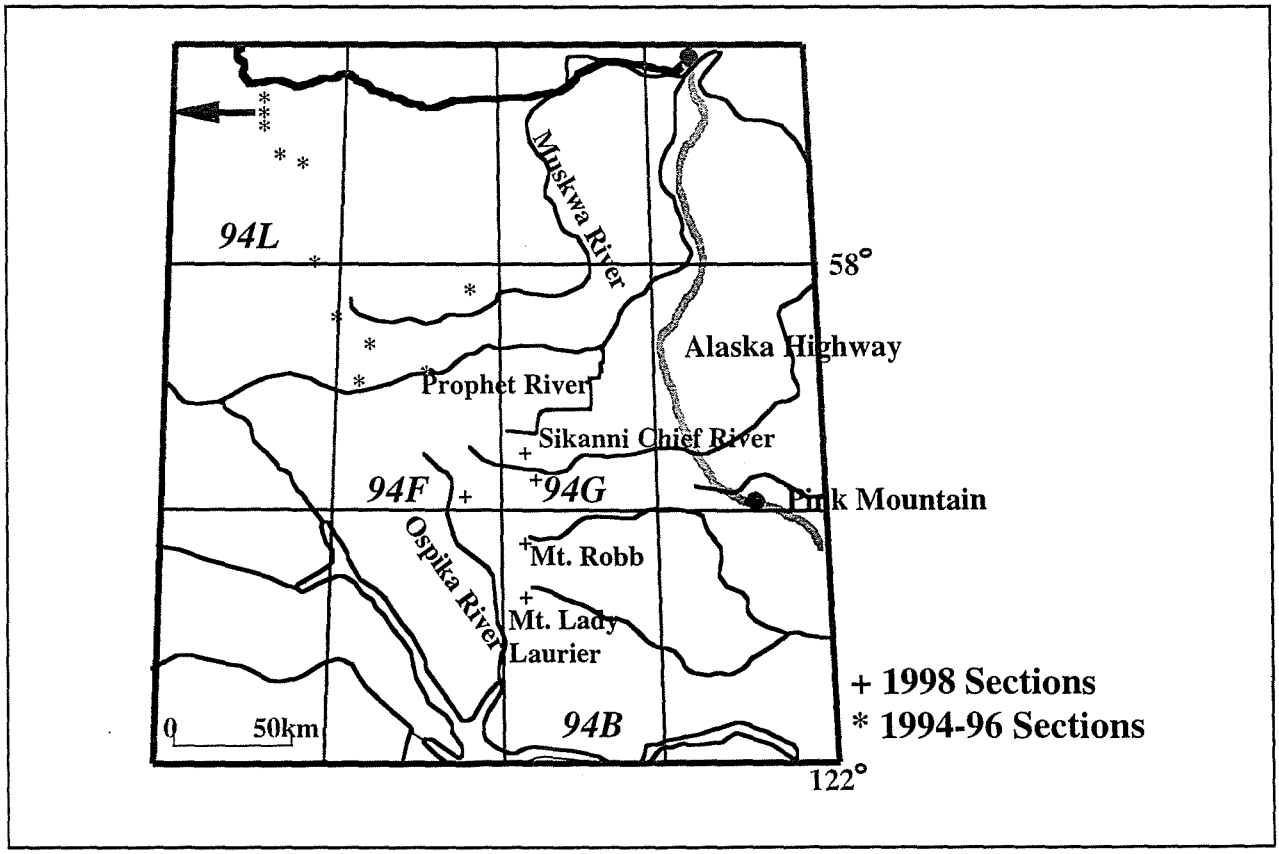

Fig. 1: Location map for stratigraphic sections

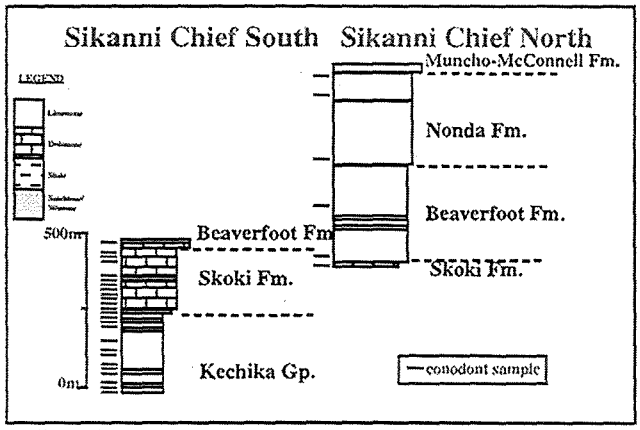

Fig. 2: Stratigraphy and conodont samples, Sikanni Chief North and South sections, Trutch map area

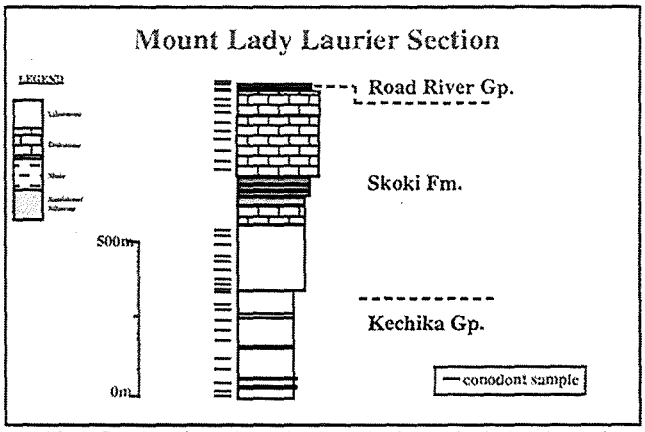

Fig. 3: Stratigraphy and conodont samples, Mount Lady Laurier section, Halfway River map area

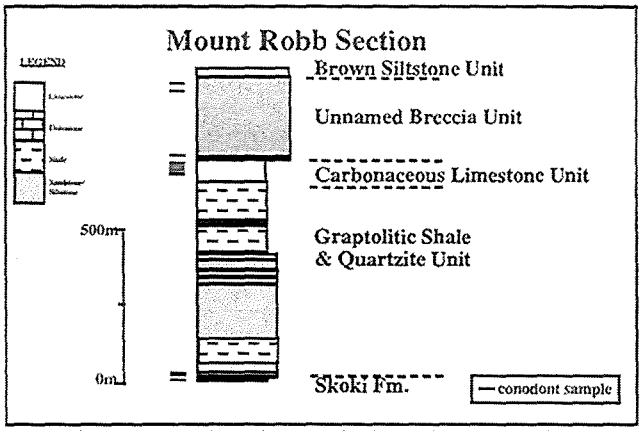

Fig. 4: Stratigraphy and conodont samples, Mount Robb section, Halfway River map area

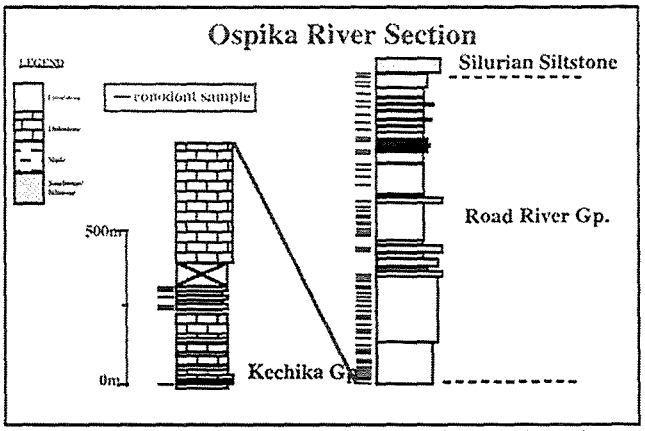

Fig. 5: Stratigraphy and conodont samples, Ospika River sections, Ware map area

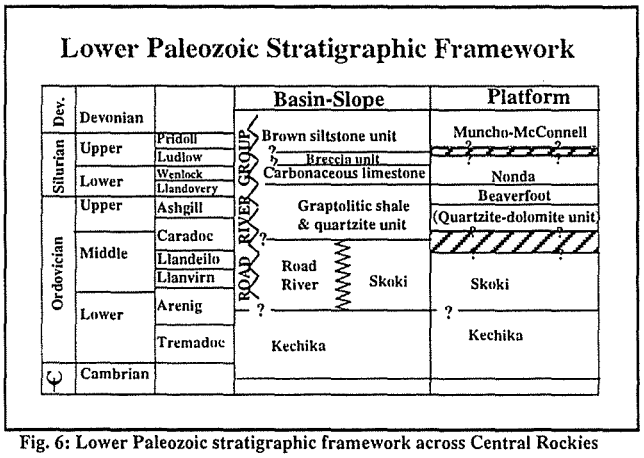

Fig. 6: Lower Paleozoic stratigraphic framework across Central Rockies transect

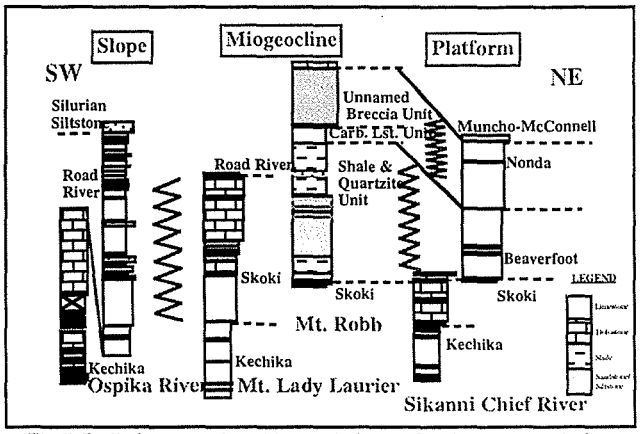

Fig. 7: Preliminary stratigraphic correlations and facies changes, platform to basin transect, central Rockies

STRATIGRAPHIC/TECTONIC ISSUES

Stratigraphic Units	Questions
Nonda	Scale of Silurian hiatuses?
Unnamed Breccia Unit	Equivalent to which part of Nonda? Possible margin extension?
Carbonaceous limestone unit	Equivalent to basal Nonda?
Unnamed shale/quartzite unit	Equivalent to Mount Wilson Quartzite? Relationship to Advance Formation?
Road River	Scale of potential internal hiatuses? Scale and cause of Middle-Upper Ord. hiatuses?
Skoki/Road River	Volcanics: same age in both units?
Kechika/Skoki	Change of platform sedimentation? Ramp to defined shelfbreak change?
Kechika/Road River	Modification of margin? Phase of extension? Timing: Tremadoc, Arenig, Llanvirn? Hiatus?

Fig. 8: Tectono-stratigraphic issues requiring resolution, platform to basin transect, central Rockies

Tectono-stratigraphic framework of Triassic strata, northeastern British Columbia: ichthyolith biostratigraphy and regional thermal maturation studies.

M.J. Johns[1], Barnes, C.R.[2], and M.J. Orchard[3]

[1]Pacific PaleoQuest, P.O. Box 220, Brentwood Bay, B.C. V8M 1R3
[2]School of Earth and Ocean Sciences, University of Victoria, P.O. Box 3055, Victoria, BC V8W 3P6
[3]Geological Survey of Canada, 101-605 Robson Street, Vancouver, BC V6B 5J3

INTRODUCTION

Ichthyoliths (microscopic fish teeth and scales; Fig. 1) are a new tool for the development of a tectono-stratigraphic framework for Triassic rocks and in future hydrocarbon exploration in northeastern British Columbia (NEBC). Ichthyoliths have utility in biostratigraphic, paleoenvironmental, and thermal maturation assessments. They have a broad distribution in pelagic environments, may be recovered from small samples in both marine and nonmarine sedimentary rocks, have a long range (Cambrian to Recent), and are naturally resilient during diagenetic and laboratory processes.

This report summarizes progress on a new project initiated in 1998 on Triassic ichthyolith biostratigraphy and thermal maturation studies in the Trutch and Halfway River map areas, NEBC. The study is supported through the LITHOPROBE SNORCLE and the G.S.C. Central Foreland NATMAP projects.

PROJECT OBJECTIVES

The principal objectives of this project are to:

1) test, calibrate, and refine the provisional Middle and Upper Triassic ichthyolith zonation of NEBC (Johns, Barnes, & Orchard, 1997) and extend stratigraphic coverage to include the Lower Triassic and Lower Jurassic;
2) recognize and interpret regional variations in ichthyolith successions and biofacies along and across the strike of the foreland belt;
3) develop an ichthyolith colour alteration index and recognize regional thermal maturation patterns;
4) analyze differences between faunas recovered from shale and limestone beds;
5) investigate key stratigraphic and biological event intervals (e.g. Phosphate Zone; Norian/Carnian boundary, Jurassic/Triassic boundary); and
6) compare NEBC results with other Triassic ichthyolith data from B.C. miogeoclinal and outboard terrane sections to better understand terrane motions from ichthyolith distributions.

The combination of the ichthyolith studies with other stratigraphic and biostratigraphic work should help to resolve the regional tectono-stratigraphic framework for the western margin of the Western Canada Sedimentary Basin during the early Mesozoic.

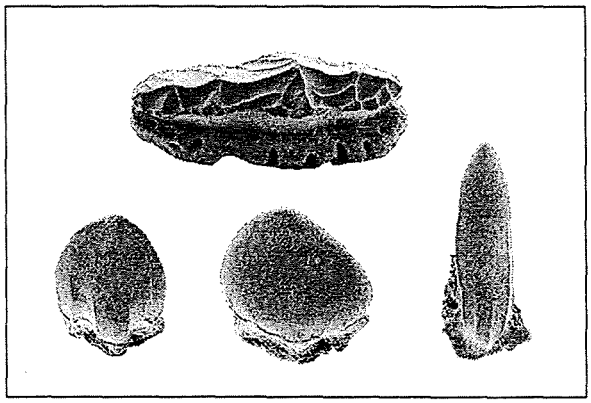

Figure 1. *Synechodus incrementum* Johns (shark tooth) and three forms of elasmobranch (shark) scales diagnostic of the Norian *Synechodus incrementum* ichthyolith zone, northeastern B.C. All specimens are from GSC loc. C-303445, Moose Lick Creek ridge.

1998 AND 1999 FIELD WORK

Joint 1998 field work (M.J. Orchard, M.J. Johns, and J. Dixon) in the southern Trutch and northern Halfway River map areas resulted in the collection of approximately 140 limestone and 75 shale samples, and description and interpretation of Triassic strata. Important sites and formations sampled are shown in figures 2 and 3.

Plans for 1999 field work will be based on microfossil recovery and results from 1998 samples. Sites with good microfossils may warrant a revisit for more detailed sampling. Geological mapping during 1998 and 1999 will assist in locating the best new Triassic and Lower Jurassic sections for microfossil sampling. Suggested new site targets for 1999 sampling are shown in Figure 2. Similar to 1998, emphasis will be placed on joint field work and collaboration.

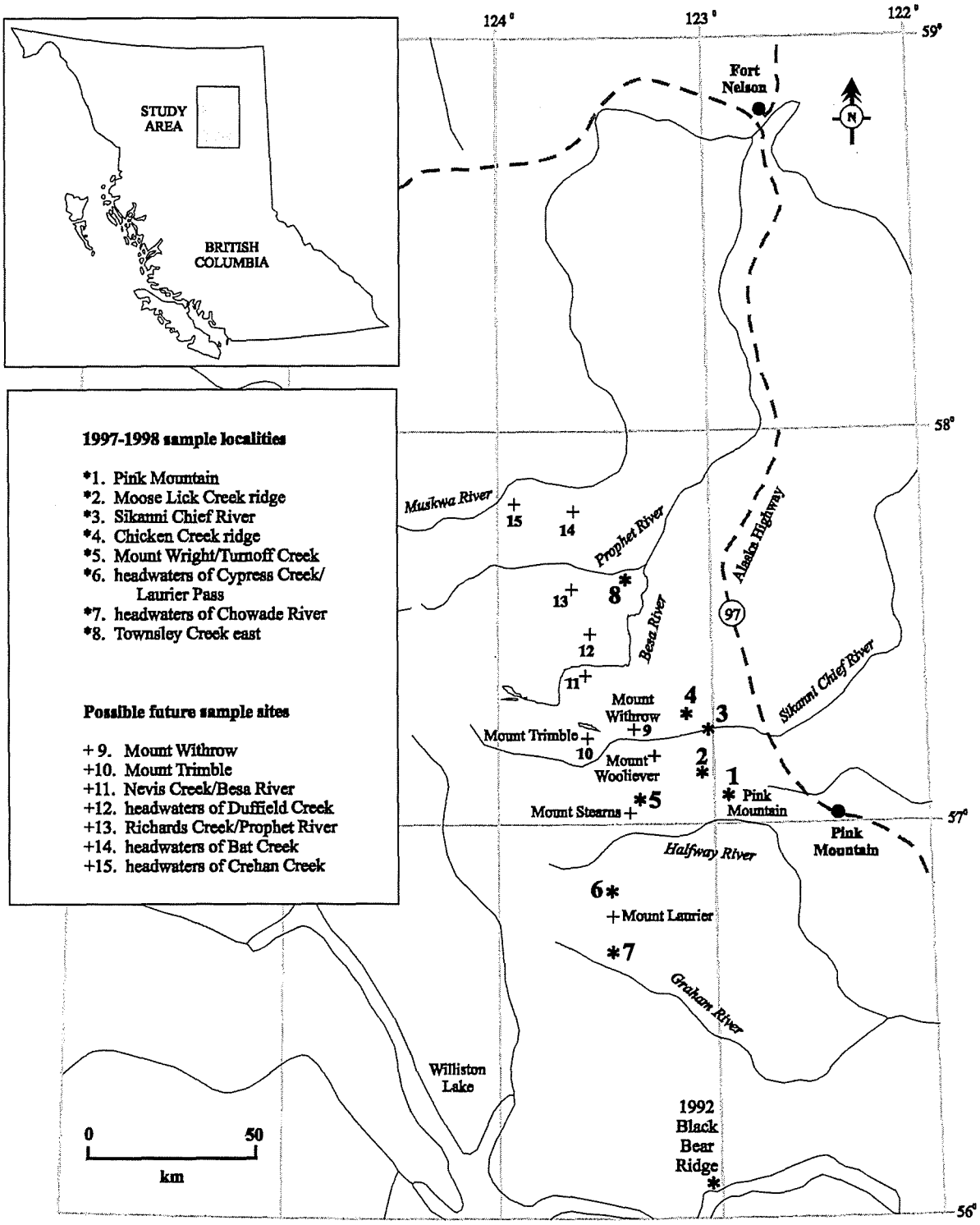

Figure 2. Index map of northeastern British Columbia illustrating sites where microfossil samples were collected in 1997 and 1998, and possible future collection sites.

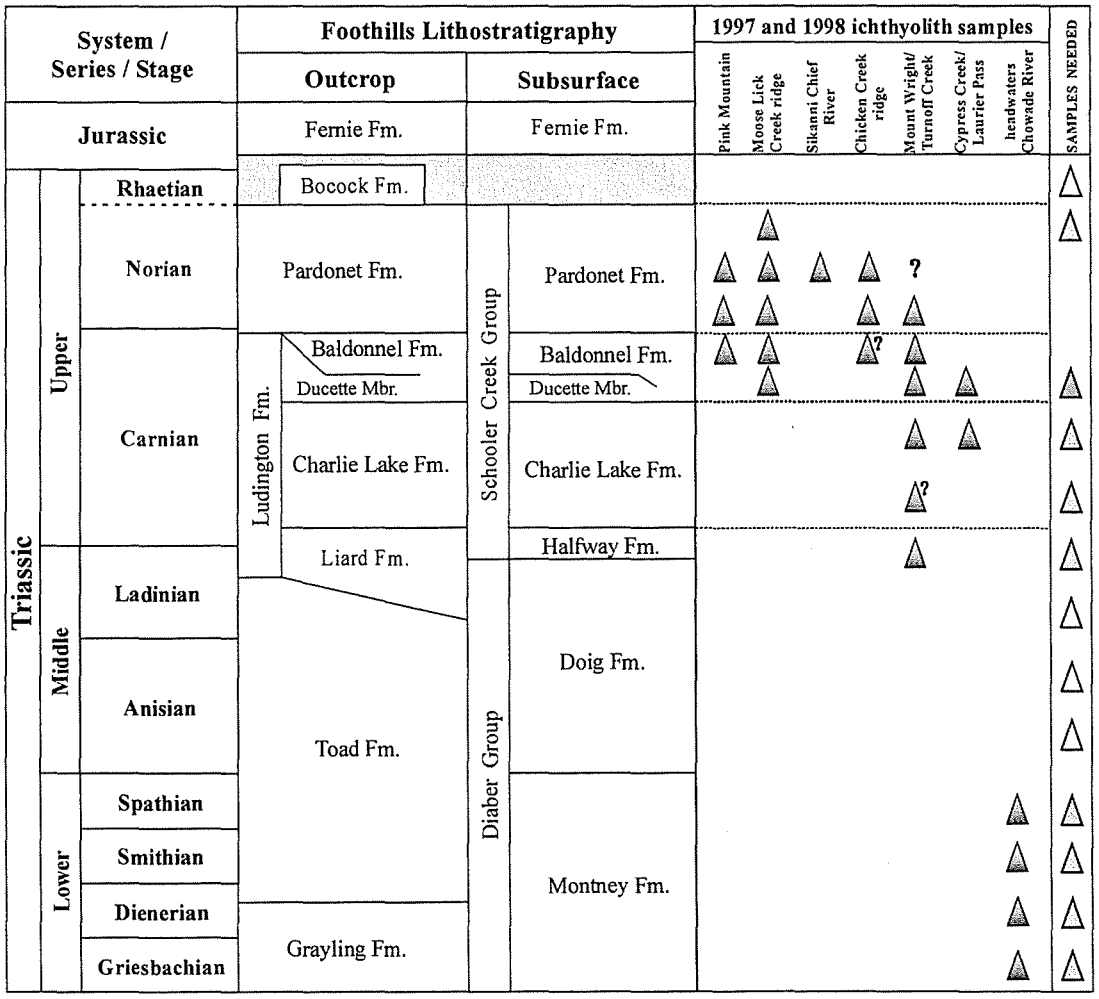

Figure 3.

Triassic stratigraphy of northeastern British Columbia (after Gibson, 1993).

Indicates locations and geological formations sampled for ichthyoliths in 1997 and 1998. Good sample coverage is in the Middle and Lower Norian, and the Carnian.

The need for future ichthyolith samples is shown at the right. The least amount of triangle shading indicates the greatest need for samples.

Sampling in 1999 could focus on upper and middle Toad Formation strata (lower Ladinian, Anisian, and Spathian) so that the ichthyolith zonation could be extended below the Ladinian.

ICHTHYOLITH FAUNAS

Limestone and shale samples collected in 1998 are currently being processed and picked. Preliminary results are based on good ichthyoliths recovered from eleven 1997 spot-samples collected at Pink Mountain and Moose Lick Creek ridge, and some of the first processed samples from each of the 1998 sites (Fig. 2). Early results indicate excellent ichthyolith data for Norian, Carnian, and Ladinian studies.

New ichthyoliths (Fig. 4) have been recovered from samples in the Upper Norian at Moose Lick Creek ridge. The specimens are small (200-300 microns) and consist of elasmobranch (shark) teeth and scales. In addition, two other new ichthyolith assemblages are thought to be Lower Norian and/or Upper Carnian (Fig. 5). One of these assemblages recovered from samples at Pink Mountain contains new elasmobranch scales. A second slightly older fauna consists mainly of elasmobranch teeth that were found at Moose Lick Creek and Chicken Creek ridges.

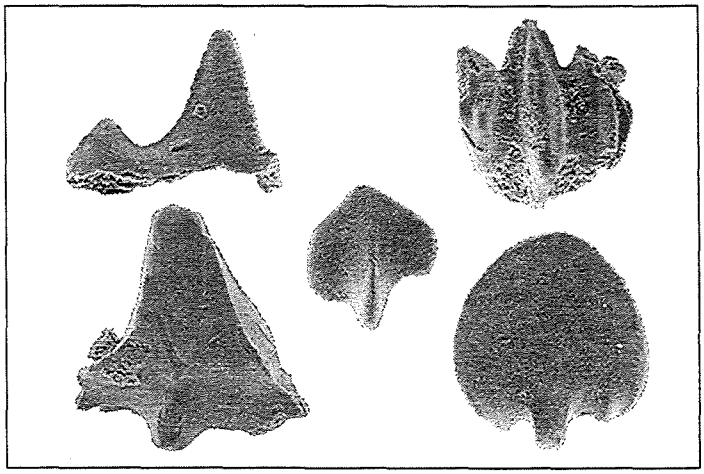

Figure 4. Unidentified new species of Upper Norian ichthyoliths from Moose Lick Creek ridge, GSC. Loc. C-303449.

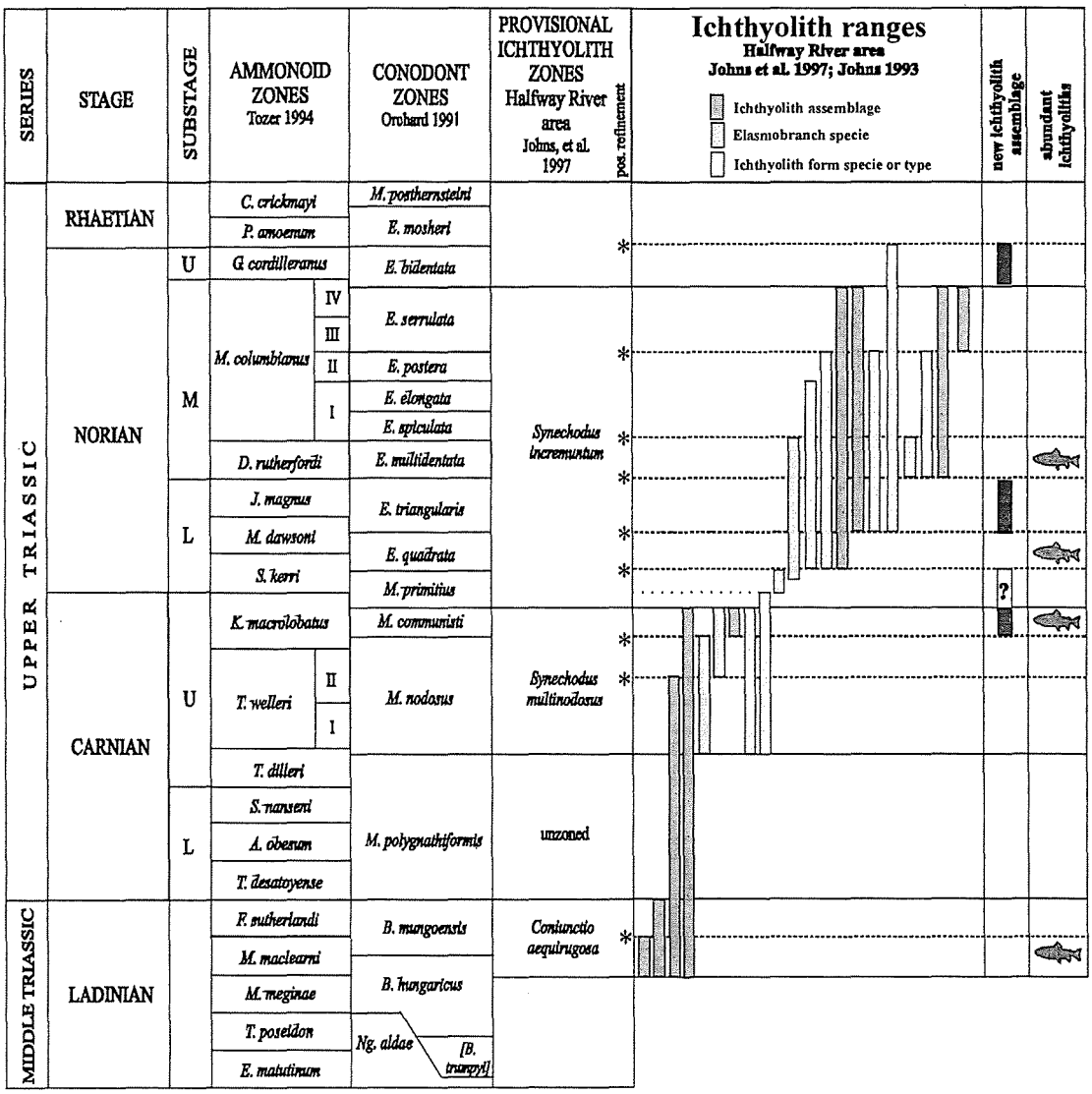

Figure 5.
A provisional ichthyolith zonation (Johns et al., 1997) is calibrated with the conodont (Orchard, 1991) and ammonoid (Tozer, 1994) zonations.

Possibilities for refinement of the ichthyolith zonation (*) will be based on good recovery from 1997/98 samples of previously and newly identified ichthyoliths.

New ichthyoliths have been found in the Upper Norian, uppermost Lower Norian, and near the Norian/Carnian boundary.

Some beds of ichthyoliths are extremely abundant and appear to be widespread. They occur in the lowermost Middle Norian, Lower Norian, uppermost Upper Carnian, and the upper Ladinian.

Some beds in the Middle and Upper Triassic contain abundant ichthyoliths (Fig. 5) that are correlated in the Halfway River and Trutch areas and also correspond to known sequence boundary events in the Western Canada Sedimentary Basin. Abundant upper Ladinian ichthyoliths (*Coniunctio aequirugosa* ichthyolith Zone) are currently known from sections in the Halfway River area and the Trutch Mount Wright section. Ichthyoliths near the Norian/Carnian boundary (lower Pardonet and upper Baldonnel formations) in the Halfway River area show a significant change that is indicated by the disappearance of the *Synechodus multinodosus* ichthyolith Zone fauna in the Carnian, appearance of the *Synechodus incrementum* ichthyolith Zone fauna in the Lower Norian, and an extremely abundant bed of *Birgeria* sp. teeth in the Lower Norian. This *Birgeria* sp. bed is widespread and found at locations in the Halfway River area, at Pine Pass to the south, and at Pink Mountain and Mount Wright (Trutch map). Early Middle Norian ichthyoliths of the *Synechodus incrementum* ichthyolith Zone are abundant, diverse, and also occur at several locations in the Halfway River map area and in the Trutch area at Pink Mountain, Moose Lick Creek ridge, Sikanni Chief River, and Chicken Creek Ridge.

There may be several reasons for ichthyolith abundant beds. Some examples include: a lag deposit at the contact of two sedimentary facies; winnowing and concentration of coarser, heavier, and more resistant particles; concentration resulting from long periods of slow deposition; and mass mortality perhaps caused by upwelling and associated phytoplankton blooms, biogenic toxins, and/or anoxia. With future study and sampling in NEBC, ichthyolith fauna types, abundance, and preservation, as well as ichthyolith-bearing strata and bed lithology, will be analyzed in more detail so that interpretations can be made on facies type and depositional environment. In addition, it would be interesting to sample Triassic subsurface core materials to see if ichthyolith abundant beds and zones correlate with high gamma log deflection levels measured in subsurface wells.

Comparison of Triassic ichthyoliths from NEBC ancestral North America strata with suggested Panthallasan terrane strata is an important future study. Observations of ichthyoliths recovered from the Upper Triassic Tyaughton Formation (Cadwallader terrane) and the Nicola Group (Quesnellia) in southern British Columbia show good ichthyolith recovery, unique new faunas, and also some common faunas with NEBC.

THERMAL MATURATION STUDIES

Conodonts show progressive and irreversible chemical and colour change in response to burial time and thermal conditions in sedimentary basins (Epstein et al., 1977; Legall et al., 1981; Nowlan and Barnes, 1987; Rejebian et al., 1987; Orchard and Forster, 1991). This is useful for assessing organic maturation and hydrocarbon potential (Fig. 6).

CAI	Temperature °C	Hydrocarbon generation	Conodont and ichthyolith alteration range
1.0	- 50	under-mature	
1.5	50 - 90	early dry gas, wet gas, oil	
2.0	60 - 140	heavy to light oil, wet gas	
3.0	110 - 200		
4.0	190 - 300	dry gas	Moose Lick Creek ridge and Pink Mountain
5.0	300 - 480	barren	
6.0	360 - 550		
6.5	440 - 610		
7.0	480 - 720		
8.0	600 -		

Figure 6. Correlation of temperature values with conodont colour alteration index (CAI) ranges (Epstein et al., 1977; Rejebian et al., 1987), hydrocarbon generation values (Legall et al., 1981), and conodont and ichthyolith colour alteration range from samples at Moose Lick Creek ridge and Pink Mountain.

Like conodonts, ichthyoliths show similar colour change patterns in response to heating. An actinopterygian (bony fish) tooth, *Birgeria* sp.1 is particularly useful for colour and thermal analyses.

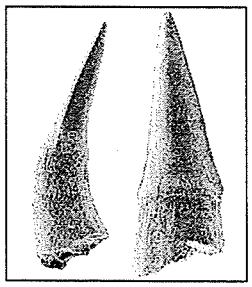

Figure 7.
Two orientations and specimens of *Birgeria* sp. 1

Birgeria sp. 1 has a simple form, is abundant, and is long ranging – it occurs in most of the samples so far studied in the Middle and Upper Triassic (Fig. 7). Using this species in thermal assessments will provide consistent results. An ichthyolith colour alteration index is currently under development.

Ichthyolith colour changes in northeastern British Columbia occur within a spectrum of conodont colour alteration indices (CAI) ranging from about 1.5 to 5.0 (Johns et al., 1997). Triassic samples from the eastern Peace Reach (Williston Lake, 94B) area containing both ichthyoliths and conodonts are less altered than those in western sections.

Initial analyses of ichthyolith colour in the 1997 spot samples (Fig. 6) correlate with a conodont CAI of 1.5 to 2.0 at Moose Lick Creek ridge and Pink Mountain. Both sites are in the oil window.

REFERENCES

Epstein, A.G., Epstein, J.B., and Harris, L.D.
1977: Conodont color alteration - an index to organic metamorphism; U.S. Geological Survey Professional Paper 995, United States Department of the Interior, 27 p.

Gibson, D.W.
1993: Upper Triassic coquina channel complexes, Rocky Mountain foothills, northeastern British Columbia; Bulletin of Canadian Petroleum Geology, v. 41, no. 1, p. 57-69.

Johns, M.J., Barnes, C.R., and Orchard, M.J.
1997: Taxonomy and biostratigraphy of Middle and Late Triassic elasmobranch ichthyoliths from northeastern British Columbia; Geological Survey of Canada, Bulletin 502, 235 p., 38 pl., 14 fig.

1999: Triassic ichthyolith biostratigraphy and regional thermal maturation studies, Trutch and Halfway map areas, northeastern British Columbia; in Current Research 1999-A, Geological Survey of Canada.

Legall, F.D., Barnes, C.R., and Macqueen, R.W.
1981: Thermal maturation, burial history and hotspot development, Paleozoic strata of southern Ontario – Quebec, from conodont and acritarch colour alteration studies; Bulletin of Canadian Petroleum Geology, v. 29, no. 4, p. 492-539.

Nowlan, G.S. and Barnes, C.R.
1987: Thermal maturation of Paleozoic strata in eastern Canada from conodont colour alteration index (CAI) data with implications for burial history, tectonic evolution, hotspot tracks and mineral and hydrocarbon exploration; Geological Survey of Canada, Bulletin 367, 47 p.

Orchard, M.J.
1991: Upper Triassic conodont biochronology and new index species from the Canadian Cordillera; in Ordovician to Triassic Conodont Paleontology of the Canadian Cordillera, M.J. Orchard and A.D. McCracken (ed.), Geological Survey of Canada, Bulletin 417, p. 299-335.

1999: Triassic conodont biostratigraphy and Upper Triassic stratigraphy, Trutch map area, British Columbia; in Current Research 1999-A, Geological Survey of Canada.

Orchard, M.J. and Forster, P.J.L.
1991: Conodont colour and thermal maturity of the late Triassic Kunga Group, Queen Charlotte Islands, British Columbia; in Evolution and Hydrocarbon Potential of the Queen Charlotte Basin, British Columbia, G.J. Woodsworth (ed.); Geological Survey of Canada, Paper 90-10, p. 453-464.

Rejebian, V.A., Harris, A.G., and Huebner, J.S.
1987: Conodont color and textural alteration: An index to regional metamorphism, contact metamorphism, and hydrothermal alteration; Geological Society of America Bulletin, v. 99, p. 471-479.

Tozer, E.T.
1994: Canadian Triassic ammonoid fauna; Geological Survey of Canada, Bulletin 467, 663 p., 148 pl.

A Re-Examination of the Type Section of the Backbone Ranges Formation, Mackenzie Mountains, NW Canada: Stratigraphic and Tectonic Implications

Robert B. MacNaughton[1], Guy M. Narbonne, and Robert W. Dalrymple
Department of Geological Sciences, Queen's University
Kingston, Ontario, CANADA K7L 3N6
([1]E-mail: macnaugh@geol.queensu.ca)

INTRODUCTION

The Backbone Ranges Formation is one of the most widely recognized but poorly understood formations in the Mackenzie Mountains. The type section was defined by Gabrielse *et al.* (1973) and remeasured by Fritz (1982), but both studies were at a reconnaissance level and did not utilize sequence stratigraphy or process sedimentology. The type section has not yielded fossils, and hence its age can only be bracketed between the early Ediacarian (terminal Neoproterozoic) Sheepbed Formation below and the Middle Cambrian Avalanche Formation above. Strata referred to the Backbone Ranges Formation in the June Lake area (100 km to the northwest) contain a rich assemblage of sub-trilobite Lower Cambrian trace fossils (Fritz, 1980; Fritz et al., 1983; MacNaughton and Narbonne, 1999), but correlation of these strata with the formation's type section is controversial (e.g. Aitken, 1984, 1989; Fritz *et al.*, 1984, 1991).

Despite these uncertainties, the type area of the Backbone Ranges Formation has been thought to hold a key to interpreting the age of breakup of the western margin of Laurentia. Early Cambrian extensional tectonism is well documented in the southern Canadian Cordillera (Devlin and Bond, 1988; Devlin, 1989; Lickorish and Simony, 1995; Warren, 1997), and has been interpreted by some of these authors as evidence for earliest Cambrian separation of western Laurentia (but see Ross, 1991, for a conflicting interpretation). In contrast, evidence of deep-water passive-margin sedimentation (including true turbidites and contourites) in the Sheepbed Formation led Dalrymple and Narbonne (1996) to support Ross' (1991) view that continental separation occurred earlier in the Neoproterozoic, and that by middle Ediacarian time northwestern Canada was separated from its conjugal margin by a significant distance of ocean floor. Despite ongoing investigations over nearly thirty years, the only report of possible Early Cambrian extensional tectonics from the Mackenzie Mountains is Fritz's (1982) report of rapid thickness variations and synsedimentary breccias (interpreted as mass flow deposits) in the upper

member of the Backbone Ranges Formation at its type section and at the Brokenskull River section 30 km to the south. These have been interpeted as indicating latest-Neoproterozoic to earliest-Cambrian syn-depositional normal faulting (Fritz, 1982; Fritz *et al.*, 1991).

In an effort to clarify these issues, and as part of our group's project to develop a Neoproterozoic-Cambrian sequence-stratigraphic framework for northwestern Canada (Dalrymple and Narbonne, 1996; MacNaughton *et al.*, 1997, 1998), we spent ten days in the summer of 1998 restudying the the type section of the Backbone Ranges Formation. In this contribution we present a preliminary report of the sedimentological and sequence-stratigraphic results of this study. Based upon our observations, we propose a novel lithostratigraphic correlation scheme for these strata and comment on their probable tectonic significance.

THE CORRELATION PROBLEM

The type section of the Backbone Ranges Formation lies within the Brokenskull anticline, several kilometres north of Avalanche Lake and about forty kilometres east of the Brokenskull River (Figure 1). The type section (Figure 2) consists of three informal members— a basal, quartz arenite-dominated member (approx. 270 m thick), a middle dolostone member (approx. 200 m thick), and an upper quartz arenite member (approx. 850 m thick) that are readily mappable throughout the Brokenskull anticline (Gabrielse *et al.*, 1973). However, the type section has proven undatable and the three members cannot be physically traced from the Brokenskull anticline into other structural panels. The type section lies above the siltstone-dominated Sheepbed Formation and the upper contact of the Backbone Ranges Formation is with the Middle Cambrian Avalanche Formation. Regional stratigraphic correlations indicate that the latter contact represents a significant disconformity (Gabrielse *et al.*, 1973, Fritz *et al.*, 1991).

This succession is different from the relatively complete succession preserved in the June Lake and Sekwi Brook areas (Figure 1), where formations (Figure 2) are readily datable using fossils and C-isotope chemostratigraphy. In these areas, the Sheepbed Formation is a unit of continental-slope origin (Dalrymple and Narbonne, 1996) that contains Ediacaran body fossils (Narbonne and Aitken, 1990; Narbonne, 1994) and distinctive C-isotopic signatures (Narbonne *et al.*, 1994) indicative of an early Ediacarian (terminal Neoproterozoic, ca. 590-550 Ma) age. The succession between the Sheepbed Formation and the Cambrian contains additional units

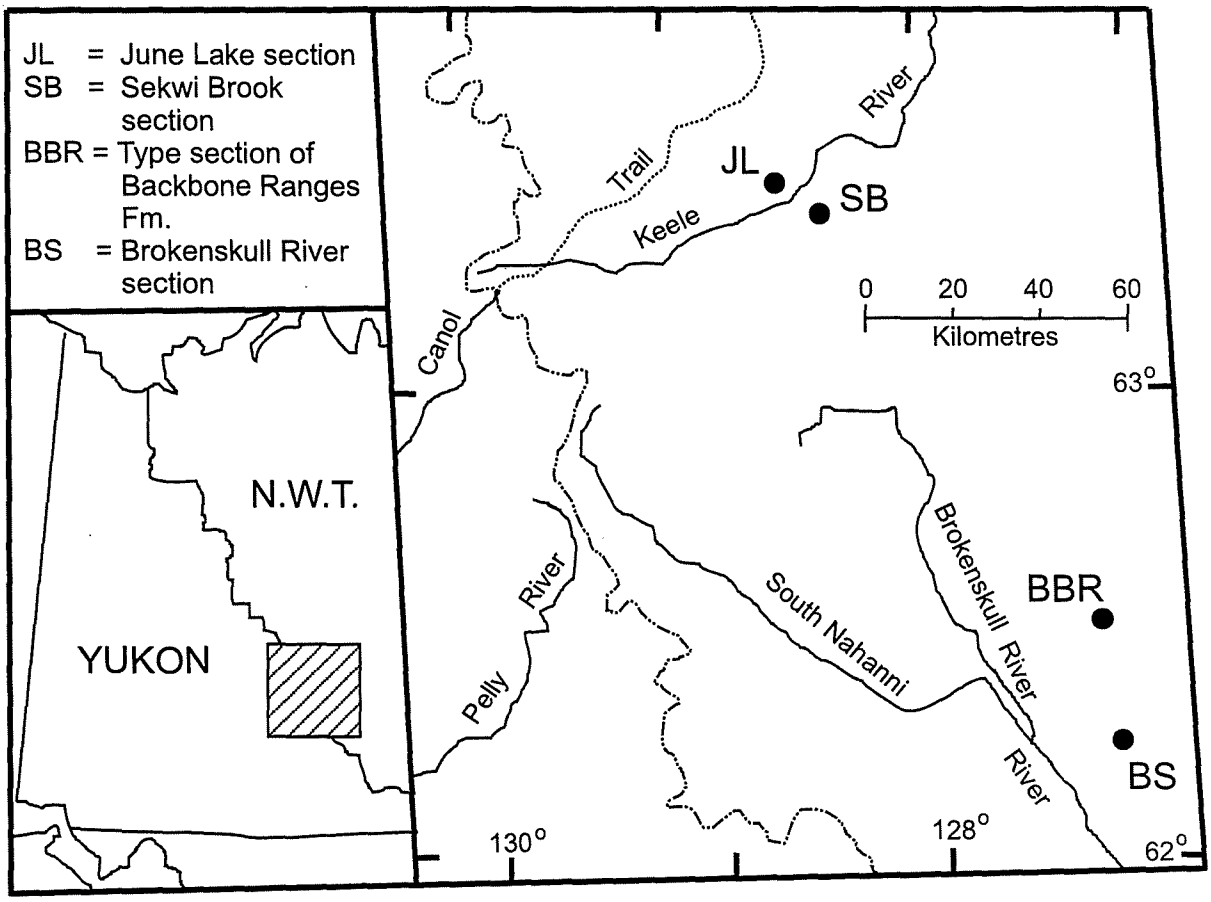

Figure 1: Map showing the location of the stratigraphic sections referred to in this paper. Dashed line shows the position of the Yukon-Northwest Territories border. SNORCLE seismic reflection corridor 31 begins along the Canol Trail, at the western edge of the map area, and continues to the west.

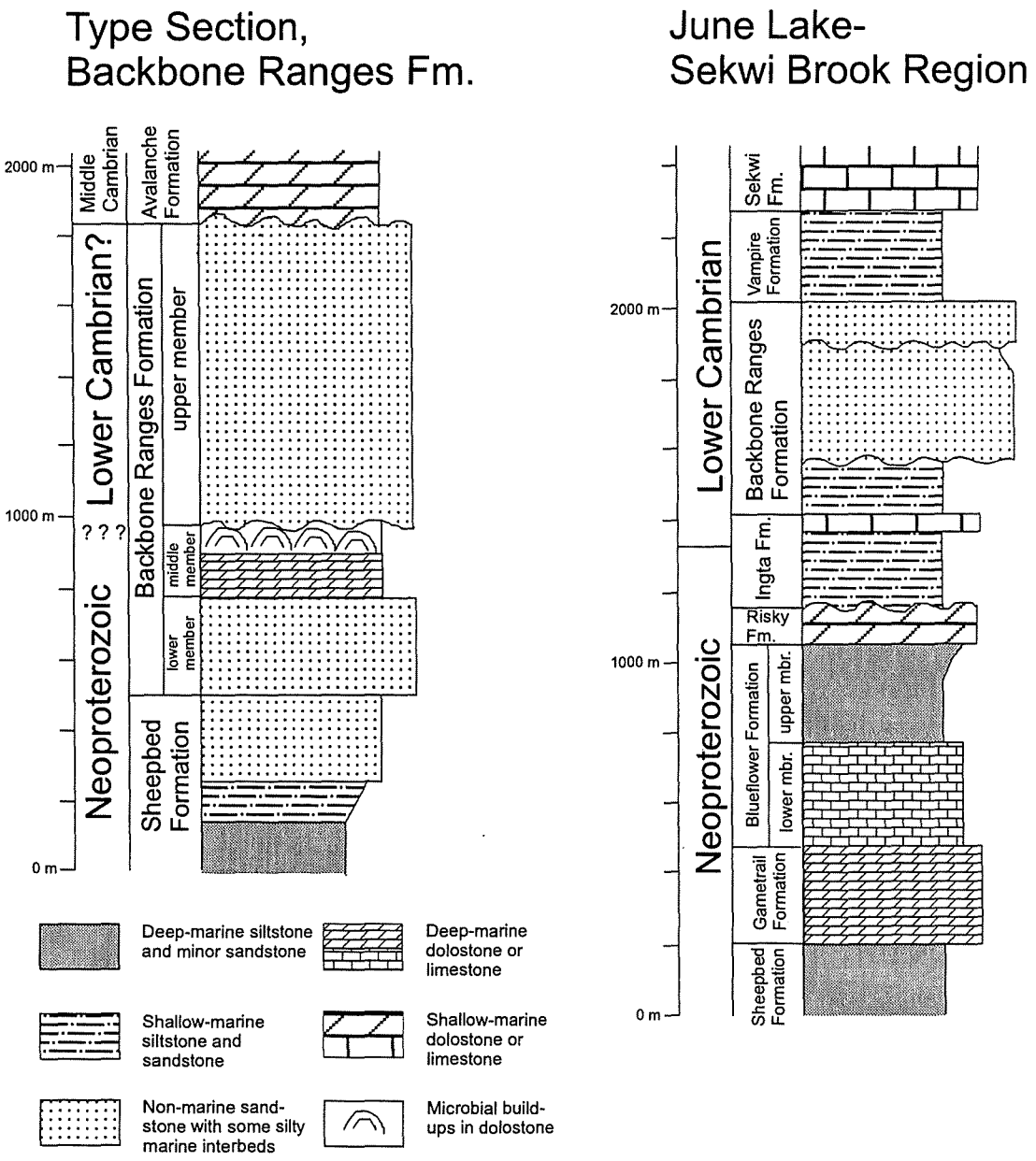

Figure 2: Simplified stratigraphic sections for the type section of the Backbone Ranges Formation (left) and for the June Lake-Sekwi Brook region (right). Note the much larger number of stratigraphic units in the latter area. Lithostratigraphy for Backbone Ranges Formation based on Gabrielse *et al.* (1973), Fritz (1982), and our field work: lithostratigraphy for June Lake-Sekwi Brook after Aitken (1989), Narbonne and Aitken (1995), Dalrymple and Narbonne (1996), MacNaughton *et al.* (1997), and our field work. Position of Neoproterozoic-Cambrian boundary in June Lake-Sekwi Brook region based on trace-fossil assemblages reported by MacNaughton and Narbonne (1999).

(Narbonne and Aitken, 1995). In ascending order, these are the Gametrail Formation (continental slope carbonates), the Blueflower Formation (slope-carbonate lower member and slope-siliciclastic upper member), the Risky Formation (shelf carbonates and sandstones), the Ingta Formation (distal-shelf, fine siliciclastics), the "Backbone Ranges Formation" (shallow-shelf to non-marine siliciciclastics), and the Vampire Formation (mid-shelf, fine siliciclastics). The first trilobites (*Fallotaspis* Zone) occur high in the Vampire Formation, which is conformably overlain by the Sekwi Formation, a carbonate-dominated unit containing *Bonnia-Olenellus* and *Nevadella* Zone trilobites (Fritz, 1980). A mild disconformity separates the Sekwi Formation from the overlying Middle Cambrian Hess River Formation (Fritz *et al.*, 1991). The sub-Cambrian unconformity in this region occurs at the top of the Risky Formation.

The differences in stratigraphic succession between the June Lake-Sekwi Brook region and the type section of the Backbone Ranges Formation may simply indicate very different depositional histories. However, they may also indicate erosional removal of several units in the type area of the Backbone Ranges Formation, perhaps in response to tectonic events. Any effort to determine which is the case requires accurate correlation of the two successions. Fritz *et al.* (1991) correlated the middle member with the Risky Formation (Figure 2), and proposed raising the Backbone Ranges Formation to group status. In this view, the lower member of the Backbone Ranges Formation would correlate with the siliciclastic-dominated upper member of the Blueflower Formation. The upper member of the Backbone Ranges Formation would be correlative with some or all of the Ingta, Backbone Ranges, and Vampire formations. (The Gametrail Formation and the carbonate-dominated lower member of the Blueflower Formation would seem to be absent from the Brokenskull River region under this interpretation.) Our observations in the type section and in the June Lake-Sekwi Brook region suggest another correlation that should resolve certain difficulties inherent in the present correlation.

DESCRIPTION OF THE TYPE SECTION

The type section of the Backbone Ranges Formation (Figure 2) contains deposits of numerous siliciclastic and carbonate depositional environments. Here, we provide a brief, preliminary description of the section's sedimentology and sequence stratigraphy, as determined from our 1998 field observations.

The oldest strata examined in the immediate vicinity of the type section are in the Sheepbed Formation. In this area the lower part of the Sheepbed Formation consists of several hundred metres of dark brown to grey siltstone and shale of marine (possibly upper-slope to distal-shelf) origin. The upper part of the Sheepbed Formation consists of roughly 350 m of interbedded siltstone and quartz sandstone that define an overall upward-coarsening succession. The sandstones in this part of the Sheepbed Formation contain hummocky and swaley cross-stratification, indicating shoreface deposition. Trough cross-bedded fluvio-deltaic sandstones become common near the formation's top. This facies appears abruptly in the succession and a sequence boundary is probably present at the level of its first appearance.

The contact with the overlying Backbone Ranges Formation is gradational. The lower member of the Backbone Ranges Formation is at least 350 m thick and is dominated by medium to thick-bedded quartz sandstone with lesser siltstone. The sandstones display a variety of sedimentary structures indicating deposition in environments ranging from shallow, storm-influenced shelf to tidal-channel to fluvio-deltaic (including floodplain). With the exception of rare thin dolostone beds, the lower member is composed entirely of siliciclastic material. Evidence for subaerial exposure (mudcracks, redbeds, and variably developed paleosols) is present throughout the member but is best developed in its upper 150 m.

The middle member is approximately 200 m thick and is characterised by orange- to pink-weathering microcrystalline dolostone. Its base is abrupt and locally marked by a thin conglomerate of reworked siltstone clasts that probably represents erosional reworking of underlying beds during transgression. The basal 10 to 20 m of the member contain hummocky cross-stratification and edge-wise flat-pebble conglomerates that were probably deposited in a mid-ramp setting above storm wave-base. The middle part of the member (at least 80 m thick) lacks wave-formed structures, contains abundant soft-sediment slump folds, and was probably deposited below storm wave-base in an outer ramp setting. This in turn is overlain by roughly 60 m of shallow-marine dolostone containing hummocky cross-stratification and flat-pebble conglomerates that passes upward into a complex of stromatolite mounds. Individual mounds range from 1 to greater than 20 m in diameter and have coalesced laterally and stacked to form a continuous, 60 m-thick unit of stromatolitic dolostone. The top of this mound complex is a major sequence boundary that is marked by a 30 to 40 m unit of breccia consisting of angular

boulders up to 3 m in diameter in a matrix of fine-grained quartz sandstone. Solution-collapse cavities displaying keystone-collapse breccias and karst pipes up to 22 m deep into the underlying stromatolite mounds also attest to a long period of surface and subsurface karst. Five metres of flat-laminated to hummocky cross-stratified sandstone separate this karst surface from the highest dolostones of the middle member (10 m thick), which also show evidence of karst, including up to 2 m of relief on their upper surface.

The upper member is 850 m thick and sits sharply on the upper surface of the middle member. The upper member is dominated by medium- to very thick-bedded quartz sandstone. Trough cross-bedding is abundant and shows unimodal paleocurrents, suggesting deposition in a sandy, braided-fluvial system. Rare, siltstone-dominated intervals with wave and current ripples and tidal rhymites represent marine incursions.

Conglomerates are common at several levels in the upper member. Some of the conglomerates contain metre-scale blocks of laminated mudstone and siltstone that lie at the base of fluvial channels. Comparable beds from a nearby section were described by Fritz (1982) and interpreted as mass-flow deposits (Fritz *et al.*, 1991). However, the conglomerates are not sufficiently muddy or disorganised to be debris flows. Also, in several cases they occur laterally adjacent to siltstone facies identical to the reworked blocks. Thus, the conglomerates are best interpreted as locally derived blocks of siltstone that were produced during bank collapse of fluvial channels, and as such have little or no tectonic significance.

No definite fossils have been found in the Backbone Ranges Formation in its type area.

ASSESSING THE PRESENT CORRELATION

The correlation scheme of Fritz *et al.* (1991) has two main arguments in its favour. First, it correlates two strongly developed disconformities: the sub-Cambrian unconformity above the Risky Formation in the June Lake-Sekwi Brook region (Narbonne and Aitken, 1995; MacNaughton *et al.*, 1998) and the karst surface atop the middle member of the type Backbone Ranges Formation. Second, for both regions this correlation produces a broadly similar succession, with two siliciclastic units separated by a dolomitic unit.

However, there are several difficulties with this proposal. First, Aitken (1989) has argued that the Risky Formation and the middle member of the Backbone Ranges Formation contain

very different carbonate facies, a contention we support. The Risky Formation consists, in large part, of oolitic and pisolitic carbonate, with abundant quartz sand (including sandstone and dolomitic sandstone), whereas these facies are essentially absent from the middle member of the Backbone Ranges Formation.

Second, the correlation produces additional stratigraphic complications. It implies that the Gametrail Formation and the Blueflower Formation's carbonate-dominated lower member are absent in the Brokenskull River area, an interpretation that seems unlikely in view of their kilometre-scale thickness in the Sekwi Brook area (Figure 2) and the apparent absence of a significant disconformity in the lower member of the Backbone Ranges Formation. This correlation also implies that, in the Brokenskull River region, the time of greatest erosion was partway through the deposition of the Windermere Supergroup, whereas elsewhere in the Mackenzie Mountains the greatest erosion occurred at the end of Windermere deposition, before the onset of basal Cambrian deposition (Aitken, 1989; Narbonne and Aitken, 1995).

Third, in the June Lake-Sekwi Brook area, the Risky Formation represents shallow-shelf conditions and the underlying Blueflower Formation is slope-deposited unit. The upward transition is thus regressive. By contrast, the lower member of the Backbone Ranges Formation contains shallow-marine to non-marine facies and the middle member is of deep ramp origin. The upward transition here is transgressive, the opposite of that in the suggested correlative units.

AN ALTERNATE CORRELATION

In view of these difficulties, we suggest an alternate possibility (Figure 3). The Gametrail Formation (and the basal part of the Blueflower Formation) show several similarities with the middle member of the Backbone Ranges Formation. These include a predominantly thin-bedded depositional style and an absence of ooids or other coated carbonate grains. As a result, the Gametrail Formation provides a better homotaxial correlation with the middle member than does the Risky Formation. A correlation between the middle member and the Gametrail Formation is also supported by the transgressive Sheepbed-to-Gametrail transition, which corresponds to transgression from the lower member into the middle member.

In the Sekwi Brook region, the upper part of the Sheepbed Formation was deposited during a lowstand and contains a sequence boundary (Dalrymple and Narbonne, 1996). In the

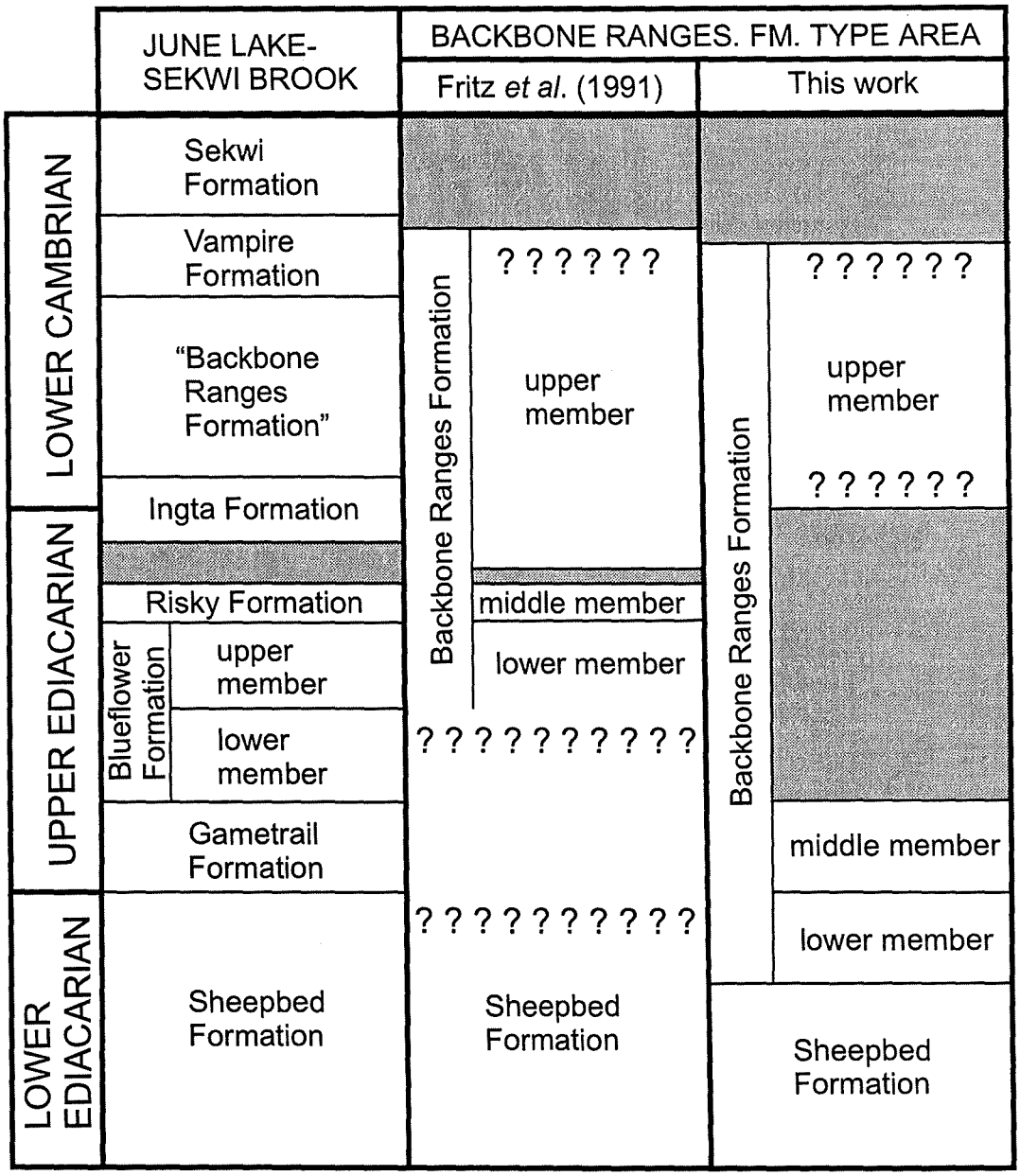

Figure 3: Comparison of two proposed correlations between the type section of the Backbone Ranges Formation and the well-constrained June Lake-Sekwi Brook succession. Note that Fritz *et al* (1991) did not propose specific correlations for units below the middle member of the Backbone Ranges Formation. Times of non-deposition and erosion are shown in grey.

Brokenskull River region, the upper part of the Sheepbed Formation and the lower member of the Backbone Ranges Formation are also regressive deposits. Additionally, there is almost certainly a sequence boundary in the upper part of the Sheepbed Formation, as indicated by the transition from relatively distal marine into non-marine facies. Thus, the Sheepbed Formation of the Sekwi Brook region is probably equivalent to the Sheepbed Formation and lower member of the Backbone Ranges Formation of the Brokenskull anticline region. This proposal is further supported by the robust correlation of the underlying Ice Brook Formation and/or Tepee Dolomite that underlie the Sheepbed Formation in both regions (Gabrielse *et al.*, 1973; Dalrymple and Narbonne, 1996; and field observations).

The absence of the Risky Formation and of part or all of the Blueflower Formation in the Brokenskull anticline is also accounted for under this proposal. The prominent karstic surface at the top of the middle member of the Backbone Ranges Formation presumably marks the erosional removal (or non-deposition) of the units. (The compound nature of this surface may indicate more than one episode of exposure.) Thus, our proposal enables us to account for the absence of these formations by invoking erosion and non-deposition at the sub-Cambrian unconformity. This is consistent with the record of erosion preserved elsewhere in northwestern Canada: (Aitken, 1989; Narbonne and Aitken, 1995). Precise correlation of the Backbone Ranges Formation's upper member is uncertain due to lack of biostratigraphic constraint. However, it is probably equivalent to part or all of the the Ingta, Backbone Ranges, and Vampire formations in the June Lake region.

This correlation is not falsified by any data of which we are aware. Efforts to test it with carbon-isotope analysis of the middle member (and isolated carbonate beds in the lower member) have not produced reliable results, probably because of diagenetic overprinting during the karst episode at the end of deposition of the middle member.

STRATIGRAPHIC AND TECTONIC IMPLICATIONS

The correlations proposed herein reinforce the fact that the Backbone Ranges Formation, as presently defined, is a problematic unit. It apparently contains a disconformity between its middle and upper members that is equivalent to at least two, kilometre-scale, Neoproterozoic formations. In view of the important role it plays in basal Cambrian stratigraphy, a formal

reassessment of the formation's status is needed. Whether it is preferable to abandon the name or to redefine it is a matter for further consideration. However, we believe the well-characterised and well-dated earliest Cambrian quartz arenites in the June Lake-Sekwi Brook region that are currently assigned to the Backbone Ranges Formation (Aitken, 1989; MacNaughton *et al.*, 1997), should probably be given a new and distinctive name. We can see no advantage in elevating the Backbone Ranges Formation to group status, as suggested by Fritz *et al.* (1991).

Our observations also imply that the Brokenskull River region, in common with much of northwestern Canada, was an area of net erosion and/or nondeposition during the late Neoproterozoic and earliest Cambrian. The strong karst features atop the middle member suggest prolonged, and possibly repeated, subaerial exposure during this interval.

Finally, our observations indicate that the conglomerates and breccias in the upper member of the Backbone Ranges Formation are not mass-flow deposits. The reinterpretation of these conglomerates as coarse-grained fluvial deposits removes a major piece of evidence for latest Neoproterozoic to earliest Cambrian extensional tectonism in northwestern Canada. This lends further support to models that place the onset of rifting and the breakup of Rodinia in northwestern Canada at the same time as the onset of Windermere Supergroup deposition (Ross, 1991; Ross et al., 1995; Dalrymple and Narbonne, 1996).

ACKNOWLEDGEMENTS

This project was funded by a LITHOPROBE grant to GMN and RWD and by NSERC Operating Grants to GMN and RWD. Donald Simmons is thanked for cheerful and reliable assistance in the field. Tim Simmons provided stellar helicopter support and Erica Tamboline is thanked for daily wireless dispatches. We thank W.H. Fritz for his interest in this project, for freely sharing his own observations with us, and for his advice prior to the 1998 field season. We also gratefully acknowledge the consent granted to our research by various bodies in northwestern Canada.

REFERENCES

Aitken, J.D., 1984. Strata and trace fossils near the Precambrian-Cambrian boundary, Mackenzie, Selwyn, and Wernecke mountains, Yukon and Northwest Territories: Discussion. *Current Research, Part B, Geological Survey of Canada Paper 84-1B*, p. 401-407.

Aitken, J.D., 1989. Uppermost Proterozoic formations in central Mackenzie Mountains, Northwest Territories. *Geological Survey of Canada Bulletin 368*, 26 p.

Dalrymple, R.W., and Narbonne, G.M., 1996. Continental slope sedimentation in the Sheepbed Formation (Neoproterozoic, Windermere Supergroup), Mackenzie Mountains, N.W.T. *Canadian Journal of Earth Sciences*, v. 33, p. 848-862.

Devlin, W.J., 1989. Stratigraphy and sedimentology of the Hamill Group in the northern Selkirk Mountains, British Columbia: evidence for latest Proterozoic-Early Cambrian extensional tectonism. *Canadian Journal of Earth Sciences*, v. 26, p. 515-533.

Devlin, W.J., and Bond, G.C., 1988. The initiation of the early Paleozoic Cordilleran miogeocline: evidence from the uppermost Proterozoic-Lower Cambrian Hamill Group of southestern British Columbia. *Canadian Journal of Earth Sciences*, v. 25, p. 1-19.

Fritz, W.H., 1980. International Precambrain-Cambrian Working Group's 1979 field study to MacKenzie Mountains, Northwest Territories, Canada. *Current Research, Part A, Geological Survey of Canada Paper 80-1A*, p. 41-45.

Fritz, W.H., 1982. Vampire Formation, a new upper Precambrian(?)/Lower Cambrian formation, Mackenzie Mountains, Yukon and Northwest Territories. *Current Research, Part B, Geological Survey of Canada Paper 82-1B*, p. 83-92.

Fritz, W.H., Cecile, M.P., Norford, B.S., Morrow, H., and Geldsetzer, H.H.J., 1991. Cambrian to Middle Devonian assemblages. In: H. Gabrielse and C.J. Yorath (eds.), *Geology of the Cordilleran Orogen in Canada.* Geological Survey of Canada, Geology of Canada no. 4, p. 151-218.

Fritz, W.H., Narbonne, G.M., and Gordey, S.P., 1983. Strata and trace fossils near the Precambrian-Cambrian boundary, Mackenzie, Selwyn, and Wernecke mountains, Yukon and Northwest Territories. *Current Research, Part B, Geological Survey of Canada Paper 83-1B*, p. 365-375.

Fritz, W.H., Narbonne, G.M., and Gordey, S.P., 1984. Strata and trace fossils near the Precambrian-Cambrian boundary, Mackenzie, Selwyn, and Wernecke mountains, Yukon and Northwest Territories: Reply. *Current Research, Part B, Geological Survey of Canada Paper 84-1B*, p. 409-412.

Gabrielse, H., Blusson, S.L., and Roddick, J.A., 1973. Geology of Flat River, Glacier Lake, and Wrigley Lake map-areas, District of Mackenzie and Yukon Territory. *Geological Survey of Canada, Memoir 366*, 153 p.

Lickorish, H.W., and Simony, P.S., 1995. Evidence for late rifting of the Cordilleran margin outlined by stratigraphic division of the Lower Cambrian Gog Group, Rocky Mountain Main Ranges, British Columbia and Alberta. *Canadian Journal of Earth Sciences*, v. 32, p. 860-874.

MacNaughton, R.B., Dalrymple, R.W., and Narbonne, G.M., 1997. Multiple orders of relative sea-level change in an earliest Cambrian passive-margin succession, Mackenzie Mountains, northwestern Canada. *Journal of Sedimentary Research*, v. B67, p. 622-637.

MacNaughton, R.B., and Narbonne, G.M., 1999. Evolution and ecology of Neoproterozoic-Lower Cambrian trace fossils, NW Canada. *PALAIOS*, in press.

MacNaughton, R.B., Narbonne, G.M., and Dalrymple, R.W., 1998. Developing a sequence-stratigraphic framework for the Neoproterozoic-Cambrian evolution of the northwestern margin of North America. In: F. Cook, and P. Erdmer (compilers), *Slave-Northern Cordillera Lithospheric Evolution (SNORCLE) Transect and Cordilleran Tectonics Workshop Meeting*. Lithoprobe Report no. 64, p. 109.

Narbonne, G.M., 1994. New Ediacaran fossils from the Mackenzie Mountains, northwestern Canada. *Journal of Paleontology*, v. 68, p. 411-416.

Narbonne, G.M., and Aitken, J.D., 1990. Ediacaran fossils from the Sekwi Brook area, Mackenzie Mountains, northwestern Canada. *Palaeontology*, v. 33, p. 945-980.

Narbonne, G.M., and Aitken, J.D., 1995. Neoproterozoic of the Mackenzie Mountains, northwestern Canada. *Precambrian Research*, v. 73, p. 101-121.

Narbonne, G.M., Kaufman, A.J., and Knoll, A.H., 1994. Integrated chemostratigraphy and biostratigraphy of the Windermere Supergroup, northwestern Canada: implications for Neoproterozoic correlations and the early evolution of animals. *Geological Society of America Bulletin*, v. 106, p. 1281-1292.

Ross, G.M., 1991. Tectonic setting of the Windermere Supergroup revisited. *Geology*, v. 18, p. 1125-1128.

Ross, G.M., Bloch, J.D., and Krouse, H.R., 1995. Neoproterozoic strata of the southern Canadian Cordillera and the isotopic evolution of seawater sulfate. *Precambrian Research*, v. 73, p. 71-99.

Warren, M.J., 1997. *Crustal extension and subsequent crustal thickening along the Cordilleran rifted margin of ancestral North America, western Purcell Mountains, southeastern British Columbia*. Queen's University (Kingston, Ont.), unpublished Ph.D. dissertation, 361 p.

TECTONOSTRATIGRAPHIC FRAMEWORK OF THE MESOPROTEROZOIC MUSKWA ASSEMBLAGE, NORTHERN BRITISH COLUMBIA.

D. G. F. Long, **J. R. Devaney**, Department of Earth Sciences, Laurentian University, Sudbury, Ont. P3E 2C6, dlong@nickel.laurentian.ca and **B. R. Pratt**, Department of Geological Sciences, University of Saskatchewan, Saskatoon, SK, S7N 5E2.

ABSTRACT.

Strata within the Mesoproterozoic Muskwa Assemblage in the Tuchodi Lakes area of northern British Columbia appear to have been developed by repeated progradation of storm-influenced carbonate and siliciclastic ramp facies over deeper water muds in an inner to outer shelf setting within an extensional or transtensional basin. Major transgressive phases may have been triggered by reactivation of basement faults during extension, rather than by large scale eustatic sea-level change. Persistent SW-facing paleoslopes are reflected by uniform orientation of gutter casts, domal stromatolites and rectilinear molar tooth structures. Orientation of cross-stratification and slump axes are less consistent. There is no evidence at present to suggest that a segmented continental margin was developed in the area prior to the Racklan orogeny. Basin closure at ~1.2 Ga, possibly related to far-field tectonic influences, is suggested by small-scale open folding of the sequence. This was followed by an extensional phase, marked by intrusion of as yet undated dikes which were later sheared during the Hayhook orogeny at ~0.8 Ga.

INTRODUCTION

Strata within the Muskwa Assemblage (Aitken and McMechan, 1991) are considered to be stratigraphic equivalents to Mesoproterozoic (1.7-1.2 Ga) strata in the middle and lower parts of the Belt-Purcell Supergroup in southeastern British Columbia and southwestern Alberta, and strata of the Wernecke Supergroup in north-central Yukon (Young et al., 1982; Aitken and McMechan, 1991). While the general stratigraphy of the succession has been outlined by Taylor and Stott (1973), study of the sedimentology of these units has been minimal. Bell (1966, 1968) recognised that at least part of the succession was of deep-water origin, a thesis supported in a brief review by Aitken (1975) and Aitken and McMechan (1991). In the Tuchodi Lakes area, the sequence is at least 6 km thick, and is thought to thin cratonwards in the subsurface to the NE and to the SE towards the Peace River arch (Fig. 1, 2).

SEDIMENTARY FRAMEWORK

Bell (1966, 1968), building on earlier mapping by Taylor (1963), divided the Precambrian rocks, first recognised by Williams (1944), into seven distinct formations (Fig. 2). Bell suggested that all of the preserved sequence was of probable Helikian age, and that an angular unconformity was present at the base of the Tetsa Formation.

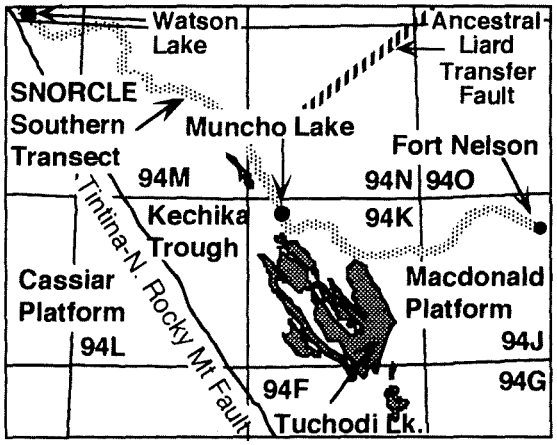

Fig 1. Distribution of Mesoproterozoic strata of the Muskwa Assemblage in the Tuchodi Lakes area.

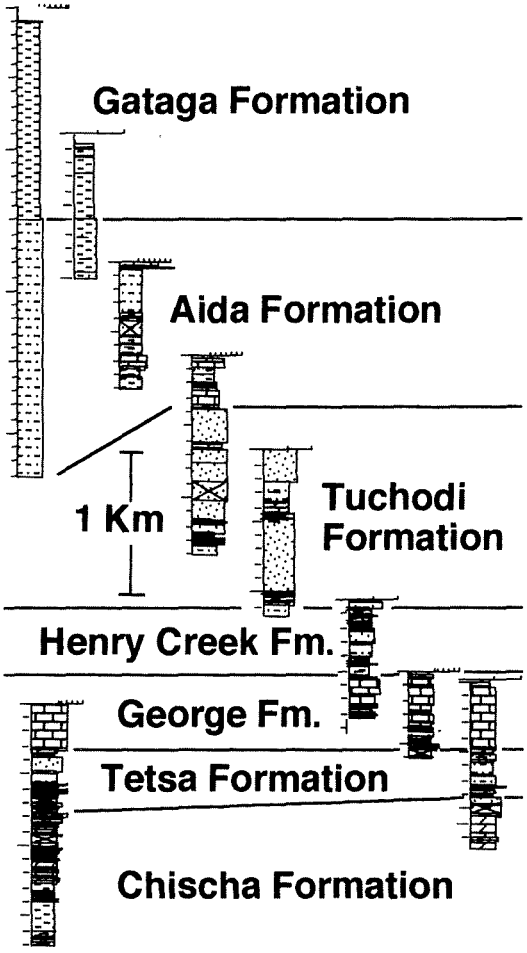

Fig 2. (Right) Stratigraphy of the Muskwa Group (after Bell 1968).

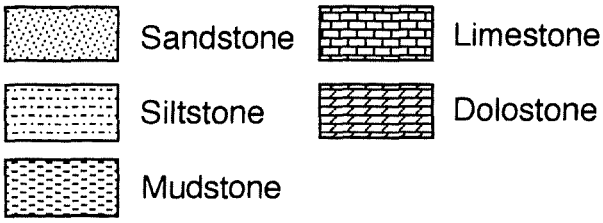

As the base of the sequence is not exposed, the total thickness of Neoproterozoic strata in the area remains unknown. New observations on the lower five formations are summarised below.

Chischa Formation.

The lowermost exposed strata in the Muskwa Assemblage are the Chischa Formation. This consists predominantly of fine grained dolomicrites, with stromatolites, flat-pebble conglomerates, gutter-casts and hummocky cross-stratification, indicating a shallow-water, storm-influenced ramp environment. Molar-tooth structures are abundant: these early pre-diagenetic features of enigmatic origin (Pratt, 1998; Furniss et al., 1998), in places resemble extensional vein arrays and parts of ductile shear zones which have subsequently undergone compaction and thinning. Our studies show that they have a preferred (shore-parallel) plan-view orientation of 130/310°, approximately 90° to the paleoslope direction of 220° indicated by gutter casts and 230° stromatolite elongation (Fig. 3). Fine-grained quartz arenites in the upper part of the Chischa Formation are characterised by abundant hummocky cross-stratification suggesting marked storm influence in water depths typically less than 30 m. Slump structures, scours and intraformational breccias at the top of the formation suggest major, perhaps catastrophic, collapse and deepening of the basin prior to

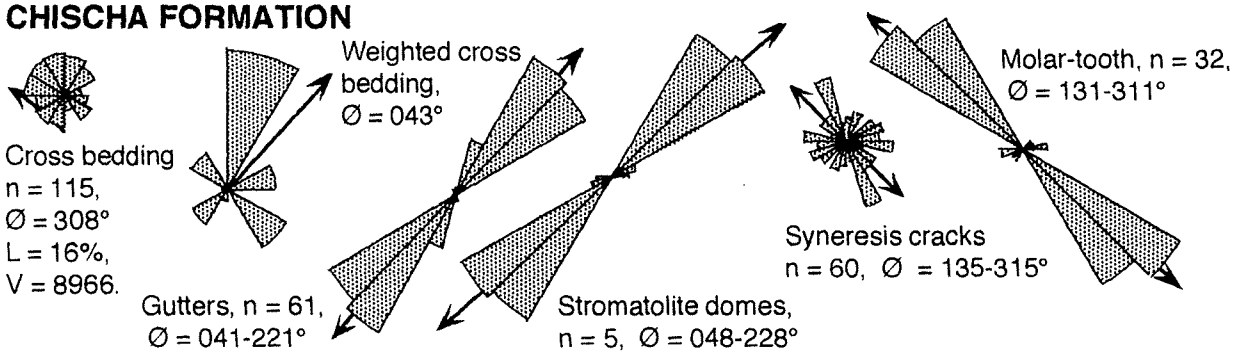

Fig. 3. Paleocurrent data for the Chischa Formation

deposition of the overlying Tetsa Formation.

Tetsa Formation.

Bell (1966, 1968) suggested that an angular unconformity exists between the Tetsa Formation and underlying strata of the Chischa Formation. Our observations indicate that the contact is essentially conformable. Sandstones at the top of the Chischa Formation appear to have been scoured and reworked by submarine density currents, with synchronous deposition of both channel and subaqueous levee facies following rapid (extensional-fault related) collapse of the basin. The contact at Bathtub Creek (Fig 4.) is a sharp, major flooding surface, with deep-water mudstones draped over the underlying topography. Conglomeratic strata in Bell's (1968) section 2 (unit 5) at Chischa River are here interpreted as coarse-grained sediment gravity-flow deposits. Siltstone, sandstone, dolostone and mudstone clasts in these conglomerates, and in conglomeratic sandstones in the Bathtub Creek section, were derived by reworking the upper few tens of metres of the Chischa Formation by scouring along the walls of submarine canyons developed across the footwall of a normal fault. The apparent absence of basement clasts suggests that fault displacement here, and further up the paleoslope, must have been only a few hundred metres.

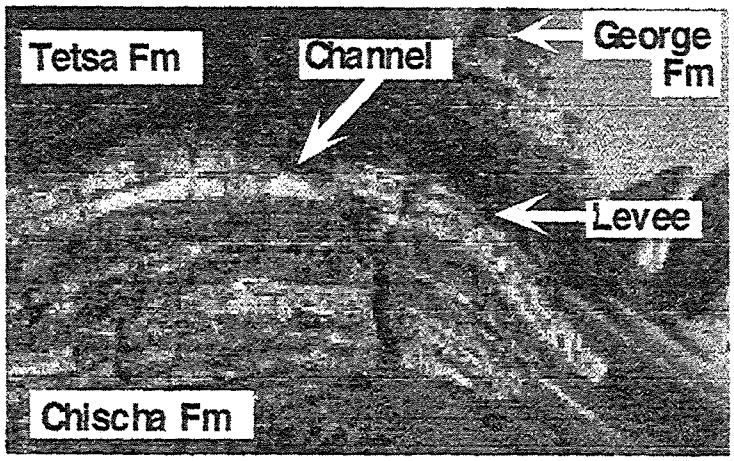

Fig. 4. Submarine channel at the top of the Chischa Formation, draped by mudstones of the Tetsa Formation, Bathtub Creek, 58°31'N, 124°39'W.

Mudstones at the base of the Tetsa Formation appear to have been deposited in a distal ramp setting, in waters more than a hundred metres deep. Thin beds of fine- and very fine-grained sandstone (quartz arenite) contain climbing ripples and other evidence of reworking by traction currents, reflecting geostrophic currents or storm-induced underflows rather than distal turbidites. Carbonate content increases up-section, as does evidence of soft-sediment deformation.

George Formation.

Strata of the Tetsa Formation are conformably overlain by muddy carbonates of the George Formation. These pass upsection from laminated carbonate mudstones with abundant soft-sediment deformation features, to predominantly thick-bedded carbonate-mudstones, with parallel lamination, ripple cross-lamination, hummocky cross-stratification, flat pebble conglomerates, stromatolites and abundant molar-tooth structures, reflecting deposition in a prograding ramp setting. Carbonate composition changes radically over short distances along strike, with limestones passing laterally to more steeply dipping dolostones within a few decimetres of faults (spaced at 200-300 m apart). Gutters indicate paleoslopes trending to 220°, with molar-tooth structures striking quasi-orthogonally at 150/330° (Fig. 5). Aitken and McMechan (1991) note the presence of diamictite-like beds near the top of the formation. These are of uncertain origin and were not seen in 1998. They may be fluvial or tidal channel fills, related to partial exposure of the ramp, or may be deeper-water debris flows or seismites.

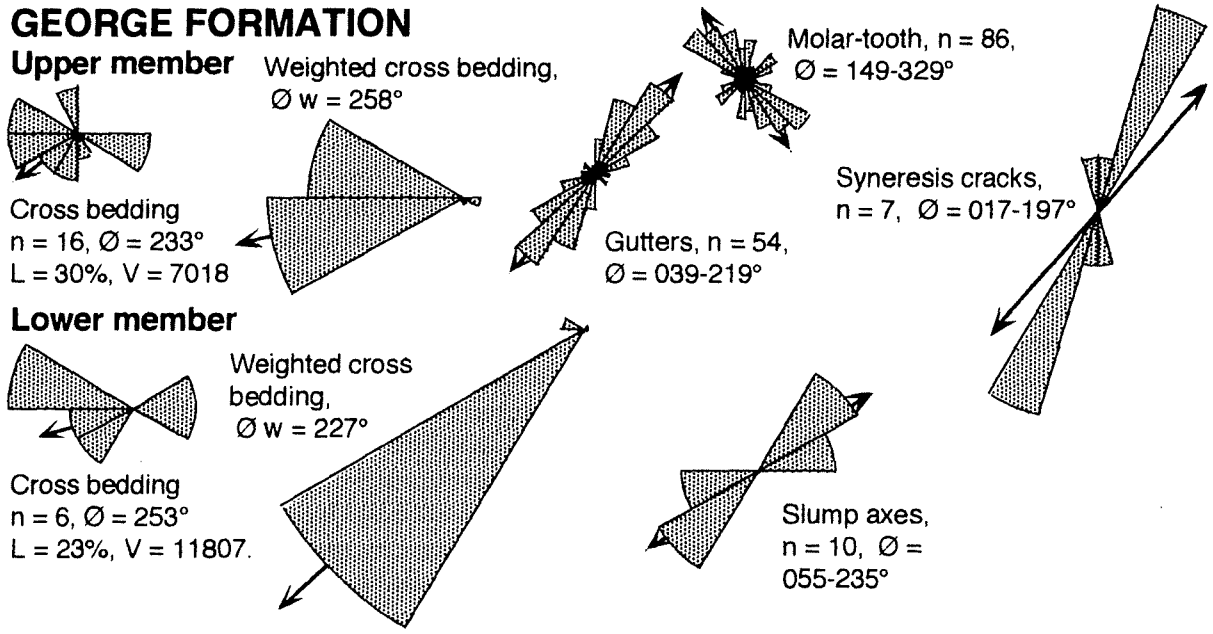

Fig. 5. Paleocurrent data from the George Formation.

Henry Creek Formation.

Mudstones and minor sandstones of the Henry Creek Formation reflect transgression, with a return to a deeper-water siliciclastic dominated setting following deposition of the George Formation. It is unclear if this transition is due to repeated faulting, triggered by extension related basement collapse, as at the Chischa/Tetsa contact, or if it reflects eustatic processes. Abundant slumps and gravity-flow deposits suggest continued progradation in an unstable ramp setting. Molar-tooth structures and domal stromatolites, developed locally in carbonates near the top of the formation, suggest continued progradation in a ramp setting. Siltstone and very fine-grained sandstone increase in abundance in the upper 200 m of the formation, and represent a distal (storm influenced) equivalent to the predominantly siliciclastic facies in the overlying Tuchodi Formation. Paleocurrent data are as yet ambiguous, with limited observations of gutter casts and domal stromatolites suggesting paleoslopes at a high angle to those in underlying units (Fig. 6).

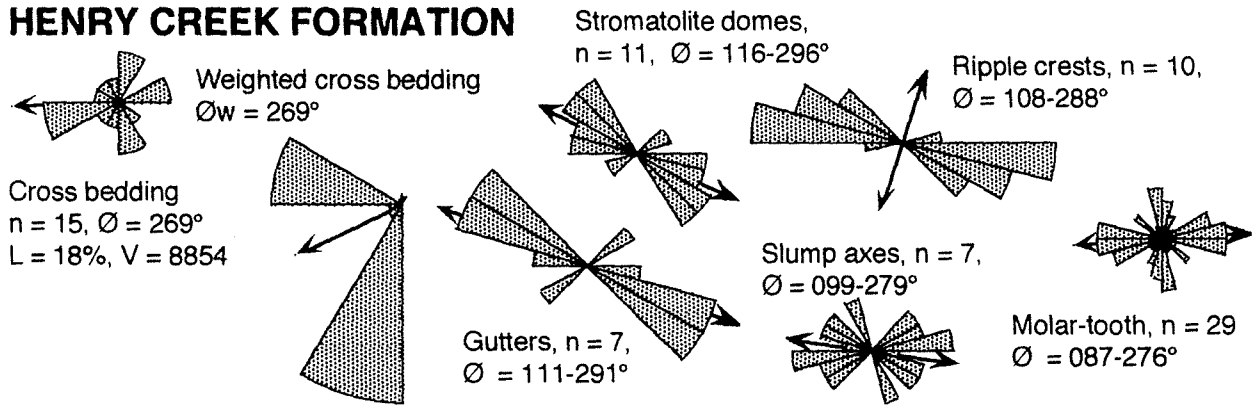

Fig. 6. Paleocurrent data from the Henry Creek Formation.

Tuchodi Formation.

The predominantly wavy and ripple cross-laminated sandstones of the Tuchodi Formation reflect a return to shallower-water conditions on a wave and storm influenced graded siliciclastic shelf. While large scale cross-stratification (>6 m) reflects local progradation of Gilbert-type deltaic facies at the lower contact of the formation south of Tuchodi Lake, in most sections the contact appears more transitional. Paleocurrent data from the formation are diffuse, suggesting weak currents directed NW-SE. Syneresis cracks are roughly parallel to ripple crests and may reflect a shore-parallel orientation, but are oblique to slump axes and are therefore ambiguous (Fig. 7).

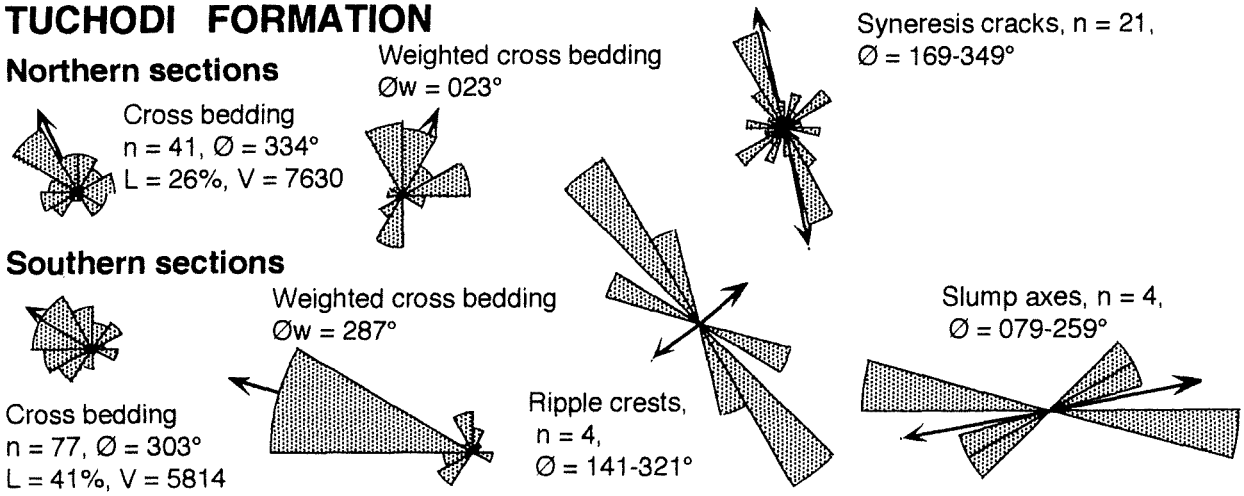

Fig. 7. Paleocurrent data from the Tuchodi Formation.

Aida and Gataga Formations.

Overlying strata of the Aida and Gataga Formations were not examined. The Aida contains a thick assemblage of sandy calcareous mudstones that apparently represent a return to deeper-water conditions, with local evidence of slumping and turbidites (Aitken, 1975). The Gataga is dominated by mudstones with minor sandstones of either distal-storm or turbidite origin.

TECTONIC FRAMEWORK.

The configuration of the western margin of ancestral North America at the time of deposition of the Belt-Purcell Supergroup remains problematic (Gabrielse and Yorath, 1991, p. 819). While this sequence is interpreted by some to represent an early rift-drift sequence, Winston (1990) and Ross et al. (1992), argue that early rifting was followed by thermal relaxation with sag-basin development, and that no major continental separation occurred. The more than six kilometres of strata preserved in the Muskwa Ranges is suggestive of extensional basin development, although there is no clear evidence to date if this is rift related extension or might be tied to transtensional strike slip mechanisms. Using concepts outlined by Cloetingh (1988) and Ziegler et al. (1995), we theorize that some North American Mesoproterozoic basins, including the Muskwa basin, formed via intracontinental rifting (extension perpendicular to local structures) and widespread intracontinental transtensional wrenching ("extension" oblique to local structures) processes which resulted from long-range (1000-5000 km) transmission of stresses from plate margin collisional areas. There is no evidence for direct influence of NE-SW directed faults during deposition of the Muskwa Assemblage. Inferred NW-SE paleo-shorelines roughly parallel the strike of the modern Cordillera.

Closure of the basin, in response to far-field tectonic stress, may have occurred

during the Racklan orogeny at ~1.2 Ga, but is as yet unconfirmed by direct dating. Closure led to localised uplift and erosion during deposition of the overlying Mackenzie Mountains Supergroup and its equivalents north of the study area (Young, 1979; Young et al., 1982). This latter group also appears to have developed in an extensional or transtensional basin setting with little to no evidence of a drift phase. The absence of equivalent strata in the study area may indicate that the MacDonald platform (Fig. 1) acted as a high or horst, controlled by deep-seated faults inherited from the earlier basin or initiated during a rifting-spreading event. Extension in the Muskwa Ranges is marked by the intrusion of as yet undated diabase dikes along high angle faults.

A second phase of folding, the ~0.8 Ga Hayhook orogeny of Young et al. (1982), separates the above strata from a well defined continental margin sequence which reflects rift and drift conditions in the late Paleoproterozoic. It is uncertain if this phase involved only minor separation of Australia and Laurentia, or if a broad ocean basin was developed (Dalziel, 1991; Moores, 1991; Young, 1992). This phase may be reflected in the Muskwa Assemblage by reactivation and shearing along the trend of the high-angle faults which host the diabase dikes. Local dolomitization of the George Formation adjacent to high-angle reverse faults may have occurred at this time.

Cecile et al. (1997) and others have suggested that renewed rifting along the margin occurred in Early Cambrian time. They suggest that his later event is best modeled using a crustal-attenuation model involving asymmetrical extensional break-up, delamination and sub-crustal shear. In this model, upper plate segments (crust above a deep detachment fault) may alternate with lower plate segments (consisting of the footwall of detachment, overlain by faulted upper plate remnants). While there is some evidence to suggest that this framework existed during deposition of the Rapitan and Windermere Supergroups and possibly the underlying Mackenzie Mountain Supergroup, there is no clear evidence as yet to support the concept that upper and lower plate segmentation developed in early Mesoproterozoic time.

FUTURE WORK

Additional stratigraphic observations need to be made in the lower part of the succession to confirm tentative paleogeographic and tectonic reconstructions presented herein. The nature of the contact between the George and Henry Creek Formations needs to be documented at several locations to determine if it reflects an allocyclically controlled sequence boundary or a tectonically induced transgressive surface. The Aida and Gataga Formations need to be examined in detail.

ACKNOWLEDGEMENTS

We thank Renée D. Brickner and Katherine M. Gerein for their able assistance in the field, and NSERC, Lithoprobe and the Northern Science Training Program for funds in support of this research.

REFERENCES.

Aitken, J.D., 1975. Proterozoic stratigraphy and sedimentology, Tuchodi Lakes Map-area, B.C. (94K). Geological Survey of Canada, Paper **75-1A:** 511.

Aitken and McMechan, M.E., 1991. Middle Proterozoic Assemblages. *In* H.Gabrielse and C.Yorath (editors) Geology of the Cordilleran Orogen in Canada, Geological Survey of Canada, Geology of Canada **4:** 97-124.

Bell. R.T. 1966. Precambrian rocks of the Tuchodi Lakes map-area, northeastern British Columbia. Ph. D. thesis, Princeton University 138 p.

Bell. R.T. 1968. Proterozoic stratigraphy of northeastern British Columbia. Geological Survey of Canada, Paper **67-68.**

Cecile, M.P., Morrow, D.W., and Williams, G.K., 1997. Early Paleozoic (Cambrian to Early Devonian) tectonic framework, Canadian Cordillera. Bulletin of Canadian Petroleum Geology **45:** 54-74.

Cloetingh, S., 1988. Intraplate stresses: a new element in basin analysis. Chapter 10 in K.Kleinspehn and C.Paola (editors) New perspectives in basin analysis. Springer-Verlag, New York, N.Y., p. 205-230.

Dalziel, W.D. 1991. Pacific margins of Laurentia and East Antarctica-Australia as a conjugate rift pair: evidence and implications for an Eocambrian supercontinent. Geology **19:** 589-601.

Furniss, G., Rittel, J.F., and Winston, D., 1998. Gas bubble and expansion crack origin of "Molar-tooth" calcite structures in the Middle Proterozoic Belt Supergroup, Western Montana. Journal of Sedimentary Research **68**: 104-114.

Gabrielse, H., and Yorath, C.J., 1991. Geology of the Cordilleran orogen in Canada. Geological Survey of Canada, Geology of Canada **4**, 844 p.

Moores, E.M. 1991. Southwest U.S.-East Antarctic (SWEAT) connection: a hypothesis. Geology **19:** 425-428.

Pratt, B.R., 1988. Molar-tooth structures in Proterozoic carbonate rocks: origin from synsedimentary earthquakes, and implications for the nature and evolution of basins and marine sediment. Geological Society of America, Bulletin **110**: 1028-1045.

Ross, G.M., Parish, R.R., and Winston, D., 1992. Provenance and U-Pb geochronology of the Mesoproterozoic Belt Supergroup (northwestern United States): implications for age of deposition and pre-Panthalassa plate reconstructions. Earth and Planetary Science Letters **113:** 57-76.

Taylor, G.C., 1963. MacDonald Creek, British Columbia. Geological Survey of Canada, Map **28-1963.**

Taylor, G.C. and Stott, D.F. 1973. Tuchodi Lakes map-area, British Columbia. Geological Survey of Canada, Memoir **373.**

Williams, M.Y., 1944. Geological reconnaissance along the Alaska highway from Fort Nelson, B.C., to Watson Lake, Yukon. Geological Survey of Canada, Paper **44-28.**

Winston, D.,. 1990. Evidence for intracratonic, fluvial and lacustrine settings of Middle to Late Proterozoic basins of western U.S.A., in C.F.Gower, T.Rivers and B.Ryan (editors) Mid-Proterozoic Laurentia-Baltica. Geological Association of Canada, Special Paper **38**: 535-564.

Young, G.M., 1979. Correlation of middle and upper Proterozoic strata of the northern rim of the North American craton. Transactions of the Royal Society of Edinburgh **70:** 323-336.

Young, G.M. 1992. Late Proterozoic stratigraphy and the Canada-Australia connection. Geology **20:** 215-218.

Young, G.M., Jefferson, C.W., Delaney, G.D. and Yeo, G.M., and Long, D.G.F., 1982. Upper Proterozoic stratigraphy of northwestern Canada and Precambrian history of the North American Cordillera. in Society of Economic Geologists, Coeur d'Alene field conference, Idaho, 1977. Edited by R.R.Reid and G.A.Williams. Idaho Bureau of Mines and Geology, Bulletin **24:** 73-96.

Ziegler, P.A., Cloetingh, S., and van Wees, J.-D., 1995. Dynamics of intra-plate compressional deformation: the Alpine foreland and other examples. Tectonophysics **252:** 7-59.

Mid-Cretaceous Granites of the southern Yukon: Initial report.

George A. Morris and Robert A. Creaser
Department of earth and Atmospheric Sciences, University of Alberta, Edmonton, AB, T6G 2E3, Canada. e-mail: george.morris@ualberta.ca; robert.creaser@ualberta.ca

During the summer of 1998 over 100 samples were collected from mid-Cretaceous plutons along SNORCLE transect #3 for geochemical and isotopic analysis. Plutons were divided into eight groups divided largely on a geographical basis. These are: Whitehorse area, including the Whitehorse and Mt. McIntyre suites of Hart (1995); Surprise Lake batholith; Teslin - west, four plutons on the west side of the Teslin fault; Teslin - east, mid-Cretaceous rocks of the Deadman Batholith (Gordey et al., 1998); the Quiet Lake Batholith; the Nisutlin Batholith; the Anvil Batholith; and plutons in the area of MacMillan Pass on the Yukon / NWT border.

All granitoids are sub-alkaline and lie close to the metaluminus - peraluminous boundary and there is a general increase in K_2O/Na_2O from west to east. Most significantly, there are three distinct strontium isotope initial ratio groups; a group with primitive values and two groups of more evolved values (figure 1). Primitive values (Sr_i: 0.70287 to 0.70527) encompass almost all samples west of the Teslin Fault, as well as some samples from the Teslin - east and Quiet Lake groups. The first group of crustal values (Sr_i: 0.71694 to 0.72076) encompass some rocks of the Teslin - east group, the Nisutlin Batholith, all samples from the Anvil Batholith and some samples from the MacMillan Pass group. Elevated Sr_i values in some plutons of the Teslin -west group could indicate mixing between primitive magmas and these more evolved magmas. The second group of crustal values (Sri: 0.72751 to 0.73539). These two crustal groups potentially match two groups identified by Driver (1998) in the Cassiar Batholith, south of the Anvil and Nisutlin batholiths of this study. Sm-Nd isotopic analysis is ongoing. Initial results support the primitive nature of low Sr_i samples on both sides of the Teslin Fault (4.6 to 5.1 εNd_T). Three recently published εNd_T numbers from the Cassiar, Anvil and Glenlyon (north of the Nisutlin) batholiths also suggest two crustal sources, one at approx. -9.6 and the other at -14.2 to -16.6 (Patchett et al., 1998), again correlating well with the substantive database from the Cassiar batholith (Driver, 1998).

Our initial data suggests that three distinct sources exist for mid-Cretaceous granites along the SNORCLE transect #3. A primitive source exists beneath western end of the transect, extending east as far as Quiet Lake. A more evolved crustal source contributes magmas to plutons from the Teslin - east, and possibly mixing with magmas from the Teslin - west group, to MacMillan Pass. A second, much more evolved (cratonic North American?) source contributes to plutons from the Nisutlin batholith, east.

Gordey, S.P., McNicoll, V.J., & Mortensen, J.K., 1998. New U-Pb ages from the Teslin area, southern Yukon, and their bearing on terrane evolution in the northern Cordillera. in Radiogenic Age and Isotope Studies: Report 11; Geological Survey of Canada, Current Research 1998-F.

Hart, C.J.R., 1995. Magmatic and tectonic evolution of the Intermontane Superterrane and Coast Plutonic Complex in southern Yukon Territory. unpublished MSc thesis, University of British Columbia, 189p.

Driver, L.A., 1998. Petrogenesis of the Cretaceous Cassiar Batholith, Yukon - B.C., Canada: Implications for Magmatism in the North American Cordilleran Interior.

unpublished MSc thesis, University of Alberta, 80p.

Patchett, P.J., Gehrels, G.E., & Isachsen, C.E., 1998. Nd isotopic characteristics of metamorphic and plutonic rocks of the Coast Mountains near Prince Rupert, British Columbia. Canadian Journal of Earth Sciences, v. 35, p. 556-561.

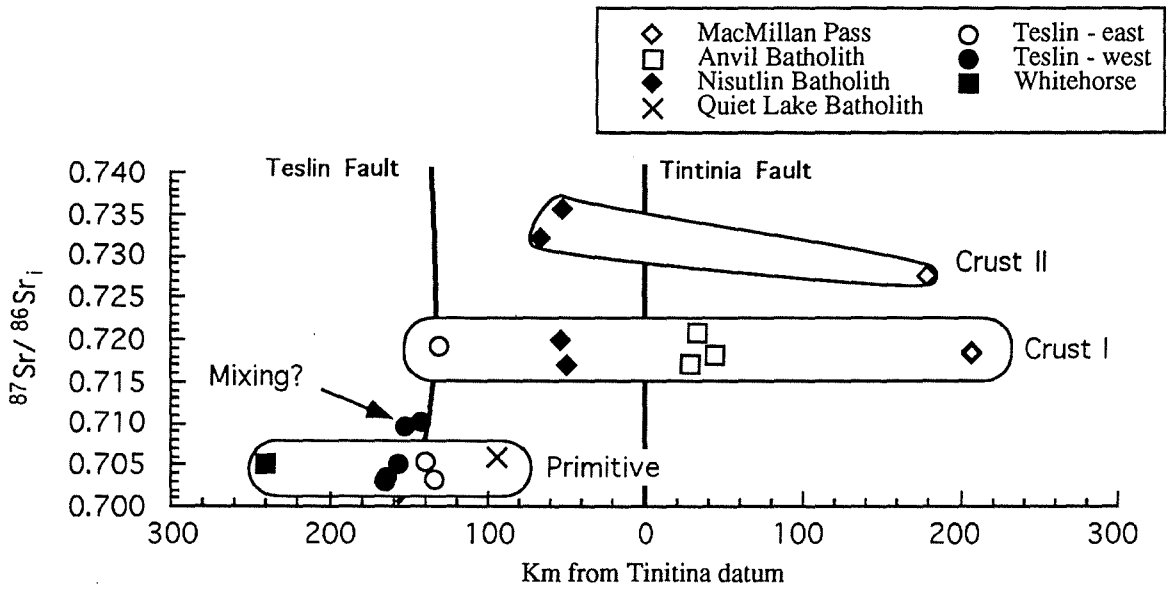

Figure 1. Variation in strontium initial ratiosfor mid-Cretaceous granitoids along SNORCLE transect #3. All distances are taken perpendicular to a baseline drawn along axis of the Tintina Fault at Ross River, Yukon Territory.

Cretaceous extension and regional calcic metasomatism in the Cassiar terrane south of the d'Abbadie pluton, south-central Yukon

Martin de Keijzer and Paul F. Williams
Department of Geology, University of New Brunswick, Fredericton, N.B., E3B 5A3, n29r@unb.ca

FOREWORD

Eastward accretion and obduction of the Yukon-Tanana Nisutlin and Slide Mountain / Anvil assemblages onto parautochthonous miogeoclinal strata of the Cassiar terrane (CT) is manifested by klippen of the former overlying the latter throughout south-central Yukon (Tempelman-Kluit 1979; Wheeler et al. 1991). Some of the klippen contain eclogite fragments spatially associated with ultramafic rock (e.g., the St. Cyr klippe; Erdmer 1992) thus providing strong evidence of obduction rather than these rocks being, for example, (layered) intrusions. In the Last Peak area (NTS sheet 105E/9), obduction was achieved by ductile thrusting and transposition folding, which affected both the hanging- and footwall rocks (de Keijzer et al. in press). During this crustal thickening event the footwall rocks (i.e. the CT) experienced prograde amphibolite facies metamorphism. Most workers believe this occurred in the Early to Middle Jurassic (e.g., Hansen et al.1991; Stevens et al. 1996). However, de Keijzer et al. (in press) proposed that emplacement related deformation may be as old as the Middle Permian, based mainly on a ~239 Ma cooling age of white mica in the western Teslin zone (Erdmer et al. 1998), which is syn-kinematic with amphibolite-grade fabric development (Erdmer et al., pers. comm. 1998). Similar Middle Permian cooling ages of muscovite and biotite have been reported in the St. Cyr klippe (Fallas et al. 1998).

On the other hand, the western CT records cooling through 500–300 °C from c. 145 to 110 Ma (Hansen et al. 1991). Hansen (1992) interpreted this mid-Cretaceous cooling event as representing a static process "consistent with a lack of ductile deformation during retrograde metamorphism or cooling". However, ductile to brittle deformation recording the uplift and predominantly SW-NE-directed extension of the western part of the CT is ubiquitous, and is closely related in time to the intrusion of the mid-Cretaceous d'Abbadie pluton (U-Pb zircon age ~110 Ma; Carr and de Keijzer, 1998). This extensional deformation was briefly described by de Keijzer and Williams (1997), and is described here in more detail. The present observations favour an interpretation of crustal scale extension of the CT in the Cretaceous. Contrary to most other parts of the Omineca Belt, this has not yet been documented in the Omineca Belt in southern Yukon Territory. Extension was accompanied by low pressure - high temperature metamorphism. The spatial distribution and composition of minerals crystallized during this metamorphic event requires regionally extensive fluid flow and mass transport of, amongst others, Ca. Accordingly, a case is presented here for regional-scale fluid flow and calcic metasomatism associated with the uplift and

extension of the Cassiar rocks.

STRUCTURE

The CT between the southern margin of the d'Abbadie pluton and the Dunite klippen (cf. Tempelman-Kluit 1979) ($\sim$ 40 km^2) comprises an approximately 4 km thick, strongly transposed, gently WSW- to SSW-dipping sequence. This sequence is dominated by quartzofeldspathic schist and pelite at low structural levels ("low level"), (calcic) pelite and marble in the "middle level", and pelite, siliceous graphitic schist, marble and quartzite at high structural levels ("high level"). Transposition with folds up to km-scale was accompanied by intense non-coaxial flow as indicated by, for example, sheath fold formation. This occurred during prograde metamorphic conditions (snowball garnets with prograde growth zoning). Transposition folds typically have their axes (sub)parallel to a SW-plunging mineral lineation (L_M). Kinematics during this prograde shearing event have been largely obliterated by pervasive static recrystallization (e.g., quartz shape fabrics) prior to and(?) during subsequent deformation (see below). However, shear bands defined by dynamically recrystallized regional peak-metamorphic minerals in probable correlative rocks in the western Teslin zone (de Keijzer et al. in press), and sense of rotation of garnets with spiral and sigmoidal inclusion patterns, suggest easterly directed shear during prograde amphibolite facies metamorphism.

Zone of extension

Various structures at outcrop scale indicate predominantly SW-NE-directed ductile to brittle extension of the pre-existing transposition foliation (S_T) in a km-wide zone. These include (i) top-to-the-SW,-S, and conjugate shear bands and boudins up to decameter scale, (ii) progressively more brittle-ductile and brittle, commonly conjugate shears and normal faults, and (iii) joints and dilational veins, principally filled with quartz, at high angle to S_T and L_M ("extension veins"). The middle and high levels preserve the highest concentration of retrograde shear bands, most of which accommodated final movement at low temperatures ($< \sim 300$ °C, as indicated by unannealed biotite and muscovite).

Continuous variations in the orientation of L_M, and various orientations of retrograde shear bands, in Cassiar rocks close to, and within, the Dunite klippen, delineate areas with triaxial (rather than monoclinic) fabric symmetry. In one area, a change in the orientation of retrograde shear bands is not accompanied by a change in the orientation of L_M, and an overprinting scenario between the two fabric elements is suggested. The various shear band orientations in the Cassiar rocks close to the (ultra)mafic klippe rocks can be explained by heterogeneous deformation around the presumably more competent klippe rocks during the waning stages of ductile deformation. The complex lineation distribution could be a result of triclinic flow (Jiang and Williams 1998; this volume), either during ductile thrusting or during subsequent extension but more work is required on this problem.

E- and W-dipping, commonly conjugate, brittle normal faults are most extensively developed in the easternmost and westernmost parts of the Cassiar mapping area. Recorded normal displacements are up to 100 m. The d'Abbadie fault system forms part of the western 'system' and, based on the similar orientation of mesoscopic brittle normal faults close by, a large component of brittle normal (latest) movement (west-side-down) on the d'Abbadie fault system is proposed. The d'Abbadie fault system could be a subsidiary zone of normal faults above the main extension zone and, if so, could shallow out at depth. Apparently undeformed pegmatite sills and dykes spatially related to the d'Abbadie pluton are offset by the normal faults.

METAMORPHISM

The common occurrence of garnet and staurolite in pelitic rocks, and garnet, dark green hornblende, and oligoclasic plagioclase in mafic rocks indicates that the CT has experienced pervasive amphibolite facies metamorphism in the study area. A sample ~1 km from the d'Abbadie pluton contains the peak metamorphic M_I assemblage biotite-garnet-staurolite-kyanite in the presence of quartz and muscovite. Geothermobarometry on garnet-amphibolites in the middle level yields estimated peak-metamorphic conditions of 770 +/- 100 MPa (garnet-amphibole-plagioclase calibration of Kohn and Spear 1990) and 610 +/- 30 °C (garnet-amphibole and plagioclase-amphibole calibrations of Graham and Powell [1984] and Blundy and Holland [1994], respectively). The temperature estimate is in good agreement with (i) the absence of epidote in the hornblende+oligoclase–andesine amphibolites, indicative of temperatures above ~575 °C (e.g., Bégin 1992), (ii) preservation of prograde zoning profiles in the amphibolitic garnets (therefore temperatures below ~650 °C, given their 0.5–3 mm size), and (iii) the occurrence of staurolite (generally considered to have a small temperature range of ~560–630 °C) and absence of sillimanite and K-feldspar (and no evidence for the initiation of muscovite-out reactions) in surrounding pelites. Obtaining quantitative peak-metamorphic conditions from the pelitic rocks is severely hindered by the Cretaceous metamorphic overprint, which is more pervasive in these rocks.

Replacement textures clearly distinguish the formation of a mid-Cretaceous low pressure - high temperature M_{II} assemblage at the expense of the M_I assemblage. Cordierite, andalusite, and, more rarely, fibrolitic sillimanite occur as M_{II} phases in pelites in a ~ 1.5 km wide zone along the southern margin of the d'Abbadie pluton. ***Regionally extensive*** M_{II} phases in pelitic rocks are oligoclase–andesine (Pl_{II}), biotite (Bt_{II}), and muscovite (Ms_{II}). Other locally significant M_{II} phases are clinozoisite, calcite, tourmaline, and chlorite. M_{II}-related alteration in amphibolitic dykes, though generally less profound than in surrounding pelitic rocks, resulted in the formation of oligoclase–andesine (Pl_{II}), sphene (Spn_{II}), calcite, apatite, and clinozoisite.

Mineral textures suggest that the M_{II} assemblage formed syn- to postkinematic with respect to

extension. For example, andalusite locally has pull-apart structures and is affected by shear bands (de Keijzer and Williams 1997). More commonly, however, M_{II} phases form randomly oriented, apparently undeformed aggregates armouring strongly corroded M_I phases. Garnet resorption is ubiquitous especially in the low and middle levels. In the low level Bt_{II} and Ms_{II} (also Bt_I and Ms_I?), and to a lesser extent Pl_{II}, abut garnet and the percentage of biotite-garnet contacts (relative to Pl_{II}-garnet contacts) is generally high. This in contrast to various samples in the middle level in the vicinity of the d'Abbadie pluton. There, Pl_{II} typically forms irregular moats or coronas between garnet and Bt_{II} / Ms_{II}, corroding both minerals and commonly completely separating garnet from Bt_{II} and Ms_{II}. It appears therefore that garnet resorption in the middle level was a two-stage process; first formation of Bt_{II} and Ms_{II}, followed by Pl_{II} formation at the expense of both garnet and Bt_{II}/Ms_{II}. In all three levels, matrix biotite and muscovite are extensively mimetically overgrown by Pl_{II}. Most analysed Pl_{II} grains, both those replacing garnet and matrix phases, show a profound outward increase in An-content: Rim compositions are typically An_{4-20} higher than core compositions, with core compositions ranging mostly between An_{18} and An_{36}, and rim compositions between An_{25} and An_{52}.

DISCUSSION

Crustal extension

Extension of a (transposed) regional layering, with recorded normal movement ***in its present orientation***, need not necessarily imply ***crustal*** extension (e.g., Wheeler and Butler 1993, 1994). Could the zone of extension, as described above, represent a tilted thrust and actually shorten the crust? As pointed out by Wheeler and Butler (1994), criteria strongly suggestive of a regional-scale shear zone truly extending the crust include (i) faster decompression of the footwall than the hanging wall (requires pressure-time histories), (i) intersection of the fault zone with the paleosurface in a direction opposite to that of hanging wall transport (i.e. to the northeast of the study area), and (iii) juxtaposition of rocks with old cooling ages in the hanging wall against rocks with young cooling ages in the footwall. Data either consistent or inconsistent with these criteria are insufficient or lacking at the present time. For example, information on the cooling history of Cassiar rocks (Hansen et al. 1991) is confined to a restricted area in the high to middle level south of the Dunite klippen.

Given the present data set, however, we propose that the zone of extension in the CT (and in the klippen) represents a low-angle detachment fault, recording Cretaceous crustal extension (i.e. thinning of the lithosphere), for the following reasons. First, there is no evidence that the SW-dipping retrograde fault zone re-emerges at the surface to the southwest by either later folding or due to original orientation changes (i.e. no evidence for a thrust scenario). Second, in a thrusting scenario, the footwall rocks (represented by the low level) are expected to show metamorphic evidence for renewed, or continued, burial superposed

on early obduction-related M_I metamorphism. This has not been observed. The Cretaceous M_{II} overprint has the same general characteristics in all three levels. Third, extensional structures throughout this portion of the CT record a progressive change from ductile to brittle deformation and, albeit localization of deformation, the area as a whole appears to have been uplifted to higher crustal levels during the same event. Fourth, regionally voluminous Cretaceous intrusions, and the elongate shape of some of these plutons (e.g., the d'Abbadie and Big Salmon plutons) is in accordance with a E–NE to W–SW dilating crust. (And there is no evidence for these being sheet-like intrusions.) Fifth, whatever the underlying driving force(s), thinning of the lithosphere is expected after profound crustal thickening (e.g., Dewey 1988), and the proposed extension in the CT agrees well with Mesozoic-Cenozoic extension prevalent across almost the entire length of the Cordilleran Omineca Belt (e.g., Coney and Harms 1984; Pavlis 1989).

Regional metasomatism.

Crystallization of large quantities of calcic Pl_{II} (together with other calcic phases like clinozoisite, calcite, sphene, and apatite) ***throughout*** the CT in a variety of rock types, many of which lacked a (sufficient) Ca nutrient source, can only be explained by open system behaviour of Ca. Mobility of Ca in the presence of a fluid phase is well-recognized in, for example, skarn environments and fault zones. Several workers (e.g., Carten 1986; Ague 1997) have reported calcic(-sodic) alteration that is characterized by large increases of Na/K and Ca/K ratios, and the formation of oligoclase–andesine. Based on mass-transfer and time-integrated fluid flux calculations, Ferry and Dipple (1991) and Dipple and Ferry (1992) proposed that increasing Na/K and Ca/K ratios record fluid flow in a direction of increasing temperature. The same relationship between direction of fluid flow and calcic(-sodic) alteration was suggested by Carten (1986) and Ague (1997).

In the CT, evidence for the presence of a fluid phase ***during*** extension and M_{II} metamorphism includes (i) primary fluid inclusions in quartz and Pl_{II}, both of which replace the rims and interior parts of garnet, (ii) an abundance of quartz-filled extension veins, indicating high fluid pressure (e.g., Etheridge et al. 1983), and (iii) an abundance of felsic pegmatites spatially associated the d'Abbadie pluton. The following characteristics strongly suggest the applicability of a model of dominantly subhorizontal advection-dominated regional fluid flow up a temperature gradient for the (western) CT in the Cretaceous, similar to that proposed in Vermont by Ferry (1992); (i) the presence of fluids during M_{II} metamorphism, (ii) the extensional tectonic setting (therefore highly permeable rocks), (iii) the shallow orientation of transposed layering, and (iv) intrusion of large felsic plutons (which provided a heat source to establish, or modify existing, regional temperature gradients). It is therefore suggested that regional-scale fluid flow towards the d'Abbadie pluton resulted in the widespread crystallization of the conspicuously calcic M_{II}

assemblage, Pl_{II} being its main constituent. Leaching of Ca from marble, present in all three levels, probably provided the Ca required for the observed metasomatic reactions in the other rock types. Transport of the necessary nutrients is believed to have occurred through early tensile (micro)fractures (e.g., Etheridge et al. 1983), most of which are sealed now (as indicated by bands of fluid and mineral inclusions at high angle to S_T in Pl_{II} and quartz) or are quartz veins.

Conditions of metasomatism

The association of Pl_{II} with andalusite and cordierite (close to, or just in, the sillimanite stability field) near the d'Abbadie pluton suggests temperatures of ~525–600 °C (e.g., Barker 1990) at a maximum pressure of ~375 MPa (Holdaway and Mukhopadhyay 1993). The pressure was probably between 200 and 300 MPa. Because of the uniform Pl_{II} compositions in the oligoclase–andesine field, it is believed that the prevailing temperatures during Pl_{II} growth further away from the pluton were of the order of 475–550 °C. These regionally elevated lower amphibolite facies temperatures agree well with those proposed for calcic metasomatism elsewhere (van Marcke de Lummen and Verkaeren 1987; Carten 1986). Thus Pl_{II} development probably predates many of the *preserved* retrograde shear bands, boudins, and extension veins, which formed at lower temperatures (<300–350 °C, as indicated by unannealed micas) and are the manifestation of the later part of extension.

Pl_{II} grew in a dynamic tectonic setting, with strong coupling between ductile–brittle deformation, plutonism, regional fluid flow, varying fluid pressures on many scales (repeated hydrofracturing and healing of fractures), mass transport, crystallization of Pl_{II} and other M_{II} phases, and breakdown of M_I phases such as garnet (providing some Ca). The outward increasing An-content in Pl_{II} is probably governed by a combination of one or more of the following processes; decreasing pressure (e.g., Barker 1990), increasing temperature (observed both in closed systems [e.g., Spear et al 1991] and open systems [e.g., Ferry 1992]), or increasing availability of Ca (e.g., Crawford 1977). Localized controls on the bulk availability of Ca probably existed, since a correlation between An-content and proximity to the d'Abbadie pluton is not apparent (with the present data set). One possible scenario is that Pl_{II} zoning was controlled principally by a temperature increase as a result of a regionally elevated geothermal gradient caused by the d'Abbadie pluton. The pluton may have intensified the convection of hydrothermal fluids together with heating of these fluids progressively further away from it.

Regional implications of metasomatism

It is considered highly unlikely that in a region with widespread and voluminous Cretaceous plutonism, the profound regional-scale fluid flow, as reported here, is an isolated case. More hydrothermal systems, possibly with similar metasomatic effects, are expected to have been present elsewhere in the region in the Cretaceous.

Open-system processes need to be characterized before an attempt can be made to decipher the pressure-temperature-time-deformation history of a region (e.g., Ague 1997). Of particular importance in this respect is the calcic nature of M_{II} metamorphism/metasomatism since plagioclase is of fundamental importance in geothermobarometry of amphibolite grade rocks. In the study area, Pl_{II} and garnet growth are clearly not coupled, and can therefore not be used together in thermobarometrical calculations. Indeed, unrealistically high pressure and temperature estimates (1.0–1.3 GPa and 675–800 °C) are obtained using these minerals. The generally complex reaction kinetics of plagioclase, the common mimetic growth of Pl_{II}, and the lack of Pl_{I} inclusions in pelitic garnet, prevent the selection of garnet and plagioclase analyses that can with a reasonable level of confidence be interpreted as having been in chemical equilibrium during the peak of metamorphism. (The peak-metamorphic conditions reported above are obtained from carefully selected grains in garnet-amphibolites that have largely escaped M_{II} metamorphism.)

Hansen (1992) obtained peak-metamorphic pressure and temperature estimates ranging from 0.7 to 1.3 GPa and 550 to 750 °C , respectively, using rim-rim analyses in samples collected from a small area (4 by 4 km) south of the Dunite klippen. However, there is no detailed description of microtextures in support of the inferred equilibrium between mineral phases, and chemical zoning data of, for example, plagioclase are absent. Most interestingly, Hansen (1992) reported plagioclase with An_{22-26} and An_{50} from within the same unit. This compositional range is strikingly similar to that of Pl_{II} north of the Dunite klippen. It is therefore considered very likely that the high calcic plagioclase rim reported by Hansen (1992) reveals the presence of Pl_{II} there too. If this is the case, then mid-Cretaceous metasomatism also occurred south of the Cassiar study area, and the geological significance of Hansen's pressure and temperature estimates should be questioned.

The regional extent of elevated temperatures in the CT associated with M_{II} metamorphism sheds new light on the preservation of Cretaceous cooling ages (Hansen et al. 1991) in the CT versus older (pre-Late Jurassic) cooling ages in the Teslin zone (e.g., Hansen et al. 1991) and in some of the klippen (e.g., the St. Cyr klippe; Fallas et al. 1998). Isotopic systems that close below 500 °C have probably been reset in the mid-Cretaceous, whereas in areas less affected or unaffected by M_{II} metamorphism, older cooling ages may have been preserved and/or possibly partially reset. Resetting of isotopic systems with low blocking temperatures, but not the ones with higher blocking temperatures (≥500 °C), opens up the possibility for reinterpretation of the slow cooling history of the CT proposed by Hansen (1992), especially if considered in light of the active extension and uplift experienced by these rocks as reported here.

REFERENCES

Ague, J.J. 1997. Geology, 25: 73-76.
Barker, A.J. 1990. Blackie, London.
Bégin, N.J. 1992. Journal of Metamorphic Geology, 10: 685-704.
Carr, S., and de Keijzer, M. 1998. Lithoprobe Report, 64: p. 228.
Carten, R.B. 1986. Economic Geology, 81: 1495-1519.
Coney P.L., and Harms, T.A. 1984. Geology, 12: 550-554.
Crawford, M.L. 1977. Canadian Mineralogist, 15: 243-249.
de Keijzer, M. and Williams, P.F. 1997. GAC/MAC Annual Meeting, Abstract Volume, pp. A
de Keijzer, M., Williams, P.F., and Brown, R.L. In press. Kilometre-scale folding in the Teslin zone, northern Canadian Cordillera, and its tectonic implications for the accretion of the Yukon-Tanana terrane to North America. Canadian Journal of Earth Sciences.
Dewey, J.F. 1988. Tectonics, 7: 1123-1139.
Dipple, G.M., and Ferry, J.M. 1992. Contributions to Mineralogy and Petrology, 112: 149-164.
Erdmer, P. 1992. Canadian Journal of Earth Sciences, 29: 1296-1304.
Erdmer, P., Ghent, E.D., Archibald, D.A., and Stout, M.Z., 1998. GSA Bulletin, 110: 615-629.
Etheridge, M.A., Wall, V.J., and Vernon, R.H. 1983. Journal of Metamorphic Geology, 1: 205-226.
Fallas, K., Erdmer, P., Archibald, D., Heaman, L., and Creaser, R. 1998. Lithoprobe Report, 64: 131-138.
Ferry, J.M. 1992. Journal of Petrology, 33: 45-94.
Ferry, J.M., and Dipple, G.M. 1991. Geology, 19: 211-214.
Graham, C.M., and Powell, R. 1984. Journal of Metamorphic Geology, 2: 13-21.
Hansen, V.L. 1992. Journal of Metamorphic Geology, 10: 239-263.
Hansen, V.L., Heizler, M.T., and Harrison, T.M., 1991. Tectonics, 10: 51-76.
Holdaway, M.J. and Mukhopadhyay, B. 1993. American Mineralogist, 78: 298-315.
Holland, T., and Blundy, J. 1994. Contributions to Mineralogy and Petrology, 116: 433-447.
Jiang, D., and Williams, P.F. 1998. Journal of Structural Geology, 20: 1105-1120.
Kohn, M.J., and Spear, F.S. 1990. American Mineralogist, 75: 89-96.
Pavlis, T.L. 1989. Geology, 17: 947-950.
Spear, F.S., Kohn, M.J., Florence, F.P., and Menard, T. 1991. Journal of Metamorphic Geology, 8: 683-696.
Stevens, R.A., Erdmer, P., Creaser, R.A., and Grant, S.L., 1996. Canadian Journal of Earth Sciences, 33: 103-116.
Tempelman-Kluit, D.J. 1979. Geological Survey of Canada, Paper 79-14, 27p.
van Marcke de Lummen, G., and Verkaeren, J. 1987. Chemical Transport in Metasomatic Processes (ed. H.C. Helgeson), 669-679.
Wheeler, J., and Butler, R.W.H. 1993. Earth and Planetary Science Letters, 117: 457-474.
Wheeler, J., and Butler, R.W.H. 1994. Journal of Structural Geology, 16: 1023-1027.
Wheeler, J.O. Brookgield, A.J., Gabrielse, H., Monger, J.W.H., Tipper, H.W. and Woodworth, G.J. (comp.) 1991. Geological Survey of Canada, Map 1713A, scale 1:2 000 000

NEW TERRANE INTERPRETATION FOR THE ST. CYR KLIPPE, SOUTH-CENTRAL YUKON.

[1]**Karen M. Fallas** (e-mail: karen.fallas@ualberta.ca)
[1]**Philippe Erdmer** (e-mail: p.erdmer@ualberta.ca)
[1]**Robert A. Creaser** (e-mail: robert.creaser@ualberta.ca)
[2]**Douglas A. Archibald** (e-mail: archiba@geol.queensu.ca)
[1]**Larry M. Heaman** (e-mail: larry.heaman@ualberta.ca)

[1] Dept. of Earth and Atmospheric Sciences, University of Alberta, Edmonton, AB, T6G 2E3.
[2] Dept. of Geological Sciences, Queen's University, Kingston, ON, K7L 3N6.

The St. Cyr klippe (SCK) lies between the Teslin Tectonic Zone (TTZ) and the Tintina Fault in south-central Yukon, and was originally mapped at a regional scale by Tempelman-Kluit (1979). He recognized two sheared metamorphic assemblages preserved in the hanging wall of the klippe: the metasedimentary Nisutlin allochthon, and the metaigneous Anvil allochthon of oceanic affinity. Detailed mapping in the SCK requires that these two units be redefined. Sedimentary rocks of the Cassiar Terrane are preserved in the footwall of the klippe

The Nisutlin allochthon can be subdivided into two units: structurally higher garnet-muscovite schist which underlies the Anvil allochthon, and a structurally lower psammite, quartzite, and phyllite assemblage which locally preserves primary sedimentary structures and is indistinguishable from the rocks of the Cassiar terrane which underlie them (Fig. 1). The former are referred to as the Nisutlin assemblage, and the latter are now grouped with the Cassiar terrane. The boundary between the two is the basal thrust of the SCK.

The Anvil allochthon of Tempelman-Kluit (1979) includes two mappable units: a greenschist-grade metavolcanic unit with volcanic textures and a poorly developed strain fabric, and a mixed unit of amphibolite, peridotite, muscovite quartzite, calc-silicate, eclogite, and rare marble displaying a strong penetrative foliation and stretching lineation. Within the SCK, greenschist metavolcanic rocks are referred to here as the Tower Peak assemblage, and the mixed amphibolite unit is called the Indian Mountain assemblage.

Regional correlations and Geochemistry

The Nisutlin assemblage is correlated with similar deformed metasedimentary rocks in southern Yukon which Tempelman-Kluit (1979) included in the Nisutlin allochthon. Using terrane terminology, the Nisutlin assemblage is the metasedimentary portion of the Yukon-Tanana terrane (Hansen, 1989), or the Nisutlin subterrane of the Kootenay terrane (Wheeler and McFeely (1991). Locally, the Nisutlin assemblage of the SCK is correlated with the Nisutlin assemblage of the TTZ (Stevens and Erdmer, 1996). Although the rocks of the TTZ are of lower metamorphic grade than those of the SCK, Sm-Nd geochemistry indicates similar provenance for these rocks (Fallas et al., 1998, and Creaser et al., 1997), supporting their correlation.

The Tower Peak assemblage and the Indian Mountain assemblage are correlated with the Anvil allochthon (Tempelman-Kluit, 1979), and the Anvil assemblage (Creaser et al., 1997) in southeast Yukon. Regionally, the Anvil assemblage has been correlated with the Slide Mountain terrane of British Columbia (Wheeler and McFeely, 1991). This correlation is problematic because Slide Mountain terrane rocks are unmetamorphosed whereas Anvil assemblage rocks are greenstones. Recent geochemical studies of the Anvil assemblage (Creaser et al., 1997, and Plint and Gordon, 1997) have helped in defining its tectonic

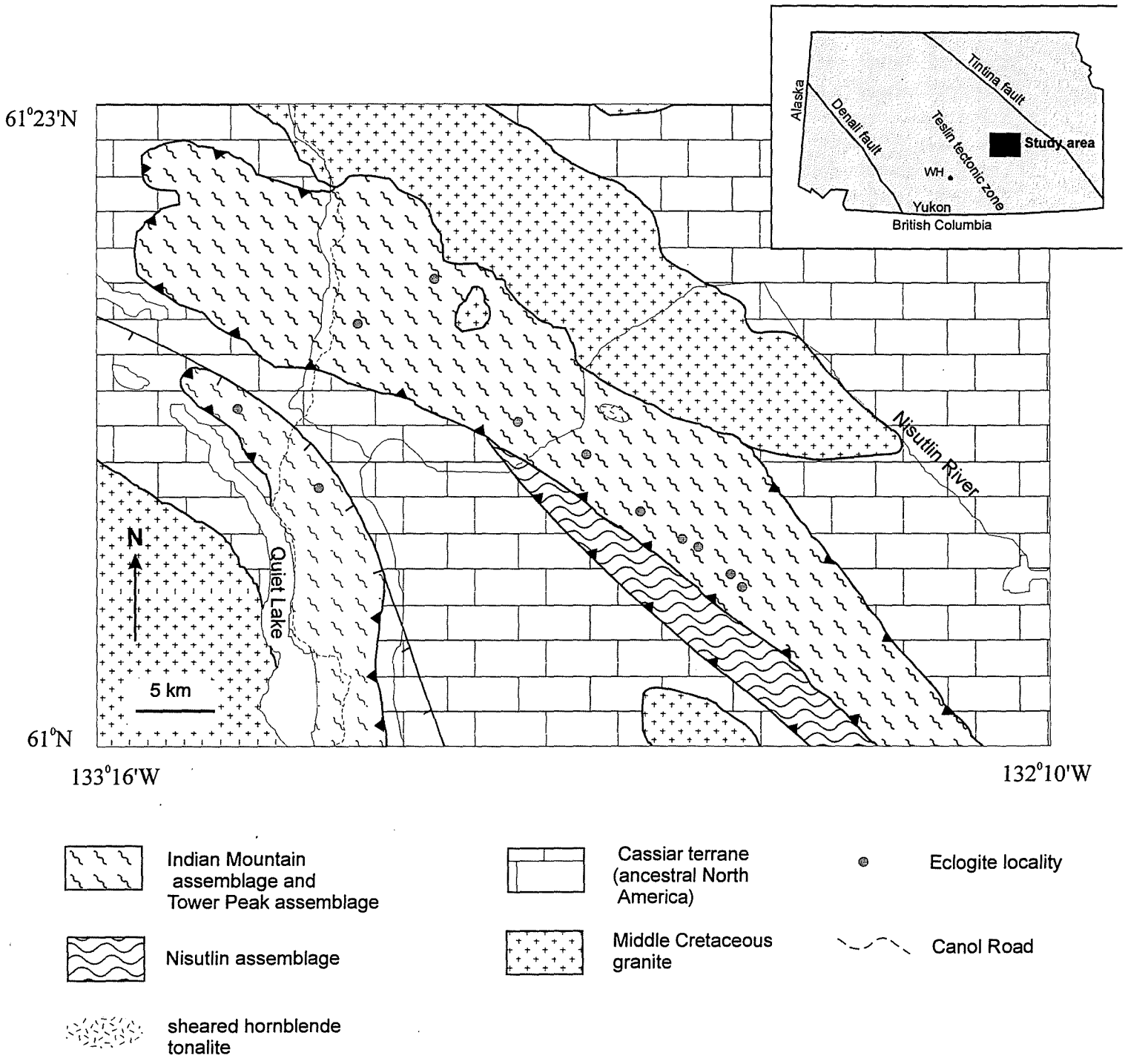

Figure 1. Simplified geology of the St. Cyr and Quiet Lake klippen showing the revised geology of the area, including the newly defined Indian Mountain assemblage and Tower Peak assemblage.

affinity, and will aide regional correlations.

Figure 2 shows representative incompatible element plots for the Indian Mountain assemblage and the Tower Peak assemblage of the SCK. Elements considered to be immobile during metamorphism are considered. It is clear that the two units have different geochemical characteristics. The Indian Mountain assemblage has a flat pattern near 1 relative to MORB, demonstrating its MORB-like protolith. In contrast to the Indian Mountain assemblage, the Tower Peak assemblage records an arc affinity with very high Th, low Ta and Nb, and high La and Ce ratios relative to MORB. This pattern is matched in trace element discrimination diagrams, with Indian Mountain assemblage rocks consistently plotting in the MORB or within-plate basalt fields, and Tower Peak assemblage rocks plotting in arc andesite fields.

Indian Mountain assemblage rocks have a similar geochemical signature to Slide Mountain terrane rocks such as the Fennel Formation (Smith and Lambert, 1995), the Kaslo Group (Roback et al., 1994), and the Nina Creek Group (Ferri, 1997). Division II of the Sylvester Allochthon (Nelson, 1993) makes a poor match with the Indian Mountain assemblage. In the Yukon, Indian Mountain assemblage rocks geochemically resemble mafic metavolcanic rocks in the Finlayson Lake area (Plint and Gordon, 1997), the Anvil Range Group basalts (L. Pigage pers. comm., 1998), as well as selected eclogites from Faro, Ross River, and Simpson Range areas (Creaser et al., in review).

Other parts of the Anvil assemblage record an arc affinity such as: the Money klippe (Grant, 1997), the Stewart Lake eclogites (Creaser et al., in review), the TTZ (Creaser et al., 1997), and a sample from the Casino area (D. Selby pers. comm., 1998). These rocks more closely resemble geochemically the Tower Peak assemblage of the SCK.

Clearly, the rocks that have been mapped as the Anvil assemblage include two distinct tectonic assemblages. Greenstone units throughout or associated with the Yukon-Tanana terrane should be correlated with care and with the aid of trace and rare-earth element geochemistry.

Metamorphism

Reconnaissance mapping of the SCK by Erdmer (1992) discovered the presence of eclogites associated with amphibolites of the Indian Mtn assemblage. Detailed mapping coupled with P-T work on the Indian Mountain assemblage and Nisutlin assemblage has shown that high-pressure metamorphism is widespead in the SCK. Figure 3 shows the results of P-T calculations for an eclogite of the Indian Mountain assemblage, a calc-silicate schist of the Indian Mountain assemblage and metapelite from the Nisutlin assemblage. All 3 samples record pressures of at least 10 kbar and temperatures between 450 and 600°C. The pressure of ~23 kbar for the sample from the Nisutlin assemblage is geologically implausible, possibly due to limitations of the plagioclase activity model. The result for the eclogite sample matches with results from other eclogites in the Yukon (Erdmer et al., 1998). The age of peak eclogite metamorphism is 260-265 Ma, on the basis of U-Pb zircon dating and Ar-Ar mica cooling ages (Fallas et al., 1998).

The distinction between the Indian Mountain assemblage and the Tower Peak assemblage is further emphasized by the contrast in metamorphic grade. The Tower Peak assemblage records greenschist facies metamorphism with chlorite +/- epidote dominating the mineral assemblage. The timing of metamorphism is not constrained but is younger than Permian and older than MiddleCretaceous (the age of local post-tectonic contact metamorphism).

Rocks in the footwall of the SCK record greenschist to lower grade metamorphism, with only minor chlorite and white mica growth. Locally, these rocks reach amphibolite facies in the contact aureoles of the Nisutlin batholith and Red plug. On the basis of mica Ar40/Ar39 cooling ages of phyllite in the footwall regional

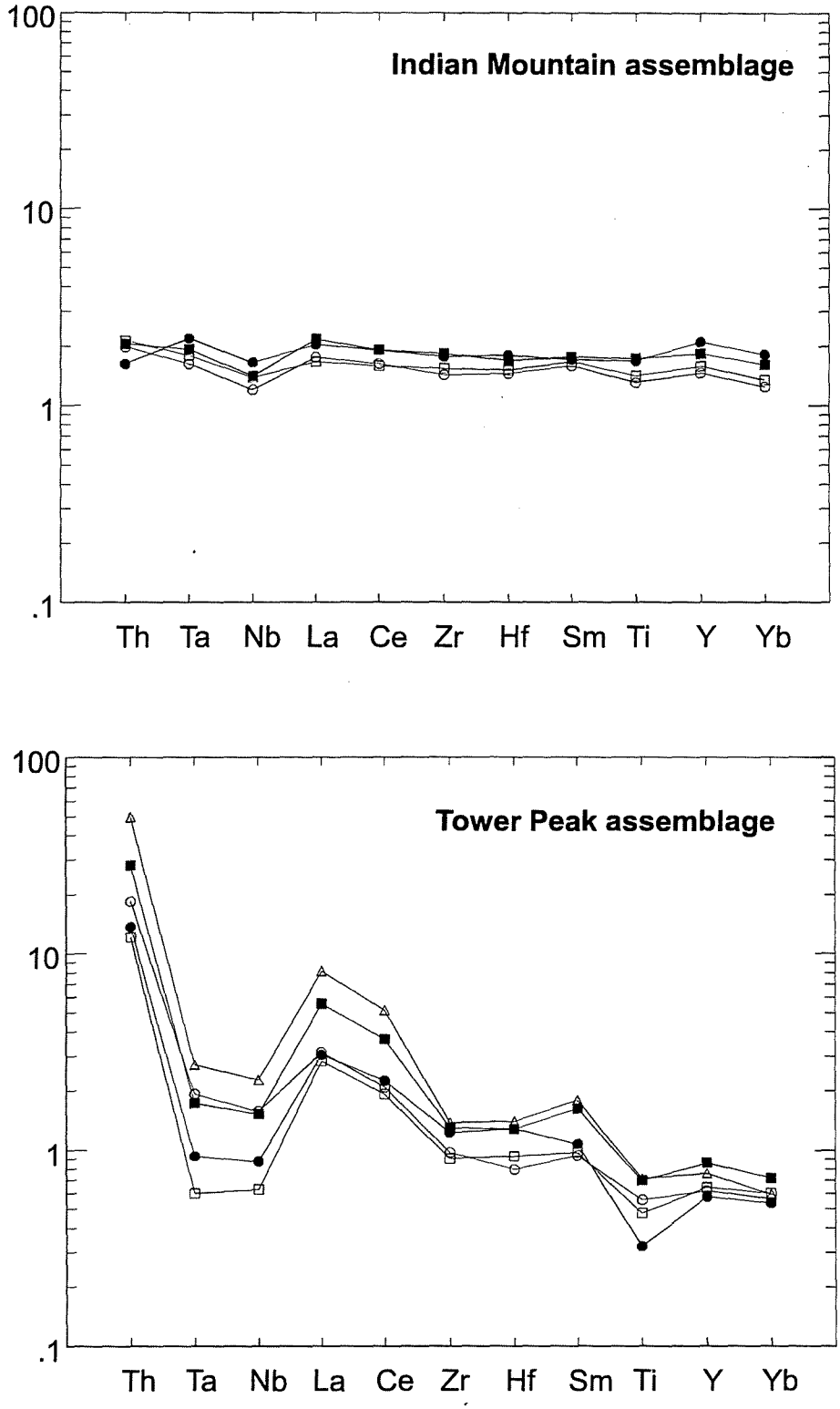

Figure 2. Incompatible element plots relative to MORB for the Indian Mountain assemblage and the Tower Peak assemblage of the St. Cyr klippe.

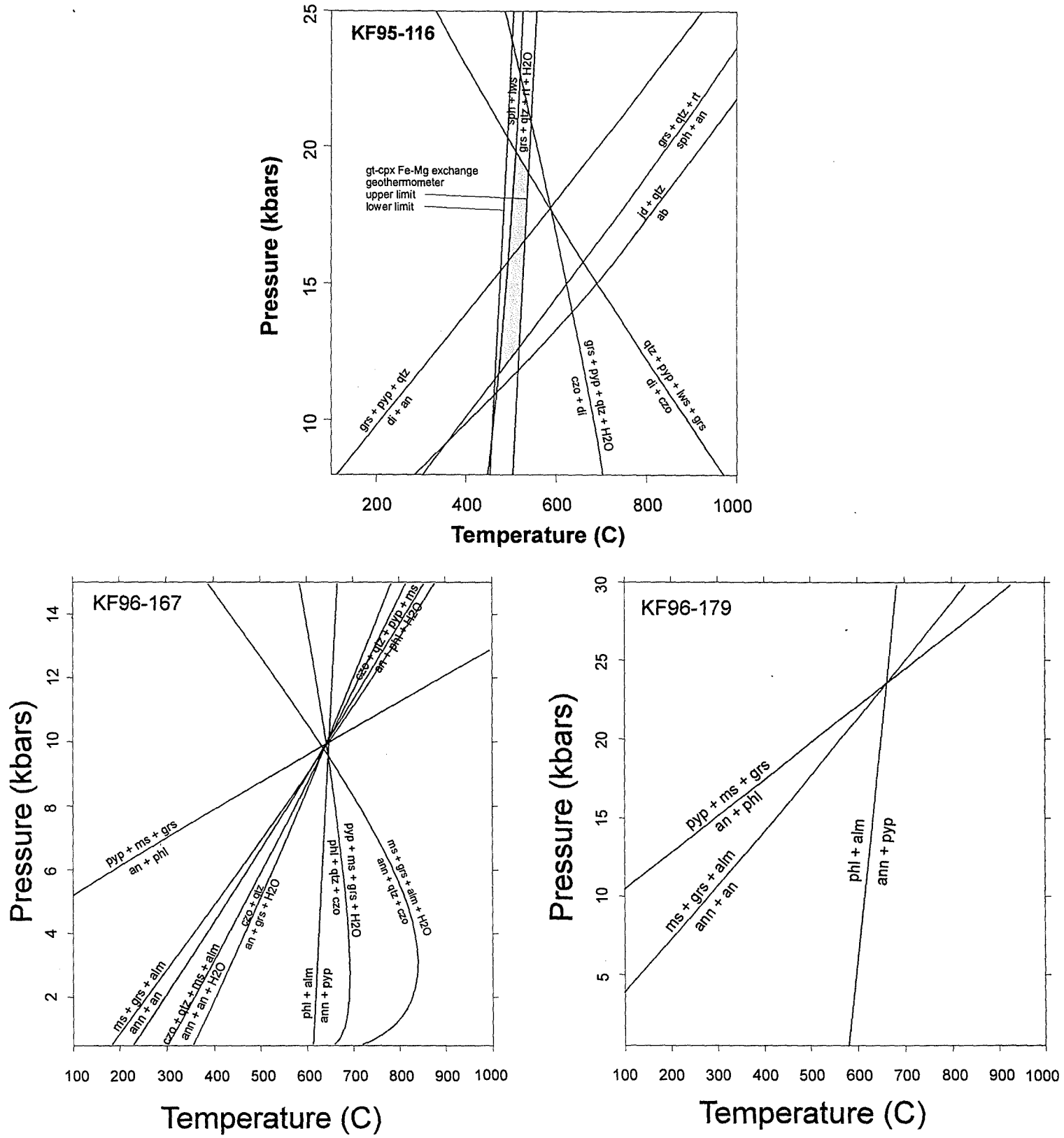

Figure 3. P-T constraints for the Indian Mountain assemblage (KF95-116 - eclogite and KF96-167 - calcsilicate) and Nisutlin assemblage (KF96-179 - garnet-muscovite schist).

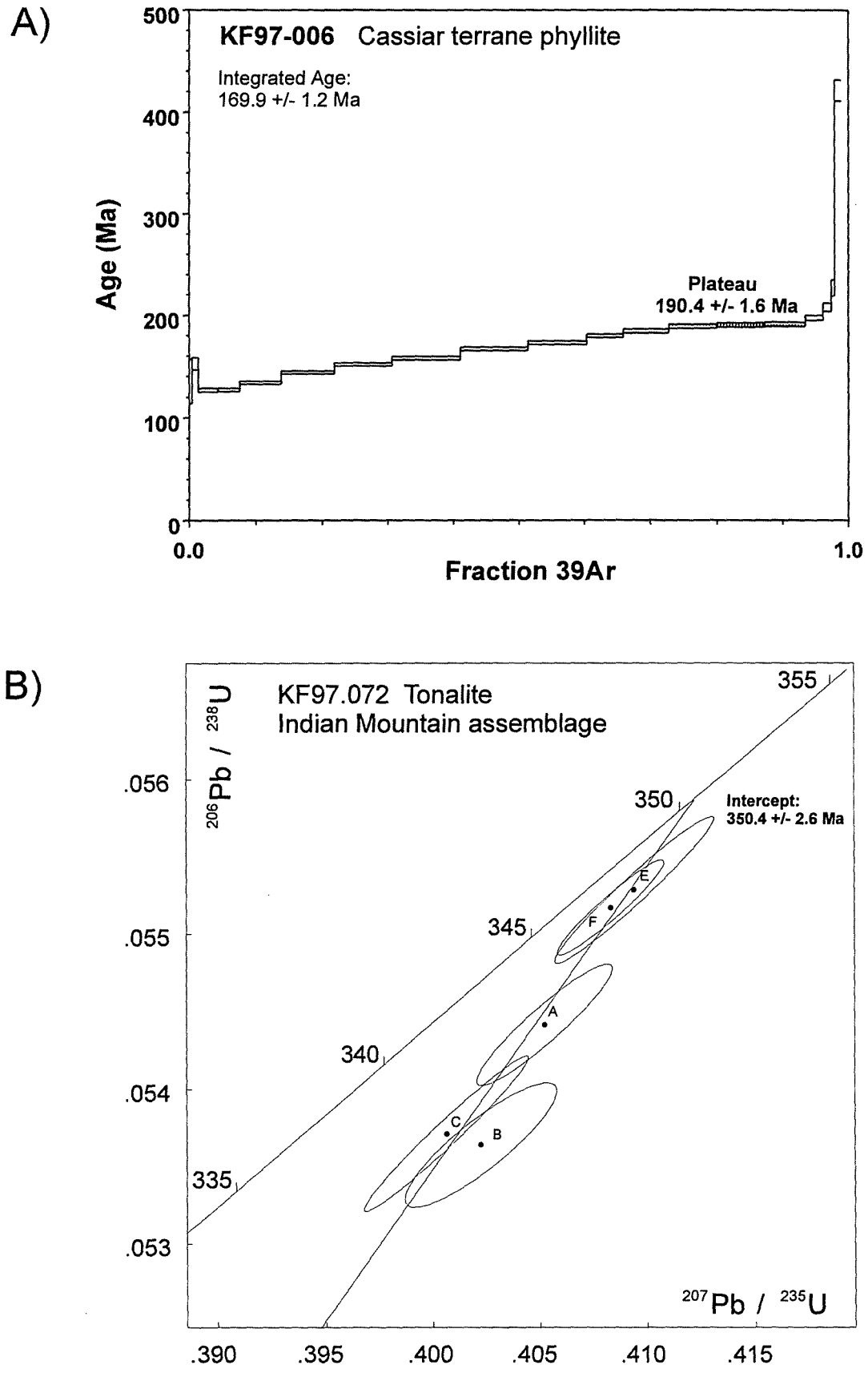

Figure 4. a) Argon release spectrum for a phyllite from the Cassiar terrane rocks of the footwall of the St. Cyr klippe. b) Revised U-Pb age for sheared tonalite of the Indian Mtn assemblage.

metamorphism of footwall rocks occurred in the Late Triassic to Early Jurassic. Integrated ages cluster around 210 Ma, with some spectra showing a complicated thermal history with possible Permian or older ages overprinted by a Late Triassic-Early Jurassic event, in turn overprinted by a Middle Cretaceous event (Fig.4). Excess Ar may further complicate interpretation of the calculated ages.

Tectonic history

From the early Mississippian sheared tonalite found within amphibolite (concordia plot shown in Fig.4) the ocean basin recorded by the Indian Mountain assemblage was likely of lower Paleozoic age. Based on their correlation with the Nisutlin assemblage of the TTZ (Stevens et al., 1996) the metasedimentary rocks of the Nisutlin assemblage were deposited by Early Mississippian time. ϵNd values for the Nisutlin assemblage (Fallas et al., 1998) indicate that these sedimentary rocks were being deposited not far from a cratonic source, interpreted as North America. The Indian Mountain and Nisutlin assemblages together may represent a back-arc basin.

Destruction of this basin began before 265 Ma (from the age of eclogite metamorphism), and the Indian Mountain and Nisutlin assemblages were exhumed by ~260 Ma (from mica cooling ages). Structural imbrication of the Indian Mountain assemblage likely occurred during the subduction event, as contacts are now annealed by metamorphism. Ductile fabrics in these rocks also formed during subduction. Late in the subduction-and-exhumation history, or during subsequent deformation at shallow levels in the crust, the ductile fabrics were folded about NW-SE (present day co-ordinates) axes (Fallas, 1997). Oblique NW-SE mineral lineations may record either oblique transpression during subduction or reorientation into parallelism with fold axes during later folding.

Although there are no direct age constraints on the Tower Peak assemblage, it is folded together with the Indian Mountain assemblage. It appears to have been juxtaposed (structurally or stratigraphically) with the Indian Mountain assemblage after subduction but before thrusting (fold limbs are cut by thrusts). The Late Triassic to Early Jurassic cooling ages of Cassiar terrane rocks in the footwall of the SCK as well as rocks of the Nisutlin assemblage in the TTZ (Hansen et al., 1991) may record obduction of the SCK over the Cassiar terrane.

The next event recorded in the SCK is Middle Cretaceous plutonism. The ~ 90Ma Nisutlin batholith (Tempelman-Kluit, 1979) cuts the NE side of the SCK, placing a minimum age on the obduction event. It gave rise to contact metamorphism within a few hundred meters of the batholith. Minor normal faults in the area are likely related to either Cretaceous strike-slip faulting or younger extension.

References

Creaser, R.A., P. Erdmer, R.A. Stevens, and S.L. Grant (1997) Tectonic affinity of Nisutlin and Anvil assemblage strata from the Teslin Tectonic Zone, Northern Canadian Cordillera: constraints from neodymium isotope and geochemical evidence. *Tectonics,* vol.16, pp.107-121.

Creaser, R.A., J. S. Goodwin-Bell, P. Erdmer (in review) Geochemical and Nd isotopic constraints for the origin of eclogite protoliths, Northern Cordillera: implications for the Paleozoic tectonic evolution of the Yukon-Tanana terrane. *Can. J. Earth Sci.,* submitted 1998.

Erdmer, P. (1992) Eclogitic rocks in the St. Cyr klippe, Yukon, and their tectonic significance. *Can. J. Earth Sci.,* vol.29, pp.1296-1304.

Erdmer, P., E.D. Ghent, D.A. Archibald, M.Z. Stout (1998) Paleozoic and Mesozoic high-pressure metamorphism at the margin of ancestral North America in central Yukon. *GSA Bulletin,* vol.110, pp.615-629.

Fallas, K.M. (1997) Preliminary constraints on the structural and metamorphic evolution of the St. Cyr klippe, south-central Yukon. in F. Cook and P. Erdmer (compilers), *Slave-Northern Cordilleran Lithospheric Evolution (SNORCLE) and Cordilleran Tectonics Workshop Meeting (March 7-9), University of Calgary, Lithoprobe Report No. 56,* pp.90-95.

Fallas, K.M., P. Erdmer, D.A. Archibald, L.M. Heaman, and R.A. Creaser (1998) The St. Cyr klippe, south-central Yukon: an outlier of the Teslin Tectonic Zone? In F.Cook and P.Erdner (compilers), *Slave-Northern Cordilleran Lithospheric Evolution (SNORCLE) and Cordilleran Tectonics Workshop Meeting (March 6-8), Simon Fraser University, Lithoprobe Report No.64,* pp.131-138.

Ferri, F. (1997) Nina Creek Group and Lay Range Assemblage, north-central British Columbia: remnants of late Paleozoic oceanic and arc terranes. *Can. J. Earth Sci.*, vol.34, pp.854-874.

Grant, S.L. (1997) Geochemical, radiogenic tracer isotopic, and U-Pb geochronological studies of Yukon-Tanana terrane rocks from the Money klippe, southeastern Yukon, Canada. Unpub. MSc .thesis., Univ. of Alberta, 177p.

Hansen, V.L. (1989) Structural and kinematic evolution of the Teslin suture zone, Yukon: record of an ancient transpressional margin. *Journal of Structural Geology,* vol.11 (6), pp.717-733.

Hansen, V.L. (1991) Mesozoic thermal evolution of the Yukon-Tanana composite terrane: new evidence from 40Ar/39Ar data. *Tectonics*, vol.10 (1), pp.51-76.

Nelson, J.L. (1993) The Sylvester Allochthon: upper Paleozoic marginal-basin and island-arc terranes in northern British Columbia. *Can. J. Earth Sci.*, vol.30, pp.631-643.

Plint, H.E., and T.M. Gordon (1997) The Slide Mountain Terrane and the structural evolution of the Finlayson Lake Fault Zone, southeastern Yukon. *Can. J. Earth Sci.*, vol.34, pp.105-126.

Roback, R.C., J.H. Sevigny, and N.W. Walker (1994) Tectonic setting of the Slide Mountain terrane, southern British Columbia. *Tectonics,* vol.13 (5), pp.1242-1258.

Smith, A.D., and R.St J. Lambert (1995) Nd, Sr, and Pb isotopic evidence for contrasting origins of late Paleozoic volcanic rocks from the Slide Mountain and Cache Creek terranes, south-central British Columbia. *Can. J. Earth Sci.,* vol.32, pp.447-459.

Stevens, R.A., and P. Erdmer (1996) Structural divergence and transpression in the Teslin tectonic zone, southern Yukon Territory. *Tectonics,* vol.15 (6), pp.1342-1363..

Stevens, R.A., P. Erdmer, R.A. Creaser, and S.L. Grant (1996) Mississippian assembly of the Nisutlin assemblage: evidence from primary contact relationships and Mississippian magmatism in the Teslin tectonic zone, part of the Yukon-Tanana terrane of south-central Yukon. *Can. J. Earth Sci.,* vol.33, pp.103-116.

Tempelman-Kluit, D.J. (1979) Transported cataclasite, ophiolite and granodiorite in Yukon: evidence of arc-continent collision. *Geological Survey of Canada,* Paper 79-14.

Wheeler, J.O., and P. McFeely (1991) Tectonic Assemblage Map of the Canadian Cordillera and adjacent parts of the United States of America. *Geological Survey of Canada Map* 1712A.

Yukon-Tanana terrane and its relationship to Slide Mountain 'terrane', Finlayson Lake area, southeastern Yukon

Donald C. Murphy
Yukon Geology Program
Yukon Government
Box 2703 (F-3)
Whitehorse, Yukon Y1A 2C6
don.murphy@gov.yk.ca

Geological mapping of Yukon-Tanana terrane near Finlayson Lake (Murphy, 1997, 1998; Murphy and Piercey, 1998, 1999; Murphy and Timmerman, 1997a, b) has outlined the stratigraphy and structure of the terrane in this area, and clarified the relationship of the terrane to the overlying rocks of the Campbell Range belt, previously correlated with Slide Mountain terrane.

Yukon-Tanana terrane in this area is composed of two stratigraphic successions inferred to be separated by a regional angular unconformity. The succession beneath the unconformity consists of four polydeformed stratigraphic units intruded by Early Mississippian orthogneiss. Unit 1 comprises muscovite-quartz schist and pelitic schist of predominantly clastic protolith but also includes some felsic meta-volcanic rocks. A regionally extensive marble and calc-schist unit occurs near the top of unit 1. Unit 2 consists of biotite-chlorite schist and is interpreted as a mafic meta-volcanic unit. Locally, unit 2 is spatially associated with layer-conformable bodies of ultramafic rock that are inferred to be comagmatic sills. Unit 3 consists of muscovite-quartz schist and augen schist of felsic meta-volcanic protolith and variable amounts of carbonaceous phyllite and marble. The youngest unit beneath the unconformity comprises biotite-chlorite schist, carbonaceous phyllite, quartzite and quartz grit. Yukon-Tanana terrane rocks above the unconformity are less deformed than the lower succession and consist primarily of carbonaceous metaclastic rocks and quartz- and feldspar-phyric felsic metavolcanic rocks. The basal part of the sequence consists of quartzofeldspathic grit and sandstone interbedded with carbonaceous phyllite (unit 5l). Quartz and feldspar pebble conglomerate occurs locally in the basal unit. Quartz-feldspar meta-porphyry (unit 5qfp) and carbonaceous phyllite (unit 5cp) overlie the basal clastic unit; the amount of porphyry is laterally variable and generally decreases upsection. The top of this unit is marked by a laterally persistent siliceous exhalite unit (unit 6) containing baritic magnetite iron formation. The siliceous exhalite unit is overlain by a carbonaceous phyllite and gritty quartz sandstone unit with lesser diamictite and mafic meta-volcanic rock (unit 7). The top

of this unit is marked by a green chert and tuffaceous chert and greywacke member which is overlain by pillow breccias at the base of the Campbell Range basalt.

Early Mississippian orthogneiss, intruding only the lower succession, is predominantly granite to quartz monzonite in composition in this area but rare bodies of biotite-hornblende meta-diorite also occur. The larger bodies of orthogneiss have undergone all the phases of deformation experienced by the layered rocks of the lower succession. However, some smaller bodies, originally considered to be Cretaceous yet have preliminary Early Mississippian ages (J. Mortensen, personal communication), are discordant to the main phase foliation yet folded and weakly foliated. The significance of this Early Mississippian deformation implied by these relationships is as yet unclear but the nearby occurrence of eclogite with Mississippian cooling ages (Erdmer et al, 1998) suggests an event of regional tectonic significance.

The interpretation that the two successions are separated by an unconformity is based on several key observations. First of all, the overlying succession is less deformed than the lower succession. Secondly, the underlying succession strikes east-west and the overlying succession strikes northwest-southeast. Hence, the basal unit of the younger succession overlies different units of the underlying succession. Thirdly, quartz and feldspar pebble meta-conglomerate at the base of the overlying succession is a proximal deposit as indicated by angularity of clasts and euhedral detrital zircons and an obvious source is the coarse-grained orthogneiss and augen schist of the underlying succession. Fourthly, the late kinematic nature of weakly deformed Early Mississippian granite implies that some deformation occurred before the intrusion of this granite, which only occurs with rocks of the lower succession. Fifthly, there are no structural features at or near the contact suggesting a faulted or sheared contact. Sixthly, quartz-feldspar meta-porphyry inferred to be a subvolcanic feeder to the voluminous felsic meta-volcanic rocks of the younger succession is less highly deformed than adjacent felsic meta-volcanic rocks of the older succession.

In contrast to previous interpretations (e.g. Plint and Gordon, 1997 and references therein), the contact between unit 7 and the Campbell Range basalt is inferred to be depositional. First of all, the top of unit 7 includes pale green siliceous phyllite and meta-sandstone as well as some of the rock types of the Campbell Range belt such as thin-bedded chert and rare fragmental meta-basalt with carbonate cement. The occurrence of these rock types at the top of unit 7 suggests a transitional contact with Campbell Range meta-basalt. Secondly, the contact exhibits

no structural evidence of a fault or shear zone. The base of the sheet of Campbell Range meta-basalt has been observed with relatively good exposure both along strike and across strike in anticlinal hinge zones. Everywhere along this contact, the meta-basalt sits above the transitional-looking upper part of unit 7 and there are no increases in the amount of fracturing or strength of foliation, slickensides or gouge. Meta-basalt and unit 7 are folded conformably around first-order upright to southwestwardly overturned, southwest-vergent folds with a gently dipping enveloping surface.

If this new interpretation that the Campbell Range meta-basalt is depositionally linked to Yukon-Tanana terrane is correct, then the contact cannot be a terrane boundary. Rocks of the Campbell Range belt must be now be considered in the context of Yukon-Tanana terrane and not as part of a separate allochthonous Slide Mountain 'terrane'. This contact would therefore mark a profound shift in the tectonic evolution of the Yukon-Tanana crustal block. Rocks of Yukon-Tanana terrane below this contact represent a mid-Paleozoic continental magmatic arc (Mortensen and Jilson, 1985; Mortensen, 1992). Rocks above this contact formed in an oceanic or marginal basin setting. This transition, which occurred sometime in the Pennsylvanian or Permian, can be explained in many ways, none of which can be reasonably constrained with current information.

References

Erdmer, P.; Ghent, E.D.; Archibald, D.A.; and Stout, M.Z.; 1998. Paleozoic and Mesozoic high-pressure metamorphism at the margin of ancestral North America in central Yukon. Geological Society of America Bulletin v. 110, p. 615-629.

Mortensen, J.K., 1992. Pre-mid-Mesozoic tectonic evolution of the Yukon-Tanana Terrane, Yukon and Alaska. Tectonics, v. 11, p. 836-853.

Mortensen, J.K. and Jilson, G.A., 1985. Evolution of the Yukon-Tanana terrane: evidence from southeastern Yukon Territory. Geology, v. 13, p. 806-810.

Murphy, D.C., 1997. Preliminary geological map of Grass Lakes area, Pelly Mountains, southeastern Yukon (105G/7). Exploration and Geological Services Division, Yukon, Indian and Northern Affairs Canada, Open File 1997-3, scale 1:50 000.

Murphy, D.C., 1998. Stratigraphic framework for syngenetic mineral occurrences, Yukon-Tanana Terrane south of Finlayson Lake: A progress report. In: Yukon Exploration and Geology 1997, Exploration and Geological Services Division, Indian and Northern Affairs Canada, p. 51-58.

Murphy, D.C. and Piercey, S.J., 1998. Preliminary geological map of northern Wolverine Lake area (NTS 105G/8, north half). Exploration and Geological Services Division, Indian and Northern Affairs Canada, Open File 1998-4.

Murphy, D.C. and Timmerman, J.R.M., 1997a. Preliminary geological map of part of Grass Lakes area, Pelly Mountains, southeastern Yukon (105G/7). Exploration and Geological Services Division, Yukon, Indian and Northern Affairs Canada, Open File 1997-1, scale 1:50 000.

Murphy, D.C. and Timmerman, J.R.M., 1997b. Preliminary geology of the northeast third of Grass Lakes map area (105G/7), Pelly Mountains, southeastern Yukon. In: Yukon Exploration and Geology 1996, Exploration and Geological Services Division, Yukon, Indian and Northern Affairs Canada, p. 62-73.

Plint, H.E. and Gordon, T.M., 1997. The Slide Mountain Terrane and the structural evolution of the Finlayson Lake Fault Zone, southeastern Yukon. Canadian Journal of Earth Sciences, v. 34, p. 105-126.

Volcanic Probes of the Craton's Edge Beneath the Northern Canadian Cordillera

Francis, Don, Abraham, Anne-Claude, Earth & Planet. Science, McGill Uni. Montréal, and Polvé, Mireille, Université Paul Sabatier, Toulouse, France.

Distinct isotopic (Sr, Nd, and Pb) discontinuities exist in two of the three volcanic provinces that have spanned the width of the northern Canadian Cordillera since the mid-Cretaceous. The most important of these isotopic breaks corresponds to the position of the boundary between the Intermontane and Omenica Belts, indicating the occurrence of a fundamental lithospheric transition across this boundary, which may correspond to the edge of the North American craton.

Since their assembly in the mid-Creaceous, three episodes of volcanism have spanned of the disparate terranes of the northern Canadian Cordillera:

- *Recent Alkaline Volcanism (0-15 Ma)*

  Numerous small alkaline volcanic centres of late Tertiary to Recent age occur along the length of the northern Canadian Cordillera, many of which host spinel lherzolite mantle xenoliths. Lava compositions range from olivine nephelinites to hyperstene-normative basalts, in some cases in single vents. This recent alkaline volcanism is thought to be associated with localised zones of trans-tension caused by the relative dextral motion between the Pacific and North American plates (Souther, 1992).

- *Eocene Magmatism (40-50 Ma)*

  Eocene volcanic successions outcrop along the length of the western Intermontane Belt (IMB), adjacent to coeval granitoid plutons of the Coast Plutonic Belt (CPB) to the West, and isolated erosional remnants occur across the Cordillera, from west of Carmacks to the Tintina trench. Lava compositions range from basalt to rhyolite, and are characterized by chemical affinities that change from alkaline and tholeiitic to calc-alkaline in time and space. The intensity of magmatism in the Eocene is believed to be related to the change in relative motion of the North American plate with respect to the Kula-Farallon plate, from dominantly orthogonal to oblique (Gabrielse and Yorath, 1991).

- *Late Cretaceous Carmacks Volcanics (70 Ma)*

  Remnants of thick successions of high-K to shoshonitic lavas stretch from Dawson to Whitehorse. These lavas have calc-alkaline chemical signatures, including: enrichment in large ion lithophile and light rare earth elements (REE), relative depletion in high field strength elements, and flat heavy REE patterns. In the central part of the Carmacks province, high-Mg ankaramites (15 wt.% MgO) have erupted on both sides of the Yukon River. Despite their "calc-alkaline" signature, the Carmacks magmas appear to reflect melting in the lithospheric mantle, possibly over the Yellowstone hotspot (Johnston et al. 1996).

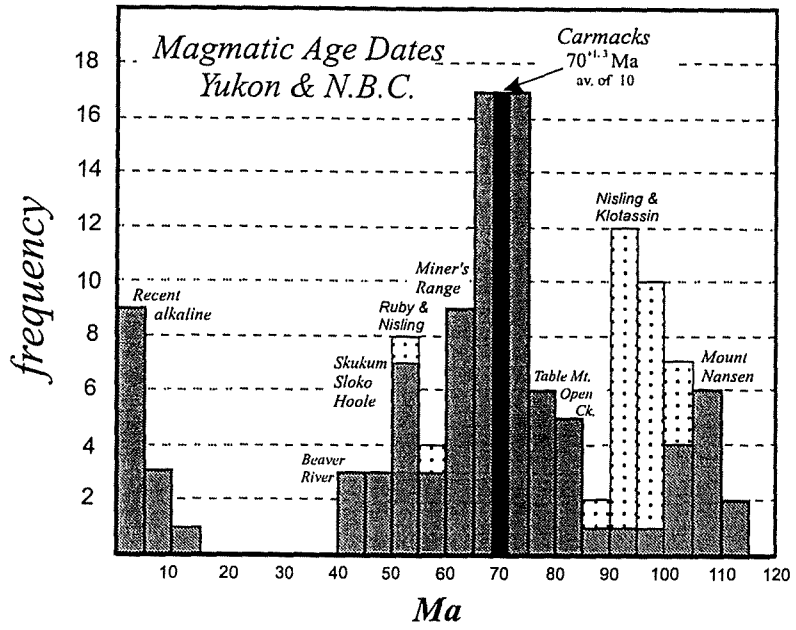

Figure 1: Magmatic age dates in the northern Canadian Cordillera.

Our studies of the regional variations across the northern Canadian Cordillera show evidence for a coincident isotopic discontinuities in both the recent alkaline basalts and the late-Cretaceous Carmacks volcanics that corresponds with the boundary between the Intermontane (IMB) and Omenica (OMB) belts.

1. Recent Alkaline Volcanism

There are three discontinuities in the isotopic and chemical signatures of the recent alkaline basalts across the northern Canadian Cordillera:

- One occurs at the Tintina Fault, a major transcurrent fault separating the assembled terranes of the Cordillera from the North American Craton. Basaltic lavas of the east side of the fault are characterized by significant higher Ca, Zr, and $^{143}Nd/^{144}Nd$, and lower heavy rare-earth elements (HREE) and $^{87}Sr/^{86}Sr$ than their equivalents erupted on the west side of the fault. These results suggest that the Tintina Fault is a high angle fault that penetrates the upper mantle and separates 2 distinct lithospheric roots.
- The most pertinent to this talk occurs between the Cassiar and Teslin Faults, approximately 20 km to the East of the surface expression of the boundary between the IMB and Omineca Belt (OMB), along the Stikine volcanic belt. Samples erupted to the East of the Cassiar Fault have higher Rb, $^{87}Sr/^{86}Sr$ and Pb isotopic ratios, but lower $^{143}Nd/^{144}Nd$ ratios than their equivalents in the westernmost OMB and the IMB.

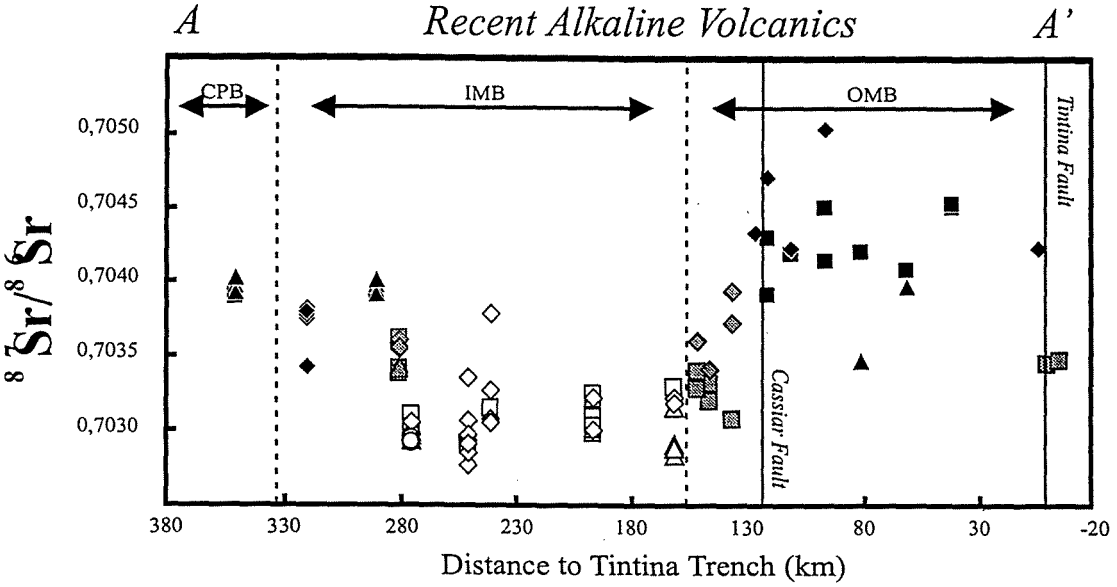

Figure 2: Projection of the isotopic variation in recent alkaline basalts across the Cordillera

- A third occurs in the alkaline basalts of the IMB, to the east of its boundary with the Coast Plutonic Belt (CPB). The central IMB alkaline lavas have distinctly lower $^{87}Sr/^{86}Sr$, Nb/Zr, and Rb/Zr ratios than basalts erupted near its western margin or within the CPB to the West. The alkaline basalts of the western IMB and the CPB do not, however, share the high $^{207}Pb/^{204}Pb$ and $^{208}Pb/^{204}Pb$ ratios of the alkaline basalts of the OMB to the East. These results indicate that the relatively radiogenic source region of the CPB alkaline basalts extends beneath the western margin of the IMB.

In general, there is a striking overall correspondence between the regional variation in $^{87}Sr/^{86}Sr$ in the recent alkaline basalts and the Sr line defined by Armstrong on the basis of regional variations in the isotopic composition of Mesozoic and Tertiary granitoids. The alkaline basalt Sr isotopic compositions are, however, are systematically less radiogenic than adjacent Mesozoic granitoids.

2. *Carmacks Volcanism*

New isotopic results for the late Cretaceous Carmacks volcanics (Francis and Johnston, 1998) indicate the existence of an isotopic discontinuity across the boundary between the Intermontane and Omenica Belts long the Yukon River, near the town of Carmacks. From the west to the East sides of the Yukon River, there is a discontinuous increase in $^{87}Sr/^{86}Sr_i$ and decrease in $^{143}Nd/^{144}Nd_i$, which lines up with the northward projection of the Teslin fault to the South. Although the isotopic data for the Carmacks volcanics to the East of the Yukon River are still scarce, it would appear that both the recent alkaline volcanics and the late Cretaceous Carmacks volcanics have detected a significant lithospheric change corresponding approximately to the IMB - OMB boundary. Unlike the case for the recent alkaline basalts, however, the Sr isotopic composition of the Carmacks lavas closely approximates that of adjacent Mesozoic granitoid plutons.

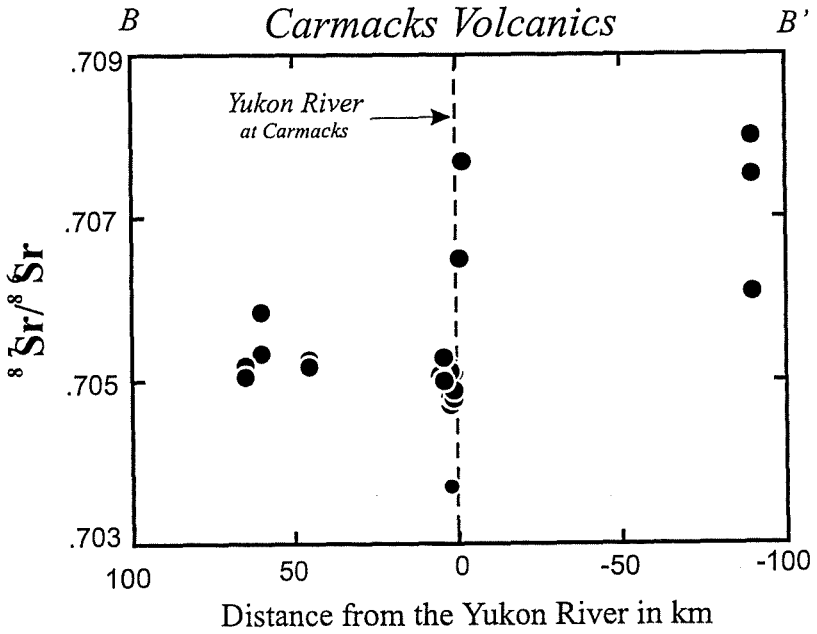

Figure 3: Projection of the isotopic variation in the Carmacks lavas across the Cordillera.

Unfortunately, there is not enough isotopic data at the moment to determine whether similar isotopic discontinuities exist in the Eocene calc-alkaline lavas across the northern Canadian Cordillera. The regional isotopic variations in the Mesozoic and Tertiary granitoids, the late-Cretaceous Carmacks volcanics, and the recent alkaline basalts, however, all clearly detect a major lithospheric change at the IMB – OMB boundary, which may correspond to the edge of the North American craton.

Mantle Signature versus Crustal Contamination in Arc-Magmatism: An Example from Zippa Mountain

M. Westphal, I.M. Coulson, G.M. Dipple, and J.K. Russell

Department of Earth and Ocean Sciences
The University of British Columbia
Vancouver, B.C. V6T 1Z4

Introduction

The Zippa Mountain pluton is the best-exposed example of a suite of zoned silica-undersaturated alkaline plutons (ZSAP) that intrude the Stikine and Quesnel terranes (e.g., Coulson et al., 1999 and this volume). The distinctive chemistry and mineralogy of this suite and the short time-span of emplacement for these plutons have been marshaled as evidence for a shared or similar tectonic history of the Quesnel and Stikine Terranes in late Triassic to Jurassic times (Lang et al., 1995; Coulson et al., this volume). However, the Zippa Mountain pluton is also ringed by a series of skarn deposits that record extensive chemical interaction of the magma chamber with Paleozoic limestone at shallow crustal levels. The mechanisms of interaction are preserved in these deposits because they have been frozen mid-stream. Here we describe these deposits and comment on the nature and consequences of chemical interaction between the Zippa Mountain pluton and Paleozoic limestone of the Stikine assemblage. Future work on these deposits will identify those chemical attributes of the ZSAP that are indicative of source region (mantle) from those that result from crustal interactions.

Geologic Setting

The Zippa Mountain intrusion is of late Triassic age and is situated in the Iskut River area (NTS 104 B 11) of northwest British Columbia (Kerr, 1948; Woodsworth et al., 1991; inset of Fig. 1). The pluton is elliptical in shape and 3.5 by 5 km in diameter, and is compositionally zoned from clinopyroxenite, at the pluton margins, through mela-syenite to a core of syenite (e.g., Coulson et al, this volume). It intrudes the Paleozoic and Mesozoic stratigraphy of Stikinia (Fig. 1). These strata include limestone, schist, phyllite, and calc-silicate of the Stikine assemblage, and interbedded pyroxene porphyritic tuff and lava of the late Triassic Stuhini group. Both the Stikine assemblage and the Stuhini Group have been interpreted to be remnants of magmatic island arcs (Monger, 1977; Brown et al., 1991; Anderson, 1993).

Wollastonite +/- diopside, grossular, and andradite skarn is developed peripheral to the Zippa Mountain intrusion (Fig. 1; Jaworski and Dipple, 1996). Skarn typically contains greater than 80% wollastonite by volume and many zones exceed 95% in purity. Skarn is hosted by limestone of the Paleozoic Stikine assemblage and occurs as isolated rafts enclosed within clinopyroxenite of the Zippa Mountain pluton (e.g., Cliff and Glacier deposits, Fig. 1) and as replacement bodies adjacent to the pluton (e.g., Bril and Bartnick

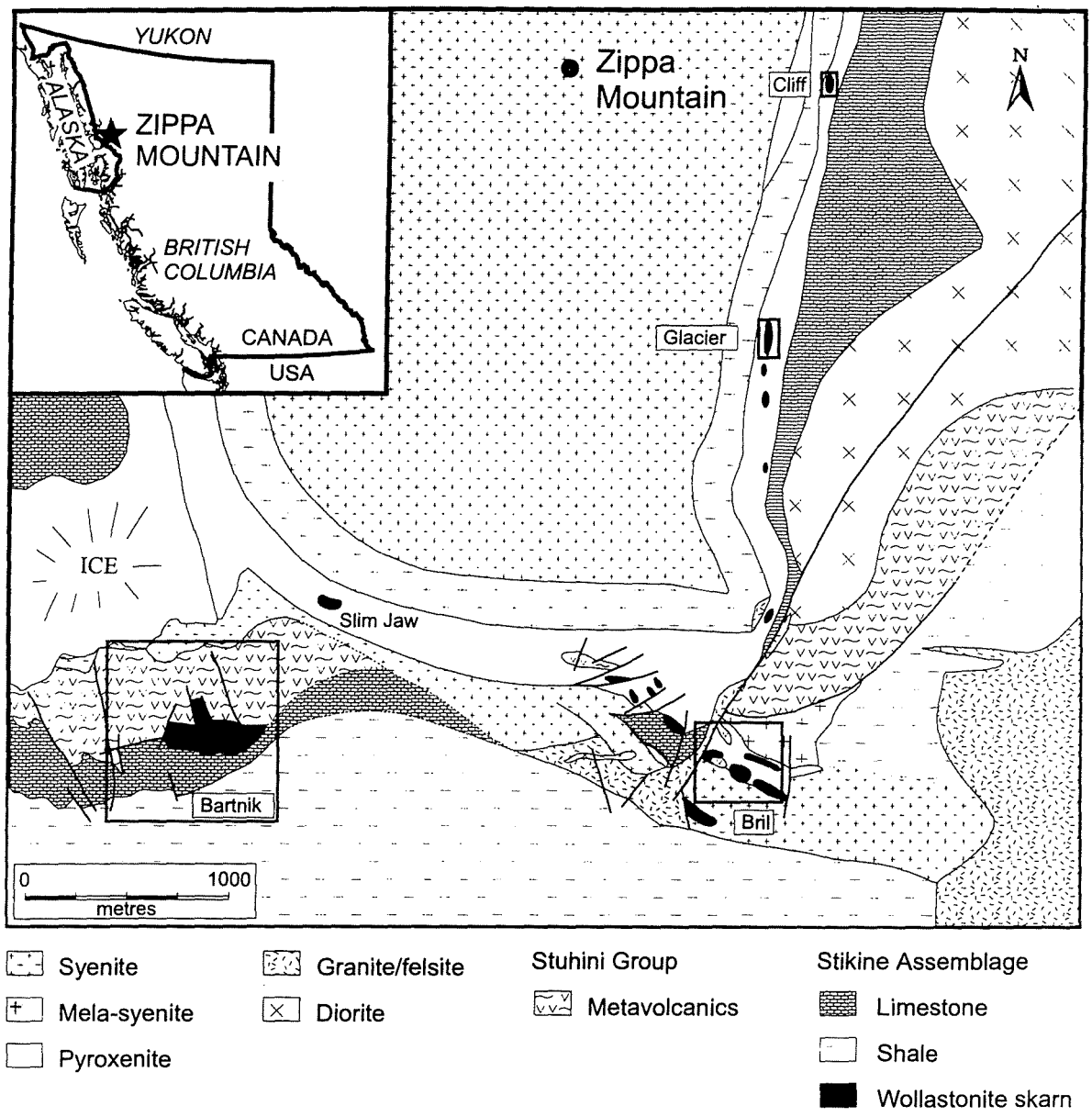

Figure 1. Geological map of the Zippa Mountain intrusion and adjacent region (modified from Lueck and Russell, 1994; Jaworski and Dipple, 1996; Westphal et al., in prep.).

deposits). Figure 2 presents schematic representations of skarn geometry that is based on our deposit maps (Jaworski and Dipple, 1996; Westphal et al., in prep.).

Diking, Stoping and Assimilation

The Glacier, Cliff, and Bril deposits record the physical and chemical erosion of limestone that occurs where it is in contact with the Zippa Mountain pluton. Rafts and xenoliths of skarn were incorporated into the pluton by a combination of dike injection and chemical reaction (assimilation). Further reaction between skarn and magma is evident as reaction zones around xenoliths and rafts.

The Cliff deposit consists of a single large raft of metasediment (Fig. 2a) about 160 meters long, 100 meters high and 15 to 30 metres thick that survived intact within the enclosing pyroxenite. In contrast, the Glacier deposit contains xenoliths of skarn that have been dissected by dikes and chemically reacted with magma after being enclosed by magma (Fig. 2b). Xenolith diameter ranges from centimeters to tens of metres; the deposit extends for more that 300 metres up-slope. The Bril deposit is hosted in steeply dipping marble (formed by contact metamorphism of the limestone from the Stikine assemblage) at the southeast corner of the pluton, outside of the pluton proper (Fig. 1). Detailed mapping and extensive drilling of the deposit has constrained its geometry in three dimensions (Westphal et al., in prep.). The skarn extends at least 150 metres at depth into pyroxenite and syenite but remains attached to the host strata of the Stikine assemblage at the highest elevations (Fig. 2c). The prevalence of pyroxenite dikes and the rounded and embayed skarn boundaries at the Bril deposit are indicative of detachment by a combination of dike injection and chemical reaction.

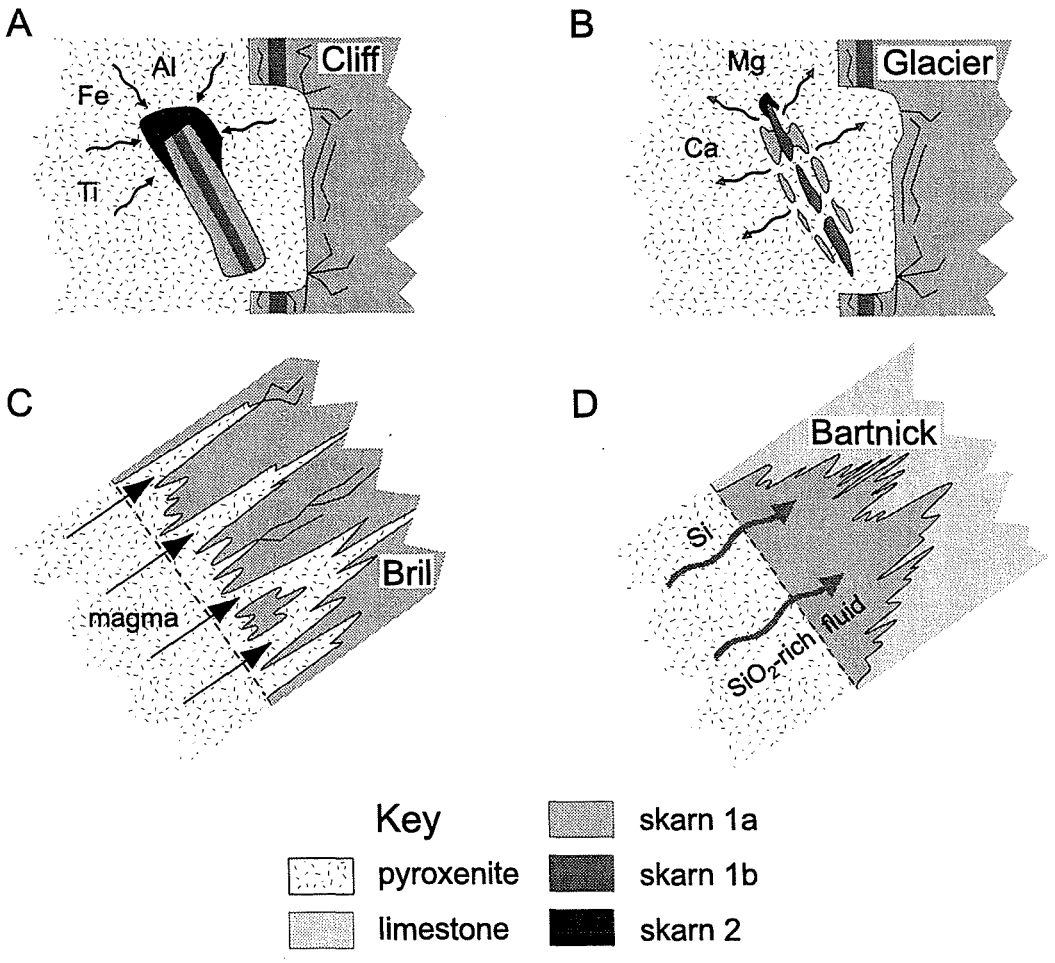

Figure 2. Styles of magma-wall rock interaction at Zippa Mountain.

The latest stages of skarn formation at the Glacier and Cliff deposits clearly postdate stoping. Andradite-wollastonite skarn is developed on the margins of small (metre-scale) xenoliths (Fig. 2b) at the Glacier deposit and around the large raft at the Cliff deposit (Fig. 2a). These skarn zones occur on a scale of centimetres to metres which suggests that mass transport was controlled by diffusional exchange between the xenoliths and the pyroxenite. Contamination of pyroxenite (see below) may record bi-directional mass transport that is the hallmark of diffusional exchange.

These observations and interpretations allow the stoping process to be generalized:

1. Marble and skarn are stoped as large rafts and further dissagregated within the pluton.
2. Detachment and dissagregation occurs via a combination of physical (diking) and chemical (reaction and assimilation) erosion.
3. Continued reaction between xenoliths and magma results in further skarn formation and magma contamination.

Magma Contamination

Lueck and Russell (1994) and Coulson et al. (1999, this volume) argue that some of the chemical zonation of ZSAP plutons derives from fractional crystallization. In their model, the pyroxenite border phase forms by crystal settling at the margins of the pluton. However, not all of the petrologic features of the Zippa Mountain pluton result from magmatic differentiation processes. Our studies of pluton-skarn interaction have uncovered two features that require a different origin for some pyroxenite. At the glacier deposit, pyroxenite occurs as dykes that dissect and fragment rafts of skarn (Fig. 2b). The disaggregation of metasediments by the pyroxenite requires that it be liquid, rather than crystal-rich mush. Moreover, Westphal et al. (1998) proposed that some pyroxenite is a product of carbonate contamination of the Zippa Mountain pluton (Fig. 2b). This hypothesis is supported by the observation that pyroxenite is prevalent at all skarn deposits (Fig. 1) and by anomalous Ca-enrichment trends in some Zippa pyroxenite (Fig. 3).

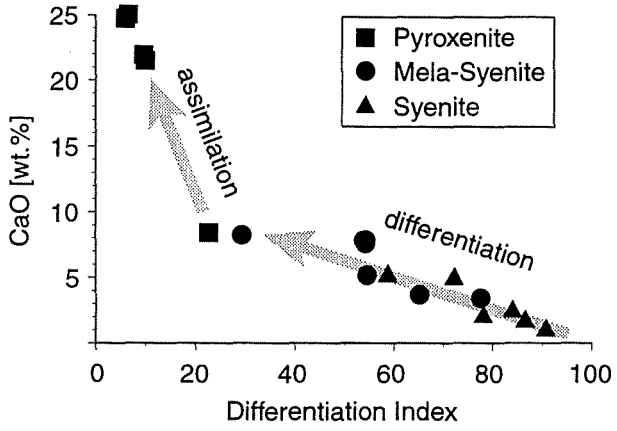

Figure 3. Plot of Wt. % CaO vs. Differentiation Index for Zippa Mountain plutonic rocks (after Coulson et al., 1999).

Loss of Chemical Species from the Magma

Loss of chemical species from the magma chamber is evident in the metasomatic rinds that formed on the xenoliths at the Glacier and Cliff deposits. In this instance, the lost components include Fe, Ti, and Al (Fig. 2a). A more dramatic example of lost chemical species is the formation of large skarn deposits external to the magma chamber by fluid expulsion. Skarn formation is a highly metasomatic process by which considerable chemical species are lost by the pluton to the enclosing wall rocks. This loss of chemical species is another manifestation of magma alteration by crustal interaction.

More than 500 vertical metres through the Bartnik deposit are exposed on an east-facing slope located about 2 km west of the Bril deposit (Fig. 1). Skarn is hosted within a thick sequence of Permian limestone that is probably correlative with the limestone sequence at the Bril deposit (Fig. 1). Marble dominates the upper levels of the deposit, where centimetre to decimetre thick skarn layers are restricted to fingers within massive marble (Fig. 2d) and to envelopes around folded and boudinaged calc-silicate layers. The lower levels of the deposit consist of massive wollastonite skarn generally metres in thickness, intercalated with calcsilicate. Marble occurs as centimetre to decimetre wide lenses. Sub-vertical drill holes intersect pyroxenite below the lower levels of the Bartnick deposit at a depth of about 60 metres.

The reaction boundary that separates marble from skarn demarcates an abrupt change in SiO_2 content. Jaworski and Dipple (1996) and Westphal et al. (1998 and in prep.) argued that the SiO_2 must have been metasomatically introduced because the metasedimentary protolith to the skarn is too poor in silica to form wollastonite isochemically (also see Dipple and Gerdes, 1998). Westphal et al. (1998) further argued that the scale of alteration requires advective transport of material and that the Zippa Mountain pluton was the source of metasomatic fluid. They present whole rock stable isotopic ratios demonstrating that wollastonite skarn is at or near isotopic equilibrium with pyroxenite and far from equilibrium with the host marble (Fig. 4). The host marble retains a $\delta^{18}O$ signature typical of marine limestone (c.f., Nabelek, 1991 and Westphal et al, 1998).

The formation of extensive wollastonite skarn exterior to the Zippa Mountain pluton marks significant loss of SiO_2 from the magma chamber, presumably as magmatically equilibrated fluid was expelled upwards from the pluton. It is not clear if wollastonite skarn formation at the other deposits occurred prior to, during, or after stoping. However, the scale of mass transport required by the size of these deposits implicates advective mass transport which restricts skarn formation to periods of exsolution of magmatic fluid. Wollastonite formation prior to stoping would require pluton emplacement at or near volatile saturation so that sufficient fluid was expelled to form skarn prior to the solidification of the margins of the pluton (Podladchikov and Wickham, 1994). The possibility that reaction between syenite and marble drove volatile saturation remains untested.

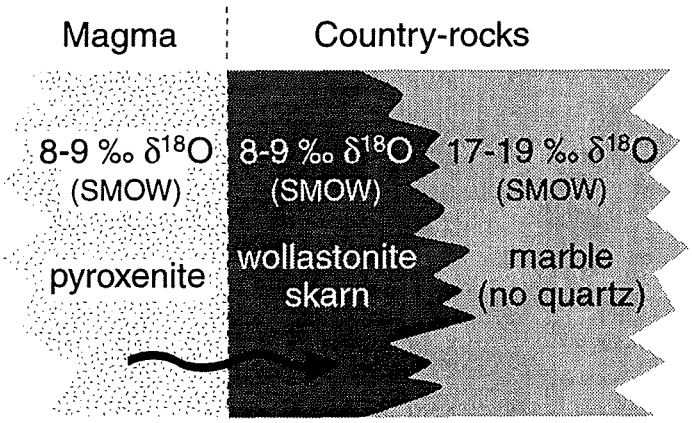

Figure 4. Oxygen isotope ratios in whole rock samples of igneous pyroxenite, wollastonite skarn, and marble (after Westphal et al., 1998).

Conclusions

Zippa Mountain provides us with an excellent in situ record of the processes of magma/crustal interaction, frozen mid-stream. These interactions between dominantly calcareous country rocks and alkaline magmas, during or shortly after emplacement demonstrate a coupled system of internal and external processes that influence the bulk composition of the igneous rocks.

The main internal process was fractional crystallization of a mantle derived, silica-undersaturated, potassic magma, which resulted in pluton-scale zonation from syenite in the core to pyroxenite at the rim (Coulson et al., this volume). The two main external processes were (i) gain of elements by assimilation of country rocks and (ii) loss of elements to the country rocks by fluid egress and metasomatic reaction. As a result, the Zippa Mountain igneous rocks show both a mantle-like signature and significant crustal contamination. To date, evidence of contamination is restricted to the border phases of the pluton. Future work on the Zippa Mountain pluton and skarn will further constrain those chemical and petrologic attributes that are indicative of source region (mantle) from those that result from crustal interactions.

Acknowledgements

This research is supported by Whitegold Resources Inc. and NSERC, in the form of an Industry Orientated Research grant held by Dipple and Russell.

References

Anderson, R.G. 1993. A Mesozoic stratigraphic and plutonic framework for northwestern Stikinia (Iskut River map area), northwestern British Columbia, Canada. In Mesozoic Paleogeography of the Western United States –II (G. Dunne and K. McDougall, Eds.) Pacific section of the SEPM: vol. 71, p. 477-494.

Brown, D.A., Logan, J.M., Gunning, M.H., Orchard, M.J., and Bamber, W.E. 1991. Stratigraphic evolution of the Paleozoic Stikine Assemblage in the Stikine and Iskut rivers area, northwestern British Columbia. Canadian Journal of Earth Sciences 28: 958-972.

Coulson, I.M., Russell, J.K. and Dipple, G.M. (1999, accepted pending revisions). The Zippa Mountain intrusion: A zoned, silica-undersaturated alkaline pluton from the Cordillera of British Columbia. Canadian Journal of Earth Sciences.

Coulson, I.M., Westphal, M., Russell, J.K., and Dipple, G.M. (this volume) Primitive arc-magmatism in Stikinia: implications from the Zippa Mountain Pluton.

Dipple, G.M. and Gerdes, M., (1998) Reaction infiltration feedback and hydrodynamics at the skarn front. In: Mineralized Intrusion-Related Skarn Systems. Mineralogical Association of Canada Short Course Volume 26. D.R. Lentz, (Ed.) Mineralogical Association of Canada, p. 71-97.

Jaworski, B.J. and, Dipple, G.M. 1996. Zippa Mountain wollastonite skarns, Iskut River map area (104B/11). Geological fieldwork 1995, Paper 1996-1.

Kerr, F.A. 1948. Lower Stikine and Western Iskut River Areas, B. C.: Geological Survey of Canada, Memoir 246.

Lang, J.R., Lueck, B., Mortensen, J.K., Russell, J.K., Stanley, C.R., and Thompson, J.F.H. 1995. Triassic-Jurassic silica-undersaturated and silica-saturated alkalic intrusions in the Cordillera of British Columbia: Implications for arc magmatism. Geology, 23:5, 451-454.

Lueck, B.A., and Russell, J.K. 1994. Geology and origins of the Zippa Mountain igneous complex with emphasis on the Zippa Mountain pluton, northern British Columbia. In Current research 1994-A. Geological Survey of Canada, pp.77-85.

Monger, J.W.H. 1977. Upper Paleozoic rocks of the western Canadian Cordillera and their bearing on Cordilleran evolution. Canadian Journal of Earth Sciences, 14: 1832-1859.

Nabelek, P.L., (1991) Stable isotope monitors. Mineralogical Society of America Reviews in Mineralogy Volume 26. D.M. Kerrick, (Ed.) Mineralogical Society of America, p. 395-435.

Podladchikov, Y.Y. and Wickham, S.M. 1994. Crystallization of hydrous magmas: calculation of associated thermal effects, volatile fluxes, and isotopic alteration. Journal of Geology, 102: 25-45.

Westphal, M., Dipple, G.M., and Kyser, K. 1998. Documenting the plumbing system of the Isk Wollastonite Skarn, Zippa Mountain, British Columbia, Canada. Geological Society of America, Abstracts with Programs, 30, A279.

Woodsworth, G. A., Anderson, R. G., and Armstrong, R. L. 1991. Chapter 15, Plutonic Regimes, In Geology of the Cordilleran Orogen in Canada, Geology of Canada, no. 4. Edited by H. Gabrielse and C.J. Yorath. Canada Geological Survey , pp. 491-531.

Geotectonic motion history of the Yukon-Tanana Terrane: Preliminary paleomagnetic results from the Big Creek and Seymour Creek intrusions.

D.T.A. Symons[1], P.J.A. McCausland[2], C.J.R. Hart[3], W.H. Blackburn[4], M.J. Harris[2], and P.R. Williams[1]

[1]Earth Sciences, University of Windsor, Windsor, Ontario N9B 3P4
[2]Earth Sciences, University of Western Ontario, London, Ontario N6A 5B7
[3]Yukon Geology Program, Government of Yukon, Box 2703 [F-3], Whitehorse, YT Y1A 2C6
[4]Royal Roads University, 2005 Sooke Rd., Victoria, BC V9B 5Y2

1. Introduction

Assembly models of the North American western Cordillera differ regarding the role of the Yukon-Tanana Terrane (YTT) in the margin's accretionary history. The YTT is an assemblage of rocks with apparent continental North American affinity (Lowe et al., 1994) that may be: 1) far-traveled along the North American margin, perhaps associated with the Intermontane Belt terranes (e.g. Irving et al., 1996; Johnston et al., 1996); or, 2) in situ with respect to North America, having acted as a 'bumper' to halt the northward motion of the Intermontane Belt terranes (e.g. McLelland et al., 1992; Mihalynuk et al., 1994). Therefore a key question to be investigated by this and further studies is: Did the YTT (or parts of it) participate in the motion of the Intermontane Belt terranes relative to North America? This study presents preliminary paleomagnetic evidence that suggests the YTT's tectonic motion history since the Early Jurassic. The appendix briefly summarizes the status of other collections being analysed paleomagnetically as part of the overall project.

2. Geological setting

The enigmatic Yukon-Tanana Terrane underlies much of south-central Yukon and eastern Alaska (Figure 1). In this study it is considered to have been a relatively coherent block since Early Jurassic time that is composed of metamorphosed Paleozoic-Triassic passive margin and continental arc assemblages of North American heritage (Mortensen, 1992; Lowe et al., 1994). Mesozoic and younger evolution of the central YTT involves Late Triassic-Early Jurassic plutonism and uplift, with subsequent regional Late Jurassic-Early Cretaceous southeast-directed extension. This was followed by the emplacement of mid Cretaceous and Late Cretaceous-Tertiary plutonic and volcanic rocks (Hansen et al., 1991; Hansen and Dusel-Bacon, 1998).

The Big Creek and Seymour Creek intrusions are located in the south-central YTT, about 200 km northwest of Whitehorse. The Early Jurassic Big Creek batholith outcrops over ~400 km^2 and is generally elongated NW-SE, bounded to the northeast by the Big Creek fault (Figure 2). It consists of variably coarse-grained hornblende syenites and monzogabbros that intrude metamorphic host rocks of the YTT and the Early Jurassic Granite Mountain batholith. U-Pb ages of 197 +/- 1 Ma from zircon and 184 +/- 2 Ma from

titanite (Mortensen and Jilson, 1985), and a K-Ar age on hornblende of 188.8 +/- 3.8 Ma (Hunt and Roddick, 1987) put the emplacement of the Big Creek batholith at about ~190 Ma. Younger K-Ar hornblende ages of 152 +/- 7 Ma and 142 +/- 10 Ma obtained from the more altered rocks at the southeast end of the batholith (Stevens et al., 1982) likely reflect thermal resetting due to regional extension in the south-central YTT (Hansen et al., 1991).

The Seymour Creek stock is a 4 km^2 ovate body emplaced into the Big Creek and Early Cretaceous Dawson Range batholiths, stitching the Big Creek Fault (Figure 3). It is a massive granodiorite to quartz monzonite pluton with ubiquitous biotite and accessory apatite and magnetite. Hornblende is rare, but locally abundant. A K-Ar biotite age of 85.2 +/- 2.6 Ma (Tempelman-Kluit and Wanless, 1975) was determined for quartz monzonite from the Seymour Creek stock.

3. Paleomagnetism

The Big Creek batholith yielded a collection of 236 specimens from 21 sites (Figure 2), while 154 specimens were obtained from 16 sites in the Seymour Creek stock (Figure 3). Both collections were subjected to standard AF and thermal demagnetization methods at the Paleomagnetic Laboratory of the University of Windsor using a Sapphire Instruments SI-4 alternating-field (AF) demagnetizer, a Magnetic Measurements MMTD1 thermal demagnetizer, and an automated CTF DRM-420 cryogenic magnetometer that are set inside a magnetically-shielded room which has 0.2% of the Earth's ambient magnetic field intensity.

Saturation isothermal remanent magnetization (SIRM) testing was performed on 12 specimens from each collection with a Sapphire Instruments SI-6 pulse magnetizer and AF demagnetization. Thermal decay curves show that the characteristic remanent magnetization (ChRM) in both the Big Creek and Seymour Creek collections is carried by titanomagnetite or magnetite, while SIRM acquisition and decay curves indicate the magnetic carriers are stable multi- to pseudosingle-domain magnetite.

Preliminary paleomagnetic analysis of the Big Creek batholith collection (Williams, 1998) found a steep normal-polarity ChRM in 16 sites and an antiparallel reversed-polarity ChRM in two sites. Three sites were randomly oriented without a mean direction. A mean direction of D=305.6°, I=72.1°; α_{95}=3.9°, k=82 is calculated from 18 sites for the Big Creek batholith (Figure 4a). For the Seymour Creek stock, 14 sites carried a steep, reversed ChRM, while two sites exibited normal-polarity magnetizations, together comprising a single bipolarity distribution with mean (reversed) direction D=87.7°, I=-83.4°; α_{95}=5.0°, k=55.5 (Figure 4b).

The age of normal-polarity magnetization for the Big Creek batholith is inferred to be related to early Middle Jurassic uplift, since preliminary Al-in-hornblende geobarometry (Schmidt, 1992) shows a depth of emplacement ~20 km, where high ambient crustal

temperatures would forestall the acquisition of a permanent magnetization. The Seymour Creek stock was emplaced at ~10 km depth, and its dominantly-reversed ChRM direction is different from that of the Big Creek batholith, thus providing a contact test. While no paleomagnetic tests for primary remanence are available for the ~85 Ma Seymour Creek stock, its dominantly-reversed ChRM is consistent with primary remanence acquisition during the Earth's 83-79 Ma period of reversed polarity (Jacobs, 1994). Primary remanence is likely for the Seymour Creek stock since it postdates regional deformation events and it shows no mineralogical evidence for post-emplacement metamorphism or tectonic displacement.

4. Discussion

These preliminary paleomagnetic results from the Early Jurassic Big Creek batholith and intruding Late Cretaceous Seymour Creek stock yield paleopoles of 63°N, 147°E (*dp*=6°, *dm*=7°) and 59°N, 197°E (*dp*=10°, *dm*=10°), respectively (Figure 5). Comparison of these paleopoles with the North American APWP (Besse and Courtillot, 1991) reveals a consistent relationship between the YTT and North America, distinct from that reported for accreted terranes of the Canadian Cordillera. Both YTT paleopoles are slightly *near-sided* with respect to their cratonic reference poles, and both indicate ~30°+/-15° *counterclockwise* rotation of the YTT relative to North America. They imply that the YTT has been more or less in its present position relative to cratonic North America since the Early Jurassic, in accord with the pericratonic YTT interpretation of McLelland et al. (1992) and Mihalnyuk et al. (1994). Specifically, models of terrane accretion for the Cordillera may have to accomodate: 1) a YTT that does not seem to have participated in the Late Cretaceous northward transport of the terranes comprising the Intermontane Belt; and 2) a net ~30°+/-15° counterclockwise rotation of the YTT since the Late Cretaceous that is unlike the ~60°+/-15° clockwise rotation inferred for terranes of the Intermontane Belt (Irving et al., 1996; Harris et al., 1997a; Harris, 1998).

Along with studies from the Intermontane Belt (e.g. Irving et al., 1996; Harris et al., 1997a; Harris, 1998), these preliminary results from the south-central YTT are in sharp disagreement with those from the nearby and presumably overlying ~70 Ma Carmacks volcanics (Johnston et al., 1996; Wynne et al., 1998). The latter place the Intermontane Belt terranes and south-central YTT some 1900 km south of their present position in the latest Cretaceous. This discrepancy is perplexing, and will require in part further paleomagnetic study of the YTT's motion history to clarify its post-Triassic relationships to North America and the Intermontane Belt terranes. To this end, paleomagnetic work on Early Jurassic, Middle Cretaceous and Eocene plutons of the YTT is in progress.

Appendix

During the past summer collections were made from the ~190 Ma Granite Mountain batholith, the ~105 Ma Dawson Range batholith, and the ~56 Ma Pattison pluton from the YTT. The purpose of these collections, when combined with the ~190 Ma Big Creek and ~85 Ma Seymour Creek work, is to provide poles to define an apparent polar wander path for the central YTT. Comparison of the YTT to cratonic North America's path should fully confirm or deny the conclusion reached in the preceeding section that the YTT has always been proximal to the craton at about its present location. A fourth collection was made from the ~54 Ma Flat Creek batholith with cross-cutting Eocene dikes in the Stikine terrane. Its purpose is to check the conclusion reached from the White Pass dikes near Skagway in the Coast Plutonic Complex (CPC) that northward translation had ended by ~52 Ma in the CPC and inboard Intermontane terranes but that ~41°+/-15° clockwise rotation occurred subsequently. The four collections have an average of 289 specimens from 23 sites.

Prior to the current year, results from the Whitehorse pluton and Mount McIntyre pluton had been published in papers (Harris et al., 1996, 1997a) as well as in abstracts. During the year the results from several collections in the Intermontane terranes were set out in a Ph.D. thesis by Harris (1998). They have been circulated quickly in abstract format for the most part (Harris et al., 1997b; Harris et al., 1998a,b,c,d,e,f; Symons et al., 1997, 1998a,b) and are in the process of being published as papers (Harris et al., 1999a,b,c). Also, initial results from the YTT are being made available (McCausland et al., 1998; Symons 1998; Symons et al., 1998c; Williams, 1998).

References

Besse, J., and Courtillot, V., 1991. Revised and synthetic apparent polar wander paths of the African, Eurasian, North American and Indian plates, and true polar wander since 200 Ma. Journal of Geophysical Research, 96, B3, pp 4029-4050.

Johnston, S.T., Wynne, P.J., Francis, D., Hart, C.J.R., Enkin, R.J., and Engebretson, D.C., 1996. Yellowstone in Yukon: The Late Cretaceous Carmacks Group. Geology, 24, pp 997-1000.

Hansen, V.L., and Dusel-Bacon, C. 1998. Structural and kinematic evolution of the Yukon-Tanana upland tectonites, east-central Alaska: A record of late Paleozoic to Mesozoic crustal assembly. GSA Bulletin, 110(2), pp 211-230.

Hansen, V.L., Hietzler, T.M., and Harrison, T.M. 1991. Mesozoic thermal evolution of the Yukon-Tanana terrane: New evidence from ^{40}Ar-^{39}Ar data. Tectonics, 10, pp 51-76.

Harris, M.J., Symons, D.T.A., Blackburn, W.H., and Hart, C.J.R., 1996. Paleomagnetic study of the mid-Cretaceous Mount McIntyre pluton, Whitehorse map area (105D), southern Yukon Territory. Yukon Exploration and Geology 1996, p. 124-132.

Harris, M.J., Symons, D.T.A., Blackburn, W.H., and Hart, C.J.R., 1997a. Paleomagnetic and geobarometric study of the mid-Cretaceous Whitehorse Pluton, Yukon Territory. Can. Jour. Earth Sci., 34. pp 1379-1391.

Harris, M.J., Symons, D.T.A., Blackburn, W.H., and Hart, C.J.R., 1997b. Tectonic motion of the Jurassic Fourth of July batholith, northern British Columbia, from paleomagnetism. Am. Geophys. Un., EOS, 78, p. F188

Harris, M. J., 1998. Geotectonic motions of northern Canadian Cordilleran terranes from paleomagnetic measurements with geobarometric corrections. Ph.D. thesis, University of Western Ontario, Department of Earth Sciences, 206 p.

Harris, M.J., Symons, D.T.A., Blackburn, W.H., and Hart, C.J.R., 1998a. Late Cretaceous-Eocene motion of the Stikine terrane: Paleomagnetic evidence from the 75Ma Mount Lorne stock, Yukon, Canada. Am. Geophys. Un., EOS, v. 80, in press.

Harris, M.J., Symons, D.T.A., Blackburn, W.H., and Hart, C.J.R., 1998b. Jurassic motions of the Canadian Cordillera: Paleomagnetic evidence from the Guichon batholith, B.C. and the Teslin Stock, Y.T. Geol. Assoc. Can. Abst., A-73.

Harris, M.J., Symons, D.T.A., Hart, C.J.R., and Blackburn, W.H., 1998c. An early Eocene end for northward displacement of the Coast Plutonic Complex in northern Canada and Alaska from paleomagnetism. Geol. Assoc. Can. Abst., A-73.

Harris, M.J., Symons, D.T.A., and Blackburn, W.H., 1998d. Guichon and Endako intrusives of British Columbia revisited: Geothermobarometric data for tilt-corrections on the paleomagnetic results. Am. Geophys. Un. EOS, v. 79, p. S61.

Harris, M.J., Symons, D.T.A., Blackburn, W.H., and Hart, C.J.R., 1998e. Late Cretaceous motions "North of 60°": Paleomagnetic evidence from the Mount Lorne stock, Yukon. Am. Geophys. Un. EOS, v. 79, p. S63.

Harris, M.J., Symons, D.T.A., Blackburn, W.H., and Hart, C.J.R., 1998f. The northern Canadian Cordillera: Paleomagnetic evidence for NAFTA. Geol. Assoc. Am., Abst. v. 30, p. A355.

Harris, M.J., Symons, D.T.A., and Hart, C.J.R., 1999a. A regional paleomagnetic conglomerate test for Laramide orogenic remagnetization of plutons in the Cordillera. Jour. Geophys Res., under revision.

Harris, M.J., Symons, D.T.A., Blackburn, W. H., and Hart, C.J.R., 1999b. Paleomagnetic and geobarometric study of the Late Cretaceous Mount Lorne stock, southern Yukon Territory. Can. J. Earth Sci., minor revisions in progress.

Harris, M.J., Symons D.T.A., Hart, C.J.R., and Blackburn, W.H., 1999c. Jurassic plate motions in the Yukon: a paleomagnetic and geothermobarometric study of the Teslin Crossing Stock (NTS 105E/7). Yukon Geol. And Exploration, in press.

Hunt, P.A., and Roddick, J.C. 1987. A compilation of K-Ar ages, Report 17. Geological Survey of Canada, pp 143-210.

Irving, E., Wynne, P.J., Thorkelson, D.J., and Schiarizza, P. 1996. Large (1000 to 4000 km) northward movements of tectonic domains in the northern Cordillera, 83 to 45 Ma. Jour. Geophys. Res., 101(B8), pp 17901-17916.

Jacobs, J.A. 1994. Reversals of the Earth's Magnetic Field. (2nd ed., Cambridge University Press, 346 p.

Lowe, C., Horner, R.B., Mortensen, J.K., Johnston, S.T. and Roots, C.F. 1994. New Geophysical data from the northern Cordillera: preliminary interpretations and implications for the tectonics and deep geology. Can. Jour. Earth Sci. 31, pp 891-904.

McCausland, P.J.A., Symons, D.T.A., and Hart, C.J.R., 1998. Post-Cretaceous geotectonic motion of the Yukon-Tanana Terrane from paleomagnetism of the Seymour Creek stock, Yukon Territory. Am. Geophys. Un., EOS, v. 80, in press.

McLelland, W.C. et al. 1992. Upper Jurassic-Lower Cretaceous basinal strata along the Cordilleran margin: Implications for the accretionary history of the Alexander-Wrangellia-Peninsular terrane Tectonics, 11, pp 823-835.

Mihalynuk, M.G., Nelson, J.L., and Diakow, L.J. 1994. Cache Creek terrane entrapment: Oroclinal paradox within the Canadian Cordillera. Tectonics, 13, pp 575-595.

Mortensen, J.K., and Jilson, G.A. 1985. Evolution of the Yukon-Tanana Terrane: Evidence from southeastern Yukon Territory. Geology, **13**: pp 806-810.

Mortensen, J.K. 1992. Pre-mid-Mesozoic evolution of the Yukon-Tanana Terrane, Yukon and Alaska. Tectonics, 11, pp 836-853.

Schmidt, M.W. 1992. Amphibole composition in tonalite as a function of pressure: an experimental calibration of the Al-in-hornblende barometer. Contrib. Min. Petrol. 110, pp 304-310.

Stevens, R.D., Delabio, R.N., and Lachance, G.R. 1982. Age determinations and geological studies: K-Ar isotopic ages, Report 15. GSC Paper 81-2, pp 18-19.

Symons, D.T.A., Blackburn, W.H., Harris, M.J., and Hart, C.J.R., 1997. Paleomagnetic and geobarometric study of the Teslin Crossing stock, Stikine terrane, Yukon, Canada. Am. Geophys. Un, EOS 78, p. F188.

Symons, D.T.A., 1998. Sole-fault deflection tectonics and clockwise rotation in the allochthonous Canadian Cordillera. Am. Geophys. Un., EOS, v. 80, in press (invited).

Symons, D.T.A, Harris, M.J., Hart, C.J.R., and Blackburn, W.H., 1998a. Geotectonics in the northern Cordillera from paleomagnetism and geobarometry: Progress report and recent results from the Eocene White Pass dikes and Jurassic Fourth of July batholith. LITHOPROBE Rept. 64, p. 171-180.

Symons, D.T.A., Harris, M.J., Hart, C.J.R., and Blackburn, W.H., 1998b. Paleomagnetism of the Eocene White Pass dikes: End of northward translation for the accreted terranes inboard of the Coast Shear zone. Am. Geophys. Un. EOS, v. 79, p. S63.

Symons, D., Williams, P.R., and Hart C.J.R., 1998c. Whence came the Yukon-Tanana terrane?: Paleomagnetism of the Jurassic Big Creek batholith, Y.T., Am. Geophys. Un., EOS, v. 80, in press (invited).

Tempelman-Kluit D.J., and Wanless, R.K. 1975. Potassium-Argon Age Determinations of Metamorphic and Plutonic Rocks in the Yukon Crystalline Terrane. Can. Jour. Earth Sci., 11, pp 1895-1909.

Williams, P.R., 1998. Measuring the geotectonic motion of the Yukon-Tanana terrane, B.Sc. thesis, Univ. of Windsor, 38 p.

Wynne, P.J., Enkin, R.J., Baker, J., Johnston, S.T., and Hart, C.J.R. 1998. The big flush: paleomagnetic signature of a 70 Ma regional hydrothermal event in displaced rocks of the northern Canadian Cordillera. Can. Jour. Earth Sci. 35, pp 657-671.

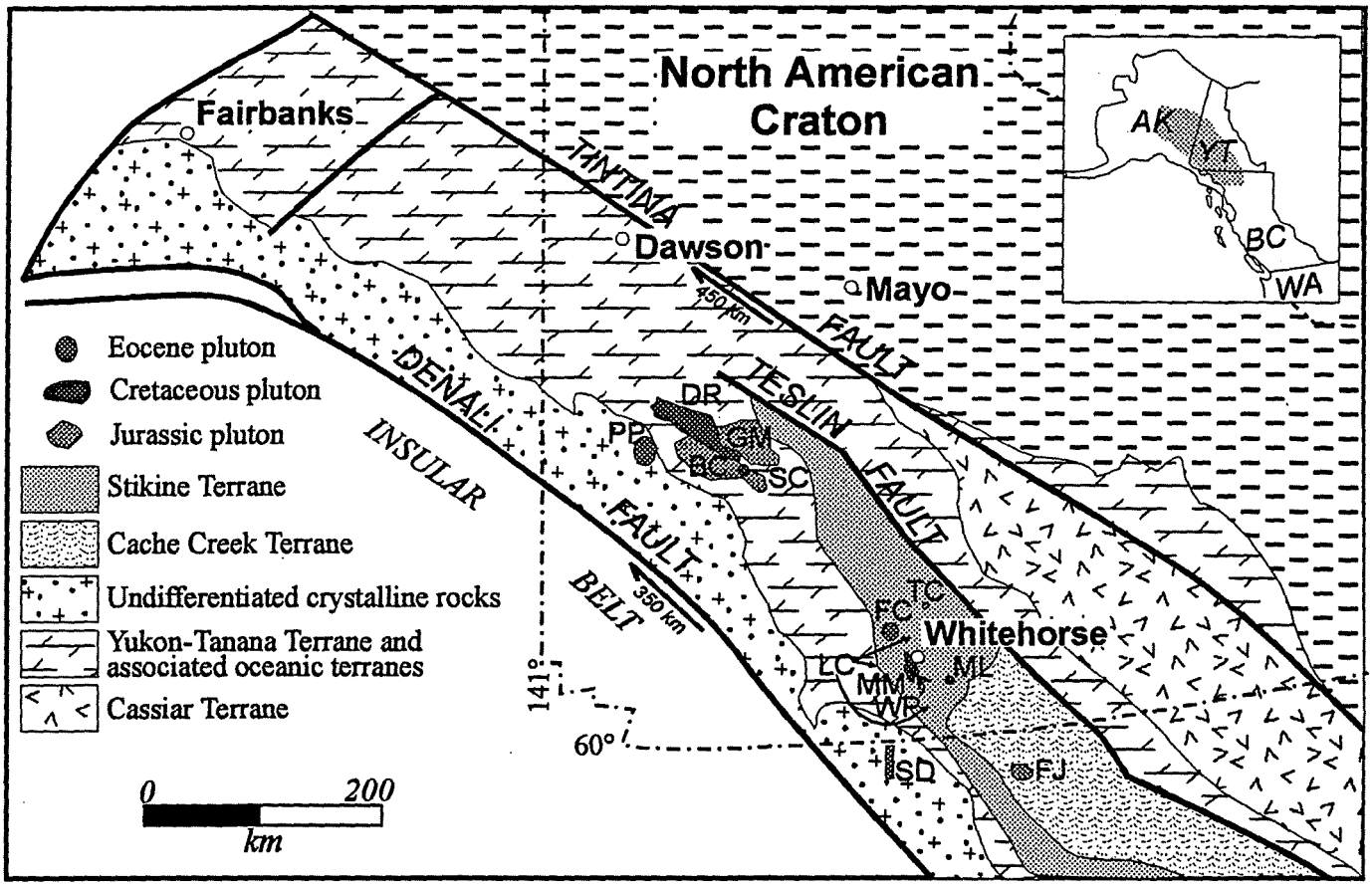

Figure 1. Yukon-Tanana Terrane: regional setting in the Canadian Cordillera. Abbreviations are: BC- Big Creek batholith; DR- Dawson Range batholith; FC- Flat Creek pluton; FJ- Fourth of July batholith;GM- Granite Mountain batholith; LC- Laberge Conglomerate; ML- Mount Lorne pluton; MM- Mount McIntyre pluton; PP- Pattison pluton; SC- Seymour Creek stock; SD- Skagway dikes; TC- Teslin Crossing; WP- Whitehorse pluton.

Legend

Late Cretaceous

Carmacks Group Volcanics (~70 Ma)

Seymour Creek Stock (~83 Ma)

Early Cretaceous

Mount Nansen Volcanics (<105 Ma)

Dawson Range Batholith (~105 Ma)

Early Jurassic

Big Creek Batholith (~190 Ma)

Granite Mountain Batholith (~191 Ma)

Paleozoic

Paleozoic host metasediments

contact

fault

1, 2 Paleomagnetic sampling sites

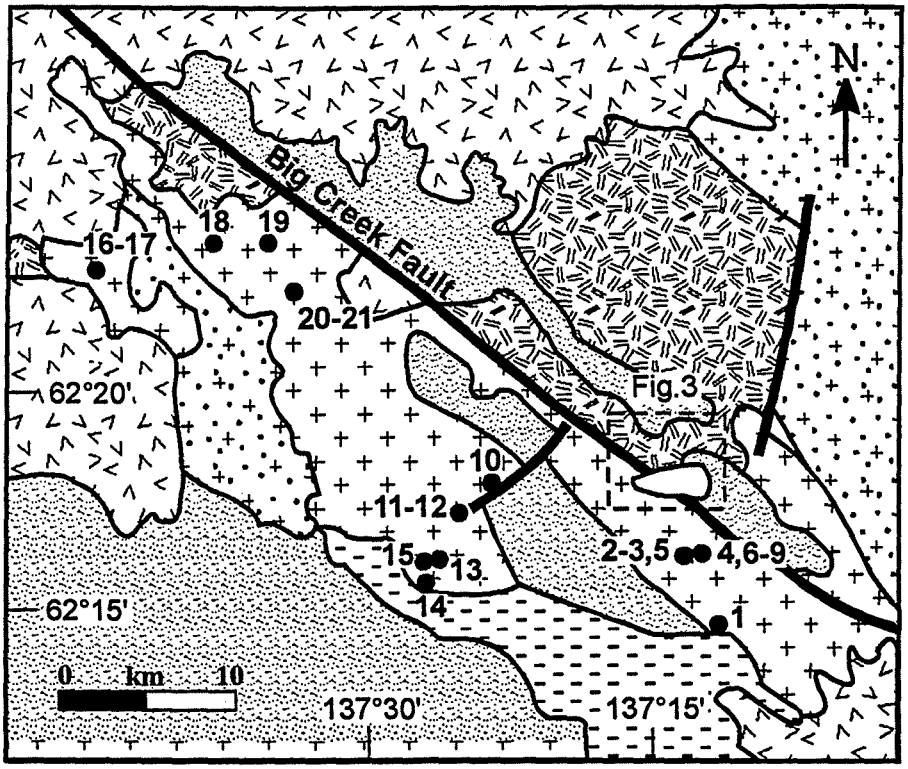

Figure 2: Big Creek Batholith -general geology and site map

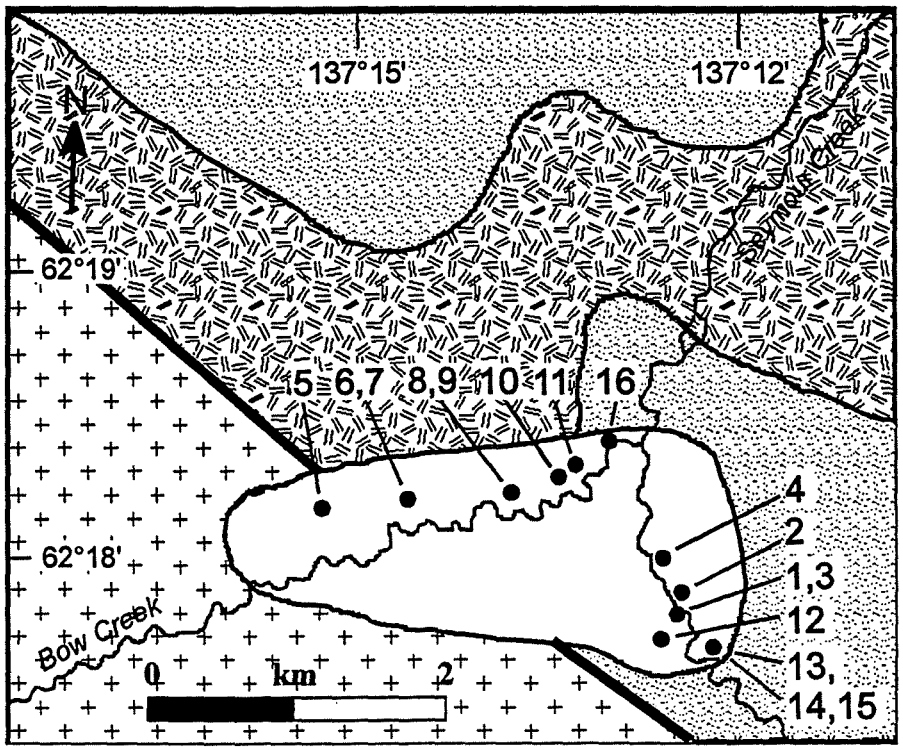

Figure 3: Seymour Creek Stock -local geology and site map

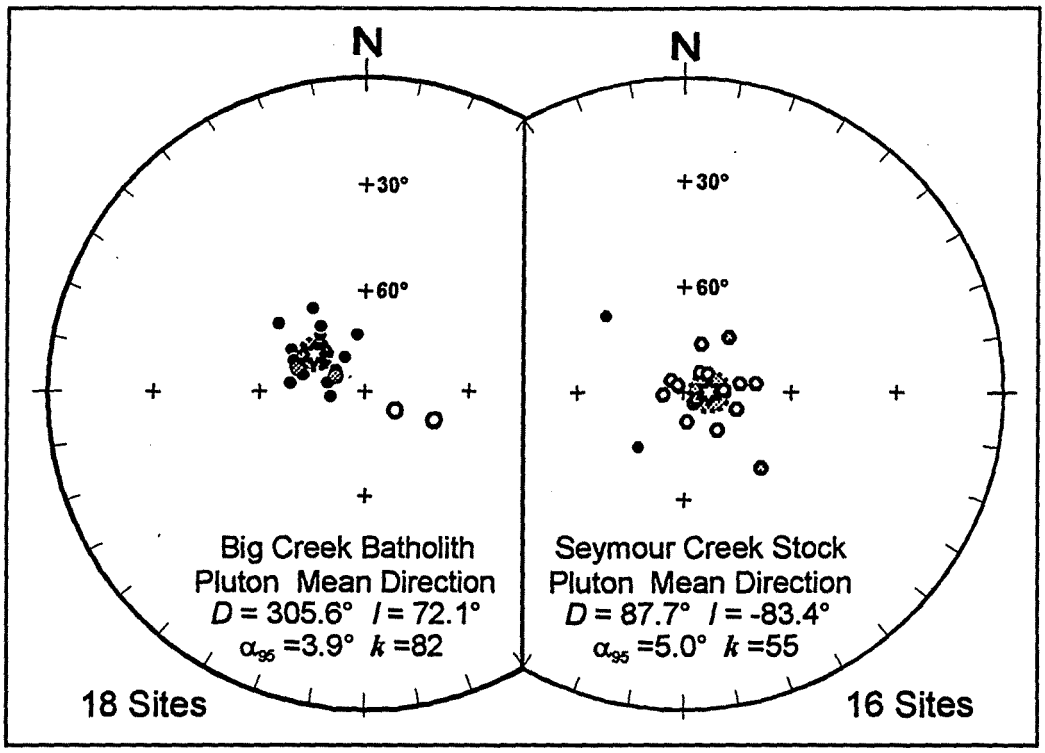

Figure 4: Preliminary site and unit mean ChRM directions

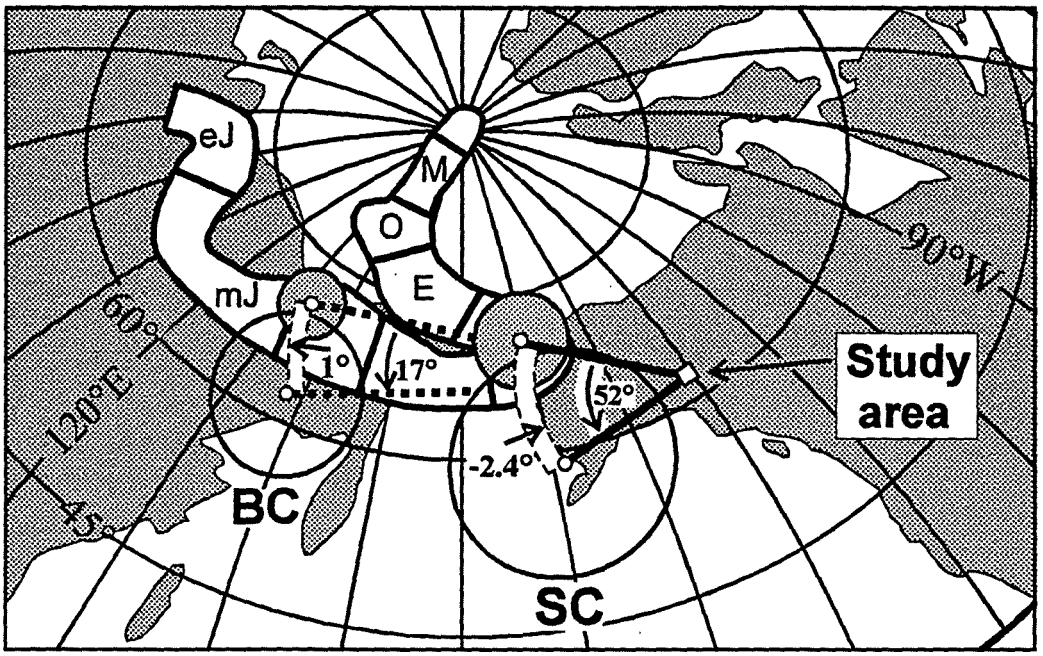

Figure 5: Yukon-Tanana Terrane Geotectonic Motion since the Early Jurassic relative to North America (Besse and Courtillot, 1991).

Crustal Seismic Velocity Structure of the Northern Cordillera, Southern Yukon Territory - LITHOPROBE SNoRE Line 31

Brian Creaser and George Spence
School of Earth and Ocean Sciences, University of Victoria, P.O. Box 3055, Victoria, BC, V8W 3P6, Phone: 250-721-6120, Fax: 250-472-4620, E-mail: bcreaser@uvic.ca

Abstract

A seismic refraction/wide-angle reflection profile was collected in the summer of 1997 across the southern Yukon Territory in northwestern Canada. The data were acquired by LITHOPROBE as part of the Slave-Northern Cordillera Lithospheric Evolution (SNorCLE) transect Refraction Experiment (SNoRE). From east to west, Line 31 extends from the deformed miogeocline of ancestral North America (Omineca belt), across the Tintina fault (TF), through displaced continental margin terranes, and into pericratonic and accreted terranes of the Cordillera (Intermontane superterrane). The Tintina fault is a major intercontinental transform characterized by at least 400 km of late Cretaceous to Oligocene dextral strike-slip movement. Little is known about the subsurface expression of this feature. The profiled region has a complex geologic history, including phases of extension, contraction, accretion and lateral displacement. Models of crustal structure are essential to advance our understanding of the tectonic evolution of the northern Cordillera.

The 360 km-long seismic profile was comprised of 7 shot points (1000 - 2000 kg of T3 explosive). Data were recorded by 403 seismographs (PRS, REFTEK and SGR) spaced approximately 0.8 km apart. The Line 31 data quality is excellent. Numerous refracted and reflected phases are easily identified, including refracted energy from the shallow crust (Ps), upper crust (Pg) and upper mantle (Pn), as well as reflected energy from a mid-lower crustal reflector (R1) and the base of the crust (PmP). Forward modelling and travel-time inversion indicate significant structural differences across the TF. The upper crust east of the TF has slower apparent velocities than that west of the TF, and the crust immediately west of the TF is thicker (~40 km) than the crust to the east (~36 km).

Introduction

The purpose of this study is to determine the seismic velocity structure of the crust below the southern Yukon Territory. This information is relevant for the investigation of several geological problems in the Northern Cordillera and may be used to constrain future studies in the area. The Tintina Fault, for example, is a well known major structural feature in the area but is poorly understood at depth. Seismic refraction/wide-angle reflection data record large-scale velocity features of the crust and upper mantle. Such information will provide new insight on the development the northern Cordillera.

The velocity structure of the crust is derived from forward modelling and inversion of observed traveltimes (Zelt and Smith, 1992) combined with forward amplitude modelling (Zelt and Ellis, 1988). A "layer-stripping" approach is used where shallow layers remain fixed while deeper layers are inverted. The main criterion for determining model "correctness" is the minimization of the root-mean-square traveltime residual (RMS) and normalized $\chi 2$ misfit. Attempts are made so that the RMS value is as close to 0 as possible, and that the $\chi 2$ value is as close to 1 as possible.

Geological Setting

The northern Cordillera is characterized by phases of extension, contraction, and accretion. Passive margins developed after the dispersal of the Late Proterozoic supercontinent. These passive margins experienced several phases of extension before western North America built outward by the accretion of terranes during the Cordilleran orogeny.

Line 31 of SNoRE is contained entirely within the Yukon Territory. The main tectonic units crossed by the refraction profile, from east to west, include the miogeocline of Ancestral North America, displaced continental margin terranes, pericratonic terranes, and accreted terranes (see map). Line 31 also crosses two major faults within the study area. The Tintina Fault is thought to be a major intracontinental transform that has experienced several hundred kilometers of Cretaceous to Oligocene dextral displacement. Line 31 also crosses the Teslin Fault near shot point 7. The Teslin Fault represents the eastern boundary of the Cache Creek terrane and has been interpreted as the transition between the accreted and autochthonous sections of the Cordillera. This structure may be a shallowly dipping near surface feature.

Preliminary Results

Combined forward and inverse modelling of refraction data has revealed several preliminary results:

1. Upper and middle crustal velocities generally increase from east (North American miogeocline) to west (accreted terranes of the Cordillera).
2. The Tintina Fault does not appear to be associated with any significant deep penetrating velocity anomaly. Although a local velocity high is centered below the surface expression of the fault.
3. The mid-lower crust is characterized by two weakly reflective boundaries.

4. The base of the crust (Moho) is a significant velocity discontinuity.
5. The Moho shows significant topography across the profile. The crust appears to be thickest (~37-38 km) just west of the Tintina Fault. Minimum crustal thickness (~32-33 km) occurs to the east of the Tintina Fault.

Future work will include: (1) continued modelling of the refraction data to improve the velocity model, (2) modelling of gravity data, (3) comparisons with other geophysical data, (4) reprocessing of refraction data to obtain a standard reflection profile.

References

Zelt, C.A. and Smith, R.B. 1992. Seismic traveltime inversion for 2-D crustal velocity structure. Geophysical Journal International, 108: 16-34.

Zelt, C.A. and Ellis, R.M. 1988. Practical and efficient ray tracing in two dimensional media for rapid traveltime and amplitude forward modelling. Canadian Journal of Exploration, 24: 16-31.

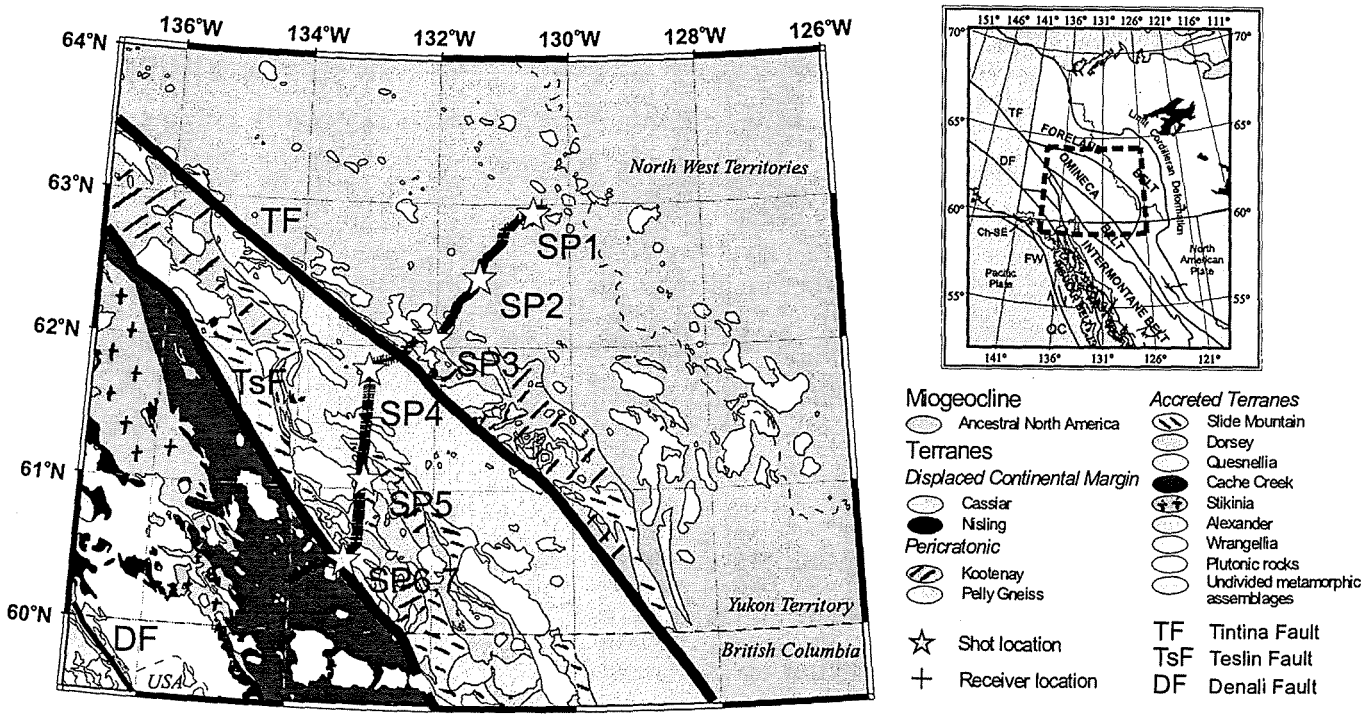

Geological map of the study area. The refraction profile extends from the miogeocline (east), through displaced continental margin and pericratonic terranes into accreted terranes (west). SP, shot point. **Top right**: Map showing the location of the study area (thick dashed line) and morphogeological boundaries in northwestern Canada. TF, Tintina Fault; DF, Denali Fault; FW, Fairweather Fault; Ch-SE, Chugach-St. Elias Fault; QC, Queen Charlotte Fault.

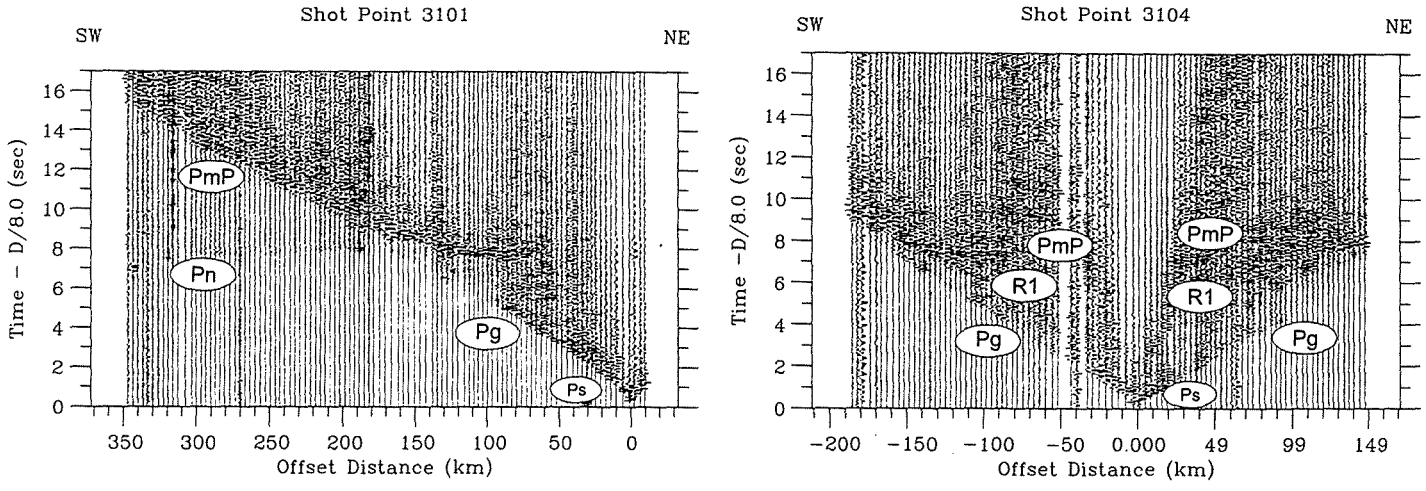

Examples of data collected along line 31.

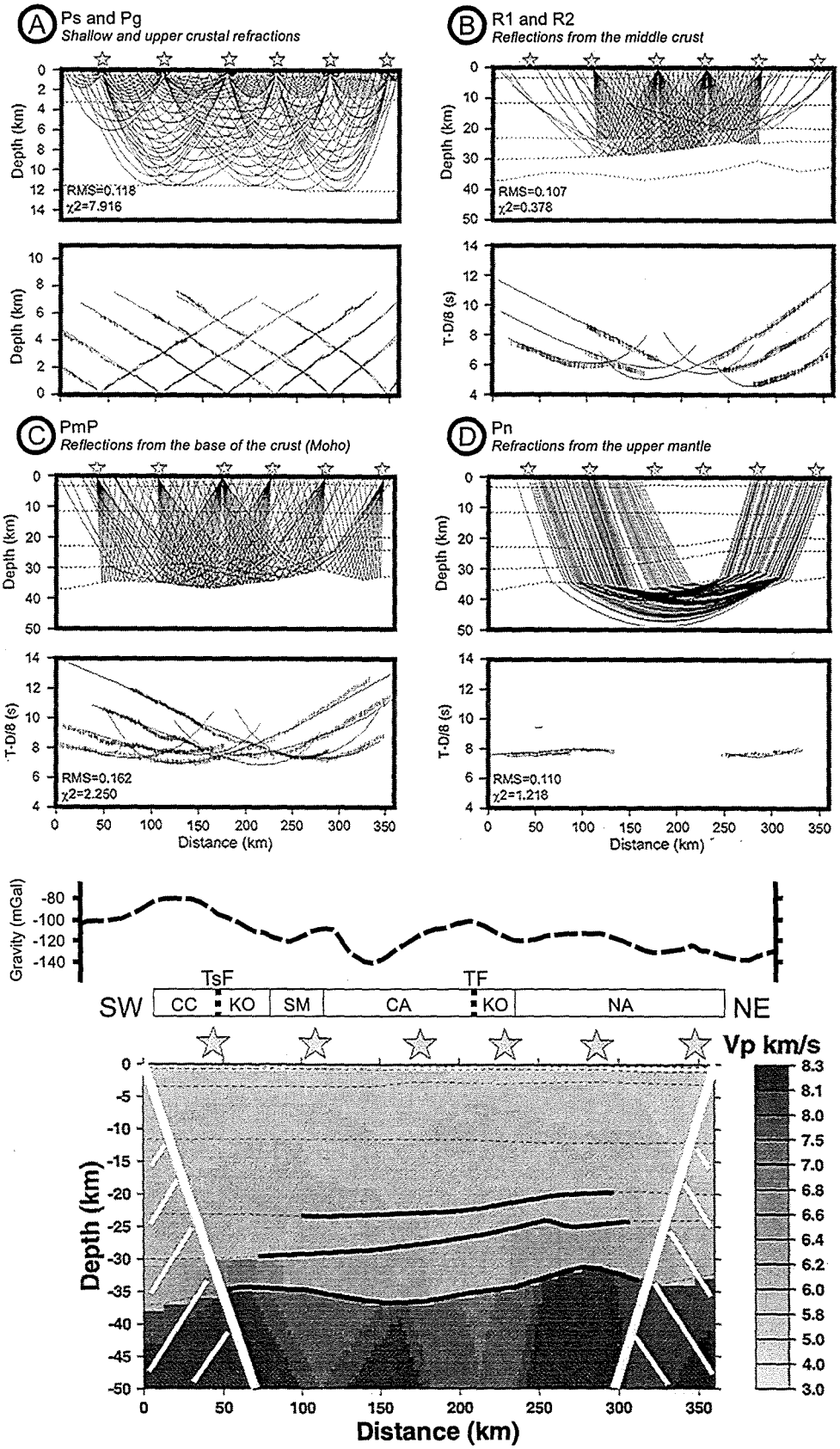

Top: Ray tracing diagrams for various crustal and upper mantle phases (A-D). **Bottom**: Preliminary velocity model plotted with simplified surficial geology and Bouguer gravity. Thick black lines indicate potential reflective boundaries. Thin dashed lines indicate model boundaries. Slanted white lines indicate unconstrained areas of the model. CC, Cache Creek; KO, Kootenay; SM, Slide Mountain; CA, Cassiar; NA, Ancestral North America; TF, Tintina Fault; TsF, Teslin Fault..

Deformation Processes Along the Denali Fault System

Joseph Clancy White
Department of Geology
University of New Brunswick

The objectives of this project have been threefold: (1) to examine the kinematics of faults associated with the Denali fault system in southwestern Yukon (2) to compare existing seismic records with the fault distributions and surface-mapped kinematics and (3) to examine in detail the fault rock textures and deformation mechanisms in order to establish the rheological nature of displacements.

Faults, as previously described, are orogen-parallel (oblique strike-slip, normal and thrust faults) or NNW-trending, parallel to topographic breaks across which there is often no clear disruption of orogen-parallel lithologies. Fault rocks cover the range from discrete polished planes through thin brecciated zones to thick mature fault zones. Zeolite mineralization is common throughout the fault rocks. Ubiquitous throughout the fault rocks, as well as significant volumes of host rock, is the introduction of extensive calcite veining that controls subsequent rheological response. The intimate association of calcite veining, a proxy for the hydrologic system, and the faults has been similarly documented in upper crustal fault systems from the Southern Cordillera Transect (Kennedy & Logan 1998; White and Kennedy, 1998). The carbonate infiltration and precipitation is not simply a passive record of the faulting, but instead serves as a determining factor in the crustal architecture and presumably, the sub-surface record; that is, the micromechanical processes affect the overall response of a fault zone - strength, storage and release of seismic energy and induced dilatancy as well associated fluid flow.

Many of the orogen-parallel faults are localized at lithostratigraphic contacts, demonstrating the typical control of mechanical contrast on faulting. Because the calcite (with minor quartz) veins can in the extreme resemble host rock, it is presumed that some degree of brittle displacement serves a the precursor for subsequent faulting i.e. dilatant faulting, increased permeability and precipitation of carbonate. The latter is believed to be fluid pressure-controlled and is consistent with the extensive evidence of fluid transport (veins). Estimates of fluid pressure on the order of 0.7 - 0.8 lithostatic pressure have been given previously (White 1998). The effect of coarse-grained calcite precipitation is to move the fault zone from the brittle to the ductile regime. Subsequent deformation is predominantly crystal-plastic with extensive dynamic recrystallization to 1-30μm grain size. This can produce extreme localized displacement within the fault zone with eventual strain hardening of the fine-grained material (Hall-Petch relationship) leading to brittle displacement.

The consequence of this deformation sequence is that coarse-grained, high porosity carbonate zones are transformed to fine-grained, low porosity, denser carbonate zones. In the context of relating seismic reflection architecture to geology, this raised the question of whether fault zones of this type would image well. Unlike layered sedimentary packages, carbonate units of this type are equally well developed in crystalline rocks, and at least after recrystallization have not dissimilar impedances. This would seem to provide an interesting problem for synthetic seismogram modelling.

References

Kenndy, L.A. & Logan, J.M 1998. Tecontophysics 295, 167-186.
White, J.C. 1998. Lithoprobe Report No. 64, 327-331.
White, J.C. & Kennedy 1998. Geol. Soc. Am. Abst. Progm. 30, A-325.

MIGMATIZATION IN THE CENTRAL GNEISS COMPLEX, COASTAL NORTHWESTERN BRITISH COLUMBIA AND SOUTHEASTERN ALASKA

SOKOL, Nikolas K. and CRAWFORD, Maria L., Department of Geology, Bryn Mawr College, Bryn Mawr, PA, 19010, nsokol@brynmawr.edu

Migmatite genesis has long perplexed igneous and metamorphic petrologists. Leucosome segregation has been shown to result from numerous different open- and closed-system processes such as *in situ* partial melting, melt injection, subsolidus segregation, and metasomatism. These processes are manifested in sundry migmatites with contrasting structural, textural, and chemical characteristics. This study is founded in the idea that migmatites with different qualities result from distinct mechanisms, the origins of which can be tested.

This paper investigates the petrogenesis of two migmatite suites from the Central Gneiss Complex (CGC) of southeastern Alaska and coastal northwestern British Columbia. Field, petrologic, and chemical data and observations are combined to make inferences regarding the migmatization mechanisms for both suites. The two migmatite suites have markedly different compositional and structural characteristics. Suite A migmatites are garnetiferous, biotite-rich metagreywackes and are characterized by layer-parallel leucosomes that are deformed along with host rocks. In contrast, Suite B migmatites are garnet-poor, pyroxene-bearing, range in composition from metagreywackes (Suite B-MG) to amphibolites (Suite B-A), and show variable structures. Many of the Suite B migmatites comprise rafts or large flecks of fine grained melanosome 'floating' in a coarse grained plagioclase- and quartz-rich leucosome. Amphibolite melanosomes have well defined boundaries with the leucosomes whereas metagreywackes show gradational boundaries between them. We hypothesize that the layer-parallel leucosomes in Suite A were formed by solid state processes and that the cross-cutting leucosomes of Suite B were formed by processes involving melt. Furthermore, the variety of structures observed in Suite B migmatites are attributed to multiple migmatite forming processes and/or variable mechanical responses resulting from different starting materials.

These hypotheses are tested using petrographic and structural observations, geothermobarometry, mineral compositions, and major- and trace-element partitioning between leucosomes and melanosomes. K-spar and muscovite are absent in both suites. Garnet is abundant in Suite A and scarce in Suite B. Plagioclase is preferentially aligned in the leucosomes of Suite A but randomly arranged in Suite B leucosomes. The composition of plagioclase is the same in leucosomes and melanosomes of Suite A (An 32) but different in Suite B (L = An 33; 37; 47 and M = 33; 33; 35). In addition, some leucosomes of Suite B are enriched in anorthite relative to melanosomes (fig. 1). Major- and trace-element partitioning between melanosomes and leucosomes from the Suite B migmatites show ambiguous signatures not compatible with those predicted by the existing published models of leucosome segregation. Geothermobarometric results indicate a P-T of 725 +/- 75°C and 6.5 +/- 1.0 kbars for Suite A and 850 +/- 100°C and 5.5 +/- 1.0 kbars for Suite B.

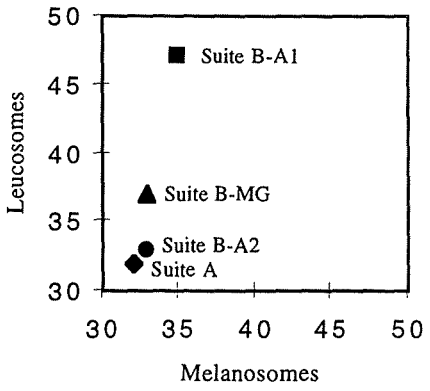

Figure 1. Anorthite percentage in leucosomes and melanosomes.

The amphibolite facies temperatures inferred for suite A are on the lower cusp of those determined experimentally to induce significant partial melting of metagreywackes. This and other characteristics of Suite A: 1) layer parallel nature of leucosomes; 2) constant plagioclase compositions throughout all aspects of the migmatites; and 3) layer parallel plagioclase growth in leucosomes are considered to indicate closed-system internal differentiation processes for leucosome segregation. The higher temperatures and granulite facies mineral assemblages achieved in Suite B are sufficient for anatexis in rocks of both metagreywacke and amphibolite composition. Considering this with the aforementioned properties: 1) cross-cutting leucosomes; 2) anorthite enrichment in leucosomes; 3) the absence of K-spar in leucosomes; and 4) ambiguous trace-element signatures, an open-system melt injection is proposed for the genesis of Suite B migmatites. The presence of two plagioclase compositions in leucosomes of Suite B-A may represent multiple leucosome forming processes, i.e. a melt injection heats the host rocks and they subsequently partially melt. The leucosome formed from partial melt retains a similar plagioclase composition to that of the melanosome while plagioclase in the leucosome formed from injected melt has a very different anorthite percentage.

Key words: migmatite, Central Gneiss Complex, subsolidus segregation, partial melting, leucosome

Implications of Early Miocene or younger normal faults on interpretation of ACCRETE reflection data, northwest Canadian Cordillera

C.A. Evenchick, Geological Survey of Canada, 101-605 Robson St. Vancouver, B.C. V6B5J3
M.L. Crawford, Bryn Mawr College, Bryn Mawr, PA 19010
V.J. McNicoll, Geological Survey of Canada, 601 Booth St. Ottawa, On. K1A0E8

The ACCRETE seismic project crosses a corridor 200 km long from Dundas Island (Queen Charlotte Sound) to Stewart, British Columbia. The northern 110 km of the corridor is along Portland Canal. The fjord trends in 2 directions, northeast and about N10W. Northerly trending segments of the fjord coincide with a newly recognized system of steep brittle faults which cut early Tertiary and older rocks along and east, and west of, Portland Canal (Evenchick et al., 1999). Significant offset can be demonstrated on two north-trending faults: the Portland Canal and Big Dam faults. The Portland Canal Fault separates migmatitic granitoid rocks and ca. 22 Ma massive granite on the west from greenschist facies rocks, massive ca. 58-60 Ma granite, and ca. 22 Ma volcanic rocks on the east. The difference in metamorphic grade, and position of volcanics 500 m above a coeval (and assumed comagmatic) pluton, requires that Portland Canal Fault be an east-side-down fault of post-22 Ma age. Farther east, the Big Dam Fault is a brittle fault zone 2 km wide which cuts ca. 53-61 Ma granite in Observatory Inlet. To the north, where the fault cuts greenschist facies stratified rocks, contacts are offset with a west-side-down sense. Parallel faults in early Tertiary granite between northerly projections of the Portland Canal and Big Dam faults are steeply east and west dipping, and extensional. Therefore, although dip directions of the Big Dam and Portland Canal faults are unknown, they are assumed to be related to the other post-early Tertiary faults of similar character, and therefore extensional.

The Portland Canal Fault is approximately in the plane of the ACCRETE seismic line for at least 50 km, and another northerly trending fault is inferred to be in the southern north-trending segment of Portland Canal. Reflectors in the northern half of the ACCRETE line have previously been inferred to represent northeast dipping early Tertiary shear zones and/or layers of tonalite and gabbro projected into the section from more than 100 km to the south (Hollister, 1996; Morozov et al., in press). Recognition that the Portland Canal Fault is steep, likely deep, and approximately coplanar with the seismic dataset, poses problems for interpretation of seismic reflection data for much of the northern part of the line. Previous interpretations can neither be supported or rejected, and will only be resolved with thorough field study. Post- 22 Ma brittle extension faults are one facet of what is likely a rich late Tertiary history; ongoing studies are aimed at resolving the timing of young features.

REFERENCES

Evenchick, C.A., Crawford, M.L., McNicoll, V.J., Currie, L.D., and O'Sullivan, P.B., 1999, Early Miocene or younger normal faults and other Tertiary structures in west Nass River map area, northwest British Columbia, and adjacent parts of Alaska; in Current Research 1999-A, Geological Survey of Canada, p. 1-11.

Hollister, L.S., 1996, Correlation of Deep Crustal Reflectors of the ACCRETE Seismic Section With Surface Exposures of Rocks Formed in the Lower Crust; in AGU, 1996 Fall Meeting Vol. 77, No. 46, p. F651.

Morozov, I., Smithson, S.B., Hollister, L.S., and Diebold, J.B., in press, Wide-Angle Seimic Imaging across Accreted Terranes, Southeastern Alaska and Western British Columbia; Tectonophysics.

Crustal Structure across the Coast Plutonic Complex and Stikinia in Northwestern British Columbia: Wide-angle P- and S-wave Velocity Models from ACCRETE and LITHOPROBE SNORE Line 22

Philip T C Hammer and Ron M Clowes

Department of Earth and Ocean Sciences
University of British Columbia
2219 Main Mall, Vancouver, Canada V6T 1Z4
hammer@eos.ubc.ca

Introduction

The crustal structure beneath the transition from the Intermontane superterrane to the Coast Belt of the northern Canadian Cordillera is interpreted from the inversion of refraction and wide-angle reflection (R/WAR) seismic data. The profile (**Fig. 1**) traverses the suture zone resulting from the mid-Cretaceous collision between the exotic Insular superterrane (Alexander and Wrangellia terranes) and the previously accreted Intermontane superterrane (Stikinia, Taku and Yukon terranes) [*Gabrielse and Yorath*, 1992]. During accretion, Stikinia was collapsed more than 160 km by thin-skinned thrusting and folding [*Evenchick*, 1991]. The resulting Skeena Fold Belt is truncated to the west by the overprinting Coast Plutonic Complex (CPC), a rapidly uplifted and exhumed subduction arc. In the early Paleogene, the majority of magmatic and deformational events ceased and transcurrent motion was established between the Kula/Pacific and North American Plates. Neogene to Quaternary crustal extension has been documented within the CPC on the basis of mapped faults (*Hollister and Andronicos* [1997], *Evenchick et al.* [1999], *Morozov et al.* [1999] and *Diebold et al.* [1998]). The ACCRETE and LITHOPROBE investigations along this corridor are directed toward understanding the tectonic history and 3-d structure of Stikinia and the CPC. Broader questions being addressed concern the growth of continents by magmatic and terrane accretion.

Experiments: ACCRETE and SNORE Line 22

The 1994 ACCRETE seismic refraction/wide-angle reflection (R/WAR) experiment and the 1997 SNorCLE R/WAR Experiment (SNORE) provide a continuous survey across the CPC-Stikinia transition (**Fig. 1**). Using coastal fjords for access to the interior of the orogen, ACCRETE profiled with a towed 132ℓ airgun array (50-150 m shot spacing). An inline, wide-angle seismic dataset was recorded by Reftek 3-component seismographs deployed along the 180 km-long Portland Inlet. In order to sample the eastern CPC and into Stikinia, 17 additional seismographs were deployed northeast from the head of the fjord (5-15 km receiver spacing), extending the in-line profile 105 km (**Fig. 1**). This northern ACCRETE dataset provides coverage across the transition but the unreversed airgun shots limit shallow velocity control within Stikinia. Therefore, SNORE Line 22 was designed to improve coverage across the CPC-Stikinia transition and to directly link the ACCRETE and SNorCLE Transects. Line 22, described in detail by *Hammer and Clowes* [this volume], incorporated nine explosive shots that were recorded by one-component (PRS1 and SGR) and 3-component (Reftek) seismographs. Two of these shots were included in the combined analysis; Shot 2 (2400 kg) was positioned directly inline with the ACCRETE corridor and Shot 3 (2000 kg), while slightly offline, provides deeper reversed ray coverage. SNORE data included in this analysis were recorded by seismographs located between Shots 2 and 3 along the primary Line 22 corridor. In

addition, data were recorded by a secondary splay of 42 PRS1s positioned at ~1.8 km intervals along the ACCRETE line (Fig. 1). This overlapping extension down Portland Inlet yields reversed coverage and greatly improved upper crustal resolution across the CPC-Stikinia transition. The full ACCRETE/SNORE dataset provides a 360 km-long, densely sampled, inline profile.

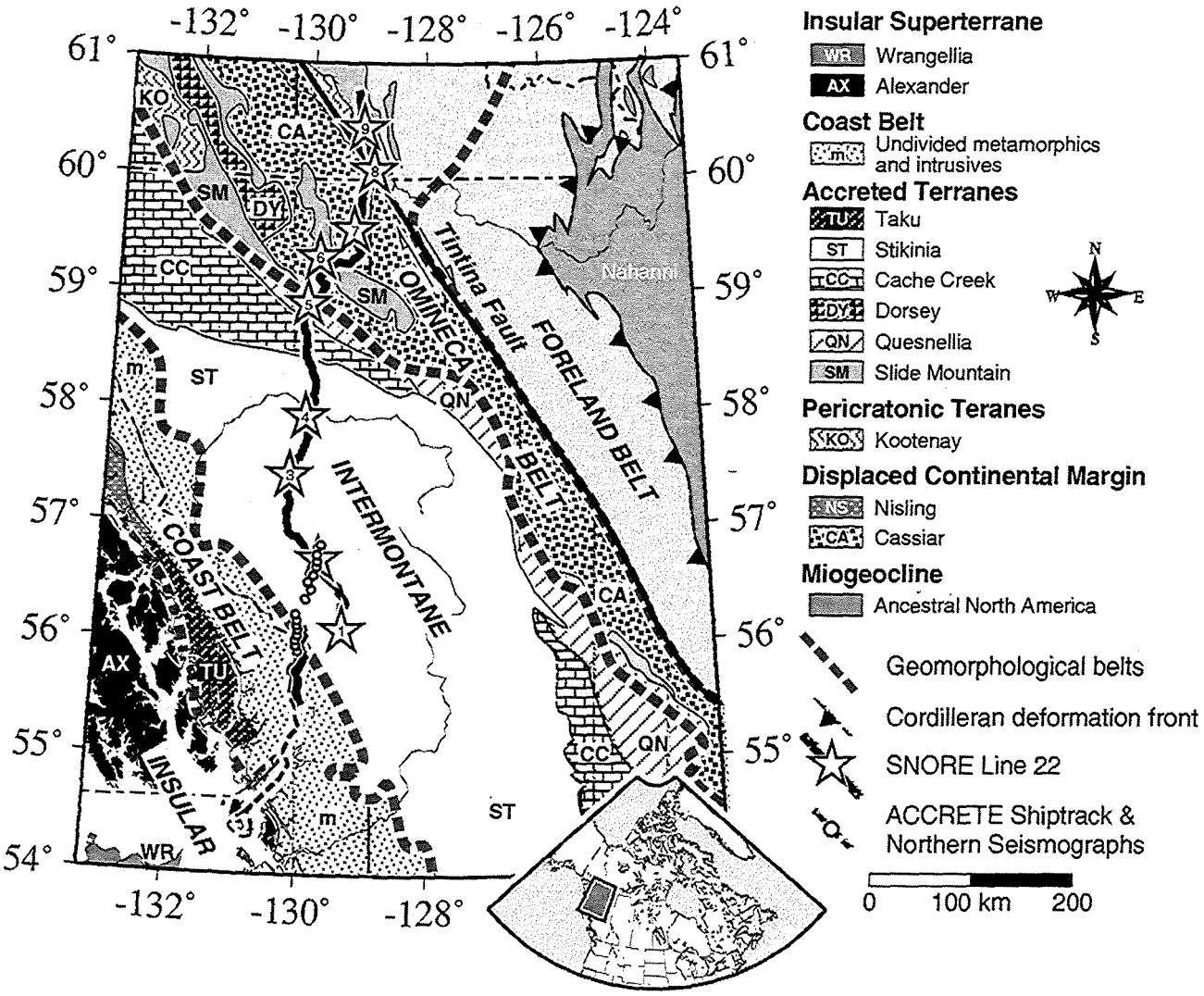

Figure 1: SNORE Line 22 location map. Terranes and geomorphological belts of the northwestern Canadian Cordillera are shown. Line 22 energy generated by explosive shots ( ) was recorded by receiver arrays (▬▬). Accrete airgun shots (O) along Portland Inlet were recorded by inline seismographs (- - -). To locate Line 22 relative to the other SNORE lines, see Figure 1 in *Fernandez Viejo et al.* (this volume).

Data and Modeling

Data quality from both experiments is generally excellent and a rich suite of P- and S-wave arrivals are observed. The ACCRETE dataset, in particular, includes strong S-wave arrivals. These are indicative of efficient P-to-S conversion along the fjord sediment/basement interface.

Refracted arrivals include upper crustal refractions (Pg, Sg) and upper mantle refractions (Pn). Intracrustal reflections are observed in the upper crust (PcP1), at the base of the upper crust (PcP2, PcP3, ScS3) and within the mid-lower crust (PcP4). Strong Moho reflections are also observed (PmP, SmS). In addition, the ACCRETE dataset includes converted Moho reflections (SmP); this unusual phase is observed on several adjacent receivers at ~80 km offset.

P- and S-wave arrivals were analyzed using a combination of 1-d τ-p velocity modeling [*Gorman and Clowes*, 1999] and subsequent 2-d traveltime inversion and forward amplitude modeling [*Zelt and Smith*, 1992]. Velocity and reflector depth resolution varies throughout the model. In general, upper crustal velocities have uncertainties of 0.1-0.2 km/s and lateral resolution of 3-35 km. Lower crustal velocties exhibit 0.2-0.3 km/s uncertainty and lateral resolution of 20-75 km. Moho depth is constrained to 1.5-3 km and upper mantle velocities to 0.1 km/s. For a detailed discussion of the modeling procedure and uncertainty analysis, please see *Hammer and Clowes* [1999b]

P-wave and S-wave Velocity Structure Models

The P-wave velocity model was first constructed (**Fig 2a**). Using this layered model parameterization, the S-wave velocity model was then developed (**Fig. 2b**). These structural models exhibit a well-defined transition from the CPC to Stikinia. A number of robust features are required by the data:

Crustal velocities:

- Extremely slow velocities (Vp: 4.0-5.7 km/s) are observed in the uppermost Stikinia crust. These constrain the thickness (0-4 km) of the sedimentary Bowser Lake assemblage that overlies western Stikinia basement. Spectral analysis of magnetic data yields a similar depth to basement [*Lowe et al.*, 1998].
- The upper crust in the uplifted plutonic complex is significantly faster than the upper crust of Stikinia (Vp: 6.2 km/s vs. 5.8 km/s).
- CPC mid-lower crustal velocities are also faster than equivalent Stikinia velocities.
- Average crustal P-velocities are 6.55 km/s for the CPC and 6.4 km/s for Stikinia. These values are slower than mean P-velocities in continental crust (6.7 km/s) and are generally consistent with velocities characteristic of other young orogenic belts or extensional environments.

Crustal thickness:

- Thin crust beneath the CPC (31.5-32 km) thickens beneath Stikinia (35-36 km). This is consistent with geologic and seismic observations (*Evenchick et al.* [1999] and *Morozov et al.* [1999]) suggesting recent extension beneath the CPC.

Moho characteristics:

- Wide-angle Moho reflections (PmP and SmS) are strongly multicyclic, suggesting that for these wavelengths and incidence angles, the crust-mantle "boundary" is a layered transition zone.
- This model is complicated by the presence of converted Moho reflections (SmP) that require a sharp impedance contrast. These reflections are only observed over a limited offset range. The observations suggest significant laterally variability in Moho structure. Converted Moho reflections have been linked to magmatic underplating in the Basin and Range and at

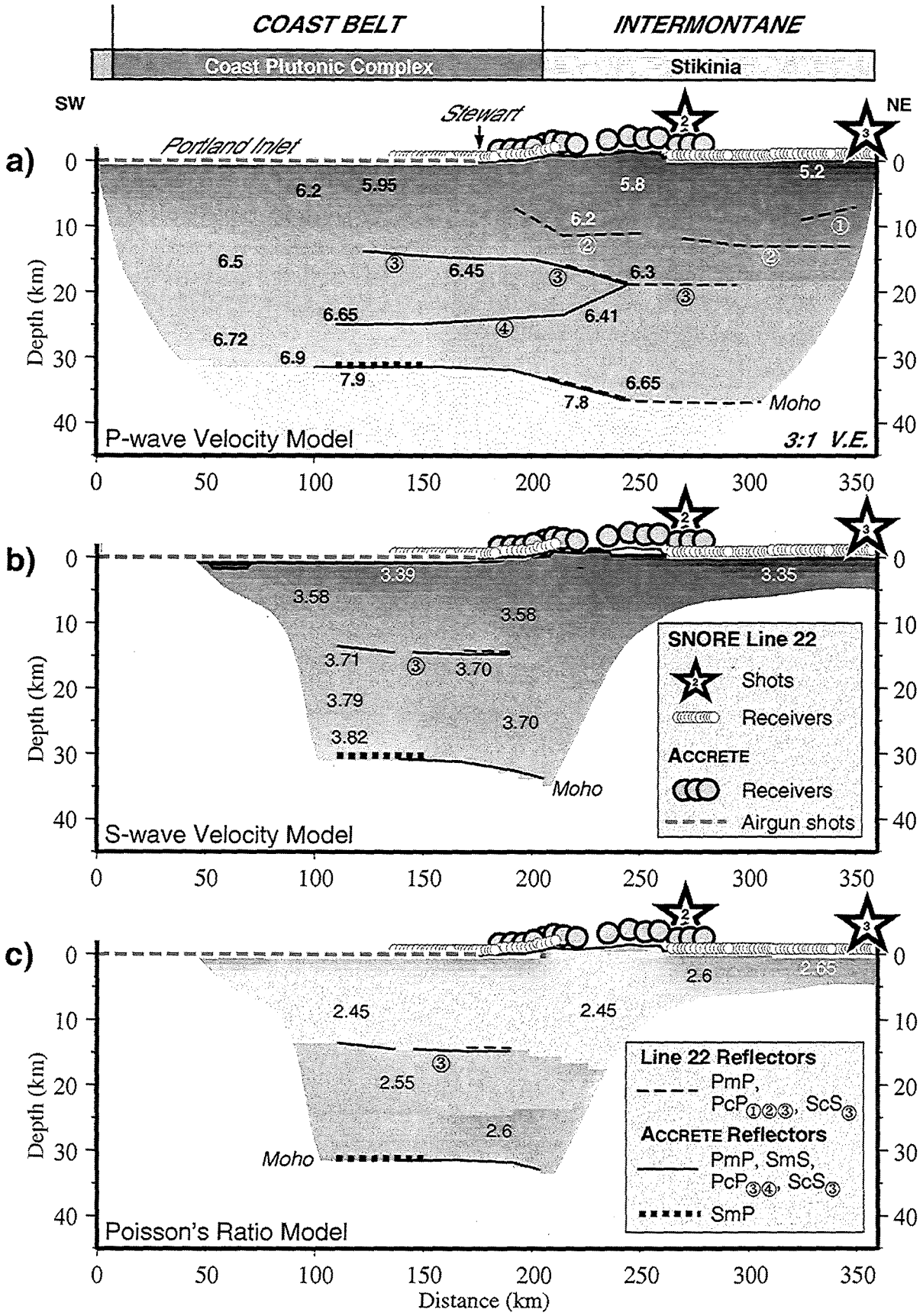

Figure 2. a) P-wave velocity model. **b)** S-wave velocity model. **c)** Poisson's ratio model. Velocities in km/s. Regions without ray coverage are masked out. Reflectors are numbered.

Mid-ocean Ridges. Underplating is consistent with recent extension beneath the CPC.

Intracrustal reflections:

- ➢ The short, SW-dipping (in the profile plane) PcP1 reflector is only observed in the Line 22 Shot 3 gather. It has not been correlated with a mapped fault within Stikinia.
- ➢ The upper-midcrustal reflectors (PcP2, PcP3, ScS3) may represent:
  - the thermal boundary between the brittle and ductile crustal regime, or
  - a compositional change between felsic and mafic dominated rocks. The Poisson's ratio analysis suggests this may be the situation in the CPC (see below).
- ➢ A mid-lower crustal reflector (PcP4) is consistently observed. This impedance contrast may be associated with:
  - the proposed detachment beneath Stikinia [*Evenchick*, 1991] or,
  - extensional faults (Neogene?) soling within the crust, or
  - a compositionally layered structure.

Poisson's Ratio Model

The P- and S-velocity models were combined to generate a Poisson's ratio model for the ACCRETE/SNORE profile (**Fig. 2c**). Poisson's ratio (σ) is proportional to Vp/Vs and improves constraints on crustal composition. That is not to say that composition can be precisely identified as a number of factors complicate the analysis. These include: a) combined velocity errors lead to relatively large errors in σ, b) rock types have variable properties and are typically intermingled on the scales sampled by seismic energy, and c) anisotropy and fluid pore pressure can have significant effects on velocities. However, general conclusions can be drawn from comparisons of the Poisson's ratio model with laboratory measurements of rocks tested at different pressures. In **Figure 3**, Vp and Vs values from a variety of depths within the models are plotted beside average values dervied by laboratory measurements for appropriate rock types [*Christensen*, 1995 and personal communication].

- ➢ Vp/Vs analyses and comparison with laboratory measurements of rock types observed in the ACCRETE corridor lead to several conclusions:
  - The upper crust of the CPC is felsic and of low metamorphic grade (σ=0.250 ± 0.005).
  - The shallow crust in Stikinia is felsic and of low metamorphic grade (σ=0.265 ± 0.005). As would be expected, the modeled values indicate significantly different composition than the neighboring CPC upper crust.
  - Lower resolution models of average mid-lower crustal structure in the CPC indicate composition is mafic and of high metamorphic grade (σ=0.26 ± 0.01).
- ➢ The felsic upper crust within the CPC thins to the southwest along the ACCRETE corridor. This may support non-uniform exhumation of the CPC.

References

Diebold, J.B., L.S. Hollister & T. Das, 1998. ACCRETE MCS data synthesis reflects tectonic history of the northern continental margin of British Columbia. *EOS Trans.*, AGU: T71E-05.

Evenchick, C. A., 1991. Geometry, evolution and tectonic framework of the Skeena Fold Belt, north central British Columbia. *Tectonics*, **10**: 527-546.

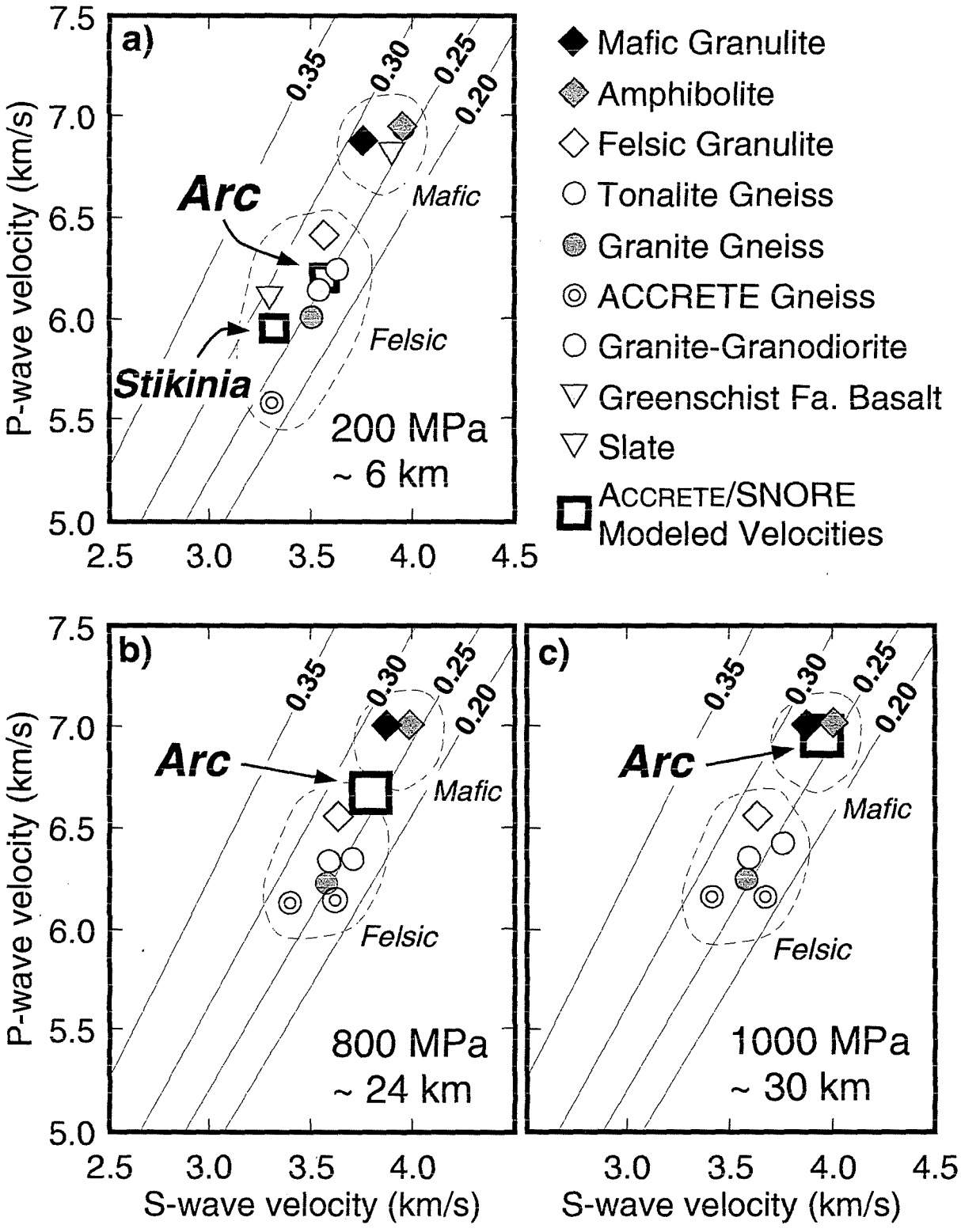

Figure 3. P- and S-wave velocity at pressures characteristic for the **a)** upper crust, **b)** middle crust and **c)** lower crust. Velocities determined from ACCRETE/SNORE velocity models are given by □ (size represents estimated error). Symbols represent values for laboratory measurements on rock samples [*Christensen*, 1995 and personal communication]. Diagonal lines represent constant Poisson's Ratios. Dashed lines indicate approximate felsic (low- to medium-grade metamorphism) and mafic (granulite metamorphism) fields.

Evenchick, C.A., M.L. Crawford, V.J. McNicoll, L.D. Currie & P.B. O'Sullivan, 1999. Early Miocene or younger normal faults and other Tertiary structures in west Nass River (103P) map area, northwest British Columbia, and adjacent parts of Alaska. In Current Research 1999-A, GSC, submitted.

Gabrielse, H. & C. J. Yorath *(editors)*, **1992**. Geology of the Cordilleran Orogen in Canada. GSC, *Geology of Canada No. 4*, **G-2:** 844 p.

Gorman, A.R. & R.M. Clowes, 1998. Wavefield tau-p analysis for 2-D velocity models: Application to western North American lithosphere. *Geophys. Res. Lett.*, in press.

Hammer, P.T.C. & R.M. Clowes, 1999a. Crustal Structure across the Cordilleran Orogen of Northwest British Columbia - Preliminary Results of LITHOPROBE SNorCLE Refraction Experiment Line 22. *in LITHOPROBE SNorCLE Transect Workshop Volume.*

Hammer, P.T.C. & R. M. Clowes, 1999b. Crustal Velocity Structure across the Coast Orogen of Northwest British Columbia. *J. Geophys. Res.*, submitted.

Hollister, L.S. & C.L. Andronicos, 1997. A candidate for the Baja British Columbia Fault System in the Coast Plutonic Complex. *GSA Today*, **7**: 1-7.

Morozov, I.B., S.B. Smithson & L. Hollister, 1999. Wide-angle seismic imaging across accreted terranes, southeastern Alaska and western British Columbia. *Tectonophys.*, submitted.

Zelt, C.A. & R.B. Smith, 1992. Seismic traveltime inversion for 2-d crustal velocity structure. *Geophys. J. Int.*, **108**: 16-34.

The Omineca Belt: a crustal scale shear zone or a zone of thrusting?

Paul F. Williams and Dazhi Jiang

Department of Geology, University of New Brunswick, Fredericton, NB, Canada E3B 5A3

The Omineca Belt is generally characterised by transposition-by-folding at outcrop scale. In some areas, such as the Monashee Complex (MC) and the Selkirk allochthon (SA) to its immediate W, transposition folds are of regional scale. In the MC there is an unconformity between Palaeoproterozoic and Neoproterozoic and layering on both sides of the unconformity and the unconformity itself are all transposed into parallelism. These structural observations have generally been interpreted in terms of a thrust model and the Monashee Décollement (MD) has been considered one of the major thrusts.

Small scale transposition may be explicable by ductile thrusting as has been suggested for the MC. However, consideration of the geometry leads us to the conclusion that the large scale structure cannot be explained by such a model. The only model considered feasible involves the development of upright folds of one or more generations followed by horizontal shear in a major crustal detachment zone. The shear modifies all earlier structures and generates new ones. New structures may include F_3 folds and C and C' surfaces, the C' surfaces appearing as zones of higher than background shear. Anything that can be explained by thrusting can be explained by this model, but in addition the model can explain the various structures that cannot be explained by the thrust model.

The model has considerable significance for regional reconstruction of the tectonic history. For example, if the MD exists, it would be better interpreted as some upright structure such as a transcurrent fault. The klippe-to-fenster method of palinspastic reconstruction is invalid in this area as are stratigraphic arguments including the interpretation of the MD as a topographic high, an interpretation which is inconsistent with the structural evidence.

Slip and Deformation Path Partitioning in Orogenic Belts: Implications for Kinematic Analysis of Geological Structures

Dazhi Jiang and Paul F. Williams

Department of Geology, University of New Brunswick, Fredericton, NB, Canada E3B 5A3

Deformation in orogenic belts can be organized, on all scales, into zones of high strain bounding domains of undeformed or weakly-deformed rocks. An important goal of structural analysis is to establish a model that can account for different scale observations. Current paradigms for structural synthesis are monoclinic shear zone models. While these models have served as the frameworks in which many deformation features in natural shear zones are understood, they fail to explain certain strain geometry observed in recent years.

Both natural examples and theoretical investigation have led us to conclude that natural deformation generally follows triclinic deformation paths; monoclinic paths are special end members. Consideration of slip partitioning in transpressional regimes further demonstrates that triclinic deformation is inevitable in such environments. We therefore believe that the current methodology of kinematic analysis based on the assumption of monoclinic deformation path needs to be modified. For example, stretching lineations are not simply parallel to the tectonic transport direction, dragfolds may or may not evolve into sheath folds, and dragfold-derived sheath folds exhibit asymmetry when viewed normal to their axial planes. Kinematic indicators recording different values of strain are expected to show their axes of asymmetry oblique to one another. Furthermore, slip partitioning generally expected on all scales implies that only when the deformation paths across the whole orogenic belt are integrated can reliable inference be made regarding the net plate motion leading to the mountain building. Although this is theoretically possible, problems of challenging complexity are encountered when this is attempted in practice.

Tectonics of central British Columbia and a proposal for a three-dimensional mapping transect across the Cordillera at 55^0 latitude.

L.C. Struik
Geological Survey of Canada
605 Robson Street, Vancouver, B.C. V6B 5J3

Transect proposal

Pre-Middle Jurassic tectonostratigraphic terranes and their extensive overlap assemblages and structures have been newly mapped and studied under the central British Columbia Nechako NATMAP project. These studies have contributed many new suggestions on the tectonic evolution in the Intermontane Belt of the central Canadian Cordillera (see Struik and MacIntyre, 1999, and references there in). Certain crustal-scale interpretations remain unresolved. Now is a good time to do seismic and ancillary studies across the Cordillera at approximately 55^0 latitude.

Excellent control on the surface geology at this latitude between the Omenica and Rockies belts to the east and Coast Mountains to the west makes it possible to interpret reflection and refraction layers and other geophysical parameters of the sub-surface of the Intermontane. In addition, the modern geological and geophysical data bases provide an opportunity to focus detailed surface studies on various geological questions. With three-dimensional maps it would be possible to address the distribution and accretion of the terranes, their mineral and hydrocarbon resources, and how those terranes have been involved in post-accretion deformation and resource formation and concentration. In addition it would address the variations in neotectonic processes from the Coast Mountains to the Rockies.

Questions to be answered through a crustal transect include:

1. Is Cache Creek Terrane detached from its basement and resting as a thrust sheet on Quesnel and Stikine terranes that have underthrust from the east and west, respectively?
2. How deep are the crustal roots to Stikinia and how far do those roots extend to the east and west in the subsurface?
3. How thick is the crust across the Cordillera in central B.C. in comparison to the north and south?
4. What is the density - velocity structure of the crust in the Intermontane Belt?
5. Is the sub-crust stable (constant velocity increase to depth) or is it soft?
6. What is the composition and nature of the Miocene and older mantle?
7. Can a Miocene Mantle Plume be detected and the related question: is there sub-crustal erosion or underplating in the Intermontane?
8. Can Eocene northwest-directed crustal extension be detected?
9. Can the boundaries of Eocene core complexes such as the Vanderhoof and Wolverine metamorphic complexes be detected to depth?
10. Does the Pinchi fault transect the Cache Creek and Quesnel Terrane boundary or does it form that boundary?
11. How far westward does the North American basement underlie accreted terranes and old marginal arc terranes?

12. Does the blueschist terrane of the Cache Creek Group continue to the east under Quesnel terrane?
13. How deep is the Molybdenum rich Endako Batholith and what are its underlying contacts?
14. What is the subsurface nature of the Coast Belt Intermontane contact?
15. What is the huge gravity anomaly cutting the Pinchi Fault east of Fort St. James?
16. Can the Cretaceous east-directed thrust structure be imaged on a crustal scale?
17. With a grand enough plan, the question of basement involvement in the thrusting of the western Rocky Mountains could be addressed.

Some techniques to be used to address these questions include:
1. seismic reflection
2. seismic refraction
3. seismic tomography
4. studying mantle nodules in Miocene basalt flows and centres.
5. detailed mapping of fault zones, including isotopically dating them.
6. gravity profiles over the Pinchi anomaly.
7. isotopic characterization of magmatic rocks.

Summary of the tectonics of central Canadian Cordillera

Central Cordillera is underlain by 3 upper Paleozoic to early Jurassic tectonostratigraphic terranes, which, from east to west are Quesnel (extension margin and arc), Cache Creek (ocean) and Stikine (arc). These terranes can be traced north to the Yukon and south into the United States (Nokleberg et al., 1998). The geological history of the central Cordillera is the development of these three terranes and their subsequent collision, accretion and subsequent deformation and overlap from Jurassic to Recent time. Ideas about the geological history in the region as presented here rely heavily on the work of the Nechako NATMAP project team.

The three terranes were apparently imbricated during Triassic and Jurassic plate convergence. Remnants of the convergence are evident in the eclogite-blueschist belt of the Cache Creek Terrane (Paterson, 1973), the overthrusting of Cache Creek Terrane westward onto Stikinia (Schiarizza and MacIntyre, 1999; Hrudey et al., 1999) and the Early and Middle Jurassic compressional structures within Stikine and Cache Creek terranes (ibid).

The geometry of the subduction zones active during the convergence are not clearly known. Extrapolation from the south would indicate Cache Creek Terrane subducted eastward under Quesnellia. The west side of Cache Creek may have subducted under Stikinia (see Mihalynuk and Nelson, 1997 for discussion). In central and northern British Columbia the subduction was followed by westerly obduction of Cache Creek onto Stikinia (Gabrielse and Yorath, 1991; Schiarizza and MacIntyre, 1999).

Magmatism associated with each of the terranes in central British Columbia is in the process of being chemically and isotopically characterized and dated. That information, in conjunction with the field relationships, has led, and will lead in the next few years, to

a reasonably good understanding of the paleo-environments and the genetics that led to the magmatism. The plutonic suites have been used to confine the age of terrane imbrication and convergence deformation.

Extensive plutonic and volcanic suites were emplaced, and some sedimentary basins formed, during and after collision of the terranes. These events happened in at least 5 significant episodes. Terrane collision occurred during the Early and Middle Jurassic. That collision was followed by 1) Middle Jurassic to Early Cretaceous post-accretion crustal thickening, magmatism and sedimentation; 2) mid-Cretaceous possible crustal thinning and magmatism; 3) Late Cretaceous crustal thickening, magmatism and sedimentation; 4) Eocene crustal thinning, magmatism and minor sedimentation; and 5) Miocene crustal fracturing and mafic volcanism. In addition, the crustal architecture and physiography of the area was altered by the Pleistocene ice age.

When subduction stopped after collision of the Stikine, Cache Creek and Quesnel terranes, compression and magmatism continued. The Jurassic terrane-collision may have transferred directly into the protracted Middle Jurassic to Early Cretaceous compressional/crustal thickening event. From the current age constraints on the magmatism of the region, there is a lull of activity from approximately 200 to 180 Ma; and then for a short time from 180 to 170 Ma. It is during this time (from 200 to 170 Ma) when much of the westerly directed thrusting of Cache Creek onto Stikine Terrane is interpreted to have occurred. Middle Jurassic to Early Cretaceous magmatism has a subduction chemical signature. However, it is not clear that this signature was generated over a subduction zone, as subduction must have jumped far to the west; to the western edge of Stikinia. It was during the Late Jurassic – Early Cretaceous transition that the extensive molybdenum mineralization of the Endako camp is interpreted to have been deposited.

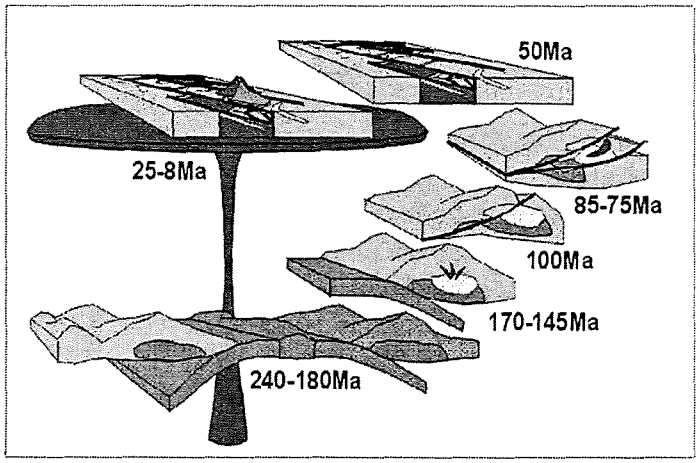

Mid-Cretaceous granite and rhyolite occurs in several areas in central British Columbia. They appear to be volumetrically minor compared to older and younger magmatic rocks. A period of crustal thinning is speculated to coincide with the generation of these rocks. This is based mainly on negative evidence for compression, here or to the east in the Rocky Mountains belt.

The Upper Cretaceous event is marked by some plutonism, extensive dacite to rhyolite volcanism, wide spread (though volumetrically minor) sedimentation and some

interpreted thrust faulting. From extrapolation of similarly aged thrust tectonics to the south and north is it interpreted that the Upper Cretaceous is a time of compression.

Eocene tectonism is a marked departure from the Mesozoic events. It is a time of extensive bimodal volcanism, minor sedimentation, north-northwesterly trending strike-slip and extensional faulting and the uplift and exposure of metamorphic core complexes. The event is short-lived, being mainly from 55 to 45 Ma.

Miocene tectonism, represented primarily by extensive thin basalt flows and scattered eruptive centres, is thought to have been a process of crustal fracturing, either related to distant crustal extension (Rohr and Currie, 1998), or more speculatively a mantle plume. Some Miocene volcanoes are built along Tertiary fault zones, and are interpreted to have been localized by motion on the those faults. The basalt flows are mostly flat lying, and as such extensive crustal rearranging has been ruled out in this part of the Intermontane Belt.

The area was completely covered by glacial ice during the Pleistocene and in particular during the later Wisconsin stage. The upper surface of the ice was over 2500m above sea level and thick enough to flow independently of surrounding Mountains. Such masses of ice reshaped the landscape, redistributed surface material and created a very large load on the underlying crust. Melting of that ice must have been accompanied by some isostatic rebound.

Acknowledgments
Many thanks to all the people involved in the Nechako NATMAP project who have contributed ideas and information that have led to this summary (see Struik and MacIntyre, 1999 for an outline of their research and for references to their work). I am grateful to Marianne Quat for helping with the preparation of this abstract.

References

Gabrielse, H. and Yorath, C.J. (Editors)
1991: Geology of Canada no. 4; Geology of the Cordilleran Orogen in Canada; Geological Survey of Canada, 844 p.

Hrudey, M.G., Struik, L.C., and Whalen, J.B.
1999: Geology of the Taltapin Lake map area, central British Columbia; in Current Research 1999-A; Geological Survey of Canada, p. 85-96.

Mihalynuk, M.G., Nelson, J., and Diakow, L.J.
1994: Cache Creek Terrane entrapments; oroclinal paradox within the Canadian Cordillera; Tectonics, v.13, no. 3, p. 575-595.

Nokleberg, W.J., Parfenov, L.M., Monger, J.W.H., Norton, I.O., Khanchuk, A.I., Stone, D.B., Scholl, D.W., and Fujita, K.
1998: Phanerozoic tectonic evolution of the circum-north Pacific.; U.S. Geological Survey Open File 98-754.

Paterson, I.
1977: The geology and evolution of the Pinchi Lake Fault zone at Pinchi Lake, central British Columbia; Canadian Journal of Earth Sciences, v. 14, p. 1324-1342.

Rohr, K.M.M. and Currie, L.
1997: Queen Charlotte Basin and Coast Mountains: Paired belts of subsidence and uplift caused by low-angle normal fault; Geology, v. 25, p. 819-822.

Schiarizza, P. and MacIntyre, D.G.
1999: Geology of the Babine Lake - Takla Lake area, central British Columbia (93K/11, 12, 13, 14; 93N/3, 4, 5, 6); in Geological Fieldwork 1998; British Columbia Ministry of Energy and Mines, Paper 1999-1.

Struik, L.C. and MacIntyre, D.G.
1999: Nechako NATMAP Project overview, central British Columbia, year four: part 1; in Current Research 1999-A; Geological Survey of Canada, p. 71-78.

MID-JURASSIC HOBSON LAKE PLUTON OF THE CENTRAL CARIBOO MOUNTAINS, BRITISH COLUMBIA: RE-EXAMINATION OF CRITICAL FIELD RELATIONSHIPS

Reid, Leslie, Department of Geology and Geophysics, University of Calgary, Calgary, Alberta. (reid@geo.ucalgary.ca)

The Hobson Lake Pluton has been used as a structural lynch pin to constrain the timing of regional deformation in the western Cariboo Mountains. In recent years there has been controversy regarding the relationship of the pluton to regional structural fabrics and folds (Ferguson, 1994). Field research carried out in the summer of 1998 east of Hobson Lake has ascertained the structural relationship of the Hobson Lake Pluton to the main regional structures in the central Cariboo Mountains of British Columbia. This was accomplished by tracing regional southwest-verging structures from the northern Cariboo Mountains south into the region where the Hobson Lake Pluton occurs.

The Hobson Lake Pluton is a granodioritic sill-like intrusion that is approximately 400m thick and covers 500km^2 and intrudes the carbonate-rich Cunningham Formation of the Neoproterozoic Windermere Supergroup. The pluton is undeformed and unmetamorphosed and apophyses of the main body cross-cut regional deformation structures that include metre to kilometre-scale southwest-verging folds and an associated axial planar cleavage. The folds that are cross-cut by the Hobson Pluton can be traced along axial surfaces to the northwest where they comprise the main regional kilometre-scale anticlinoria and synclinoria structures that dominate the structural style in the northern and central Cariboo Mountains.

Both the upper and lower contacts of the Hobson Lake Pluton are well exposed. The upper contact shows a gradational change in mineralogy and texture from a medium to coarse-grained hornblende-biotite granodiorite to leucogranite that is aplitic in texture and composition. This change occurs over five metres at the margin of the pluton where there is a sharp contact with the surrounding host rock. The lower contact shows no mineralogical or textural change towards the margin, but does clearly cross cut folded layers in the Cunningham Formation. Epidote-garnet skarn rock is present within marble rock of the Cunningham Formation up to two metres from the contact. This alteration is found for approximately two meters into the Cunningham Formation. Approximately five kilometers south of the Hobson Lake Pluton, are three mineralogically distinct plutonic bodies that all show the same structural relationship to the surrounding country rock as the Hobson Lake Pluton (i.e. they cross cut regional folds). These plutonic bodies include a leucogranite feldspar porphry pluton, a diorite pluton and a hornblende gabbro pluton.

Based on new mapping it can be shown conclusively that the Hobson Lake Pluton cross-cuts the main regional structures and thus post-dates the main deformation and metamorphism in the area. This implies that the main regional structures in the north and central Cariboo Mountains are indeed older than 174 Ma (mid-Jurassic), the age obtained for the Hobson Lake Pluton by previous workers (Gerasimoff, 1988). Other post-tectonic plutonic bodies mapped during this season are the focus of U-Pb geochronological work to determine whether they are similar in age to the Hobson Lake Pluton.

Ferguson, C.A., 1994, **Structural Geology and Stratigraphy of the northern Cariboo Mountains between Isaac Lake and Fraser River, British Columbia**. unpublished Ph.D. thesis, University of Calgary, Calgary, Alberta.

Gerasimoff, M.D., 1988, **The Hobson Lake Pluton, Cariboo Mountains, British Columbia, and its significance to Mesozoic and early Cenozoic cordilleran tectonics**. unpublished M.Sc. thesis, Queens University, Kingston, Ontario.

New Structural and Stratigraphic Data from the Purcell Thrust Zone and Some Implications

Simony, P.S., Boggs, K.J.E. and Acton, S.L., Department of Geology and Geophysics. University of Calgary, Calgary, Alberta T2N 1N4

The Purcell Fault is an out-of-sequence, southwest-dipping thrust between the fold and thrust structures of the Purcell Mountains in its hanging wall and the fold and thrust structures of Western Ranges of the Rocky Mountains in its footwall. Its trace corresponds approximately with the west wall of the southern Rocky Mountain Trench. It is defined by mapping for a strike length of only 200 km from the vicinity of Radium at Lat. 50° 30′N to Bush Arm (mouth of the Bush River) at Lat. 51° 41′N. Linkages with faults to the NW and the SE are interpretations. For the northwestern 50 km of its trace, from the Trans-Canada Highway northwestward, the same strata and the same structural elements continue on either side of the fault. In its footwall it follows black argillaceous slate that weathers to a soft soil. This explains why the fault is generally not exposed. The slate is a unit within the calcareous slates of the Upper Cambrian, Canyon Creek Formation. In its hanging wall lie Lower Cambrian quartzite, slate and limestone of the deepest, most easterly horse of the Dogtooth Duplex (Kubli and Simony 1994). This implies that in these 50 km, the stratigraphic throw remains the same and possibly, therefore, the net slip at Bush Arm is approximately 10 km, the same magnitude as was determined near the Trans-Canada Highway, in the Dogtooth Range (Simony and Wind, 1970; Kubli and Simony, 1994). At Bush Arm the thrust therefore maintains an important displacement to the northwest of where it is cut by a west-side-down fault that down-throws the thrust one or two kilometres into the sub-surface. The Trench follows that normal fault northwestward to the Big Bend of the Columbia where the normal fault ends.

At the headwaters of Blackwater Creek (Long. 117° 25′W – Lat. 51° 38′N, the Purcell thrust as well as bedding and cleavage in its hanging wall and footwall are folded by a kink band with a width of some 300 m, nearly vertical axial planes that strike at 030°-040° and with nearly vertical kink axes. This orientation is similar to that of mesoscopic kink bands common in the region near the Trench. They therefore probably also post-date the Purcell Thrust.

The Lower Cambrian succession in the immediate hanging wall of the Purcell Thrust to the west of Succour Arm and Succour Creek (between Lat. 51° 40′N and 51° 46′N) consists of 170 m of quartzite and siliceous slate of the uppermost unit of the Hamill Group. That unit is equivalent to the Poker Member at the top of the Upper McNaughton Formation in the western Rockies. It is overlain by 20 m of brown slate and 20 m of Archaeocyathid limestone of the Donald Formation that is equivalent to the Mural Formation in the western Rockies. The 170 m quartzite and slate unit has basal beds of gritty, feldspathick sandstone that lie directly and unconformably on slate and grit of the Horsethief Creek Group equivalent to the Neoproterozoic Middle Miette Group of the western Rockies.

In the same thrust slice, 50 km to the southeast, the Hamill Group is 900 m thick and lies on slates of the Horsethief Creek Group equivalent to the Upper Miette

of the Rockies. The 900 m of Hamill is considered to have been deposited on the "Easterly High" (Kubli and Simony 1992) because it is thinner than, and lacks units present in, Hamill Group in a more westerly thrust sheet. Clearly the Easterly High, subtle in the northeastern Dogtooth Range, becomes more pronounced northwestward with the sub-Hamill unconformity eroded more deeply into the underlying strata and with onlap of the highest unit of the Hamill Group. The thin stratigraphy west of Succour Arm could represent the most uplifted portion of the western Rocky Mountains "high" described in the Solitude Range by Lickorish and Simony (1995) and transported eastward on the Purcell Thrust.

References

Kubli, T.E. and Simony, P.S. 1992, The Dogtooth High, northern Purcell Mountains, British Columbia. Bulletin of Canadian Petroleum Geology, **40**, p. 36-51.

Kubli, T.E. and Simony, P.S. 1994. The Dogtooth Duplex, a model for structural development of the northern Purcell Mountains. Canadian Journal of Earth Sciences, **31**, p. 1672-1686.

Lickorish, W.H. and Simony, P.S. 1995. Evidence for late rifting of the Cordilleran margin outlined by stratigraphic division of the Lower Cambrian Gog Group, Rocky Mountain Main Ranges, British Columbia and Alberta. Canadian Journal of Earth Sciences, **32**, p. 860-874.

Simony, P.S. and Wind, G. 1970. Structure of the Dogtooth Range and adjacent portions of the Rocky Mountain Trench. *In* Structure of the Southern Canadian Cordillera, J.O. Wheeler (ed.) Geological Association of Canada Special Paper No. 6, p. 41-51.

The Josh Creek Diorite, Christina Lake, southeastern British Columbia: A deformed Late Triassic body within Quesnellia

Acton, S.L., Simony, P.S., and *Heaman, L. Department of Geology and Geophysics, The University of Calgary, Calgary, AB, T2N 1N4; *Department of Earth and Atmospheric Sciences, The University of Alberta, Edmonton, AB T6G 2E5

The correlation of supracrustal assemblages within the southwestern Omineca Crystalline Belt remains a problem. The age and extent of strata underlying Triassic-Jurassic assemblages of Quesnellia is unknown in many locations due the presence of unmapped geology, complex stratigraphy, structure, and the superposition of Omineca Belt metamorphism and plutonism on the eastern part of the Intermontane Superterrane. Until recently, little detailed geologic work had been completed in the Christina Lake area, therefore it was not known if the pre-Jurassic rocks in this area represent an older part of Quesnellia or strata of North American affinity. Initial U-Pb geochronology of a deformed diorite body and detailed geologic mapping strongly suggest that the supracrustal rocks in the Christina Lake area are a part of Quesnellia.

Supracrustal rocks in the Christina Lake area consist of compositionally banded metamorphosed siltstone, coarse-crystalline marble, and lithologically variable semipelitic schist and metasandstone of the Mollie Creek Assemblage. These rocks are extensively intruded by the foliated Josh Creek Diorite, which is Late Triassic using U-Pb zircon geochronology. Two multigrain zircon fractions were analyzed, consisting of small, cloudy, fractured prisms. The fractions are slightly discordant and give a lower concordia intercept age of 215.9 ± 1.9 Ma (2□ error), which is interpreted as the time of emplacement of the diorite. Because the diorite intrudes the Mollie Creek Assemblage, the assemblage is older than Late Triassic. The age cannot be further constrained since older rocks were not documented, strain and low-pressure metamorphism have destroyed fossils, and stratigraphic relationships have been disrupted by several phases of deformation and plutonism. A sample of less deformed diorite related to the Early Jurassic Rossland Group was also analyzed. Using U-Pb zircon geochronology, the age of the diorite is constrained to 197 ± 5 Ma (2□ error), which is similar to the ages of a suite of diorite bodies in southeastern British Columbia inferred to be related to the volcanic rocks of the Rossland Group.

The Josh Creek Diorite and Mollie Creek Assemblage have undergone at least four phases of deformation since the Late Triassic. Post-Late Triassic Deformation (D_1) resulted in the folding of the Mollie Creek Assemblage. Mesoscopic-scale folding of the Mollie Creek Assemblage and Josh Creek Diorite into west verging F_2 folds, which deform F_1 folds and foliation (S_1), occurred in response to the obduction and accretion of the Intermontane Superterrane onto North America in the Early to Mid-Jurassic. Minor refolding of F_2 folds (D_3) may have occurred as a result of the emplacement of the Mid-Jurassic Nelson Suite. D_1, D_2, and possible D_3 structures are cut by syenitic intrusions of the Coryell Suite and the north-trending Kettle River and McRae Creek normal faults related to Eocene extension.

The Josh Creek Diorite had previously not been recognized in the Christina Lake region. The Late Triassic age of the Josh Creek Diorite and its similarity to other Late Triassic dioritic bodies within Quesnellia implies that the Mollie Creek Assemblage was part of Quesnellia during the Late Triassic. The Josh Creek Diorite may represent the early stages of island-arc tectonism and magmatism within Quesnellia prior to the accumulation

of the Rossland Group in the Early Jurassic. The Mollie Creek Assemblage is either the equivalent of pericratonic assemblages deposited on the western margin of ancient North America, rifted off and later incorporated into Quesnellia, or is a western continuation of the Pennsylvanian to Early Triassic Mount Roberts Formation defined in the Rossland area. The Late Triassic age of the Josh Creek Diorite, which intrudes the Mollie Creek Assemblage, does not resolve this problem. Typically, North American strata that have been metamorphosed below the obducted sheet record high pressure (500-800 Mpa) Jurassic and/or Cretaceous metamorphism within the kyanite zone of the amphibolite facies (Colpron et al. 1996, Read et al. 1991, Ghent et al. 1982). Low-pressure metamorphism of the Mollie Creek Assemblage is consistent with the Christina Lake area lying above the obduction surface. Rocks of the Rossland Group lie topographically and structurally above the Mollie Creek Assemblage, a relationship that can be interpreted as a stratigraphic contact consistent with the unconformity at the base of the Rossland Group. The obduction surface would then have to lie below the Mollie Creek Assemblage or at a deeper structural level, suggesting that the supracrustal rocks of the Christina Lake area are a part of Quesnellia.

References:

Colpron, M. Price, R.A., Archibald, D.A. and Carmichael, D.M. 1996. Middle Jurassic exhumation along the western flank of the Selkirk fan structure: Thermobarometric and thermochronometric constraints from the Illecillewaet synclinorium, southeastern British Columbia. Geological Society of America Bulletin, v. 108, p. 1372-1392.

Ghent, E.D., Knitter, C.K., Raeside, R.P. and Stout, M.Z. 1982. Geothermometry and geobarometry of pelitic rocks, upper kyanite and sillimanite zones, Mica Creek area, British Columbia. Canadian Mineralogist, v. 20, p 295-305.

Read, P.B., Woodsworth, G.J., Greenwood, H.J., Ghent, E.D. and Evenchick, C.A. 1991. Metamorphic map of the Canadian Cordillera. Geological Survey of Canada, Map 1714A, scale 1:200000.

U-TH-PB GEOCHRONOLOGIC CONSTRAINTS ON DIACHRONOUS METAMORPHISM AND DEFORMATION IN THE MICA CREEK AREA, SOUTHEASTERN CANADIAN CORDILLERA

Crowley, J.L.[1], Ghent, E.D.[1], Carr, S.D.[2], Hamilton, M.A.[3], Simony, P.S.[1]
[1]Department of Geology and Geophysics, University of Calgary, Calgary, AB T2N 1N4; [2]Ottawa-Carleton Geoscience Centre and Department of Earth Sciences, Carleton University, Ottawa, ON K1S 5B6; [3]Geological Survey of Canada, 601 Booth Street, Ottawa, ON K1A 0E8

U-Th-Pb data from isotope dilution and SHRIMP dating indicate that the ages of metamorphism and deformation vary in the Mica Creek area, southeastern Canadian Cordillera. Three, km-scale age domains exist in a region with apparent metamorphic, structural, and stratigraphic continuity. In domain 1, most monazite and xenotime in garnet schist grew at ~163 Ma and underwent minor to moderate recrystallization or overgrowth at ~70 Ma. Growth also occurred at 90 and 70 Ma. Electron microprobe analysis shows that garnet grew during a single phase and temperatures were not high enough to modify the growth zoning patterns. In domain 2, matrix monazite in migmatitic kyanite schist mostly grew at 83-70 Ma, and some grains contain minor amounts of younger (61 Ma) or older monazite. Monazite inclusions in garnet and kyanite grew at 110 and 83-73 Ma, respectively. Temperatures were high enough to homogenize garnet zoning patterns. In domain 3, monazite in migmatitic kyanite and sillimanite schists mostly grew at 99-93 Ma, and growth also occurred at ~163, 110, and 70 Ma.

These data indicate that kyanite growth during peak metamorphism in domain 2 occurred after 73 Ma, possibly during leucosome crystallization at 61 Ma. We suggest that peak metamorphism in domains 1 and 3 occurred during the dominant periods of monazite growth at ~163 and 99-93 Ma, respectively, but younger metamorphism cannot be ruled out. Our interpretations require that (i) the age of peak metamorphism differs in each domain and (ii) secondary thermal events were synchronous with peak events in other domains. Timing constraints on the dominant foliation (S_{1+2}) are provided by the strained states of dated granitoids; S_{1+2} developed before 72 and 63 Ma in domains 1 and 3, respectively, whereas at least some development occurred at 61-58 Ma in domain 2.

The Mica Creek area is the only known region in the southeastern Canadian Cordillera that was tectonized during the three major periods of orogenesis (170-160, 100-90, and 75-60 Ma). It is difficult to explain a diachronous history in an area with apparent geologic continuity. If the continuity exists as mapped, then metamorphic heat sources were localized (e.g., related to plutonism) and the young deformation associated with S_{1+2} in domain 2 was insignificant (e.g., related to reactivation of preexisting S_{1+2}). If the continuity is only apparent, the domains may have been tectonized, at least in part, at different times and places in the orogen and then assembled into their present positions via cryptic, complex structures. The occurrence of common periods of monazite growth suggests that the domains have similar thermal histories, possibly indicating that they were never greatly separated.

THE NICOLA HORST: AN UPDATE AND UNRESOLVED PROBLEMS

John M. Moore
Adjunct Professor
Earth Sciences Program
Simon Fraser University
Burnaby, BC V5A 1S6

The Nicola Horst, a prominent feature of the Southern Cordillera LITHOPROBE transect at *ca.* Long. 120° 40'W, was mapped in 1988-89 at 1:100,000 scale (Moore and Pettipas, 1990). Since then there have been no systematic geological studies of the area.

The Nicola Horst comprises granitic rocks ranging in age from Palaeocene to at least as old as early Jurassic; metavolcanic units correlated with the surrounding late Triassic Nicola Group; and probably older metapelite and quartzite metaconglomerate. The volcanic and sedimentary rocks, along with tonalite of uncertain age, are strained, metamorphosed to low amphibolite facies and apparently truncated by less deformed plutonic units. These deformed supracrustal rocks have recently become a matter of special interest because they have been tentatively correlated by Erdmer et al. (1999) with Palaeozoic pericratonic rocks around the northern Okanagan Valley to the east (Tsalkom, Sicamous, Eagle Bay, Chapperon units). These rocks are postulated to represent a stratigraphic link between the Triassic rocks of Quesnellia and the late Proterozoic-early Palaeozoic margin of North America. If the proposed correlations are valid, then it is indicated that Nicola rocks were deposited on North American basement that extends at least as far west as the Nicola Horst and, by extension, that Quesnellia is not exotic.

In light of the importance of this hypothesis to regional Cordilleran tectonics, it is proposed to restudy critical parts of the Nicola Horst and its surroundings in detail. Areas to map and supporting techniques will be chosen in order to address the following problems:

1) *Is there evidence of a pre-Nicola metamorphism and deformation in the Horst?* Planar and linear fabrics of similar orientation to those seen in the metasediments also exist in the metavolcanic units of the Horst, that are at least lithologically correlative with Nicola units at much lower grade outside the boundary faults. As yet there is also no evidence of any difference in metamorphic grade between these "meta-Nicola" rocks (unit TNm of Moore and Pettipas, 1990) and the metasediments; the lower strain in them may be only a reflection of their basaltic composition. As there is clearly pre-Nicola metamorphism and deformation in the Chapperon group beneath the sub-Nicola unconformity, 35 km east of the Horst and 50 km west of the localities discussed by Erdmer et al., the features of the Chapperon associated with this locality should be compared with those in the Horst.

2) *Is the P-T-t path of metamorphism in the Horst comparable to that observed by Erdmer and co-workers to the east?* The existence of andalusite (after kyanite) in the lower amphibolite facies of the Horst indicates a similar metamorphic history to that of the supposed pre-Triassic metamorphism in the Vernon area, but P-T-t studies would be required to support this contention.

3) *What is the provenance of the metaconglomerate in the Horst?* The discovery of ca. 560 Ma granite debris in strained metaconglomerate of the Fowler Creek area (Erdmer et al., 1999) provides a potential "fingerprint", as plutons of that age are distinctive, being as yet unrecorded in the region. There are granitic clasts in the Nicola Horst metaconglomerate and their age should be determined.

4) *What is the tectonic regime of the deformed rocks in the Horst and how does it compare with that recorded in similar units to the east?* Mapping by Moore in 1989 indicated easterly transport, but additional data collected in 1990 yielded a mix of shear senses. Further fabric studies are in order.

5) *What is the plutonic history of the Horst?* The highly strained tonalites in the west margin of the Horst are of unknown age and affinity. Their age and contact relationships with the metasediments and the other plutonic rocks will help to constrain the tectonic history.

6) *Are the Nicola Horst rocks correlative with metamorphic units yet further west?* The Mount Lytton/Eagle Complex rocks have been tentatively correlated with those in the Nicola Horst (Monger and McMillan, 1989). If this is so, and units in the Horst can be correlated with Palaeozoic units to the east, then continental basement is indicated all the way to the Fraser fault system.

References

Erdmer, P., Thompson, R.I. and Daughtry, K.L., 1999: Pericratonic Paleozoic succession in Vernon and Ashcroft map areas, British Columbia; *in* Current Research 1999-A; Geological Survey of Canada, p. 205-213.

Monger, J.W.H. and McMillan, W.J., 1989: Geology, Ashcroft, British Columbia; Geological Survey of Canada, Map 42-1989, sheet 1, scale 1:250,000.

Moore, J. M. and Pettipas, A. R., 1990: Geological Studies in the Nicola Lake Region (92I/SE); Part A *in* Nicola Lake Region Geology and Mineral Deposits; British Columbia Geological Survey Branch, Ministry of Energy, Mines and Petroleum Resources, Victoria, Open File 1990-29, p. 3-11 and 1:100,000 map.

Tracking North American Basement west of the Okanagan Valley: insights from the Vernon, Ashcroft, and Hope map areas

R. I. Thompson[1], P. Erdmer[2], K. L. Daughtry[3], L. Heaman[2], and R. A. Creaser[2]

[1]Geological Survey of Canada, 9860 W. Saanich Road, P.O. Box 6000, Sidney, B.C. V8L 4B2
[2]Department of Earth & Atmospheric Sciences, University of Alberta, Edmonton, AB, T6G 2E3
[3]Discovery Consultants, P.O. Box 933, Vernon, B.C. V1T 6M8

Strata that formed part of the ancient Pacific margin of south-central British Columbia have been mapped from east of the Okanagan Valley more than 100 kilometers west to the Nicola horst near Merritt. A distinctive pericratonic succession of quartzite- and granite-pebble conglomerate (~50 m), amphibole schist (~500 m), and marble (~40 m) of probable Lower Paleozoic age overlies a thick succession of quartzofeldspathic schist, quartzite, pegmatite, and paragneiss (Silver Creek Formation) that forms part of the Neoproterozoic (Windermere) succession deposited along the continental margin about 550 to 750 million years ago. The pericratonic succession is overlain along a stratigraphic contact by Permian and Triassic volcanic arc and sedimentary rocks. This tripartite regional stratigraphy crosses the Okanagan Valley without significant offset.

There is a notable change in grade of metamorphism as well as intensity and style of deformation between the pericratonic succession and overlying rocks, indicating a regional ductile deformation and accompanying metamorphism at mid-crustal levels prior to deposition of Permian and younger strata. This distinction is veiled by later metamorphism and deformation near the Okanagan Valley.

The implications of this find are huge. For example, the region west of the Okanagan Valley was until now thought to be underlain by more juvenile crust belonging to the Quesnellia terrane, a volcanic arc accreted to the North American margin during Jurassic time. Mapping reveals that the pericratonic succession, i.e., North American rocks which are tied depositionally to the ancient margin, underlies a stratigraphic cover of Quesnellia terrane strata, consisting of the Permian Harper Ranch Group and the Upper Triassic Nicola Group which include carbonaceous shale, volcanic strata and thin carbonate members. We see no reason why the stratigraphy that underlies the Nicola Group should stop at the Nicola horst. To the west, metamorphic rocks that underlie the Nicola Group are known adjacent to the Fraser fault. Our conclusion is that Permian and Upper Triassic volcanic arcs were active at a continental margin that extended at least as far west as the Nicola horst, likely as far as today's Fraser fault, and possibly beyond.

Preliminary U-Pb Geochronology Results from the Vernon area, British Columbia

L.M. Heaman[1], P. Erdmer[1], R.I. Thompson[2] and K.L. Daughtry[3]

[1] Department of Earth and Atmospheric Sciences, University of Alberta, Edmonton, AB
[2] Geological Survey of Canada, Sidney, B.C.
[3] Discovery Consultants, P.O. Box 933, Vernon, B.C.

Recent field work and mapping initiatives in the Vernon area (see Erdmer et al., 1999 for references) have identified a distinctive pre-Triassic pericratonic supracrustal package that can be traced across the Omineca/Intermontane Belt boundary implying that the margin of autochthonous North American basement may extend much further west than previously thought. As part of a companion isotopic study, six samples have been selected for U-Pb study in an attempt to provide further temporal constraints for the age of both pre- and post-Triassic magmatism, sedimentation, and deformation/ metamorphism. Three of the samples were collected from the Kalamalka Lake area with an aim to constrain the timing of pre-Eocene deformation. These include a granodiorite sample from the Cosens Bay pluton (PE97-28), a Coryell monzonite dyke showing no superimposed fabric (PE97-7), and a two-mica aplite dyke (PE97-7A) that clearly truncates regional schistosity but itself contains a tectonic fabric which may be contemporaneous with development of a major shear zone along Kalamalka Lake. U-Pb results for two samples from the Fowler Creek area, a metaconglomerate (97TW-173) and foliated granodiorite (PE98-33), were obtained in an attempt to constrain the age of the pre-Triassic supracrustal assemblage mentioned above. Work is currently in progress on a granitic sill that intrudes, but is concordant with, the pericratonic package from the Bob Lake area in the Nicola horst (PE98-27A).

U-Pb Results from the Kalamalka Lake Area

Cosens Bay Granodiorite (PE97-17)

The Cosens Bay pluton is truncated by a major shear zone and its emplacement age provides a maximum estimate for the timing of shearing. This granodiorite sample contains abundant colourless zircon and the results offour U-Pb zircon analyses are displayed on a concordia diagram in Figure 1. A number of zircon grains are subhedral, exhibiting significant resorption with visible milky white cores. These are interpreted as xenocrysts and the single grain analysis #4 with a $^{207}Pb/^{206}Pb$ age of 531 Ma represents a minimum estimate for the age of this inheritance. Three multi-grain fractions (#1-3) of slender needles are also shown in Figure 1. Two possible reference lines are shown and demonstrate that the data are consistent with either a 90 or 104 Ma lower intercept age. At the present time we interpret the emplacement age of the Cosens Bay pluton to be constrained to this 90-104 Ma age bracket and hence shear zone development must post-date this.

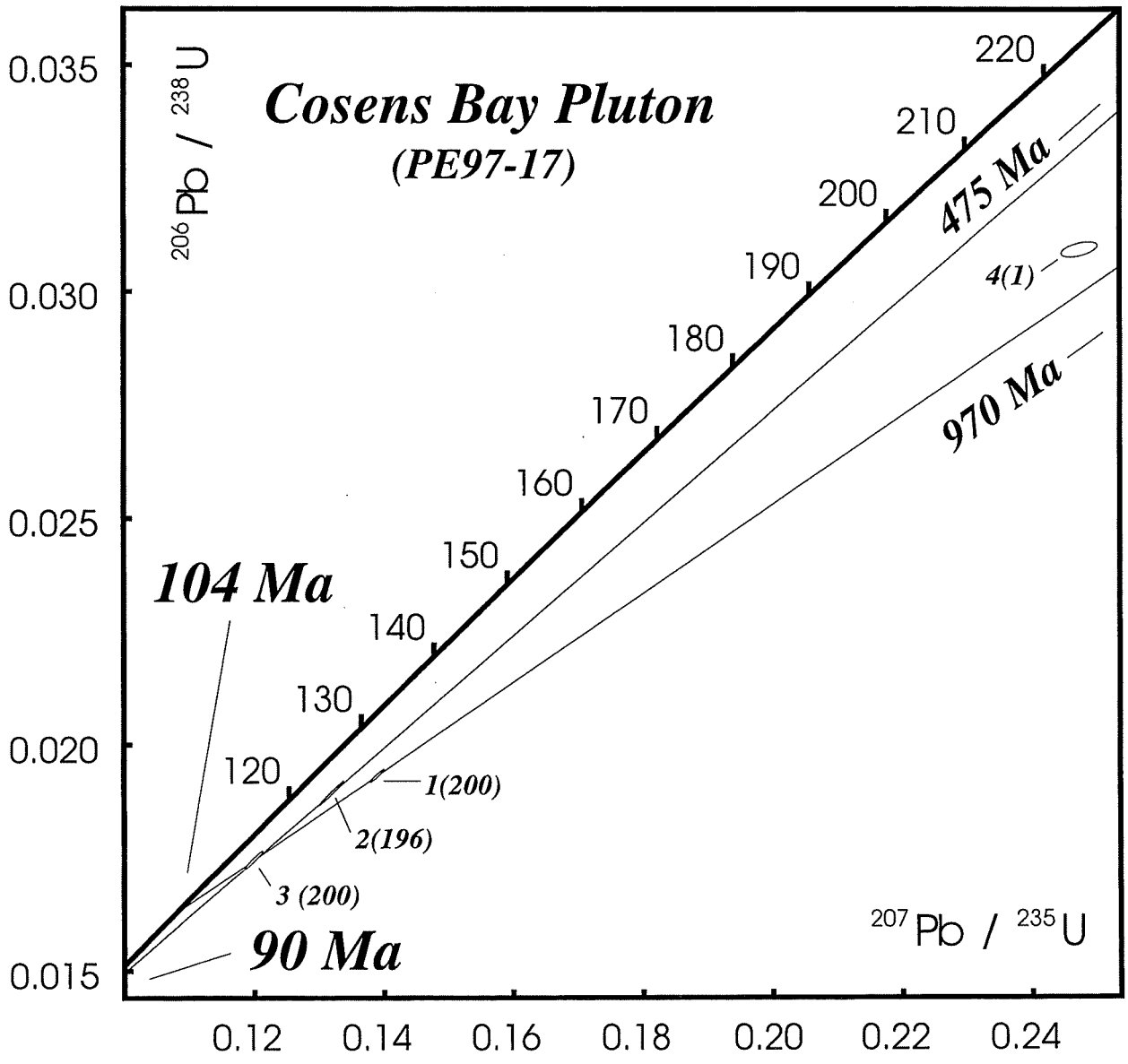
Cosens Bay Pluton
(PE97-17)
$^{206}Pb / ^{238}U$
$^{207}Pb / ^{235}U$
0.035
0.030
0.025
0.020
0.015
0.12
0.14
0.16
0.18
0.20
0.22
0.24
220
210
200
190
180
170
160
150
140
130
120
475 Ma
970 Ma
104 Ma
90 Ma
4(1)
1(200)
2(196)
3 (200)

Figure 1

Coryell Dyke (PE97-28)

A sample of an undeformed dyke, presumed to be a Coryell dyke, was processed to provide a minimum age constraint for the time of shear zone development. As in the case of the Cosens Bay granodiorite sample, two distinct populations of colourless zircon are present; 1) resorbed prismatic grains and 2) slender needles. The results for two fractions from this sample are shown in Figure 2. Fraction #1 consisted of 80 minuscule colourless needles which has indistinguishable $^{206}Pb/^{238}U$ and $^{207}Pb/^{235}U$ ages of 46.3±0.4 Ma and 47.1±0.6 Ma, respectively (two sigma uncertainties). If there is negligible inheritance present in this analysis then the best estimate for the emplacement age of the dyke is 47 Ma. A colourless irregular prismatic single grain (#2) has a significantly older $^{207}Pb/^{206}Pb$ age of 182 Ma and is interpreted as an indication of Jurassic inheritance in this sample.

Two-mica aplite dyke (PE97-7A)

This sample was selected because it is in close proximity to the Coryell dyke discussed above, truncates the regional schistosity but itself contains a fabric which might be contemporaneous with shear zone development. The results for four U-Pb zircon analyses are also shown in Figure 2. Once again two populations of colourless zircon are present. The younger two analyses (#2,4) represent multi-grain fractions of slender needles while the older analyses (#1,3) are single prismatic grains. The youngest analysis (#4) yields identical $^{206}Pb/^{238}U$ and $^{207}Pb/^{235}U$ ages of 49.8±0.2 Ma and 50.3±0.4 Ma, respectively (two sigma uncertainties) and the best estimate for the emplacement age of this dyke is 50 Ma. Similar to the Coryell dyke, Jurassic inheritance is implicated from the single prismatic zircon analyses. Assuming that the fabric present in this sample is not of a primary nature, then its development must have occurred sometime before 47 Ma (the age of the undeformed Coryell dyke).

Fowler Creek Area

Granodiorite (PE98-33C)

The Fowler Creek granodiorite intrudes the pericratonic supracrustal package and therefore provides a minimum estimate for the depositional age of these units. A single multi-grain analysis of colourless needles indicates a $^{207}Pb/^{206}Pb$ age of 359 Ma (10.5% discordant). We tentatively interpret this granodiorite to be Devonian in age and part of a more regional suite of Devonian plutonism. If this interpretation is correct then the depositional age of the pericratonic supracrustal rocks is pre-Devonian.

Metaconglomerate (97TW-173)

This metaconglomerate locally contains a preponderance of deformed granite clasts and was investigated to identify the age and nature of the basement that the pre-Triassic supracrustal package was eroded from. As a starting point, a sample of the metaconglomerate was crushed without any effort to isolate individual clasts. A portion

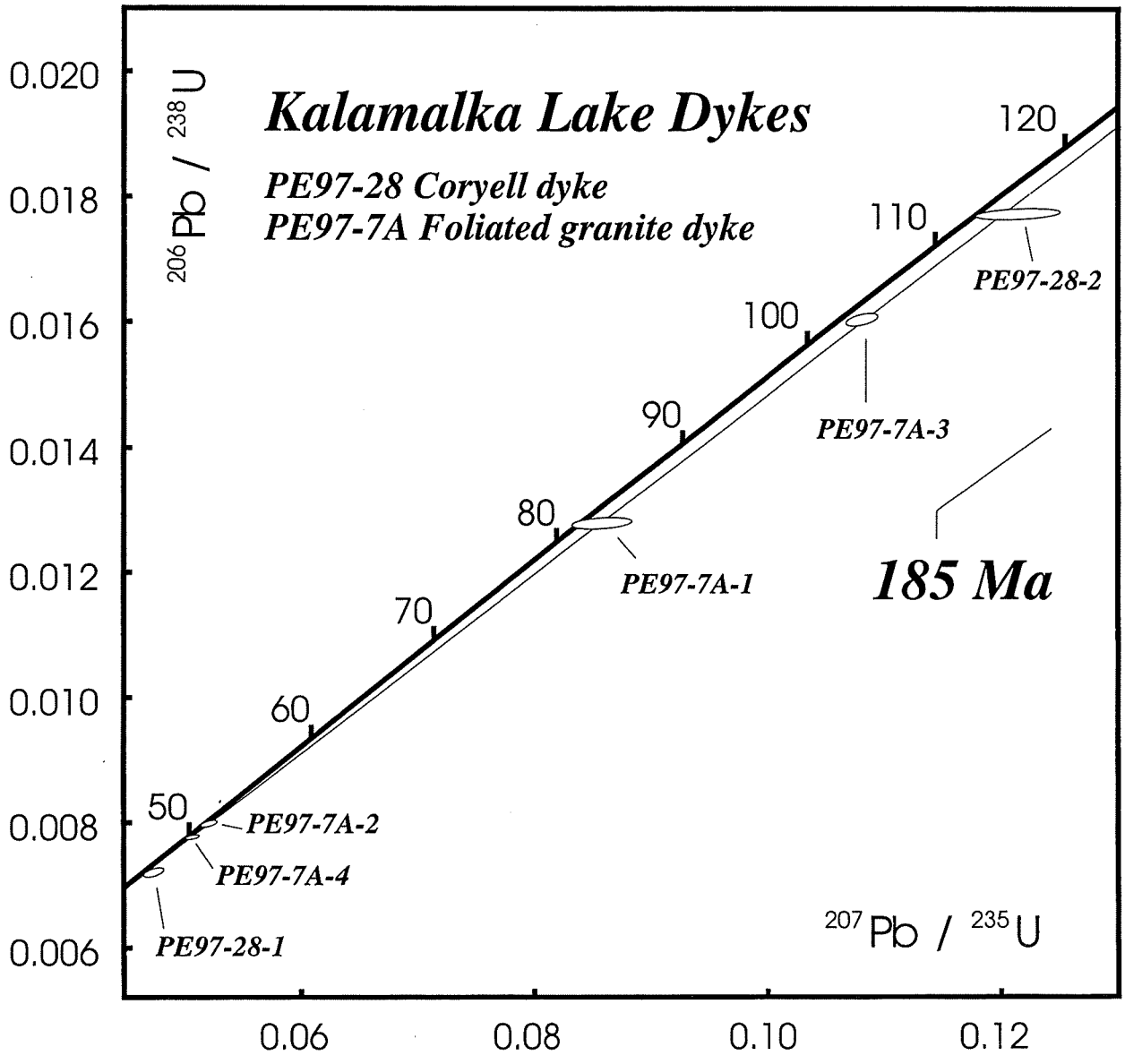
Kalamalka Lake Dykes
PE97-28 Coryell dyke
PE97-7A Foliated granite dyke
185 Ma
PE97-28-1
PE97-7A-4
PE97-7A-2
PE97-7A-1
PE97-7A-3
PE97-28-2
50
60
70
80
90
100
110
120
0.020
0.018
0.016
0.014
0.012
0.010
0.008
0.006
0.06
0.08
0.10
0.12
206Pb / 238U
207Pb / 235U

Figure 2

of the uncrushed sample was kept in order to determine the age of individual clasts if necessary. The results for three zircon analyses are presented in Figure 3. Two of the analyses are unabraded multi-grain fractions (#1,3) and fraction #2 represents a single abraded colourless blocky fragment. The $^{207}Pb/^{206}Pb$ ages for these fractions are 560, 554 and 623 Ma, respectively and all are less than 10% discordant. From these data we can constrain the depositional age to be younger than 554 Ma and older than the 360 Ma Devonian granodiorite discussed above. Considering that there is very little age variation in the detrital zircon analyses and there is a preponderance of granitic clasts, we interpret that this conglomerate primarily reflects erosion of a nearby Precambrian granite and that the depositional age is likely close to 560 Ma, because we otherwise would anticipate a more diverse age profile in the zircon population.

Erdmer, P., Thompson, R.I., Daughtry, K.L., 1999. Pericratonic Paleozoic succession in Vernon and Ashcroft map areas, British Columbia. In Current Research 1999-A, Geological Survey of Canada, p. 205-213.

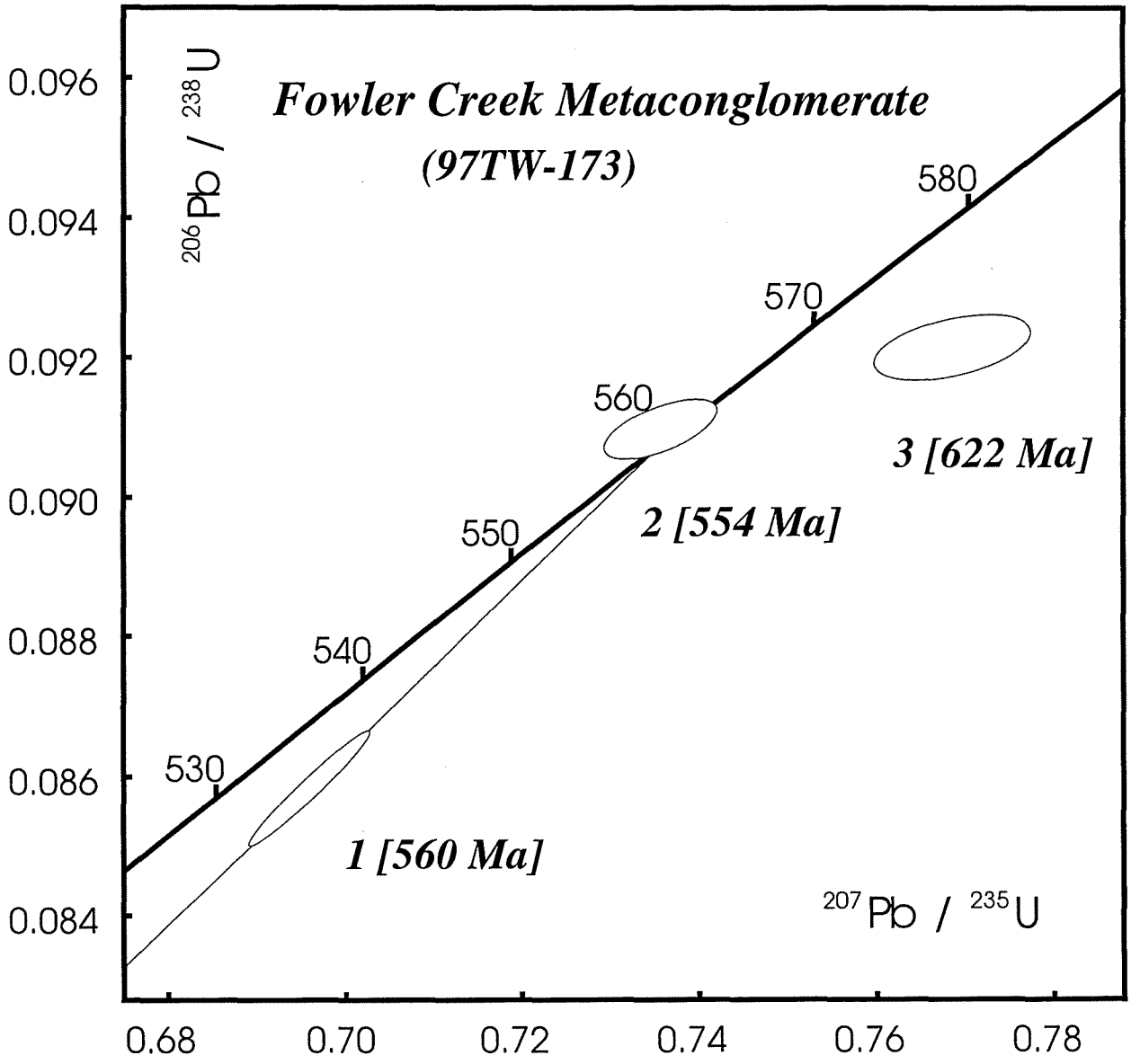
Fowler Creek Metaconglomerate
(97TW-173)
^{206}Pb / ^{238}U
^{207}Pb / ^{235}U
0.096
0.094
0.092
0.090
0.088
0.086
0.084
0.68
0.70
0.72
0.74
0.76
0.78
530
540
550
560
570
580
1 [560 Ma]
2 [554 Ma]
3 [622 Ma]

Figure 3

Spatial relations between a mid-crustal ductile shear zone, the sub-Eocene unconformity, and asymmetric Eocene normal faults, Vernon Map Area

Paul Glombick[1]

A high-grade paragneiss assemblage intruded by a variety of plutonic bodies is exposed east of Kalamalka Lake in the Vernon area (Figure 1). The assemblage includes biotite-sillimanite schist, calc-silicate, marble, calcareous quartzite, amphibolite, and is inferred to be Neoproterozoic to Early Paleozoic in age. A granodiorite pluton and a heterogeneous diorite/granodiorite body truncate the primary foliation in the paragneiss. A ductile west-dipping shear zone, more than 20 kilometres long and several hundred metres thick, postdates the emplacement of the plutons. It is characterized by a shallowly west-plunging stretching lineation, synkinematic sillimanite, and a hanging-wall-down sense of shear. Isolated erosional outliers of dacite inferred to be Eocene in age rest unconformably on the high-grade rocks. At one location, a dacite flow directly overlies a regolith developed in mylonitic biotite-sillimanite schist. At several other localities, dacite breccia contains randomly oriented foliated gneiss clasts. The Eocene dacite rests unconformably on basement gneiss and is not in the immediate hanging-wall of a crustal scale detachment zone as proposed in the Kelowna area. At one locality, on the western shore of Kalamalka Lake, an outcrop of high-grade gneiss is truncated by a steeply dipping west-side down brittle normal fault. The unconformable contact between the Eocene strata and the high-grade basement and the observed faulting suggest that the high-grade basement and low-grade cover are juxtaposed through steep normal faults with local displacement rather than a shallowly west-dipping detachment with regional displacement.

A sample of biotite-sillimanite-garnet schist from the mylonitic paragneiss succession on Kalamalka Lake was selected for P-T analysis. The sample contains the mineral assemblage quartz-plagioclase-potassium feldspar-biotite-sillimanite-garnet-magnetite-zircon. The garnet is characterized by concentric reverse zoning with extreme Mn-enrichment in the rim due to resorbtion. The plagioclase and biotite do not show zoning and only minor compositional variation. Pressures and temperatures were estimated using the GASP geobarometer and garnet-biotite Fe-Mg exchange thermometer. The garnet core composition combined with the matrix plagioclase and biotite yielded a pressure and temperature of 7.8 kbar and 790 °C. Calculations using the garnet rim composition resulted in a pressure and temperature of 4.3 kbar and 650 °C. Pressures and temperatures estimated using the matrix plagioclase and biotite and five equally spaced positions within the garnet from core to rim yielded a nearly isothermal decompression path.

These observations need to be reconciled with present tectonic models for the Okanagan Valley.

[1] Department of Earth and Atmospheric Sciences, University of Alberta, Edmonton, Alberta T6G 2E3
E-mail: glombick@gpu.srv.ualberta.ca

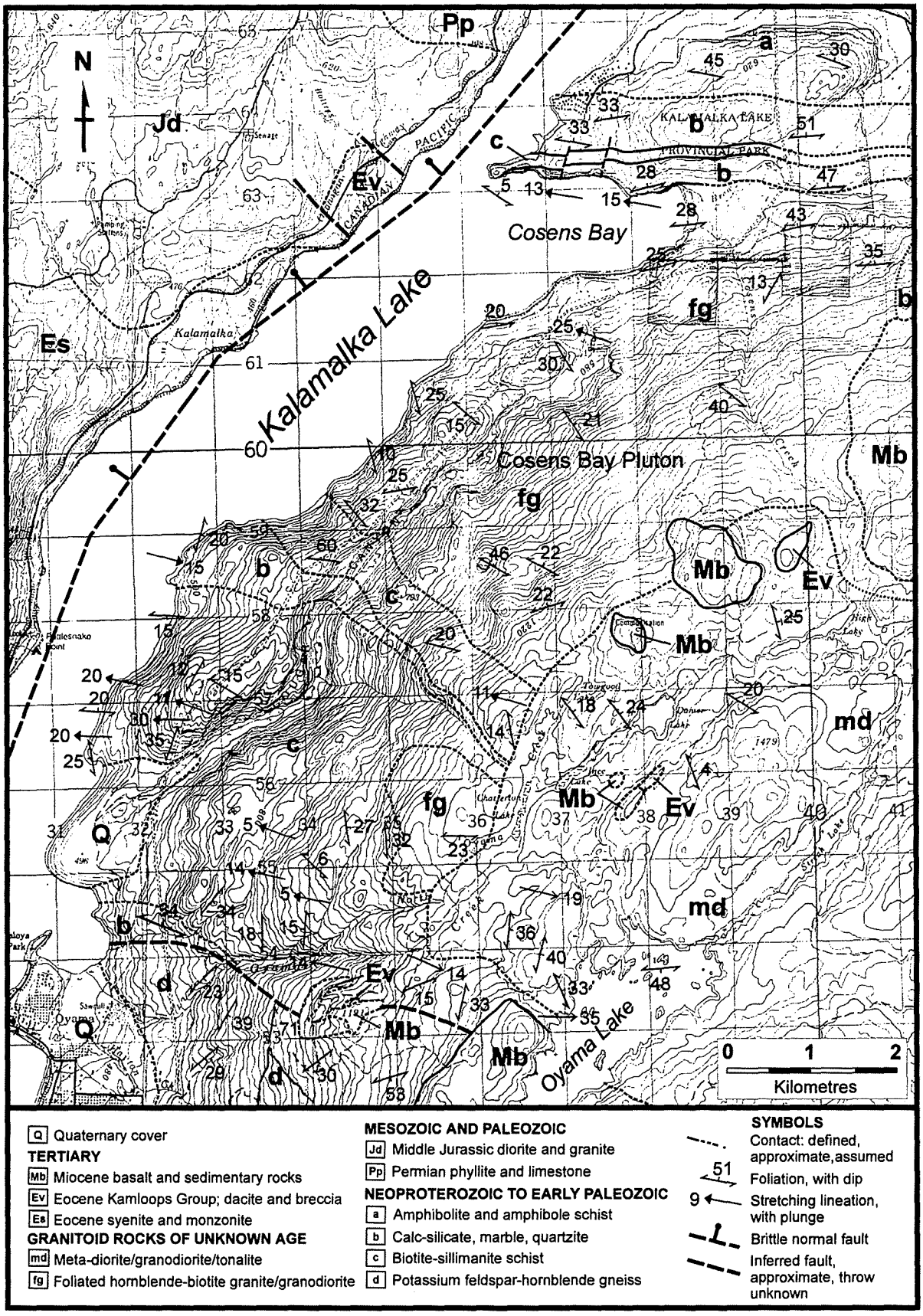

Figure 1. Geological map of the area east of Kalamalka Lake, central Okanagan Valley. Data are from this study and previous mapping for the Vernon Project. topographic base is NTS 82 L/3, 1:50 000 scale map.

Transition from Proterozoic to Triassic stratigraphy, Vernon map sheet: Is the Quesnellia terrane autochthonous or allochthonous on Silver Star Mountain?

Jennifer Unterschutz, Univeristy of Alberta,
Department of Earth and Atmospheric Sciences, email:jenunter@ualberta.ca

Vernon map area is located within the Omineca Belt of the Canadian Cordillera (Fig. 1). The boundary between ancestral North American Proterozoic to Paleozoic pericratonic sediments of the Kootenay terrane and Triassic arc volcanic and sedimentary strata of the Quesnellia terrane transects the area in an east-southeast direction. Terrane maps and regional structure cross-sections show this boundary as a crustal-scale thrust fault with more that 200 km of west-to-east overlap, juxtaposing a 30 km-thick block of crust on top of pericratonic North American crust (Varsek and Cook, 1994; Monger and Nokleberg, 1995; and references therein). The nature of this contact is not well described or defined. Recent work by Thompson and Daughtry (1996, 1997) suggests that the boundary separating Quesnel terrane rocks from pericratonic North American rocks is stratigraphic. More detailed work by Unterschutz *et al.* (1999) aimed at testing this hypothesis has revealed no evidence for a structural contact between the two successions, and suggests that Quesnel terrane rocks may be part of pericratonic North America in the Vernon area.

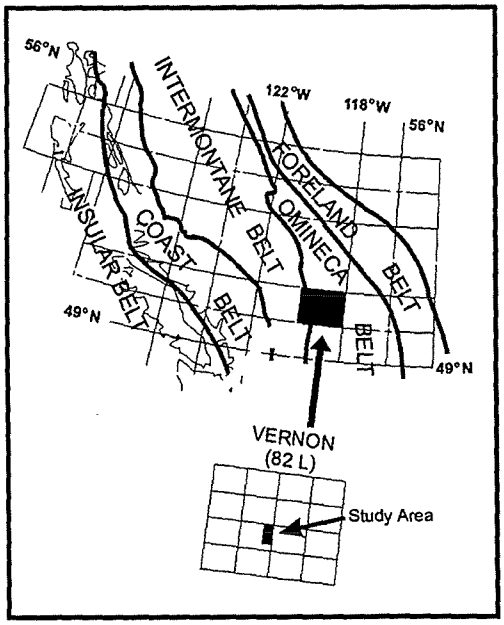

Figure 1: Terrane map of the Canadian Cordillera showing location of study area, Vernon map area (82 L).

Unit Descriptions

Rocks within the study area (Fig. 2) form part of the Shuswap metamorphic complex. Strata can be divided into three regional units.

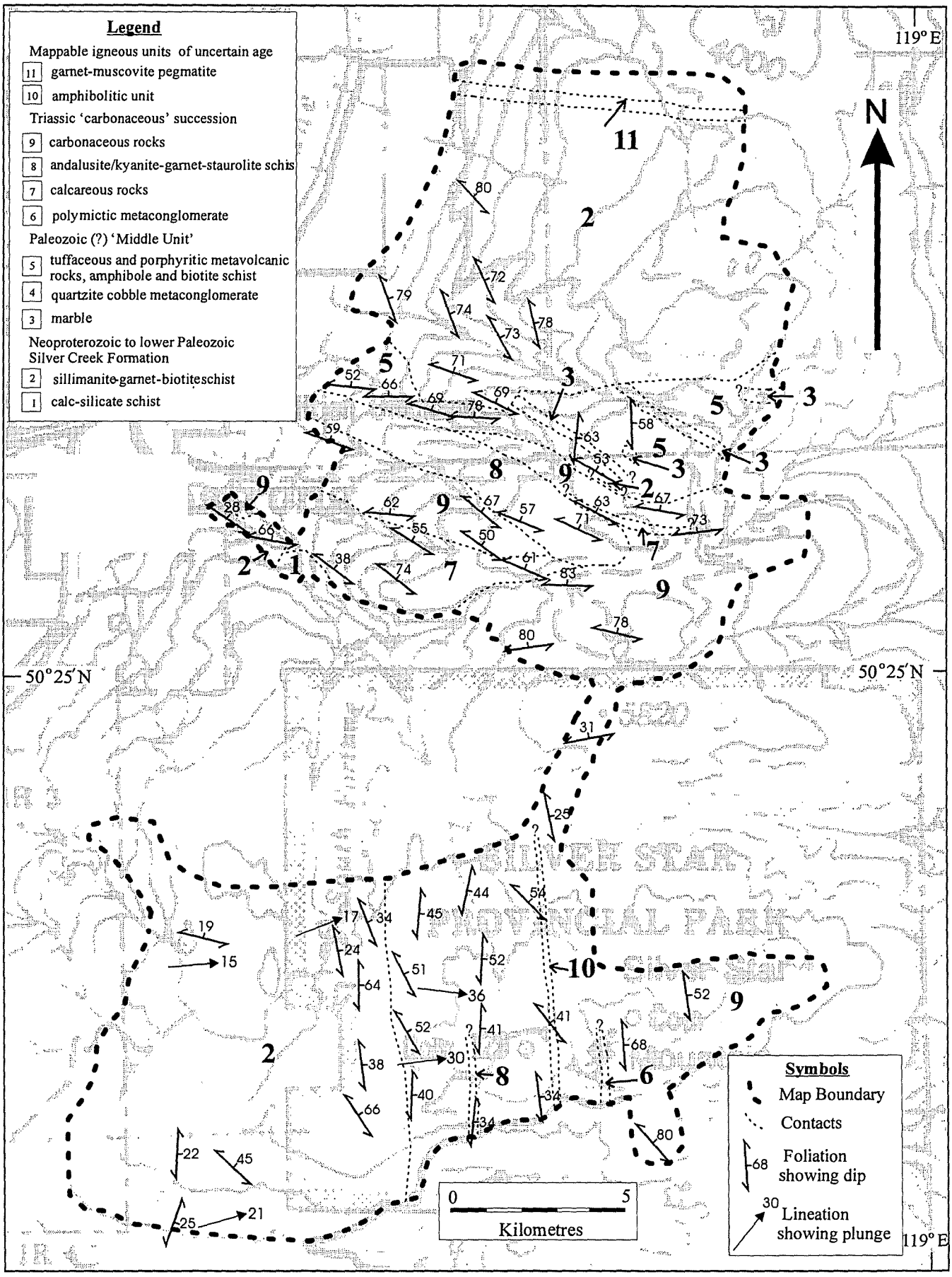

Figure 2: Geological map of study area including the Silver Star region east of Armstrong, British Columbia. Topographic base is 82 L, Vernon 1:250 000 scale NTS mapsheet.

Silver Creek Formation

The lowermost unit is the (inferred) Neoproterozoic to lower Paleozoic Silver Creek Formation (Read and Okulitch, 1977) dominated by biotite- and amphibole-rich quartzofeldspathic schist with local garnet, muscovite, and sillimanite. Less abundant rock types in this heterolithic unit include fine- to coarse-grained calc-silicate and calcareous schist, and silvery garnetiferous muscovite schist. Migmatite between 1 and 10 m in thickness is common.

Pegmatite is common within the Silver Creek Formation as 5cm to 3m thick tabular bodies that cut the regional schistosity. These massive bodies consist of quartz, feldspar, muscovite, and occasionally garnet. Two phases of pegmatite intrusions are visible based on crosscutting relationships. Fine- to medium-grained granite also intrudes the Silver Creek formation and may contain garnet, muscovite, biotite, hornblende, and tourmaline as accessory minerals. Some granite bodies are strongly foliated and lineated while others are massive recording pre- syn- and post-tectonic emplacement.

'Middle Unit'

The 'Middle Unit' overlies the Silver Creek Formation. The contact has yet to be discovered in outcrop, although its location can be determined to within metres in some areas. The 'Middle Unit' possibly correlates with the Lower Paleozoic Tsalkom Formation as suggested by Jones (1959) and Read and Okulitch (1977), with correlation extending to the Sicamous and Eagle Bay formations as suggested by Thompson and Daughtry (1998).

The 'Middle Unit' consists of tuffaceous, ignimbritic, and porphyritic metavolcanic strata of felsic to mafic compositions, stretched quartzite-cobble metaconglomerate, marble, amphibole-and biotite schist, and pelitic to semipelitic units interlayered at centimetre to metre scales. Static garnet porphyroblasts overprint schistosity in the matrix of the metaconglomerate.

Triassic Strata

The uppermost map unit is a carbon-rich succession, correlating with the Triassic Nicola Group and (or) Slocan Group, consisting largely of dark layers of metamudstone, metasiltstone, and metasandstone, with less abundant layers of metavolcanic rocks, marble, and metaconglomerate. Static porphyroblasts of garnet, staurolite, kyanite, muscovite, and biotite can be observed to have grown across foliation in various layers.

Structure

Map scale data and outcrop pattern suggests the presence of a map-scale northeast plunging synform defined by layering. In upper layers of the Triassic succession just outside the map area trace fossil borings suggest that the strata are overturned at that location. Foliation attitude does not appear to change across boundaries between units.

A stretching lineation plunging to the east, expressed as rodding of quartz and feldspar in foliated granite cutting Triassic and Silver Creek rocks, is visible locally in the southern part of the map area. A mineral lineation defined by secondary biotite growth parallel to the above mentioned stretching lineation is locally visible in this area as well, along foliation surfaces within the Triassic succession. A stretching lineation is also defined by the shape of quartzite clasts in the metaconglomerate of the 'middle unit'.

A zone of mylonite and cataclasite occurs in the southeast portion of the area within the Silver Creek Formation. Broken and winged feldspar porphyroblasts between 0.5 and 4 cm in diameter are common within a schistose to finely ground matrix. The thickness and extent of this zone have yet to be determined, but the zone occurs below the Silver Creek-Triassic contact and is at least several hundred metres thick. Sillimanite fibres form a crude linear fabric aligned with the direction of stretching.

Metamorphism

Metamorphic grade varies from sillimanite in the Silver Creek Formation to kyanite in Triassic rocks. Regional deformation and metamorphism imposed tectonic fabrics on the Silver Creek Formation, the 'middle unit', and the Triassic strata. The growth of static kyanite, staurolite, biotite, muscovite, and garnet in the Triassic strata, and of garnet in the 'middle unit', records a metamorphic event subsequent to latest folding.

In the Triassic succession metamorphic grade decreases upward from kyanite-grade near the basal contact with the older rocks, to chlorite grade approximately five kilometres upsection. In the lowest grade part, a fusilinid has been discovered within a carbonate clast from the metaconglomerate, and is predicted to be Permian in age.

P-T Analysis

P-T analysis of two samples of maximum-phase metamorphic assemblages was undertaken in hopes of resolving the question of whether the contact between the Triassic succession and ancestral North American rocks is structural or stratigraphic. Sample 98JU312b is a staurolite-muscovite-sillimanite-garnet-biotite schist, believed to represent

the majority of the Silver Creek Formation. PE 98-4 is a kyanite-chlorite-muscovite-garnet-biotite-staurolite schist from the metamorphosed Triassic succession.

In order to determine pressure and temperature estimates for these samples, the solid solution series of garnet, plagioclase, muscovite, and biotite were analyzed using an electron microprobe. Garnets from both samples were found to be zoned in a systematic concentric pattern to varying degrees in the concentration of minerals Fe, Mg, Mn, and Ca. Garnet was the only mineral to display significant and systematic zoning. The compositional profile strongly suggests growth zoning is the major cause of zoning in PE 98-4. The flat profile of 98JU312b suggests that peak metamorphic conditions were hot enough for diffusion to homogenize the garnet's composition.

Once the nature of the zoning within the garnets was determined, compositions of the mineral phases were processed and input into the program TWEEQU designed by Robert Berman of the Geological Survey of Canada. The results are displayed in figure 3. The significance of these results has yet to be determined, as the two samples are from locations separated by approximately ten kilometres. Further geothermobarometry is underway in order to help resolve questions surrounding these results.

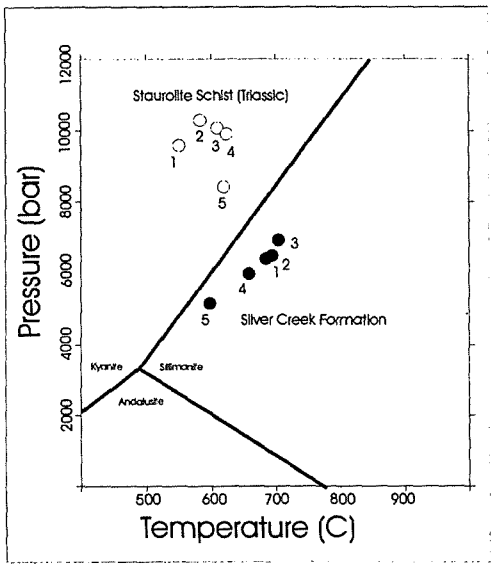

Figure 3: Pressure-temperature results using garnet compositions from core (1) to rim (5) of PE 98-4 (Triassic succession) and 98 JU 312b (Silver Creek Formation)

Discussion

Mapping in the Silver Star Region did not reveal evidence of tectonic contacts between any of the units. Contacts are sharp or mixed gradational, consisting of interlayering of rocks typical of upper and lower succession. A disconformity appears to separate the Triassic carbonaceous rocks from underlying units.

Future Work

The following research is planned to help resolve geologic uncertainties in the Vernon area:

1. By sampling clasts from metaconglomerates within the Triassic succession we hope to ascertain the provenance of the succession, and test the hypothesis that Nicola Group (Quesnel terrane) sedimentary rocks were derived from, and deposited onto, the outer margin of ancestral North America.
2. All units will be examined for dateable minerals in hopes of determining ages of intrusions, deformation, and metamorphism. Particular emphasis will be placed on determining the age of mylonite and cataclasite development and stretching lineation development.
3. Sr - Nd analyses of rocks are planned in order to clarify their juvenile vs. evolved nature.
4. Further geothermobarometry is planned.
5. Future fieldwork will focus on better defining the nature of the contact between the Triassic succession and underlying units, and between the 'middle unit' and Silver Creek Formation.

References

Jones, A. G., 1959, Vernon map-area, British Columbia; Geological Survey of Canada, Memoir 296, 186 p.

Monger, J.W.H. and Nokleberg, W.J., 1995, Evolution of the northern North American Cordillera: generation, fragmentation, displacement and accretion of successive North American plate-margin arcs; *in* Geology and Ore Deposits of the American Cordillera, A.E. Coyner and P.L.Fahey (ed.); Geological Society of Nevada Symposium Proceedings, Volume III, p. 1133-1152.

Read, P.B. and Okulitch, A.V., 1977, The Triassic unconformity of south-central British Columbia; Canadian Journal of Earth Science, v. 14, p. 606-638.

Thompson, R.I., and Daughtry, K.L., 1996, New stratigraphic and tectonic interpretations, North Okanagan Valley, British Columbia; *in* Current Research 1996-A; Geological Survey of Canada, p.132-141.

Thompson, R.I., and Daughtry, K.L., 1997, Anatomy of the Neoproterozoic-Paleozoic continental margin, Vernon map area, British Columbia; *in* Current Research 1997-A; Geological Survey of Canada, p 145-150.

Thompson, R.I., and Daughtry, K.L., 1998, Stratigraphic linkages across Vernon map area, British Columbia; *in* Current Research 1998-A; Geological Survey of Canada, p 145-150.

Unterschutz, J., Erdmer, P., Thompson, R.I., and Daughtry, K.L, 1999, Transition from Neoproterozoic to Triassic stratigraphy, Silver Star Mountain, Vernon map area, British Columbia; *in* Current Research 1999-A; Geological Survey of Canada, p 199-204.

Varsek, J.L., and Cook, F.A., 1994, Three-dimensional crustal structure of the Eastern Cordillera, southwestern Canada and northwestern United States; *in* Geological Society of America Bulletin, v. 106, p. 803-823.

Devonian plutonism and pre-Devonian tectonism, Vernon map area, British Columbia

N. Slemko, University of Alberta

INTRODUCTION

In the Shuswap Lake region, the greenschist-grade Silver Creek, Sicamous, and Eagle Bay formations are overlain by an amphibolite-grade succession termed the Queest Mountain assemblage. The contact between the low- and high-grade rocks is sharp, planar, and mylonitized, and has been interpreted as a contraction fault, the Queest Mountain fault. An intrusion of granite to granodiorite, dated at 364 Ma by U-Pb in zircon, cuts foliation and syn-tectonic minerals in the Queest Mountain assemblage and apparently crosses the fault without offset, demonstrating pre-Devonian deformation and metamorphism. Thin section petrography shows that the Queest Mountain assemblage has higher-grade peak metamorphic assemblages and preserves more episodes of deformation than the lower-grade rocks beneath it. Analysis of orientation data shows that the map can be divided into three domains with distinct structural histories. I discuss here the relationship between the low- and high-grade rocks, the relationship between Unit Dg and the country rock, the age of Unit Dg, and the structural and metamorphic history of the area.

STRATIGRAPHY

Queest Mountain Assemblage

The Queest Mountain assemblage rocks were previously mapped as part of the Eagle Bay Formation, however, on the basis of protolith composition and metamorphic grade, these rocks have affinity with older (Neoproterozoic) quartz- and feldspar-rich assemblages such as the Silver Creek Formation. The Queest Mountain assemblage includes garnet-biotite-muscovite- feldspar-quartz +/- staurolite schist and marble to calcsilicate with grossular, tremolite, diopside, and locally quartz and feldspar, recording amphibolite facies metamorphism. The contact between the Queest Mountain assemblage and the lower grade Eagle Bay Formation is sharp and planar. Thin section textures record two phases of deformation. The first episode produced a schistosity and the second a crenulation. Some samples also display a moderately developed gneissosity defined by the segregations of layers rich in quartz and feldspar from layers rich in biotite. Peak metamorphic mineral growth appears to have been syn-tectonic.

Silver Creek Formation

The miogeoclinal Neoproterozoic Silver Creek Formation is composed mainly of biotite-muscovite-quartz schist, with minor calcareous mica schist. The formation displays moderately- to well-developed foliation, consisting of mica schistosity and compositional layering. The Silver Creek Formation is characteristically intruded by numerous pegmatite and aplite sills and dykes. The Sicamous-Silver Creek contact along the Trans Canada Highway is interfingered and inferred to be depositional. The Silver Creek Formation is at greenschist grade within the map area.

Sicamous Formation

The Lower? Paleozoic Sicamous Formation underlies the Eagle Bay Formation. This eugeoclinal unit is a fine- to medium-grained metamorphosed carbonaceous limestone, with distinctive black and white layering in outcrop. It was likely deposited outboard of the North American miogeocline. The Sicamous Formation has one foliation, defined by elongate calcite grains and compositional layering or streaking of graphite-rich layers. The Sicamous-Eagle Bay contact is interfingered near Old Town Bay, and is inferred to be depositional.

Eagle Bay Formation

The Lower? Paleozoic Eagle Bay Formation contains fine-grained chlorite schist, chlorite-sericite schist, biotite-muscovite schist, and volcanic greenstone. One or more streaked white to black marble marker horizons, typically 100 to 200 m thick, are present. Variations in metamorphic grade from lower greenschist to upper greenschist facies occur within the Eagle Bay Formation, possibly the result of retrogression. The Eagle Bay Formation is characterized by a weakly to moderately developed foliation defined by mica schistosity and compositional layering.

Unit Dg

An intrusion 20 km across of biotite-hornblende, equigranular to megacrystic granite to granodiorite, correlated by Okulitch (1975) with the Devonian Mount Fowler Batholith, cuts the Eagle Bay Formation and the Queest Mountain assemblage. Some phases are chloritized and/or metamorphosed. Strain is heterogeneous, varying from none to strongly penetrative. Fabrics range from massive igneous texture in some of the undeformed and unmetamorphosed samples to schistosity or gneissosity in other phases. Schistosity and metamorphic layering within host rocks is clearly cut by the granodiorite.

STRUCTURAL GEOLOGY

Queest Mountain contraction Fault

The contact between the high-grade Queest Mountain assemblage and the lower-grade Eagle Bay Formation is sharp, planar, west-northwest striking, and moderately north-northeast dipping. It is interpreted as a southwest-verging contraction fault. Both the Eagle Bay Formation (footwall) and the Queest Mountain assemblage (hanging wall) near the contact contain fibrolitic sillimanite, suggesting that later metamorphism may be associated with the faulting. Quartz layers on either side of the contact show weak to strong mylonitization. The Queest Mountain fault would have resulted from northeast compression, and placed the higher-grade Queest Mountain assemblage over the lower-grade Eagle Bay Formation. The strike of the fault is parallel to the axial traces of large open folds on the east side of Shuswap Lake, and the fault and the folds may be kinematically related.

Foliations

Stereographic plots of foliation in mica-rich metasedimentary rocks show that the map area can be broken into three domains. The Silver Creek, Sicamous, and Eagle Bay formations have foliations that plot as a cluster, indicating that either these formations were not folded, or that the folding is at such a large scale that only one fold limb is present. The Queest Mountain assemblage has foliations that may outline two limbs of a mesoscopic fold, which agrees with a marker pattern that suggests a large open fold in the northeast corner of the map area. Foliation in Unit Dg, which ranges from weak to strongly penetrative, plots with some scatter, which may indicate syn-emplacement foliation development or the warping of post-emplacement foliation at the edges of the pluton, possibly by Mesozoic strain.

GEOCHRONOLOGY

Four zircon fractions from two samples of Unit Dg have been dated using U-Pb analysis. Fractions NS97-14-1 (colourless zircons) and NS97-14-2 (pink zircons) are from a felsic sample from south of the Queest Mountain fault, while fractions NS97-83-1 (yellow zircons) and NS97-83-2 (colourless zircons) are from a more mafic sample from north of the fault. All fractions are somewhat discordant, and plot on a discordia line with an upper intercept of ~364 Ma.

SUMMARY

1) The Queest Mountain assemblage and the Eagle Bay Formation have different protolith compositions and were metamorphosed to different grades, and were therefore deformed and metamorphosed separately before being juxtaposed by the Queest Mountain Fault.

2) The Queest Mountain Fault and foliation in the Queest Mountain assemblage are both cut by Unit Dg, and are therefore older than Late Devonian.

3) The Queest Mountain assemblage is at a higher metamorphic grade than Unit Dg. The metamorphic minerals in the Queest Mountain assemblage are syn-tectonic, and the foliation is cut by Unit Dg. Therefore, at least some of the metamorphism of the Queest Mountain assemblage pre-dates Unit Dg.

4) A second episode of deformation occurred, affecting all the rocks and producing a weak to moderate foliation in Unit Dg and a second foliation in some of the metasedimentary rocks. It may be of Mesozoic age.

ABSTRACTS of POSTER PRESENTATIONS

INVESTIGATION OF STRAIN RELATED TO DISPLACEMENT-TRANSFER AND ALONG-STRIKE STRUCTURAL VARIATION BY 3-D SEISMIC INTERPRETATION, PHYSICAL MODELLING AND COMPUTER-GRAPHICS VISUALIZATION

Evsen O. Aydemir* and John M. Dixon

Experimental Tectonics Laboratory, Dept. of Geological Sciences,
Queen's University, Kingston, Ontario K7L 3N6

A 3-d seismic volume from the Rocky Mountains Foothills of northeastern British Columbia was interpreted to image zones of displacement transfer between several foreland- and hinterland-vergent thrusts. Buckle folding and thrust faulting are both important shortening mechanisms in this geological setting. The centrifuge technique was used to produce scaled physical models with similar structural features displaying along-strike variation. Hinterland-vergent faults appear to play an important role in overall shortening, but the physical models suggest that back-thrusts may be restricted to the cores of folds.

A new method allows for detailed monitoring of strain within the mid-plane of a competent stratigraphic unit in a model. During model construction, galena markers are placed in a grid along coloured plasticine strips within the unit. The marker points are located in plan view by x-ray, and their location in the third dimension is derived from the locations of the coloured strips determined in serial sections of the model.

Computer representations of the marker grid plane before and after deformation are constructed using GOCAD 3-d visualization software. The shapes of corresponding planar elements in the two planes are compared to calculate strain ellipse axes. This yields values of strain intensity for each deformed planar element. GOCAD is then used to generate strain-intensity contours on the plane.

Strain distribution was analyzed along faulted folds similar to those in the natural prototype. Distributed strain in the marker-grid plane is concentrated in different locations as fold geometry changes along strike and displacements on individual faults vary. The fold hinge is transported toward the foreland at some positions by a tightening of the fold as its forelimb rotates into an overturned orientation; at others, displacement is transferred to increased offset on foreland-vergent faults that cut the forelimb. Distributed strain is concentrated in the forelimb where it has been rotated to near vertical. The presence of a back-thrust cutting the back-limb may locally lower strain intensity in its footwall as the fault takes up a higher proportion of total shortening.

Strain intensity is presumably linked to fracture intensity, which is an important issue in choosing oil/gas well locations. While the in-plane strain analysis presented here cannot provide direct information on fracture orientations, the geometry of structures and the known positions of high strain concentrations may shed light on where different fracture patterns are more likely to develop along a fold that may trap hydrocarbons.

Acknowledgements: This work was conducted as part of the Foothills Research Project. Financial support from the FRP's Oil Industry sponsors and NSERC is gratefully acknowledged.

*current address: Conoco Canada Ltd., Calgary, Alberta

Deformation features, and rheological behaviour of the Slave Upper Mantle

Michael J. Begbie and Lori A. Kennedy
Earth and Ocean Sciences, The University of British Columbia,
6339 Stores Rd, Vancouver, B.C., V6T 1Z4

The microstructures and fabrics (crystallographic preferred orientations, or CPO's) of mantle xenoliths sampled by the Jericho kimberlite are currently being analysed with the aim of: (1) inferring the rheological behaviour of the upper mantle along a depth profile of the Northern Central Slave, and (2) testing the hypothesis that foliated eclogites are responsible for the continuous, shallowly dipping reflector imaged in the upper mantle beneath SNORCLE 1 Corridor (Bostock, 1997; Cook, 1997). Samples for this study are from the same suite as that investigated by Kopylova et al (1998;1999), whose geothermobarometric studies provided a detailed mantle stratigraphy of the Northern Central Slave Province. Our objective is to correlate the stratigraphic column as determined by Kopylova et al (1998,1999) and chemical composition of the upper mantle (Kopylova and Russell, *this volume*), with deformation microstructures, fabrics, inferred mechanisms of deformation and ultimately the rheological behaviour of the upper mantle. Our poster will present the results of fabric analyses of peridotites and eclogites and microstructural observations (optical and TEM) in conjunction with the petrological and geochemical data of Kopylova and Russell (this volume)

Seismic and teleseismic images of the Slave lithosphere (Cook, et al. 1997; Bostock, 1998) suggest that the Slave mantle is heterogeneous and locally, strongly anisotropic; an observation supported by petrological studies (Kopylova et al., 1999). The strongly anisotropic layers documented by Bostock (1997) may represent foliated eclogite layers within the Slave mantle, which is compatible with petrographic observations. Since anisotropic seismic reflectors may result from (1) compositional layering of garnet and clinopyroxe, and/or (2) a CPO of clinopyroxenes, we will measure cpx fabrics from foliated eclogites to evaluate if a CPO may responsible for the seismic anisotropy. Our CPO data will be compared to Vp/Vs measurements of foliated eclogite samples (to be measured by N. Christensen, U of Wisconsin at Madison). This exercise will be particularly useful if a weak to non-existent CPO is found for the eclogites.

Preliminary Results:

Peridotites

Peridotite samples are diverse in textural habit, including: protogranular(undeformed), porphyroclastic non-fluidal and, less commonly, porphyroclastic fluidal (mylonitic; classification of Hart, 1977). Protogranular peridotites are characterized by a lack of foliation and lineation, coarse grains, curved grain boundaries, and rare kink bands. Non-fluidal porphyroclastic are likely the deformed equivalents of protogranular peridotite and are typified by an alignment of elongate

olivine, together with the formation of dynamically recrystallized grains. Mylonitic or fluidal samples, have a well-developed foliation, and show evidence for grain size reduction (to ~10 _m) by dynamic recrystallization. Both the porphyroclastic peridotites and mylonitic peridotites appear to have well-developed fabrics, although more data is necessary to substantiate this statements(Fig. 1a &b). CPO's in general, suggest the activity of dislocation creep during deformation. Estimates of formation P-T conditions indicate that porphyroclastic peridotites formed deeper than undeformed, coarse peridotite, indicating a high stress and/or strain rate for the formation of the porphyroclastic peridotites, and a very low stress and or strain rate for the formation of protogranular peridotites.

Eclogites

Eclogite xenoliths are abundant and can be massive or foliated; most eclogite samples are foliated and the foliation is defined by mineralogical banding (interlayering garnet and clinopyroxene) or an apparent preferred mineral orientation. Clinopyroxene in foliated eclogites ranges from basically undeformed to flattened and elongated, with the development of dynamically recrystallized grains. Garnets also range from unreformed too highly flattened. As discussed by Ji et al. (1998), highly strained eclogites are the exception and most previous microstructural analyses have been performed on relatively undeformed eclogites. Our poster will present results of fabric analyses for clinopyroxene and TEM studies of deformed garnet to evaluate the role of CPO of eclogites in contributing to seismic anisotropy.

References

Bostock, M.G. 1997. Anisotropic upper mantle stratigraphy and architecture of the Slave craton. Nature, 390, 392-395.

Cook, F.A., van der Veldon, A.J., Hall, K.W., and Roberts, B.R. 1997. Transect and Cordilleran Tectonics Workshop Meeting, 58-62 (Lithoprobe Report No. 56).

Harte, B., 1977. Rock nomenclature with particular relations to deformation and recrystallization textures in olivine-bearing zenoliths. J. Geol. 85, 279-288.

Ji, S., Wang, Z., and Saruwatari, K. 1998. Plasticity of eclogite: Implications for rheology and seismic reflectivity of the subducting slab. In: Cook, F and erderm p (compilers), 1988, Slave-Northern Cordillera Lithospheric Evolution (SNORCLE) Transect and Cordilleran Tectonics Workshop Meeting (March 6-8), Simon Frazer University, Lithoprobe Report No. 64, 331p.

Kopylova, M.G., Russell, J.K. and Cookenboo, H. 1999. Petrology of peridotite and pyroxenite xenoliths from the Jericho kimberlite: Implications for the thermal state of the mantle beneath theSlave Craton, northern Canada. J. of Petrol. 40, 1, 173-208.

Kopylova, M.G., Russell, J.K. and Cookenboo, H. 1998. Upper-mantle stratigraphy of the Slave craton, Canada: Insights into a new kimberlite province. Geology, 26, 315-318.

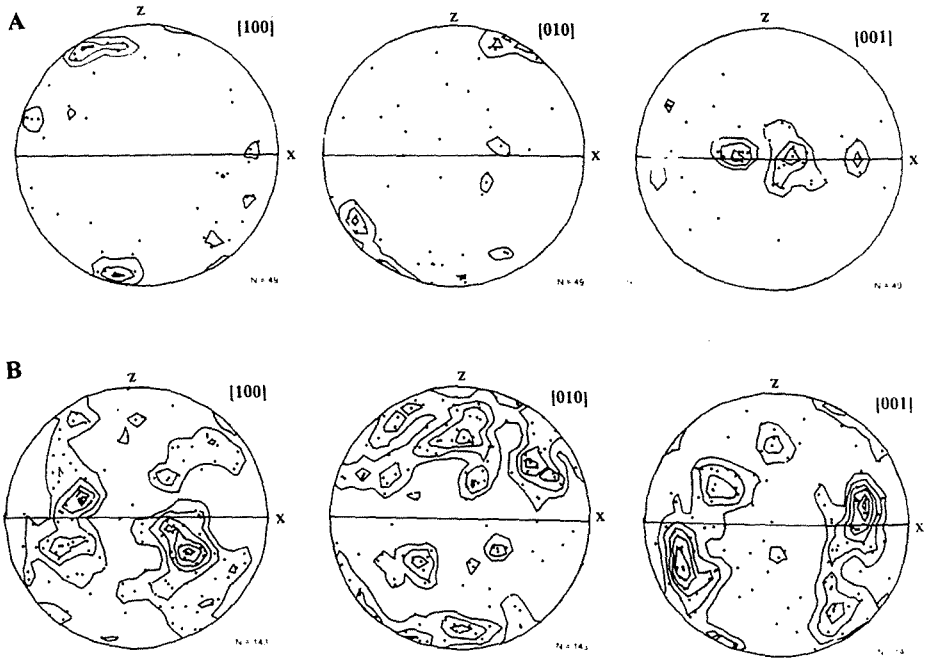

Figure 1: Olivine fabric diagrams for porphyroclastic peridotites. (a) mylonitic peridotite. Horizontal line represents the foliation. (b) less deformed porphyroclastic peridotite.

Meso- and Paleoarchean Basement Rocks of the Slave Province: Distribution in Space and Time

Wouter Bleeker[1], John Ketchum[2], Bill Davis[1], and Richard Stern[1]

[1]*Geological Survey of Canada, 601 Booth Street, Ottawa, ON, K1A 0E8 (wbleeker@nrcan.gc.ca)*
[2]*Memorial University of Newfoundland, St. John's, NF, A1B 3X5*

The Slave craton of the Canadian Shield hosts the oldest terrestrial rocks yet identified (Bowring et al., 1989; Stern and Bleeker, 1998). Furthermore, no less than one third of the craton appears to be underlain by Paleo- and Mesoarchean crust. Arguably, the Slave is also one of the best exposed Archean cratons in the world, thus providing unique opportunities to study pre-2.7 Ga crustal evolution.

To gain a better understanding of Meso- and Paleoarchean rocks underlying parts of the Slave Province, all presently available U-Pb ages, other relevant age data, and some preliminary data sets have been compiled. These ages span a record from 4041±12 Ma, the oldest identified zircon in an Acasta gneiss (R. Stern and W. Bleeker, unpublished data), to 2734±2 Ma, the age of a mafic dyke swarm heralding the break-up of Mesoarchean crust in the southern Slave Province (Bleeker et al., 1999b). The age data, organized by age, location, and data type provide a fascinating record of episodic crustal growth and (or) crustal reworking. A minimum of ten "events" (*I* to *X*) can be recognized, with individual events typically lasting ca. 40-60 m.y. and being spaced at ca. 100 m.y. intervals. For example, some characteristic ages are: 4025±12 Ma, ca. 3600 Ma, ca. 3350 Ma, 3250 Ma, 3155 Ma, 2950 Ma, 2880 Ma, 2835 Ma, and 2734 Ma.

The spatial distribution of many of these age groupings appear to outline overlapping patterns, except for those of a "ca. 2950 Ma tonalite event" and a "ca. 2880 Ma granite event". To date, the former event appears to be restricted to the Central Slave Basement Complex south of Point Lake (Bleeker et al., 1999a), whereas the latter has been recorded from the Acasta Gneiss Complex (R. Stern and W. Bleeker, unpublised data) to the Eokuk Uplift on the Coronation Gulf (e.g., Emon et al., 1999). A mutually exclusive age distribution may point at the presence of a cryptic domain or terrane boundary in Mesoarchean crust of the Slave craton. In this respect it is interesting to note that all basement occurrences from Point Lake to the south are associated with the occurrence of a thin but diagnostic cover sequence—the ca. 2.8 Ga Central Slave Cover Group (Bleeker et al., 1999a; unpublished field data, 1998). This cover sequence has not (yet?) been found overlying the northwestern part of the basement. However, given the relatively small number of samples at each locality, it is too early to tell whether these apparent differences are real or merely a consequence of poor statistics. With future addition of relevant age data, the ten or so "events" may become more distinct or, alternatively, may blur into a single, more complex history.

References

Bleeker, W., Ketchum, J.W.F., Jackson, V.A., and Villeneuve, M.E., 1999a. The Central Slave Basement Complex, Part I: Its structural topology and autochthonous cover sequence. Canadian Journal of Earth Sciences, *in press*.

Bleeker, W., Ketchum, J.W.F., and Davis, W.J., 1999b. The Central Slave Basement Complex, Part II: High-strain zones along the basement/cover contact. Canadian Journal of Earth Sciences, *in press*.

Bowring, S.A., Williams, I.S., and Compston, W. 1989. 3.96 GA gneisses from the Slave province, Northwest Territories, Canada. Geology, **17**: 971-975.

Emon, K.A., Jackson, V.A., and Dunning, G.R., this volume. Geology and U-Pb geochronology of rocks of the Eokuk Uplift: a pre-2.8 Ga basement terrane in the northwestern Slave Structural Province, Northwest Territories, Canada. Canadian Journal of Earth Sciences, *in press*.

Stern, R.A., and Bleeker, W. 1998. Age of the world's oldest rocks refined using Canada's SHRIMP: the Acasta Gneiss Complex, Northwest Territories, Canada. Geoscience Canada, **25**: 27-33.

PROGRESS REPORT ON U-Pb GEOCHRONOLOGY STUDIES - TESLIN ZONE AND WESTERN CASSIAR TERRANE, YUKON; TIMING CONSTRAINTS ON DEFORMATION AND THERMAL HISTORY

S. D. Carr[1], M. de Keijzer[2] and C. Gallagher[1]

[1]Ottawa-Carleton Geoscience Centre and Department of Earth Sciences, Carleton University, Ottawa, ON, Canada K1S 5B6; [2]Department of Geology, University of New Brunswick, Fredericton, N.B. E3B 5A3

On the basis of mapping of a 50 x 20 km area in the Big Salmon Range in the Teslin zone and adjacent rocks to the east (Brown et al. 1995, 1998; de Keijzer and Williams, 1996, 1997a, b, 1998; de Keijzer et al. 1999; Harvey et al. 1996, 1997a, b; Gallagher et al. 1998, 1999), the Teslin zone is reinterpreted as a zone of ductile thrusting, and includes thrust sheets of North American affinity and allochthonous rocks that have been complexly folded and displaced northeastward. This deformation resulted in a gently dipping, regionally pervasive, synmetamorphic transposition foliation (S_T). S_T was rotated into a steep orientation on the short limbs of km-scale post-transposition folds such as the Grizzly synform (de Keijzer and Williams 1997a; de Keijzer et al. 1999) and the Late Cretaceous Two Cub Antiform (Gallagher et al. 1998, this volume). The steep limb of these regional-scale structures explains the steep attitude of most Teslin zone rocks. Late Cretaceous structures include ductile to brittle-ductile shear bands and boudins indicating predominantly NE-SW-directed extension in the Cassiar terrane (de Keijzer and Williams, this volume), local ductile dextral strike slip faults (Gallagher et al., this volume), as well as ductile-brittle strike-slip,oblique-slip and normal offsets on the N-S D'Abbadie fault zone.

U-Pb studies are designed to determine the timing of metamorphic events, ductile thrusting and transposition folding, and post-transposition folding in structural domains of the Teslin zone and adjacent Cassiar rocks to the east. The domains are: the western and eastern Teslin zone, which broadly correspond to the Anvil and Nisutlin assemblages, respectively, the Cassiar terrane, and the ultramafic-bearing klippen (Figure 1; see also de Keijzer and Williams 1997a; de Keijzer et al. 1999; Brown et al. 1998). We are testing the model that rocks in the Teslin zone and Cassiar terrane share a common transposition folding history.

Zircon- and monazite-bearing samples have been dated. Crystallization ages of granitoids in the Teslin zone, ultramafic-bearing klippe and Cassiar terrane are Late Devonian - Early Mississippian (358 Ma), Early Permian (267 Ma) and Early Mississippian (331 Ma), respectively. Late Cretaceous granitoids place constraints on late folding and strike slip faulting (Gallagher et al., this volume). Titanites from samples representative of each structural domain are being processed to place constraints on cooling history. Similar high temperature cooling ages will support the interpretation that all domains have undergone a similar deformation history; different ages may indicate, multiple metamorphic events in one or more of the domains (such as is the case in the Cassiar terrane; de Keijzer and Williams, this volume) and/or post-S_T displacement on domain bounding structures.

East of the d'Abbadie fault, the 110 Ma d'Abbadie pluton and a 110 Ma late planar andesite dyke postdated regionally penetrative transposition fabrics in the

surrounding amphibolite-facies metasedimentary rocks of the Cassiar terrane. Boudinaged andalusite in pelitic schist, interpreted as having grown in the contact aureole together with cordierite, calcic plagioclase, and rare fibrolitic sillimanite, indicates that intrusion of the d'Abbadie pluton may be synchronous with the later stages of NE-SW extension in the Cassiar terrane (de Keijzer and Williams 1997b). A detailed description of the regional mid-Cretaceous low pressure - high temperature metamorphism, characterized primarily by calcic metasomatism away from the contact aureole is provided by de Keijzer and Williams (this volume). This M_{II} metamorphic event overprinted earlier prograde amphibolite facies M_I regional metamorphism, which is related to the thrusting of the Yukon-Tanana Nisutlin and Anvil rocks onto the Cassiar terrane. De Keijzer and Williams (this volume) also briefly discuss the preservation of the various cooling ages (pre-Late Jurassic and mid-Cretaceous) recorded in different parts of the region.

REFERENCES

Brown, R. L., Carr, S. D., Harvey, J. L., Williams, P. F and de Keijzer, M. 1995. Structure and tectonic significance of the Teslin suture zone. LITHOPROBE Report No. 44, 1995 SNORCLE Transect Meeting, Calgary, AB, 56-62.

Brown, R. L., De Keijzer, M., Carr, S. D. , Williams, P. F. and Gallagher, C. S. 1998. Structure of the Teslin Zone, Yukon, Canada. LITHOPROBE Report. 1998 SNORCLE and Cordilleran Tectonics Workshop, Vancouver, B. C., 152-157.

de Keijzer, M. and Williams, P. F. 1996. Structural analysis in the Teslin Tectonic zone, south-central Yukon. LITHOPROBE Report No. 50, 1996 SNORCLE and Cordilleran Tectonics Workshop, Calgary, AB, 45-53.

de Keijzer, M and Williams, P .F. 1997a. A new view on the structural framework of the Teslin Zone, south-central Yukon. LITHOPROBE Report No. 56, 1997 SNORCLE and Cordilleran Tectonics Workshop, Calgary, AB., 96-102.

de Keijzer, M. and Williams, P. F. 1997b. Fabric development in the Cassiar terrane, Yukon Territory: A response to terrane accretion or subsequent extension? GAC-MAC Abstracts, 22: A36.

de Keijzer, M, Williams, P .F. and Brown, R. L. 1999. Kilometre-scale folding in the Teslin zone, northern Canadian Cordillera, and its tectonic implications for the accretion of the Yukon-Tanana terrane to North America. Canadian Journal of Earth Sciences, In press.

de Keijzer, M., and Williams, P .F. 1999 (**this volume**). Cretaceous extension and regional calcic metasomatism in the Cassiar terrane south of the d'Abbadie pluton, south-central Yukon. LITHOPROBE REPORT. 1999 SNORCLE and Cordilleran Tectonics Workshop, Calgary, AB.

Gallagher, C., Brown, R. L. and Carr, S. D. 1998. Geometry of the Dycer Creek map area, Teslin zone, Yukon. LITHOPROBE REPORT. 1998 SNORCLE and Cordilleran Tectonics Workshop, Vancouver, B. C., 139-151.

Gallagher, C., Carr, S. D. and Brown, R. L. 1999 (**this volume**). U-Pb geochronologic evidence of Early Cretaceous Large-Scale Folding in the Dycer Creek area, Pelly Mountains, Yukon. LITHOPROBE REPORT. 1999 SNORCLE and Cordilleran Tectonics Workshop, Calgary, AB.

Harvey, J. L., Brown, R. L., and Carr, S. D. 1996. Progress in structural mapping in the Teslin Suture Zone, Big Salmon Range, Central Yukon Territory. LITHOPROBE report No. 50, 1996 SNORCLE and Cordilleran Tectonics Workshop, Calgary, AB, 33-41.

Harvey, J. L., Carr, S. D., Brown, R. L., and Gallagher, C. 1997a. Deformation history and geochronology of plutonic rocks near the D'Abbadie fault, Big Salmon Range, Yukon. LITHOPROBE report No. 56. 1997 SNORCLE and Cordilleran Tectonics Workshop, 103-114.

Harvey, J. L., Carr, S. D., and Brown, R. L. 1997b. Ages of deformed plutonic rocks along the D'Abbadie fault, Teslin zone, Big Salmon Range, Yukon: Implications for timing of strike-slip deformation. GAC-MAC Abstracts: 22: A23.

Preliminary stratigraphy and structure of Yukon-Tanana terrane, Little Kalzas Lake area, central Yukon (NTS 105L/13)

Maurice Colpron
Yukon Geology Program, Box 2703 (F-3), Whitehorse, Yukon Y1A 2C6

INTRODUCTION

A 1:50,000-scale bedrock mapping program of the Little Kalzas Lake area (105L/13) was initiated during the summer of 1998 (Colpron, 1998, 1999). The Little Kalzas Lake area occupies the northwest corner of the Glenlyon map-area, which was previously mapped at the scale of 1:253,440 by Campbell (1967). Campbell's work identified a 30-50 km-wide, NW-trending belt of metasedimentary, metavolcanic and metaplutonic rocks SW of Tintina Trench in the centre of Glenlyon map-area which has been correlated with Yukon-Tanana terrane (Fig. 1; Tempelman-Kluit, 1979; Coney et al., 1980; Wheeler et al., 1991). Restoration of 450 km of dextral displacement along the Tintina Fault juxtaposes this belt of rocks with Yukon-Tanana terrane rocks in the Finlayson Lake area in which numerous volcanic-hosted massive sulphide deposits and occurrences have been found (e.g. Kudz Ze Kayah, Wolverine, Fig. 1; Hunt, 1997). These new discoveries have increased the need for a better understanding of the stratigraphy and tectonic evolution of the terrane as a whole but in particular of nearby areas about which little is known, such as the Little Kalzas Lake area.

SUMMARY OF STRATIGRAPHIC RELATIONS

Yukon-Tanana terrane in the Little Kalzas Lake area comprises a lower quartzite package (Unit 1) and an upper metavolcanic package (Units 2 and 4) containing a conspicuous marble marker (Unit 3; Fig. 2). Up to nine mappable units were identified in alpine exposures along ridges north of Macmillan River (Figs. 2 and 3). However, only a four-fold subdivision of the layered rocks could be traced into the heavily forested areas which cover much of the Little Kalzas Lake map area.

Metasedimentary and metavolcanic rocks in the area generally are pervasively deformed (strongly foliated and lineated) and metamorphosed to greenschist facies. Although pristine primary textures are preserved sporadically, the facing direction of the stratigraphic sequence could not be determined with certainty. Therefore, stratigraphic units are described below according to their structural position (assuming an upright stratigraphic sequence prior to dominant regional deformation). This stratigraphic sequence is provisional and most likely will be revised after further field, biostratigraphic and geochronologic studies are completed.

UNIT 1 (QUARTZITE UNIT)

The lowest stratigraphic unit in the Little Kalzas Lake area consists predominantly of massive to well-bedded quartzite (Figs. 2 and 3). The quartzite commonly displays white to medium grey wispy banding. It is progressively more micaceous up-section, where it is commonly intercalated with dark grey phyllite. The quartzite unit includes a middle metavolcaniclastic unit (Unit 1v) around Dillweed Plateau. The metavolcaniclastic unit consists primarily of light green chloritic phyllite intercalated with light green quartzite and feldspathic grit. South of Pelmac Ridge, the quartzite is inferred to pass laterally into coarse-grained dolomitic grit and beige weathering, medium to dark grey quartz-muscovite-dolomite schist (Unit 1gr; Fig. 3).

UNIT 2 (LOWER METAVOLCANIC UNIT)

Unit 1 is transitionally overlain by a lithologic assemblage which is dominated by rocks of volcanic parentage (Unit 2). North of Macmillan River, the base of Unit 2 corresponds to a sequence of intercalated tan weathering, 'waxy', quartz-muscovite-feldspar (±chlorite) schist (felsic metavolcanic rock), carbonaceous phyllite and minor gritty quartzite (Unit 2fv).

The most prominent rock type in Unit 2, north of Macmillan River, is massive to foliated, dark green to black, fine-grained, plagioclase-epidote-hornblende-biotite-calcite meta-andesite (Unit 2iv, Fig. 2). A white to dark grey cherty quartzite and minor dark grey phyllite unit (Unit 2q) occurs in the middle of the meta-andesite. Above the quartzite, the meta-andesite is intercalated with dark grey phyllite and passes eastward into a tan weathering, light grey, calcareous muscovite-chlorite phyllite and minor felsic, quartz-muscovite-feldspar schist (Fig. 2).

Near Macmillan River, and on Pelmac Ridge to the south, Unit 2 is dominated by light to medium green, muscovite-quartz-chlorite phyllite and micaceous quartzite (metavolcaniclastic rocks) with minor intermediate to mafic metavolcanic rocks and felsic quartz-muscovite-feldspar schist. The top of Unit 2 locally is marked

by a foliated white to medium grey quartzite intercalated with 1-5 mm thick beds of dark grey carbonaceous phyllite.

UNIT 3 (MARBLE)

A conspicuous laterally persistent marble divides metavolcanic rocks of Unit 2 from those of Unit 4. The marble is typically light grey to white and locally weathers to a light buff colour. Near Macmillan River, the marble occurs in large masses in the hinge zone of folds. It commonly contains well-preserved crinoids and is locally cherty. North of Macmillan River, the marble is much thinner and extensively recrystallized. It is locally phyllitic and closely associated with meta-andesite and carbonaceous phyllite.

UNIT 4 (UPPER METAVOLCANIC UNIT)

Unit 4 is generally poorly exposed and comprises a mixture of metasedimentary and metavolcanic rocks. North of Macmillan River, Unit 4 includes carbonaceous phyllite and quartzite, meta-andesite and felsic metavolcanic rocks. On Pelmac Ridge, Unit 4 is dominated by light green quartz-muscovite-chlorite phyllite and light green quartzite and grit (metavolcaniclastic rocks) intercalated with minor intermediate to mafic metavolcanic rocks. The highest stratigraphic unit consists of white, green and pink dolomitic quartzite intercalated with 0.5-5 cm-thick brown weathering dolomitic beds (Unit 4q; Fig. 3).

INTRUSIVE ROCKS

The layered metamorphic rocks are intruded by at least three suites of intrusive rocks. The oldest suite is penetratively deformed with the country rocks; the two younger suites postdate deformation.

In the northeastern part of the map area, along the southwestern side of Tintina Trench, the multi-phase Little Kalzas orthogneiss complex, of uncertain age (possibly Mississippian ?), comprises an older granodioritic gneiss (Mgd) which is intruded by a granitic gneiss (Mg). Both phases contain abundant xenoliths of country rock.

The post-kinematic Cornolio pluton intrudes the layered metamorphic rocks in the north-central part of the map area (Jqm; Fig. 3). It is an unfoliated to weakly foliated medium-grained hornblende ± biotite quartz monzonite. The age of the Cornolio pluton is uncertain. The southwest corner of the map area is underlain by the Tatlmain batholith (Tempelman-Kluit, 1984, JTd, Fig. 3). It is composed of medium to coarse-grained, equigranular hornblende ± biotite quartz diorite. A Jurassic age is assigned to the Tatlmain batholith based on similarity in composition with the Tatchun batholith in the southern part of Glenlyon map area (Campbell, 1967) which yielded Middle Jurassic K-Ar dates from hornblende and biotite (Tempelman-Kluit, 1984).

The youngest intrusive rocks in the Little Kalzas Lake area are small plugs of quartz-feldspar porphyry (Tp; Fig. 3).

STRUCTURE

The dominant tectonic fabric in the area is a pervasive transposition foliation and mineral lineation. Although primary layering has generally been transposed parallel to foliation, primary textures are preserved in local low-strain domains. The intense deformation recorded by the dominant structures has not disrupted the stratigraphic sequence at the scale of the map area (Fig. 3), in contrast to regional models previously suggested for Yukon-Tanana terrane (e.g., Tempelman-Kluit, 1979).

The transposition foliation is axial-planar to tight, gently WNW- or SSE-plunging, SSW-verging folds (Fig. 4). The foliation and axial surfaces progressively change toward the northeast from NNE-dipping to upright to SSW-dipping (Fig. 4). A mineral lineation, defined by orientation of elongate minerals (primarily micas and quartz) on planes of the dominant foliation, is generally parallel to fold axes and bedding/foliation intersections. The dominant structures are deformed by a younger crenulation cleavage which strikes to the southeast and dips moderately to the northeast.

The dominant SSW vergence of the major structures in the Little Kalzas Lake area differs from recent structural interpretations proposed for the Teslin zone, approximately 150 km to the southeast, where major structures have a predominant NE vergence (e.g., Gallagher et al., 1998; de Keijzer et al., *in press*). However, the style of deformation recorded in the Little Kalzas Lake area is consistent with that of the Big Salmon Complex farther south, near the 60th parallel, where major folds are SW- and WSW-verging (Mihalynuk et al., 1998). At this stage, our limited knowledge of the regional geology of Yukon-Tanana terrane precludes a proper resolution of the apparent variability in the style and orientation of deformational features reported from various locations along strike.

DISCUSSION

Although with important differences, the stratigraphy and structural style of the rocks of Little Kalzas Lake area are similar to those of Yukon-Tanana terrane across the Tintina Trench. Precise correlation between

the rocks of Little Kalzas Lake area and elsewhere in Yukon-Tanana terrane cannot be attempted until the necessary geochemical, biostratigraphic, and geochronological studies have been done. However, some general statements can be made on the basis of field relationships:

- The occurrence of voluminous clean quartzite is perhaps one of the most distinguishing character of the stratigraphic sequence mapped in the Little Kalzas Lake area (Figs. 2 and 3). Clean quartzite is a relatively uncommon lithology in Yukon-Tanana terrane; it is a minor constituent of the Nasina assemblage west of Dawson, approximately 280 km to the northwest (Mortensen, 1988a; 1988b; 1992). The presence of clean quartzite in the Little Kalzas Lake area therefore suggests a possible correlation with the Nasina assemblage of west-central Yukon.
- The crinoidal marble of Unit 3 is the most promising horizon for stratigraphic linkage with other parts of Yukon-Tanana terrane. Latest Mississippian to Early Permian fossiliferous marble occurs sporadically throughout Yukon-Tanana terrane (cf. Mortensen, 1992, Fig. 5). Latest Mississippian marble occurs below an important unit of mafic to intermediate metavolcanic rocks in the Big Salmon complex of northern British Columbia and southern Yukon (Mihalynuk et al., 1998). Upper Paleozoic marble are also present in the Finlayson Lake District (Tempelman-Kluit, 1977; Mortensen, 1992). Several samples of Unit 3 marble are being analyzed for microfossils. If the Unit 3 marble yields a Late Mississippian-Pennsylvanian age, then the upper metavolcanic sequence (Units 2 and 4) of the Little Kalzas Lake area is most likely coeval with the upper part of Yukon-Tanana stratigraphy (which hosts the Wolverine deposit) as defined by Murphy and Piercey (1999) in the Finlayson Lake District.

REFERENCES

Campbell, R. B., 1967, Geology of Glenlyon map-area, Yukon Territory (105 L): Geological Survey of Canada, Memoir 352, 92 p.

Colpron, M., 1998, Preliminary geological map of Little Kalzas Lake area, central Yukon (NTS105L/13): Exploration and Geological Services Division, Yukon, Indian and Northern Affairs Canada, Open File 1998-3, 1:50 000.

Colpron, M., 1999, Glenlyon Project: Preliminary stratigraphy and structure of Yukon-Tanana terrane, Little Kalzas Lake area, central Yukon (105L/13), *in* Yukon Exploration and Geology 1998: Exploration and Geological Services Division, Yukon, Indian and Northern Affairs Canada, p. 63-72.

Coney, P. J., Jones, D. L. and Monger, J. W. H., 1980, Cordilleran suspect terranes: Nature, v. 288, p. 329-333.

de Keijzer, M., Williams, P. F. and Brown, R. L., *(in press)*, Kilometre-scale folding in the Teslin zone, northern Canadian Cordillera, and its tectonic implications for the accretion of the Yukon-Tanana terrane to North America: Canadian Journal of Earth Sciences.

Gallagher, C. S., Brown, R. L. and Carr, S. D., 1998, A structural re-evaluation of the Teslin Zone, Yukon, Canada: Geological Society of America Abstracts with Program, v. 30, p. A-177.

Hunt, J. A., 1997, Massive sulphide deposits in the Yukon-Tanana and adjacents terranes, *in* Yukon Exploration and Geology 1996: Exploration and Geological Services Division, Yukon, Indian and Northern Affairs Canada, p. 35-45.

Mihalynuk, M. C., Nelson, J. and Friedman, R. M., 1998, Regional geology and mineralization of the Big Salmon Complex (104N NE and 104O NW), *in* Geological Fieldwork 1997: B.C. Ministry of Employment and Investment, Geological Survey Branch, Paper 1998-1, p. 6-1 - 6-19.

Mortensen, J. K., 1988a, Geology of southwestern Dawson map area (NTS 116 B, C): Geological Survey of Canada, Open File 1927, 1:250 000.

Mortensen, J. K., 1988b, Geology of southwestern Dawson map area, Yukon Territory (NTS 116 B, C), *in* Current Research, Part E: Geological Survey of Canada, Paper 88-1E, p. 73-78.

Mortensen, J. K., 1992, Pre-Mid-Mesozoic tectonic evolution of the Yukon-Tanana terrane, Yukon and Alaska: Tectonics, v. 11, p. 836-853.

Murphy, D. C. and Piercey, S., 1999, Finlayson Project: Geological evolution of Yukon-Tanana terrane and its relationship to Campbell Range belt, northern Wolverine Lake map area, southeastern Yukon, *in* Yukon Exploration and Geology 1998: Exploration and Geological Services Division, Yukon, Indian and Northern Affairs Canada, p. 47-62.

Tempelman-Kluit, D. J., 1977, Quiet Lake (105F) and Finlayson Lake (105G) map areas, Yukon Territory: Geological Survey of Canada, Open File 486, 1:250 000.

Tempelman-Kluit, D. J., 1979, Transported cataclasite, ophiolite and granodiorite in Yukon: evidence of arc-continent collision: Geological Survey of Canada, Paper 79-14, 27 p.

Tempelman-Kluit, D. J., 1984, Geology, Laberge (105E) and Carmacks (105I), Yukon Territory: Geological Survey of Canada, Open File 1101, 1:250 000.

Wheeler, J. O., Brookfield, A. J., Gabrielse, H., Monger, J. W. H., Tipper, H. W. and Woodsworth, G. J., 1991, Terrane Map of the Canadian Cordillera: Geological Survey of Canada, Map 1713A, 1:2 000 000.

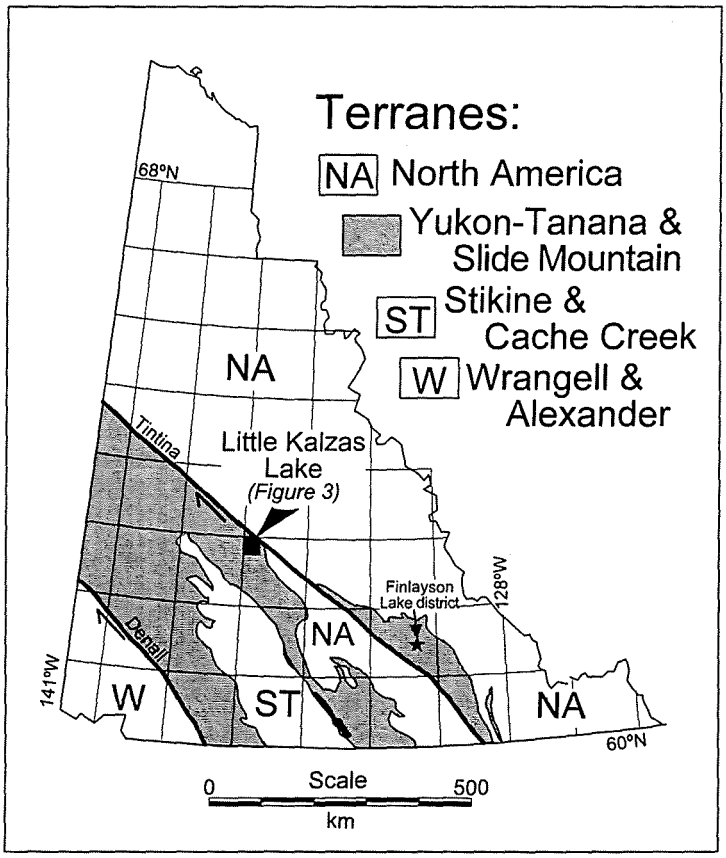

Figure 1. Location of the Little Kalzas Lake area with respect to distribution of Yukon –Tanana terrane in Yukon and to syngenetic sulphide deposits of the Finlayson Lake district.

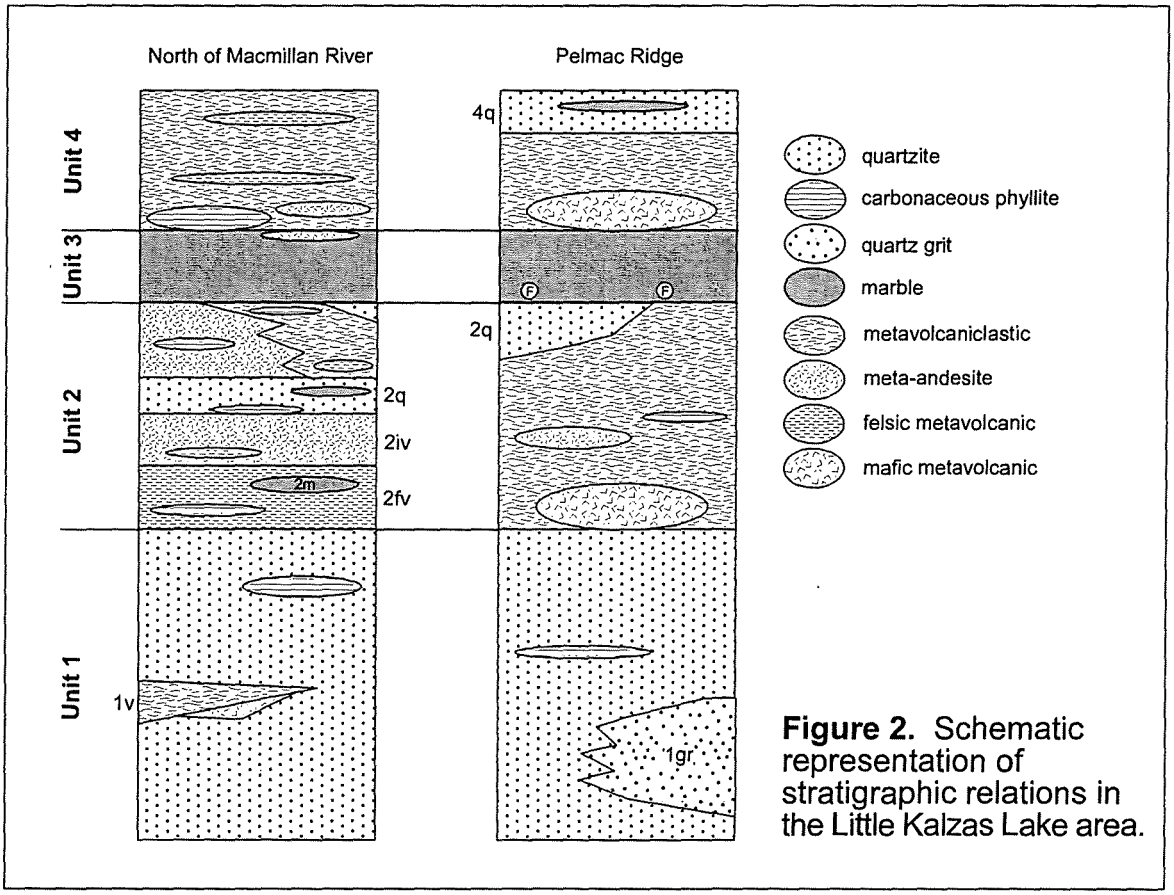

Figure 2. Schematic representation of stratigraphic relations in the Little Kalzas Lake area.

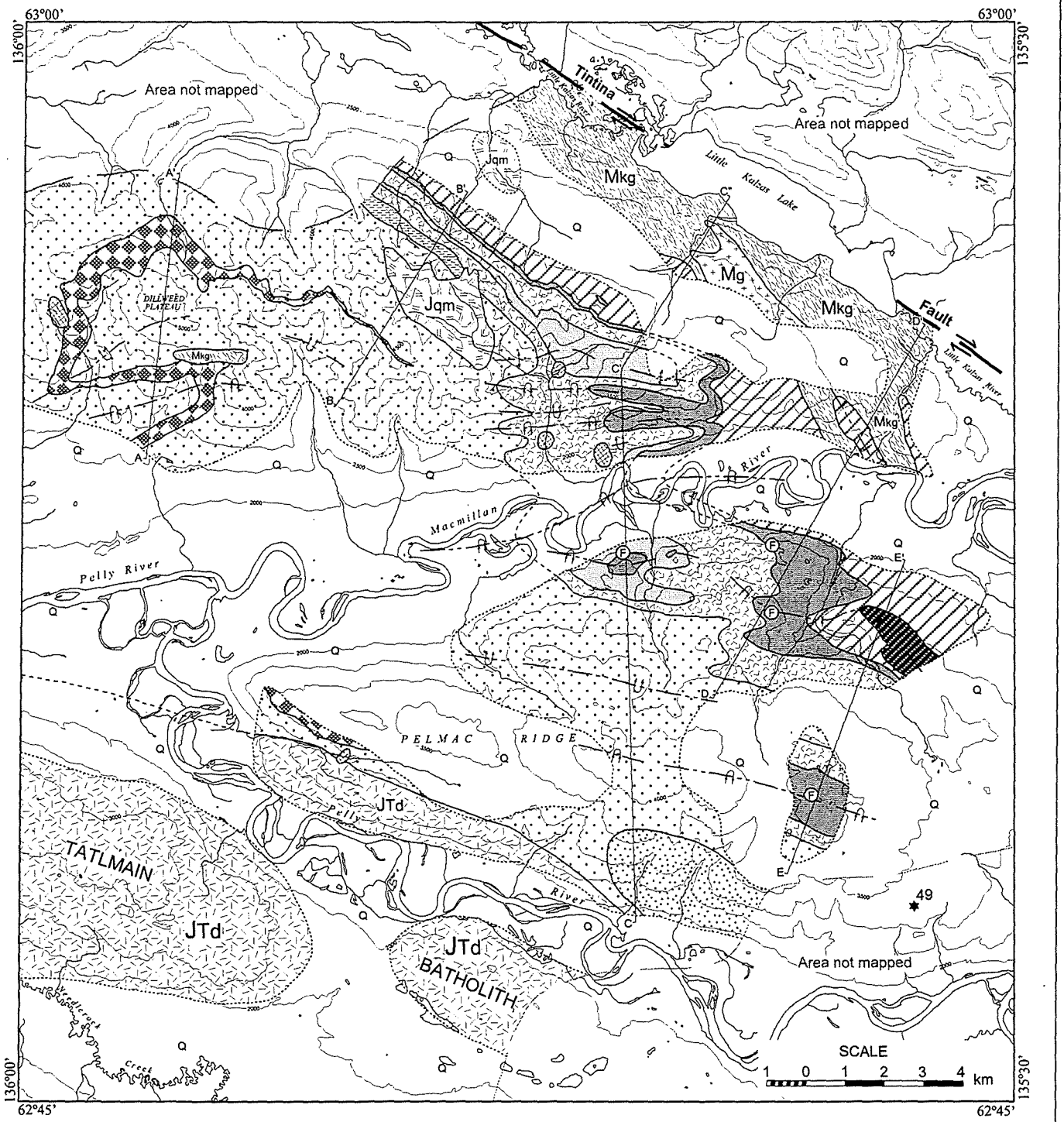

LAYERED METAMORPHIC ROCKS

- Unit 1 - quartzite
- Unit 1v - metavolcaniclastic rocks
- Unit 1gr - quartz grit
- Unit 2 - intermediate to mafic metavolcanic rocks
- Unit 2fv - felsic metavolcanic rocks
- Unit 2q - quartzite
- Unit 3 - marble
- Unit 4 - felsic to intermediate metavolcanic rocks
- Unit 4q - quartzite

INTRUSIVE ROCKS

- Tp - Tertiary porphyries
- JTd - Jurassic (?) quartz diorite (Tatlmain batholith)
- Jqm - Jurassic (?) quartz monzonite (Cornolio pluton)
- Mgd - Mississippian (?) granodiorite gneiss
- Mg - Mississippian (?) granite gneiss

Figure 3. Geological map of the Little Kalzas Lake area (105L/13). F = occurrences of crinoidal marble in Unit 3. Number 49 indicates location of Yukon Minfile occurrence 105L-049 (Hugh, Gal).

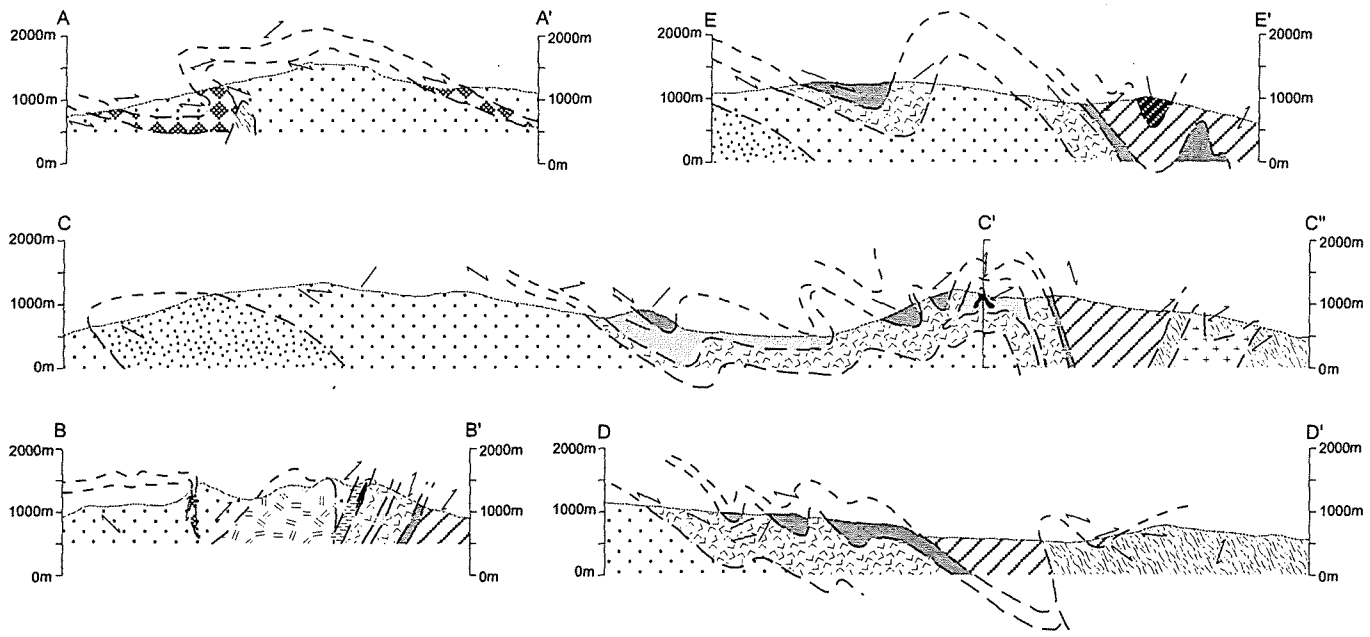

Figure 4. Vertical cross-sections for the Little Kalzas Lake area. Line of sections are located in Figure 2. See Figure 2 for legend.

Primitive arc-magmatism in Stikinia: implications from the Zippa Mountain Pluton.

I.M. Coulson, M. Westphal, J.K. Russell & G.M. Dipple

Geological Sciences Division, Department of Earth & Ocean Sciences, The University of British Columbia, Vancouver, British Columbia, Canada, V6T 1Z4.

Introduction

This paper discusses the nature, origin and mantle sources of a suite of Late Triassic to Jurassic alkaline intrusions distributed throughout the Stikine and Quesnel Terranes of the Canadian Cordillera (Fig. 1). These intrusions share a unique set of structural, lithological, petrological and mineralogical traits (Lueck et al. 1993). Specifically, the individual plutons comprise syenite, melasyenite and pyroxenite, show a concentric zonation in rock types, contain mineralogical layering, and exhibit well-developed planar mineral fabrics. The intrusions are silica-undersaturated based on modal mineralogy and rock compositions.

Detailed study of one of these intrusions, the Zippa Mountain pluton (Fig. 2), demonstrates its chemical affinity to 'shoshonitic' magmas formed in an island-arc system. The similarities between these alkaline intrusions are strong enough to suggest that they derive from similar source regions, represent similar tectonic settings, and have shared a common style of emplacement and differentiation. Such implications are significant because these petrologically distinctive plutons appear to have intruded the Paleozoic to Mesozoic stratigraphic packages of the Quesnel and Stikine terranes over a relatively narrow period of time (Woodsworth et al. 1991, Lang et al. 1995). This simple fact suggests that these terranes are the same or shared similar magmatic events in their makeup.

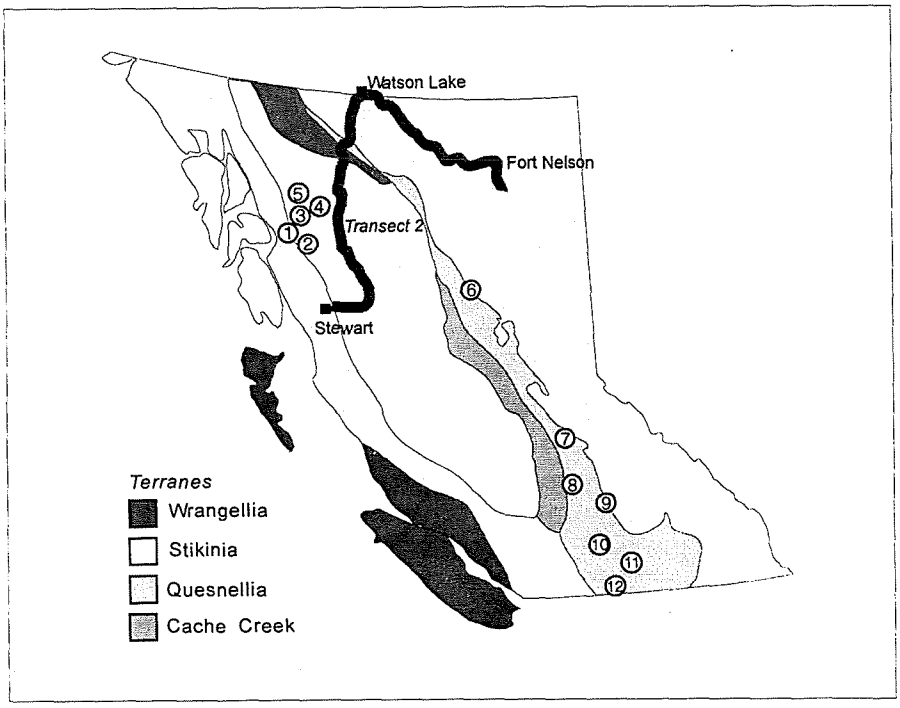

Figure 1. Location of early Mesozoic silica-undersaturated alkaline intrusive complexes in the Cordillera of British Columbia (after Lang et al. 1995 & references therein). Key: 1. Butterfly Pluton, 2. Zippa Mountain, 3. Galore Creek, 4. Ten Mile Creek, 5. Rugged Mountain, 6. Duckling Creek, 7. Mount Polley, 8. Rayfield River, 9. Kamloops Syenite, 10. White Mountain, 11. Averill Pluton, and 12. Kruger Mountain. The position of the SNORCLE Transect 2 is indicated.

ZSAP Intrusions in the Cordillera

Alkalic intrusions of Mesozoic age are common throughout the Intermontane Belt of the Canadian Cordillera (Barr et al. 1976, Woodsworth et al. 1991) and define a period of magmatism from 210 to 155 Ma (Armstrong 1988, Lang et al. 1995). In British Columbia, alkalic plutonic rocks of Late Triassic to Early Jurassic age are found in both the Quesnel and Stikine terranes of the Canadian Cordillera (Fig. 1). Recent work (Keep & Russell 1992, Lueck & Russell 1994*b*, Lang et al. 1995) has recognized that this period of alkalic magmatism has produced both silica-undersaturated and silica-saturated suites of intrusive rock types. The zoned, silica-undersaturated, alkaline plutons (ZSAP) are particularly distinctive in mineralogy and structure and, although many of the general characteristics have been described (Keep & Russell 1992, Neill & Russell 1993, Lueck & Russell 1994*b*, Coulson et al. 1999), the origin of these intrusions and the broader tectonic implications have not been resolved.

Distinguishing Characteristics

There are at least 12 major intrusions which constitute the silica-undersaturated suite as described by Lueck et al. (1993), and Lueck and Russell (1994*a,c*) (Fig. 1). The intrusions comprise rock types that span the compositional range from clinopyroxenite to syenite. As a group, they are chemically alkaline, potassic (Fig. 3*a*), and all are strongly silica-undersaturated (Fig. 3*b*) and contain nepheline (Kruger syenite, Currie 1976), pseudo-leucite (Mount Polley and Galore Creek, Currie 1976), and vishnevite (Zippa Mtn., Lueck & Russell 1994*a,b*). The presence of accessory titanian andradite is another clear indication of silica-undersaturation and occurs in most intrusions.

The combination of large-scale petrological zoning, small-scale mineral layering and a mappable igneous foliation suggest that these rocks may have formed dominantly by gravitational settling of minerals crystallizing from a strongly undersaturated alkaline magma. The continuity in mineral assemblage, continuum in modal proportions and chemical characteristics further suggests a cogenetic relationship between all phases of the intrusion (Coulson et al. 1999).

These alkaline intrusions range in age from Latest Triassic to Jurassic. They occur in both the Stikine and Quesnel Terranes and intrude Paleozoic to Triassic assemblages. The fact that these intrusions share so many field, petrographic and geochemical attributes suggests a common mechanism operating throughout time and space.

Zippa Mountain: an example of the ZSAP

The Zippa Mountain intrusion in northwestern British Columbia intrudes stratigraphy within Stikinia (Figs. 1 & 2), and is typical of these Mesozoic, undersaturated, alkaline plutons. It exhibits the most complete range of features characteristic of the group, whereas other intrusions display them to varying degrees. It is, therefore, an excellent example to explore the nature of the suite as a whole.

Geology

Zippa Mountain is an elliptical laccolith about 14 km^2 in area situated in the Iskut River map area (NTS 104 B 11) of northwest British Columbia, within the western margins of the

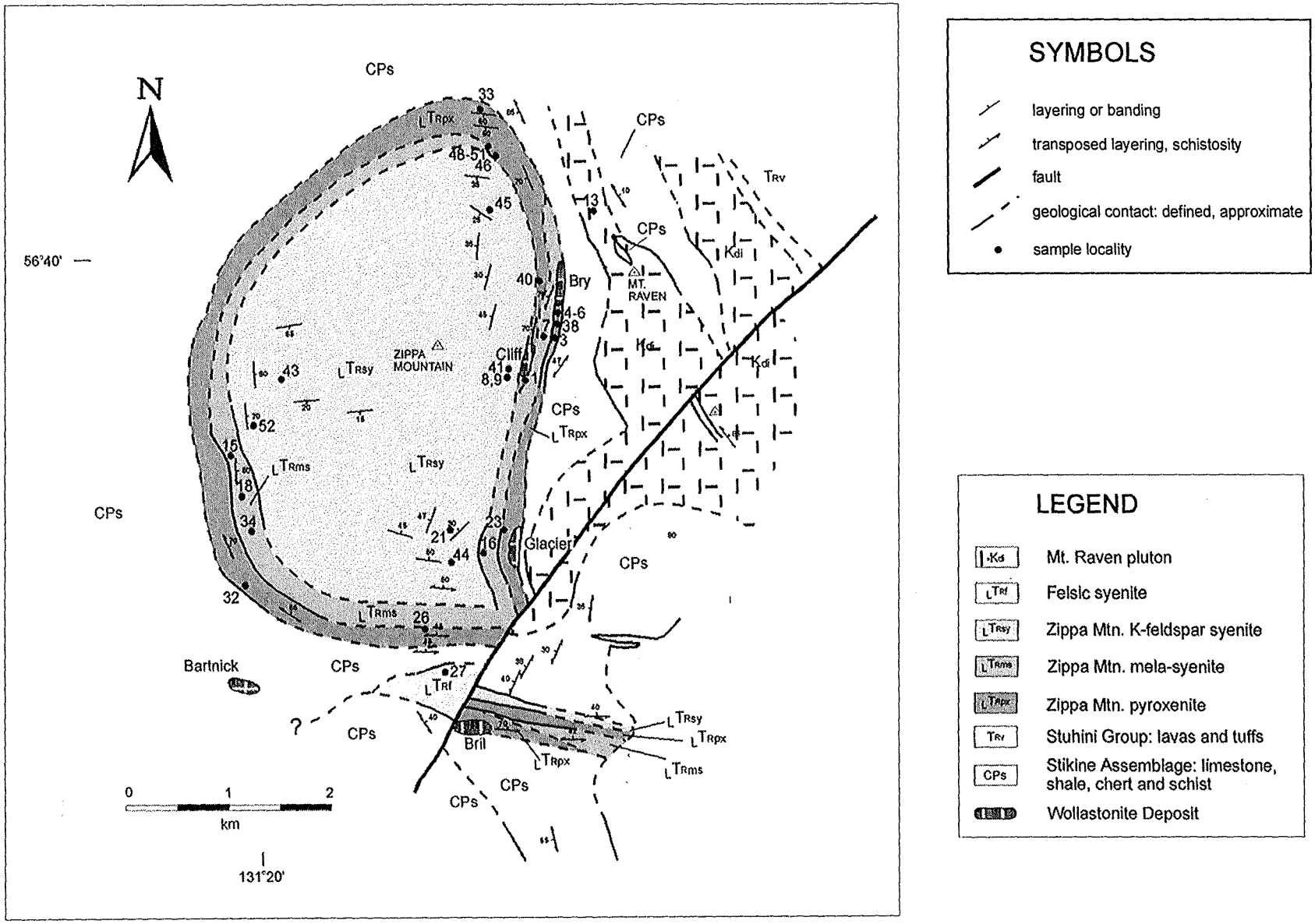

Figure 2. Simplified geological map of the Zippa Mountain intrusion (modified Coulson et al. 1999).

Intermontane Belt (Kerr 1948, Woodsworth et al. 1991) (Figs. 1 & 2). The intrusion has an U-Pb (zircon) emplacement age of 210 ± 2 Ma (Bevier & Anderson, unpubl. data), intrudes Paleozoic and Mesozoic stratigraphy of Stikinia, and has a well developed skarn zone showing evidence of magma-crustal rock interactions (see Westphal et al. *This Volume*).

The pluton is zoned from a clinopyroxenite border phase, to mela-syenite and to K-feldspar megacrystic syenite in the core (Fig. 2). Clinopyroxenite forms an inwardly-dipping marginal phase which grades through mela-syenite to the core syenite. The silica-undersaturated nature of the pluton is manifest in abundant and widespread modal vishnevite (after feldspathoid) and titanian andradite. Wollastonite skarn is developed peripheral to the Zippa Mountain intrusion. The skarn formed by infiltration of marble by SiO_2-bearing aqueous fluid (Jaworski & Dipple 1996). The close association of skarn development with the Zippa Mountain intrusion and the similarity of oxygen isotopic compositions of Zippa syenite and wollastonite skarn argue for the Zippa Mountain pluton as the source of that fluid (Westphal et al. *This Volume*).

Geochemistry

The Zippa Mountain plutonic rocks span a wide range in SiO_2 (45-60 wt.%). Chemically, they are silica-undersaturated and strongly alkaline (Fig. 3*a*). There is a smooth trend of increasing fractionation for the Zippa plutonic suite: the oxides TiO_2, FeO(T), MnO, MgO, CaO, and P_2O_5 show continuous and negative correlations with increasing fractionation. In addition to being peralkaline, many of the Zippa rocks are also strongly potassic, reflecting the dominance of K-feldspar in the mode (Coulson et al. 1999)

Trace element data for Zippa Mountain rocks show an affinity to volcanic-arc and syn-collisional granitoids (Fig. 3*c*). Incompatible element distributions are typical of arc-related rocks; they are characterized by high ratios of large-ion lithophile elements to high-field strength elements (e.g., LILE/HFSE)(Fig. 4d). Enrichment of LILE relative to HFSE is characteristic of primitive arc-magmas (Morrison 1980). Rare earth element (REE) data for the Zippa rocks show light-REE enrichment and moderately flat heavy REE patterns.

Discussion

Primitive Magmas and the Nature of the Parent Magma

Potassic magmatism, such as that found at Zippa Mountain and Rugged Mountain occurs in a diverse range of tectonic settings (Bergman 1987, Gibson et al. 1995). In addition to high K, these plutons are characterized by high concentrations of incompatible elements. These chemical attributes makes its genesis by partial melting of conventional peridotite mantle sources unlikely (Wyllie 1987). Some potassic rocks (e.g., shoshonites) are demonstrably linked to subduction-related magmas that are associated spatially and temporally with calc-alkaline volcanics (Morrison 1980). Other strongly potassic magmas, (e.g., minettes) on the other hand, result from the extension and thinning of sub-continental lithospheric mantle (Thompson et al. 1989). Smith (1972) studied some high-potassium intrusives from Southeastern Papua and demonstrated their affinity to shoshonites. These intrusives are similar to those from Zippa in that they are undersaturated and potassic, they range in composition from pyroxenite to syenite and display a wide variety of textures and

grain sizes. Smith (1972) demonstrated that high-potassium magmas can be generated in areas of active tectonism and that they are related to calc-alkaline rocks of island-arcs. More recently, Ayer (1998) in studying the Falcon Island pluton, Ontario, Canada, reported its ultrapotassic character. He noted that the intrusion was similarly zoned from clinopyroxenite to syenite and concluded, from its arc-like trace element chemistry, that it formed from in a mature island or continental arc setting.

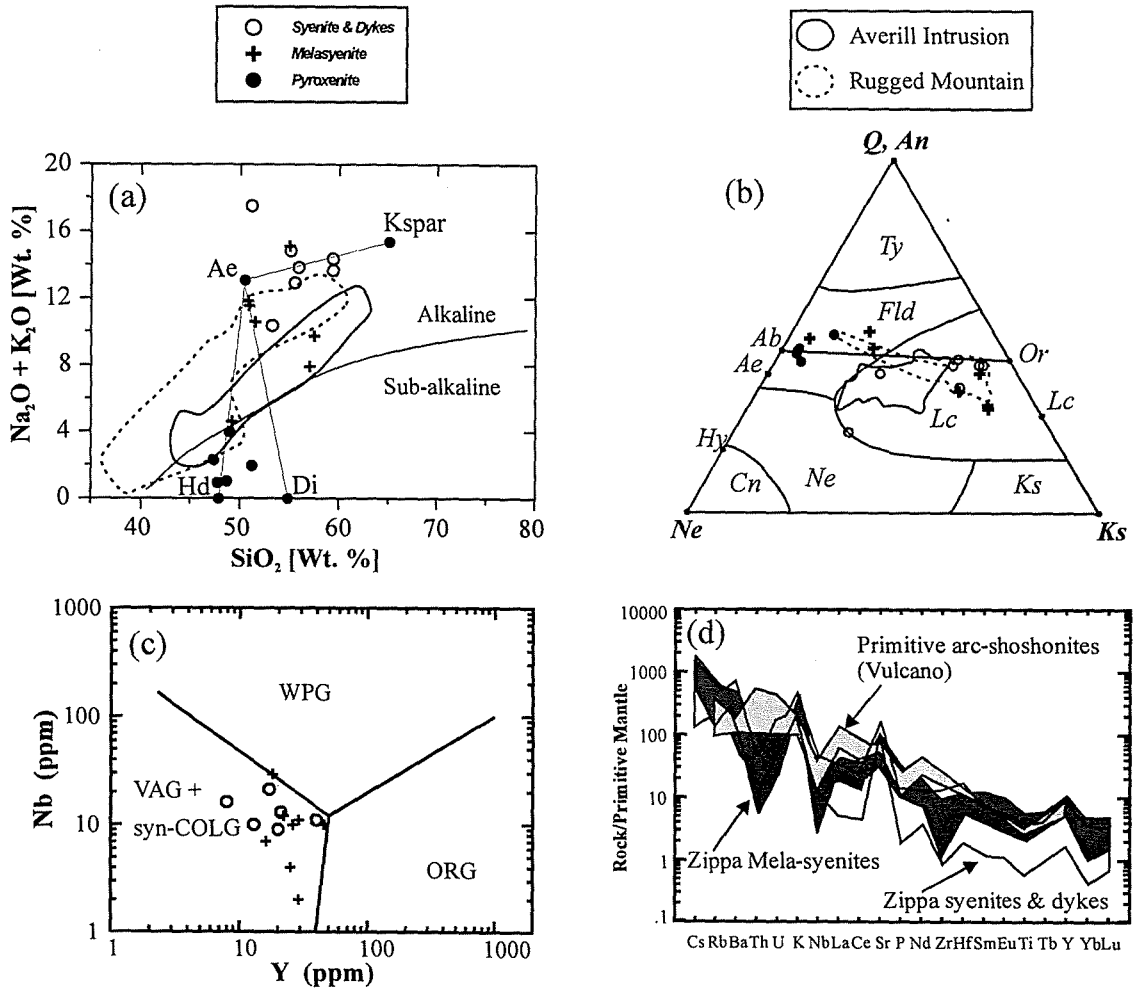

Figure 3. Chemical compositions of Zippa Mountain rocks (Lueck & Russell 1994*a, b*, Coulson et al. 1999) are plotted as: a) TAS. Tie lies are for Ae – aegirine, Di – diopside, Hd – hedenbergite and K-spar - potassium feldspar. Alkaline/subalkaline division is from Irvine & Barager (1971). Also shown for comparison are data from the Rugged Mountain (Neill & Russell 1993) and Averill (Keep & Russell 1992) complexes of the B.C. Cordillera; b) Q-Ne-Ks against the experimentally determined liquidus phase relationships (Morse 1980). Compositions are projected from ideal phase assemblage of clinopyroxene, magnetite, titanite, and apatite, which is found in all the alkalic systems investigated here, and which potentially removes effects of sorting of phases other than those lying in the plane of projection. Ab - albite, Ae - aegirine; An - anorthite, Cn - carnegeite, Fld - feldspar, Hy - haüyne; Ks - kalsilite, Lc - leucite, Ne - nepheline, Or - orthoclase, Q - quartz, Ty - tridymite.). In this projection, the majority of rocks plot within the leucite-saturated field; c) Rb vs. Y tectonomagmatic discrimination diagram for volcanic-arc (VAG), within-plate (WPG), ocean-ridge (ORG), and syncollision (Syn-COLG) granitoids (after Pearce et al. 1984); d) Primitive mantle-normalized abundance patterns. For comparison, the field for primitive island-arc shoshonitic rocks from Vulcano, Italy (Coulson 1993) are shown.

We conclude that the source of the Zippa potassic rocks (and by analogy the alkaline suite) is constrained by high LILE, LREE and K, and depletions in selected HFSE, relative to a primitive mantle composition (Sun & McDonough 1989). The presence of chemical features characteristic of subduction zone magmas (Saunders et al. 1991), suggests that the most primitive magmas present at Zippa were generated in an arc-like setting. The type of arc is not readily constrained, although is likely to be a fairly mature island-arc (e.g. Vulcano, Aeolian arc, Italy; Keller 1980, Coulson 1993) or continental-arc, because of the highly potassic (shoshonitic) nature of the magmas produced. A phlogopite bearing garnet peridotite, metasomatised to varying degrees by heterogeneous slab derived fluids, is favoured as a likely mantle source for the investigated rocks.

Tectonic Synthesis: island or continental-arc

The above model for the formation of the Zippa Mountain and ZSAP magmas is consistent with the hypothesis that in the Late Triassic, the Stikine (Zippa), and possibly the Quesnel terranes, were made up or punctuated by arc-type magmas (Mortimer 1987). The strongly potassic nature of this magmatism, implies that the arc was well developed (cf. Aeolian arc, Italy; Ellam et al. 1988), although whether this formed part of an island-, back- or continental-arc setting is not known. Lang et al. (1995) report limited isotopic data for the ZSAP suite, and infer that the primitive ε_{Nd} (+2.7 to +7.9) and initial $^{87}Sr/^{86}Sr$ ratios (0.7033 ± 0.0003) preclude their emplacement through a thickened continental crust. In other words it appears more likely that these magmas were produced in an island-, as opposed to, a continental-arc setting (cf. Smith 1972). This is significant because these magmas intrude a slightly older stratigraphic package of arc-related volcanic rocks from the Stuhini group; a series of Late Triassic calc-alkaline lavas and tuffs (Friedman et al. 1998). This may suggest that arc-magmatism began in Stikinia with the eruption of early, dominantly calc-alkaline products before maturing; resulting in the formation of a series of potassic magmas. This transition and subsequent termination of magmatism represents the last stages of arc-development before accretion onto North America in the Jurassic.

The similarities between the ZSAP intrusions throughout both the Stikine and Quesnel Terranes, are strong enough to suggest that they derive from similar source regions, represent similar tectonic settings, and have shared a common style of emplacement and differentiation. Such implications are significant because these petrologically distinctive plutons appear to have intruded the Paleozoic to Mesozoic stratigraphic packages of the Quesnel and Stikine terranes over a relatively narrow period of time (Woodsworth et al. 1991, Lang et al. 1995). This simple fact suggests that these terranes are the same or shared similar magmatic events in their makeup (Wernicke & Klepacki 1988, Mihalnyuk et al. 1994).

Conclusions

1. The Zippa Mountain pluton is a Late Triassic (210 Ma), petrologically-zoned intrusion, characteristic of the zoned, silica-undersaturated alkaline plutonic suite.
2. Chemically we demonstrate the intrusion to be silica-undersaturated, alkaline and potassic in character. We show that the potassic nature of the pluton is a characteristic of the parental magma, and that this potassic character is emphasized as a result of

strong fractionation within a closed system magma chamber.

3. The chemistry of the Zippa rocks shares similarities with alkaline potassic magmas formed in an island arc-setting (e.g., shoshonitic magma series), emphasized by high LILE, LREE, depletion of Nb and Ti, and its primitive isotopic character.

Acknowledgements

This research was made possible through the financial and logistical support of the Geological Survey of Canada (R.G. Anderson), the Mineral Deposit Research Unit (MDRU) at The University of British Columbia, and more recently through Whitegold Resources Inc. and NSERC, in the form of an Industry Orientated Research grant held by Dipple and Russell.

References

Armstrong, R.L., 1988. Mesozoic and early Cenozoic magmatic evolution of the Canadian Cordillera. *In* Processes in Continental Lithospheric Deformation. *Edited by* S.P. Clark, Jr., B.C. Burchfield & J. Suppe. Geological Society of America, Special Paper, **218**: 55-91.

Ayer, J.A. 1998. The mafic minerals of the Falcon Island ultrapotassic pluton, Lake of the Woods, Ontario: progressive reduction during fractionation. The Canadian Mineralogist, **36**: 49-66.

Barr, D.A., Fox, P.E., Northcote, K.E., & Preto, V.A. 1976. The alkaline suite porphyry deposits: a summary, *In* Porphyry deposits of the Canadian Cordillera. *Edited by* A. Sutherland Brown. Canadian Institute of Mining & Metallurgy Special Volume, **15**: p.359-367.

Bergman, S.C. 1987. Lamproites and other potassium-rich igneous rocks: a review of their occurrence, mineralogy and geochemistry. *In* Alkaline Igneous Rocks. *Edited by* J.G. Fitton & B.G.J. Upton. Geological Society Special Publication No. **30**: 103-190.

Coulson, 1993. The petrogenetic and volcanic evolution of Northern Vulcano, Aeolian Islands, Italy. Unpublished B.Sc. Honours thesis, University of Portsmouth, U.K. 100 p.

Coulson, I.M, Russell, J.K. & Dipple, G.M. 1999 (Accepted pending revisions) Origins of the Zippa Mountain Pluton: a Late Triassic, arc-derived, ultrapotassic magma from the Canadian Cordillera. Canadian Journal of Earth Sciences.

Currie, K. L. 1976. The Alkaline Rocks of Canada; Geological Survey of Canada, Bulletin 239.

Ellam, R.M., Menzies, M.A., Hawkesworth, C.J., Leeman, W.P., Rosi, M., & Serri, G. 1988. The transition from calc-alkaline to potassic orogenic magmatism in the Aeolian islands, Southern Italy. Bulletin of Volcanology, **50**: 386-398.

Friedman, R.M., Schiarizza, P., Mustard, P., van der Heyden, P., Mortensen, J.K., Thompson, J.F.H., & Deyell, C. 1998. Middle and Late Triassic arc volcanic rocks and associated intrusions in southern and central British Columbia: evidence for correlation of Stikine, Cadwallader and Methow Terranes. *In*: Cook, F. & Erdmer, P. (compilers). Slave-Northern Cordillera Lithospheric Evolution (SNORCLE) Transect & Cordilleran Tectonics Workshop Meeting (March 6-8), Simon Fraser University, Lithoprobe Report No. **64**: pp. 250.

Gibson, S.A., Thompson, R.N., Dickin, A.P., & Leonardos, O.H. 1995. High-Ti and low-Ti mafic potassic magmas: key to plume-lithosphere interactions and continental flood-basalt genesis. Earth & Planetary Science Letters **123**: 105-117.

Irvine, T.N, & Barager, W.R.A. 1971. A guide to the chemical classification of the common volcanic rocks. Canadian Journal of Earth Sciences, **8**: 523-548.

Jaworski, B.J. &, Dipple, G.M. 1996. Zippa Mountain wollastonite skarns, Iskut River map area (104B/11). Geological fieldwork 1995, Paper 1996-1.

Keep, M., & Russell, J. K. 1992. Mesozoic alkaline rock of the Averill plutonic complex: Canadian Journal of Earth Sciences, **29**: 2508-2520.

Keller, J. 1980. The island of Vulcano. Rendiconti Societa Italiana di Mineralogia e Petrologia, **36**: 369-414.

Kerr, F.A. 1948. Lower Stikine and Western Iskut River Areas, B. C.: Geological Survey of Canada, Memoir 246, 94 p.

Lang, J.R., Lueck, B., Mortensen, J.K., Russell, J.K., Stanley, C.R., & Thompson, J.F.H. 1995. Triassic-

Jurassic silica-undersaturated and silica-saturated alkalic intrusions in the Cordillera of British Columbia: Implications for arc magmatism. Geology, **23**:5, 451-454.

Lueck, B. A., & Russell, J. K. 1994*c*. Zoned, Silica Undersaturated, Alkalic Plutons of the British Columbia Cordilleran. *In* Geological Fieldwork 1994-1, British Columbia Geological Survey Branch, P-038.

Lueck, B. A., Neil, I., & Russell, J. K. 1993. The Rugged Mountain Pluton: an Example of the Melanite Bearing Pyroxenite-Syenite Association: Geological Association of Canada-Mineralogical Association of Canada, Programs with Abstracts, **18**, p. A61.

Lueck, B.A., & Russell, J.K. 1994*a*. Silica-undersaturated, zoned alkaline intrusions within the British Columbia cordillera, *In* Geological Fieldwork 1993: British Columbia Ministry of Energy, Mines & Petroleum Resources Paper 1994-1, pp. 311-315.

Lueck, B.A., & Russell, J.K. 1994*b*. Geology and origins of the Zippa Mountain igneous complex with emphasis on the Zippa Mountain pluton, northern British Columbia. *In* Current research 1994-A: Geological Survey of Canada, pp.77-85.

Mihalynuk, M.G., Nelson, J. & Diakow, L.J. 1994. Cache Creek terrane entrapment: Oroclinal paradox within the Canadian Cordillera. Tectonics, **13**: 575-595.

Morrison, G.W. 1980. Characteristics and tectonic setting of the shoshonite rock association. Lithos, **13**: 97-108.

Morse, S.A. 1980. Basalts and their phase diagrams. Springer-Verlag, New York, 493p.

Mortimer, N. 1987. The Nicola Group: Late Triassic and Early Jurassic subduction related volcanism. Canadian Journal of Earth Sciences, **24**: 2521-2536.

Neill, I., & Russell, J. K. 1993. Mineralogy and chemistry of the Rugged Mountain pluton: a melanite-bearing alkaline intrusion. *In* Geological fieldwork 1992, British Columbia Ministry of Energy, Mines & Petroleum Resources Paper 1993-1, pp. 149-157.

Pearce, J.A., Harris, N.B.W., & Tindle, A.G. 1984. Trace element discrimination diagrams for the tectonic interpretation of granitic rocks. Journal of Petrology, **25**: 956-983.

Saunders, A.D., Norry, M.J., & Tarney, J., 1991. Fluid influence on the trace element compositions of subduction zone magmas. Philosophical Transactions of the Royal Society of London, **A355**: 377-392.

Smith, I.E.M. 1972. High-potassium intrusives from southeastern Papua. Contributions to Petrology & Mineralogy, **34**: 167-176.

Sun, S-S., & McDonough, W.F. 1989. Chemical and isotopic systematics of oceanic basalts: implications for mantle composition and processes. *In* Magmatism in the ocean basins. *Edited by* A.D. Saunders & M.J. Norry. Geological Society Special Publication (London), **42**, pp. 313-345.

Thompson, R.N., Leat, P.T., Dickin, A.P., Morrison, M.A., Hendry, G.L., & Gibson, S.A. 1989. Strongly potassic mafic magmas from lithospheric mantle sources during continental extension and heating: evidence from Miocene minettes of northwest Colorado, U.S.A. Earth & Planetary Science Letters, **98**: 139-153.

Wernicke, B. & Klepacki, D.W. 1988. Escape hypothesis of the Stikine block. Geology, **16**: 461-464.

Wesphal, M, Coulson, I.M., Dipple, G.M., & Russell, J.K. *This Volume*. Mantle signature versus crustal contamination in arc-magmatism: constraints from Zippa Mountain.

Wilkins. A. L. 1981. K-Ar and Rb-Sr Dating of the Whiterocks Mountain Alkalic Complex in the Intermontane Belt West of Okanagan Lake; unpublished B. Sc. thesis. The University of British Columbia.

Woodsworth, G. A., Anderson, R. G., & Armstrong, R. L. 1991. Chapter 15, Plutonic Regimes, *In* Geology of the Cordilleran Orogen in Canada, Geology of Canada, no. 4. *Edited by* H. Gabrielse & C.J. Yorath. Canada Geological Survey , pp. 491 - 531 (also Geological Society of America, The Geology of North America, no. G-2).

Wyllie, P.J. 1987. Volcanic rocks: boundaries from experimental petrology. Fortschrifte für Mineralogie **65**: 249-284.

PHYSICAL MODELLING OF HANGINGWALL AND FOOTWALL DEFORMATION NEAR TEAR FAULTS AND LATERAL AND OBLIQUE RAMPS

John M. Dixon, Margaret Oliphant, Julia Blackburn and Simone Garneau

Experimental Tectonics Laboratory, Dept. of Geological Sciences,
Queen's University, Kingston, Ontario K7L 3N6

Physical models (scaled at approximately 1:1,000,000) of a foreland stratigraphic succession demonstrate mechanisms by which a thrust sheet accommodates itself to displacement over ramp systems consisting of two frontal-ramp segments linked by either a vertical tear fault, a gently dipping lateral ramp, or gently dipping oblique ramps with different strikes relative to the transport direction. The models include four stratigraphic units of alternating competency, composed of laminae of Plasticine and silicone putty. The ramp system was cut in the desired configuration in the basal (competent) stratigraphic unit during assembly. The models were deformed in a centrifuge at 2500-4000 ***g*** to achieve dynamic scaling. Matched models of each configuration were serial-sectioned transversely or longitudinally so that the deformation associated with the transverse or oblique structure could be well constrained in 3-d.

Structures in the hangingwall and footwall are diagnostic of the geometry of the ramp system. In the tear-fault and lateral-ramp models, the thrust sheet develops prominent structural culminations associated with the frontal ramps. The culminations terminate abruptly above the buried transverse structure, and associated folds plunge in opposite directions off the ends of the culminations. In contrast, the main thrust sheet in the oblique-ramp models develops a single anticlinal ridge which tracks the ramp system but lacks isolated structural culminations and plunge reversals.

The leading edge of the competent lowest unit in the thrust sheet tends to become overturned towards the foreland. In plan, it reflects the geometry of the ramp system. In the tear-fault and lateral-ramp cases, the leading-edge segments become curved, reflecting a decrease in thrust displacement on each frontal-ramp segment towards the lateral structure. In the oblique-ramp cases, the frontal-ramp leading edges remain straighter because thrust displacement remains constant along strike.

The transverse structures (tear fault and lateral ramp) appear to be rotated in response to 3-d strain comprising longitudinal gravitational spreading of the ramp-anticlinal culminations as well as local collapse and longitudinal spreading of the footwall of the trailing frontal ramp adjacent to the transverse structure. The models suggest that a transverse link (tear fault or lateral ramp) between two frontal ramps is unstable. By rotating out of the transport direction, the linking fault ceases to be favourably oriented to transfer slip between the frontal-ramp segments and is abandoned as the two frontal ramps propagate laterally to form a lap-joint displacement-transfer zone.

Acknowledgements: This work was conducted as part of the Foothills Research Project. Financial support from the FRP's Oil Industry sponsors and NSERC is gratefully acknowledged.

PHYSICAL MODELLING OF THE INFLUENCE OF REGIONAL LITHOFACIES GRADIENTS ON FOLD-THRUST STRUCTURES

John M. Dixon and Marie Wardman

Experimental Tectonics Laboratory, Department of Geological Sciences,
Queen's University, Kingston, Ontario K7L 3N6

We have constructed physical models of foreland stratigraphic successions in which one unit has a lateral competency gradient that simulates a regional change in lithofacies (*e.g.*, a "shale-out"). The models include three stratigraphic units of contrasting bulk competency, composed of laminae of Plasticine and silicone putty. Two units are laterally homogeneous but the alternating laminae of the two constituents in the third unit are tapered in opposite directions so that the ratio of competent to incompetent constituents varies laterally. This simulates a regional gradient of sand-shale or lime-shale ratio in the prototype system. The models were deformed in a centrifuge at 2500-4000 ***g*** to achieve dynamic scaling. In different models, shortening was directed either up, down or transversely to the regional competency gradient.

The models show that the regional mechanical gradient can combine with the across-strike gradient of horizontal compressive stress, which decreases from hinterland to foreland, to influence where fold-thrust shortening initiates and in which direction it propagates. In some circumstances the normal pattern of foreland-directed fold-thrust propagation can be overcome by the regional competency gradient, such that the deformation propagates in a retrograde (from foreland towards hinterland) or even a longitudinal (along-strike) direction. This observation is contrary to the normal regional pattern of "break-forward" structural sequence in fold-thrust belts and has important implications for the timing of formation of structures (i.e., hydrocarbon traps). This mechanism may provide an explanation for anomalous compressional structures situated well ahead of the deformation front, such as some of the isolated anticlinal structures in the easternmost Foothills of NE British Columbia.

There are also systematic differences in the style and size of structures and strain partitioning that are related to the lithological gradient. These variations are not restricted to the unit with the gradient, but can also occur in vertically adjacent units because the deformation reflects the mechanical character of the whole stratigraphic package.

Together, the timing of development as well as the size and style of structures have relevance to hydrocarbon exploration because they control trapping potential.

Acknowledgements: This work was conducted as part of the Foothills Research Project. Financial support from the FRP's Oil Industry sponsors and NSERC is gratefully acknowledged.

U-Pb Geochronologic Evidence of Early Cretaceous Large-Scale Folding in the Dycer Creek Area, Pelly Mountains, Yukon

Chris Gallagher, Sharon D. Carr and Richard L. Brown
Ottawa-Carleton Geoscience Centre and Department of Earth Sciences, Carleton University, Ottawa, Ontario, K1S 5B6

1.0 Introduction

Rocks of the Teslin Zone, located in the central Yukon, are characterized by a steeply dipping regional foliation that differentiates them from the rest of the Yukon-Tanana Terrane (Templeman-Kluit, 1979; Hansen, 1989, 1992 a,b). The zone was originally thought to represent the deep seated portion of a west-dipping Permo-Triassic subduction zone (Templeman-Kluit, 1979; Hansen, 1989). In contrast, recent work by Brown *et al.* (1998), de Keijzer *et al.* (1996, 1997, 1998, in press) and Gallagher *et al.* (1988) has shown that the Teslin Zone is a fold and thrust belt, and that the regional fabric within it developed as a near horizontal transposition fabric (S_{T2}) during northeast vergent isoclinal F_2 folding. The fabric was then rotated into it's present day steep attitude during late large-scale F_3 folding.

Timing of regional ductile deformation is poorly constrained. Hansen (1989, 1992a,b) suggests that, based on regional cooling ages and a lack of recovery microstructures in Teslin Zone rocks, regional deformation occurred in Early Jurassic time. In the hope of better constraining the timing of regional ductile D_2 and D_3 deformation, geochronology samples of four plutonic bodies have been collected during the 1995, 1996 and 1997 field seasons (Fig. 1). Initial results of the study are promising as U-Pb dating of zircons from the Mendocina Orthogneiss has confirmed the presence of Devonian orthogneiss within the Teslin Zone, and dating of monazites from the Dycer Creek Stock and Last Peak Granite has bracketed the age of regional F_3 folding between 113 and 98 Ma. These findings suggest that at least part of the regional deformation may be younger than previously proposed (Templeman-Kluit, 1979; Hansen, 1989, 1992 a,b).

2.0 Geologic Setting

The 9 km by 14 km Dycer Creek Area, located 150 km northeast of Whitehorse, straddles the d'Abbadie Fault Zone and contains rocks of the Cassiar Platform and Teslin Zone (Fig. 1). The map area has been divided into the eastern and western structural domains, located east and west of the d'Abbadie fault zone, respectively (Fig. 1). The western domain consists of polyfolded greenschist and lower amphibolite facies metasedimentary and metaplutonic rocks correlative with the Nisutlin and Anvil assemblages of the Yukon-Tanana Terrane. The eastern domain consists of greenschist facies metasedimentary and metaplutonic rocks of the Cassiar Platform. For detailed geologic descriptions of the eastern and western domains, see Gallagher *et al.* (1998).

The d'Abbadie Fault Zone was originally interpreted to represent a major structural boundary that separated flat lying rocks of the Cassiar Platform to the east from steeply dipping mylonitic rocks of the Teslin Zone to the west (Templeman-Kluit, 1979; Hansen, 1989,1992a,b). Detailed geologic mapping of the Dycer Creek Area and farther to the north at Last Peak (Harvey *et al.*, 1997; Gallagher *et al.*, 1998; Brown *et al.*, 1998) has revealed several major findings: i) rocks of the Teslin Zone and Cassiar Platform are documented on both sides of the fault; ii) regional transposition S_{T2} fabrics observed on both sides of the fault are correlative with one another; iii) late large-scale F_3 folding resulted in steeply dipping fabrics and modification of flat-lying regional fabrics on both sides of the fault. These findings lead to several conclusions. The d'Abbadie Fault Zone is not a major tectonic boundary separating terranes of contrasting tectonic history, and the entire Dycer Creek Area has undergone a common deformation history (Gallagher *et al.*, 1998).

The dominant regional fabric documented in the area consists of a variably dipping, southeast-

striking S_{T2} transposition fabric that is observed on both sides of the fault. S_{T2}, is interpreted to have developed coevally in both domains during northeast vergent isoclinal F_2 folding (Harvey *et al.*, 1997; Gallagher *et al.*, 1998; de Keijzer *et al.*, 1997,1998). The original orientation of S_{T2}, based on regional arguments and field observations, is interpreted to have been near horizontal or gently west dipping. S_{T2} has been rotated, by large-scale F_3 open folding, from a gently west dipping to a steeply dipping orientation in the eastern domain. F_3 minor open folds, observed in both domains, are correlated with zones of steeply dipping S_{T2}. These field observations, led Gallagher *et al.* (1998) to identify late regional scale F_3 folds (e.g. Two-Cub Antiform) as having been responsible for the steeply dipping fabrics of the Dycer Creek Area. These findings are consistent with those to the north at Last Peak (de Keijzer *et al.*, 1997, 1998), although the geometrical relationships between the two late folding events requires further study.

The final phase of deformation involved two Cretaceous dextral strike-slip events. A northwest striking ductile dextral strike-slip zone, concordant with the regional transposition fabric, is documented in the western domain (Fig. 1). Field relationships of the ductile shear zone are discussed in detail below. The d'Abbadie Fault Zone, is the second Cretaceous dextral strike-slip event documented in the area. It is a brittle, north-south trending, vertical fault zone, that has been assigned normal and dextral sense of displacement by various authors (Templeman-Kluit, 1979; Hansen, 1989, 1992). In the Dycer Creek area, kinematic indicators consisting of drag folds and near horizontal slickensides and fibres are consistent with dextral strike-slip motion (Gallagher *et al.*, 1998).

3.0 Plutonic Rocks of the Dycer Creek Area

3.1 Granitoids of the Western domain

Variably deformed granitoids, the mylonitic Mendocina Orthogneiss (365 Ma; this paper) and the protomylonitic Last Peak Granite (98 ± 1 Ma; Harvey *et al.*, 1997a; this paper) are parallel tabular north-northwest trending sheets of granitoids that together are ~750 metres thick and extend for at least 12 km along the eastern margin of the western domain. The contact between the two granitoids is concordant with the regional S_{T2} foliation (Fig. 1) and contact relationships between the two granitoids are not known (Harvey *et al.*, 1997a). The two granitoids and a 50 metre strip of country rock to the west are located within a ~800 metre wide dextral ductile strike-slip shear zone that is interpreted to be early Cretaceous in age (Harvey *et al.*, 1997a). Within the shear zone is a north to northwest striking near vertical mylonitic shear foliation concordant with S_{T2} and shallowly northwest or southeast-plunging stretching lineation.

3.1.1 Mendocina Orthogneiss

Contact Relationships and Lithology

The Mendocina Orthogneiss is a two mica granite that is well exposed along the western margin of the Last Peak Granite (Fig. 1). The orthogneiss weathers from dark to light grey and displays tabular K-feldspar augen, up to 1 cm in length, in a dark grey fine-grained matrix that is composed of quartz, K-feldspar, plagioclase, muscovite and biotite. Contacts between the orthogneiss and the country rocks are concordant (Fig. 1), and there is apparently no chilled margin or contact metamorphism (Harvey *et al.*, 1997a). The contact is interpreted to represent a transposed contact (Harvey *et al.*, 1997a); it is not possible to deduce if the contact is intrusive or tectonic in nature.

Structural Fabrics

The dominant fabric in the orthogneiss is defined by discontinuous north to northwest striking near vertical C-planes (Fig. 3; 1) that are concordant to the regional S_{T2} foliation. This foliation forms part of a Type I S-C fabric (Twiss and Moores, 1992) and contains a northwest to north trending, shallowly plunging stretching lineation that is defined by quartz ribbons, elongate feldspar porphyroclasts and elongate aggregates of biotite (Fig. 2;4). C-planes occur as penetrative micro-scale shear planes consisting of discrete zones of very fine grained, preferentially oriented biotite, quartz and insoluble residue. Discontinuous S-planes are defined by elongate or pulled-apart feldspar porphyroclasts, quartz ribbons,

biotite fish and sigma K-feldspar porphyroclasts (Fig. 2; 2 a,b,c). S-planes are oriented at an angle of 45° or less counter-clockwise with respect to the C-planes and feed into the C-planes (Fig. 2). Asymmetrical extensional shear bands cross-cut S-C fabrics and are oriented at an angle of ~ 30° clock-wise with respect to the C-planes (Fig. 2; 3). A poorly developed set of micro-scale conjugate extensional shear bands, whose acute angle is bisected by the vertical shear planes, are observed in the YZ plane normal to the stretching lineation (Fig. 2; 5).

Kinematic Indicators

Microstructures and their relationships are consistent with the orthogneiss having undergone general shear consisting of a component of strike-slip shear and a component of boundary normal shortening (Hamner and Paschier, 1991). Within the motion plane, S-C fabric relationships, asymmetric extensional shear bands, sigma porphyroclasts and biotite mica fish are consistent with dextral strike-slip motion (Fig. 2). The plane normal to the stretching lineation preserves conjugate shear bands that are consistent with a component of boundary normal shortening.

Timing relationships

Transposed contacts of the orthogneiss with the country rock are consistent with a pre- to syn-D_2 emplacement. Detailed kinematic analysis of fabrics within the orthogneiss reveal that it has clearly undergone general shear consisting of a major dextral strike-slip component and a minor boundary normal shortening component. Dextral ductile shear, associated with internal fabric development within the orthogneiss, is interpreted to post-date regional ductile deformation.

3.1.2 Last Peak Granite

Field relationships and lithology

The Last Peak Granite is a resistant leucogranite that weathers light grey and consists of white elongate K-feldspar megacrysts set in a fine-grained, light-grey matrix of quartz, K-feldspar and plagioclase. The well exposed western contact between the granite and country rocks of the Last Peak assemblage is typically concordant with the regional transposition fabric S_{T2}, but undeformed dykes of granite intrude and cross-cut S_{T2} and S_3. A chilled margin at the western contact, along with a thin metamorphic aureole, are consistent with intrusion into rocks located in a cool upper-crustal environment (Harvey *et al.*, 1997a,b).

The Last Peak Granite can be divided into three domains on the basis of the style of structural fabrics and degree of mylonitization (Harvey *et al.*, 1997a). The granite in the western most "contact zone" is fine grained, lacks structural fabrics and is characterized by an outcrop-scale igneous fabric (Harvey *et al.*, 1996). The main body of the granite is a protomylonite characterized by a well developed steeply dipping shear foliation containing a shallowly north to northwest-plunging stretching lineation. The eastern margin of the granite is marked by a ~100m thick mylonitic C-S tectonite containing a shallowly northwest or southeast plunging stretching lineation.

Structural Fabrics

The main body of the granite is characterized by a well developed foliation that is concordant with S_{T2} and is defined by comminuted fine grained biotite grains and quartz ribbons. The eastern mylonitic zone is characterized by S-C tectonites and a northwest to north trending, shallowly plunging stretching lineation defined by quartz and feldspar rods. The motion plane displays near vertical, C-planes, defined by very fine grained quartz, muscovite and biotite; C-planes strike northwest are sub-parallel to S_{T2}. Discontinuous S-planes defined by elongate quartz aggregates, muscovite porphyroclasts and feldspar porphyroclasts are oriented at an angle of < 45° with respect to the C-planes. Microscopic asymmetric extensional shear bands form an angle of ~30° clock-wise with respect to the C-planes. No structural fabrics are observed in the plane normal to the stretching lineation.

Kinematic Indicators

Kinematic indicators are consistent with dextral strike-slip shear, in the main body and the eastern

margin of the granite. They are best observed in the mylonitic zone where well developed S-C fabrics, observed in the plane normal to the C-plane, are consistent with dextral strike-slip shear. Asymmetric shear bands, "mica fish" and sigma and gamma K-feldspar porphyroclasts, observed in the motion plane, are all consistent with dextral shear (Harvey *et al.*, 1996). There is no evidence of any boundary normal shortening in the plane normal to the stretching lineation. Bulk shear associated with deformation of the Last Peak Granite is therefore interpreted to be of dextral strike-slip sense.

Conclusions

Cross-cutting relationships exhibited by the Last Peak Granite demonstrate an intrusive relationship with the country rock; intrusion post-dated S_3 cleavage development during D_3 deformation. Mylonitic fabric development within the granite must therefore post-date regional ductile deformation as well. Structural fabrics within the granite are interpreted to result from local dextral strike-slip motion. The west to east variation in strain observed in the granite is interpreted to represent intrusion of the magma just prior to or during displacement on the dextral strike-slip shear zone (Harvey *et al.*, 1997a).

3.2 Dycer Creek Stock

The stock is a coarse grained biotite quartz monzonite and is exposed in the eastern domain (Fig.1). It weathers dark grey and the fresh surface is light grey to white. The monzonite is typically homogenous and does not contain phenocrysts. The variably exposed contact varies from highly discordant to concordant with S_{T2}. The western margin of the stock trends roughly parallel to the regional foliation while along the eastern margin the vertical intrusive contact sharply cross-cuts an approximately 500 metre vertical exposure of country rock containing moderately southwest-dipping S_{T2}.

Variably deformed pegmatite dykes, of similar composition to the Dycer Creek Stock, intrude the country rocks. The dykes vary from undeformed and discordant to deformed and concordant with respect to the regional fabric S_{T2}. Folded and boudinaged dykes are interpreted to have intruded the country rock prior to or during D_2 deformation, while undeformed discordant dykes are interpreted to have a post-D_2 intrusive relationship with the country rocks.

Locally, just west of S677 (Fig. 1), there is a distinct contact aureole consisting of a 10 metre wide calc-silicate skarn composed of coarse grained calcite, diopside, biotite and garnet (Fig. 1). The skarn contains a well developed foliation that is concordant, on the outcrop scale, to S_{T2}. The foliation wraps around garnet porphyroblasts.

Structural Fabrics

There is a weak variably dipping southeast-striking foliation defined by preferentially oriented biotite grains averaging 1 cm in diametre. The foliation is variably southwest dipping from shallow in the east to steep in the west. This variation in fabric orientation is identical to that of S_{T2} and is interpreted to have been rotated by late F_3 folding. Southwest-plunging stretching lineations, defined by quartz rods and smeared biotite, are limited to discrete ~1m thick gently west-dipping ductile shear zones. The stretching lineations lie in gently southwest-dipping S-planes that form a small clockwise angle with respect to the shear planes, and are consistent with a top-to-the-east shear sense.

Mineralogical Characteristics

The stock consists of equigranular coarse grained microcline, quartz, biotite and minor plagioclase and muscovite. Highly fractured and serisitized microcline grains show undulose extinction, tartan twinning and weakly developed core and mantle textures. K-feldspar grains are typically highly fractured and serisitized. Plagioclase grains display undulose extinction and deformation twins. No subgrains are observed, fractures are rare and there is little alteration associated with the grains. Quartz occurs as equant fine grained aggregates displaying 120° triple point junctions, bilateral grain boundaries and little or no undulose extinction that are consistent with a significant degree of recovery. Fractures within the quartz grains are rare. Biotite and chlorite are commonly observed together and biotite often forms the cores of chlorite grains.

Conclusions

Field observations associated with the Dycer Creek Stock provide evidence pertaining to the timing of intrusion into carbonates of the Cassiar Platform. Cross-cutting contacts and pegmatite dykes along with contact metamorphism are consistent with post-D_2 intrusion into cold country rock. However, deformed pegmatite dykes and fabric relationships with contact aureoles are consistent with late-D_2 intrusive relationships. These observations are interpreted to be consistent with late syn-D_2 to post-D_2 intrusion of the monzonite into the country rock. The weak foliation within the pluton most likely developed during late D_2 deformation or may have developed at a later time during reactivation of D2 fabrics related to thermal softening at the time of pluton emplacement. Regardless, the foliation has been rotated by F_3 folding. We interpret this to be evidence that the stock intruded the country rock prior to D_3 deformation.

4.0 Age Interpretation of Geochronology Samples

4.1 Analytical Methods

Sample preparation, analytical techniques and data reduction were carried out at the Carleton University U-Pb laboratory using methods described by Krogh (1973, 1982), Roddick (1987), Roddick *et al.* (1987) and Parrish *et al.* (1987). Where available zircon and monazite crystals of the best clarity, with out visible cores, and with minimal opaque inclusions or fractures were chosen for analysis. Descriptions of zircons and monazite, outlined below, apply to the general population of crystals in each sample. A summary of U-Pb analytic data for the samples is presented in Table 1. Monazite data are reversely discordant, a common phenomena in young monazite. This is interpreted to result from the incorporation of excess ^{230}Th during monazite growth. Monazite crystallization ages are therefore estimated from the 207/235 age that does not reflect ^{206}Pb concentrations (Schärer, 1984; Parrish, 1990).

4.2 Mendocina Orthogneiss 545890, 6818900

The general population of zircons within YT95-BS082 (Mendocina Orthogneiss) occur as 170μ - 64μ diametre, euhedral to prismatic, whole or fractured zircons of poor quality and clarity. Cores, preserved as cloudy inclusions within the crystals, are common and the majority of the zircons are altered to a dark rusty red. Opaque inclusions are present within the majority of crystals. Zircons of <64μ diametre are of excellent quality and clarity. The <64μ crystals contain no visible cores or fractures, opaque inclusions are rare and alteration is nonexistant to weak. We interpret the morphology of all the zircons to reflect a magmatic origin.

Fractions A is a 6 grain fraction of equant euhedral +149 μ zircons and B is a 34 grain fraction of equant subhedral to euhedral 105 - 149 μ zircons; both are highly discordant and are interpreted to have an inherited Pb component (Fig 3). Fraction E is a 14 grain fraction of <64μ needles with a 3:1 length to width ratio. All three ages derived from U-Pb analysis of fraction E are in agreement within error and the fraction is therefore interpreted to be concordant (<0.3% discordant; Table 1). The weighted average of the 207/235 and 206/238 ages yields a crystallization age of 357.8 ± 1.2 Ma and is interpreted to represent the crystallization age of YT95-BS082 (Mendocina Orthogneiss; Fig. 3).

4.3 Last Peak Granite 545300, 6821900

Both zircons and monazites were analysed from YT95-BS107 (Last Peak Granite). Zircons, ranging 160μ to 64μ in diametre, are of poor clarity and quality. The majority of euhedral to prismatic crystals contain cores and opaque inclusions and alteration to a dark rusty red is common. Zircon morphology is interpreted to reflect a magmatic origin. Equant euhedral monoclinic monazite crystals, with diametres of >149μ were analysed. Monazite is pale yellow to gold and of excellent clarity. Opaque inclusions within the monazite are common although no cores are observed. Monazite morphology is consistent with an igneous origin.

Zircon fractions A, B, D, E, and F-1 are single grain to multigrain fractions ranging in size from 160μ to 74μ in diametre. All show various degrees of discordance and are interpreted to reflect

components of inherited Pb (Fig. 4). The pattern of discordance is consistent with multiple Proterozoic sources for the inherited Pb. Monazite fractions M1 - M3 are slightly reversely discordant (Fig. 4). The weighted average of the $^{207}Pb/^{235}U$ ages yield an age of 95.7 ± 0.6 Ma that is interpreted to represent the crystallization age of YT95-BS107 (Last Peak Granite).

4.4 Dycer Creek Stock

551500, 6813900

CG97-712 (Dycer Creek Stock) contains zircon and monazite, and both were analysed. Zircon occurs as 160μ to 64μ euhedral to prismatic crystals of poor clarity and quality. Crystals are predominantly highly altered and fractured. Large cores and opaque inclusions are common. Monazite is generally of good quality and occurs as pale yellow to gold equant euhedral crystals. Clarity of the crystals ranges from good to perfect. Cores are not observed although opaque inclusions are common. The morphology of zircon and monazite is interpreted to reflect a magmatic origin.

Multigrain zircon fraction G is discordant and is interpreted to contain a Proterozoic Pb component (Fig. 5). Monazite fractions M1 - M4 are all slightly reversely discordant with overlapping error ellipses (Fig. 5). A weighted average of monazite fractions M1 to M4 yields a $^{207}Pb/^{235}U$ age of 112.3 ± 1.3 Ma that is interpreted to represent the crystallization age of CG97-712 (Dycer Creek Stock).

5.0 Implications of U-Pb age analysis

Dating of igneous zircons from the Yukon-Tanana Terrane is problematic as a result of Proterozoic inheritance. This is reflected in the majority of the zircon fractions analysed from the Dycer Creek Area. One exception is the multigrain fraction E from YT95-BS082 that consists of <64μ prismatic needles. Inheritance of radiogenic Pb results from the nucleation of new zircon crystals on remnant xenocrystic zircons of an older population. The small grains selected for fraction E are interpreted to represent a population that nucleated after all xenocrystic material had been incorporated in previous zircon crystals. Such grains would have nucleated at new sites and are therefore free of inherited Pb. The first stage of analysis has proved promising as analytical data is consistent with >64μ grains containing no inherited Pb component. Small prismatic crystals, although difficult to work with, may represent a solution to the inheritance problem.

A 357 ± 1.6 Ma U-Pb zircon age for the Mendocina Orthogneiss confirms the presence of highly deformed Devonian orthogneiss in the Teslin Zone. A Devonian magmatic event is widely documented throughout the Yukon-Tanana Terrane (Mortensen, 1992). The age of the Mendocina Orthogneiss is consistent with the interpretation that rocks of the Teslin Zone correlate with those of the Yukon-Tanana Terrane. A Devonian age does not place limits on protolith ages of the metasedimentary country rocks as it remains unclear whether the granitoid was emplaced tectonically or intrusively.

Timing of intrusion of the Dycer Creek Stock (112.3 ± 1.3 Ma) is interpreted to pre-date large-scale F_3 folding and to be synchronous with or post-date the development of S_{T2}. We interpret intrusion of the Last Peak Granite (95.7 ± 0.6 Ma) into the western domain to post-date large-scale F_3 regional folding and to precede or be contemporaneous with development of the local dextral strike-slip shear zone. Age constraints on the timing of regional deformation can be drawn from these observations: i) regional S_{T2} transposition fabrics in the Dycer Creek area had developed by 112 ± 1.3 Ma; ii)large-scale F_3 folding occurred between 95.7 ± 0.6 Ma and 112.3 ± 1.3 Ma; iii) development of the local dextral strike-slip shear zone, in the Teslin Zone, occurred after 95.7 ± 0.6 Ma

6.0 Conclusions

1) Regional fabrics developed coevally in the Teslin Zone and eastern Cassiar Platform as near horizontal transposition fabrics (S_{T2}) during northeast vergent isoclinal F_2 folding. S_{T2} was rotated into a steep attitude by late large-scale F_3 folding (de Keijzer, 1997, 1998; Harvey 1996, 1997; Gallagher 1998).

2) Timing of the D_2 transposition event remains poorly constrained, but regional fabrics are thought to have

developed by at least 112 Ma.
3) Development of steep attitudes in the Teslin Zone and eastern Cassiar Platform occurred in the Cretaceous between 112 and 96 Ma, not in the Early Jurassic as previously proposed by Hansen (1989).
4) Ductile dextral strike-slip shear occurred in the Teslin Zone some time after 96 Ma. The shear zone is local in nature, post dates regional transposition and F_3 folding, and does not characterize regional deformation of the Teslin Zone. Protomylonitic and mylonitic foliations within the metasediments of the shear zone most likely represent reactivated steeply dipping regional transposition fabrics.

REFERENCES

Brown, R. L., Carr, S. D., Harvey, J. L., Williams, P. F and de Keijzer, M. 1995. Structure and tectonic significance of the Teslin suture zone. LITHOPROBE Report No. 44, 1995 SNORCLE Transect Meeting, Calgary, AB, 56-62.

de Keijzer, M. and Williams P.F. 1997b. Fabric Development in the Cassiar Terrane, Yukon Territory: A response to terrane accretion or subsequent extension? GAC-MAC Abstracts: 22: A36.

de Keijzer, M. and Williams, P. F. 1996. Structural analysis in the Teslin Tectonic zone, south-central Yukon. LITHOPROBE Report No. 50, 1996 SNORCLE and Cordilleran Tectonics Workshop, Calgary, AB, 45-53.

de Keijzer, M and Williams, P .F. 1997. A new view on the structural framework of the Teslin Zone, south-central Yukon. LITHOPROBE Report No. 56, 1997 SNORCLE and Cordilleran Tectonics Workshop, Calgary, AB., 96-102.

de Keijzer, M. and Williams, P.F. 1998 Kilometre-scale folding in the Teslin zone, northern Canadian Cordillera, and its tectonic implications for the accretion of the Yukon-Tanana terrane to North America. LITHOPROBE Report No. 64, 1998 SNORCLE and Cordilleran Tectonics Workshop, Vancouver, BC, 130.

de Keijzer, M., Williams, P.F. and Brown, R.L. 1999. Kilometre-scale folding in the Teslin Zone, northern Canadian Cordillera, and its tectonic implications for the accretion of the Yukon-Tanana terrane to North America. *Canadian Journal of Earth Sciences*. (in press)

Gallagher, C.S., Brown R.L., Carr S.D. 1998 Structural geometry of the Cassiar Platform and Teslin Zone, Dycer Creek area, Yukon. LITHOPROBE Report No. 64, 1998 SNORCLE and Cordilleran Tectonics Workshop, Vancouver, BC, 139-151.

Hamner, S. and Passchier, C. 1991 Shear-sense Indicators: A Review. Geological Survey of Canada Paper 90-17. 72 pg

Hansen, V. L. 1989. Structural and kinematic evolution of the Teslin suture zone, Yukon: record of an ancient transpressional margin. Journal of Structural Geology, 11: 717-733.

Hansen, V. L. 1992a. Backflow and margin-parallel shear within an ancient subduction complex. Geology, 20: 717-733.

Hansen, V. L. 1992b. P-T evolution of the Teslin suture zone and Cassiar tectonites, Yukon, Canada: evidence of A- and B-type subduction. Journal of Metamorphic Geology, 10: 239-263.

Hansen, V. L., Mortensen, J. K. and Armstrong, R. L. 1989. U-Pb, Rb-Sr, K-Ar isotopic constraints for ductile deformation and related metamorphism in the Teslin suture zone, Yukon-Tanana terrane, south-central Yukon. Canadian Journal of Earth Sciences, 26: 2224-2235.

Harvey, J. L., Brown, R. L., and Carr, S. D. 1996. Progress in structural mapping in the Teslin Suture Zone, Big Salmon Range, Central Yukon Territory. LITHOPROBE report No. 50, 1996 SNORCLE and Cordilleran Tectonics Workshop, Calgary, AB, 33-41.

Harvey, J. L., Carr, S. D., Brown, R. L., and Gallagher, C. 1997a. Deformation history and geochronology of plutonic rocks near the D'Abbadie fault, Big Salmon Range, Yukon. LITHOPROBE report No.

56. 1997 SNORCLE and Cordilleran Tectonics Workshop, 103-114.

Harvey, J. L., Carr, S. D., and Brown, R. L. 1997b. Ages of deformed plutonic rocks along the D'Abbadie fault, Teslin zone, Big Salmon Range, Yukon: Implications for timing of strike-slip deformation. GAC-MAC Abstracts: 22: A65.

Krogh, T.E. 1973. A low contamination method for hydrothermal decomposition of zircon and extraction of U and Pb for isotopic age determinations. *Geochim. Cosmochim. Acta*, 37: 485-494.

Krogh, T.E. 1982. Improved accuracy of U-Pb ages by the creation of more concordant systems using an air abrasion technique. *Geochim. Cosmochim. Acta*, 46: 637-649.

Mortensen, J. K. 1992. Pre-mid Mesozoic tectonic evolution of the Yukon-Tanana Terrane, Yukon and Alaska. Tectonics, 11: 836-853.

Parrish, R.P. 1990. Monazite U-Pb systematics and applications of monazite dating to geological problems. Can. J. Earth Sci., 27: 1431-1450.

Parrish, R.P. and Krogh, T.E. 1987. Synthesis and purification of 205Pb for U-Pb geochronology. Chem. Geol., 66: 103-110.

Roddick, J.C. 1987. Generalized numerical error analysis with applications to geochronology and thermodynamics. *Geochim. Cosmochim. Acta*, 51: 2129-2135.

Roddick, J.C., Loveridge, W.D., Parrish, R.R. 1987. Precise U/Pb dating of zircon at the sup-nanogram Pb level. Chem. Geol., 66: 111-121.

Schärer, U. 1984. The effect of initial 230^{Th} equilibrium on young U-Pb ages; the Makalu case, Himalaya. Earth Planet. Sci. Lett., 67: 191-204.

Stevens, R. A. and Erdmer, P. 1993. Geology and structure of the Teslin suture zone and related rocks in parts of the Laberge, Quiet Lake, and Teslin map areas, Yukon Territory. Geological Survey of Canada, Paper, 93-1A: 11-20.

Stevens, R.A., and Erdmer, P. 1996. Structural divergence and transpression in the Teslin Tectonic zone, southern Yukon Territory. Tectonics, 15: 1342-1363.

Tempelman-Kluit, D.J. 1979. Transported cataclasite, ophiolite, and granodiorite in Yukon: Evidence of arc-continent collision. Geological Survey of Canada, Paper 79-14, 27p.

Table 1: U-Pb Analysis of Geochronology Samples from the Dycer Creek Area

Fraction[a]	Wt. (ug)[b]	U (ppm)	Pb* (ppm)[c]	$^{206}Pb/^{204}Pb$[d]	Pb (pg)[e]	^{208}Pb %	Th/U	Corr. Coeff.	$^{206}Pb/^{238}U$[f]	$^{207}Pb/^{235}U$[f]	$^{207}Pb/^{206}Pb$[f]	$^{206}Pb/^{238}U$ Age (Ma)[g]	$^{207}Pb/^{235}U$ Age (Ma)[g]	$^{207}Pb/^{206}Pb$ Age (Ma)[g]	% Disc.
YT95-BS082: Mendocina Orthogneiss															
A	91	281	33	5181	34	11.2	.4926	.9462	0.10913±.12	1.8577±.13	0.12346±.04	667.7±1.5	1066.2±1.7	2006±1.5	70.1
B	134	373	40	6404	51	8.4	.3419	.9636	0.10332±.32	1.4049±.32	0.09861±.09	633.9±3.9	891±3.9	1598.1±3.3	63.3
E	10	676	36	1484	17	4.1	.1444	.1346	0.05708±.39	0.4225±.26	0.05369±.44	357.8±0.7	357.8±1.6	357.9±19.9	0.0
YT95-BS107: Last Peak Granite															
A	94	366	14	4984	17	8.4	.3386	.8520	0.03769±.10	0.49971±.12	0.09615±.06	238.5±0.5	411.5±0.8	1150.6±2.3	86.1
B	145	701	14	375	386	5.6	.2042	.5034	0.02133±.16	0.18391±.75	0.06253±.69	136.1±0.4	171.4±2.4	692.4±29.3	81.2
D	52	293	5	884	21	5.7	.2020	.4916	0.01916±.09	0.14205±.37	0.05376±.33	122.4±0.6	134.9±1.1	361.0 ± 15.0	66.7
E	30	1313	24	2911	17	6.1	.2162	.6480	0.01900±.09	0.13945±.16	0.05323±.13	121.3±0.4	132.5±0.5	338.7±5.7	64.8
F-1	50	603	13	2019	21	6.1	.2212	.6388	0.02246±.47	0.18874±.43	0.06092±.39	143.2±1.4	175.5±1.4	636.4±16.6	78.4
M1	15	1458	36	1892	11	43.9	2.563	.5377	0.01546±.10	0.10086±.22	0.04730±	98.9±0.2	97.6±0.4	64.2±8.7	-54.7
M2	7	2876	385	1162	17	89.4	27.66	.4465	0.01559±.10	0.10085±.40	0.04691±	99.7±0.2	97.6±0.7	44.7±17.4	-124.
M3	17	809	109	1959	7	89.6	28.27	.5929	0.01540±.18	0.10058±.30	0.04735±	98.6±0.4	97.3±0.6	66.8±11.5	-48.0
CG97-712: Dycer Creek Stock															
G	11	844	27	942	20	6.8	.2579	.8815	0.03209±.28	0.31841±.32	0.07195±.15	203.6±1.1	280.7±1.6	984.6±6.2	80.6
M1	8	3006	363	3210	9	86.6	21.12	.8379	0.01784±.49	0.11747±.53	0.04774±.29	114.0±1.1	112.8±1.1	86.6±13.9	-31.9
M2	7	2741	377	1446	16	88.2	24.40	.6776	0.01791±.24	0.11717±.34	0.04743±.25	114.5±0.5	112.5±0.7	71.1±12.0	-61.5
M3	3	2706	476	301	33	90.8	32.21	.5579	0.01786±.31	0.11568±1.1	0.04697±.98	114.1±0.7	111.1±2.4	47.8±47.0	-140.
M4	3	2736	513	1369	8	91.2	34.11	.4658	0.01807±.18	0.11838±.49	0.04749±.44	115.5±0.4	113.6±1.1	74.1±20.7	-56.3

[a] s=single crystal, Letters (A-G)=zircon, M=monazite; [b] weighing error is 1 microgram; [c] radiogenic Pb; [d] = Radiogenic Pb, corrected for spike and Pb fractionation of 0.09% ± 0.03%/amu; [e] total common Pb in analysis corrected for spike and fractionation; [f] corrected for Pb and U laboratory blank where 208/204 : 207/204 : 206/204 are 19.02:15.65:38.23, errors are 1 standard error of the mean in percent for ratios and 2 standard errors of the mean when expressed in Ma, [g] corrected for common Pb and laboratory blank, errors are 2 standard errors of the mean in Ma.

Table 1: U-Pb Analysis of Geochronology Samples from the Dycer Creek Area

Fraction[a]	Wt. (ug)[b]	U (ppm)	Pb* (ppm)[c]	$^{206}Pb/^{204}Pb$[d]	Pb (pg)[e]	^{208}Pb %	Th U	Corr. Coeff.	$^{206}Pb/^{238}U$[f]	$^{207}Pb/^{235}U$[f]	$^{207}Pb/^{206}Pb$[f]	$^{206}Pb/^{238}U$ Age (Ma)[g]	$^{207}Pb/^{235}U$ Age (Ma)[g]	$^{207}Pb/^{206}Pb$ Age (Ma)[g]	% Disc.
YT95-BS082: Mendocina Orthogneiss															
A	91	281	33	5181	34	11.2	.4926	.9462	0.10913±.12	1.8577±.13	0.12346±.04	667.7±1.5	1066.2±1.7	2006±1.5	70.1
B	134	373	40	6404	51	8.4	.3419	.9636	0.10332±.32	1.4049±.32	0.09861±.09	633.9±3.9	891±3.9	1598.1±3.3	63.3
E	10	676	36	1484	17	4.1	.1444	.1346	0.05708±.39	0.4225±.26	0.05369±.44	357.8±0.7	357.8±1.6	357.9±19.9	0.0
YT95-BS107: Last Peak Granite															
A	94	366	14	4984	17	8.4	.3386	.8520	0.03769±.10	0.49971±.12	0.09615±.06	238.5±0.5	411.5±0.8	1150.6±2.3	86.1
B	145	701	14	375	386	5.6	.2042	.5034	0.02133±.16	0.18391±.75	0.06253±.69	136.1±0.4	171.4±2.4	692.4±29.3	81.2
D	52	293	5	884	21	5.7	.2020	.4916	0.01916±.09	0.14205±.37	0.05376±.33	122.4±0.6	134.9±1.1	361.0 ±	66.7
E	30	1313	24	2911	17	6.1	.2162	.6480	0.01900±.09	0.13945±.16	0.05323±.13	121.3±0.4	132.5±0.5	338.7±5.7	64.8
F-1	50	603	13	2019	21	6.1	.2212	.6388	0.02246±.47	0.18874±.43	0.06092±.39	143.2±1.4	175.5±1.4	636.4±16.6	78.4
M1	15	1458	36	1892	11	43.9	2.563	.5377	0.01546±.10	0.10086±.22	0.04730±	98.9±0.2	97.6±0.4	64.2±8.7	-54.7
M2	7	2876	385	1162	17	89.4	27.66	.4465	0.01559±.10	0.10085±.40	0.04691±	99.7±0.2	97.6±0.7	44.7±17.4	-124.
M3	17	809	109	1959	7	89.6	28.27	.5929	0.01540±.18	0.10058±.30	0.04735±	98.6±0.4	97.3±0.6	66.8±11.5	-48.0
CG97-712: Dycer Creek Stock															
G	11	844	27	942	20	6.8	.2579	.8815	0.03209±.28	0.31841±.32	0.07195±.15	203.6±1.1	280.7±1.6	984.6±6.2	80.6
M1	8	3006	363	3210	9	86.6	21.12	.8379	0.01784±.49	0.11747±.53	0.04774±.29	114.0±1.1	112.8±1.1	86.6±13.9	-31.9
M2	7	2741	377	1446	16	88.2	24.40	.6776	0.01791±.24	0.11717±.34	0.04743±.25	114.5±0.5	112.5±0.7	71.1±12.0	-61.5
M3	3	2706	476	301	33	90.8	32.21	.5579	0.01786±.31	0.11568±1.1	0.04697±.98	114.1±0.7	111.1±2.4	47.8±47.0	-140.
M4	3	2736	513	1369	8	91.2	34.11	.4658	0.01807±.18	0.11838±.49	0.04749±.44	115.5±0.4	113.6±1.1	74.1±20.7	-56.3

[a] s=single crystal, Letters (A-G)=zircon, M=monazite; [b] weighing error is 1 microgram; [c] radiogenic Pb; [d] = Radiogenic Pb, corrected for spike and Pb fractionation of 0.09% ± 0.03%/amu; [e] total common Pb in analysis corrected for spike and fractionation; [f] corrected for Pb and U laboratory blank where 208/204 : 207/204 : 206/204 are 19.02:15.65:38.23, errors are 1 standard error of the mean in percent for ratios and 2 standard errors of the mean when expressed in Ma, [g] corrected for common Pb and laboratory blank, errors are 2 standard errors of the mean in Ma.

gure 1 - Regional geology of the Dyeer Creek Area showing U-Pb sample locations and ages. YT95-BS107 is located north of the mapping limits and is not located the map. Structural data is a compilation of Gallagher (1997) and Harvey (1995)

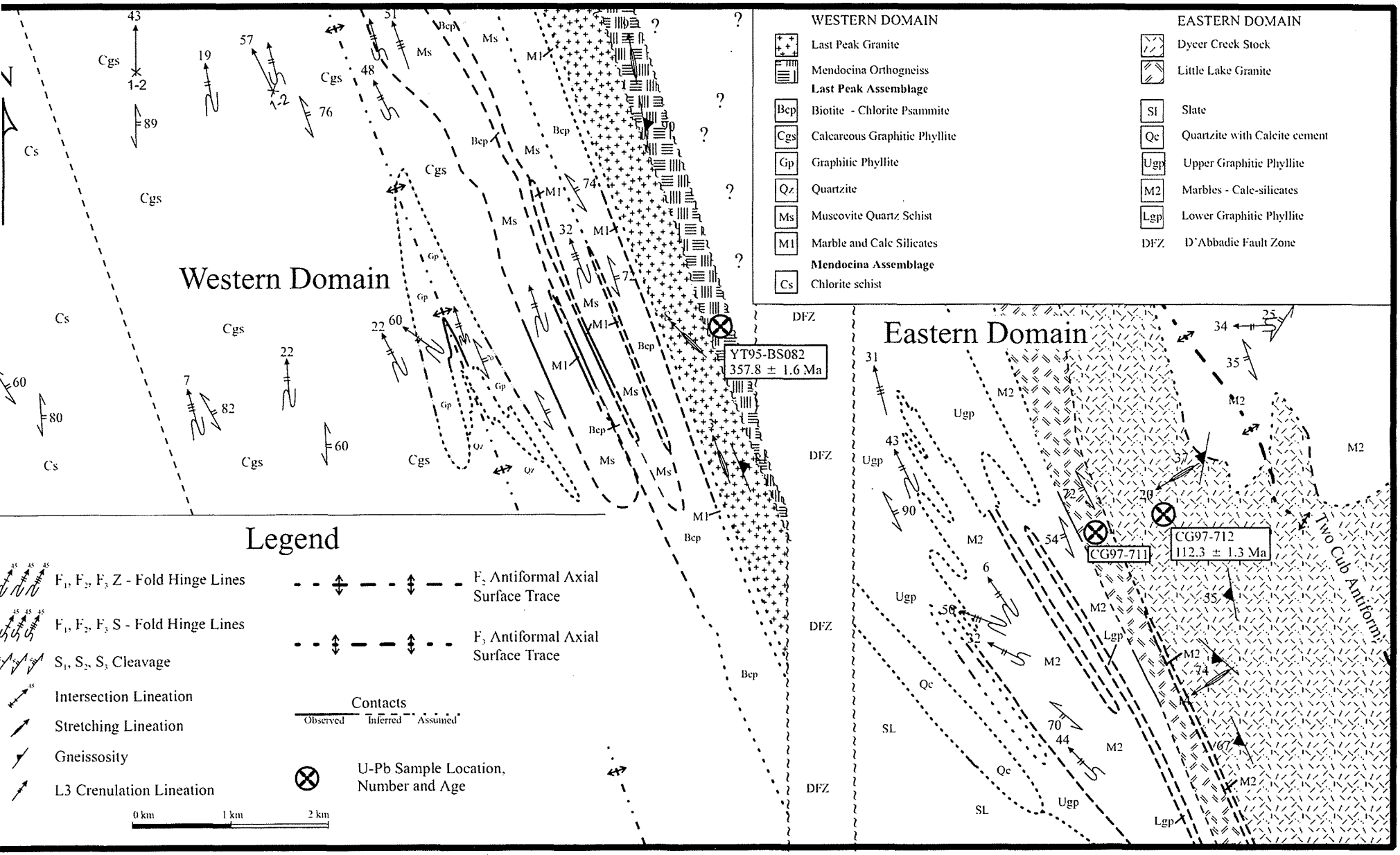

Figure 2: Simplified block diagram of the structural fabric relationships in the Mendocina orthogneiss. The shaded plane represents the plane normal to the C-plane orientation of the rock.

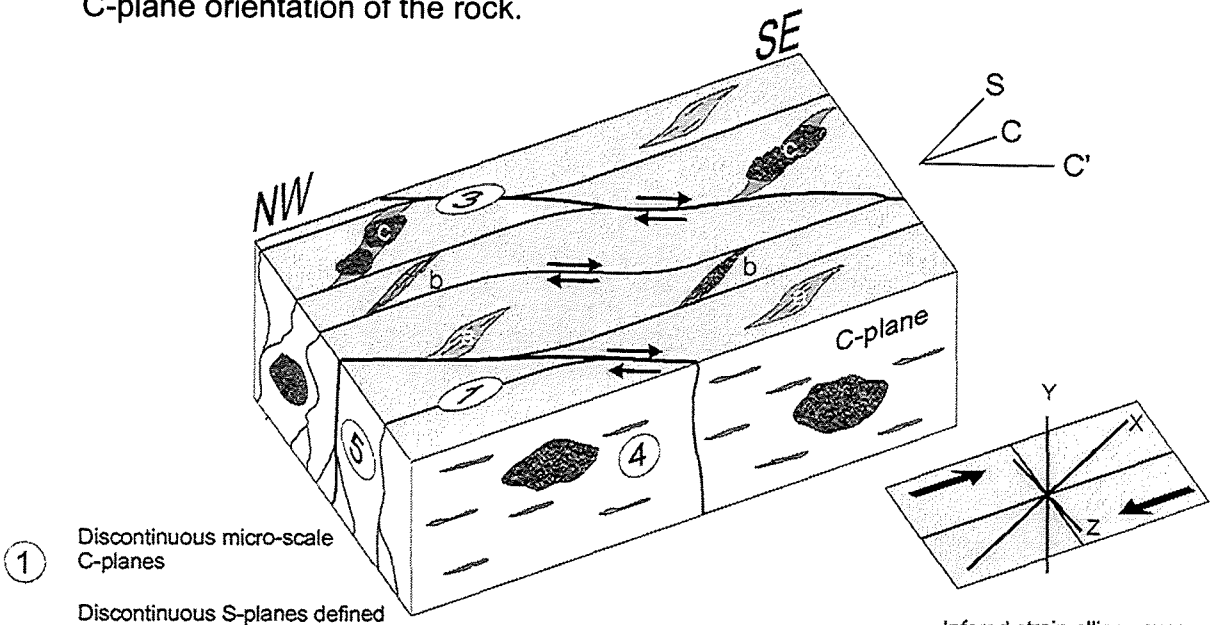

1. Discontinuous micro-scale C-planes
2. Discontinuous S-planes defined by mica (a) fish, (b) quartz ribbons and (c) pulled-apart and sigma K-feldspar porphyroclasts
3. Cm-spaced, extensional shear bands
4. Intersection lineation observed on the C-plane surface
5. Conjugate shear bands in the plane almost normal to the stretching lineation

Infered strain ellipse axes orientation in the block diagram. Shaded plane is equivalent to the plane normal to the C-fabric of the block diagram.

Figure 3: Concordia diagram of YT95-BS082 (Mendocina Orthogneiss) U-Pb zircon analyses (see text for interpretation).

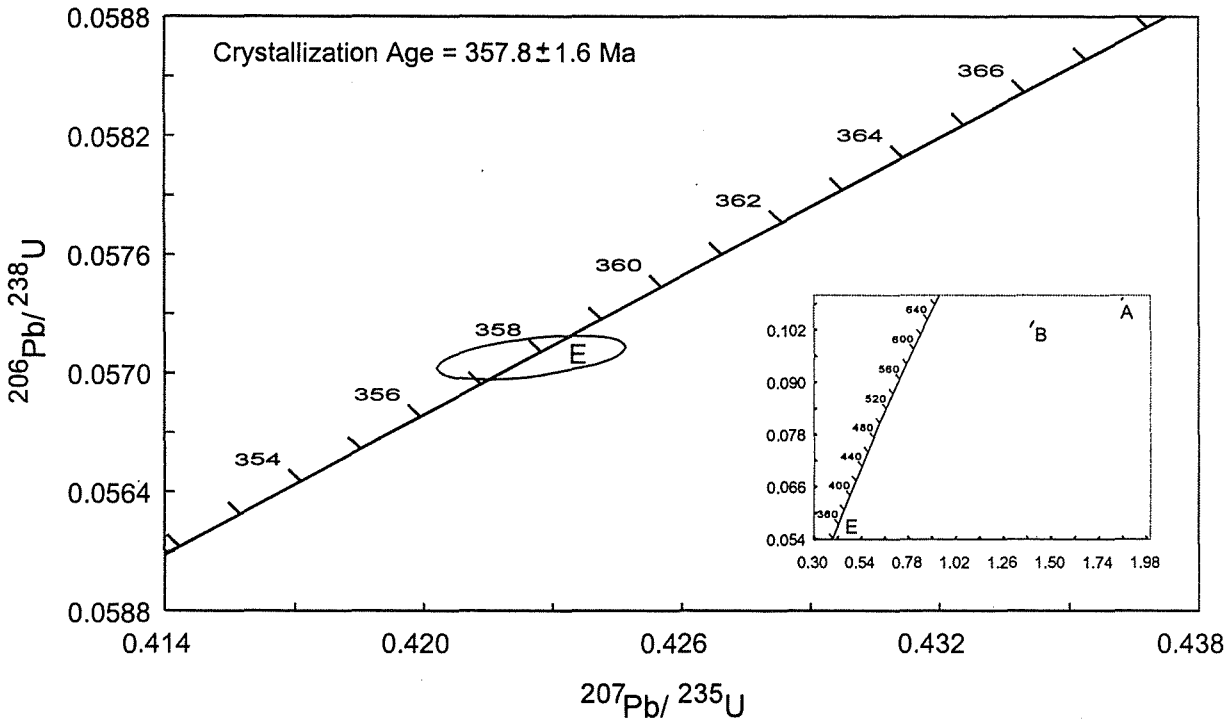

Figure 4: Concordia diagram of YT95-BS107 (Last Peak Granite) U-Pb monazite and zircon analyses (see text for interpretation).

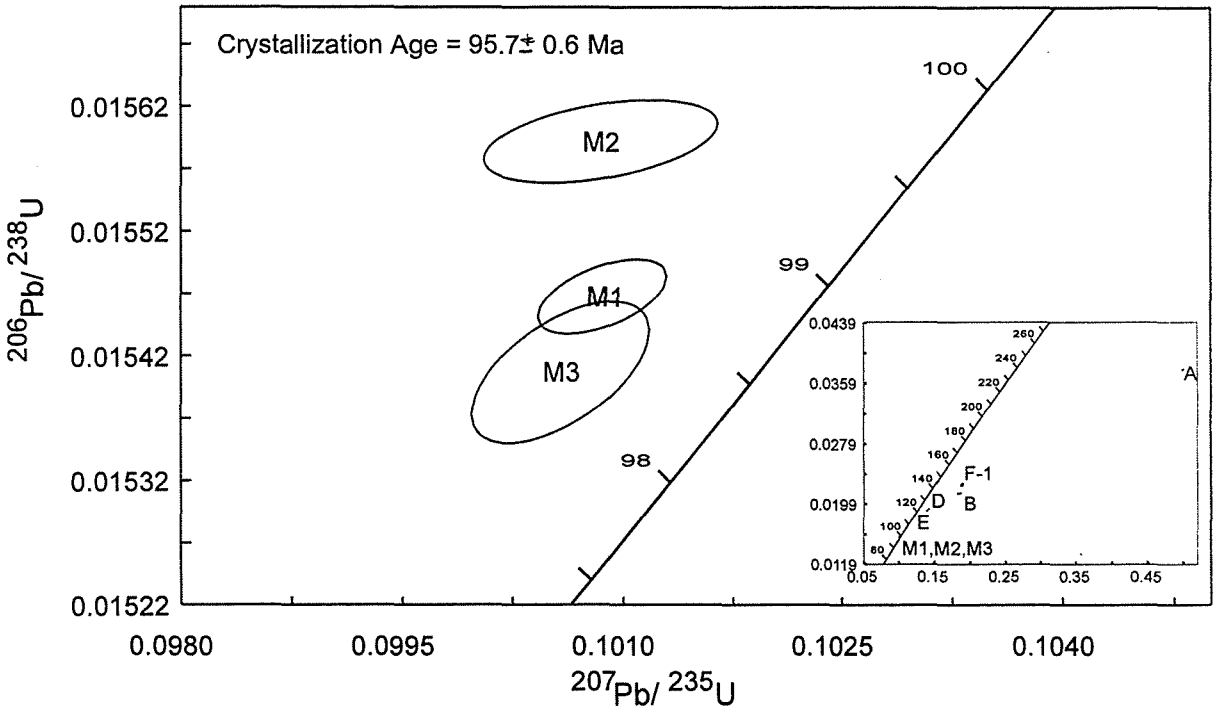

Figure 5: Concordia diagram of CG97-712 (Dycer Creek Stock) U-Pb monazite and zircon analyses (see text for interpretation).

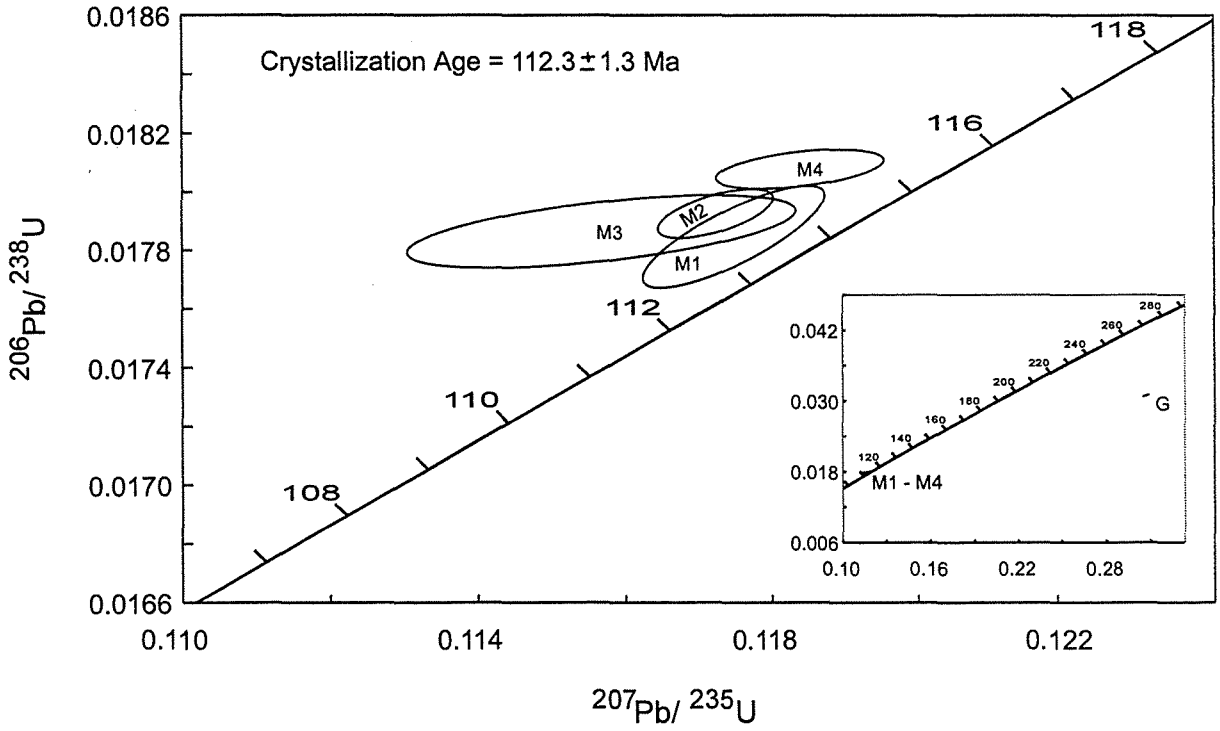

PRESTACK TIME MIGRATION WITH RELATIVE AMPLITUDE PRESERVATION: RESULTS FROM THE SNORCLE TRANSECT

Hugh D. Geiger, Rolf Maier, Arie J. van der Velden, Frederick A. Cook

Department of Geology and Geophysics

University of Calgary

Calgary Alberta T2N 1N4

ABSTRACT

A processing flow for crustal seismic reflection data is presented that attempts to preserve relative reflection strength over a wide range of dips and depths. Currently, the processing flow adopted by LITHOPROBE includes an automatic gain control (AGC) applied to input traces, stacking of common midpoint (CMP) gathers without dip moveout (DMO), poststack time migration, and coherency filtering prior to display and interpretation. This processing flow, although effective in imaging the structural relationships revealed by continuity and patterns of reflections, does not preserve relative amplitude.

The new processing flow hinges on equivalent offset migration (EOM), a fast method for prestack time migration of reflection seismic data (Bancroft and Geiger, 1994; Bancroft et. al, 1998). The method is divided into two steps: (1) a gathering process that forms common scatterpoint (CSP) gathers without requiring DMO; and (2) a simplified Kirchhoff migration which is performed on the CSP gathers. Relative amplitude is preserved by careful preprocessing of input traces, followed by theoretically correct scaling and filtering factors as required by prestack migration theory. The new flow is tested on a portion of the LITHOPROBE SNORCLE transect Line 1. The high fold of the prestack migrated output traces provides good signal to noise ratios that gives comparable results to the conventional semblance filtered result. In addition to better relative amplitude information, the new flow provides consistent imaging velocities valid over a range of dips, which provides more confidence in the interpretation of subtle concordant and discordant reflector relationships.

INTRODUCTION

The conventional approach to crustal seismic reflection processing, as currently adopted by LITHOPROBE, includes an automatic gain control (AGC) applied to input traces, stacking of common midpoint (CMP) gathers without dip moveout (DMO), poststack time migration, and coherency filtering prior to display and interpretation. This processing flow, although effective in imaging the structural relationships revealed by continuity and patterns of reflections, does not preserve relative amplitude. In addition, the image is first created as an unmigrated stack, where it is well known that reflectors and their respective imaging velocities are mispositioned. Poststack time migration attempts to accurately position dipping reflections in the image, but the final position of dipping events is a function of the migration velocity. More confidence in the imaging velocities and the relative positions of dipping events can be achieved with a prestack time migration.

Equivalent offset migration (EOM) (Bancroft and Geiger, 1994; Bancroft et. al, 1998) is a fast method for prestack time migration of reflection seismic data. The method is divided into two steps: (1) a gathering process that forms common scatterpoint (CSP) gathers without requiring DMO; and (2) a simplified Kirchhoff migration which is performed on the CSP gathers. Relative amplitude is preserved by careful preprocessing of input traces, followed by theoretically correct scaling and filtering factors as required by prestack migration theory. EOM can be efficiently applied to the large 2D data volumes typically encountered in crustal seismic reflection processing.

The 90 km portion of the LITHOPROBE SNORCLE (SLave NOrthern Cordillera Lithospheric Evolution) profile selected for this study is outlined by the yellow box in Figure 1, and shown in a variety of migrated images in Figures 3-6. The portion straddles parts of the accreted Hottah and Fort Simpson terrains as well as the Fort Simpson Basin, which developed along a west-facing passive continental margin between ~1.84-0.6 Ga (Cook et al., 1998). The test portion includes a variety of shallow and deep structures, including some of the steepest dipping reflectors imaged in the SNORCLE profile (the east or right side between 1-5 s, see Figures 3-6), a possible syncline structure (west side between 5-7 s), a clear reflection Moho (west side at 11s), and subduction plate geometries from an interpreted fossil subduction zone (east side, reflection packages at 9 s and 12 s).

CONVENTIONAL PROCESSING

The conventional processing methodology adopted by LITHOPROBE does not preserve relative amplitudes primarily because an AGC is employed in lieu of spherical divergence corrections and trace balancing. An AGC has the additional benefit of balancing traces and reducing the effort required for data cleaning (trace killing). The data are then ready for conventional velocity analysis procedures prior to stack and poststack migration (statics and

deconvolution being assumed). The poststack phase shift migration uses a constant velocity of 6 km/s. The poststack migrated result is shown in Figure 3, plotted with a trace bias to remove the trace zero line which would dominate the plot at the small plotting scale. Figure 4 is the result typically used for interpretation. The CMP stack is semblance filtered, poststack migrated using a phase-shift migration, semblance filtered again, and plotted with a trace bias.

RELATIVE-AMPLITUDE: DATA PREPARATION AND EOM

The relative-amplitude processing methodology of this study differs from conventional processing in two areas. The first is a careful statistical cleaning of the data, primarily using median filters to reject outliers, along with gather balancing in the shot and receiver domains. The second is prestack time migration by the method of equivalent offset. The following steps outline the method in detail:

Step 1: Refraction and residual statics determined by conventional means are applied to the input traces. A suitable replacement velocity and constant datum are chosen so that traveltimes are similar to those from the acquisition datum. A trace-by-trace gap deconvolution is applied.

Step 2: All traces whose amplitude (in one of 5 time windows) exceeds the median value by a chosen factor (4.5) are removed.

Step 3: All traces which show an amplitude decrease of less than 10 percent between the time windows of 4.5 - 6.5 s and 13 - 15 s respectively are killed.

Step 4: All very weak traces are killed (those with amplitudes less than 1 percent of the average trace amplitudes in the gather).

Step 5: Traces with RMS amplitudes deviating more than 3 standard deviations from the mean in the time window 6 to 10 s are killed.

Step 6: Traces are balanced in the shot domain and then in the receiver domain. The median absolute amplitude of the time window from 13 - 16 s is used. Receivers producing less than 11 live traces are considered bad and their traces killed.

Step 7: CSP gathers are formed using theoretically correct scaling factors based on Kirchhoff summation weights and Claerbout's imaging condition (Lumley, 1989; see also Hanitzsch, 1995 and Winbow, 1995).

Step 8: Prestack time migration imaging velocities are determined from constant velocity stacks of the CSP gathers.

Step 9: The final migrated image is created using Kirchhoff NMO and stack of the CSP gathers, followed by the differential filter of 2D Kirchhoff migration theory.

COMPARISON OF MIGRATED SECTIONS

At the chosen scale, the conventional poststack migrated result of AGC'd input traces without semblance filtering (Figure 3) is the better result for comparison with the EOM results (Figures 5 and 6). The semblance filtered result (Figure 4) highlights textural changes in the image by enhancing event continuity and reducing background noise. The resulting image is preferable for interpretation of large-scale crustal geometries, but lacks the fine detail visible in the other migrated images. Tests showed that variable density displays using a nonlinear greyscale produced the largest dynamic range and hence best images for comparison. However, these images could not be faithfully plotted. All figures are displayed using the identical plotting parameters optimally chosen for the conventional displays. Although this permits a comparison of relative levels of signal and noise within and amongst images, the large clip factor (trace excursion of 4) reduces the resolution of higher-amplitude steeply-dipping events in the EOM results.

The AGC'd EOM result (Figure 5) shows better imaging of reflection events in the shallow section (1-6 s). The relative-amplitude EOM result (Figure 6) shows broad light and dark regions that suggests that signal-to-noise ratios are comparable to the conventional semblance filtered result (Figure 4).

Both EOM results appear to have produced a degraded image in the very near surface (upper 0.5 seconds). Conventional 2D processing incorporates a variable cross-line bin location. EOM, which honors a true 3D geometry for sources and receivers relative to the output location, produces a poor image in the shallow section when the output locations along the CDP bin line are not close to the source-receiver pairs on the acquisition line.

CONCLUSIONS

Prestack time migration with relative-amplitude preservation is a viable alternative to conventional processing methods. Image quality is similar to and in some cases better than conventional poststack migrated results.

The main benefit of EOM is the sensitivity and accuracy of the velocity analysis in the CSP gather domain (Bancroft et al. 1998). Reflection events are imaged directly to their true time-migrated position independent of dip, without the intermediate step of event imaging in the CMP stack domain. Conventional processing, on the other hand, first images reflections in the CMP stack, then repositions the reflections during poststack migration. Using EOM, an interpreter can be more confident of concordant and discordant relationships between reflectors. Relative amplitude information provides an interpreter with additional information to differentiate reflections - information content that is diminished when data are AGC'd.

In the future, we plan to combine this processing technique with seismic skeletonization (Vasudevan and Cook 1998), which will allow the interpreter

to extract more accurate dip and amplitude information from the migrated image.

ACKNOWLEDGMENTS

This work is supported in part by the Natural Sciences and Engineering Research Council of Canada. Industry participants in this phase of the SNORCLE reflection program are UNOCAL Canada and PanCanadian Petroleum. The CREWES project at the University of Calgary generously provided computer facilities for the prestack migration. Henry Bland, Darren Foltinek and Xinxiang Li of CREWES provided valuable programming assistance. Elissa Lynn and Kris Vasudevan of LSPF provided much support during all phases of the work.

REFERENCES

Bancroft, J.C. and Geiger, H.D., 1994. Equivalent offsets and CRP gathers for prestack migration: 64th Ann. Internat. Mtg., Soc. Expl. Geophys., Expanded Abstracts, 672-675.

Bancroft, J.C., Geiger, H.D. and Margrave, G.F., 1998. The equivalent offset method of prestack time migration: Geophysics, 63, 2042-2053.

Cook, F.A., van der Velden, A.J. and Hall, K.H. and Roberts, B.J., 1998. Frozen subduction in Canada's Northwest Territories: Lithoprobe deep lithospheric reflection profiling of the western Canadian shield, Tectonics, in press.

Hanitzsch, C. 1995. Amplitude preserving prestack depth migration. Ph.D. thesis, Univ. Karlsruhe.

Lumley, D.E., 1989. Kirchhoff prestack depth migration: Imaging conditions and amplitude recovery: 59th Ann. Internat. Mtg. Soc. Expl. Geophys., Expanded Abstracts, 1336-1339.

Vasudevan, K. and Cook, F.A., 1998. Skeltons and fractals - a statistical approach to deep crustal seismic data processing and interpretation, Tectonophysics, 286, 93-109.

Winbow, G. 1995. Controlled amplitude time migration, 65th Ann. Internat. Mtg. Soc. Expl. Geophys., Expanded Abstracts, 1153-1155.

FIGURES

Figure 1: Study area (yellow box).

Figure 2a: Unscaled shot with all traces.

Figure 2b: Unscaled shot with good traces only.

Figure 2d: Automatically rejected traces.

Figure 2d: Balanced and scaled shot with good traces, input to relative amplitude EOM.

Figure 2e: Shot with AGC, input to poststack migrations (Figures 3 and 4) and the AGC EOM.

Figure 3: Poststack phase-shift migrated CMP stack (800 ms prestack AGC).

Figure 4: Semblance filtered CMP stack, phase-shift migrated, semblance filtered (800 ms prestack AGC).

Figure 5: EOM migration (800 ms prestack AGC).

Figure 6: EOM migration with relative amplitude preservation (no prestack AGC).

Input data for all displayed sections have identical refraction statics, residual statics, and gap deconvolution applied.

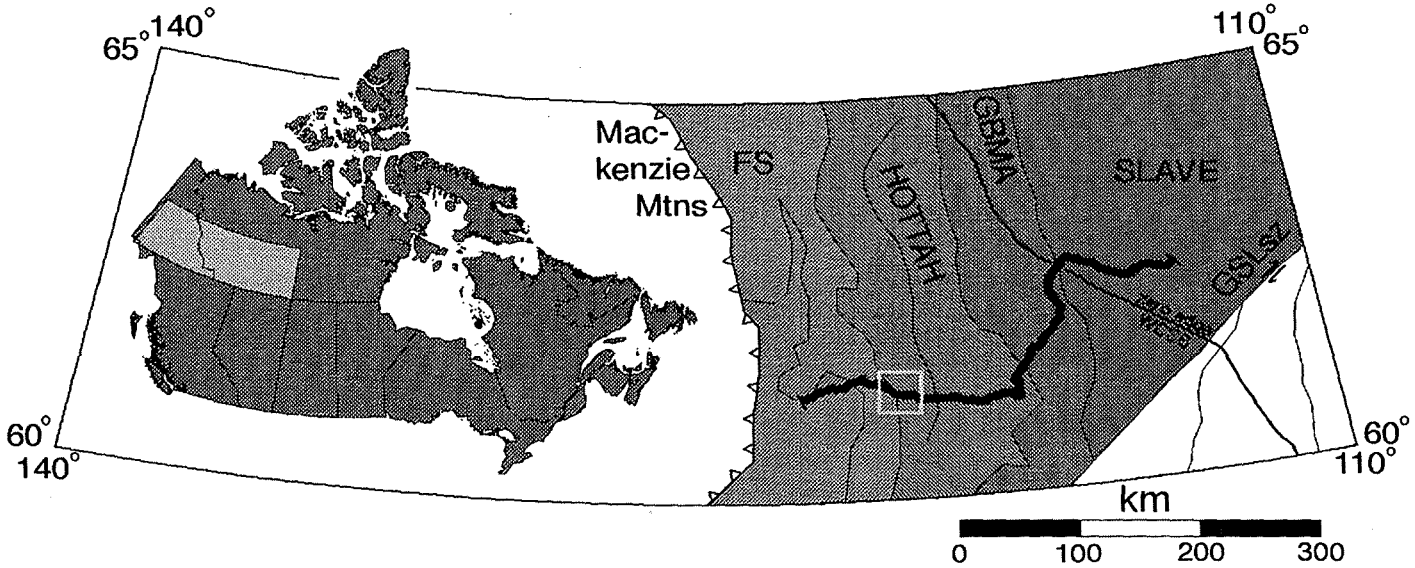
65°
140°
110°
65°
Mac-
kenzie
Mtns
FS
HOTTAH
GSBMA
SLAVE
GSLsz
60°
140°
60°
110°
km
0
100
200
300

Figure 1

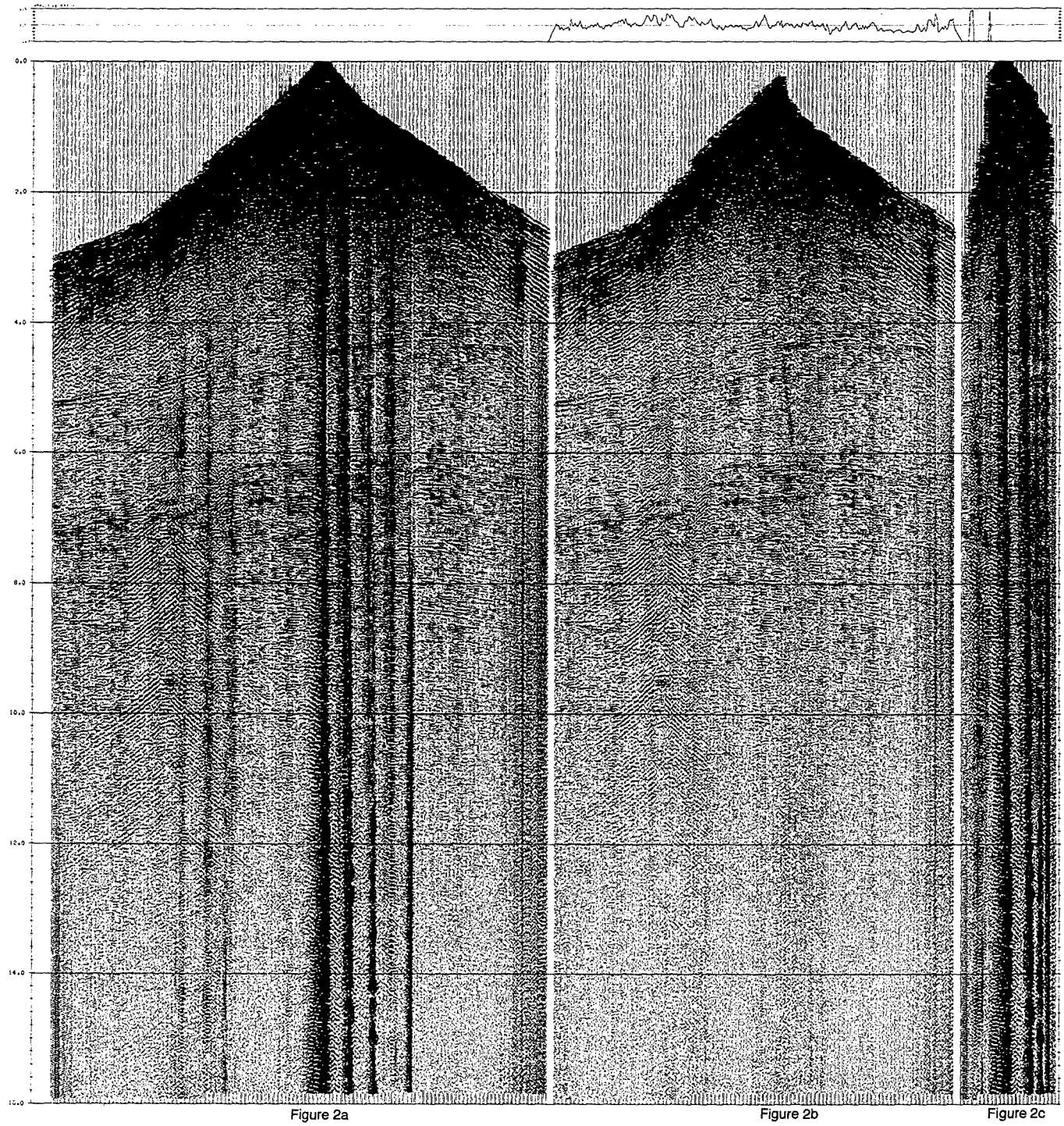

Figure 2a Figure 2b Figure 2c

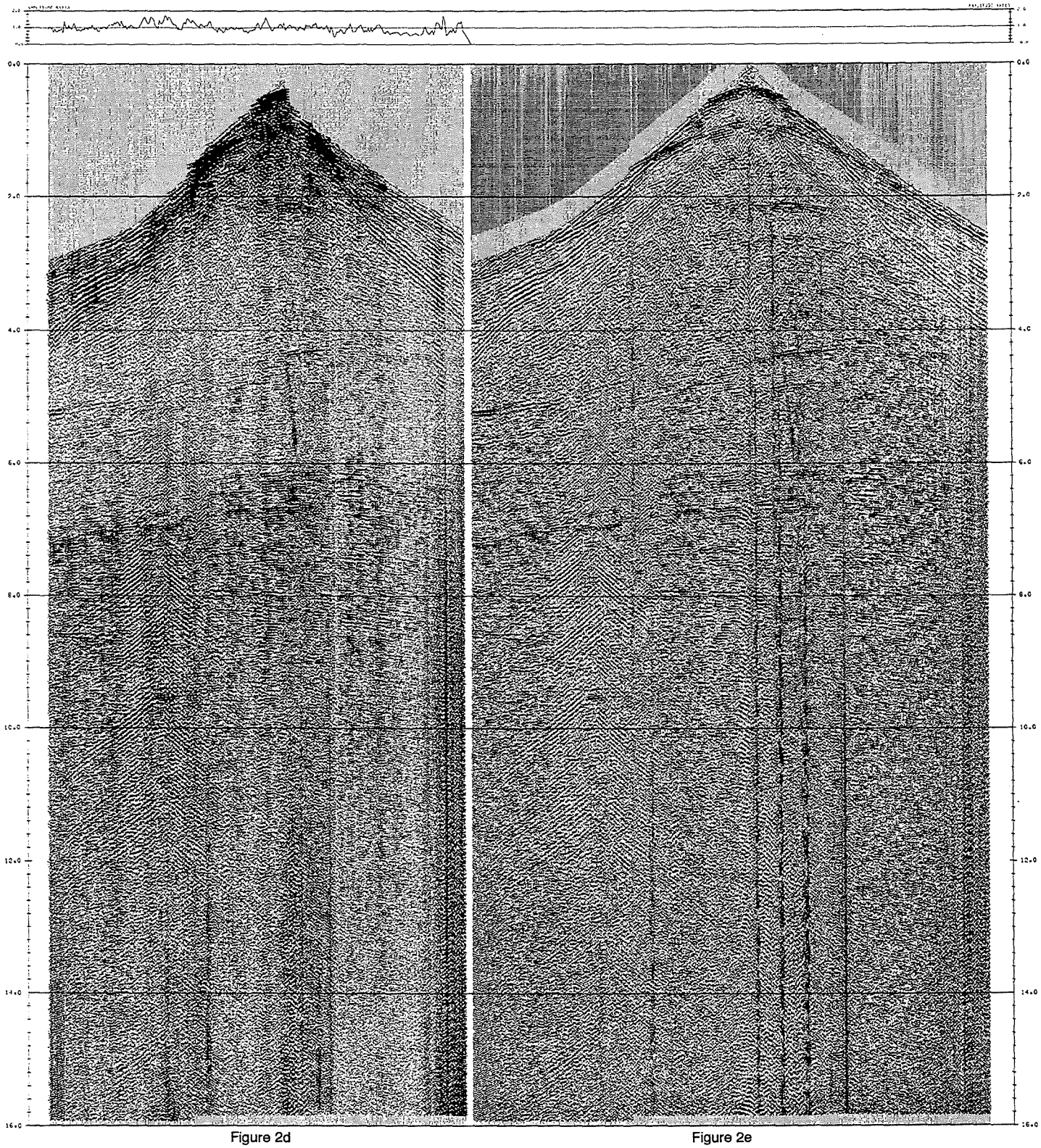

Figure 2d

Figure 2e

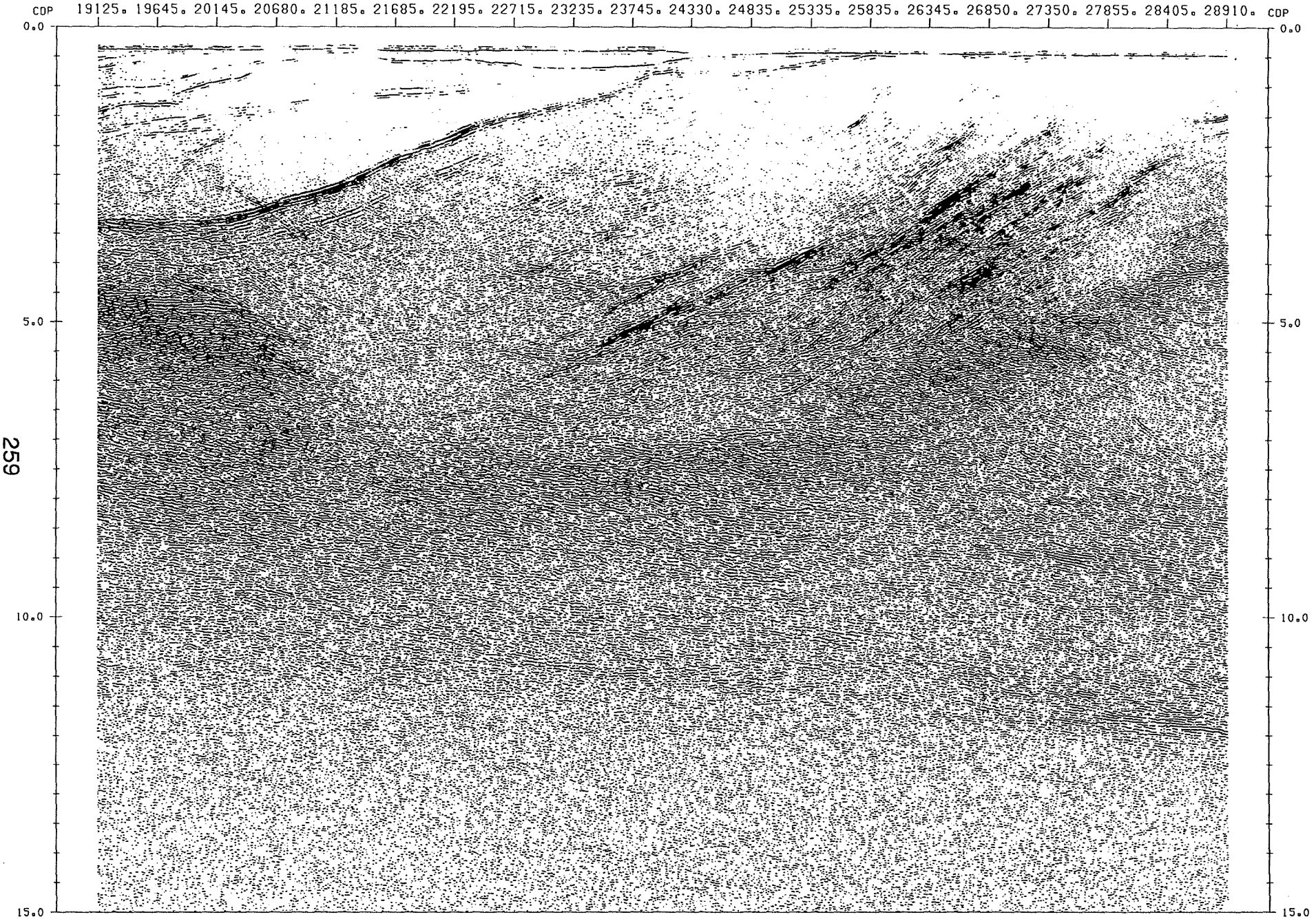
CDP 19125. 19645. 20145. 20680. 21185. 21685. 22195. 22715. 23235. 23745. 24330. 24835. 25335. 25835. 26345. 26850. 27350. 27855. 28405. 28910. CDP
0.0
5.0
10.0
15.0

Figure 3

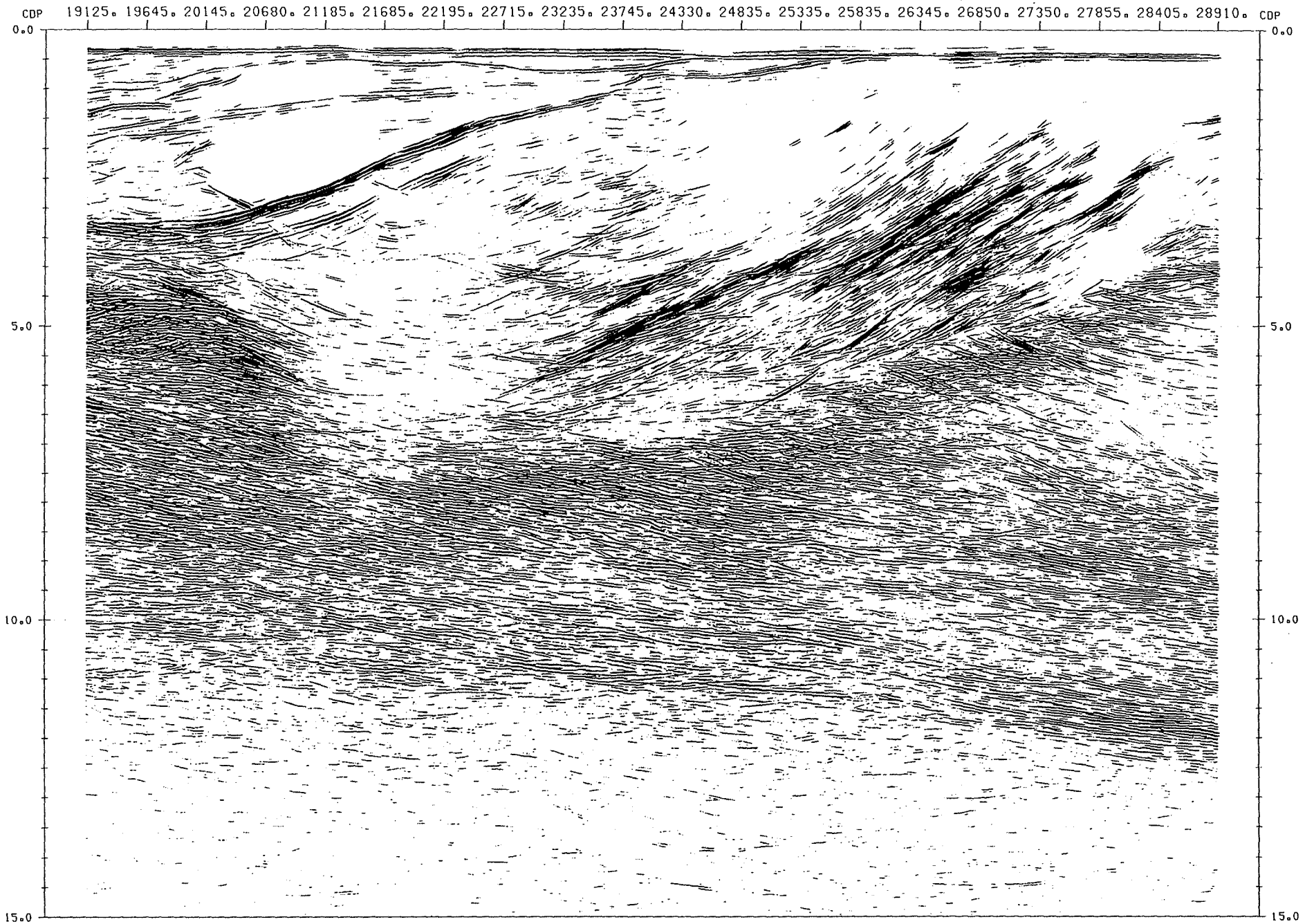
CDP 19125. 19645. 20145. 20680. 21185. 21685. 22195. 22715. 23235. 23745. 24330. 24835. 25335. 25835. 26345. 26850. 27350. 27855. 28405. 28910. CDP
0.0
5.0
10.0
15.0

Figure 4

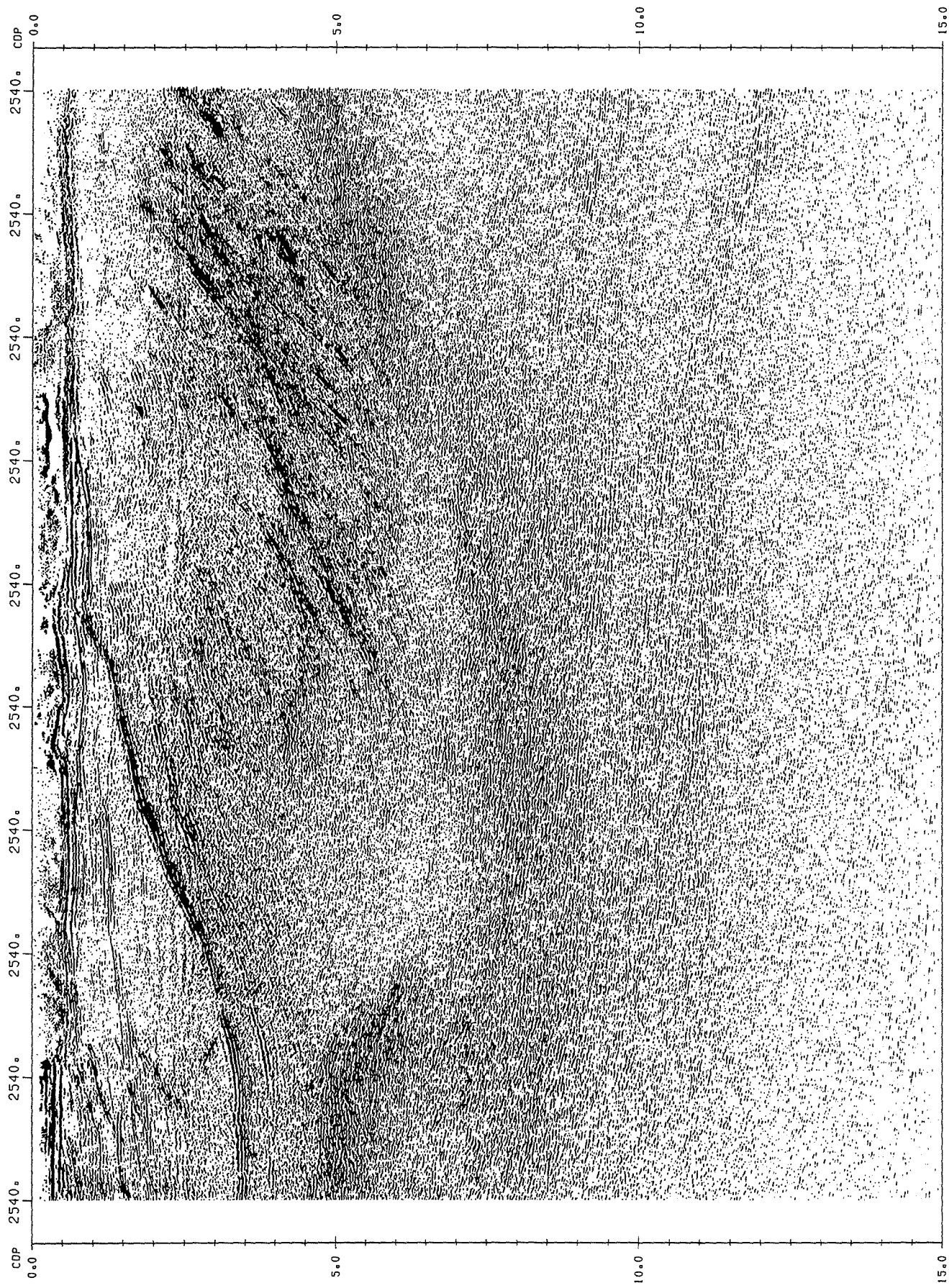

Figure 5

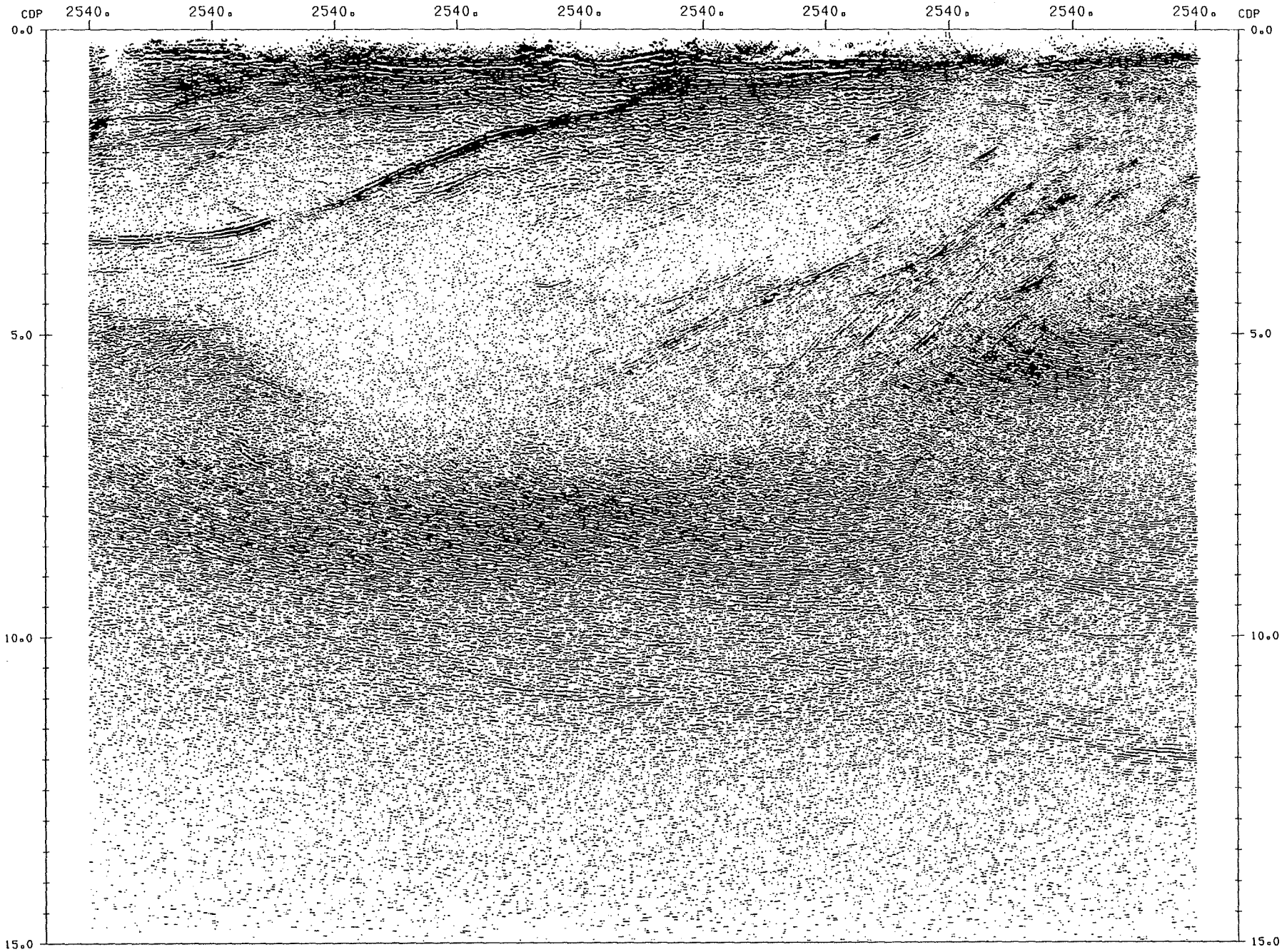
CDP
2540.
2540.
2540.
2540.
2540.
2540.
2540.
2540.
2540.
2540.
CDP
0.0
0.0
5.0
5.0
10.0
10.0
15.0
15.0

Figure 6

Eocene Ootsa Lake Group volcanics in the northern Nechako River and southern Fort Fraser map sheets, central British Columbia

Nancy Grainger, University of Alberta, 1-26 Earth Sciences Bldg, University of Alberta, Edmonton, AB, T6G 2E3 (nancy.grainger@ualberta.ca)

Bob Anderson, Geological Survey of Canada, 101-605 Robson St, Vancouver, BC, V6B 5J3 (banderson@gsc.nrcan.gc.ca)

The geology of the northern Nechako River (NTS 93F) and southern Fort Fraser (NTS 93K) map areas is dominated by the rocks of an Eocene bimodal volcano-plutonic complex. This complex developed coeval with the terminal cooling of a nearby, extensional metamorphic complex and contemporaneous with trans-tensional tectonics. Locally rocks of the predominantly felsic Ootsa Lake and overlying andesitic Endako groups are well known. Regionally, however, these rocks are poorly known and understood. In particular the relationships amongst the sequence of magmatism and the timing and structural style of extensional tectonics remain unresolved.

Recent mapping, as part of the Nechako NATMAP project, has found that the Ootsa Lake Group consists predominately of variegated, flow laminated rhyolitic flows and domes, with lesser portions of crystal and lithic-crystal tuff, pyroclastic and autoclastic breccia, and minor dacite and andesite flows. Cospatial intrusions include aphanitic or porphyritic rhyolite, miarolitic leucogranite and seriate biotite monzogranite. Local stratigraphy within the northwestern Nechako River area comprises of; a basal hb-plag porphyritic andesite, medial flow laminated rhyolites and breccia and upper felsic tuff and breccia. Distinct rhyolite ash-lignite beds mark the top of the Ootsa Lake Group and in addition to glassy quenched flow bases and reworking of lithic tuff units, suggest local shallow water environments.

Regional K/Ar and Ar/Ar age dates for the Ootsa Lake Group range from 54.0 to 47.6 Ma within the Fort Fraser and Nechako River map areas and 55.6 to 47.4 Ma within the adjacent Whitesail and Smithers map areas. Recent Ar/Ar age dating within the Hallett Lake map area (NTS 93F15) has identified a more restricted period of Ootsa Lake volcanism ca. 52-50 Ma and ca 47-51 Ma for the Endako Group (M. Villeneuve, unpub. data *in* Anderson et al., 1998). Preliminary U/Pb age dates support these age ranges for the Ootsa Lake Group.

Ootsa Lake Group rocks are silicic, calc-alkaline, very high-K and large ion lithophile-rich. Rocks of the Endako Group are mildly alkaline, transitional to calc-alkaline and high-K. Coeval miarolitic leucocratic granite and bimodal plutonic rocks are silicic, calc-alkaline, high-K, meta to peraluminous and overlap the compositional range of the Ootsa Lake Group volcanic rocks. Tracer isotope data indicates a primitive magmatic source for both the Endako and Ootsa Lake groups with Sr_i = 0.70401 to 0.70442 and ε_{Nd} = +1.3 to +3.2.

Ongoing work is focused on further constraining the timing of Ootsa Lake volcanism and related plutonism and, in particular, using geochemistry and tracer isotopes to examine the magmatic source of the Ootsa Lake Group and it's genetic relationship with the subsequent Endako Group volcanism, coeval plutonism and nearby coeval Newman volcanism.

References

Anderson, R.G., Snyder, L.D., Wetherup, S., Struik, L.C., Villeneuve, M.E., and Haskin, M.1998: Mesozoic to Tertiary Volcanism and Plutonism in Southern Nechako NATMAP Area: Part 1: Influence of Eocene tectonics and magmatism on the Mesozoic arc and orogenic collapse: New developments in the Nechako River map area; in L.C. Struik and D.G. MacIntyre, editors, New Geological Constraints on Mesozoic to Tertiary Metallogenesis and on Mineral Exploration in central British Columbia: Nechako NATMAP Project; Geological Association of Canada, Cordilleran Section, March 27, 1998, Short Course Notes, 26 pages.

Early Tertiary Forearc Igneous and Metamorphic Activity Recorded in the Leech River Complex, Southern Vancouver Island

Wesley G. Groome*[1], Derek J. Thorkelson[1], Richard M. Friedman[2], James K. Mortensen[2], Nick W. D. Massey[3]

(1) Earth Sciences Program, Simon Fraser University; (2) Department of Earth and Ocean Sciences, University of British Columbia; (3) Geological Survey Branch, BC Ministry of Energy and Mines

E-Mail : wgg@sfu.ca

Abstract

Numerous Early Tertiary intrusions are found in the Leech River Complex, located on southern Vancouver Island. In addition to igneous activity, the Leech River Complex was affected by multiple stages of deformation and metamorphic activity. Two phases of deformation are recorded in this region. Metamorphic and igneous activity are closely related to one another, as well as to deformation. Metamorphism is syn- to post-deformation, as is igneous activity. There is a strong correlation between igneous and metamorphic activity, indicating they are contemporaneous. New isotopic age determinations from intrusive rocks provide a constraint on the absolute timing of igneous and metamorphic activity in this terrane.

Igneous activity on southern Vancouver Island is part of a larger belt of early Tertiary forearc activity extending from the Chugach Terrane in Alaska to the Crescent Basalts in Washington and Oregon. Paleomagnetic and structural evidence suggests that this belt was once much less extensive, and has been smeared out by dextral strike slip faulting.

Introduction

The Walker Creek and Jordan River intrusions are found in the Leech River Complex, on southern Vancouver Island (Figure 1). The Leech River Complex is part of the Pacific Rim Terrane found on Vancouver Island and correlative in the San Juan Islands (Brandon 1989). The complex is a metamorphosed and twice-deformed package of pelitic, volcanic and arenaceous rocks, with minor intrusive rocks. Metamorphic grade ranges from a lower greenschist assemblage of chlorite-sericite to an amphibolite assemblage of staurolite-andalusite-garnet.

The Leech River Complex is fault bounded on the north, south and east, to the west, the complex lies against the Pacific Ocean. In the north and east, the Leech River Complex is separated from Wrangellian rocks by the San Juan Fault System (Muller 1980) (Figure 1). In the south, the Leech River Complex is separated from the Metchosin Igneous Complex by the Leech River Fault (Muller 1980). Both of these faults have been imaged by LITHOPROBE lines to be shallow-dipping reflectors, interpreted as thrust faults (Clowes et al. 1995). The Leech River Complex is thrust beneath Wrangellia along the San Juan-Survey Mountain fault system, and the Metchosin Igneous Complex is thrust beneath the Leech River Complex along the Leech River Fault.

Mapping for this study concentrated on an area 0-3 km north of the Diversion Reservoir, between Valentine Mountain on the east and Wye Lake on the west, herein called the *study area* (Figure 2). This region defines the area of maximum intrusive activity in the Leech River Complex. Approximately 6 weeks of mapping and sampling were completed in June and July.

The Leech River Complex is part of a larger belt that has been affected by early Tertiary forearc igneous and metamorphic activity. Presently, this belt extends from Alaska to northern California. In Alaska and British Columbia, this activity was dominantly plutonic (and associated metamorphism) with minor volcanics. From the southernmost part of Vancouver Island to northern California, activity was dominantly basaltic volcanism, with minor associated intrusions. A slab window model, utilizing the Kula-Farallon spreading ridge, is being used to explain the origin of these igneous and metamorphic rocks.

The Leech River Complex

Previous Work

The Leech River Complex consists of variably metamorphosed pelitic, volcanic and arenaceous rocks, with subordinate intrusive rocks. The Leech River Complex has been correlated with rocks of the Pacific Rim Terrane on Vancouver Island and rocks in the San Juan Islands (Fairchild and Cowan 1982, Brandon 1989). Rocks of the Pacific Rim Terrane have been metamorphosed to lawsonite grade, as have rocks in the San Juan Islands (Brandon 1989). However, rocks in the Leech River Complex have been metamorphosed up to staurolite-andalusite grade. This may be the result of high-T overprinting related to the abundant intrusive activity in the Leech River Complex.

The Leech River Complex has undergone two phases of deformation, and two periods of metamorphism. The first phase of deformation produced a slaty cleavage in lower grade rocks, and foliation, defined by micaceous minerals, in higher grade rocks (Fairchild 1979). The second phase of deformation folded the S1 foliations into tight, east-west tending folds (Fairchild 1979).

Fairchild (1979), and Fairchild and Cowan (1982) reported that metamorphic grade ranges from lower greenschist to amphibolite. They reported that metamorphic grade is lower greenschist in the north, increasing to amphibolite in the south. They attributed this to an increase in regional grade towards the Leech River Fault.

Fairchild (1979) concentrated his investigations in the Survey Mountain area for the most part, with a reconnaissance map west to Walker Creek. A K-Ar date of ca. 39 Ma was reported from biotite in schist, and interpreted as the age of metamorphism (Fairchild and Cowan 1982). Fairchild and Cowan (1982) hypothesized that the protolith for the Leech River Complex was Jura-Cretaceous, based on similar assemblages in California and Alaska. They also reported Rb-Sr data and interpretations from the Leech River Complex, indicating a Jura-Cretaceous age.

In the Leech River Complex, meta-pelitic rocks are by far the most abundant with subordinate volcanic and sandstone bodies. One large metamorphosed sandstone body occurs on Valentine Mountain, and is named the Valentine Metasandstone (Fairchild 1979) (Figure 2). A large body of volcanic rock is reported on Survey Mountain (Fairchild 1979). Another volcanic body, characterised by pillow basalts, has also been reported along Malahat Drive, northwest of Victoria, and correlated with Leech River Complex volcanics (Rusmore and Cowan 1985). Major element chemical analyses on the Survey Mountain volcanics indicates that they are basaltic, but no more information has been reported (Fairchild and Cowan 1982).

Fairchild (1979) investigated the Walker Creek Intrusions on a reconnaissance basis. He reported that a number of trondjhemitic dykes and sills occurred in the Jordan River and Walker Creek area. These rocks contain muscovite, biotite and garnet porphyroblasts and/or phenocrysts, and range from foliated to massive. A K-Ar muscovite date from one intrusion of 39 Ma was interpreted by Fairchild (1979) to be the age of intrusive activity.

Fairchild (1979) recognized two phases of deformation in the Leech River Complex. He concluded that the D1 event caused a complete transposition of bedding into elongate fragments parallel to S1 foliation. During D2, transposition was partial and strongly controlled by lithology, concentrated in pelitic layers. He recognized that D2 folds deform S1 foliations, and produce an S2 axial planar cleavage that cross-cuts the S1 foliations in fold hinges. He also reported that the S2 axial planar cleavage strikes east, with very steep dips. The D2 event was interpreted to deform isoclinal F1 folds into tight F2 folds.

Although strata of the Leech River Complex were highly disrupted by deformation and metamorphism, Fairchild proposed a generalized stratigraphic package with the volcanic unit at the base, the pelitic unit in the middle and the Valentine Sandstone on top (Fairchild 1979)

Fairchild (1979) proposed a single metamorphic event in the Leech River Complex. This event was a low-P, low-T Buchan regional event (Fairchild 1979). The grade of metamorphism ranges from greenschist to amphibolite (Fairchild 1979). Fairchild (1979) concluded that regional metamorphism was synchronous with deformation. Rusmore and Cowan (1985) reported greenschist grade metamorphism in the Leech River Complex in the Port Renfrew area. They reported that this was a single event as well.

Current Research

Field Relations

Mapping during June and July 1998 concentrated on the region between Valentine Mountain and Wye Lake (Figure 2). This region corresponds to part of Fairchild's (1979) reconnaissance area.

The area mapped for this project corresponds to the locus of maximum intrusive activity in the Leech River Complex. Previously, only one suite of intrusive rocks was recognized in this region of the Leech River Complex. Field work in 1998 indicates there may be two suites of intrusions. This possibility is being tested with geochemistry and age determinations.

The previously recognized suite is the Walker Creek Intrusions. This suite ranges from white to grey, coarse grained, foliated to unfoliated muscovite-garnet tonalite to a medium grey, medium grained, foliated granodiorite. This suite occurs as several (50-100) small dykes, roughly parallel to discordant with respect to foliation in the host rock. The dykes range in size from several centimetres to several metres thick. The largest continuous intrusion occurs on the west side of Walker Creek. It is about 100 m thick, and extends for at least 1.5 km along strike (to the east, the intrusion pinches out, but to the west the nature of the contact was not determined). Foliated dykes are generally parallel with foliation, while massive dykes are slightly discordant to foliation. Most dykes can't be traced from outcrop to outcrop. This suite has previously been dated at 39 Ma (K-Ar on muscovite reported by Fairchild 1979). This suite is most likely syn- to post- kinematic, but some of the intrusions may be pre-kinematic, as it ranges from foliated to unfoliated.

The newly recognized suite is informally termed here the Jordan River suite. This suite consists of one large body and a few smaller dykes. Outcrops of this suite can be found on the east side of Valentine Mountain as well as on the western slopes of the Jordan canyon (Figure 2). This suite consists of a dark grey, foliated to massive, fine-grained granodiorite. The large intrusion is approximately 150 m thick, 1 km wide at its widest point, and more than 2 km along strike. It is roughly tabular, and horizontally oriented, and is considered to be a sill. A number of dykes were found in the Jordan River which strike into the intrusion on the slopes of the Jordan Canyon and Valentine Mountain. These dykes are probably consanguineous with the large sill. This suite is being separated from the Walker Creek Intrusions on the basis of intrusion size and shape, lithology, and degree of alteration. Relative to the Walker Creek suite, Jordan River suite consists of one large body, is more igneous in mineral assemblage and less altered. Geochemical analyses are underway in order to establish any chemical differences between the Jordan River Sill and the Walker Creek Intrusions.

In this region of the Leech River Complex, metamorphic grade ranges from lower greenschist to lower amphibolite. In the lower amphibolite region ductile structures are dominant, while in the lower grade region structures are more brittle. During the 1998 field season, D1 and D2 features were observed. S1 foliations were observed and measured at all outcrops of schist and at many outcrops of Walker Creek dykes. S1 foliations are defined by the orientation of metamorphic minerals, in the case of the schist, and igneous minerals in the dykes. Rootless F1 folds were also observed at several outcrops. These rootless folds are commonly observed in quartz veins, and are uniformly oriented with the limbs parallel with foliation.

In the southern portion of the study area, D2 deformation can be demonstrated. In this area, S1 foliations are folded into at least three tight, map-scale D2 folds. Fold axes strike east-west and plunge to the east. In several areas, S1 foliations are folded into tight to isoclinal outcrop scale folds. It is not clear at this time if these outcrop scale folds record a D2 event or if they are the product of progressive D1 deformation.

Veining was also observed in the Leech River Complex. Quartz veins demonstrate the same general pattern as intrusions. They range from completely transposed to discordant. The veining ranges from syn- to post-kinematic. The veining is related to the intrusions both spatially and temporally. The youngest intrusions show no evidence of cross-cutting veins, while the older intrusions have some cross-cutting veins associated with them. Veining increases in abundance towards the locus of maximum igneous activity.

There are two metamorphic events recorded in this part of the Leech River Complex. The first metamorphic event produced a regional sericite-chlorite to a biotite-quartz assemblage. This event was syn-kinematic, since the metamorphic minerals define the foliation. Regional metamorphic grade

decreases to the north, from a biotite grade near the Bear Creek Reservoir, to a chlorite-sericite grade in the north of the map area.

The second metamorphic event was an amphibolite grade contact metamorphic overprint. This assemblage consists of staurolite-andalusite +/- garnet-cordierite. This overprint is syn- to post-kinematic, as porphyroblasts, primarily staurolite and andalusite, range from preferentially oriented and elongate, to euhedral and randomly oriented. This assemblage is spatially associated with the region of maximum intrusive activity. The contact nature of this event was observed at one locality on a cm-scale near a dyke in the lower grade portion of the Leech River Complex. At this location, mm-size staurolite and garnet were observed along the contacts between dyke and schist. The abundance of staurolite and garnet decreased away from the dyke, until they were completely absent approximately 25 cm from the dyke.

U-Pb Geochronology

A foliated, syn-kinematic, leucocratic garnet-muscovite tonalite dyke of the Walker Creek magmatic suite was sampled for U-Pb geochronology. The rock yielded modest quantities of both zircon and monazite. Two distinct populations of zircon were recovered, including clear, pale pink stubby prismatic grains and contrasting metamict, brown, turbid to opaque elongate euhedral prisms. No visible cores or zoning were observed within grains of either population. Monazite is clear, pale yellow, nearly inclusion-free and occurs as subhedral tabular grains.

Four analyzed fractions of the clear zircons have low to moderate uranium concentrations (~175-350 ppm) and are discordant with, $^{207}Pb/^{206}Pb$ ages of about 1150-1360 Ma, the latter suggesting that significant proportions of old inherited zircon are present (C-F, Figure 3 a). These inherited components presumably occur as cryptic cores, as no visible cores have been observed. In contrast, metamict brown grains have very high uranium concentrations (~4700 and 10,300 ppm) and at most contain only small traces of inherited zircon. These latter fractions plot just off concordia at about 47 Ma (G and H, Figure 3 b); their slight discordance is probably largely due to Pb-loss.

Three analyzed monazite fractions are reversely and normally discordant at about 50-51 Ma (M2-M4, Figure 3 b). An interpreted magmatic age of 50.9±0.6 Ma is based on the median $^{207}Pb/^{235}U$ age of reversely discordant monazite fractions M2 and M4. Normally discordant monazite fraction M3 is likely to have undergone minor Pb loss. Two chords that bound the clear zircon data array and project to the interpreted magmatic age of the rock are plotted on Figure 3 a. Upper intercept values of about 1.25-1.4 Ga provide an estimate for the ages of inherited zircon components in analyzed clear zircon fractions C-F. The interpreted magmatic age of this rock provides a constraint on the age of associated deformation and metamorphism.

Regional Setting of the Leech River Complex

Early Tertiary forearc magmatism is recorded from Alaska to California. In Alaska and British Columbia, the forearc magmatism is recorded as a series of felsic plutonic rocks, with minor volcanic rocks (Pavlis and Sisson 1995), whereas in Washington, Oregon, and California forearc magmatism is recorded as MORB to OIB type basaltic flows and related intrusions (Babcock et al. 1992).

In Alaska, forearc magmatism is localized in the Sanak-Barnoff Belt, consisting of intrusions ranging from tonalite to granite (Hill et al. 1981). Plutonic rocks in this belt range in age from 60 to 41 Ma (Hill et al. 1981). These plutons intrude into accretionary prism rocks, at the same time as volcanic arc activity occurred, approximately 100 km inland (Moll-Stalcup 1994). The intrusive rocks in the Sanak-Barnoff Belt have a MORB-like chemical signature, but $^{87}Sr/^{86}Sr$ initial ratios indicating an evolved component, probably from the accretionary prism sediments (Hill et al. 1981).
Pavlis and Sisson (1995) and Sisson and Pavlis (1993) studied the structural and metamorphic conditions in the Chugach Terrane in southern Alaska. The Chugach Terrane has undergone three phases of deformation and an Eocene high-T, low-P metamorphic event (Pavlis and Sisson 1995). The three phases of deformation record major changes in kinematic axes over an 8 my period of time (Pavlis and Sisson 1995). Pavlis and Sisson (1995) reported that the first period of deformation was pre-metamorphic, and the second and third deformational events occurred during progressive metamorphism.

Additionally, the second period of deformation is coincident with a period of melt injection in the high grade gneiss complex, as well as intrusion of several large plutons (Pavlis and Sisson 1995). Melt injection is also recorded during the third period of deformation (Pavlis and Sisson 1995). The third period of deformation caused boudinage structures in the D2 dykes (Pavlis and Sisson 1995).

Pavlis and Sisson (1995) reported that metamorphic grade is variable, with blueschist grade metamorphism restricted to a melange complex near the Border Ranges fault. The regional metamorphic grade is a sub-greenschist to greenschist (Pavlis and Sisson 1995). The highest grade metamorphism is localized in a narrow belt of voluminous granitoid plutonism (Pavlis and Sisson 1995). This high grade assemblage is a low-P, high-T amphibolite assemblage (Pavlis and Sisson 1995). Pavlis and Sisson (1995) reported that metamorphic grade decreases around this core in a concentric manner to a lower greenschist facies. This high-T, low-P metamorphism, combined with the presence of abundant granitoid intrusions, is unexpected in an accretionary prism. It is expected that in an accretionary prism, high-P metamorphism would dominate, and intrusive activity would be very rare. This high-T, low-P metamorphism is similar to what is observed in the Leech River Complex.

On Vancouver Island, the bulk of the Early Tertiary intrusive rocks fall into the "Catface" suite (Woodsworth et al. 1991). This suite occurs as several small stocks, dykes and sills extending from Nanaimo to Ucluelet, and north to Zeballos (Woodsworth et al. 1991). These intrusions are dominantly tonalite and quartz diorite with minor granite and granodiorite (Woodsworth et al. 1991). Isotopic ages (K-Ar) range from 32 to 59 Ma, with the majority falling into the 36 to 45 Ma time period (Woodsworth et al. 1991). Isachsen (1987) reported that a "Catface" intrusion on Mears Island, near Tofino, had a U-Pb age of 47 Ma, and a K-Ar (biotite) cooling age of 34 Ma, indicating a rapid cooling of this pluton. An enrichment of K, Rb, Ba, and Sr and a depletion of Nb, Ce, Nd, Zr and Y led Isachsen (1987) to conclude that this pluton formed in an arc setting, but that the proximity to the trench is "problematic."

The Flores Volcanics, near Tofino, are associated with the "Catface" intrusions (Souther 1991). These volcanics consist of dacite breccias, welded ash flows and laharic breccias (Souther 1991). Zircon fission track ages on these volcanics range from 54 to 56 Ma (Souther 1991). These volcanics are spatially associated with "Catface" plutons and related dykes (Souther 1991). Brandon (1989) constrained the age of the Westcoast Fault, which separates Wrangellia from the Pacific Rim Terrane, as being older than 50 Ma, based on the presence of undeformed 50 Ma dykes crosscutting the fault.

South of the Leech River Complex is the Metchosin Igneous Complex. This complex consists of three main parts : gabbro stocks, sheeted dykes and a submarine to subaerial basaltic sequence (Massey 1986). The K-Ar whole-rock ages on the volcanic rocks range from 57.8 to 41.9 Ma, however a U-Pb zircon age of 50.3 +/- 0.3 Ma was obtained on the Broom Hill Trondjhemite (Massey 1986). Massey (1986) interpreted this complex to be a partial ophiolite as there is a gradation from the gabbro stocks into the sheeted dykes into the volcanics on top. This complex most likely formed in an extensional environment, due to the presence of the sheeted dykes. Brandon and Massey (1985) interpreted the Metchosin Complex to have formed in a transform margin basin.

In Washington and Oregon, the forearc igneous activity produced a thick succession of basaltic flows and related intrusions, known as the Coast Range volcanic province (Babcock et al 1992). Extrusion of these basalts began in the Paleocene and continued until the late Eocene (Babcock et al 1992). Babcock et al (1992) interpreted these basalts to be the product of continental margin rifting, rather than the older interpretation of accreted seamounts.

Isotopic ages ($^{40}Ar/^{39}Ar$ whole rock) of these basalts range from 57.8 +/- 0.8 Ma to 50.3 +/- 1.5 Ma (Babcock et al 1992). However, sediments interbedded with the uppermost Crescent flows indicate a minimum age of 48 Ma (Babcock et al 1992).

Paleomagnetic data reported in Babcock et al (1992) indicates little to no northward displacement of the Crescent basalts, and minimal rotation. Additionally, the presence of terrigenous sediments preclude these basalts from forming any great distance from the continental margin.

Correlations

The Chugach Terrane and the Leech River Complex have similar deformational, intrusive and metamorphic histories. Both terranes record two periods of deformation, one accompanied by lower greenschist regional metamorphism and localized intrusive activity, followed by a period of intrusive

activity, followed by a second period of deformation and localized higher grade metamorphism associated with intrusive activity (Sisson and Pavlis 1993).

The Chugach Terrane may have been located well to the south in Eocene time. Two major faults have displaced the Chugach Terrane up to 1000 km northward between 58 and 38 Ma (Lanphere 1978; Smart et al. 1996). The Shakwak, Dalton and McKinley segments of the Denali Fault system record dextral displacements between 300 and 400 km (Lanphere 1978). This is based on correlations between the McLaren metamorphic belt in the Alaska Range and the Ruby Range metamorphic belt near Kluane Lake (Lanphere 1978). Additionally, the correlation of Mesozoic flysch sequences supports a minimum of 300 km dextral displacement in these segments (Lanphere 1978). Lanphere (1978) concluded that this displacement occurred between 55 and 38 Ma, and that only 40 km of displacement have occurred post-38 Ma.

The Border Range fault, which juxtaposes the Chugach Terrane against the Peninsular-Alexander-Wrangellia Terrane, indicates as much as 700 km of dextral displacement may be accommodated between 58 and 50 Ma (Smart et al. 1996). Direct $^{40}Ar/^{39}Ar$ dating on white mica in a mylonite shear zone indicated an age of 51 Ma for growth in the shear (Smart et al. 1996). Progressive deformation from ductile to brittle is evident along this fault, in which case the 51 Ma age would be an upper age for motion (Smart et al. 1996). Paleomagnetic displacements are in excess of 400 km for the Chugach Terrane during this time period (Smart et al. 1996). Tentative correlations between 162 Ma plutons in the Chugach Terrane and similar age plutons indicate a displacement between 150 and 800 km (Smart et al. 1996). This correlation is based on the atypical presence of 162 Ma plutonic rocks in the Glacier Bay region, which are uncommon inboard of the Border Ranges fault (Smart et al. 1996). The closest plutons of this age along strike of the Border Ranges fault are 150 km southward. However, plutons of that age also occur further south in the Queen Charlotte Islands and Vancouver Island (Smart et al. 1996).

Paleomagnetic determinations on the Flores Volcanics, on western Vancouver Island indicate that there is little to no northward displacement of these rocks (Irving and Brandon 1990). This indicates that there is no displacement of the Pacific Rim Terrane post 50 Ma. This location is then a fixed locator for our tectonic model.

If the displacements along the Border Ranges and Denali faults are accurate, then the Chugach Terrane would be located much closer to the Leech River Complex in Eocene time. Combined displacements along these faults place the Chugach Terrane somewhere between the Queen Charlotte Islands and the northern part of Vancouver Island. This indicates that the Leech River Complex and the Chugach Terrane were closer together at the time of igneous and metamorphic activity. The intrusive and metamorphic activity may have been a product of the same process in both terranes.

Preliminary Tectonic Model

Forearcs are thermaly cool parts of convergent margins. Anomalously high temperatures are required for forearc magmatism. The simplest way to rationalize high heat flow in forearc settings is to invoke a ridge-trench intersection (cf. Delong et al., 1979) and slab window formation (e.g., Pavlis and Sisson, 1995; Thorkelson, 1996). In the Cenozoic, spreading ridges between the Pacific-Kula, Pacific-Farallon, and Kula-Farallon plates are candidates for trench intersection along the coastline from California to Alaska. The location and nature of these intersections remains a matter of debate (e.g., Lonsdale, 1988).

The intrusions of the Leech River Complex may have been caused by the intersection of the Kula-Farallon ridge with the North American trench (Figure 4). Intersection of this ridge may explain some of the Eocene forearc magmatism recorded from Alaska to Oregon. If northward translation of forearc terranes and migration of the Kula-Farallon-North America triple junction are considered, then a single, diachronous slab window may explain forearc magmatism from Vancouver Island to the Chugach Terrane in Alaska.

Assuming an initial triple junction location in the vicinity of the Queen Charlotte Islands at 61 Ma, and using Engbretson et al.'s (1985) plate vectors, the Kula-Farallon-North American triple junction migrated rapidly southward between 61 Ma and 56 Ma. At 56 Ma, plate vectors indicate the triple junction reversed and migrated northward at a slightly slower rate. This is consistent with geological observations that igneous activity gets younger to the south in the Chugach Terrane (Haeussler et al.

1995). This is also consistent with data from the Crescent Terrane and the Leech River Complex indicating a major thermal event in this region around 50 Ma. At this time, the Kula-Farallon-North America triple junction may have been located near southern Vancouver Island by right-stepping, north-northwest oriented transform faults (Figure 4).

Oblique subduction of the Kula plate could cause a strike-slip regime in the North American plate, which could cause northward translation of the Chugach Terrane. This northward motion is indicated by paleomagnetic data as well as correlations along the Border Ranges and Denali fault systems (Smart et al. 1996; Lanphere 1978). This means that the Chugach Terrane would have been much closer to the Leech River Complex, and as such would have undergone forearc intrusive and metamorphic activity related to the southward migration of the Kula-Farallon-North American triple junction. Then the triple junction would have been essentially stabilized at the position of Vancouver Island.

A single triple junction would not have been able to migrate far enough southward in our model to cause the forearc magmatism in California. However, a second or even a third ridge may have been active within the Kula plate during this time if the Kula plate was an amalgamation of more than one micro-plate (Barker et al. 1994). In this scenario, an intra-Kula-North American triple junction could have been responsible for the forearc magmatism and metamorphism in the northern forearc, while the Kula-Farallon ridge would have been responsible for the southern forearc magmatism, as postulated by Thorkelson and Taylor (1989). Work is in progress to determine where an intra-Kula ridge may have been located, as all traces of this postulated ridge appear to have been consumed by subduction.

References

Babcock, R.S.; Burmester, r.F.; Engebretson, D.C.; Warnock, A. and Clark, K.P. 1992. A rifted margin origin for the Crescent Basalts and related rocks in the northern Coast Range Volcanic Province, Washington and British Columbia. Journal of Geophysical Research., vol. 97. P. 6799-6821

Brandon,M.T. and Massey, N.W.D. 1985. Early Tertiary tectonics of the Pacific Northwest: truncation and rifting with a transform plate boundary. In Symposium on the Deep Structure of Southern Vancouver Island, Results of LITHOPROBE Phase 1, Geological Association of Canada Programmes with Abstracts., 8,9

Brandon, M.T., 1989 Deformation styles in a sequence of olistostromal melanges, Pacific Rim complex, Western Vancouver Isalnd, Canada. Geological Society of America Bulletin vol. 101., p. 1520-1542

Delong, S.E., Schwarz, W.M., and Anderson, R.N., 1979. Thermal effects of ridge subduction. Earth and Planetary Science Letters., vol., 44, p. 239-246.

Engebretson, D.C.; Cox, A. and Gordon, R.G. 1985. Relative motions between oceanic and continental plates in the Pacific Basin : Geological Society of America Special Paper 206. 59p

Fairchild, L.H. 1979 The Leech River Unit and Leech River Fault, southern Vancouver Island, British Columbia. MSc Thesis, University of Washington, Seattle, WA 170 p

— and Cowan, D.S. 1982 Structure, petrology, and tectonic history of the Leech River complex northwest of Victoria, Vancouver Island. Canadian Journal of Earth Science, vol. 19., p. 1817-1835

Hill, M.; Morris, J; and Whelan, J. 1981. Hybrid granodiorites intruding the accretionary prism, Kodiak, Shumagin and Sanak Islands, southwestern Alaska. Journal of Geophysical Research., vol. 86., p. 10569-10590

Irving, E. and Brandon, M.T. 1990. Paleomagnetism of the Flores Volcanics, Vancouver Island, in plece by Eocene time. Canadian Journal of Earth Scince. Vol. 27., p. 811-817

Lanphere, M.A. 1978. Displacement history of the Denali fault system, Alaska and Canada. Canadian Journal of Earth Science vol. 15., p. 817-822.

Lonsdale, P., 1988. Paleogene history of the Kula Plate: Offshore evidence and onshore implications. Geological Society of America Bulletin, vol. 100., p. 733-754.

Massey, N.W.D. 1986. Metchosin Igneous Complex, southern Vancouver Island: Ophiolite stratigraphy developed in an emergent island setting. Geology, vol. 14. P. 602-605.

Muller, J.E., 1980 Evolution of the Pacific Margin, Vancouver Island and adjacent region. Canadian Journal of Earth Sciences., vol. 14., p. 2062-2085

Moll-Stalcup, E.J. 1994. Latest Cretaceous and Cenozoic magmatism in southeastern Alaska. In *Plafker, G. and Berg, H.C., eds., The Geology of Alaska : Boulder, Colorado, Geological Society of America, The Geology of North America,* v. G-1, p. 589-621

Pavlis, T.L. and Sisson, V.B. 1995. Structural history of the Chugach metamorphic complex in the Tana River region, eastern Alaska : A record of Eocene ridge subduction. Geological Society of America Bulletin, vol. 107. P. 1333-1355

Rusmore, M.E. and Cowan, D.S. 1985. Jurassic-Cretaceous rock units along the southern edge of the Wrangellia terrane on Vancouver Island. Canadian Journal of Earth Sciences., vol. 22, p. 1223-1232

Sisson, V.B. and Pavlis, T.L. 1993. Geological consequences of plate reorganization: an example from the Eocene southern Alaska forearc. Geology., vol. 21, p. 913-916

Smart, K.J.; Pavlis, T.L.; Sisson, V.B., Roeske, S.M. and Snee, L.W. 1996. The Border Ranges fault system in Glacier Bay National Park, Alaska: Evidence for major Early Cenozoic dextral strike-slip motion. Canadian Journal of Earth Science., vol. 33., p. 1268-1282

Souther, J.G. 1991. Volcanic Regimes, Chapter 14 in *Geology of the Cordilleran Orogen in Canada, H. Gabrielse and C.J. Yorath eds. Geological Survey of Canada, Geology of Canada no. 4* p. 457-490

Thorkelson, D.J. and Taylor, R.P. 1989. Cordilleran Slab Windows. Geology. Vol. 17. P. 833-836

Thorkelson, D.J. 1996. Subduction of diverging plates and the principles of slab window formation. Tectonophysics. vol. 255. P. 47-63

Woodsworth, G.J.; Anderson, R.G.; and Armstrong, R.L. 1991. Plutonic Regimes, Chapter 15. In *Geology of the Cordilleran Orogen in Canada, H. Gabrielse and C.J. Yorath eds. Geological Survey of Canada, Geology of Canada no. 4* p.491-531

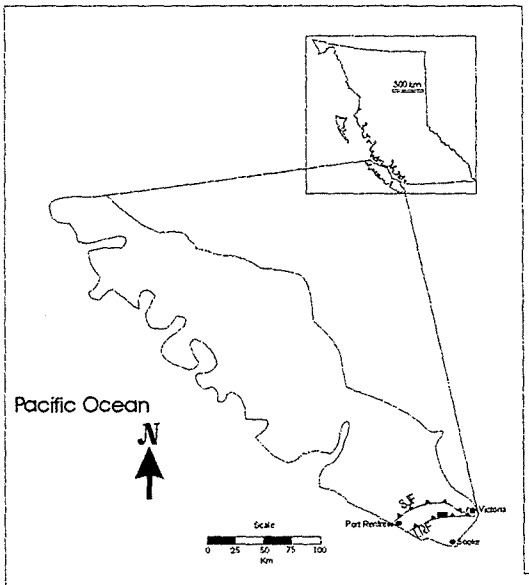

Figure 1 : Location Map : Study Area boxed in
LRF = Leech River Fault
SJF = San Juan -- Survey Mountain Fault System

Figure 2: Study Area Map

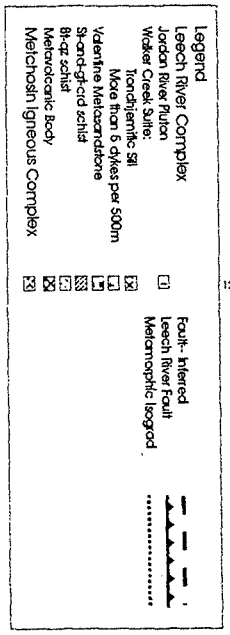

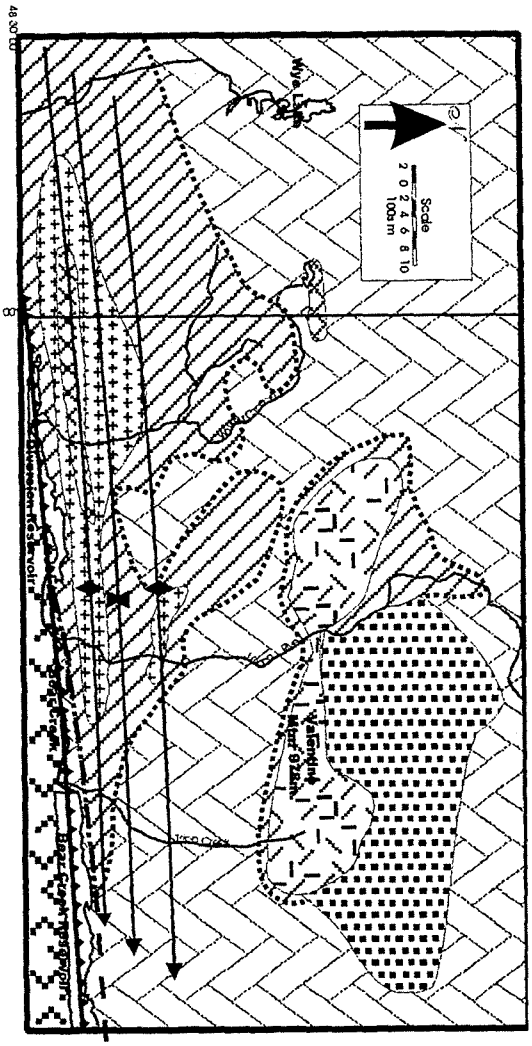

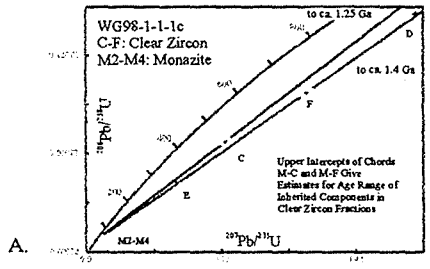

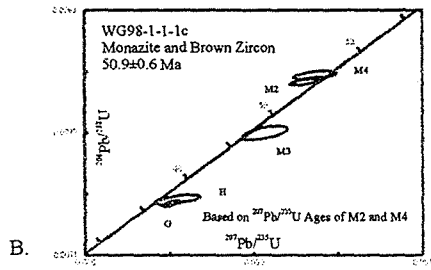

Figure 3 : Concordia plots for foliated tonalite sample WG98-1-1-1c. Error ellipses are plotted at the 2s level of uncertainty. (A) Clear zircon fraction and monazites. (B) Expanded scale showing brown zircon fractions and monazites. See text for discussion and interpretation

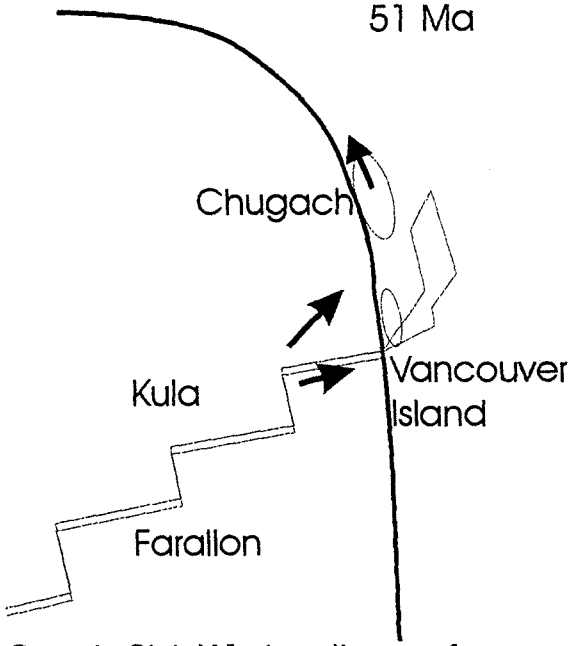

Figure 4: Generic Slab Window diagram for 51 Ma time period

Relating Potential field anomalies to Proterozoic structures in Western Canada

Kevin W. Hall, Frederick A. Cook, and C. Elissa Lynn
Department of Geology and Geophysics
University of Calgary
Calgary, Alberta T2N 1N4, Canada

Crustal-scale monoclines with up to15-20 km of vertical relief are buried beneath Phanerozoic sedimentary rocks of the Western Canada Sedimentary Basin. They are interpreted as a series of *en echelon* features that face (dip) westward and that probably formed initially as a result of lithospheric extension at about 1.8-1.7 Ga following accretion of the Paleo-Proterozoic Wopmay Orogen. Acquisition of new deep reflection profiles, particularly the LITHOPROBE Slave NORthern Cordillera Lithospheric Evolution transect (SNORCLE), provide detailed subsurface information that can be linked to regional aeromagnetic and isostatic gravity anomaly patterns to delineate the subsurface structure and along-strike variations of the monocline(s). In the northern Candian Cordillera, the monocline(s) appear to generally follow, but are situated east of, the northeastwardly convex arc of the Mackenzie Mountains, except near Great Bear lake where they may outline either the flanks of a northeast-southwest failed rift arm, or they may delineate the southern edge of a large, northwest-opening basin. In the southern Canadian Cordillera, the structure(s) were probably overridden by the thrust sheets of the Rocky Mountain foreland fold and thrust belt and thus controlled the mechanical development of the Tertiary Rocky Mountain trench extensional basin. The region in between, where the ramp(s) project beneath the Cordillera, is the locus of major changes in stratigraphy and structure from north to south.

Crustal Structure across the Cordilleran Orogen of Northwest British Columbia Preliminary Results of LITHOPROBE SNorCLE Refraction Experiment Line 22

Philip T C Hammer and Ron M Clowes

Department of Earth and Ocean Sciences
University of British Columbia
2219 Main Mall, Vancouver, Canada V6T 1Z4
hammer@eos.ubc.ca

Abstract

In 1997, LITHOPROBE conducted a seismic refraction/wide-angle reflection (R/WAR) experiment in NW Canada. The experiment was one component of the multidisciplinary Slave-Northern Cordillera Lithospheric Evolution (SNorCLE) transect. The SNorCLE Refraction Experiment (SNORE) included four R/WAR profiles. Line 22 traverses the western Cordillera, a complex assemblage of terranes accreted to North America during two distinct periods (**Fig. 1**). In the early Jurassic, the Intermontane superterrane (Stikinia, Cache Creek, Quesnellia, Slide Mountain and Cassiar terranes) was thrust over the western margin of North America (Omineca belt). During the mid-Cretaceous, the exotic Insular superterrane (Alexander and Wrangellia terranes) collided with North America, further deforming the Intermontane terranes and producing the Coast orogen. Investigations along this transect corridor are directed toward understanding the tectonic history and 3-d structure of the accreted terranes. Broader questions being addressed concern the growth of continents by magmatic and terrane accretion.

Line 22 follows the Stewart-Cassiar Highway, crossing the Tintina fault system close to the British Columbia/Yukon border. The profile continues south-southwest, traversing the Omineca belt and Intermontane terranes and extending into the Coast orogen suture zone (**Fig. 1**). Nine explosive shots (1000-3000 kg) were detonated along the 600 km profile. The primary inline dataset was acquired by 456 seismographs positioned with the 1-component (PRS and SGR) and 3-component (Reftek) instruments interspersed. An additional 42 instruments were deployed to the southwest of the primary line, crossing from the Intermontane into the Coast Belt and providing a direct overlap with the ACCRETE seismic experiment (**Fig. 1**). Data quality is superb; numerous reflected and refracted P- and S-phases are identifiable and are observed to 550 km offset. Coincident vibroseis reflection and magnetotelluric profiles will be acquired in 1999-2000.

Data analyses include initial 1-d velocity modeling using τ-p techniques and subsequent 2-d velocity modeling using traveltime inversion and ray amplitude forward modeling. Preliminary velocity structure models exhibit a strongly heterogeneous upper crust; the velocity variations correlate directly with mapped geologic and terrane elements. Preliminary model features include:

1) a crustal-scale transition between the Coast Belt and Stikinia,
2) slow shallow velocities in western Stikinia that constrain the thickness of the Bowser Lake assemblage,
3) fast upper crustal velocities in northern Stikinia and Cache Creek terranes, similar to intrusive structures imaged in the southern Cordillera and,
4) lateral velocity contrasts across the Kechika and Tintina faults.

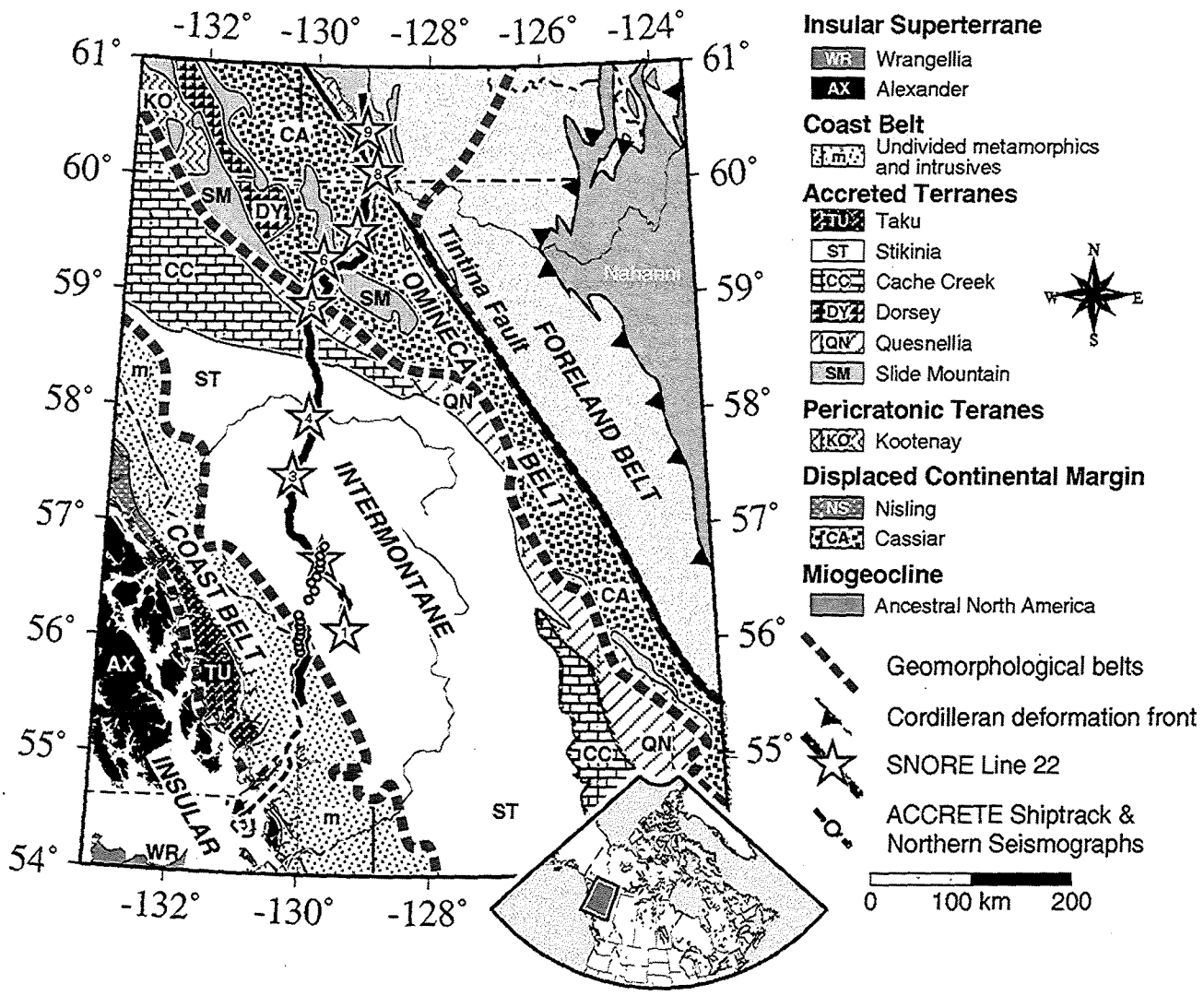

Figure 1: SNORE Line 22 location map. Terranes and geomorphological belts of the northwestern Canadian Cordillera are shown. Line 22 energy generated by explosive shots ( ) was recorded by receiver arrays (▬▬). Accrete airgun shots (O) along Portland Inlet were recorded by inline seismographs (- - -). To locate Line 22 relative to the other SNORE lines, see Figure 1 in *Fernandez Viejo et al.* (this volume).

Geotectonic Setting

The Canadian Cordillera can be divided into five subparallel geomorphological belts (**Fig. 1**) developed through a complex history of Mesozoic and Cenozoic collision and deformation (*Gabrielse and Yorath*, 1992). The northwestern Cordillera (British Columbia and SE Alaska) comprise a complex assemblage of terranes accreted to North America during two distinct periods. In the early Jurassic, the Intermontane superterrane (Stikinia, Cache Creek, Quesnellia, Slide Mountain and Cassiar terranes) was thrust eastward over North America. The Omineca belt represents the suture zone of this collision and straddles autochthonous terranes to the east and allochthonous Intermontane terranes to the west. During the mid-Cretaceous, the exotic Insular superterrane (Alexander and Wrangellia terranes) collided with North America, further deforming the Intermontane terranes and producing the Coast orogen. The history and 3-d geometry of many of these terranes are poorly understood.

Intermontane Superterrane and Omineca Belt (SNORE Line 22):

- This zone of allochthonous and autochthonous terranes (**Fig. 1**) has undergone an extremely complex history of deformation. Determining the sub-surface geometry of the terranes is necessary to advance tectonic reconstructions.
- Significant variations in structures, stratigraphy and geophysical characteristics exist along the strike of the orogen. Understanding this variability is essential for improving orogenic-scale models of accretion.
- The Northern Cordilleran Volcanic Province (NCVP) overlaps virtually all of Line 22. A diverse assemblage of large Neogene-Quaternary volcanic centres are scattered throughout the profile. There is no clear linkage of the NCVP to tectonic forces [*Edwards and Russell*, 1999].
- The Omineca belt is bounded to the west by the 1900 km-long Tintina fault zone. The geometry of this intracontinental, dextral strike-slip fault is unknown, but may penetrate the lithosphere [*Price and Carmichael*, 1986].

Line 22 Goals:
- ❖ Determine the lower boundaries of the terranes.
- ❖ Obtain information regarding the affinity of the lower crust (North American? Transitional? Oceanic?).
- ❖ Determine the nature and causes for along-strike orogen variations.
- ❖ Provide insights regarding the mechanism(s) driving the NCVP.
- ❖ Provide constraints for the structure of the Tintina fault zone at depth.

Coast Belt - Intermontane Transition (SNORE Line 22 and ACCRETE):

- The SNORE Line 22 and ACCRETE profiles overlap across the transition between the Coast orogen and the Intermontane superterrane. The high grade metamorphic orogen core is bounded on the east by the thin-skinned Skeena thrust and fold belt (Stikinia, **Fig. 1**) and on the west by a thick-skinned thrust belt. The Skeena belt developed between 140 and 65 Ma, coeval with the west-vergent thrust belt. Stikinia spans most of the width of the northern Intermontane superterrane and experienced more than 160 km of shortening through thin-skinned thrusting and folding [*Evenchick*, 1991]. Understanding the development of the Skeena belt is a key to unravelling the tectonic history of the region.

Line 22 Goals:
- ❖ Characterize the transition between Stikinia and the overprinting magmatic arc.
- ❖ Constrain the location of the proposed detachment fault beneath the Skeena fold and thrust belt.
- ❖ Determine the thickness of Bowser Basin sediments overlying Stikinia basement.
- ❖ Examine the orientation of crustal reflectors to test a hypothesis of regional Miocene extension (*Hollister et al.*[1997], *Morozov et al.*, [1999], and *Evenchick et al.* [1999]).

Experiment: SNORE Line 22

The SNorCLE Refraction Experiment included four R/WAR profiles acquired along three transect corridors (**Fig. 1**). Lines 21 and 22 were deployed simultaneously to provide both inline and broadside coverage. The primary inline dataset for Line 22 is discussed in this poster.

Acquisition Parameters for Line 22:

- ➢ Participants: 87 people from 15 institutions
- ➢ Sources:
  - 9 shots (1000-3000 kg of Hydromex T3)
  - Shot depth: 35 m

➢ Recording: 594 seismographs
- 212 Refteks and 20 PRS4s (3-component)
- 179 PRS1s and 182 SGRs (1-component)
  - The SGR data are now available for analysis. The inline Line 22 dataset used in this poster will be supplemented by 88 SGRs.

➢ Deployment:
- Station spacing:
  - Main profile: ~1.0 km (456 seismographs)
  - Extension for ACCRETE overlap: ~1.8 km (42 seismographs)
  - Broadside deployment along Line 21 for coverage across Tintina fault: ~2.0 km (94 seismographs; data now available).
- Line 22 profile length: 600 km
  - Combined length with ACCRETE: 730 km
  - Overlap with ACCRETE provides reversed coverage and greatly improved upper crustal resolution across the Coast Belt - Stikinia transition.

Data

Principal phases identified in the sections (**Fig. 2**):
- Pg: P-wave refractions through upper and middle crust.
- Pn: P-wave refractions in upper mantle
- PcP:P-wave reflections within the crust.
- PmP: P-wave reflections from Moho.
- PnP: P-wave mantle reflections
- Sg: S-wave refractions through upper and middle crust
- SmS: S-wave reflections from Moho (ACCRETE primarily).
- SmP: S-to-P conversion reflected from Moho (ACCRETE only).

Note: S-wave data discussed *Hammer and Clowes* [this volume].

Processing and 2-D Modeling

Data processing:
- All data manipulation (filtering, scaling, muting, killing, picking, plotting, nmo, semblance, etc.) was done using PLOTSEC [*Amor*, 1996]

Full waveform τ-p inversion was used to generate starting models:
- The technique is described by *Gorman & Clowes* [1999] following theoretical development by *McMechan et al.* [1982].
- The method requires no traveltime picks and provides a quick way to obtain 1-d velocity models that can then be combined into a preliminary 2-d model.
  a) First, the uninterpreted data are transformed into the τ-p domain.
  b) The data are are then downward continued into the z-p space using an arbitrary 1-d velocity function. This velocity function is modified until the amplitudes in the z-p space are maximized.
  c) The velocity model fit is tested by comparing WKBJ synthetic arrivals with the data.
  d) The resulting set of 1-d velocity models are combined into a 2-d velocity model that is used as the starting point for subsequent modeling.
- At present, the approach does require subjective iteration to improve the 1-d velocity models. However, a reasonable velocity model is quickly derived.

Figure 2. Representative receiver gathers:
Data have been band-pass filtered (1-12 Hz) and amplitudes are trace-normalized.
Traveltimes are reduced to 8.0 km/s.

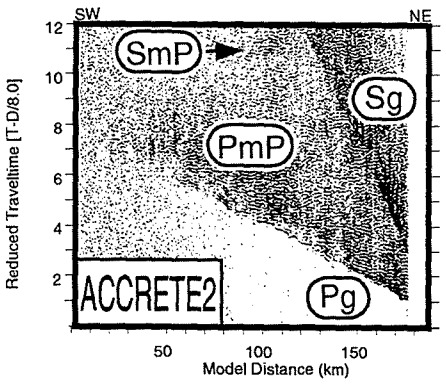

- ➡ SNORE Line 22:
  - Shot locations: see **Figs. 1, 3**
  - SNORE data section do not include SGRs. As a result, trace density is halved north of 550 km.
- ➡ ACCRETE:
  - Receiver location: ACCRETE2 is the second seismograph from the south end of the line (see **Figs. 1, 3**).
  - Dense airgun data is decimated by 3x.

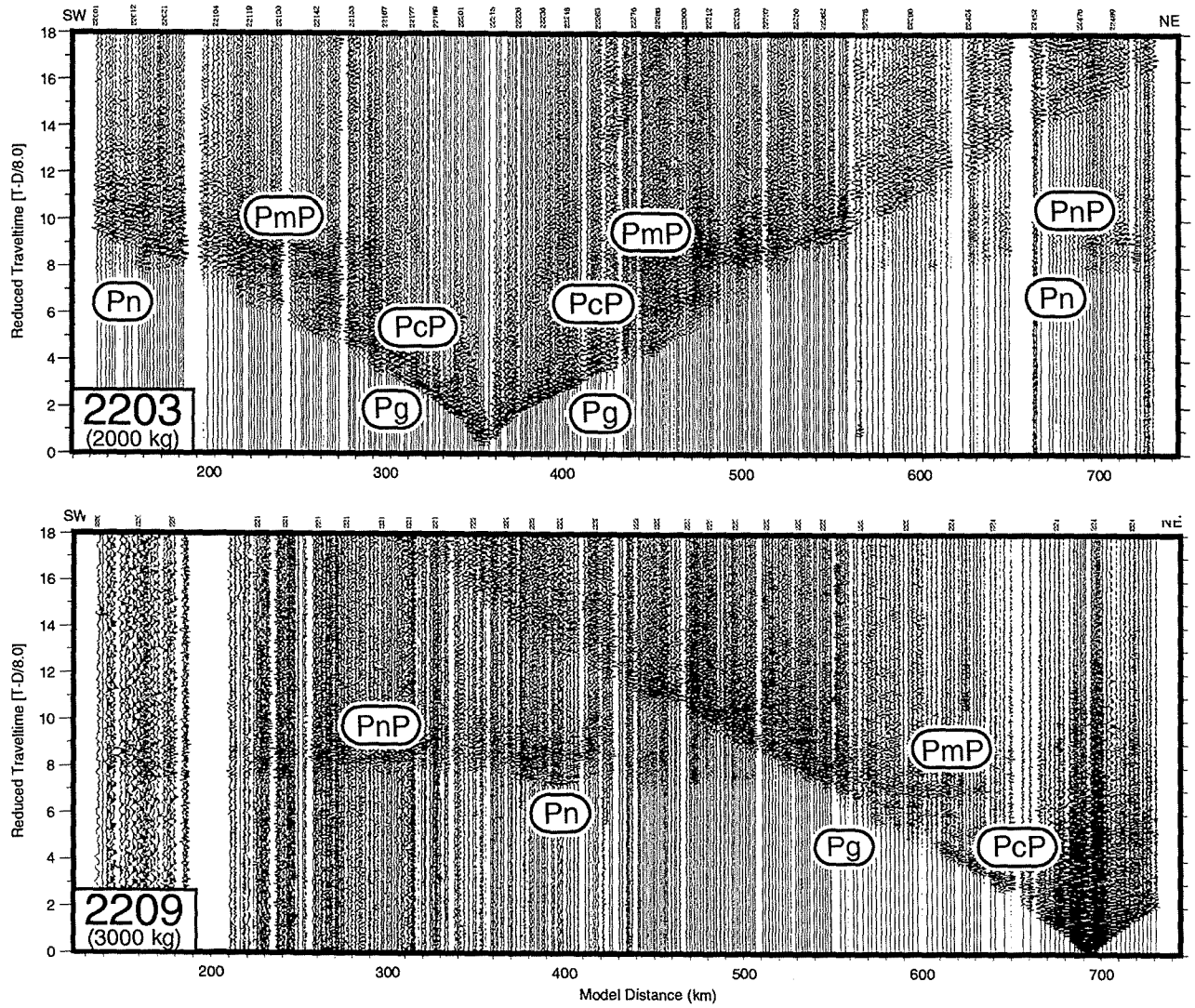

Model geometries:

a) SNORE Line 22: The model incorporates all nine shots and the receivers between shot 1 to north of shot 9 (**Figs. 1, 3**)

b) ACCRETE / SNORE Line 22: The data used to model structure across the Coast Belt/Stikinia transition includes:

- The ACCRETE dataset (airgun source along Portland Canal and 15 receivers to the NNE of the fjord (dashed line and circles in **Figs. 1, 3**).
- SNORE shots 2 and 3 shooting into seismographs:
  i) on the main Line 22 between shot sites 2 and 3
  ii) along the Line 22 extension subparallel to Portland Canal and ACCRETE (**Figs.1, 3**).

2-d modeling and inversion:

RAYINVR [*Zelt and Smith*, 1992] was used for traveltime inversion and ray amplitude forward modeling.

Preliminary Velocity Structure Model

Model features (**Fig. 3**):

- ➢ Primary Line (Line 22):
  - ❖ Laterally heterogeneous upper crustal velocities. Velocity variations correlate closely with terrane and/or geological boundaries.
  - ❖ Slow velocities in uppermost Stikinia define the base of the Bowser Lake assemblage (Bowser Basin).
  - ❖ High velocities in the lower crust between Shots 4 and 5 correlate with mapped intrusives and are similar to features observed in the Southern Cordillera [*Clowes et al.*, 1995].
  - ❖ Large lateral velocity contrast beneath Shot 7 may define the Kechika fault.
  - ❖ Extremely slow near-surface velocities (2 km/s) are observed across and to the southwest of the Tintina Fault.
  - ❖ Lower crustal/Moho/mantle features are still preliminary.
- ➢ ACCRETE Overlap (Line 22 extension and ACCRETE):
  - ❖ See *Hammer and Clowes* [this volume] for model and detailed summary.

Future Work

- ➢ Incorporate the SGR data into the velocity models
- ➢ Refine the 2-d SNORE models. Lower crust/mantle, S-wave and amplitude modeling are still at an early stage.
- ➢ Compare velocity structure models with results from the southern Cordillera and Alaska.
- ➢ Analyze broadside data collected across the Tintina fault zone.
- ➢ Integrate R/WAR results with other geophysical data (gravity, magnetic, seismic reflection and magnetotelluric) and geological studies.
  - Coincident, near-vertical incidence, vibroseis seismic reflection data to be acquired in late-1999.
  - Coincident, deep-penetrating magnetotelluric data to be acquired in 2000.

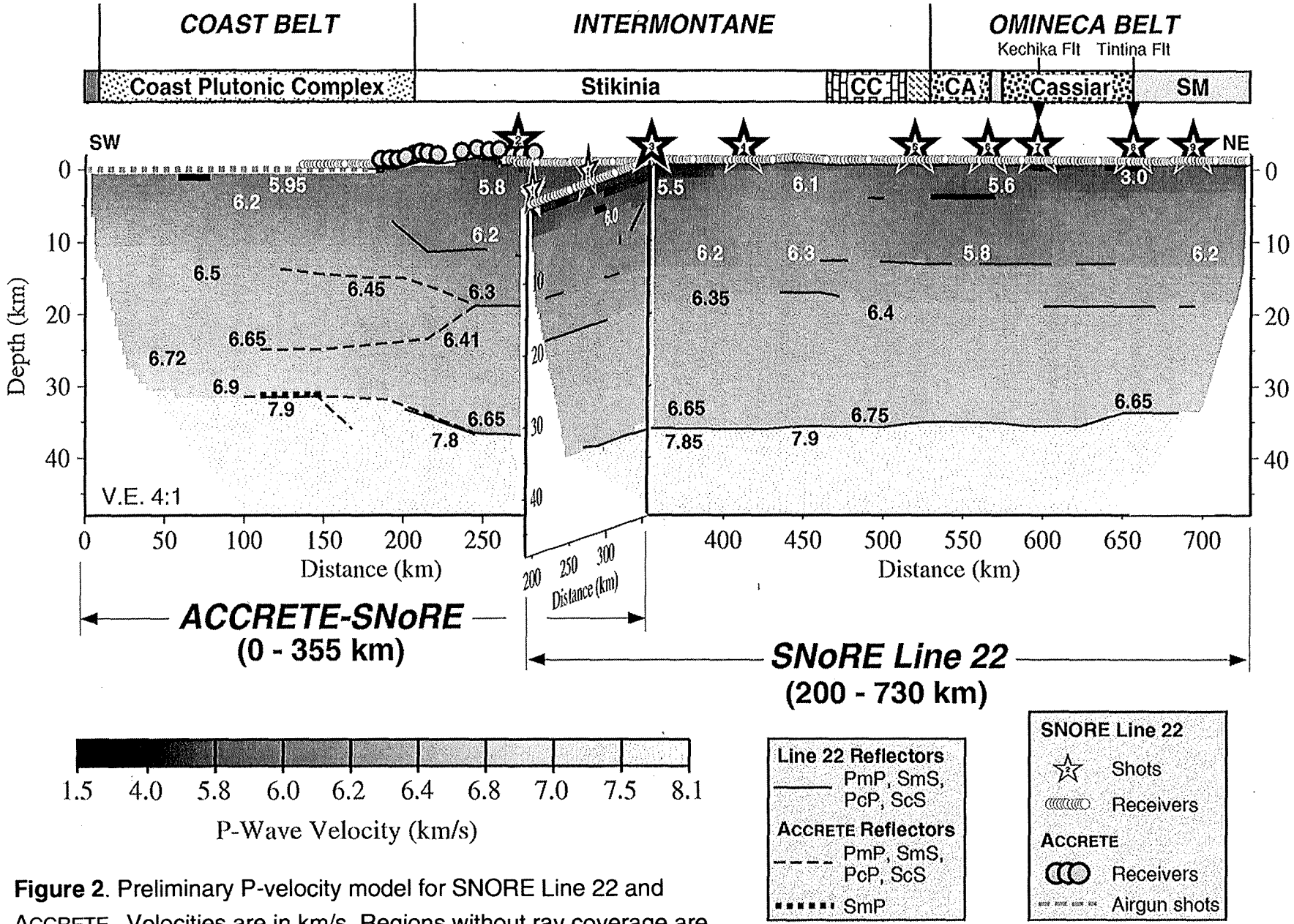

Figure 2. Preliminary P-velocity model for SNORE Line 22 and ACCRETE. Velocities are in km/s. Regions without ray coverage are masked out.

References

Amor, J.R., 1996. PLOTSEC: generalized software for seismic refraction data. LSPF Newsletter, **9:** 24-31 (see *www.geop.ubc.ca/~amor/plotsec*).

Diebold, J.B., Hollister, L.S. & Das, T., 1998. ACCRETE MCS data synthesis reflects tectonic history of the northern continental margin of British Columbi*a. EOS Trans.*, AGU: T71E-05.

Edwards, B. R. & Russell, J. K., 1999. The distribution, nature and origin of Neogene-Quaternary magmatism in the Northern Cordilleran Volcanic Province,Canada. *GSA Bull.*, submitted.

Evenchick, C. A., 1991. Geometry, evolution and tectonic framework of the Skeena Fold Belt, north central British Columbia. *Tectonics*, **10**: 527-546.

Evenchick, C.A., Crawford, M.L., McNicoll, V.J., Currie, L.D., & O'Sullivan, P.B., 1999. Early Miocene or younger normal faults and other Tertiary structures in west Nass River (103P) map area, northwest British Columbia, and adjacent parts of Alaska. In *Current Research 1999-A*, GSC, submitted.

Fernandez Viejo, G., Clowes, R.M., & Amor, J.R., 1999. Lithospheric Velocity Structure beneath the Slave Province and Wopmay Orogen from the SNorCLE Refraction Experiment. In *SNorCLE Transect Workshop Volume.*

Gabrielse, H. & Yorath, C.J. *(editors)*, **1992**. Geology of the Cordilleran Orogen in Canada. GSC, *Geology of Canada No. 4*, **G-2:** 844 p.

Gorman, A.R. & Clowes R.M., 1998. Wavefield tau-p analysis for 2-D velocity models: Application to western North American lithosphere. *Geophys. Res. Lett.*, in press.

Hollister, L.S. & Andronicos, C.L., 1997. A candidate for the Baja British Columbia Fault System in the Coast Plutonic Complex. *GSA Today*, **7**: 1-7.

Hammer, P.T.C. & Clowes, R.M., 1999. Crustal Structure across the Coast Plutonic Complex and Stikinia in Northwestern British Columbia: Wide-angle P- and S-wave Velocity Models from ACCRETE and LITHOPROBE SNORE Line 22. In *SNorCLE Transect Workshop Volume.*

McMechan, G.A., Clayton, R.W. & Mooney, W.D., 1982. Application of wavefield continuation to the inversion of refraction data. *J. Geophys. Res.*, **87**: 927-935.

Morozov, I.B., Smithson, S.B., and Hollister, L., 1999. Wide-angle seismic imaging across accreted terranes, southeastern Alaska and western British Columbia, *Tectonophys.*, submitted.

Price, R.A. & Carmichael, D.M., 1986. Geometric test for Late Cretaceous-Paleogene intracontinental transform faulting in the Canadian Cordillera. *Geology*, **14**: 468-471.

Zelt, C.A. & Smith, R.B., 1992. Seismic traveltime inversion for 2-d crustal velocity structure. *Geophys. J. Int.*, **108**: 16-34.

Reconstruction of Motion Along the Great Slave Lake Shear Zone, Northwestern Canada, using Regional Aeromagnetic Data.

Karen A.B. Hendry [1,2] and Walter R. Roest [2]

[1] Ottawa-Carleton Geoscience Centre and Department of Earth Sciences,
University of Ottawa, Ontario, K1N 6N5

[2] Geological Survey of Canada, 615 Booth St., Ottawa, Ontario, K1A 0E9

The Great Slave Lake Shear Zone (GSLSZ) is approximately 1000 km long and 25 km wide and is a prime example of a crustal-scale deformation zone (Hanmer and Lucas, 1985). Displacement along the zone is dextral and has been estimated to be as much as 700 km. The GSLSZ formed during the convergence and subsequent collision of the Slave Province with the Western Churchill Province at around 2.0 Ga (Hoffman, 1987; Hanmer, 1988; Henderson et al., 1990; and Ross et al., 1991). Subsequent to ductile deformation, a brittle phase involved the younger Bathurst and MacDonald fault systems. These systems form a 1.8 Ga conjugate set of faults, which are likely the result of indentation due to subduction beneath and collision with another continental block to the west (Henderson et al., 1990).

A digital technique, developed by Roest and Pilkington (1994), was used to reconstruct the large-scale strike-slip motions in the region of the Great Slave Shear Zone. The method allows for reconstruction of the horizontal motion along discrete faults, as well as distributed ductile deformation. Using regional aeromagnetic data, the technique used here in correlating and juxtaposing equivalent units on either side of the deformation zone.

Following Gibb (1978), we propose a model in which the younger indentation of the Slave Craton was accommodated by compression of material at the apex of the wedge as well as the escape of some material. Faults that allowed for the escape are inferred from magnetic lows in the regional magnetic data. In addition, the rotation of a small block has been predicted along the McKee fault. The geometry of our model suggests that the indentation was directed more toward the NE than in Gibb's model, where he assumed indentation normal to the Slave-Churchill boundary, i.e. in a more east-west direction.

After restoring the younger, brittle deformation, we can use this reconstruction as a starting point for restoring the motion along the GSLSZ itself. In addition to locating areas of compression and/or subduction, further investigation is required to identify possible routes for extrusion of material as a result of the collision between the Slave and Churchill Provinces. Such a model has been proposed for the India-Eurasia collision (e.g. Tapponnier et al., 1982) in which

the extrusion of material propagates as the indentation proceeds. This model accounts for large strike-slip fault systems such as the Red River fault and the Altyn Tagh fault in Asia, as well as for the opening of the South China Sea and the Andaman Sea.

The present study will provide a better understanding of the regional structure prior to shearing. It may also aid in understanding how such large displacements were accommodated in the more orthogonal convergent segment occupied by the Thelon Magmatic zone. We hope to get a clearer picture of the types of displacement that the GSLSZ accommodated. It has been proposed that the GSLSZ is a transcurrent shear zone with a dextral sense of movement (Hoffman, 1987; Hamner, 1988; and Henderson et al., 1990). However, the correlation of some of the terranes to the south of the shear zone, such as the Buffalo Head Terrane and the Chinchaga low, with units to the north remains unclear. Furthermore, the GSLSZ may also have accommodated a significant vertical component of movement.

Acknowledgments

This research is supported by an NSERC-Lithoprobe grant to Benn, Roest and Bleeker. K. Hendry acknowledges the use of GSC facilities to carry out her research.

References

Gibb, R.A., 1978. Slave-Churchill collision tectonics. Nature, v.271, p. 50-52.

Hanmer, S., 1988. Great Slave Lake shear zone, Canadian Shield: reconstructed vertical profile of a crustal scale fault zone. Tectonophysics, v. 149, p. 245-264.

Hanmer, S. and Lucas, S.B., 1985. Anatomy of a ductile transcurrent shear: the Great Slave Lake Shear Zone, District of MacKenzie, NWT (preliminary report). In Current Research, Part B, Geological Survey of Canada, Paper 85-1B, p. 7-22.

Henderson, J.B., McGrath, P.H., Theriault, R.J., and van Breemen, O., 1990. Intracratonic indentation of the Archean Slave Province into the Early Proterozoic Thelon Tectonic Zone of the Churchill Province, northwestern Canadian Shield. Can. J. Earth Sci., v. 27, p. 1699-1713.

Hoffman, P.F., 1987. Continental transform tectonics: Great Slave Lake shear zone (ca. 1.9 Ga), northwest Canada. Geology, v. 15, p. 785-788.

Roest, W. and Pilkington, M., 1994. Restoring post-impact deformation at Sudbury: A circular argument. Geophys. Res. Lett., v. 21, p. 959-962.

Ross, G.M., Parrish, R.R., Villeneuve, M.E., and Bowring, S.A., 1990. Geophysics and geochronology of the crystalline basement of the Alberta Basin, western Canada. Can. J. Earth Sci., v. 28, p. 512-522.

Tapponnier, P., Peltzer, G., Le Dain, A.Y., Armijo, R., and Cobbold, P., 1982. Propagating extrusion tectonics in Asia: New insights from simple experiments with plasticine. Geology, v. 10, p. 611-616.

Plasticity of Forsterite-Enstatite Composites at High Temperature

Shaocheng Ji & Zichao Wang

Department of Geology, University of Montreal, C.P. 6128, Succ. Centre-ville, Montreal, Quebec, H3C 3J7, CANADA

Abstract

Our knowledge of the flow properties of the lithosphere is largely constrained by comparing creep experimental data and deformation style of natural rocks observed in field. Flow properties of proposed mineral assemblages are generally calculated from laboratory measured flow laws of constituent minerals and appropriate rules of mixtures. The rules of mixtures describe variations of the flow properties of polymineralic composites as a function of their end-member flow properties and volume fraction. A common practice of the above thought is to predict the flow strengths of the crust and the upper mantle by evaluating laboratory determined steady-state flow laws of quartz/plagioclase and olivine/pyroxene with mixing rules. However, the success of such modeling depends on not only an accurate knowledge of the plasticity of the proposed minerals but also the relevance of the rule of the mixtures used. However, it is difficult to estimated the bulk plasticity of composites by using mixing rules when our knowledge of the mixing rules are limited. In this study, high-temperature creep experiments were performed on fine-grained forsterite (Fo) and enstatite (En) two phase aggregates. These two phases are common stable mineral phases in the lower crust and upper mantle, and the high temperature plasticities of both phases are well-known from previous studies. The purpose of this study is to investigate experimentally the bulk plasticity of Fo-En composite and search for the appropriate mixing rules, which works best for the mineral assemblages with similar rheological properties to the Fo-En.

Polycrystalline aggregates with forsterite volume fraction (V_f) of 0 (En), 0.2, 0.4, 0.5, 0.6, 0.8, and 1.0 (Fo) were prepared through a two-step sintering-hot pressing procedure. Creep tests were performed on these samples at the conditions of T=1463-1573 K in air. The measured creep rates $\dot{\varepsilon}$ at steady-state stage can be described by a power law relation

$$\dot{\varepsilon} = A\sigma^n d^m \exp(-Q/RT)$$

where d is grain size, A is the pre exponential factor, n is the stress exponent, m is grain size exponent, Q is the activation energy and RT has the usual meaning. We found that most of the deformed specimens reached the steady-state creep within 1% strain after loading. Specimens deformed at the given temperature range showed completely ductile behavior. No creep acceleration was observed even total strain greater than 30%, and we did not see evidences of micro cracking and partial melting. The deformation in general was stable. Most of the experiments were terminated at total strain less than 10% with a few exceptions, for which larger strain (>20%) was reached to examine microstructures. The mechanical data were summarized as follows:

Forsterite: For the Fo end-member, the creep rates, measured at the T = 1463 - 1558 K and σ = 27 - 84 MPa varied within one order of magnitude ranging from 2.3×10^{-7} s^{-1} to

2.96×10^{-6} s^{-1}. The *n*, determined at T = 1503 K, was 1.3±0.1. The activation energy (Q), determined at a constant stress of 45 MPa, was 406±25 kJ/mol (Fig. 2).

Enstatite: For the En end-member, the creep rates, measured at the T = 1483 - 1505 K and σ = 31 - 80 MPa, varied from 3.50×10^{-6} s^{-1} to 8.14×10^{-6} s^{-1}. The *n*, determined at T = 1503 K, was 1.0±0.1. The activation energy (Q), determined at a constant stress of 45 MPa, was 451±28 kJ/mol (Fig. 2).

Fo-En composites: For the Fo-En composites, the creep rates, measured at T = 1473 - 1573 K and σ = 17 - 74 MPa, varied from 3×10^{-8} s^{-1} to 8.24×10^{-6} s^{-1}. The *ns*, determined at T = 1503 K, were in the range of 0.8±0.1 - 1.4±0.1. The lowest *n* was observed in the specimen with Fo:En = 50:50, and the highest n was observed in the specimen with Fo:En = 20:80. The activation energies (Q), determined at a stress of 45 MPa, varied from 546±35 kJ/mol (specimen with Fo:En = 20:80) to 744±40 kJ/mol (specimen with Fo:En = 50:50) (Fig. 2).

Variation of bulk creep strength with the composition:: The Fo and En, in general, showed the highest and lowest creep strengths among the Fo-En composites at a comparable condition, they were considered as the strong and weak phases in Fo-En composites, respectively. However, the bulk creep strengths of the Fo-En composites did not show a linear variation with the end-member content. The bulk strength of the Fo-En composites showed first a slight decrease with Fo-content until Fo-content exceeds 40%, at which a faster increase in bulk strength was observed. The composite containing 80% Fo showed a comparable bulk strength with that of Fo end-member (Fig. 3). This general non-linear behavior in bulk property is true for the Fo-En composites tested at the conditions given in this study.

The results showed exclusively a n value close to 1, suggesting the diffusion creep as the deformation mechanism for the Fo-En composites. However the activation energies are differ among the samples suggesting a change in rate-controlling process. We further compared the experimental data with various proposed models for predicting the bulk strength of two-phase composites. Our experimental data can be much better described by the shear-lag made than by the commonly used simple models such as Eudier-Tharp's model, Duva's model and the model suggested by Tullis et al.. We interpreted this as a result from the strong interface interaction involving enhanced grain boundary diffusion.

BAJA BC AND BAJA CALIFORNIA: AN EVALUATION OF DOCKING LATITUDES

J. D. Keppie[1] , J. Dostal[2] and E. Centeno-Garcia[1]

[1] Instituto de Geologia, Universidad Nacional Autonoma de Mexico, Mexico D. F., Mexico
[2] Department of Geology, Saint Mary's University, Halifax, Nova Scotia B3H C3C

Currently, there is much debate about the late Mesozoic paleogeography of the western margin of North America. A mid-Cretaceous palinspastic reconstruction based solely on paleomagnetic data suggests that (i) the Insular Belt and Coast Mountain Orogen in Alaska and British Columbia (Baja BC) were about 3,000-5,000 km to the south, adjacent to northern Mexico; (ii) Baja California was at least 1,000 km to the south, next to southern Mexico and the Chortis block; and (iii) Baja BC and Baja California may have been along-strike continuations of one another. Comparison of their geological records are compatible with this reconstruction and indicate that (1) both the Coast Mountain Orogen and Baja California consist of a Jurassic-Cretaceous magmatic arc complex that may have changed from an oceanic arc in Baja BC to a continental-fringing arc in Baja California; and (2) a source for the Upper Cretaceous, easterly-derived sediments found along the eastern margin of Baja BC (Methow-Tyaughton basin) may be found in the northwestern Guerrero terrane (Cortez terrane).

However, comparison of Mesozoic-Cenozoic paleomagnetic data for Baja BC with latitudinal constraints, provided by faunal provinces and terrane tracks across the Pacific, is most consistent with accretion of Baja BC at approximately their present locations on the North American margin. Thus, in the Triassic and Lower Jurassic, all parameters agree and lie on an extension of a northern track where the terranes accrete with the North American margin approximately at their present location. In the Upper Jurassic and Cretaceous, the paleomagnetic data diverge from the terrane tracks and faunal data, a feature most likely attributable to the lack of paleomagnetic tilt correction in intrusive rocks and compaction shallowing in the stratified rocks. It should be noted that errors in the terrane tracks at 100 Ma allow 500-1000 km, so only an approximate position of accretion of Baja BC to the North American margin can be determined.

The occurrence of the Pliensbachian ammonite faunal province boundary between Tethyan and Mixed Tethyan and Boreal in Stikinia and Quesnellia may be used in a similar fashion. Moores (1998) suggests that these terranes were accreted to the North American margin at ~170 Ma. At this time, Cape Mendocino lay at 28°N paleolatitude, and so may have been the approximate docking position of Stikinia and Quesnellia.

Comparison of paleomagnetic data and terrane tracks for Baja California suggests that it lay either on the North American margin near the Viscaino Peninsula or on a northern terrane track with accretion approximately at its present location on the North American margin. The spread of Upper Cretaceous-Lower Cenozoic paleomagnetic data does not permit determination of the amount of latitudinal movement relative to North America.

Moores, E.M. 1998. Ophiolites, the Sierra Nevada, "Cordilleria," and orogeny along the Pacific and Caribbean margins of North and South America: International Geology Review, v. 40, p. 40-54.

Composition of peridotitic mantle from below the Slave craton.

Maya G. Kopylova and J.K. Russell

Geological Sciences Division, Earth and Ocean Sciences, The University of British Columbia, 6339 Stores Road, Vancouver, Canada, V6T 1R9.

Introduction

Our previous research on mantle xenoliths from the Mid-Jurassic Jericho kimberlite pipe elucidated the thermal state of the lithosphere underlying the north central Slave craton (Kopylova et al., 1998; Russell and Kopylova, 1999). Our analysis of P-T data from peridotitic xenoliths showed the Slave craton to be characterised by "hot" crust and "cool" mantle (Kopylova et al., 1999). The craton supports high surface heat flow (54 mWm^{-2}) because the upper crustal rocks of the craton are radiogenically-enriched, relative to other cratons. In contrast, the P-T array for the lithosphere shows the Slave mantle to be cooler than that underlying South Africa (Kopylova et al., 1999; Russell and Kopylova, 1999).

These geothermobarometric studies also allowed a stratigraphic column to be made for the lithosphere beneath the north central Slave (Kopylova et al., 1998). The resulting stratigraphic reconstruction showed the lithosphere to be dominated by coarse spinel + garnet peridotite over the depth interval of 45 to 180 km. Garnet peridotite derives from depths of 110 to 180 km and high-temperature, porphyroclastic peridotite is found at depths greater than 190 km. Furthermore, we were able to demonstrate that eclogite xenoliths derive mainly from depths between 90 and 195 km and may explain, in part, the layering in the mantle defined from teleseismic survey results (Bostock, 1997).

The purpose of this paper is to report on the chemical composition of the peridotitic mantle to the Slave craton. Specifically, we aim to characterize the chemical composition of the deep lithosphere, to compare its chemical composition to other cratonic lithosphere, and to show the variation in mantle composition with depth. Our analysis is based on chemical analyses of 39 samples of fresh peridotite xenoliths. The sample suite includes spinel peridotite, low-T garnet peridotite, and high-T garnet peridotite. Our data set includes both chemical analyses of bulk rock samples and measured modal mineralogy from thin section analysis. These results are also presented in poster format (cf. Begbie and Kennedy, this volume).

Sample Preparation

Preparation of samples for major element chemical analysis was as follows. All samples used were 400 to 500 g in size as suggested by Boyd and Mertzman (1987); restricting the sample suite to large samples was an attempt to eliminate the effects of small-scale (< cm) heterogeneity. The samples were pulverized incrementally, beginning with a jaw crusher and followed by grinding in a tungsten-carbide ring mill. In order to preserve the original redox state of

iron in the powders, grinding times were held to a minimum (generally under 90 s). All powders were analysed by X-ray fluorescence spectrometry at the Geochemical Lab of McGill University (Montreal, Canada). Several peridotite xenoliths were split into a 500 g and 100 g sample and then analysed separately to investigate the impact of sample weight on measured composition. The maximum variation between samples was found to be approximately 1 wt. % in SiO_2 and MgO and is attributable to small variations (5-6 vol %) in modal amounts of olivine and orthopyroxene.

Calculated Modal Mineralogy

The chemical compositions of peridotite samples were converted into an equivalent mineral norm using mass balance relationships that reflect the observed mineralogy (spinel, garnet, and spinel-garnet peridotite). The calculated modes are highly dependent on which elements are considered immobile (e.g., not introduced by metasomatism). We used a subset of samples for which bulk rock compositions, mineral compositions and mineral modes were known independently to identify the "optimum" immobile elements. Based on our analysis all elements except for Na and Fe^{3+} showed good agreement between calculated and measured values. Ferric iron correlated with Loss-on-Ignition and therefore was thought to reside mainly in fine oxides associated with development of secondary serpentine. Measured values of sodium are always higher than the corresponding values calculated from modes (Fig. 1) indicating the possible effects of late-stage sodium metasomatism. Our best results derived from using silica, magnesium+ ferrous iron, alumina and chromium for norm recalculation purposes.

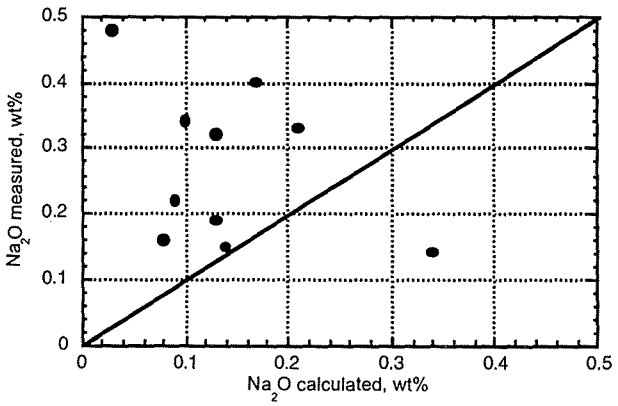

Fig. 1. A plot of measured wt. % Na2O for bulk peridotite samples versus Wt. % Na2O calculated from the modal mineralogy and mineral compositions for same samples.

Measured Modal Mineralogy

We have also estimated the modal abundance of each phase using image analysis techniques applied to scanned images of thin sections of

Table 1. Average bulk and modal compositions of Slave peridotites in comparison with other cratonic and abyssal peridotites.

Sample	Jericho Low T Gar Pd		Kaapvaal [1] Low-T Gar Pd	Udachnaya [2] Low T Gar Pd		Jericho Spinel Pd		Udachnaya [2] Spinel Pd		Abyssal [3]	Jericho High T Gar Pd		Udachnaya [2] High T Gar Pd	
	Av. of 15	St Dev	Av. of 28	Av. of 12	St Dev	Av. of 10	St Dev	Av. of 10	St Dev	Average	Av. of 9	St Dev	Av. of 20	St Dev
SiO2	44.37	1.46	46.57	39.65	1.99	44.47	1.85	40.35	1.68	43.6	42.03	0.74	40.36	1.56
TiO2	0.07	0.10	0.04	0.06	0.05	0.03	0.01	0.02	0.01	0.02	0.09	0.05	0.11	0.04
Al2O3	1.52	1.98	1.46	1.18	1.02	0.77	0.38	0.85	0.37	1.18	1.44	1.00	0.93	0.47
FeO	5.72	0.39		3.79	1.86	5.29	0.28	3.74	0.98		6.59	0.50	3.77	1.23
Fe2O3	1.26	0.48		3.39	1.92	0.97	0.28	2.72	0.99		1.74	0.33	3.98	1.26
MnO	0.12	0.02	0.12	0.13	0.04	0.10	0.00	0.11	0.04	0.14	0.13	0.01	0.12	0.03
MgO	42.68	4.41	44.05	40.71	4.15	45.40	1.58	40.98	2.57	45.2	43.17	2.68	40.10	2.42
CaO	1.31	1.39	0.79	0.98	0.59	0.51	0.22	0.68	0.41	1.13	1.21	0.95	1.13	0.49
Na2O	0.26	0.17	0.09	0.07	0.02	0.16	0.06	0.06	0.02	0.02	0.28	0.13	0.09	0.04
K2O	0.17	0.09		0.12	0.06	0.10	0.04	0.11	0.05		0.23	0.20	0.09	0.06
P2O5	0.03	0.02		0.01	0.01	0.02	0.01	0.01	0.01		0.04	0.03	0.01	0.01
LOI	1.57	1.00		9.73	5.73	1.48	0.56	10.37	2.84		1.71	0.68	9.11	3.55
Total	100.25	0.29		99.86	0.30	100.41	0.25				99.97	0.24	99.79	0.24
Cr203	0.406	0.140	0.4	0.175	0.079	0.369	0.088	0.143	0.029	0.22	0.463	0.157	0.141	0.008
NiO	0.271	0.044	0.27	0.161	0.023	0.288	0.026	0.176	0.018	0.22	0.293	0.039	0.211	0.054
Fe tot as FeO	6.77	0.60	6.24	6.80	0.40	6.10	0.45	6.09	0.37	8.22	8.05	0.60	7.37	0.64
Mg/Mg+Fe	0.918	0.014	0.926	0.915	0.007	0.931	0.004	0.924	0.005	0.908	0.906	0.010	0.907	0.010
Ca/Al	1.309	0.501	0.730	1.406	0.671	0.986	0.371	1.169	0.565	1.290	1.104	0.318	1.785	0.620
Mg/Si	1.239	0.142	1.220	1.320	0.107	1.316	0.095	1.307	0.088	1.340	1.321	0.088	1.277	0.055
Ol (%)	67.8	7.3	61.0			69.9	9.6			78.6	75.1	6.9		
Cpx (%)	20.7	6.6	31.4			27.1	9.7			12.5	14.0	4.8		
Opx (%)	5.2	3.8	1.8			2.4	2.2			4.4	3.9	3.5		
Spl (%)	0.3	0.2									0.3	0.2		
Gar (%)	6.2	3.6	5.8			0.7	0.1			4.5	6.7	5.3		

1 and 3 - from Boyd (1989)
2 - from Boyd et al., (1997)
3 - from Dick and Fisher (1984)

peridotite. Digital images were acquired using a Polaroid Sprintscan® 35 on thin sections of peridotite that were cut thicker than normal (>30 microns) to give pyroxenes a stronger body colour. The images were collected using a polarized light source. Digital images were then enhanced by changing the colours of individual minerals to a false-colour scale using ADOBE PHOTOSHOP® 4.0. The resulting images were analysed for the modal proportions of each mineral using free image analysis software distributed by the National Institute of Health. Areas of serpentine (normally < 5 %) were interpreted as replacing either olivine and/or orthopyroxene. Mineral modal abundances estimated by this procedure totalled to 100 +/- 2.5 % which provides a measure of uncertainty for the technique. The effects of sample heterogeneity were estimated by measuring mineral modes for 7 thin sections from a single sample. The variance due to sample heterogeneity was approximately 7% for olivine and orthopyroxene and 3% for clinopyroxene and garnet. Thus, variances due to uncertainties in this image analysis technique (+/- 2.5 %) are less than the variances attributable to sample heterogeneity.

Comparison of Calculated and Measured Modes

Each of these two methods of estimating modal mineral proportions has its own attributes. Image analysis methods can provide more rapid and economical modal data, but are affected more by small scale mineralogical variations. Conversely, modes calculated from bulk rock analyses can be less subjective and are based on a larger sample size. We have compared our measured and calculated mineral modes. For 65% of the peridotite samples modal mineralogy fits the calculated mineral norm within the limits established for sample heterogeneity. The remainder of peridotite samples (35%) show pronounced differences between the two modes. Many of these samples have high values of LOI (> 4%) and, thus, the calculated mode may not reflect the primary mineralogy. In such samples mineral modes determined in thin sections are more accurate. Another group of xenoliths showing a misfit between image analysis modes and modes calculated from chemical analyses include high-T fluidal peridotite that are very fine-grained. For these samples, the calculated norm is interpreted to be more reliable than the results from image analysis.

Results

Table 1 summarizes results of this study. It shows the average bulk chemical compositions and modal mineralogy for spinel peridotite, low-T garnet peridotite and high-T garnet peridotite from Jericho versus corresponding compositions for peridotite from the Kaapvaal and Siberian craton. Our results show that the high-T peridotite from the north central Slave craton is very similar to oceanic abyssal peridotite (Table 1) in terms of major element composition and modal mineralogy. In contrast, low-T garnet peridotite and spinel peridotite from Jericho are substantially more depleted in basaltic components.

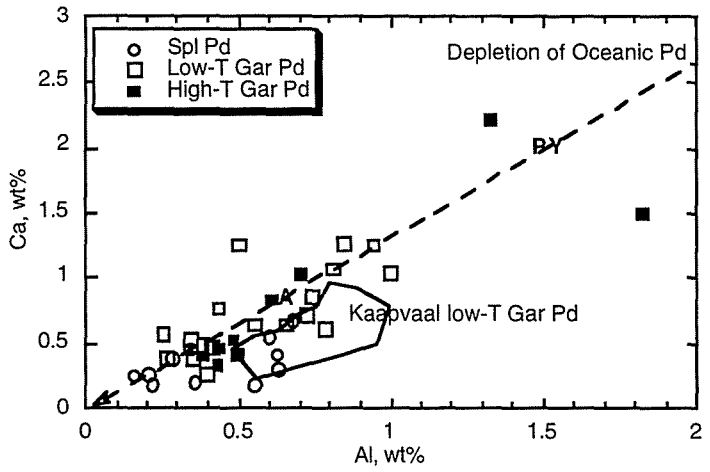

Fig. 2. A plot of Ca and Al for spinel (open circles), low-T garnet (open squares), and high-T garnet (solid squares) Slave peridotites. A solid line delineates a field for low-T Kaapvaal peridotite (Boyd, 1989). Dashed arrow marks a depletion trend for oceanic peridotite (Boyd, 1989). Also shown are average compositions of abyssal peridotite **A** (Dick and Fisher, 1984)and pyrolite **PY** (Ringwood, 1979).

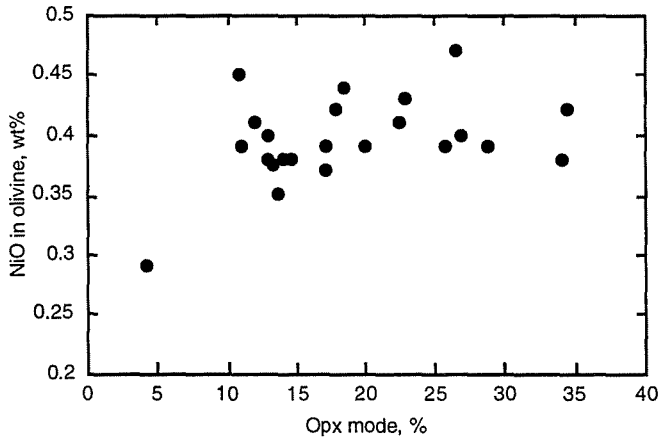

Fig. 3. Plot of NiO in olivine against modal orthopyroxene (wt%) for Jericho peridotite.

This is shown clearly in Fig. 2, where the trend established for oceanic peridotite that has undergone depletion by melt extraction (Boyd, 1989) is compared to compositions of cratonic peridotite. Oceanic peridotite compositions form a positively correlated array stretching from primitive mantle (PY) to the origin where alpinotype harzburgite plots. Slave peridotite compositions range from depleted alpinotype harzburgite to compositions more fertile than an average abyssal oceanic peridotite (A; Fig. 2). Several high-T garnet peridotites show chemical compositions as fertile as pyrolite although they differ somewhat in the Ca/Al ratio from pyrolite (PY). Slave peridotite clusters along the oceanic trend and has high Ca/Al values (Table 1, Fig. 2). It

defines a slope of 1.15, which is significantly higher than the Ca/Al ratio (0.73) defined by Kaapvaal cratonic peridotite. This correlates with the Slave peridotite containing more clinopyroxene (5.2±1.9%) than Kaapvaal low-T garnet peridotite (1.8%, Boyd, 1989). The Ca/Al ratio also distinguishes distinct groups of Slave peridotite (Table 1). Ca/Al values are highest for low-T garnet peridotite (1.31), intermediate in high-T garnet peridotite (1.10), and lowest in spinel peridotite (0.99)

The correlation between Ni in olivine and orthopyroxene modes found in some cratonic xenolith suites (Boyd et al., 1997) is absent at Jericho (Fig. 3). Here, the correlation coefficient is equal to 0.408 and the vast majority of samples contain olivine with 0.37-0.45 wt% NiO which is independent of orthopyroxene content.

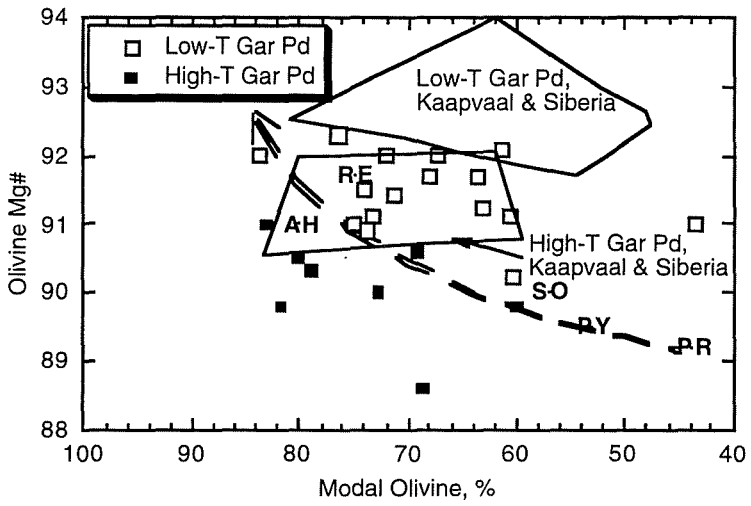

Fig. 4. Modal abundance of olivine (vol. %) is plotted against olivine composition (Mg#). Samples include low-temperature peridotite (open squares) and high-temperature peridotite (solid squares). Also shown are fields for low-temperature and high-temperature peridotites from the Kaapvaal and Siberian craton (Boyd et al., 1997). Other symbols include: **PR,** primitive upper mantle (Palme and Nickel, 1985); **PY,** average pyrolite (Ringwood, 1979); **SO** and **RE,**model source and residue for MORB (Cox et al., 1973); and **AH,** average Troodos harzburgite representing depleted upper mantle (Loney et al., 1971). A dashed arrow designates the "oceanic trend" of Boyd (1989).

The Slave peridotitic mantle differs from the mantle below other cratons in that it comprises less magnesian olivine and the low-T peridotite contains more olivine. Fig. 4 shows Mg-number (MG#) of olivine versus olivine modes for the Slave craton in comparison to those from the Kaapvaal and Siberian cratons. Low-T peridotite from the Slave has an average Mg# of 91-92 and contains ~68% of olivine in contrast to other cratonic low-temperature peridotite which have average Mg#'s of 93 and slightly less modal olivine. The Slave low-temperature peridotite is, in fact, closer to high-temperature peridotite from other cratons and to the "oceanic trend" defined by Boyd (1989) (Fig. 4). Olivine found in high-T peridotite from the Slave also has a lower average Mg# (90)

than olivine in high-temperature peridotite from other cratons (91.5). The modal abundances of olivine are similar and lie between 84 and 60%.

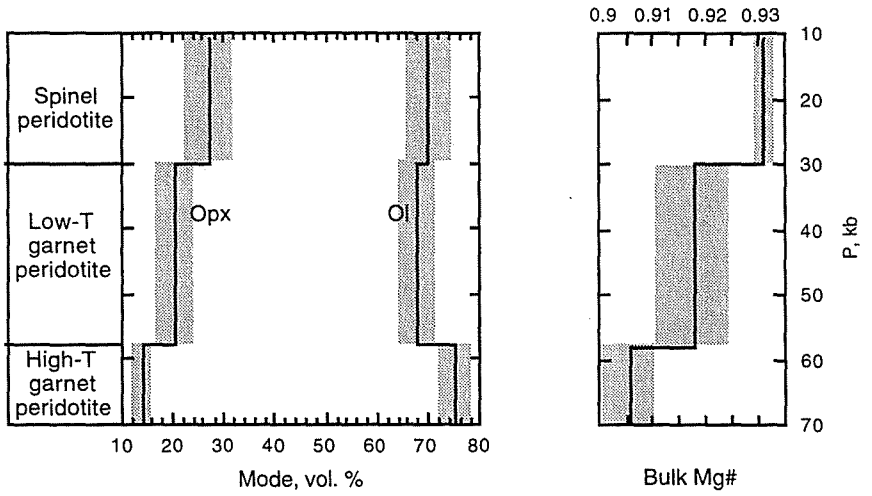

Fig. 5. Petrological characteristics of peridotite xenoliths from the Jericho kimberlite are plotted against equilibration pressures calculated in Kopylova et al. (1999). Mineralogical and chemical attributes include: modal proportions of orthopyroxene and olivine and Mg/(Mg+Fe) for bulk rocks. Shaded regions denote 1 standard deviation.

There is a marked depth-dependence to the chemical and mineralogical characteristics of the Slave peridotitic mantle (Fig. 5). Bulk rock chemical compositions show a pronounced decrease in Mg# with depth. The highest Mg#'s are found in spinel peridotite (shallowest xenoliths) and the lowest Mg#'s are found in high-T peridotite at depths greater than 170 km. The Mg-rich bulk chemistry of spinel peridotite is consistent with the presence of highly magnesian olivine found in spinel peridotite and described by Kopylova et al. (1999). Low-T garnet peridotite shows higher Ca and Al contents than spinel peridotite (Table 1), we attribute this to the presence of modal garnet. The transition from low-T to high-T garnet peridotite is also corresponds to an increase in FeO and decrease in SiO2 (Table 1).
Modal olivine is relatively constant with depth, but deeper mantle (High-T peridotite) appears to have the highest olivine contents (Fig. 5). Lastly, modal orthopyroxene in mantle rocks decreases with depth from 30 - 12 vol. %. Shallower mantle (spinel peridotite) has the highest content, low-T peridotite contains intermediate amounts of orthopyroxene and high-T peridotite has the lowest abundance (Fig. 5).

Conclusions

Our results show the Slave peridotite mantle to be chemically and mineralogically distinctive with respect to the peridotitic mantle below other

cratons. It is less depleted than other cratonic mantle as indicated by Mg#'s for bulk rock chemical analyses and compositions of olivine. Peridotite from the Slave mantle also has higher concentrations of Ti, Ca and Al. Modally, the Slave mantle is richer in olivine and clinopyroxene and contains less orthopyroxene (21% versus 31% for the Kaapvaal) than found in peridotite from other cratons. In this regard, the Slave peridotitic mantle bears a greater resemblance to moderately depleted oceanic mantle.

The character of late mantle metasomatism on the Slave also contrasts to mantle metasomatism found on other cratons. The only introduced element to the Slave mantle is sodium, whereas late Fe introduction is common beneath the Kaapvaal and Siberian cratons (Boyd et al., 1997).

Finally, the Slave mantle lithosphere appears to be chemically and mineralogically zoned with respect to depth. Both the abundance of modal orthopyroxene and the Mg#'s of bulk samples of peridotite decrease with sample depth. In summary, these data suggest that the Slave craton is unique not only with respect to the high surface heat flow and relatively cool mantle (Russell and Kopylova, in press) but also in the chemical composition of the peridotitic mantle.

Acknowledgements. This research was supported financially by NSERC-LITHOPROBE as part of the SNORCLE transect initiative.

References

Bostock, M.G., 1997. Anisotropic upper mantle stratigraphy and architecture of the Slave craton. Nature, 390, 392-395.

Boyd, F.R., 1989. Compositional distinction between oceanic and cratonic lithosphere. Earth and Planetary Science Letters, 96, 15-26

Boyd., F.R., Pokhilenko, N.P., Pearson, D.G., Mertzman, S.A., Sobolev, N.V., & Finger, L.W., 1997. Composition of the Siberian cratonic mantle: Evidence from Udachnaya Peridotite xenoliths. Contrib. Miner. Petrol., 1997, 128, 228-246

Cox K.G., Gurney, J.J., & Harte, B., 1973. Xenoliths from the Matsoku pipe, in: Lesotho kimberlites, P.H. Nixon, ed., pp 76-100. Lesotho National Development Corp., Maseru, Lesotho, 1973.

Dick, H.J.B., & Fisher, R.L., 1984. Mineralogic studies of the residues of mantle melting: Abyssal and Alpine-type peridotites, in : Kimberlites, II, The mantle and Crust-Mantle relationships, Proc. of the 3rd Intern. Kimb. Conf., J. Kornprobst, Ed., pp.295-308, Elsevier, New York, N.Y.

Loney, R.A., Himmelberg, G.R., & Coleman, R.G. 1971. Structure and petrology of the Alpine-Type peridotite at Burro Mountain, California, USA., J. Petrol., 12, 245-309.

Kopylova, M.G., Russell, J.K., & Cookenboo, H. 1998. Upper-mantle stratigraphy of the Slave craton, Canada: Insights into a new kimberlite province. Geology, 26, 315-318.

Kopylova, M.G., Russell, J.K., & Cookenboo, H. 1999. Petrology of Peridotite and pyroxenite xenoliths from the Jericho Kimberlite: Implications for the thermal stata of the mantle beneath the Slave Craton, northern Canada. J. of Petrol., 40, 1, 173-208

Palme, H. & Nickel, K.G., 1985. Ca/Al ratio and composition of the Earth's upper mantle. Geochim. Cosmochim. Acta, 49, 2123-2132.

Ringwood A.E. 1979. Origin of the Earth and the Moon, Springer-Verlag, New York, 295 pp.

Russell, J.K. & Kopylova, M.G., 1999 A steady-state conductive geotherm for the north central Slave, Canada: Inversion of petrological data from the Jericho kimberlite pipe. J. Geophys. Res., in press 01/99.

GEOCHRONOLOGICAL, PETROLOGICAL AND MICROSTRUCTURAL STUDIES ON THE THOR-ODIN DOME, MONASHEE COMPLEX, SOUTHERN CANADIAN CORDILLERA.

Kuiper, Yvette D.[1], Carr, Sharon D.[2], and Williams, Paul F.[1]

1. Department of Geology, University of New Brunswick, Fredericton, N.B., E3B 5A3
2. Ottawa-Carleton Geoscience Centre and Department of Earth Sciences, Carleton University, Ottawa, Ontario, K1S 5B6.

The basement-cored Monashee Complex of the southern Omineca Belt comprises two structural culminations; Frenchman Cap in the north and Thor-Odin in the south. The Selkirk Allochthon, which structurally overlies the Monashee Complex has been interpreted as having been emplaced onto the Monashee Complex by NE-directed transport on the Monashee Décollement (Brown et al., 1986, 1992). The location and the character of the décollement, and therefore the division between the rocks of the Monashee Complex and the Selkirk Allochthon, are based on lithologic, metamorphic, structural, geochronologic and regional arguments from a number of areas studied on the flanks of both Frenchman Cap and Thor-Odin domes (Journeay, 1986; Brown et al., 1986, 1992, and references therein; McNicoll and Brown, 1995, and references therein). However, recent work by Williams, Spark, and Johnston on the western flank of Thor-Odin has failed to reveal the décollement. Instead, a zone of uniform transposition extending throughout the exposed depth of the complex is observed. Transposition was followed by younger folds, E-W boudinage and regional extension (Johnston et al., 1996; Johnston, 1997; Spark, 1997).

U-Pb data indicate a younging of structures and thermal peak of metamorphism with decreasing structural level in the Selkirk Allochthon and Monashee Complex (Parrish, 1995, and references therein; Crowley, 1997; Gibson, 1997; Carr, 1992). Data from western Thor-Odin show the same pattern (Johnson, 1994; Johnston, 1997; Johnston et al., 1998). Metamorphic monazite ages are 94-90 Ma in the Selkirk Allochthon west of the Joss Pass brittle fault and ~57-55 Ma in the Monashee Complex east of the Joss Pass fault (Johnston, 1997). This apparent downward younging pattern may have resulted from either 1) downward heat conduction from an overthrust hot crustal slab with or without hot intrusions, 2) the juxtaposition of rocks with different metamorphic grades and ages by thrusting, normal faulting, or folding, or 3) a combination. However, enigmatic U-Pb metamorphic ages from Three Valley Gap (73.4±1.7 Ma zircon, Parkinson 1992; 89.5±0.5 Ma zircon, Wasteneys, unpublished data, 1998; ca. 72, 59.5 and 49 Ma monazite, Kuiper and Carr, unpublished data, 1998) do not fit the apparent downward younging pattern. This is being adressed by new fieldwork and laboratory studies. Samples have been collected from the western flank of Thor-Odin during summer 1998 for geochronological and geothermobarometrical studies in order to establish variation in metamorphic grade and age with structural depth, to test whether there is a gradient or whether there are two age domains present.

Detailed metamorphic and U-Pb geochronological studies are being conducted on the northwest and west flanks of Thor-Odin in order to characterize the protolith age of rocks as well as the conditions and timing of deformation, high-temperature metamorphism and cooling history at all structural levels and on both sides of identified structures. This may: 1) allow Selkirk Allochthon and Monashee Complex rocks to be distinguished, 2) establish the presence or absence of the Monashee Décollement as a syn- or post-F_1 structure, 3) deduce the thermal history throughout the structural profile, 4) place some constraints on the magnitude of displacement of structural discontinuities, 5) test ideas as to whether or not Frenchman Cap and Thor-Odin are at the same structural level, and 6) test existing tectonic models for the area (cf. e.g. Johnston et al., 1998; Parrish 1995). Research is carried out under the supervision of P.F. Williams (University of New Brunswick), S.D. Carr (Carleton University), and E.D. Ghent (University of Calgary). This project will elucidate the structural relationships between the Monashee Complex and the Selkirk Allochthon, between the Frenchman Cap and Thor-Odin culminations, and distinguish between compressional and extensional fault systems.

Central Foreland NATMAP: Preliminary results of detailed mapping in the Trutch and Toad River areas, northeastern B.C.

Lane, L.S., Geological Survey of Canada, Calgary*
Bednarski, J., Geological Survey of Canada, Calgary, Alberta T2L 2A7
Cecile, M.P., Geological Survey of Canada, Calgary, Alberta T2L 2A7
Currie, L.D., Geological Survey of Canada, Calgary, Alberta T2L 2A7
Legun, A., British Columbia Geological Survey Branch, Victoria, B.C., V8W 9N3
Okulitch, A.V., Geological Survey of Canada, Calgary, Alberta T2L 2A7
Stockmal, G.S., Geological Survey of Canada, Calgary, Alberta T2L 2A7

The Central Foreland NATMAP Project is a multidisciplinary study across two broad transects through the Cordilleran foreland near 57°N and 60°N, designed to investigate the underlying tectonic and stratigraphic controls on the transition from a narrow belt of kilometre-scale structures in the south to a broad belt of 5-10 km scale structures in the north. The region has economic importance for petroleum and base metal resources. Active gas developments exist in (among others) the Sikanni, Buckinghorse, Pocktknife, Pointed Mountain and Kotaneelee fields. In 1998, new mapping was undertaken at 1:50,000 and 1:250,000 scales in parts of the Trutch and Toad River map areas (southern transect). Also, new colour compilations of previous mapping in the Fort Nelson map area at 1:500,000, and the Toad River and Ware map areas at 1:250,000 are now available. Affiliated stratigraphic and subsurface studies were begun in 1998.

Colour compilations of 1:50,000 scale maps covering all of 94G/3 and 94G/6, parts of five adjacent map areas, as well as part of 94N/4 illustrate the stratigraphy and detailed structural geometry characteristic of the area. In Trutch, mapping focused on areas underlain by upper Paleozoic and Mesozoic strata. In most units, significant changes in facies or preserved thickness occur over distances of a few to tens of kilometres along and across strike. Fold geometries include box and chevron styles in the east. Farther west and north, folds are tight, commonly overturned, and locally disrupted by thrust faults. The folds are detached within the Besa River and Toad-Grayling formations. Individual folds are mappable for long distances, but some exhibit abrupt changes in plunge or trend, or en echelon transfer of shortening to adjacent structures. Important disparities between the trends of local structures and that of regional structures, indicate that surface structures are influenced by subsurface features, such as facies boundaries and Paleozoic structural trends. One such feature extends for more than 70 km through three map areas, and may reflect subsurface structure in the lower Paleozoic succession. In westernmost Trutch and Toad River areas, lower Paleozoic carbonate successions form rugged ranges exposing brittle, thrust-dominated structures in dolomitic units and mixed ductile shears and tight overturned folds in limestone units.

Mapping of the surficial geology, drift geochemistry and landslide hazards in the Trutch map area comprises part of this NATMAP project. Numerous stratigraphic sections in the Rocky Mountains and foothills record outwash, till and glaciolacustrine sequences related to advance and retreat of Cordilleran ice that originated west of the area, and local montane ice. Glacially scoured bedrock and erratics show that eastward-flowing Cordilleran ice reached the mountain front. Sometime after, the Laurentide Ice Sheet, advancing from the eastern plains, also reached the mountain front. In some places, the Laurentide and Cordilleran advances may have been synchronous.

Preliminary sedimentological analysis of the Cambrian Atan Group in northern B.C. - A rifted margin with fluvial cobble conglomerate to deep marine olistostromal carbonate facies

Long, D.G.F., Devaney, J.R. (Dept. Earth Sciences, Laurentian University, Sudbury, Ontario P3E 2C6) and **Pratt, B.R.** (Dept. Geological Sciences, University of Saskatchewan, 114 Science Place, Saskatoon, SK, S7N 5E2)

Sedimentary strata of the lower and/or Middle Cambrian Atan Group, exposed in the Rocky Mountains of northern British Columbia, preserve a record of rift related events along part of the northwest paleo-margin of North America. The most proximal deposits, at Muncho Lake and Mt. Roosevelt, are thick (up to ~ 1 km) linear (strike parallel), monotonous successions of polymict cobble and pebble conglomerate with minor red-bed sandstone interbeds. Predominantly quartzitic clasts within these braided river deposits were derived from partial erosion of Mesoproterozoic rocks of the Muskwa Assemblage. Boulder grade conglomerates and strata containing evidence of deposition on arid region alluvial fans adjacent to faults were not found. Two sites containing evidence of calcrete paleosols in sandy fluvial overbank deposits appear to be located near the base and top of the Group, although the age and stratigraphic context is presently poorly constrained. More distal, poorly fossiliferous marine deposits are exposed in a parallel facies belt to the west. In the northern part of the study area, west of Muncho Lake, poorly exposed muddy shelf sequences appear to shallow upwards to tidal and other sandy coastal facies, with herringbone cross-stratification, flaser bedding, syneresis cracks, *Skolithos* burrows, and rare thin beds of well sorted fine-pebble conglomerate.

In the southeastern part of the study area terrigenous (quartzitic) sand and gravel were transported to both shallow water carbonate platformal areas, with wave ripples, stromatolites and oolites, and to deeper marine slopes in which coarse mass flow deposits, including debris flows and turbidites, contain a mixture of carbonate intraclasts and extrabasinal lithoclasts. At Mount Scott, many debris-flow beds consist of large metre- to decimetre-sized blocks of microbial Girvanella-Epiphyton boundstone. These may represent building and shedding from an actively accreting upper slope reef complex. Archaeocyathids are not present. Trilobites collected from the upper part of the sequence at this locality indicate that at least part of the sequence is of Ordovician age.

Predominantly carbonate mass-flow deposits in strata to the south (W of Toad River) include olistostromal mega-blocks which may have resulted from collapse of part of the platform margin via rift-associated normal faulting of the basement. The olistoliths, previously interpreted as Archaeocyathid-reefs, consist of blocks of non-fossiliferous dolostone which are generally flat-lying and tabular, and are up to tens of metres thick and tens to hundreds of metres long. Within the blocks both tectonic and syn-sedimentary fractures (with muddy injections) can be recognised.

Exposures studied to date have not yielded full and continuous cross-sections of the Atan Group, limiting tectonostratigraphic analysis. As a preliminary interpretation it is suggested that two major regressive-transgressive cycles are present. Local evidence for rifting is presently weak and indirect: the vertical persistence of fluvial facies to the east and marine facies to the west, suggests a steep, fault controlled margin, and as noted above, evidence for a collapsed carbonate margin in the southwestern part of the study area suggests rifting of the basement.

CONTINUITY INTO THE CORDILLERAN INTERIOR FROM THE NORTH AMERICAN CRATON OF ARCHEAN AND PROTEROZOIC TRANSVERSE CRUSTAL STRUCTURES: EVIDENCE FROM GEOLOGICAL AND POTENTIAL-FIELD DATA

Henry Lyatsky
LGR&C Ltd., 4827 Nipawin Cres. NW, Calgary, Alberta T2K 2H8
ph./fax (403) 282-5873 lyatskyh@cadvision.com www.cadvision.com/lyatskyh

Summary. Steep crustal-scale faults, having their origins in the Late Archean and Early Proterozoic and trending NE-SW, which define the fundamental block structure of the North American craton, continue far into the Canadian Cordilleran interior. In the Phanerozoic, they controlled great and small transcurrent tectonic Cordilleran features, including the prominent Skeena and Stikine arches in the Intermontane Belt. Large gravity and magnetic lineaments also run across the Cordillera NE-SW. Geological and geophysical expressions of transverse ancient structures are relatively subdued in the Omineca and Coast Belt orogenic zones, where Mesozoic and Cenozoic tectonic reworking of the crust was extremely intense, but they are better expressed in the less-reworked Intermontane Belt and Yukon-Tanana massifs. In seismic reflection data, the origins and ages of low-angle reflections are unknown. These data are generally unable to detect steep crustal discontinuities, creating a false impression that the crust consists of stacked low-angle exotic-terrane thrust slices. But in reality, continuity of ancient steep transcurrent crustal structures and Paleozoic platformal sedimentary-cover units from the craton suggests that variously reworked ex-cratonic basement underlies much of the Cordillera. The western edge of the modern craton is the Rocky Mountain-Omineca belt boundary, where Cordilleran tectonic reworking of the crystalline crust is first encountered. Phanerozoic differences between the Cordilleran tectonic belts, resulting from a long, dissimilar, multi-cycle history of waxing and waning orogenesis, lie chiefly in the degree of indigenous tectonic remobilization and reworking of the ancient crust.

Steep, deep-seated, long-lived crustal weakness zones are well known to have existed in the western part of the North American craton since Late Archean or Early Proterozoic time. Their recognition is based on reliable geological field mapping, subsurface geological studies and geophysical surveys conducted for decades in the Canadian Shield and adjacent Phanerozoic cratonic platforms. These ancient weakness zones are seen to continue far into the Cordilleran interior, where they influenced many tectonic manifestations throughout the Phanerozoic.

Trending mostly NE-SW, ancient crustal weakness zones divide the North American craton into distinct large blocks. Some of these zones predate cratonization, which occurred in the Early Proterozoic in Alberta and Saskatchewan and somewhat later in much of the U.S. Many more steep brittle faults, variously following and cutting across the ancient ductile structures, were created in the upper crust after cratonization.

Being generally unable to detect high-angle rock discontinuities, seismic reflection profiles may give the unwary a false, incomplete impression that only low-angle discontinuities exist in the continental crust. The nature, origin and age of these seismically reflective low-angle crustal discontinuities are unknown, and they could be related to a multitude of

possible causes: original discontinuities in the protolith, subsequent superimposed metamorphic fronts and rheologic boundaries, ductile and brittle shearing, intrusive igneous bodies and so on. Most steep discontinuities are missed in seismic reflection images altogether, but they are better detected with potential-field data.

A geophysical anomaly, by itself, is unable to reveal the nature and age of its geologic source. Without direct geological observations, the inherent non-uniqueness of interpretations of the geophysically imaged geometries in the distribution of specific physical rock properties precludes definitive conclusions about the composition and structure of the deep crust. Even in the exposed and drilled uppermost part of the crust, every dry oil or water well, and every failed mining or geotechnical project, represents a failure of prediction.

Seismic experiments in crystalline terrains, where the multiply-reworked continental-basement rocks are exposed, show the reflectivity in these rocks to be exceedingly complex, with countless, variously oriented, unpredictable reflectors. Superdeep wells drilled into the upper continental crust in Europe, Russia and North America have also presented many surprises quite unanticipated by prior geophysical predictions, including unexpected findings about sources of seismic reflections and potential-field anomalies, as well as position of the brittle-ductile boundary and thermal and hydrologic conditions. Not even such sparse geological constraints are available for the middle and lower crust. The arbitrary and model-driven assumption that seismic-reflection geometries deep in the continental crust mostly represent thrusting contradicts the existing geological observation and leads to an incorrect perception that continental crust is usually a stack of thrust sheets.

Another false myth in modern tectonics is that continental lithosphere is essentially inert, responding only passively to external influences from plate boundaries and sub-lithospheric mantle. Having its own sources of energy, continental lithosphere is capable of indigenously driven self-development, and external plate-boundary influences (subduction, terrane collisions etc.) and mantle plumes are not required to explain all intracontinental tectonism.

Rejuvenation of old steep weakness zones and fractures, and creation of new ones, in various crustal tectonic regimes and conditions, influenced block movements and the formation of volcano-sedimentary cratonic basins in the Proterozoic and Phanerozoic. The cratonic Proterozoic Athabasca Basin in northern Saskatchewan and Alberta, for example, has a polygonal, almost N-S/E-W shape, and it is cut internally by through-going NE-SW-trending block boundaries (notably, Virgin River-Snowbird).

Cratonic crustal block movements and warping in the Phanerozoic played a crucial part in the development of the cratonic platformal basins - Alberta, Williston and others. High-angle faults, rejuvenated sporadically in favorable stress regimes, imposed the widespread NE-SW/NW-SE and N-S/E-W pattern on the distribution of lithofacies and thicknesses at various levels in the sedimentary cover and strongly affected the distribution of hydrocarbon fields. These steep cratonic basement-rooted faults are commonly unnoticed in deep seismic surveys, but they are clearly recognizable from geologic variations in the sedimentary cover, neotectonic crustal movements, and potential-field anomalies. For example, the repeatedly inverted Peace River Arch in the northern Alberta Basin has been active throughout the Phanerozoic. In it, many steep faults with offsets in the hundreds of meters are known to have accommodated multiple episodes of block uplift, subsidence and tilting.

With smaller amplitudes, similar block movements are recorded in sedimentary-cover rock units throughout the Phanerozoic all across the cratonic Alberta and Williston basins. By controlling the dissolution of Devonian salt beds, these straight, steep faults have in some cases been able to influence the Mesozoic and Cenozoic sedimentation patterns and modern topography even without any structural offsets at all.

On trend with the Proterozoic Athabasca Basin and the latest Proterozoic-Phanerozoic Peace River Arch, the prominent NE-SW-trending Skeena Arch in the Cordilleran interior has manifested its activity since at least the Mesozoic, dividing the Intermontane Belt into major crustal blocks and forming the southern boundary of the Bowser Basin. Some faults on trend with the Skeena Arch's southern boundary have been noted to continue even into the Cordilleran Coast and Insular belts farther west. The other transcurrent arch in the Intermontane Belt, Stikine, which bounds the Bowser Basin on the north, has a similar nature. Mesozoic sedimentary basins in the Intermontane Belt - Bowser, Nechako, Whitehorse Trough - owe their existence to differential uplift, subsidence and tilting of crustal blocks separated by transverse and Cordillera-parallel crustal faults. Further indications of transcurrent crustal structures, against the background of predominant NNW-SSE trends, are NE-SW gravity and magnetic lineaments crossing much of the Cordillera, E-W-elongated Mesozoic igneous plutons, and NE-SW and E-W lakes and rivers.

Wide westward extent of ancient pre-Cordilleran craton(s) is suggested by other evidence as well. Tectonically reworked Precambrian rocks of various Archean and Proterozoic ages are recognized all over the Canadian Cordillera, while paleontological, paleomagnetic and structural evidence for exoticism of assumed accreted terranes is continually revised or eliminated. The oldest known incidence of the "Cordilleran" NNW-SSE tectonic trend is the ~1,760-Ma thermally induced Kimiwan geochemical anomaly in the cratonic basement of the central and western Alberta Platform, but thereafter orogenic activity shifted to the west. Two-sided old volcano-sedimentary and sedimentary basins - Middle Proterozoic Belt-Purcell, Late Proterozoic Windermere and late Paleozoic Prophet-Ishbel - in the eastern Cordillera are known from sedimentological studies to have received sediments from land sources on the east and west. Internal variations in these basins are related to numerous faults and blocks with various orientations. The Belt-Purcell Basin, though very deep, was evidently broad, intracratonic and non-orogenic, and the ancient cratonic area to the west of it is conventionally called the Western craton. The NNW-SSE Cordilleran tectonic trend was firmly established with the onset of Windermere rifting at ~780 Ma. The Prophet-Ishbel trough was probably a foredeep to the Antler orogen, whose continuation into Canada lay in the Cordilleran regions to the west. The NNW-SSE and transverse Phanerozoic tectonic zonation in the Canadian Cordillera was inherited from Precambrian time.

In the cratonic Alberta Basin, many Paleozoic platformal sedimentary units are laterally monotonous and fail to exhibit a wedge-like thickening to the west. Occasional westward continuation of cratonic platformal depositional settings far into the Cordilleran interior is indicated by the presence even on the west side of the Omineca Belt of Paleozoic carbonate-platform remnants similar to the coeval carbonate platforms in the cratonic Alberta Basin. Contrary to a common assumption, at no time did the eastern Canadian Cordillera contain a one-sided, passive Atlantic-type continental margin.

Geochemical evidence of reworked, ex-cratonic ancient basement rocks is well

known from the metamorphic complexes in the southern Omineca Belt. Highly metamorphosed former supracrustal rocks are known in these complexes as well. To achieve their high metamorphic grades, in the Mesozoic and early Cenozoic these rocks were first lowered to great crustal depths of 20-30 km, and then rapidly returned to the surface. Mapped tectonic manifestations (magmatic, metamorphic, structural and sedimentary) indicate that intense Nevadan and Columbian orogenic episodes occurred in that region in the Middle Jurassic and mid-Cretaceous, each ending with decompression and crustal extension. The Late Cretaceous-Early Tertiary Laramian orogenic cycle, with its own well-recognized extensional pulse in the end, was only one in this long series. This repetitive, multi-cycle orogenic tectonic history contradicts the commonly assumed scenario with a passive continental margin in the eastern Cordillera before the mid-Mesozoic, compression and exotic-terrane accretion and stacking from then till the Early Tertiary, and extension thereafter.

The Laramian Rocky Mountain fold-and-thrust belt is known from outcrop, drillhole and seismic data to be a thin-skinned, rootless thrust stack that does not involve the cratonic basement, which in that region is not tectonically reworked. Cordilleran tectonic reworking of the ancient crystalline-crust basement begins at the Rocky Mountain-Omineca belt boundary, and that line should be considered the modern edge of the North American craton.

In contrast to the recurrent, strong crustal tectonic reworking in the Omineca and Coast Belt orogenic zones, metamorphism and deformation were comparatively slight in the more-rigid crustal blocks of the Intermontane Belt and Yukon-Tanana massifs: their volcano-sedimentary cover is preserved largely intact, its upper parts are metamorphosed only weakly or not at all, and block faulting is common. The magmatism in that region was largely teleorogenic, induced by orogenesis in adjacent regions (mostly, Coast Belt). Preserved blocks of rigid, semi-reworked ex-cratonic Precambrian crust probably lie beneath the exposed Late Proterozoic and Phanerozoic volcano-sedimentary cover (the oldest known cover rocks are Devonian in the Intermontane Belt and Late Proterozoic in the Yukon-Tanana massif). Presence of an older continental basement is suggested by radiometric inheritance (Early Proterozoic in the Yukon-Tanana massif), seismic-velocity structure of the crust, and long-time rigidity of these crustal blocks that saved them from a more profound orogenic reworking.

The Skeena and Stikine arches in the Intermontane Belt follow the ancient NE-SW cratonic tectonic trends, regardless of assumed Cordilleran terranes. Ex-cratonic crystalline basement, tectonically reworked to various degrees, seems to continue at least as far west as the Intermontane-Coast belt boundary. Local rifts, Mediterranean- or Red-Sea-type deep marine basins and even ephemeral minor subduction zones might nonetheless have existed in the Canadian Cordillera at various times and in various localities; the inversion and closure of these marine basins took place largely in late Paleozoic (Antler-Teslin) time. Such pre-Mesozoic events, during which the main active crustal weakness zones were the ones oriented NNW-SSE, may account for the partition of the Intermontane Belt into the Stikine and Quesnel crustal blocks. This Paleozoic division was quite different than the subsequent, Mesozoic partition into blocks defined by the reactivated but ancient, transcurrent Stikine and Skeena arches. Because crustal blocks with a shared ancient crustal ancestry in the Cordilleran interior developed throughout the Phanerozoic side by side, roughly *in situ*, the postulated multiple big former oceans (Cache Creek, Teslin, Anvil) are improbable. The Omineca, Intermontane and Coast belts developed essentially *in situ*, but the Intermontane

Belt has retained more of its ancient ex-cratonic crustal inheritance than the neighboring Omineca and Coast Belt orogenic zones.

Outward-verging Mesozoic and Cenozoic fold-and-thrust zones in the Cordilleran interior are known to bilaterally flank the Coast Belt and Omineca orogens. Like the big Rocky Mountain fold-and-thrust belt on the east side of the Omineca orogen, these zones are probably rootless. These shallow deformation zones on the orogens' flanks partly obscure the deep, steep crustal boundaries of the Coast and Omineca orogenic belts.

Seismic evidence that the Cordilleran crust is a stack of exotic-terrane thrust sheets is unconvincing. Geophysical anomalies carry useful but indirect information about the spatial distribution of specific physical properties of rocks. Yet, they say nothing about the imaged discontinuities' geologic nature, genesis or age. High-angle crustal discontinuities are usually missed in seismic reflection images altogether, and the geologic origin of low-angle reflections is unknown. Correlation of seismic events is complicated by these events' unknown nature, common lack of continuity, reflection-character variations and gaps in the data. In a strongly deformed and magmatized region like the Cordillera, many off-line arrivals and other hard-to-identify forms of coherent noise contaminate the seismic data at short and long traveltimes. The technical need for road access during data acquisition in the mountains required the Lithoprobe seismic reflection profiles to be shot largely along passable valleys, which tend to follow steep NNW-SSE-trending and transcurrent crustal faults; as a result, some of the seismic lines were shot not across but along the strike of large-scale crustal structures.

Comprehensive analysis and synthesis of various geological and geophysical evidence has previously shown that, contrary to the conventional model, no ongoing subduction is currently taking place off Vancouver Island, and the modern Cascadia subduction zone does not reach north into Canada. Postulations of trans-Cordilleran subhorizontal crustal detachments similarly rely on assumption-based correlations of selected, disconnected low-angle seismic events and their assignment to faults that at the surface are known to be variously low-angle or steep. Principal significance in these interpretations is assigned, arbitrarily, only to those reflections that seem to fit the assumed structural geometry, while the numerous other reflections are disregarded as unimportant. The Slocan Lake and Monashee faults, for example, are correlatable with any confidence only with reflections that dissipate in the upper and middle crust. The use of discontinuous "floating" events to justify these faults' presumed trans-crustal continuity is unfounded, and it contradicts the results of refraction seismic surveys. Instead, the biggest, steep fault system in the southern Omineca Belt region seems to be the one along the Kootenay Lake, which forms the western boundary of the Kootenay Arc and is associated with big seismic-velocity changes even in the lower crust.

The profound, multi-cycle tectonic reworking of the entire crust and perhaps deeper lithosphere in the Omineca orogenic belt included Mesozoic and Cenozoic differential subsidence and uplift of big crustal zones by tens of kilometers. Therefore, the postulated preservation and direct continuity from the craton of Proterozoic features in the middle and lower crust across the eastern Cordillera are implausible. In particular, there is no geological or geophysical evidence for the assumed creation and preservation within the eastern Cordilleran crust since the Proterozoic of an ancient passive-margin ramp. Due to strong, extensive and repeated Late Proterozoic and Phanerozoic whole-crust tectonic reworking of huge tec-

tonic zones in the Cordillera, direct and unbroken continuity from the craton of an unaltered ancient basement under the Cordilleran interior is impossible. Neither is the Cordilleran Moho a Proterozoic relic: indeed, COCORP seismic interpretations just south of the Canada-U.S. border note that the Cordilleran Moho truncates the seismically-inferred orogenic crustal structural patterns, and regard the Moho as probably a product of Cenozoic regeneration. The presumed trans-Cordilleran low-angle crustal detachments are likewise not supported by compelling correlations of unquestionably interpreted primary seismic reflections, and they contradict the geological evidence for large-scale vertical crustal movements in Late Proterozoic, Paleozoic, Mesozoic and Cenozoic time.

The Proterozoic Laurentian and possibly Western cratons in pre-Cordilleran time continued far into the modern-day Cordilleran interior. Today, their semi-reworked remnants are found in the comparatively stable Intermontane and Yukon-Tanana crustal massifs, which are surrounded by orogenic zones where multi-cycle crustal tectonic reworking was much greater. The main differences between tectonic zones in the Cordilleran interior lie not in their assumed exotic-terrane composition but in the degree of *in situ* multi-aspect orogenic reworking of the indigenous, ex-cratonic North American lithosphere and crust.

COMPARATIVE ANALYSES OF REGIONAL GEOLOGICAL AND GEOPHYSICAL DATA SETS BY APPLICATION OF GEOGRAPHICAL INFORMATION SYSTEMS

C. Elissa Lynn(1), Kevin W. Hall (2) and Frederick A. Cook (3)

Department of Geology and Geophysics, University of Calgary, 2500 University Dr. NW
Calgary, Alberta, Canada (403) 220 7920
(1) lynn@litho.ucalgary.ca, (2) hall@litho.ucalgary.ca, (3) cook@litho.ucalgary.ca

Analyses of regional geophysical (primarily gravity and magnetic) maps in western Canada using various filtering techniques provides opportunities to relate the anomaly patterns to surface geological data, as well as to seismic profiles. Maps of common geological features (e.g., faults, plutons, geotectonic belts) are individually overlain on different bandpass and directionally filtered versions of the gravity and aeromagnetic maps. Important features that are observed include: (1) northeast striking anomalies of the Canadian Shield that can be followed through the young Cordillera to nearly the Pacific coast, and (2) a north-striking anomaly associated with the Eocene Fraser River strike-slip faults that can be followed for more than 600 kilometers north of its known exposure. These patterns indicate that surface structures of the Cordillera have different orientations from deep structures, and are likely detached from them.

The Burmis Thrust: A blind thrust in the southern Canadian Cordillera

Paul A. MacKay
Northstar Energy, Suite 3000, 400 – 3rd Ave SW, Calgary, Alberta, T2P 4H2

The Burmis Thrust is a blind thrust in the southern Canadian Cordillera. The thrust carries Paleozoic strata in its hanging wall with approximately 10 kilometers of displacement at the Paleozoic level. The thrust has a lateral extent greater than 50 kilometers from the Oldman River in the north to south of the Castle River. The Coleman and Burmis gas fields are within these thrusted Paleozoic Strata and are prolific producers of H_2S enrich natural gas from fractured Devonian and Mississippian carbonate rocks. To the foreland the Burmis Thrust merges with the Fernie Detachment and the motion is accommodated into the leading edge of the orogenic wedge.

The Livingstone Thrust is immediately above the Burmis Thrust. The Livingstone Thrust has approximately 40 kilometers of displacement at the Paleozoic level. The hanging wall cutoff of the Paleozoic strata of the Livingstone Thrust is exposed at the Livingstone Range. The Livingstone Thrust is generally undeformed by the shape of the Paleozoic cutoff of the underlying Burmis Thrust, suggesting that the two faults are partially coeval. Field relationships and symmetry between the Livingstone Thrust and the Lewis Thrust to the west also show coeval characteristics. Thus the Front Ranges and Foothills of the southern Canadian Cordillera appear to have formed as one large wedge with a pre-established finite width and grew to a specific taper rather than having pre-established taper that migrates to the foreland.

The Volcanic Creek Centre, northern British Columbia and the nature of the underlying lithosphere

J Nicholls and MZ Stout, Department of Geology and Geophysics, University of Calgary, Calgary, Alberta T2N 1N4

Ultramafic xenoliths in Quaternary volcanic rocks of northern British Columbia and the Yukon document lateral and/or vertical heterogeneity in the underlying mantle (Francis *et al.*, 1997; Francis *et al.*, 1996). The trace element and isotopic variations between xenoliths from different volcanic centres reflect differences in mantle composition in the lithosphere under the various centres. The chemical variations are also reflected in the mineral assemblages and compositions. Differences occur over a relatively small distance in the Atlin area of northern British Columbia. This area contains several Quaternary centres with distinctive and different mineral compositions in the xenoliths and xenocrysts. Four localities (Figure 1) are 1: Volcanic Creek, 2: Ruby Mountain, 3: Llangorse Mountain and 4: Hirshfield Creek approximately 50 km east of the town of Atlin (Aitken, 1959; Nicholls *et al.*, 1982; Francis and Ludden, 1995; Edwards *et al.*, 1996; Higgins and Allen, 1985). This paper provides data on chemical variations in the mineral assemblages and compositions.

Distinct differences in spinel compositions, and to a lesser extent in pyroxene and olivine compositions occur amongst the xenoliths found at these localities. Xenoliths from Llangorse Mountain can be divided most easily on spinel compositions; Cr_2O_3-rich compositions from 38-43 wt. % and Cr_2O_3-poor from 9-15 wt. %. Table 1 lists the compositions of minerals that accompany the spinels.

Table 1	Olivine compositions	Orthopyroxene compositions
Cr_2O_3-rich	Fo91-92	MgO: 35-36 wt. %
Cr_2O_3-poor	Fo89	MgO 35 wt. %

Xenoliths from Ruby Mountain contain Cr_2O_3-poor spinels. The centre at Volcanic Creek lacks complete xenoliths but does contain xenocrysts of olivine (Fo91.5) and orthopyroxene (MgO = 35 Wt. %). These values are consistent with a mantle source that contains Cr_2O_3-rich spinels. The centre at Hirshfield still needs sampling for mineral analysis of spinel, olivine and pyroxenes.

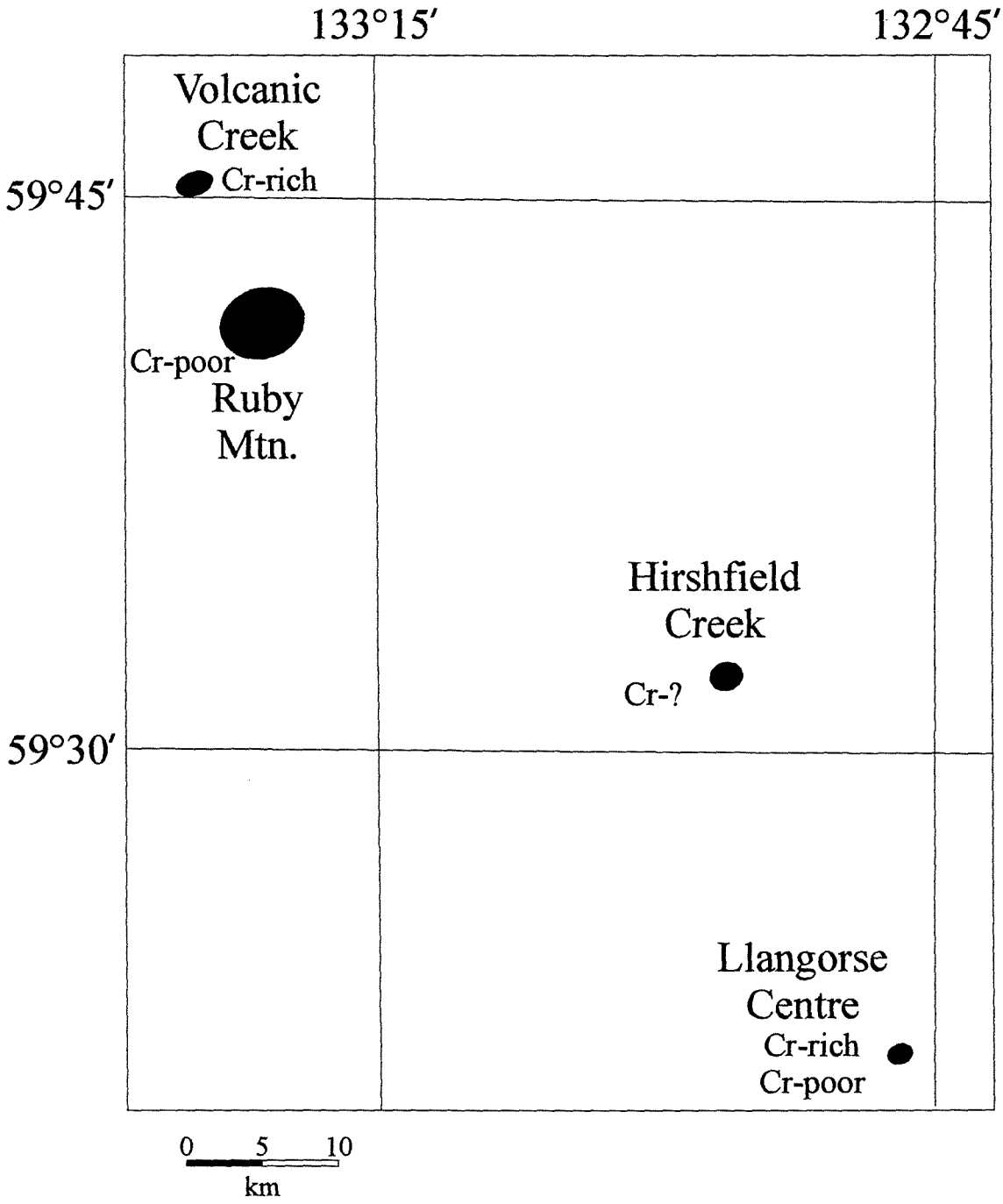

Figure 1: Locations of ultramafic xenolith locations in the Atlin area, northern British Columbia.

METAMORPHIC CONSTRAINTS ON THE TECTONIC EVOLUTION OF THE THOR-ODIN DOME, SHUSWAP METAMORPHIC CORE COMPLEX

NORLANDER, Britt H., WHITNEY, D. L., and TEYSSIER, C., Department of Geology and Geophysics, University of Minnesota, Minneapolis, MN 55455, norl0033@tc.umn.edu.

The Shuswap metamorphic core complex of the southern Omineca belt straddles the suture between allochthonous terranes and the North American paleomargin, exposing a ~15 km thick crustal section of high-grade metamorphic rocks bounded by detachment faults. The complex has been divided into three crustal units. The upper unit lies in the hanging walls of the shallowly dipping detachment faults and comprises low-grade metasedimentary units overlain by Eocene sedimentary basins. The middle unit consists of rocks associated with the Selkirk allochthon including discontinuous layers of amphibolite facies metasediments including metapelite, calc-silicate, marble, amphibolite, and quartzite. The lower unit is exposed as domes of complexly deformed, polymetamorphic Precambrian basement of metapelitic and migmatitic gneisses.

Temperatures and pressures are constrained by thermobarometric results and inferences from petrogenetic grids from metapelitic rocks and garnet amphibolites of the lower unit and metapelitic rocks of the middle unit in the Thor-Odin dome. Assemblages that were used in thermobarometric calculations include garnet-plagioclase-sillimanite-quartz, garnet-plagioclase-hornblende-quartz, garnet-biotite, garnet-hornblende, garnet-cordierite, and hornblende-plagioclase. Rocks of the lower unit record peak conditions of 750-850°C and 6-7.5 kbar. In the middle unit, garnet+sillimanite+K-feldspar±cordierite bearing metapelites yield peak conditions of 625-725°C and 6-7 kbar, suggesting that pressures at peak temperature were similar for the middle and lower units. In a garnet-gedrite amphibolite of the lower unit, a higher pressure history is suggested by distinct tabular shaped regions cored by corundum+cordierite symplectites with spinel+cordierite symplectitic rims inferred to be pseudomorphs of kyanite. Relatively high-temperature decompression is suggested by these reactions and by the partial replacement of garnet by cordierite. Garnet in hornblende amphibolites has been partially replaced at the rims by symplectitic plagioclase+hornblende+quartz suggesting decompression at high temperatures in the lower unit. This high-temperature decompression path is consistent with the occurrence of cordierite in both the lower and middle unit metapelitic rocks.

Although reaction textures indicate that the lower unit experienced $P > 9$ kbar, the data show that the primary difference between recorded metamorphic conditions of the lower and middle units is peak temperature. Both units experienced high temperature decompression, resulting in a sequence of mineral reactions from > 7 kbar to $\sim 3 \pm 1$ kbar. These high-temperature pressure paths are critical for understanding the development of the Shuswap metamorphic core complex. Furthermore, the evolution of metamorphic core complexes provides important insight into crustal rheology during both crustal thickening and exhumation.

Cyperus papyrus, A Key to the Tectonic Elucidation of the Northern Cordillera and Contiguous Canada Basin*

D.K. Norris
444 Okaview Road, Kelowna, B.C. V1W 4L4

The location of the Euler pole of relative rotation for the Arctic Alaska plate away from ancestral North America has been designated over a large area in northern Northwest Territories and adjacent Yukon Territory and Alaska, from as far east as the Eskimo Lakes Fault Zone on the Northern Interior Platform (Grantz and May, 1983), to as far west as Fairbanks, Alaska (Carey, 1955); and from as far south as upper Mackenzie Delta (Rickwood, 1970); to as far north as southern Beaufort Sea (Stephenson et al., 1994). The wide range in such locations would suggest that few investigators have taken into account the true effects of rotation on the structural geometry of the supracrustal wedge, let alone on the crystalline basement, at the pole. A number of criteria may be used collectively to identify a pole and such criteria may have application to orogenic belts worldwide.

Consider a curvilinear orogenic belt with a strong, longitudinal structural grain most probably delineating the initial shape of a shelf-miogeocline, as well as the grain of the underlying crystalline basement. Midway along it a rising temperature anomaly (following Falvey, 1974) leads to domal uplift, followed by rifting and widening biaxial subsidence, proceeding to breakup and splitting of the orogen into two arms along a spreading axis parallel to the structural grain. With the symmetrical introduction of new oceanic crust above the rising thermal anomaly, the spreading axis extends in the one direction to terminate at a major transform fault, and in the other to perpetuate the spreading process lengthwise within the orogen. Should the introduction of new crust continue at a constant rate, whereas the extension of the spreading axis halts, an Euler pole of relative rotation is created automatically and the two arms begin to rotate away from one another. Left-hand shear will occur on the inside of the curvature of the right-hand arm and right-hand shear will occur in the left-hand arm, as interstructural adjustments take place due to flexural slip. The net result is a "flower structure" in plan, herein termed a Papyrus Structure" (*Cyperus papyrus*), where the Canada Basin is embraced within the Alaskan and Innuitian arms, and the apex of the Porcupine Syntaxis (virgation; Norris, 1987) coincides with the Euler pole.

Criteria for the location and recognition of a pivotal axis, therefore, include 1) the splitting and divergence of the structural grain within an orogen at the apex of a syntaxis; 2) the matching of structural and stratigraphic features facing one another across the syntaxis; 3) the presence of contractional and oblique-slip faulting and *en echelon* folding on the inside of the curvature in the arms, on both sides of the spreading axis; 4) the limited strike length of these adjustment features as the spreading axis and, in turn, the Euler pole for the two arms migrates progressively away from the point of initiation of spreading. This gives the orogen a shredded appearance; 5) with a constant rate of injection of new crust, the separation of the two arms (S) is a function of the product of the radius of gyration (R) and the angle of rotation (θ, in radians), centred about the Euler pole ($S = R \cdot \theta$). Both contractional and extensional deformation, therefore, are zero at the Euler pole and are a maximum at the transform fault on the opposite side of the initiating thermal anomaly.

*first presented at the GSA Penrose conference on "The Tectonic Development of the Canada Basin and Surrounding Regions", September 30, 1995

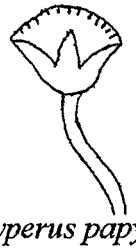

Cyperus papyrus

The Role of Overturned Panels in the Tectonic Evolution of the Phanerozoic Section on the North Flank of the Central Anticlinorium, Ostrov Vrangelya

D.K. Norris,
444 Okaview Road,
Kelowna, B.C. V1W 4L4

Ostrov Vrangelya, better known in the Western World as Wrangel Island, lies in the Arctic Ocean 140 km north of mainland Siberia. It is a structural uplift within the western limit of the Arctic Alaska Plate and is most probably underlain by continental crust. As such, Ostrov Vrangelya is part of the Frontal Belt of the North American Cordilleran Orogenic System, its counterpart being the Innuitian Arm of the Arctic Archipelago. The island comprises five, east-trending domains, named in order from south to north: Krasina Homocline (new name), Central Anticlinorium, Medvzh'ya Synclinorium, Northern Anticlinorium, and Tundra Homocline (new name). The two homoclines are mostly covered with Quaternary deposits so that currently it is impossible to evaluate precisely their structural geometry and stratigraphy.

In the Central Anticlinorium, however, the internal structure of Wrangel Uplift is spectacularly displayed (see Kos'ko et al., 1993). There, the whole of the exposed stratigraphic section, from Upper Proterozoic to Upper Triassic, has been deformed to varying degrees by the Chukotkan (Columbian) Orogeny, from north-verging open folds to isoclinal folds, and from north-verging contraction faults to folded thrusts. All of the uplift appears to have been cleaved, and overprinted with a family of northwest-trending, Laramidian(?), near-vertical faults, some with right-lateral, horizontal separations.

Of particular importance are the large, overturned and refolded panels of sedimentary rocks exposed in the Northern Anticlinorium, not only because of the large horizontal shortening and crustal thickening implied for the associated thrust faults, but also because they may indicate the one-time existence of northward migrating, frontal triangle zones in which hydrocarbons may have been trapped. Two panels are notable on Ostrov Vrangelya: one on Naskhok River and another at the junction of the Neizvestnaya and Lemmingovaya Rivers. These Chukotkan panels are geometrically similar to the large, overturned panels (peels) in both the hanging- and footwalls of the Lewis Thrust in the Frontal Belt of the Cordilleran Orogen, and to the great flap structures in the Zagros Mountains of southwest Iran. They played passive roles in the delamination of the supracrustal wedge as their upper detachments and hanging-walls were rotated progressively through the vertical, became overturned and were refolded at or near their deformation fronts.

Geochemistry of Metavolcanic Rocks from the Yukon-Tanana Terrane and Campbell Range Belt, Finlayson Lake Region, Southeastern Yukon Territory: Preliminary Results

Stephen J. Piercey[1], Donald C. Murphy[2], James K. Mortensen[1], Julie A. Hunt[2]

1-Mineral Deposit Research Unit / Geochronology Laboratory
Department of Earth and Ocean Sciences, University of British Columbia
spiercey@eos.ubc.ca, jmortens@eos.ubc.ca

2-Yukon Geology Program
Whitehorse, Yukon
huntj@inac.gc.ca, don.murphy@gov.yk.ca

Abstract

Preliminary lithogeochemical data from stratigraphically constrained samples in the Yukon-Tanana Terrane of the Finlayson Lake region in southeastern Yukon reveal a complexity of signatures and possible paleotectonic affinities for metavolcanic rocks of this region. Stratigraphically low mafic metavolcanic rocks consist predominantly of high Mg, low TiO_2, HFSE depleted and Ni-Cr enriched boninitic and island-arc tholeiitic rocks. This suite is spatially, and possibly genetically, associated with ultramafic massifs and grades laterally into a moderate TiO_2 suite that comprises variably LREE-enriched and LREE-depleted transitional (OIB?) tholeiites and normal mid-ocean ridge basalts (N-MORB), respectively. These rocks have strong similarities to mafic magmatism in forearc regions (e.g., Tonga, Izu-Bonin) and suprasubduction zone ophiolites (e.g. Betts Cove Complex, Troodos), and may represent the initiation of subduction-related magmatism in the Yukon-Tanana Terrane. Stratigraphically overlying these mafic metavolcanic rocks are two successions of Mississippian felsic metavolcanic and metaplutonic rocks, which are separated by an angular unconformity. Both successions are characterized by low Th/Nb ratios and Ti* values, and have overall LREE-enrichment consistent with mature calc-alkaline continental arc magmatism. This magmatism may represent the more evolved stages of Mississippian arc development built upon continental crust. Pennsylvanian-Permian mafic magmatism in the Campbell Range belt, which stratigraphically overlies the upper sequence of felsic metavolcanic rocks, represents a shift in magmatism to predominantly enriched mid-ocean ridge basalts (E-MORB) which spatially (and temporally?) grade into N-MORB type magmatism. This magmatism likely represent arc-rifting and back-arc basin development, respectively. It is clear from these results that the Yukon-Tanana Terrane and related rocks in the Finlayson Lake region represent a complex tectonic evolution within an arc system.

Stratigraphy of the Hazelton Group of southwestern Nechako River map area, central British Columbia.

M.B. Quat and L.C. Struik

Geological Survey of Canada, Vancouver, B.C. (email:mquat@gsc.nrcan.gc.ca and bstruik@gsc.nrcan.gc.ca)

ABSTRACT

Hazelton Group in southwestern Nechako River includes a suite of volcanic and sedimentary rocks formed in a volcanic arc of Early to Middle Jurassic age. It consists of a succession of subaerial and submarine volcanic rocks interbedded with marine sediments. This Group is the oldest sequence of rock in the area and is overlain by Eocene Ootsa Lake Group rhyolite and Miocene basalt and intruded by Jurassic(? currently being dated by J. Mortensen and S. Billesberger, UBC) diorite and granodiorite.

This study concentrates on the Hazelton Group stratigraphy of Tetachuck Lake, 93F/5 with comparisons to work done by Larry Diakow in the Fawnie and Nechako Ranges (93F/2,3,6,7) (Diakow et al., 1997) and the Whitesail Reach (93E/10)-Troitsa Lake (93E/6) (Diakow and Mihalynuk, 1987) map areas as well as work by Bob Anderson in the Iskut River map area (Anderson, 1993).

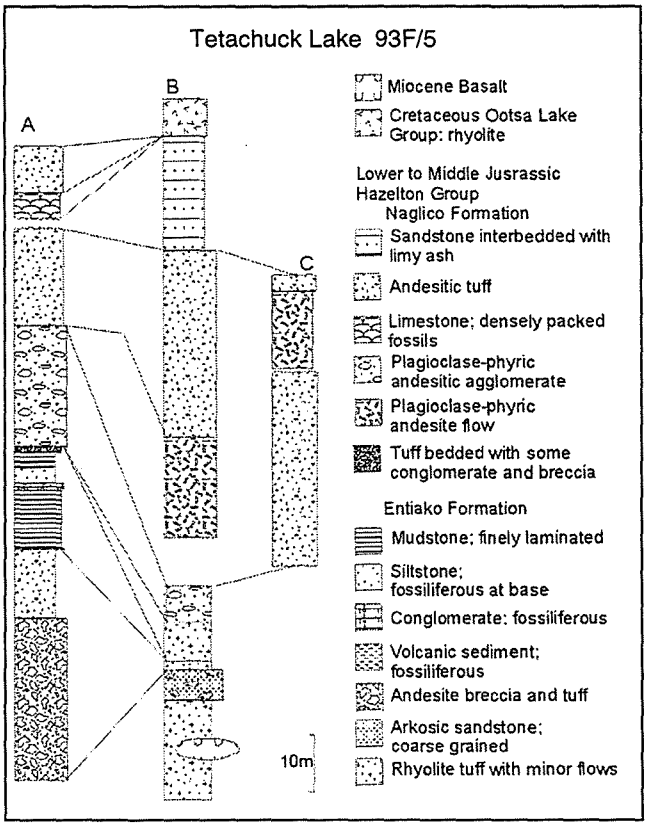

The group ranges in age from the Toarcian (late Early Jurassic) to the Bajocian (early Middle Jurassic) and is divided into two formations, Entiako and Naglico (Diakow et al. 1997). These divisions will be used here as well as new subdivisions proposed by Struik et al. (1999). The contact between the Entiako and Naglico formations is paraconformable. Entiako clasts are often found in Naglico boulder conglomerates. In the area north of the Chelaslie River it is conformable.

In the Tetachuck area the older Entiako Formation can be grouped into two facies: 1) a near shore and distal marine sedimentary facies characterized by volcanic-derived sandstones, conglomerates and tuffaceous siltstones, and mudstones and 2)a subaerial felsic volcanic facies containing rhyolite tuff, minor rhyolite flows and maroon and green air-fall tuffs. The Entiako Formation correlates to the Telkwa Formation in the Whitesail Reach map area and to the Unuk River and Betty Creek Formations in the Iskut River area.

The Naglico Formation of the Tetachuck area is differentiated into three units. One unit is an andesite flow and tuff containing massive andesite crystal tuff and agglomerate and plagioclase/augite-phyric andesite flows. Andesite agglomerate and conglomerate forms a second unit that occurs within the flow and tuff unit. The third unit of feldspathic sediments consists of sandstone interbedded with unconsolidated limy ash and tuff. The Naglico Formation roughly correlates to the Smithers Formation in the Whitesail Reach map area and to the Salmon River Formation of the Iskut River/Telegraph Creek map areas.

The formations of the Hazelton Group record island arc volcanism and associated sedimentation. The Entiako Formation records a time of subaerial volcanic deposition associated with felsic volcanism and a period of marine deposition marking the top of the formation. The Naglico Formation marks a time of plagioclase-phyric andesite flows and tuffs containing interbeds of marine volcanically derived sediments.

Diorites and granodiorites of Jurassic age(?) are scattered throughout the area and intrude into the Hazelton Group. These rocks are fine to medium-grained equigranular, contain biotite and hornblende, are slightly foliated and contain local andesite and rhyolite dykes.

References

Anderson, R.G., 1993: A mesozoic stratigraphic and plutonic framework for northwestern Stikinia (Iskut River Area), northwestern British Columbia, Canada; in Mesozoic Paleogeography of the Western United States--II, G. Dunne and K. McDougall(eds.); Pacific Section SEPM, vol.71, p.477-494.

Diakow, L. and Milhalynuk, M., 1987: Geology of Whitesail Reach and Troitsa Lake map areas (93E/10W, 11E); in Geological Fieldwork 1986, British Columbia Ministry of Energy, Mines and Petroleum Resources, Paper 1987-1,p.171-179.

Diakow, L.J., Webster, I.C.L., Richards, T.A. and Tipper, H.W., 1997: Geology of the Fawnie and Nechako Ranges, southern Nechako Plateau, central British Columbia(93F/2,3,6,7); in Interior Plateau Geoscience Project: Summary of Geological, Geochemical and Geophysical Studies, L.J. Diakow and J.M. Newell(eds.); British Columbia Survey Branch, Paper 1997-2, p. 7-30.

Struik, L.C., Anderson, R.G., and Plouffe, A.,1999: Geology of the Euchiniko map area, central British Columbia; in Current Research 1999-A; Geological Survey of Canada.

Upper crustal structure in the Southwestern Slave Province - a detailed look at the seismic results from SNORCLE line 1.

Brian Roberts, David Snyder, Erick Adam
Geological Survey of Canada
615 Booth St., Ottawa, K1A 0E9
roberts@cg.NRCan.gc.ca

Reprocessing of the seismic data from the easternmost part of line 1 of the SNORCLE transect has now been completed. We have focussed on the upper crustal section in the Slave province, from the Anton Domain west of Yellowknife to the end of the line at Tibbit Lake (~70 km), in order to correlate the seismic data with mapped geological structures and to understand the nature of the Central Slave Basement Complex below the metasediments of the Yellowknife supergroup. The major reflecting horizons were well imaged in the first round of processing and reported on by Cook et al. (1999). The target for the reprocessing was to better define the upppermost strong reflector (marked as Y1 on Figure 1) and to enhance any reflectivity in the basin-like feature it defines.

The emphasis in the reprocessing has been on; 1) defining a suitable CDP binning line, 2) pre-stack noise elimination, 3) application of a dip moveout correction, and 4) detailed velocity analysis.

1) To enhance the near-surface reflectivity as much as possible, a CDP processing line was chosen that closely follows the seismic line and a bin width of 1 km was used so that the areal extent of midpoints contributing to the individual CDP bins is limited. A binning strategy like this reduces the CDP fold, however this is compensated by the high overall data quality.

2) The amount and severity of noise in the raw shot gathers along this portion of line 1 varies significantly. Near Yellowknife high levels of cultural noise affect the data while the data to the east contain strong coherent shear wave noise. The cultural noise is partially removed by bandpass filtering the data in the approximate range of the input sweep frequencies (10-80 Hz) and notch filtering the data to remove 60 Hz noise. Noise that remains is in the same frequency range as the seismic energy but more random, so it is hoped that it is further reduced during the stacking process. The shear wave energy is reduced by performing spectral balancing on the individual shot gathers. This process does not remove the shear wave, but drastically reduces it's amplitude relative to the rest of the coherent signal.

3) A dip moveout correction (DMO) is applied in the shot gather domain and has the result of producing a zero-offset section. Events are often better defined (especially diffractions) and velocities can be selected which properly stack both flat lying and dipping events.

4) A detailed velocity analysis was performed on the non-DMO corrected data and then repeated after DMO to define the final velocity function.

Results:

Reflector Y1 has been imaged upward to a depth of approximately 300 m (100 ms TWT) and can be extrapolated to the surface at or near station 11200. We believe this correlates with a mafic-ultramafic intrusion, previously named the Duck Lake intrusive sheet (Gibbins, 1987) (Figure 1).

Above reflector Y1 we see some coherent reflectivity which is either sub-horizontal or sub-parallel to Y1. There are no strong events which extend to the surface in the eastern end of this line. It seems likely that this reflectivity represents off-line reflections from the large granitic plutons which lie both to the south and north of the seismic line and intrude the deformed metasediments. This is an indication of some high interval velocities which suggest the metasediments are interlayered with mafic units, producing reflections at locations where the geometry is favourable.

Velocity analysis indicate that Y1 and the strong west-dipping reflector below it (Y2) are associated with high interval velocities (6600-6700 m/s). This would be consistent with relatively thick layers of mafic-ultramafic material at these boundaries.

The crooked nature of the seismic line in this area give us an opportunity to make a good estimate of the true attitude of the major reflecting horizons. It appears Y1 has an general NE strike direction with a 20 degree dip to the SE. Y2 has more of an EW strike dipping gently to the S.

References:

Cook, F.A., A. van der Velden, K.W. Hall, B.J. Roberts, 1999, Frozen subduction in Canada's Northwest Territories: LITHOPROBE deep lithospheric reflection profiling of the western Canadian Shield, *Tectonics,* in press.

Gibbins, W.A., 1987, The Duck Lake Intrusive Sheet, Yellowknife Guide Book, Edited by W.A. Padgham, 209 pp.

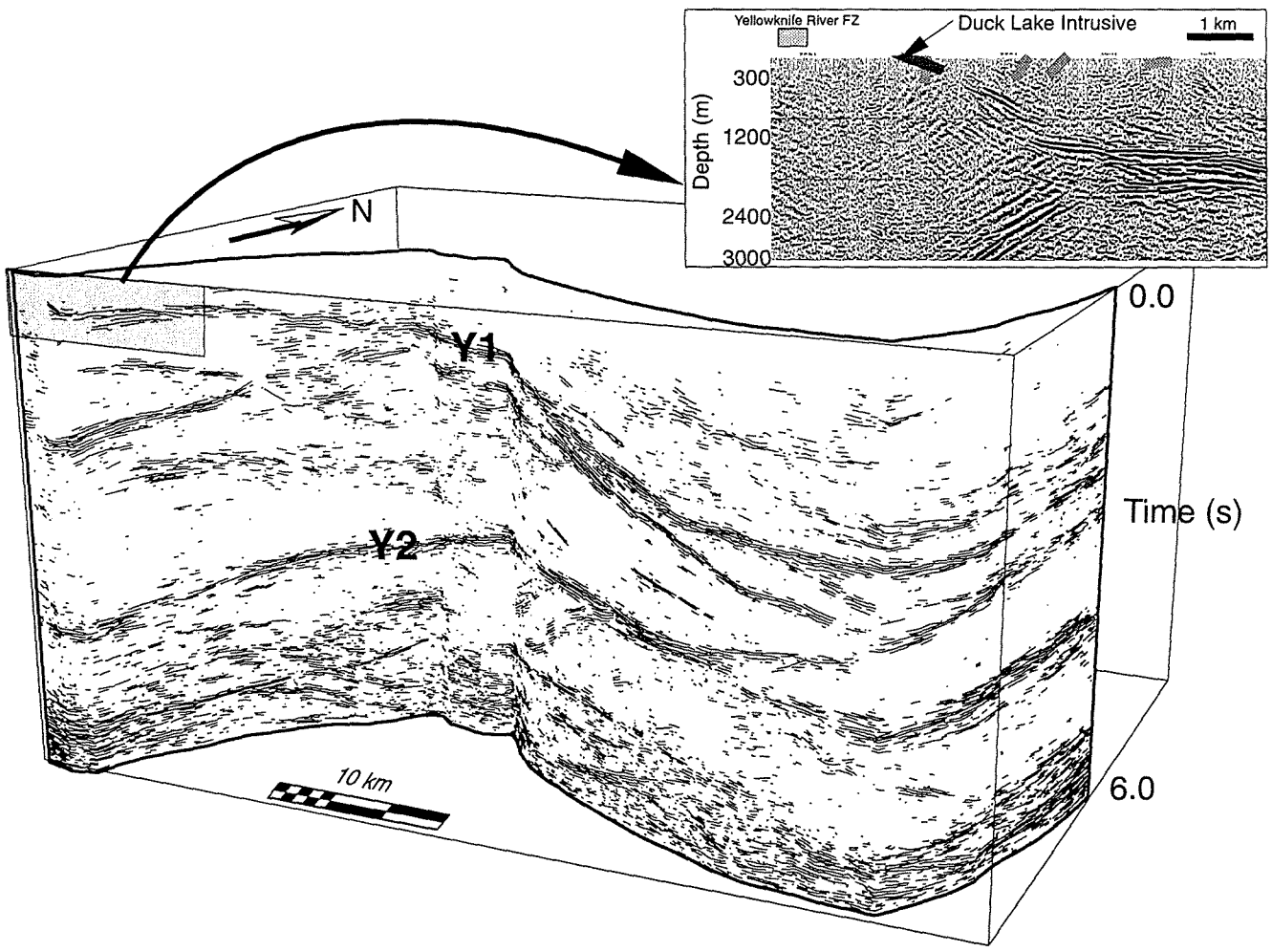

Figure 1. SNORCLE line 1 from Yellowknife to the end of the line plotted in 3D space as defined by the CDP processing li
Inset shows closeup of correlation of Y1 reflector with surface expression of the Duck Lake Intrusive.

Faults in Lansing map area, Selwyn Basin, Yukon: A transpressive squeeze

C.F. Roots, *GSC and Yukon Geology Program, 2099 2nd Ave., Whitehorse, Yukon Y1A 1B5*

Lansing map area (105N), midway between Macmillan Pass and Mayo, contains belts of deformed Late Proterozoic through Triassic deep-water strata separated by several northwest-trending faults. The sequence and nature of these faults as determined by the distribution and structures in adjacent bedrock must be determined before Selwyn Basin paleogeography can be interpreted.

In the southwestern third of the map area the Late Proterozoic to Cambrian Hyland Group is repeated by the Moose Lake and other thrusts (Fig. 1); in the northeast corner the Einarson Decollement (M. Cecile, pers. comm., 1995) also lies within the Hyland Group. Between these areas lies Paleozoic and Mesozoic strata, bounded to the south by the mid-Jurassic (?) Robert Service Thrust (RST) which was later steepened to overturned (particularly in adjacent northeastern Mayo (105M) map area) and has been fault-offset between Fairweather and Penape lakes. Some, if not all, deformation of the RST is attributed to later Tombstone thrusting, in particular the 90 km northwestward displacement (indicated in northern Mayo map area). The eastern limit of the hanging-wall Tombstone strain zone is the 'Mount Osgoode Deformation Front', although its physical connection to the Tombstone Thrust is unknown.

Both the Macmillan and Hess faults have late Devonian syndepositional and metallogenetic significance near Macmillan Pass but are dextrally reactivated and extend westward across Lansing map area. The Hess Fault lies beneath a broad valley without exposure, but the Macmillan Fault is flanked to the south by a 2-10 km wide belt of overturned and tightly folded, southwest-verging Devonian through Triassic strata suggestive of a partial flower structure.

Lansing map area therefore occupies a location of transpression where northward and northwestward displacement of regional scale thrust sheets is transferred to conjugate strike slip faults and southeast-directed contraction in the Macmillan Fold Belt.

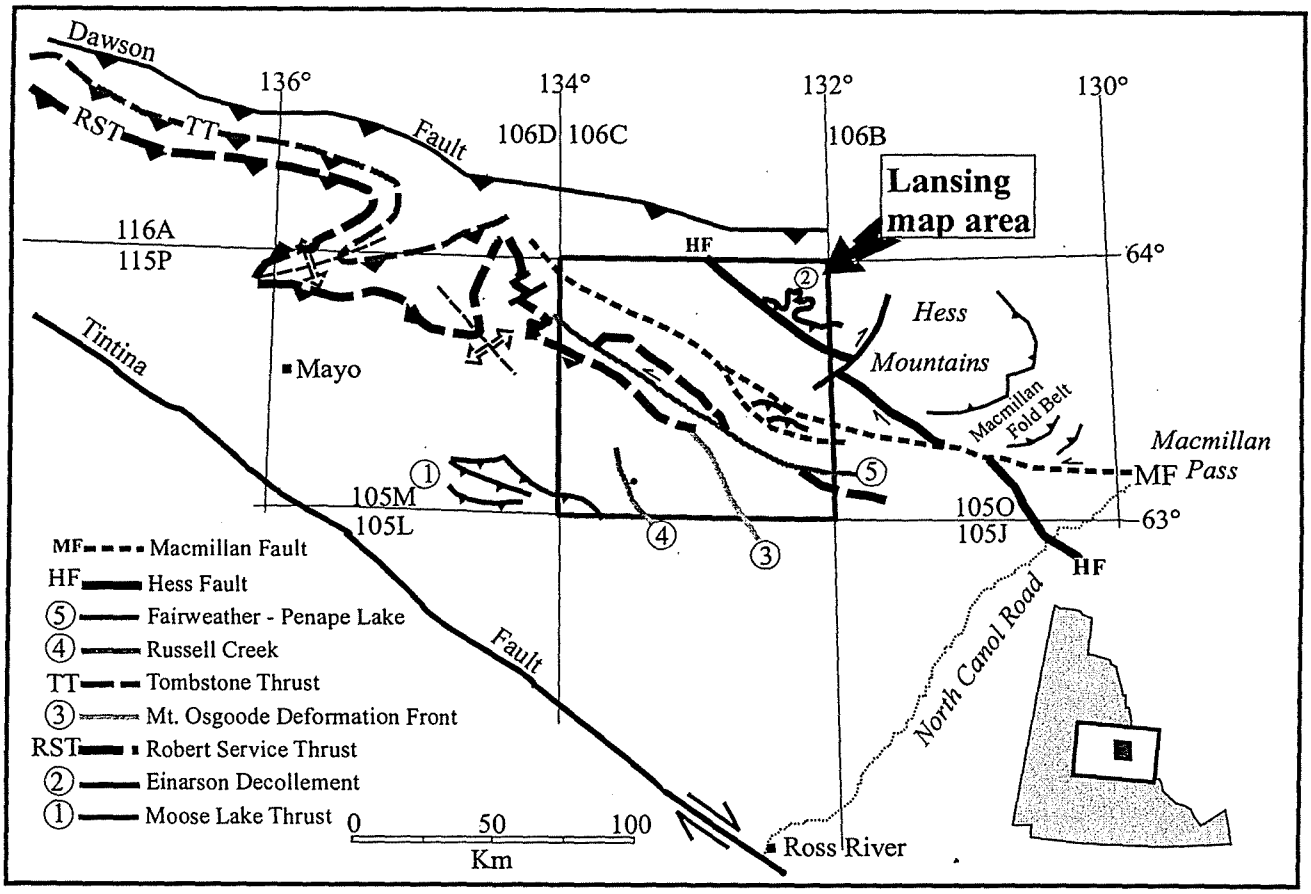

Figure 1. Distribution of regional faults in east-central Yukon. The key shows their approximate sequence from bottom to top.

RAPID EOCENE COOLING FROM PEAK METAMORPHIC TEMPERATURES IN THE NORTHERN MONASHEE COMPLEX, SOUTHERN CANADIAN CORDILLERA: EVIDENCE FROM $^{40}AR/^{39}AR$ AND U-PB DATA

Sanborn, N.M.[1*], Crowley, J.L.[2], and Archibald, D.A.[1]
[1]Department of Geological Sciences, Queen's University, Kingston, ON K7L 3N6;
[2]Department of Geology and Geophysics, University of Calgary, Calgary, AB T2N 1N4; *now at Department of Earth Sciences and Ottawa-Carleton Geoscience Centre, Carleton University, Ottawa, ON K1S 5B6

A temperature-time cooling path for an intermediate structural level in the northern Monashee complex is compiled from new hornblende and biotite $^{40}Ar/^{39}Ar$ data and previously obtained xenotime and monazite U-Pb isotopic data. The $^{40}Ar/^{39}Ar$ dates were obtained from amphibolitic gneisses collected from the Monashee cover sequence on both sides of Frenchman Cap dome. Cooling from a thermal peak of ~600-650°C, the timing of which is interpreted from the U-Pb dates and the conditions of which are interpreted from mineral assemblages in pelitic schist, through the hornblende Ar closure temperature (~530°C) occurred in a few million years and cooling through the biotite Ar closure temperature (~280°C) occurred a few million years later. This relatively rapid cooling, estimated at a rate of ~50°C/Ma, took place between 58 and 48 Ma, immediately after cessation of thrusting on an overlying crustal scale ductile thrust fault and during extension on overlying normal faults that are largely attributed with exhumation of the complex.

The hornblende $^{40}Ar/^{39}Ar$ dates from this intermediate structural level are ~6 Ma older than monazite U-Pb dates from structurally deeper rocks and the biotite dates are slightly younger than the monazite dates. Given that the monazite dates are interpreted as thermal peak ages, the intermediate structural level must have cooled significantly (by up to 400°C) during the period in which deeper rocks were heating toward peak temperatures. Therefore, we conclude that the thermal gradient during metamorphism was normal (i.e., warmer rocks were overlain by cooler rocks) rather than inverted, as was previously proposed. Hornblende and biotite $^{40}Ar/^{39}Ar$ dates obtained from Paleoproterozoic basement rocks (deepest structural level) are up to 15 Ma older than $^{40}Ar/^{39}Ar$ dates from the cover sequence and monazite U-Pb dates from nearby pelitic schists. This age conflict is attributed to the presence of excess Ar in the hornblende and biotite from the basement.

Progress Report: Geoscience Studies in the Northern Cordillera

Velma Z. Sterenberg
DIAND NT Geology Division, P.O. Box 1500, Yellowknife, NT X1A 2R3
email:sterenbergv@inac.gc.ca

Studies initiated during 1998 in the Northwest Territories segment of the Canadian Cordillera are:

1. Investigation of the nature of relationships between gold, precious gems and Cretaceous granitoid intrusions.

2. The examination of barite-bearing black shale sequences from the Caribou River area for their SEDEX potential.

3. A geochemical sampling orientation survey in the Macmillan Pass area in preparation for a future regional sampling programme to cover NTS 105P, Sekwi Mountain Map Sheet.

Only item number two will be dealt with in detail here.

A Barite-Bearing Black Shale Sequence Within Mattson Formation and Its Potential For Base Metal Mineralization

During data review for intrusive-related mineralization (Study 1), an area of black shales of uncertain age was noted in the Coal River (95D) map sheet. The units outcrop near the southern boundary of the Mielleur River Embayment of the Selwyn Basin, 150 kilometres north of the magnetic expression of the of the Liard Line. The Liard Line is thought to represent a Proterozoic transform fault, reactivated during the Ordovician and at younger times. The occurrence of both bedded and concretionary barite, and ribbon-banded, black cherty argillite within units mapped as Carboniferous Mattson Formation, their proximity to units possibly equivalent to the Road River Formation or Earn Group, and similarities to strata hosting SEDEX deposits a minimum of 250 kilometres away, along strike both to north and south, warranted further investigation. Two days of field examination led to the following preliminary assessments:

The barite-bearing, ribbon-banded, black, cherty argillite unit may be either Ordovician or Upper Devonian in age. The unit is lithologically similar to either Road River Group Duo Lake Formation or Earn Group Portrait Lake or Prevost Formations. The Mississippian Tsichu formation, which is also somewhat similar, is not reported to contain barite. Identification of spiriferid brachiopods and possible plant remains are under way. Further work on this sequence, planned for 1999, includes conodont studies and additional mapping.

Over seventeen discrete occurrences of ferricrete were observed in an area underlain by both the Carboniferous clastic unit and a unit mapped by GSC as either Road River or Besa River Formation. Citing a cautionary note in regards to significance of ferricrete analyses, grab samples taken from springs and cemented material are all weakly to moderately anomalous in zinc (39 - 1036 ppm), and barium(13 - 942 ppm), with local weak anomalies of copper (112 ppm), cobalt (124 ppm) and silver (1.4 ppm). Stream sediment samples taken from creeks draining the strike extension of the same units immediately to the south in Yukon Territory are anomalous in barium (1,100 - 12,500ppm) and weakly anomalous in zinc (124 - 850ppm), with isolated, anomalous SEDEX pathfinder elements. Assessment report records indicate that the NWT area has seen a small amount of exploration between 1960-1984. Advances in the theory of SEDEX deposit formation and emplacement might justify another pass by explorationists.

New Geological Maps of the Wernecke Mountains, Yukon Territory (106D/16, 106C/13, 106C/14)

Derek J. Thorkelson* and Carol A. Wallace

Yukon Geology Program
Canada/Yukon Geoscience Office
Whitehorse, Yukon

*now at: Earth Sciences, Simon Fraser University
dthorkel@sfu.ca

ABSTRACT

Three new geological maps of the northeastern Wernecke Mountains have been recently published by Indian and Northern Affairs Canada. They result from geological fieldwork undertaken from 1992-1995 as part of the Canada/Yukon Economic Development Agreement. The maps are companions to a comprehensive bulletin by Thorkelson which will be published later this year.

The study area provides a clear record of the Proterozoic geological evolution of northern and central Yukon Territory. The area lies in the Wernecke Mountains of east-central Yukon, approximately 150 km north-northeast of the town of Mayo, and 20 km west of the Yukon-Northwest Territories border. The area records events of sedimentation, magmatism and deformation ranging in age from the Early Proterozoic to the Tertiary. Rocks of Early Proterozoic age predominate, but strata of Middle Proterozoic, Late Proterozoic, and Early Paleozoic ages are also abundant.

The oldest strata belong to the Wernecke Supergroup which is divided into the Fairchild Lake Group (lowest), the Quartet Group (middle), and the Gillespie Lake Group (highest). These strata form two clastic-to-carbonate grand cycles, apparently recording two periods of subsidence and basinal infilling. Stratigraphic thickness is estimated at about 13 km, inferring deposition on a passive continental margin or intracratonic rift basin.

The Wernecke Supergroup was crosscut by dioritic to syenitic dykes and stocks (ca. 1.71 Ga), then folded and kinked during Racklan orogeny, and then intruded by the phreatic Wernecke breccias (ca. 1.6 Ga). The dioritic dykes, herein named the Bonnet Plume River intrusions, may be correlatative with a newly recognized stratigraphic unit, the Slab volcanics. The volcanics sit as a 250 m-thick megaclast in one of the Wernecke breccia zones, at the Slab mineral occurrence. The Wernecke breccias and adjacent country rocks have been variably metasomatized and locally mineralized. The breccias are coeval with similar phreatic and metasomatic rocks at the Olympic Dam mine, in South Australia, and may have been generated in the same general magmatic and hydrothermal regime.

The Pinguicula Group unconformably overlies the Wernecke Supergroup. The Pinguicula Group, which contains three formations, consists of mainly siltstone and shale overlain by dolostone, some of which displays prominent zebra texture. The unconformity truncates not only folds, foliations, and kink bands in the Wernecke Supergroup, but also the Bonnet Plume River intrusions and zones of Wernecke breccia. These relations confirm that Racklan orogeny was an Early Proterozoic event, and constrain the age of the Pinguicula Group to <1.6 Ga. Pinguicula strata range up to 3.5 km thick, and were apparently deposited in rift basins produced in a cycle of modest crustal extension associated with emplacement of the nearby Hart River sills (ca. 1.38 Ga). One of the sills crosscuts the lowest formation of the Pinguicula Group.

The dioritic Bear River dykes (ca. 1.27 Ga) intrude the Gillespie Lake Group and have the same age as the Mackenzie Dyke Swarm in cratonic rocks of the Northwest Territories. This event was followed by sedimentary deposition of the Hematite Creek Group, formerly the upper part of the Pinguicula Group. The Hematite Creek Group, which is up to 1 km thick, contains abundant detrital zircon (beyond the study area) and muscovite grains of Grenvillian age. The grains range as young as ca.1033 Ma, constraining Hematite Creek Group deposition to no earlier than the late Middle Proterozoic. The Hematite Creek Group, and several other broadly correlative successions extending from Alaska to the Northwest Territories, apparently received sediment from the Grenville orogen via trans-continental river systems.

The Windermere Supergroup unconformably overlies the Hematite Creek Group in the study area. The deformational event recorded by this unconformity is herein named the Corn Creek orogeny, and represents the second of two important periods of Proterozoic contraction in Yukon. The Windermere Supergroup, which is about 2.5 km thick in the study area, displays prominant facies changes involving glacial, conglomeratic, silty and dolomitic deposits. Deposition began sometime after ca. 755 Ma and ended sometime after ca. 600 Ma, spanning the Sturtian and Varangian glaciations. The facies changes in the Windermere are abrupt and imply a protracted history of synsedimentary crustal extension, possibly generated during separation of the North American and Australian continents.

Upper Proterozoic to Lower Paleozoic strata overlie the Windermere succession in the eastern part of the study area. In the west, however, Lower Paleozoic rocks lie directly on the Wernecke Supergroup, revealing a prominant lacuna of about 1 Ga. The Paleozoic strata represent mainly a carbonate bank environment – part of Mackenzie Platform – which extends from the Northwest Territories to the western Yukon.

All geological units in the study area were folded during the Cretaceous to Early Tertiary Laramide orogeny. In the northeastern corner of the study area, dextral transpression along the Snake River fault, probably in the Early Tertiary, produced southwest-verging folds and thrust faults in Upper Proterozoic and Lower Paleozoic rocks. The degree to which strike-slip deformation in the Tertiary and possibly earlier times has affected the geology of the study area is uncertain.

Mineral occurrences are numerous and belong to three general types. Sedimentary exhalative Pb-Zn occurrences are the oldest, and are restricted to the Gillespie Lake Group in the south-central part of the map area. Hydrothermal

disseminations and veins (Cu-Co-Au-Ag-U) related to Wernecke breccia are widespread. These occurrences are metallogenetically similar to those at the Olympic Dam deposit. Base-metal and rare gold-rich veins are the youngest occurrences. They crosscut geological units as young as the Windermere Supergroup, and may be as young as Tertiary. The veins are concentrated in the eastern part of the map area and appear to form the northern end of a long belt of similar occurrences.

Map References

Thorkelson, D.J., and Wallace, C.W., 1998. Geological map of Slats Creek area, Wernecke Mountains, Yukon (106D/16). Indian and Northern Affairs Canada, Exploration and Geological Services Division, Geoscience Map 1998-9, scale 1:50,000.

Thorkelson, D.J., and Wallace, C.W., 1998. Geological map of Fairchild Lake area, Wernecke Mountains, Yukon (106C/13). Indian and Northern Affairs Canada, Exploration and Geological Services Division, Geoscience Map 1998-10, scale 1:50,000.

Thorkelson, D.J., and Wallace, C.W., 1998. Geological map of "Dolores Creek" area, Wernecke Mountains, Yukon (106C/14). Indian and Northern Affairs Canada, Exploration and Geological Services Division, Geoscience Map 1998-11, scale 1:50,000.

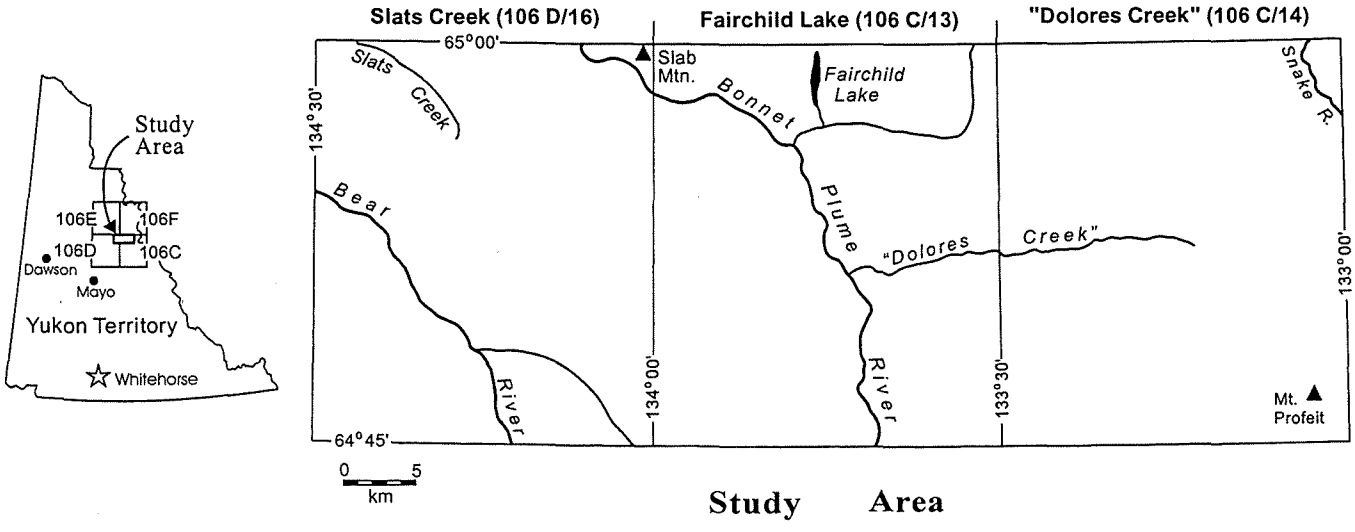

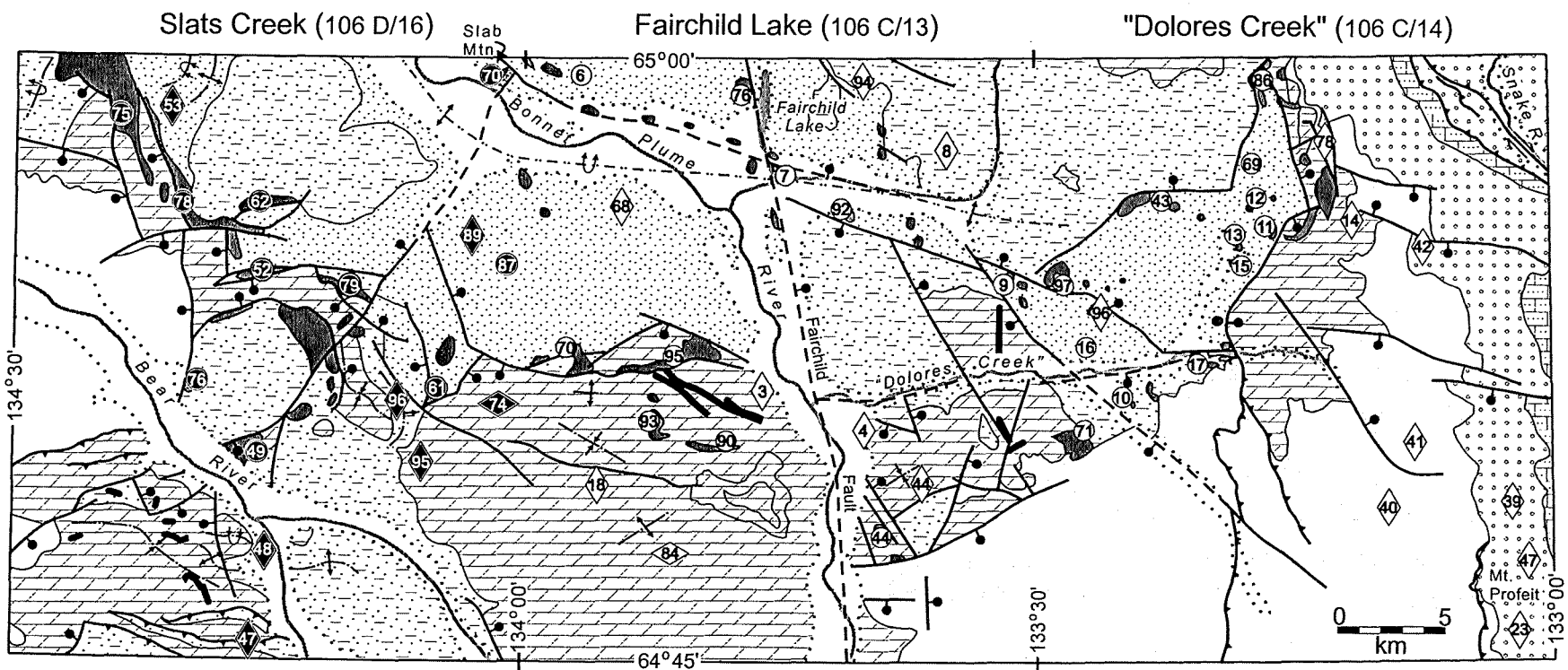

QUATERNARY
- Alluvium, Colluvium, Glacial deposits

CAMBRIAN TO DEVONIAN
- Carbonate and Sandstone

UPPER PROTEROZOIC TO LOWER PALEOZOIC
- Carbonate and Sandstone

UPPER PROTEROZOIC
- *WINDERMERE SUPERGROUP*

MIDDLE TO UPPER PROTEROZOIC
- *PINGUICULA and HEMATITE CREEK GROUPS*

LOWER PROTEROZOIC
- SLAB VOLCANICS

WERNECKE SUPERGROUP
- *GILLESPIE LAKE GROUP*
- *QUARTET GROUP*
- *FAIRCHILD LAKE GROUP*

INTRUSIVE ROCKS

MIDDLE PROTEROZOIC
- BEAR RIVER DYKES (ca. 1.27 Ga)
- WERNECKE BRECCIA (ca. 1.6 Ga)

- normal fault (peg on hanging wall)
- thrust fault (teeth on hanging wall)
- stratigraphic or intrusive contact
- extent of outcrop
- anticline: upright, overturned
- syncline: upright, overturned

MINERAL OCCURRENCES

MINFILE 106D

SLATS CREEK 106D/16
- 49 PAGISTEEL
- 52 FORD
- 61 FOUND
- 62 GNUCKLE
- 70 SLAB
- 75 BLAND
- 76 FACE
- 78 PITCH
- 79 CHIEFTAIN
- 87 SNOWSTAR
- 47 GRAY
- 48 NEW JERSEY
- 53 SLATS
- 89 ZELON
- 95 WALLACE
- 47 CORD

MINFILE 106C

FAIRCHILD LAKE 106C/13
- 6 PLUME
- 7 FAIRCHILD
- 9 DOLORES
- 44 LEARY
- 70 NORANDA
- 76 OTTER
- 90 TOW
- 95 OLYMPIC
- 92 WHALE
- 53 ATHENS
- 3 GILLESPIE
- 4 GEORDIE
- 8 BIBBER
- 18 KIDNEY
- 44 LEARY
- 68 LAW
- 94 CAROL
- 84 GOODFELLOW

"DOLORES CREEK" 106C/14
- 10 KEY MOUNTAIN
- 11 MAMMOTH
- 12 CIRQUE
- 13 PORPHYRY
- 15 AIRSTRIP
- 16 MUELLER
- 17 DOBBY
- 43 DOWSER
- 69 PTERD
- 71 PIKA
- 96 ANOKI
- 97 BEL
- 14 TETRAHEDRITE CREEK
- 23 COB
- 39 PROFEIT
- 40 POO
- 41 CARNE
- 42 DAN
- 47 COAST
- 78 BLUSSON
- 96 JULIE

KEY
- 49 6 *BRECCIA-RELATED: Cu-Co-Au-Ag-U*
- 95 3 *VEINS: Pb-Zn-Ag or Cu +/- Au, Sb, Bi, U*
- 47 84 *STRATAFORM: Pb-Zn-Ag*

Role of partial melting during late-orogenic collapse: Structural and geochronological constraints in the Shuswap metamorphic core complex, Canadian Cordillera

[1]Vanderhaeghe O., [2]Teyssier C., [3]Dunlap W.J., [3]Wysoczansky R., and [3]McDougall I.

[1] Oceanography and Earth Sciences, Dalhousie University, Halifax, NS B3H 4J1, Canada
[2]Geology & Geophysics, University of Minnesota, 310 Pillsbury Dr. SE, MN 55455 USA
[3]Research School of Earth Sciences, Australian National Univerisity, Canberra, ACT Australia

At the latitude of the Thor-Odin dome, the Shuswap Metamorphic Core Complex (MCC) displays a ~15 km structural section composed of an upper unit that preserved Mesozoic metamorphic assemblages, structures and cooling ages, separated from the exhumed metamorphic core by a low-angle detachment zone. Below the detachment, the core of the complex consists of an amphibolite-facies middle unit overlying a migmatitic lower unit exposed in the Thor-Odin dome. Combined structural study and U-Pb geochronology using the SHRIMP analytical facility indicate that pervasive shallowly-dipping foliation and east-west lineation developed in the presence of melt during Paleocene time.

The elliptical shape of the Thor-Odin dome is delineated by the metatexite-diatexite transition across which the rocks lose their solid framework and behave like a viscous magma. Leucogranite probably generated dominantly by partial melting in the migmatitic lower unit, migrated upward through a network of dikes and sills that permeated the middle unit, and ponded to form laccoliths spatially related to the detachment zone.

SHRIMP analysis of complexly zoned zircons from two migmatitic leucosomes and one leucogranite sample yield a crystallisation age of ~ 56 Ma for the migmatites and ~ 60 Ma for the syntectonic granite in the detachment zone. The similarity in age between inherited cores in the migmatite and leucogranite samples suggests a genetic link consistent with the structural analysis.

Argon thermochronology performed on samples from the footwall of the detachments provide some insights on the cooling history of the area. Hornblende yield scattered ages and irregularities in the 40Ar/39Ar age spectra indicate a component of excess argon. Nevertheless, 40Ar/39Ar ages suggest cooling below ~500°C between 60 and 55 Ma. Muscovite and Biotite provide similar ages clustering at ~ 50 Ma. These ages indicate that following the crystallization of migmatites, the footwall of the detachments cooled rapidely. Thermal modelling of K-feldspars age spectra suggest a complex low-temperature cooling history with events at ~ 45 Ma and at ~ 33 Ma.

Based on these data, we propose that exhumation of the core of the Canadian Cordillera during the formation of the Shuswap MCC occurred from 60 to 56 Ma at a time when the crust was significantly partially molten. The structural and temporal relationships between partial melting and exhumation of high-grade rocks suggest a genetic link between mechanical weakening of the crust and late-orogenic collapse in the hinterland of a thermally mature orogenic belt.

Seismic skeletonization + Empirical Mode Decomposition = A new hybrid approach to deep crustal seismic data interpretation

Kris Vasudevan and Frederick Cook
Lithoprobe Seismic Processing Facility
Department of Geology and Geophysics
The University of Calgary
Calgary, Alberta, T2N 1N4
Canada
(E-mail: vasudeva@litho.ucalgary.ca; cook@litho.ucalgary.ca)

Summary

A new decomposition method which combines the features of the seismic skeletonization and empirical decomposition methods is introduced. This forms the basis for analyzing deep crustal seismic reflection data with a view to understanding the decomposition products and the reflected wave-field. A segment of the stack from the Slave-Northern Cordillera Lithosphere Evolution transect line 1 is used to explore the usefulness of the method.

Introduction

Signal decomposition is the separation of a waveform into components that can be used for analysis and interpretation. One such decomposition method for seismic waveform is seismic skeletonization (Li et al., 1997; Vasudevan and Cook, 1998a, 1998b) that separates data traces into cycles or waveforms. Comparing cycles with neighbouring traces by using a pattern recognition method allows extraction of reflectivity patterns, thus providing the basis for seismic interpretation. This method, however, is restrictive in its present form in that it is not conducive to an analysis of frequency variation of an event in time and space. For instance, computing the instantaneous frequency attribute directly from skeletonization results is not possible. Furthermore, for non-stationary data such as deep crustal seismic data, the conditions for a strict definition of instantaneous frequency are not met. To obviate these difficulties, we propose merging a new decomposition method, recently introduced by Huang et al., (1998) with seismic skeletonization. This new decomposition method, empirical mode decomposition (EMD), splits the data into components, "intrinsic mode functions" (IMF), in such a way that for each component the instantaneous frequency could be exactly derived.

In this presentation we introduce a hybrid decomposition method to analyze deep crustal seismic reflection data. We demonstrate with data examples from the Slave-Northern Cordillera Lithosphere Evolution (SNORCLE) seismic reflection line 1 (Cook et al., 1998) that this method affords a mechanism which provides the superposition of the time-frequency representations of the individual components. Furthermore, it consolidates an understanding of the geometry-oriented reflectivity patterns.

Each intrinsic mode function is characterized by a time scale defined by the time lapse between the extrema of amplitudes. Therefore, the set of intrinsic mode functions which result from the new hybrid approach can be used to investigate the scaling behaviour of the seismic reflected wave-field.

The empirical mode decomposition segment of the new hybrid approach is a linear operation. This means that the skeletonized results of the data can be expressed as the skeletonized results of the intrinsic mode functions . Consequently, statistical methods used for the earlier version of skeletonization (Vasudevan and Cook, 1998a) are applicable to the results of the hybrid approach.

Hybrid Method

Deep crustal seismic reflection data are represented in the time domain as a collection of traces. Each trace is expressed in wiggle trace forms with varying peak and trough amplitude widths which is equivalent to a series of cyclic waveforms. Each cycle is made up of a peak and a trough which have properties such as amplitude, width, and location in a seismic profile. Recognizing coherent events in a seismic profile is thus tantamount to recognizing similar features between adjacent cycles that connect to form events, and is the basis of the skeletonization method (Li et al., 1997). Cycles from the same trace are also used in our adaptation of the empirical mode decomposition method (Huang et al. 1998) to generate a set of intrinsic mode functions (decomposition products):

(1) Apply cubic spline method (Press et al., 1992) to connect all the local maxima and minima of a seismic trace using the cycle file. The "maximum"envelope and the "minimum" envelope cover all the data.
(2) Compute the maximum and the minimum envelope;
(3) Take the difference between the data and the mean;
(4) Repeat the sifting procedure with the residue only identical to steps (2) and (3) until the difference in results between the sifting steps is small. This yields the first intrinsic mode function from the data;
(5) Subtract the first intrinsic mode function from the data.
(6) Repeat the sifting procedure on the residue from (5) as outlined in steps (2), (3), (4) and (5) to obtain the second and higher order intrinsic mode functions;
(7) Repeat the above procedure until you are left with the trend.

Following Huang et al., (1998), each intrinsic mode function, $s_j(t)$, can be expressed as

$$s_j(t) = (a_j(t))exp(i \int_{-\infty}^{\infty} w_j(t)\, dt) \tag{1}$$

where the amplitude, $a_j(t)$ and the frequency, $w_j(t)$ are functions of time. The original seismic trace, s(t) is given as

$$s(t) = \sum_{j=1}^{n} s_j(t) \tag{2}$$

Since each intrinsic mode function, $s_j(t)$ has a well-behaved Hilbert transform (Huang et al., 1998), instantaneous frequencies are calculated using it. In our earlier work (Li et al., 1997; Vasudevan and Cook, 1998), we have shown that skeletonization yields an event file which can then be used to carry out a statistical analysis of the seismic attributes associated with the reflected wave-field. The event file after skeletonization of each intrinsic mode function of the data is now updated with the instantaneous frequency attribute information.

Data

A segment of stacked section of the Fort Simpson Crustal Block of the SNORCLE profile 1 (Cook et al., 1998) was considered for analysis using the new hybrid approach (Figure 1). The entire processed data length of 32 s with 4 ms. sampling was used. There are 3000 traces utilized in this study. The stack used here (van der Velden and Hall, LSPF SNORCLE Processing Report, 1997) had not gone through any final post-stack processing such as coherency filtering and migration.

The original profile (Figure 1) exhibited reflectivity in the upper mantle between 25.0 s and 29.0 s (TWT) (highlighted in a rectangle in Figure 1). This subset (1024 traces with a time-window running from 25.0 to 29.092 s) was subjected to the new decomposition method.

Results and Discussion

Skeletonization results of the stack and the first three intrinsic mode functions are shown in Figures 1 to 4. They indicate that both the upper and middle crustal features are well-pronounced in the first three intrinsic modes of the data. The first intrinsic mode has essentially all the structural features that are present in the original data. The second intrinsic mode has a very small contribution to the reflectivity in the middle and lower crust, and the upper mantle. The third mode has negligible contribution below the upper crust.

To understand the results in Figures 1 to 4 a single trace selected from the data and its empirical mode decomposition products are closely examined. From Figure 5 it can be deduced that from one intrinsic mode function to the next, the amplitudes and frequency band-widths decrease. However, within each mode the seismic trace is made up of "waveform packets", with each waveform packet intrinsically associated with major reflection boundaries.

Another general feature that is evident in Figure 1 is the variation in the strength of the signal between stack traces. Not surprisingly, this trend is also present in all the intrinsic modes. One enigmatic feature in this data set is a reflective feature in the upper mantle. It is present in the skeletonization result of the first intrinsic mode of the data (Figure 2), corresponding to data with a wide range of frequencies.

Acknowledgements

The authors would like to thank Natural Sciences and Engineering Research Council of Canada for financial support, and Lithoprobe for the use of deep crustal seismic reflection data of line 1 of the Slave-Northern Cordillera Lithosphere Evolution (SNORCLE) transect in this study. Helpful discussions with and assistance from the LSPF crew are gratefully acknowledged.

References

1. Cook, F.A., van der Velden, A.J., Hall, K.W., and Roberts, B.J., 1998, Tectonic delamination and subcrustal imbrication of the Precambrian lithosphere in northwestern Canada mapped by Lithoprobe, Geology, 26, No. 9, 839-842.

2. Huang, N.E., Shen, Z., Long, S.R., Wu, M.C., Shih, H.H., Zheng, Q., Yen, N-C, Tung, C.C., and Liu, H.H., 1998, The empirical mode decomposition and the Hilbert spectrum for non-linear and non-stationary time series analysis, Proc. Roy. Soc. London, A, 454, 903-995.

3. Li, Q., Vasudevan, K., and Cook, F.A., 1997, Seismic skeletonization: A new approach to interpretation of seismic reflection data, J. Geophys. Res. (Solid Earth), 102 (B4), 8427-8445.

4. Vasudevan, K., and Cook, F.A., 1998a, Skeletons and fractals - A statistical approach to deep crustal seismic data processing and interpretation, Tectonophysics, 286, 93-109.

5. Vasudevan, K., and Cook, F.A., 1998b, Parameterization of reflected wave-field by data decomposition: An example from crustal reflection profiling, 8th international symposium on "Deep seismic profiling of the continents and their margins" at the Platja d'Aro Conference Centre, Barcelona, Spain, September 20-25.

Figure Captions

Figure 1. Skeletonized profile of the Fort Simpson Crustal Block of the SNORCLE line 1. The boxed area is used for a detailed study with the hybrid approach. The section is shown roughly on a 1:1 geological scale. An average crustal velocity of 6500 m/sec was assumed.

Figure 2. Skeletonized profile of the first intrinsic mode function of the original stack of SNORCLE line 1.

Figure 3. Skeletonized profile of the second intrinsic mode function of the original stack of SNORCLE line 1.

Figure 4. Skeletonized profile of the third intrinsic mode function of the original stack of SNORCLE line 1.

Figure 5. Intrinisc mode functions from the new skeletonization approach. (a) Original stack trace 1000 from the Fort Simpson Crustal Block. 8001 samples of data with a sample interval of 4 ms. were considered; (b) First intrinsic mode function of trace; (c) Second intrinsic mode function of trace (a); (d) Third intrinsic mode function of trace (a); (e) Fourth intrinsic mode function of trace (a); (f) Reconstructed stack trace 1000 from the empirical modes of the original data. Results of intrinsic mode functions were obtained after four repeating the sifting procedure four times.

FORT SIMPSON BLOCK - INITIAL STACK

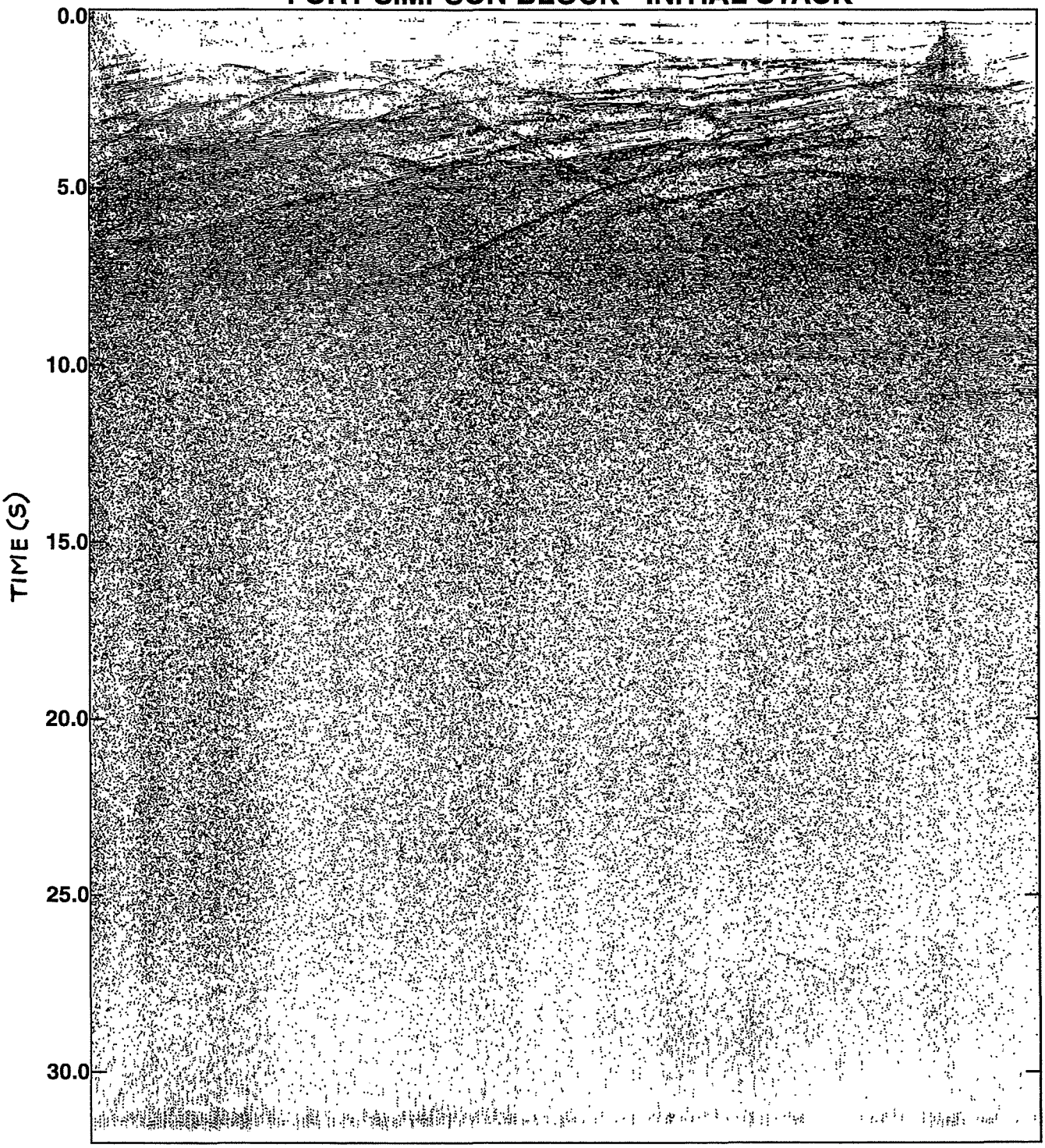

FORT SIMPSON BLOCK - INTRINSIC MODE FUNCTION ONE

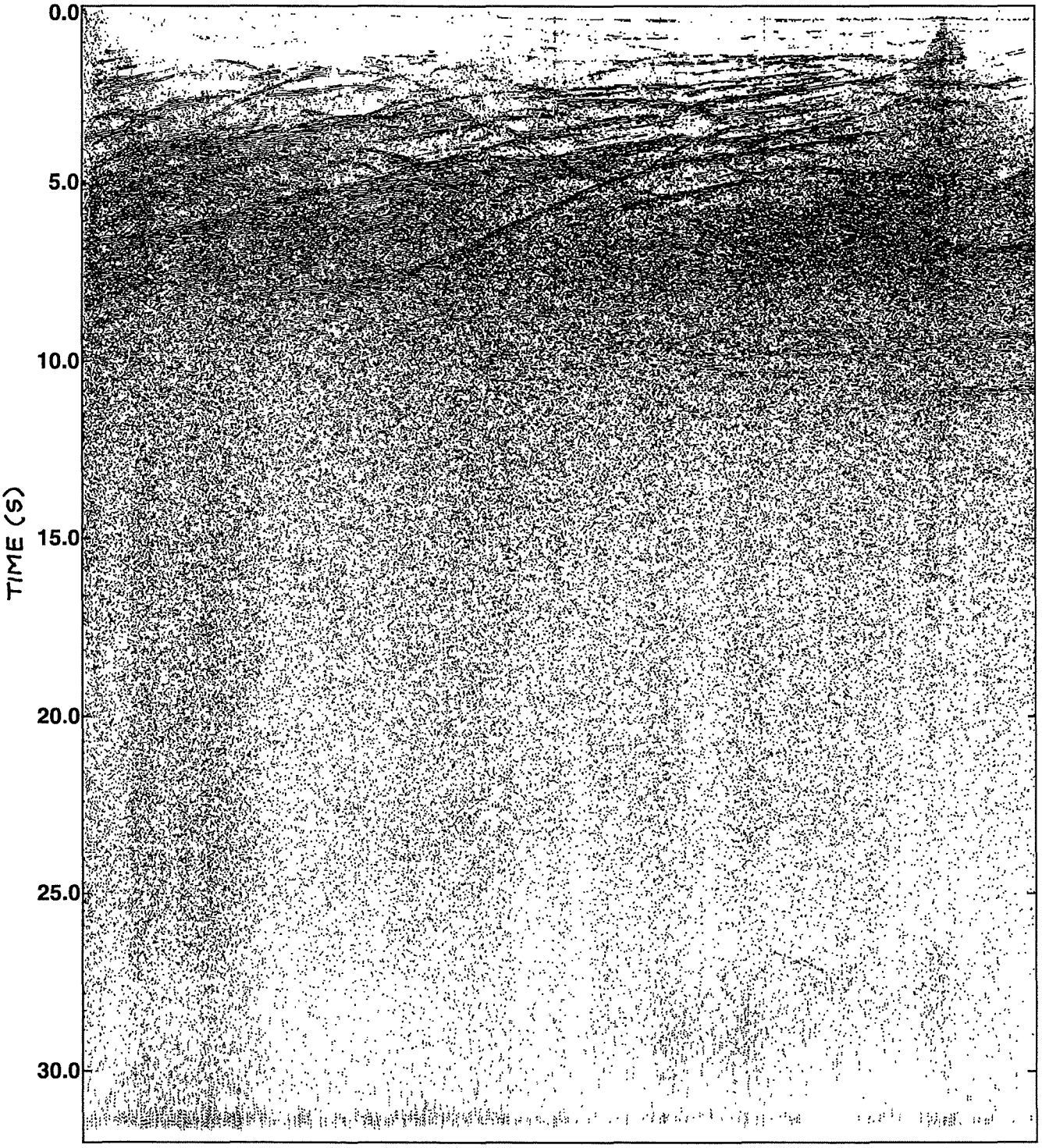

FORT SIMPSON BLOCK - INTRINSIC MODE FUNCTION TWO

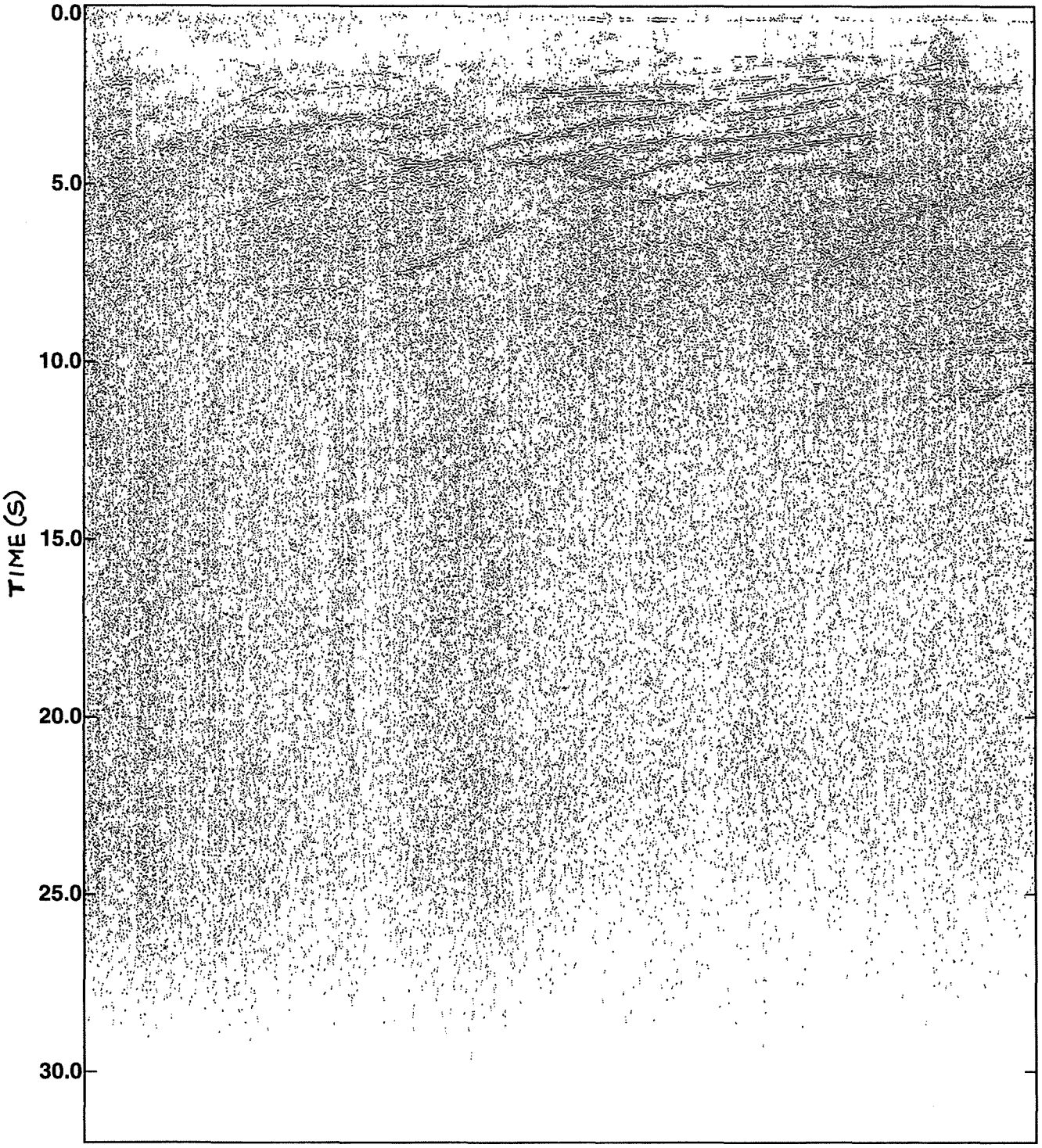

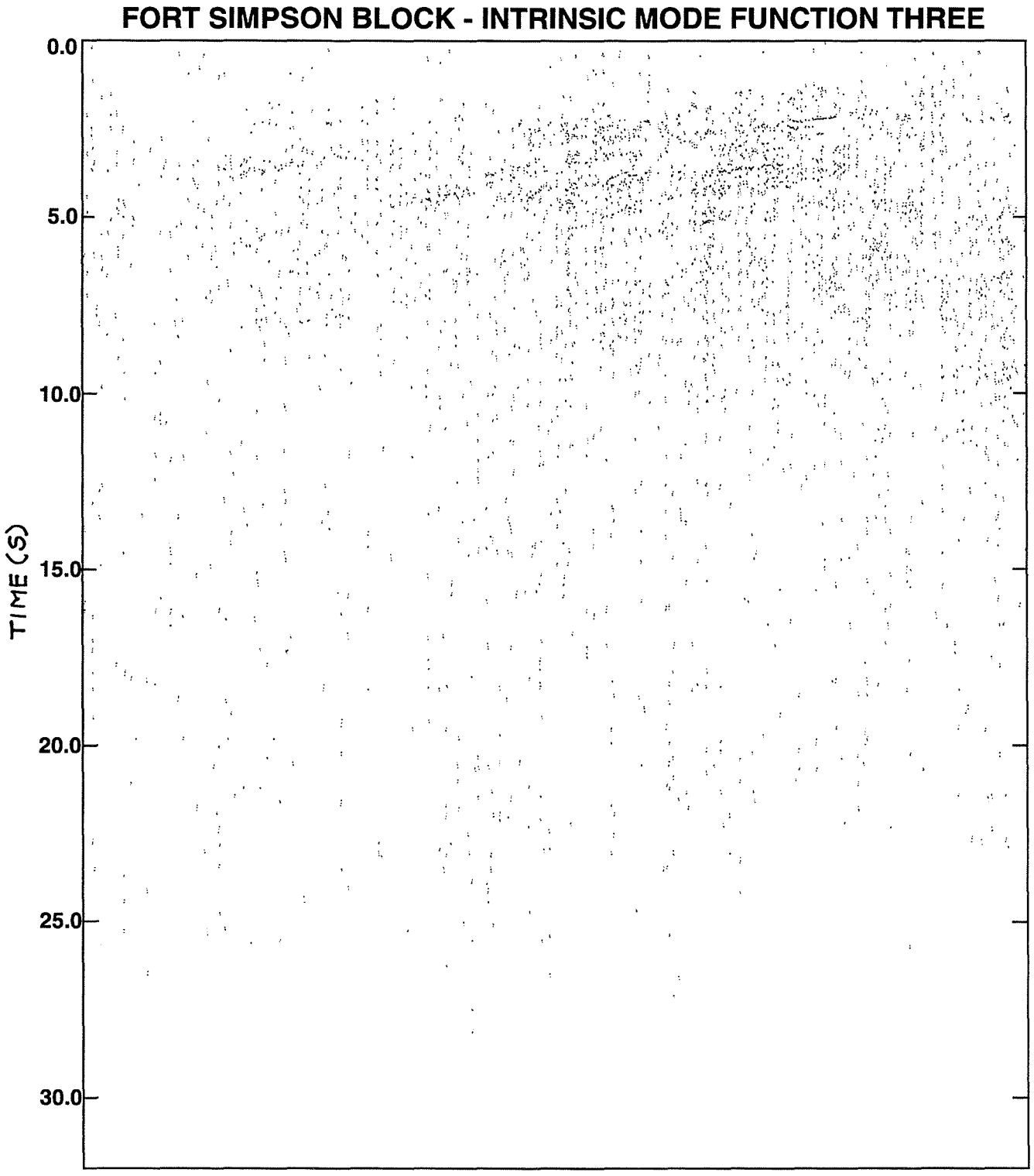
FORT SIMPSON BLOCK - INTRINSIC MODE FUNCTION THREE
TIME (S)
0.0
5.0
10.0
15.0
20.0
25.0
30.0

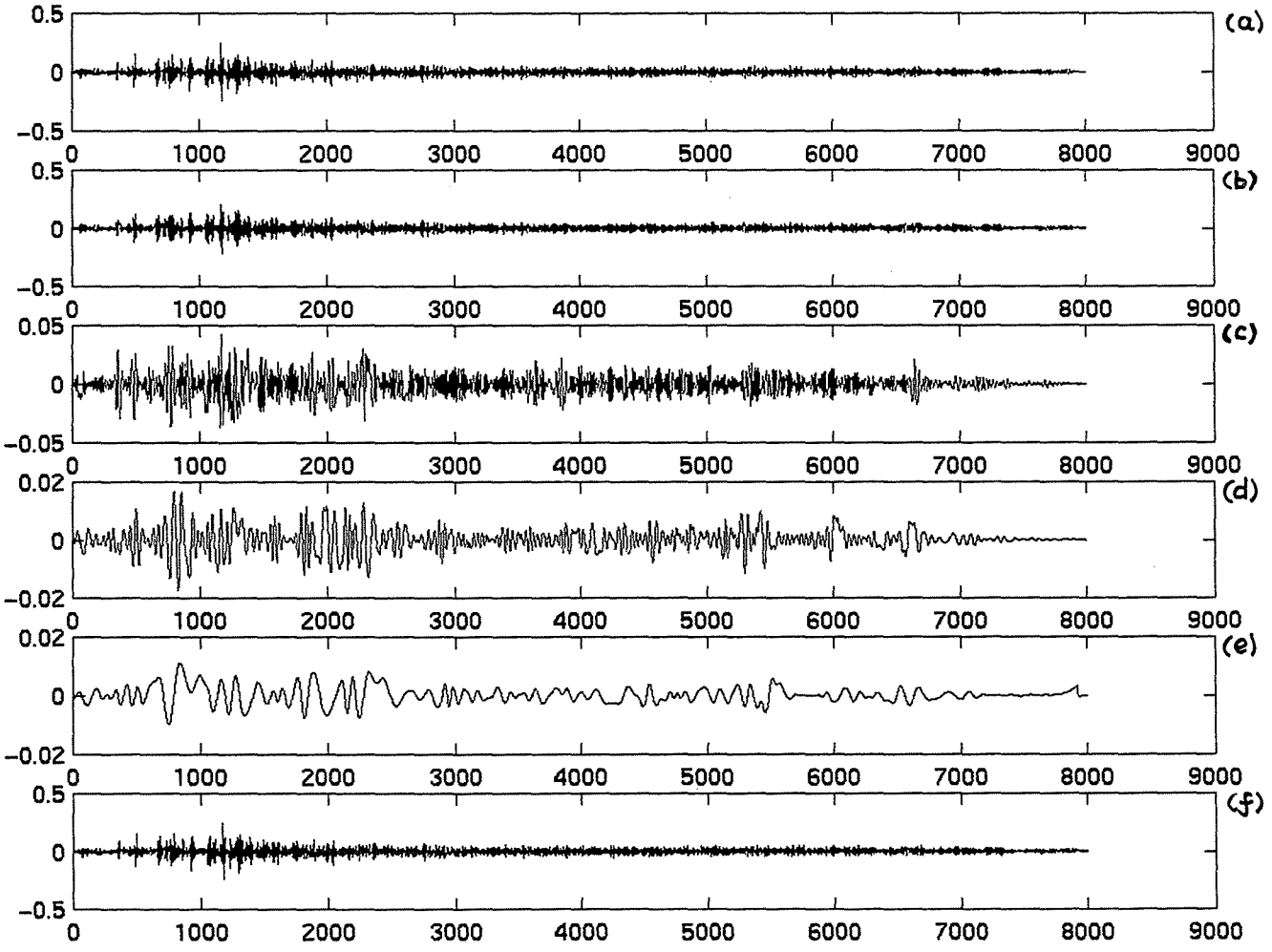
(a)
(b)
(c)
(d)
(e)
(f)
0.5
0
−0.5
0.05
−0.05
0.02
−0.02
0
1000
2000
3000
4000
5000
6000
7000
8000
9000

Towards a Transect of the North American Lithosphere

K. Vasudevan, F.A. Cook, A.J. van der Velden, E. Lynn
Lithoprobe Seismic Processing Facility
Department of Geology and Geophysics
University of Calgary, Calgary
AB T2N 1N4, Canada

and

R.M.Clowes
LITHOPROBE
University of British Columbia
357-6339 Stores Road
Vancouver
BC V6T 1Z4, Canada

LITHOPROBE, Canada's national geoscience research project, has acquired more than 10,000 km of land-based deep crustal reflection data from Vancouver Island to Newfoundland during the past 15 years. As part of its multidisciplinary scientific program, an additional 6350 km of marine-based data were acquired west of Vancouver Island, in the Great Lakes, in the Gulf of St. Lawrence, in Ungava Bay, east of Labrador and on Canada's Atlantic margin. A subset of these data are compiled into a transect that traverses the North American continent from the active Juan de Fuca Ridge in the Pacific ocean, across the southern Canadian Cordillera, the craton underlying the Western Canada Sedimentary Basin, the exposed Precambrian shield of central Canada, the southern Superior Province of Ontario and Quebec, the grenville Province, and the Appalachians of eastern Canada to the Mesozoic continental margin of the Atlantic ocean. The 5500-km long composite reflection section provides lithospheric structure over an unprecedented length scale and establishes a framework for compiling and analysing many of the LITHOPROBE geological and geophysical data sets.

Results from LITHOPROBE SNoRE 97 Experiment, Line 21: Seismic Velocity Structure across the Canadian Cordillera of Northeastern British Columbia

J. Kim Welford and Ron M. Clowes

Dept. of Earth & Ocean Sciences, Univ. of British Columbia, 6339 Stores Road, Vancouver, BC, V6T 1Z4

kwelford@geop.ubc.ca, clowes@lithoprobe.ubc.ca

ABSTRACT

The SNoRE 97 seismic refraction/wide-angle reflection (R/WAR) survey was conducted during the months of August and September 1997 in the Slave-Northern Cordillera Lithospheric Evolution (SNorCLE) transect of the LITHOPROBE project. Refraction line 21 is located in northeastern British Columbia and extends WNW to ESE for 450 km. Line 21 was designed to determine the velocity structure of the crust and upper mantle from the NW portion of the Western Canada Sedimentary Basin (WCSB), across the deformation front of the northern Cordillera into deformed North American rocks and across the Tintina Fault, the eastern boundary of accreted terranes. The goal of this investigation is to resolve the transition at depth between the eastern portion of the Cordillera and the Proterozoic-Paleozoic rifted margin of ancestral North America on which the Cordillera has been thrust. Seismic coverage along Line 21 involved 530 seismographs and a total of 8 shots detonated at spacings of $\sim$ 60 km along the line. The refraction data show good signal-to-noise ratios; primary phases (Pg, Sg, PmP and Pn) are clearly observed for most shots. A velocity structural model is achieved through tau-p analysis, forward ray trace modeling and 2-d inversion using RAYINVR. A multidisciplinary approach is undertaken by way of 2.5-d forward modeling of potential field data to show consistency with the velocity model and to provide further structural and lithological constraints for the interpretation.

GEOTECTONIC SETTING

The easternmost coverage of Line 21 extends onto the western margin of ancestral North America which developed into a passive margin sequence in Neoproterozoic time. In terms of tectonic elements (Fig. 1.1), this section of Line 21 begins in the east in the Fort Simpson terrane, extends westward across the Nahanni terrane, and then into the margin of ancestral North America. The

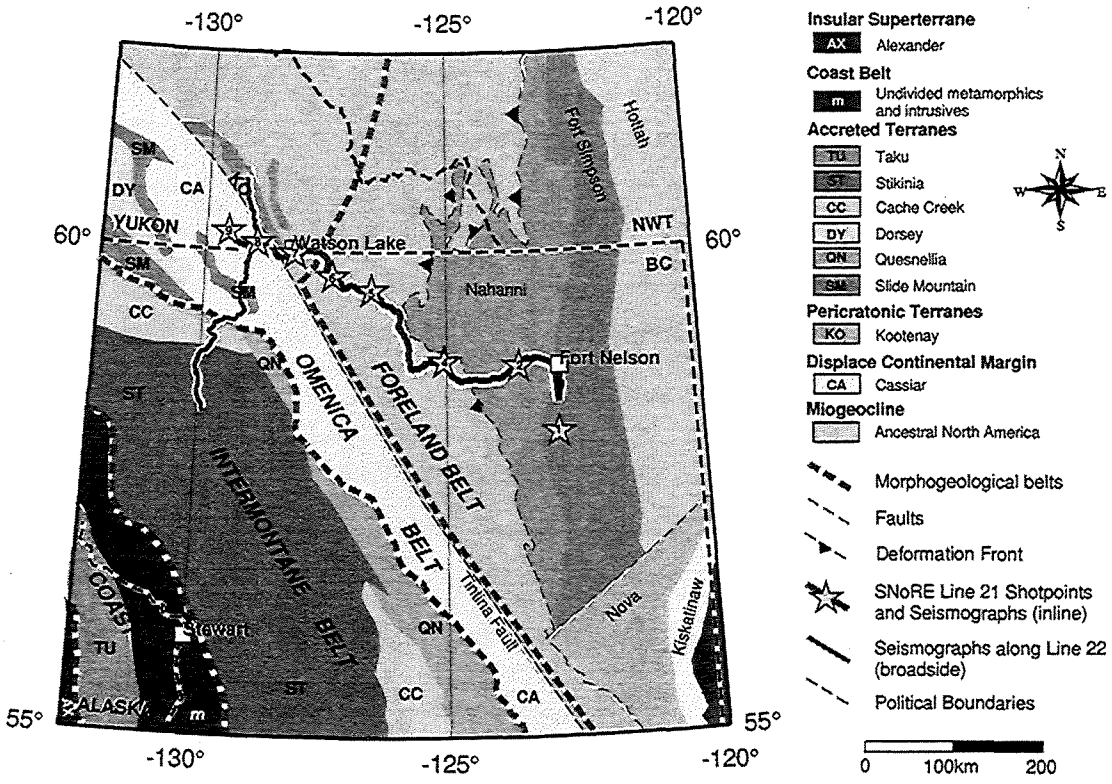

Figure 1.1: Terrane map of SNorCLE transect surrounding Line 21.

Nahanni and Fort Simpson domains were accreted as part of the Wopmay Orogen in Paleoproterozoic times.

To the west in the Cordilleran Foreland, Line 21 samples the mountainous Foreland Belt. This classic fold and thrust belt is composed of folded miogeoclinal and clastic wedge assemblages of Mesoproterozoic to Jurassic age that were deposited on and along the flank of the western passive margin of ancestral North America.

The westernmost extent of Line 21 crosses the Tintina Fault and samples the Omineca Belt which straddles the boundary between the accreted terranes and the North American miogeocline.

EXPERIMENT AND LINE 21 DESCRIPTION

The LITHOPROBE 1997 Slave-Northern Cordillera Refraction Experiment (SNoRE '97) was designed to determine the velocity structure of the crust and the upper mantle from Great Slave Lake

in the Northwest Territories to the coast of the Alaska "Panhandle". To achieve this goal, four refraction/wide-angle reflection profiles, numbered 11, 21, 22 and 31, were collected along three corridors of the SNorCLE transect.

Line 21 in Corridor 2 was designed to determine the velocity structure of the crust and upper mantle from the NW portion of the Western Canada Sedimentary Basin (WCSB), across the deformation front of the northern Cordillera into deformed North American rocks and across the Tintina Fault, the eastern boundary of accreted terranes (Fig. 1.1). The line is 450-km-long and extends along the Alaska Highway from Fort Nelson, BC, west to Watson Lake, Yukon. 594 portable seismographs were deployed along Line 21 (station spacing 1.0 km) and along the northern half of Line 22 (station spacing 2.0 km). Eight shot points along Line 21 were recorded by all stations, providing inline profiles and broadside coverage across the Tintina Fault south of Watson Lake.

DATA QUALITY AND PRELIMINARY INTERPRETATION

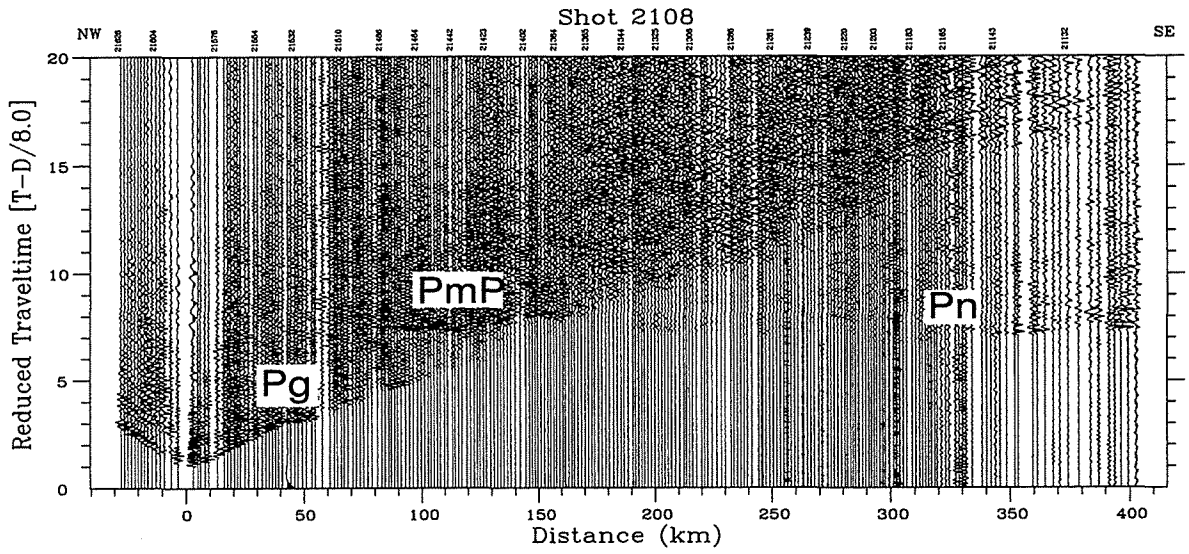

Figure 1.2: Data section for shot 2108.

The refraction data show good signal-to-noise ratios and primary phases [Pg, PmP, Pn and Sg] are observable for most shots. Highest signal-to-noise ratios occur for shots at the ends of the line (2101, 2102, 2107, 2108 (Fig. 1.2) and 2109). Shot 2104 has the noisiest data and only provides reliable Pg for near offsets. These arrivals show high velocities (6.3 km/s within 5 km of the surface). Shot 2108 shows anomalously slow velocities at the surface near the Tintina Fault.

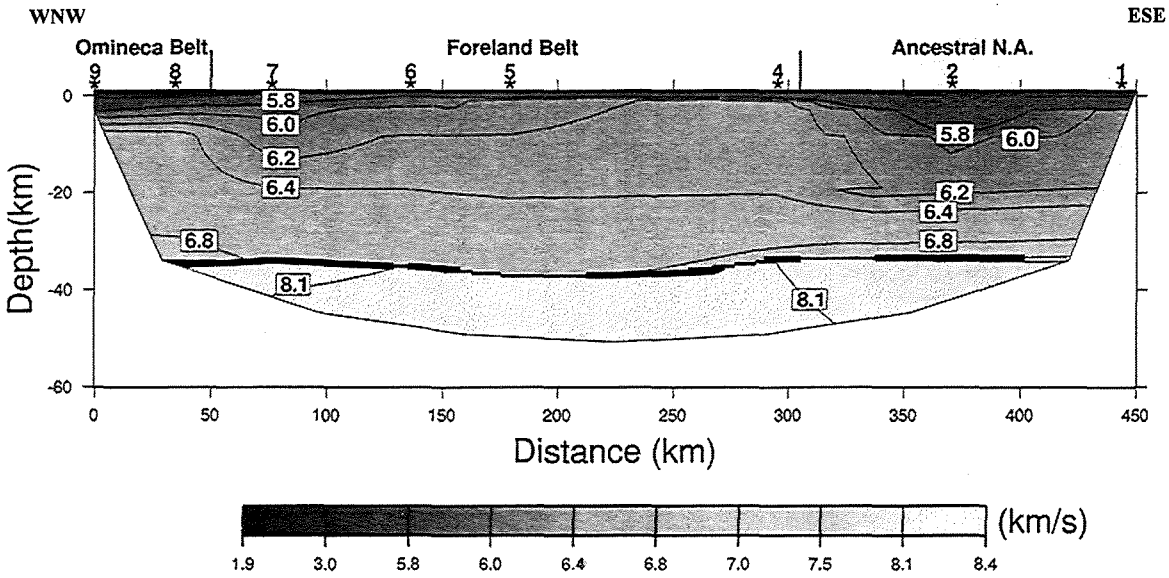

Figure 1.3: Preliminary velocity structural model for Line 21. Thin lines are velocity contours (km/s). Heavy solid lines indicate locations of wide-angle reflections from the Moho.

The preliminary velocity structural model (Fig. 1.3) was obtained using tau-p analysis (Gorman and Clowes, 1999), forward ray trace modeling and some 2-d inversion using RAYINVR (Zelt and Smith, 1992). Preliminary analyses show low upper crustal velocities (6.2 km/s and less) extending to almost 20 km depth in the east below the WCSB. These interpreted Proterozoic miogeoclinal metasediments do not extend westward into the Foreland Belt. The middle crust beneath the WCSB in the east consists of a thin layer (5-10 km) with velocities of $\sim$ 6.4 km/s; from the foreland westwards, the middle crustal layer thickens to 15-20 km and averages velocities of $\sim$ 6.5 km/s with a distinct velocity increase to $\sim$ 6.7 km/s west of the Tintina Fault. The resolved depth to Moho is $\sim$ 33 km in the east, deepening to $\sim$ 38 km beneath the Cordilleran foreland and shallowing to $\sim$ 35 km near the Omineca Belt. Upper mantle velocities beneath ancestral North America average $\sim$ 7.9 km/s, increasing to $\sim$ 8.2 beneath the Foreland Belt and returning to average values of $\sim$ 8.0 km/s beneath the Omineca Belt.

Preliminary interpretations identify the slow upper crustal velocities in the east as representing the Proterozoic and Paleozoic sediments and metasediments of the WCSB. These sediments extend to significant depths of almost 20 km but do not extend westward into the Foreland Belt. Anomalously high upper crustal velocities beneath shot 2104 are interpreted as denser uplifted sheets of middle crustal rocks that have replaced the WCSB sediments to the east.

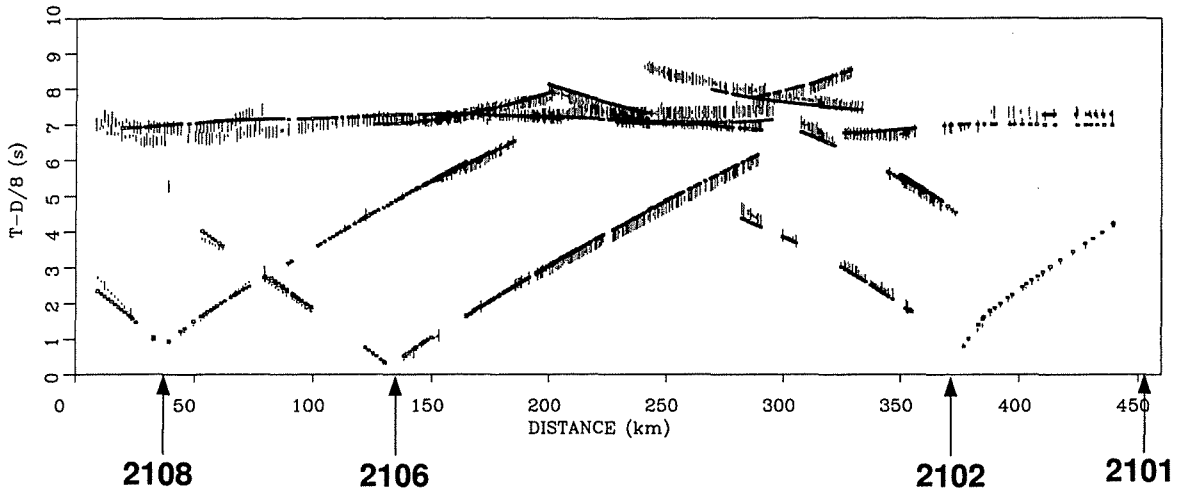

Figure 1.4: Plot of observed traveltime picks (vertical bars with length equivalent to the traveltime pick uncertainty) overlain by the calculated traveltime picks for shots 2101, 2102, 2106 and 2108.

At the Foreland/Omineca Belt transition, very slow upper crustal velocities near 2108 possibly result from saturated sediments filling in the fault scar. Higher lower crustal velocities west of the Tintina Fault may represent more mafic rock compositions. While the inline ray coverage along line 21 is unable to resolve any drastic Moho transitions beneath the Tintina Fault, the deepening of the Moho beneath the Foreland Belt is explained as isostatic support for the mountainous Foreland. Preliminary gravity field modeling using SAKI (Webring, M., 1985) supports this deepening of the Moho beneath the Foreland Belt.

FUTURE WORK

Future work will involve additional refining of the velocity structural model to incorporate all possible crustal reflectors and forward amplitude modeling. Using interpretation from Line 21 and Line 22, the broadside SGR data will be incorporated into the analysis to obtain a 3-dimensional velocity structure in the region of the Tintina Fault. Potential field modeling will be improved to incorporate 3-d forward modeling of the crust.

ACKNOWLEDGEMENTS

The funding for SNoRE 97 was provided by the NSERC Collaborative Special Projects grant to LITHOPROBE, the Geological Survey of Canada, and NSERC Research Grants to R.M. Clowes, R.M. Ellis and G. Spence. J. Kim Welford is the recipient of a CSEG Scholarship.

REFERENCES

Gorman, A.R. and R.M. Clowes, 1999. Wave-field tau-p analysis for 2-d velocity models: Application to western North American lithosphere, Geophys. Res. Lett., in press.

Webring, M., 1985. SAKI: A Fortran program for generalized linear inversion of gravity nad magnetic profiles, United States Department of the Interior, Geological Survey, Open File Report 85-122.

Zelt, C.A. and R.B. Smith, 1992. Seismic traveltime inversion for 2-d crustal velocity structure, Geophys. J. Int., 108, p.16-34.